Development and Mechanistic Elucidation of Carbonyl–Olefin Metathesis Transformations

by

Hannah L. Vonesh

A dissertation submitted in partial fulfillment
of the requirements for the degree of
Doctor of Philosophy
(Chemistry)
in the University of Michigan
2022

Doctoral Committee:

Professor Corinna S. Schindler, Chair
Assistant Professor Timothy A. Cernak
Professor Corey R. J. Stephenson
Professor John P. Wolfe

Hannah L. Vonesh

hvonesh@umich.edu

ORCID iD: 0000-0003-0448-0243

© Hannah L. Vonesh 2022

Dedication

To my parents, Mike and Anne, my siblings, Marissa, Grace, and John, my grandmother, Diane, and my anchor, Zach.

Table of Contents

Dedication ii

List of Figures vi

List of Tables viii

List of Abbreviations ix

Abstract xiii

Chapter 1: Inherent Reactivity of Carbonyls and Olefins 1

1.1 Introduction 1

1.2. Carbonyl-Ene Reactions 2

1.3 Prins Reactions 4

1.4 Carbonyl–Olefin Metathesis 5

1.5 Interrupted Carbonyl–Olefin Metathesis 7

1.6 References 10

Chapter 2: Ring-Opening Carbonyl–Olefin Metathesis 14

2.1 Introduction 14

2.2 Results and Discussion 15

2.3 Mechanistic Investigations 18

2.4 Conclusions 21

2.5 Experimental Procedures and Supplemental Information 21

2.5.1 General Information 21

2.5.2 Optimization 23

2.5.3 Mechanistic Investigations 26

2.5.4 Experimental Procedures 31

2.5.5 NMR Spectra 47
2.6 References 76
Chapter 3: Intermolecular Cross Carbonyl–Olefin Metathesis 80
3.1 Introduction 80
3.2 Results and Discussion 83
3.3 Mechanistic Investigations 87
3.4 Conclusions 89
3.5 Experimental Procedures and Supplemental Information 90
3.5.1 General Information 90
3.5.2 Optimization 91
3.5.3 Mechanistic Investigations 95
3.5.4 Experimental Procedures 104
3.5.5 NMR Spectra 115
3.6 References 140
Chapter 4: Interrupted Carbonyl–Olefin Metathesis of Cyclic, Aliphatic Ketones 144
4.1 Introduction 144
4.2 Results and Discussion 147
4.3 Mechanistic Investigations 150
4.4 Conclusions 152
4.5 Experimental Procedures and Supplemental Information 153
4.5.1 General Information 153
4.5.2 Optimization 154
4.5.3 Mechanistic Investigations 156
4.5.4 Computational Data 160
4.5.5 Experimental Procedures 160
4.5.6 NMR Spectra 182
4.6 References 225

Chapter 5: Stepwise Carbonyl–Olefin Metathesis 230
5.1 Introduction 230
5.2. Revisiting Gas Phase and Implicit Solvent DFT Computations 232
5.3 Experimental Mechanistic Investigations 233
5.4 Explicit Solvent Molecular Dynamics 237
5.5 Conclusions 242
5.6 Experimental Procedures and Supplemental Information 243
5.6.1 General Information 243
5.6.2 General Procedures 245
5.6.3 Synthesis and Characterization 247
5.6.4 Kinetic Isotope Effects 305
5.6.5 Hammett Studies 307
5.6.6 Secondary Deuterium Kinetic Isotope Effects 309
5.6.7 Computations 313
5.7 References 339

List of Figures

Figure 1.1: Reactivity between carbonyls and olefins. 1
Figure 1.2: Selected examples of carbonyl-ene reactions..... 3
Figure 1.3: Selected examples of Prins reactions. 4
Figure 1.4: Selected carbonyl–olefin metathesis examples by Schindler and co-workers. 5
Figure 1.5: Selected examples of divergent reactivity observed for interrupted carbonyl–olefin metathesis examples by Schindler and co-workers. 7
Figure 2.1: Ring-opening olefin–olefin cross-metathesis. 14
Figure 2.2: *This work:* $GaCl_3$-catalyzed ring-opening carbonyl–olefin metathesis..... 15
Figure 2.3: Reaction optimization. 16
Figure 2.4: Ring strain of cyclic olefins. 17
Figure 2.5: Aldehyde and olefin scope for ring-opening carbonyl–olefin metathesis..... 17
Figure 2.6: ^{1}H-NMR fragmentation studies of oxetanes **42** and **43**..... 18
Figure 2.7: Mechanistic investigations of aldehyde **44**. 19
Figure 2.8: ^{1}H-NMR experiment of the $GaCl_3$-catalyzed ring-opening carbonyl–olefin metathesis reaction. 20
Figure 2.9: Mass balance of ring-opening carbonyl–olefin metathesis.. 21
Figure 3.1: Traditional olefin–olefin cross metathesis. 80
Figure 3.2: Recent reports of Lewis acid-catalyzed intermolecular cross carbonyl–olefin metathesis..... 81
Figure 3.3: Activation of less reactive carbonyl substrates by stronger Lewis acids. 81
Figure 3.4: 6-membered ring formation via a superelectrophilic aluminum/silver ion pair catalyst. 82
Figure 3.5: *This work:* Intermolecular cross carbonyl–olefin metathesis promoted via an iron/silver ion pair catalyst..... 82
Figure 3.6: Reaction optimization. 83
Figure 3.7: Evaluation of active catalytic species..... 85
Figure 3.8: Evaluation of the olefin substrate scope..... 86

Figure 3.9: Aldehyde scope for intermolecular cross carbonyl–olefin metathesis. 86
Figure 3.10: Evaluation of a carbonyl-ene pathway. 87
Figure 3.11: Mechanistic investigations for intermolecular cross carbonyl–olefin metathesis... 88
Figure 3.12: ^{1}H-NMRs of oxetanes *trans*-**58** and *trans*-**59** and their subsequent fragmentation. 89
Figure 4.1: Synopsis of the reactivity between carbonyls and olefins. 144
Figure 4.2: *This work:* Iron-catalyzed carbonyl–olefin metathesis and interrupted carbonyl–olefin metathesis of cyclic, aliphatic ketones. 145
Figure 4.3: Representative natural products incorporating **15**. 146
Figure 4.4: Piers and co-workers' synthetic route to isopropyl bicyclic scaffolds. 146
Figure 4.5: Divergent reactivity of cyclic ketone **23** with distinct iron(III) sources. 146
Figure 4.6: Reaction optimization. 147
Figure 4.7: Evaluation of the olefin scope. 148
Figure 4.8: Substrate scope for cyclic, aliphatic ketones for the interrupted carbonyl–olefin metathesis reaction. 149
Figure 4.9: Deuterium labeling studies to evaluate a possible 1,2-hydride shift mechanism.... 150
Figure 4.10: Mechanistic evidence for the proposed interrupted carbonyl–olefin metathesis reaction pathway. 151
Figure 5.1: Mechanistic proposals for carbonyl–olefin metathesis. 231
Figure 5.2: Conventional DFT calculations (B3LYP-D3(BJ)/jul-cc-pVDZ) predict concerted carbonyl–olefin metathesis in implicit solvent. 232
Figure 5.3: Workflow for ^{12}C/^{13}C KIE measurements. 233
Figure 5.4: Experimental ^{12}C/^{13}C KIEs support a stepwise mechanism. 234
Figure 5.5: Hammett studies. 236
Figure 5.6: Secondary ^{1}H/^{2}H KIE studies. 237
Figure 5.7: Solvation method affects the predicted mechanism. 238
Figure 5.8: Marcus analysis. 240
Figure 5.9: Selectivity for the carbonyl–olefin metathesis pathway. 241

List of Tables

Table 2.1: Lewis acid screen. 23
Table 2.2: Solvent screen. 23
Table 2.3: Substrate ratio screen. 24
Table 2.4: Temperature screen. 24
Table 2.5: Catalyst loading screen. 24
Table 2.6: Concentration screen. 25
Table 2.7: Time point screen. 25
Table 3.1: Lewis acid screen. 91
Table 3.2: Lewis acid screen with Ag salt. 91
Table 3.3: Ag salt screen. 92
Table 3.4: AgCl recovery. 92
Table 3.5: Lewis acid and Ag salt loading screen. 93
Table 3.6: Solvent screen. 93
Table 3.7: Time point screen. 94
Table 3.8: Solvent concentration screen. 94
Table 3.9: Temperature screen. 94
Table 3.10: Starting material ratio screen. 95
Table 4.1: Preliminary Lewis acid screen. 154
Table 4.2: Extensive Lewis acid screen. 154
Table 4.3: Solvent screen. 155
Table 4.4: Catalyst loading screen. 155
Table 4.5: Temperature screen. 155
Table 4.6: Solvent concentration screen. 156

List of Abbreviations

° C	degree Celsius
Ac	acetyl
AllylOH	allyl alcohol
AllylTMS	allyltrimethylsilane
aq.	aqueous
Ar	aryl
BF_4	tetrafluoroborate anion
Bn	benzyl
BnBr	benzyl bromide
BnOH	benzyl alcohol
Bu	butyl
cm	centimeters
$CDCl_3$	deuterated chloroform
COM	carbonyl–olefin metathesis
$Cr(acac)_3$	chromium(III) acetylacetonate
DCE	1,2-dichloroethane
DCM	dichloromethane
DEPT	distortionless enhancement by polarization transfer
DFT	density functional theory
δ	chemical shift in parts per million
d	doublet
dd	doublet of doublets
DIBAL-H	diisobutylaluminium hydride
DMAP	4-(Dimethylamino)pyridine
DMF	N,N’-dimethylformamide
DMP	1,1,1-Tris(acetyloxy)-1,1-dihydro-1,2-benziodoxol-3-(1H)-one

DMS	dimethyl sulfoxide
DMSO	dimethyl sulfoxide
EDG	electron donating group
ee	enantiomeric excess
EPR	electron paramagnetic resonance
eq.	equation
equiv.	equivalents
Et	ethyl
Et_2O	diethyl ether
EtOAc	ethyl acetate
EtOH	ethanol
EWG	electron withdrawing group
$FeCl_3$	iron(III) chloride
FT-IR	Fourier Transform-infrared spectroscopy
g	grams
h	hours
H_2	hydrogen
HCl	hydrogen chloride
HRMS	high resolution mass spectroscopy
hν	light
Hz	hertz
IBX	2-iodoxybenzoic acid
*i*Pr	*iso*-propyl
*i*PrOH	isopropanol
J	coupling constant
KIE	kinetic isotope effect
K_2CO_3	potassium carbonate
LDA	lithium diisopropylamine
LED	light-emitting diode
Li	lithium
$LiAlH_4$	lithium aluminum hydride

m	multiplet
M	molar concentration
*m*CPBA	*meta*-chloroperoxybenzoic acid
Me	methyl
MeCN	acetonitrile
MeLi	methyl lithium
MeOH	methanol
MeOD	deuterated methanol
mg	milligrams
$MgSO_4$	magnesium sulfate
MHz	megahertz
min	minutes
µL	microliters
mL	milliliters
mM	millimolar concentration
mmol	millimoles
mol	moles
mol%	mole percent
MW	molecular weight
N_2	nitrogen
Na_2SO_4	sodium sulfate
NaH	sodium hydride
$NaHCO_3$	sodium bicarbonate
Na_2CO_3	sodium carbonate
n-BuLi	*n*-butyllithium
NH_4Cl	ammonium chloride
NH4OH	ammonium hydoxide
NMR	nuclear magnetic resonance
OTF	triflate anion
O_3	ozone
p	pentet

PES	potential energy surface
Ph	phenyl
PhCl	1-chlorobenzene
PhH	benzene
PhMe	toluene
$PhSiMe_3$	phenyltimethylsilane
ppm	parts per million
q	quartet
R	alkyl group
rt	room temperature
s	singlet
SDKIE	secondary deuterium kinetic isotope effect
t	triplet
TBAF	tetra-*n*-butylammonium fluoride
TBSCl	*tert*-butyldimethylsilyl chloride
TEA	triethylamine
TfOH	triflic acid
THF	tetrahydrofuran
TLC	thin layer chromatography
TMEDA	N,N,N′,N′-tetramethylethylenediamine
TMSCN	trimethylsilyl cyanide
TPP	triphenyl phosphine
TsOH	*p*-toluenesulfonic acid
RF	response factor
SCF	supercritical fluid chromatography
UPLC	ultra-high performance liquid chromatography

Abstract

Olefin–olefin metathesis has drastically changed how olefins are synthesized in materials, agrochemicals, and pharmaceuticals. An important variation of olefin–olefin metathesis is carbonyl–olefin metathesis, which provides an additional approach to access olefins, but has lacked advancements in methodology. In the last decade, the development of catalytic protocols for carbonyl–olefin metathesis has brought a renewed interest to field. The current proposed catalytic cycle for $FeCl_3$-catalyzed intramolecular ring-closing carbonyl–olefin metathesis from Schindler and co-workers in 2017 operates through an asynchronous, concerted [2+2]-cycloaddition, forming a reactive oxetane intermediate. The Lewis acid-bound oxetane fragments *via* retro-[2+2]-cycloaddition to furnish the desired metathesis product and a carbonyl byproduct. This work has been expanded to new reaction paradigms, including intermolecular ring-opening and cross carbonyl–olefin metathesis variants, as well as other Lewis acid-catalyzed interrupted carbonyl–olefin metathesis transformations. Recently, new mechanistic proposals for Lewis acid-catalyzed carbonyl–olefin metathesis have been published in the literature, and in collaboration with Merck & Co. the Schindler group reinvestigated the reaction.

Chapter 1 details the known reactivity modes for Lewis and Brønsted acids with carbonyls and olefins from their very beginnings; focused initially on carbonyl-ene and Prins chemistry, followed by the more recently discovered reactivity with carbonyl–olefin metathesis and interrupted carbonyl–olefin metathesis. Chapter 2 describes the first report of intermolecular ring-opening carbonyl–olefin metathesis between cyclic olefins and carbonyls. The reaction exclusively yields one of two metathesis products, further mechanistic investigations reveal that the transformation proceeds through a single regioisomeric oxetane to provide unsaturated ketones. A competing carbonyl-ene pathway provides two additional products.

Chapter 3 investigates the superelectrophilic $FeCl_3/AgBF_4$ ion pair-catalyzed cross carbonyl–olefin metathesis of aldehydes and tri-substituted olefins. The reaction exclusively yields (*E*)-olefin products, one of three possible metathesis products. Independently synthesized oxetane intermediates were used to study the selectivity in key mechanistic step, and only a single regio- and diastereomeric oxetane provides the observed metathesis product. Chapter 4 outlines the

synthesis of pentalenes, indenes, naphthalenes, and azulenes from cyclic, aliphatic ketones *via* a new reactivity mode of carbonyls and olefins. A distinct Lewis acid-catalyzed interrupted carbonyl–olefin metathesis furnishes the interesting bicyclic products.

Lastly, Chapter 5 details the extensive mechanistic elucidation and revision of $FeCl_3$-catalyzed intramolecular ring-closing carbonyl–olefin metathesis. Experimental ^{13}C kinetic isotope effects (KIEs), β-secondary deuterium KIEs, Hammett studies, and explicit solvent calculations all correspond to a stepwise addition mechanism, rather than an asynchronous, concerted [2+2] mechanism. This unique combination of ^{13}C natural abundance KIEs and explicit solvent molecular dynamics calculations reveals a common failure mode in routinely used implicit solvent calculations that can lead to incorrect predictions of charged intermediates along reaction pathways.

Chapter 1: Inherent Reactivity of Carbonyls and Olefins

1.1 Introduction

Lewis and Brønsted acid-catalyzed carbon-carbon bond forming transformations are powerful synthetic tools in organic chemistry.[1] Specifically of interest in this field is the reactivity between carbonyls and olefins; extensive investigations have revealed their ability to undergo a variety of carbon-carbon bond forming reaction depending on the choice of Lewis or Brønsted acid (Figure 1.1).[2-8] These functional groups typically follow carbonyl-ene (**I**)[2a] or Prins (**II**)[3a,b] reaction pathways after activation of the carbonyl moiety by a Lewis or Brønsted acid catalyst. Carbonyl-ene reactions proceed through either a stepwise mechanism, in which a discrete carbocation intermediate is formed, or a concerted mechanism, that involves a 6-membered transitions state, to furnish homoallylic alcohols (I, Figure 1.1). On the other hand, Prins reactions exclusively proceed in a stepwise fashion to form carbocation intermediates; however, these intermediates can be quenched by external nucleophiles, water, or by elimination to yield 3-sustituted alcohols, 1,3-diols, and allylic alcohols, respectively (3-substituted alcohols shown in II, Figure 1.1).

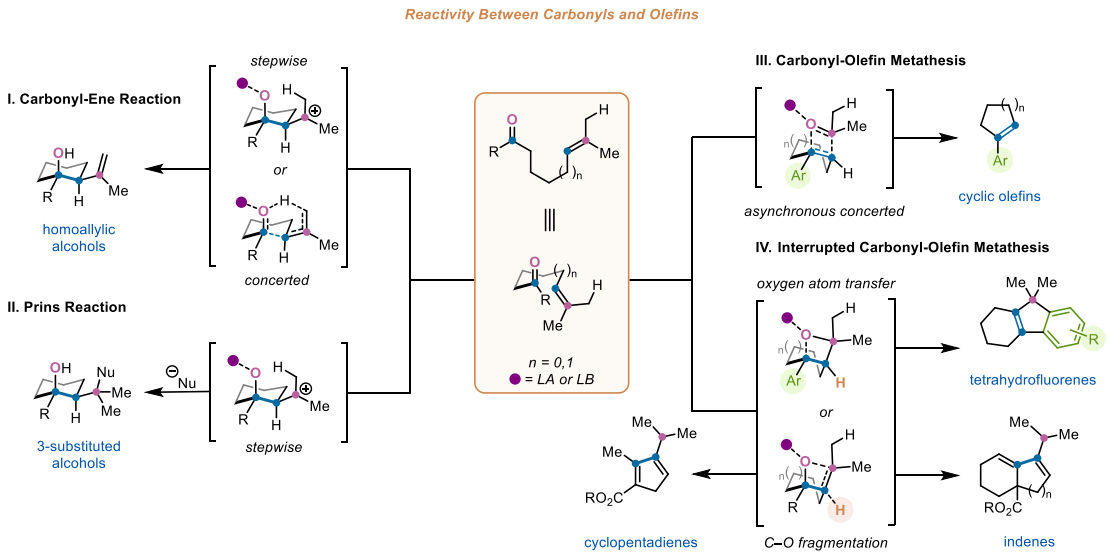

Figure 1.1: Reactivity between carbonyls and olefins.

Another well-established reaction between carbonyls and olefins is carbonyl–olefin metathesis (III, Figure 1.1).[4-7] In 2016, Schindler and co-workers had their first report on Lewis acid-catalyzed ring-closing carbonyl–olefin metathesis.[7a] They postulated that the key intermediate was a highly reactive, iron-bound oxetane. A detailed mechanistic investigation[7c] of this transformation supported the original mechanistic hypothesis involving an oxetane. In the proposed mechanism, a Lewis acid-catalyst activates the carbonyl, which then undergoes a concerted, asynchronous [2+2]-cycloaddition with the olefin subunit to form the key reactive oxetane intermediate. The newly formed oxetane subsequently fragments via a retro-[2+2]-cycloaddition to yield the cyclic olefin metathesis product and releases the Lewis acid catalyst. More recently, interrupted carbonyl–olefin metathesis has been reported as a fourth mode of reactivity between carbonyl and olefins, in which aryl ketone substrates are converted into tetrahydrofluorene products in the presence of triflic acid as a Brønsted acid catalyst (IV, Figure 1.1).[8] Under the optimized reaction conditions, triflic acid also promotes the formation of the key oxetane intermediate, which distinctly fragments through an oxygen atom transfer mechanism by cleavage of the C–O bond. However, this is not the only mechanistic pathways for interrupted carbonyl–olefin metathesis. The formation of cyclopentadienes or indene-type scaffolds can be achieved through yet another C–O oxetane fragmentation, elimination/dehydration pathway.

1.2. Carbonyl-Ene Reactions

Intramolecular carbonyl-ene and Prins reactions, as mentioned above, have been extensively investigated.[1-3] Specifically, type I intramolecular carbonyl-ene reactions follow a concerted reaction mechanism and proceed through an ordered chair transition state (**2**, Figure 1.2A).[2b] The presence of a Lewis acid catalyst can activate carbonyl **1**, and undergo the type I intramolecular carbonyl-ene reaction and yield a variety of homoallylic alcohols (**3**). Depending on the choice of catalyst, reaction conditions, and substrate, the stereochemical outcome of the products can often be manipulated.

While investigating the cyclizations of unsaturated carbonyl compounds in 1982, Snider and co-workers observed that the cyclization of the *(Z)*-isomer of an unactivated, 1,2-disubstituted aldehyde **4** with Me_2AlCl yielded *syn*-**6** as the exclusive product in 75% (Figure 1.2B).[2g] The *(E)*-isomer resulted in a mixture of products favoring the *trans*-isomer. They postulated that *syn*-**6**

forms as the exclusive product with the *(Z)*-isomer due to the rigid geometrical requirements for transitions state **5**, whereas the *(E)*-isomer is less selective.

Page and co-workers showcased the power of the type I carbonyl-ene cyclization in their 2006 report towards guaianolide natural products.[2g] Lewis acid catalysts, $Yb(OTf)_3$ or $BF_3{*}OEt_2$, promote the formation of the desired 7-membered ring scaffolds **8** and **9** (Figure 1.2C). $Yb(OTf)_3$ catalyzes a diastereoselective reaction, providing **8**, with an *anti*-fused ring junction, as the exclusive product in 46% yield. $BF_3{*}OEt_2$ leads to a mixture of products **8** (41%) and **9** (10%). Under both conditions **8** is heavily favored due to the preferred chair transition state **10**.

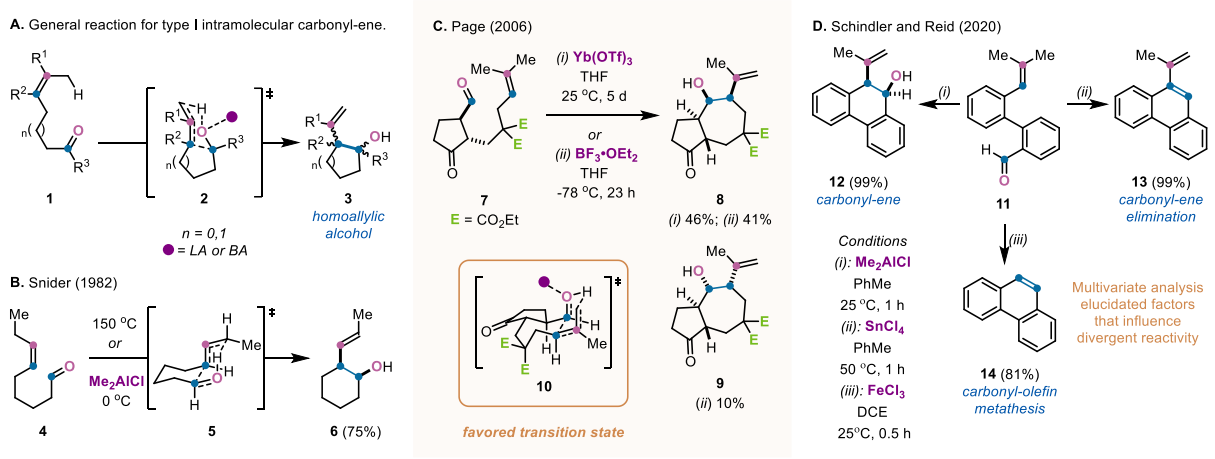

Figure 1.2: Selected examples of carbonyl-ene reactions. **A.** General reaction scheme for type I intramolecular carbonyl-ene reactions. **B.** Carbonyl-ene cyclization by Snider and co-workers. **C.** Page and co-workers' diastereoselective carbonyl-ene cyclization work towards guaianolide natural products. **D.** Schindler, Reid, and co-workers' investigations into the unique reactivity of Lewis acids.

In 2020, Schindler, Reid, and co-workers conducted an extensive study on a multitude of Lewis acids, evaluating their unique reactivities towards carbonyls and olefins; specifically looking at carbonyl-ene reactions and carbonyl–olefin metathesis (Figure 1.2D).[2j] Employing multivariate analysis and computationally derived activation barriers, a statistical model was developed that identified different parameters that were more likely to lead to either carbonyl-ene (**12** and **13**) or carbonyl–olefin metathesis (**14**) products. Carbonyl-ene reactions were more sensitive to the type of substrates utilized for the reactions, whereas carbonyl–olefin metathesis is more sensitive to catalyst effects. Specifically, when evaluating the aryl aldehyde **11**, carbonyl-ene was the dominant reaction pathway when either Me_2AlCl or $SnCl_4$ were employed as the Lewis acid catalysts, providing 99% yield of both **12** and **13**, respectively. Meanwhile, when $FeCl_3$ is used as the catalyst, carbonyl–olefin metathesis is the predominant pathway, yielding 81% of **14**.

1.3 Prins Reactions

Acid-catalyzed intramolecular Prins reactions follow a stepwise pathway that involves a discrete carbocation intermediate **15**, from which, several different products can be formed depending on the reaction conditions (Figure 1.3A). Under aqueous conditions, **15** can react with an equivalent of water to form 1,3-diols (**17**), which can undergo a subsequent elimination to form allylic alcohols (**18**). However, **18** can also be obtained directly from the carbocation via an elimination. 3-substituted alcohols **19** can also be formed by quenching **15** with an external nucleophile.

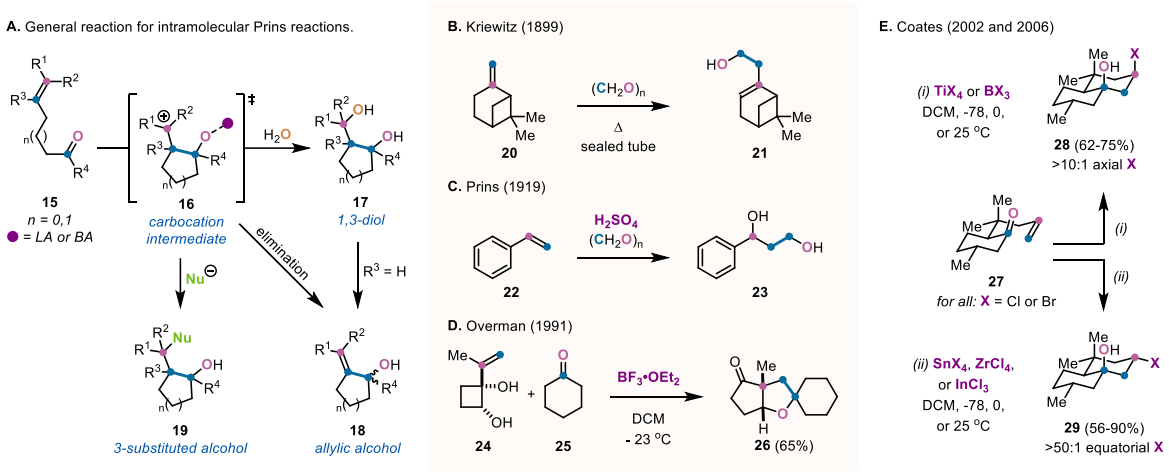

Figure 1.3: Selected examples of Prins reactions. **A.** General reaction scheme for intramolecular Prins reactions. **B.** Seminal work by Kriewitz. **C.** The first report of an acid catalyzed Prins reaction. **D.** Prins-pinacol cyclization by Overman and co-worker's. **E.** Coates and co-workers' investigations into the distinct reactivity for *syn*- and *anti*-Prins cyclizations.

The Kriewitz[3a] and Prins[3b] reactions are closely related. In the Kriewitz[3a] reaction, α-pinene **20** and paraformaldehyde, catalyzed by heat, form homoallylic alcohol **21** through a thermal ene rearrangement (Figure 1.3B). Conversely, the Prins[3b] reaction is acid-catalyzed. In the first report by Prins, styrene **22** and paraformaldehyde, catalyzed by aqueous sulfuric, form 1,3-diol **23** (Figure 1.3C). Since this seminal work in 1919, there have been numerous adaptations, including the development of the Prins cyclizations, and extensions to more complex systems.[3d-i] Overman and co-workers, in their studies on ring-enlarging tetrahydrofuran annulations, showcased the use of the Prins-pinacol reaction to quench the traditional Prins cyclization.[3d] In the presence of $BF_3{*}OEt_2$, the secondary alcohol of diol **24** reactions with cyclohexanone **25** and forms an alkoxonium ion intermediate (Figure 1.3D). This intermediate then cyclizes to produce a

tetrahydropyranyl cation, followed by a 1,2-alkyl shift to generate the ring-expanded cyclopentantone **26** in 65% yield.

Coates and co-workers demonstrated distinct reactivity for *syn*- and *anti*-Prins cyclizations products depending on the Lewis acid catalyst.[3e,f] When evaluating unsaturated ketone **27** with either TiX_4 or BX_3 (X = Cl or Br), the axial chloride or bromide product **28** is heavily favored (>10:1) in 62-75% yield (Figure 1.3E). These results are postulated to be from intramolecular halide transfer to from the activated alkoxonium (OMX_n) to the tertiary carbocation intermediate. Meanwhile other Lewis acids—SnX_4, $ZrCl_4$, or $InCl_3$—favored the equatorial halide **29** (>50:1) in 56-90% yield.

1.4 Carbonyl–Olefin Metathesis

In the last 60 years, there have been many advances in the field of carbonyl–olefin metathesis.[6] In early reports of acid-catalyzed carbonyl–olefin metathesis, superstoichiometric or equimolar amounts of the catalyst was required to provide the desired metathesis products.[4] However, in the last decade, new methods have shown that catalytic amounts of Lewis acids are effective in these transformation, and analogous strategies for ring-closing, ring-opening, and cross carbonyl–olefin metathesis have recently been developed.

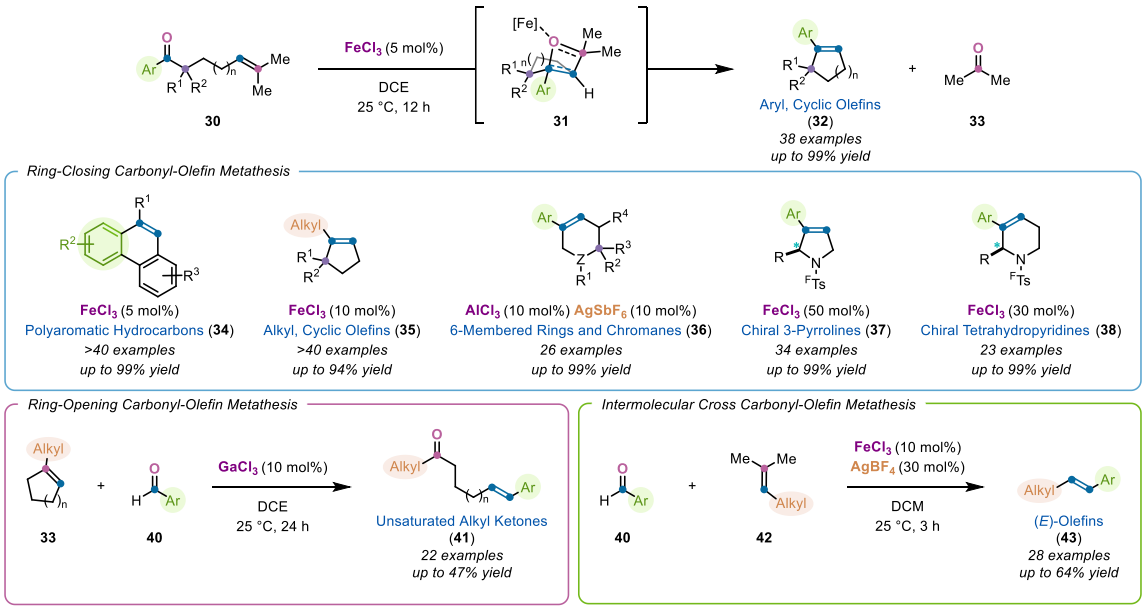

Figure 1.4: Selected carbonyl–olefin metathesis examples by Schindler and co-workers.

The Schindler lab has pioneered many of these advances, specifically for Lewis acid-catalyzed carbonyl–olefin metathesis (Figure 1.4).[7a-j] In 2016, Schindler and co-workers reported their seminal work on $FeCl_3$-catalyzed ring-closing carbonyl–olefin metathesis, providing 38 examples of 5- and 6-memebered ring metathesis products **32** from aryl ketone substrates **30**.[7a] The initially mechanistic hypothesis centered around forming a reactive oxetane intermediate **31**, that would fragment to yield the cyclic olefin product (**32**) and acetone **33** as the carbonyl byproduct. Shortly after the Schindler group's first report, they published a detailed mechanistic study on this system, in collaboration with the Zimmerman and Devery groups, that supported their original mechanistic hypothesis with DFT calculations.[7c] The currently mechanistic proposal is as follows: first, $FeCl_3$ binds to the carbonyl of **30**, promoting an asynchronous, concerted [2+2]-cycloaddition to yield **31**; oxetane **31** subsequently fragments in a retro-[2+2] fashion to provide the metathesis products **32** and **33**.

In the following years, Schindler and co-workers have significantly expanded the substrate scope of Lewis acid-catalyzed ring-closing carbonyl–olefin metathesis. In 2017, they showcased the synthesis of electronically and structurally differentiated polyaromatic hydrocarbons (**34**) with >40 examples.[7b] Two years later in 2019, they were able to expand the original 5-membered ring-closing method to now includes aliphatic ketone substrates, providing up to 94% yield of cyclic, alkyl olefins **35**.[7f] In 2020, utilizing a superelectrophilic $AlCl_3/AgSbF_6$ ion pair catalyst, challenging aryl 6-membered rings and chromanes (**36**) could reliably be accessed in yields up to 99%.[7j] Additionally, 5- and 6-membered nitrogen-containing heterocycles, 3-pyrrolines (**37**)[7d] and tetrahydropyridines (**38**),[7h] were synthesized in excellent yields utilizing $FeCl_3$ as the Lewis acid catalyst for the ring-closing carbonyl–olefin metathesis.

Branching away from the ring-closing methodologies, the Schindler group reported $GaCl_3$-catalyzed ring-opening carbonyl–olefin metathesis in 2018.[7e] Yields for the unsaturated alkyl ketone products (**41**) were on about 47% yield due to a competing carbonyl-ene pathway that accounted for the loss in the mass balance. And in 2020, utilizing $FeCl_3/AgBF_4$ as a superelectrophlic ion pair Lewis acid catalyst, the scope of (*E*)-olefins (**43**) for cross carbonyl–olefin metathesis was expanded, with increased yields of 64%.[7i] Notably, $FeCl_3$ is the optimal catalyst in almost all these systems, with 6-membered rings (Al/Ag ion pair) and ring-opening carbonyl–olefin metathesis ($GaCl_3$) as the exceptions.

1.5 Interrupted Carbonyl–Olefin Metathesis

Interrupted carbonyl–olefin metathesis transformations, as outlined below, represent new reactivity between carbonyls and olefins, and complement existing carbonyl-ene (see 1.2), Prins (see 1.3), and carbonyl–olefin metathesis reactions (see 1.4). In 2018, while investigating 6-membered ring-closing carbonyl–olefin metathesis, the Schindler group discovered divergent reactivity when evaluating different Lewis acid catalysts; ultimately leading to the first report of interrupted carbonyl–olefin metathesis (Figure 1.5A). If 6-membered aryl ketone substrate **44** was subjected to $Fe(OTf)_3$ as the Lewis acid catalyst, an unexpected tetrahydroflourene product **45** was observed. However, when employing, the expected metathesis product **46** was observed. A catalytic amount of trifilic acid was found to be the operative catalyst under these conditions, exclusively providing **45** in 48% yield. Mechanistic studies and computations suggest that the reaction proceeds via an intermediate oxetane, just like carbonyl–olefin metathesis. However, with triflic acid a the Brønsted acid catalyst, the oxetane fragmentation is hypothesized to occurs through a stepwise mechanism, thus interrupting the previously established carbonyl–olefin metathesis. A benzylic carbocation is formed, followed by intramolecular Friedel-Crafts alkylation to furnish the final products. In the end, the scope was expanding to include 30 tetrahydrofluorenes in up to 92% yield.

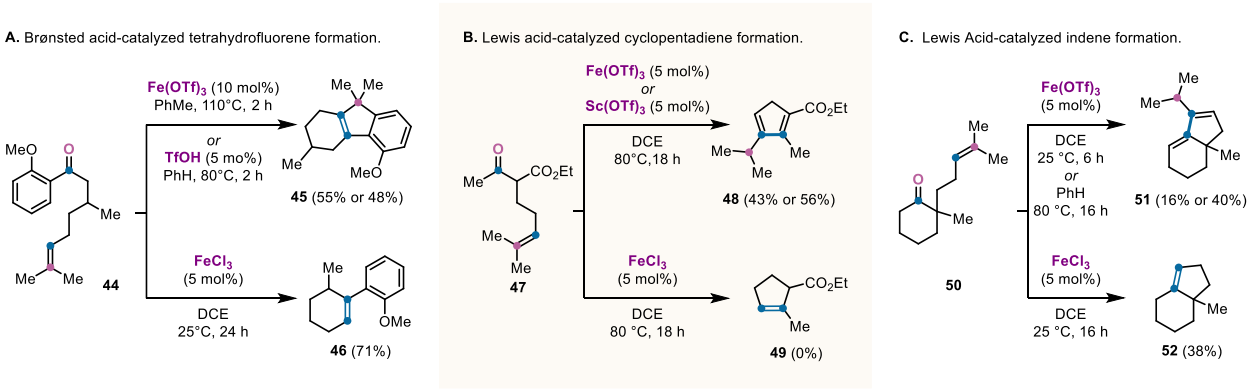

Figure 1.5: Selected examples of divergent reactivity observed for interrupted carbonyl–olefin metathesis examples by Schindler and co-workers. **A.** Triflic acid-catalyzed interrupted carbonyl–olefin metathesis for the synthesis of tetrahydrofluorenes. **B.** Synthesis of cyclopentadienes via scandium(III) triflate-catalyzed interrupted carbonyl–olefin metathesis. **C.** Iron(III) triflate-catalyzed interrupted carbonyl–olefin metathesis for indene-type scaffolds.

A similar sequence of events occurred twice more, revealing another alternative oxetane fragmentation pathway to access cyclopentadienes and indene-type products (Figure 1.5B and 1.5C, respectively, *unpublished work*). Cyclopentadienes, such as **48**, are desirable scaffolds for

uses in organic chemistry, organometallic chemistry, and catalysis.[9] Currently, methods to access functionalized cyclopentadienes are quite limited,and often rely on multi-step reaction sequences, harsh reaction conditions, and complex substrates.[10] While investigating ring-closing carbonyl–olefin metathesis for aliphatic carbonyls, such as **47**, divergent reactivity was observed (Figure 1.5B). When β-ketoester **47** was subjected catalytic amounts of $Fe(OTf)_3$, unexpected cyclopentadiene **48** was found as the exclusive product. Interestingly, when employing $FeCl_3$ as the Lewis acid catalyst, the expected metathesis product **49** was not observed. Optimizations to provide increased yields of the desirable cyclopentadiene products revealed $Sc(OTf)_3$ as the ideal catalyst, now promoting the conversion of **47** to **48** in 56%. The scope of this new strategy for accessing of 2,3,4-trifunctionalized cyclopentadienes was significantly expand and was demonstrated for 24 examples in up to 85% yield.

Again, while investigating ring-closing carbonyl–olefin metathesis for cyclic, aliphatic carbonyls, such as **50**, divergent reactivity was observed (Figure 1.5C). When cyclic ketone **50** was subjected catalytic amounts of $Fe(OTf)_3$, unexpected tetrahydroindene product **51** was observed as the exclusive product in 16%, while $FeCl_3$ provided the expected metathesis product **52**. The divergent reactivity observed in these studies ultimately lead to the development of a novel methodology allowing access to functionalized pentalenes, indenes, naphthalenes, and azulenes. These bicyclic scaffolds are desirable frameworks in the synthesis of biologically active natural products,[11] and multi-step, harsh reaction conditions[12,13] are currently required to access them. However, $Fe(OTf)_3$-catalyzed interrupted carbonyl–olefin metathesis of cyclic, aliphatic ketones provides a direct and unified method to synthesize several of these desirable bicycles. Optimizations provided increased yields of the indene-type products, the scope was significantly expanded, and the method was demonstrated for 18 examples in up to 99% yield.

Both the mechanisms for the formation of cyclopentadienes (**48**) and the indene-type products (**51**) proceeds through a distinct interrupted carbonyl–olefin metathesis (Figure 1.5B and 1.5C, respectively). The aliphatic carbonyls are proposed to undergo a [2+2]-cycloaddition to form a reactive oxetane intermediate. In contrast to the previously establish interrupted carbonyl–olefin metathesis pathway, oxetane fragmentation is proposed to occur through cleavage of the other C–O bond (Figure 1.1). For cyclopentadienes, C–O cleavage occurs through direct α-proton elimination, yielding a tetrasubstituted olefin, and for the indenes, a tertiary carbocation is formed

on the isopropyl moiety, and elimination of the adjacent α-proton in yields a tetrasubstituted olefin. Subsequent isomerizations and dehydration results in the corresponding products.

1.6 References

1. For Lewis Acids Forming Carbon-Carbon Bonds, see: *Lewis Acids in Organic Synthesis*; Yamamoto, H., Eds.; Wiley-VCH: Weinheim, 2000; Vol. 1.
2. For selected carbonyl-ene reaction, see: (a) Alder, K.; Pascher, F.; Schmitz, A. Über die Anlagerung von Maleinsäure-anhydrid und Azodicarbonsäure ester an einfach ungesättigte Kohlenwasserstoffe. Zur Kenntnis von Substitutionsvorgängen in der Allyl-Stellung *Ber. Dtsch. Chem. Ges. B Ser.* **1943**, *76*, 27–53. (b) Oppolzer, W.; Snieckus, V. Intramolecular Ene Reactions in Organic Synthesis. *Angew. Chem., Int. Ed. Engl.* **1978**, *17*, 476–486. (c) Snider, B. B.; Karras, M.; Price, R. T.; Rodini, D. J. Alkylaluminum Halide Induced Cyclization of Unsaturated Carbonyl Compounds. *J. Org. Chem.* **1982**, *47*, 4538–4545. (d) Jackson, A. C.; Goldman, B. E.; Snider, B.B. Intramolecular and Intermolecular Lewis acid Catalyzed Ene Reactions Using Ketones as Enophiles. *J. Org. Chem.* **1984**, *49*, 3988–3994. (e) Snider, B. B. in *Comp. Org. Synth.*, B. M. Trost, I. Fleming, Eds. (Pergamon, Oxford, **1991**), Vol. 2, pp. 527–562. (f) Mikami, K.; Shimizu, M. Asymmetric Ene Reactions in Organic Synthesis. *Chem. Rev.* **1992**, *92*, 1021–1050. (g) Page, P. C. B.; Gambera, G.; Hayman, C. M.; Edgar, M. An Ytterbium-Catalyzed Intramolecular Aldehyde-ene Reaction Approach to the Guaianolide and Pseudoguaianolide Diterpenoids: Synthesis of the Guaiane Skeleton. *Synlett* **2006**, 3411–3414. (h) Clarke, M. L.; France, M. B. The Carbonyl Ene Reaction. *Tetrahedron* **2008**, *64*, 9003–9031. (i) Ho, C.-Y.; Schleicher, K. D.; Chan, C.-W.; Jamison, T. F. Catalytic Addition of Simple Alkenes to Carbonyl Compounds by Use of Group 10 Metals. *Synlett* **2009**, 2565–2582. (j) Becker, M. R.; Reid. J. P.; Rykaczewski, K. A.; Schindler, C. S. Models for Understanding Divergent Reactivity in Lewis Acid Catalyzed Transformations of Carbonyls and Olefins. *ACS Catalysis* **2020**, *10*, 4387–4397.
3. For selected Prins reaction, see: (a) Kriewitz, O. Ueber Addition von Formaldehyd an einige Terpene. *Chem. Ber.* **1899**, *32*, 57–60. (b) Prins, H.J. On the Condensation of Formaldehyde with some Unsaturated Compounds. *Chem. Weekblad* **1919**, *16*, 1510. (c) Arundale, E.; Mikeska, L. A. The Olefin-Aldehyde Condensation. The Prins Reaction. *Chem. Rev.* **1952**, *51*, 505–555. (d) Brown, M. J.; Harrison, T.; Herrinton, P. M; Hopkins, M. H.; Kira D. Hutchinson, K. D.; Overman, L. E.; Mishra, P. Acid-Promoted Reaction of Cyclic Allylic Diols with Carbonyl Compounds. Stereoselective Ring-Enlarging Tetrahydrofuran Annulations *J. Am. Chem. Soc.* **1991**, *113*, 5365–5378. (e) Davis, C. E.; Coates, R. M. Stereoselective Prins Cyclizations of δ,ε-Unsaturated Ketones to *cis*-3-Chlorocyclohexanols with $TiCl_4$ *Angew. Chem. Int. Ed.* **2002**, *41*, 491–493. (f) Miles, R. B.; Davis, C. E.; Coates, R. M. Syn- and Anti-Selective Prins Cyclizations of δ,ε-Unsaturated Ketones to 1,3-Halohydrins with Lewis Acids. *J. Org. Chem.* **2006**, *71*, 1493–1501. (g) Olier, C.; Kaafarani, M.; Gastaldi, S.; Betrand, M. P. Synthesis of Tetrahydropyrans and Related Heterocycles via Prins Cyclization; Extension to Aza-Prins Cyclization. *Tetrahedron* **2010**, *66*, 413–445. (h) Greco, S. J.; Fiorot, R. G.; Lacerda, V.; dos Santos, R. B. Recent Advances in the Prins Cyclization. *Aldrichimica Acta*, **2013**, *46*, 59–67. (i) Snider, B. B. in *Comp. Org. Synth. II*, Knochel, P.; Molander, G. A. Eds. (Elsevier, Oxford, **2014**) Vol. 2, 148–191.
4. For Brønsted and Lewis acid mediated carbonyl–olefin metathesis reactions, see: (a) Schopov, I.; Jossifov, C. A Carbonyl–Olefin Exchange Reaction – New Route to Polyconjugated Polymers, 1. A New Synthesis of Polyphenylacetylene. *Makromol. Chem., Rapid Commun.* **1983**, *4*, 659−662. (b) Jackson, A. C.; Goldman, B. E.; Snider, B. B. Intramolecular and Intermolecular Lewis Acid Catalyzed Ene Reactions Using Ketones as Enophiles. *J. Org.*

Chem. **1984**, *49*, 3988–3994. (c) van Schiak, H.-P.; Vijn, R.-J.; Bickelhaupt, F. Acid-Catalyzed Olefination of Benzaldehyde. *Angew. Chem. Int. Ed.* **1994**, *33*, 1611–1612. (d) Jossifov, C.; Kalinova, R.; Demonceau, A. Carbonyl Olefin Metathesis. *Chim. Oggi* **2009**, *40*, 85−87. (e) Soicke, A.; Slavov, N.; Neudörfl, J.-M.; Schmalz, H.-G. Metal-Free Intramolecular Carbonyl–Olefin Metathesis of *ortho*-Prenylaryl Ketones. *Synlett* **2011**, *2011*, 2487−2490.

5. For Brønsted acid-catalyzed carbonyl–olefin metathesis approaches, see: (a) Catti, L.; Tiefenbacher, K. Brønsted Acid-Catalyzed Carbonyl–Olefin Metathesis Inside a Self-Assembled Supramolecular Host. *Angew. Chem., Int. Ed.* **2018**, *57*, 14589−14592. (b) To, T. A.; Pei, C.; Koenigs, R.; Nguyen, T. V. Hydrogen Bonding Networks Enable Brønsted Acid-Catalyzed Carbonyl–Olefin Metathesis. *Preprint at* https://chemrxiv.org/engage/chemrxiv/article-details/615d8156f718df1626d54e8c.
6. For a review on Lewis acid-catalyzed carbonyl–olefin metathesis, see: [‡]Albright, H.; [‡]Davis, A. J.; [‡]Gomez-Lopez, J. L.; [‡]Vonesh, H. L.; Quach, P; Lambert, T. H.; Schindler, C. S. Carbonyl–Olefin Metathesis Reactions. *Chem. Rev.* **2021**, *121*, 9359–9406. [‡]Authors contributed equally.
7. For Lewis acid-catalyzed carbonyl–olefin metathesis approaches, see: (a) Ludwig, J. R.; Zimmerman, P. M.; Gianino, J. B.; Schindler, C. S. Iron(III)-Catalysed Carbonyl–Olefin Metathesis. *Nature* **2016**, *533*, 374−379. (b) McAtee, C. M.; Riehl, P. S.; Schindler, C. S. Polycyclic Aromatic Hydrocarbons via Iron(III)-Catalyzed Carbonyl–Olefin Metathesis. *J. Am. Chem. Soc.* **2017**, *139*, 2960−2963. (c) Ludwig, J. R.; Phan, S.; McAtee, C. M.; Zimmerman, P. M.; Devery, J. J.; Schindler, C. S. Mechanistic Investigations of the Iron(III)-Catalyzed Carbonyl–Olefin Metathesis Reaction. *J. Am. Chem. Soc.* **2017**, *139*, 10832−10842. (d) Groso, E. J.; Golonka, A. N.; Harding, R. A.; Alexander, B. W.; Sodano, T. M.; Schindler, C. S. 3-Aryl-2,5-Dihydropyrroles via Catalytic Carbonyl–Olefin Metathesis. *ACS Catal.* **2018**, *8*, 2006−2011. (e) Albright, H.; Vonesh, H. L.; Becker, M. R.; Alexander, B. W.; Ludwig, J. L.; Wiscons, R. A.; Schindler, C. S. $GaCl_3$-Catalyzed Ring-Opening Carbonyl–Olefin Metathesis. *Org. Lett.* **2018**, *20*, 4954−4958. (f) Albright, H.; Riehl, P. S.; McAtee, C. M.; Reid, J. P.; Ludwig, J. R.; Karp, L. A.; Zimmerman, P. M.; Sigman, M. S.; Schindler, C. S. Catalytic Carbonyl–Olefin Metathesis of Aliphatic Ketones: Iron(III) Homo-Dimers as Lewis Acidic Superelectrophiles. *J. Am. Chem. Soc.* **2019**, *141*, 1690−1700. (g) Riehl, P. S.; Nasrallah, D. J.; Schindler, C. S. Catalytic Transannular Carbonyl–Olefin Metathesis Reactions. *Chem. Sci.* **2019**, *10*, 10267−10274. (h) Rykaczewski, K. A.; Groso, E. J.; Vonesh, H. L.; Gaviria, M. A.; Richardson, A. D.; Zehnder, T. E.; Schindler, C. S. Tetrahydropyridines via $FeCl_3$-Catalyzed Carbonyl−Olefin Metathesis. *Org. Lett.* **2020**, *22*, 7, 2844−2848. (i) Albright, H.; Vonesh, H. L.; Schindler, C. S. Superelectrophilic Fe(III)-Ion Pairs as Stronger Lewis Acid Catalysts for (*E*)-Selective Intermolecular Carbonyl−Olefin Metathesis. *Org. Lett.* **2020**, *22*, 3155−3160. (j) Davis, A. J.; Watson, R. B.; Nasrallah, D. J.; Gomez-Lopez, J. L.; Schindler, C. S. *Nat. Catal.* **2020**, *3*, 787−796. (k) Naidu, V. R.; Bah, J.; Franzén, J. Direct Organocatalytic Oxo-Metathesis, a *trans*-Selective Carbocation-Catalyzed Olefination of Aldehydes. *Eur. J. Org. Chem.* **2015**, *2015*, 1834−1839. (l) Ma, L.; Li, W.; Xi, H.; Bai, X.; Ma, E.; Yan, X.; Li, Z. $FeCl_3$-Catalyzed Ring-Closing Carbonyl–Olefin Metathesis. *Angew. Chem., Int. Ed.* **2016**, *55*, 10410−10413. (m) Ni, S.; Franzén, J. Carbocation Catalysed Ring Closing Aldehyde-Olefin Metathesis. *Chem. Commun.* **2018**, *54*, 12982−12985. (n) Tran, U. P. N.; Oss, G.; Pace, D. P.; Ho, J.; Nguyen, T. V. Tropylium-Promoted Carbonyl–Olefin Metathesis Reactions. *Chem. Sci.* **2018**, *9*, 5145−5151. (o) Tran, U. P. M.; Oss, G.; Breugst, M.; Detmar, E.; Pace, D. P.; Liyanto, K.; Nguyen, T. V. Carbonyl–Olefin Metathesis Catalyzed by Molecular Iodine. *ACS Catal.* **2019**, *9*, 912−919. (p) Hanson, C. S.; Psaltakis, M. C.; Cortes,

J. J.; Devery, J. J. Catalyst Behavior in Metal-Catalyzed Carbonyl–Olefin Metathesis. *J. Am. Chem. Soc.* **2019**, *141*, 11870−11880. (q) Djurovic, A.; Vayer, M.; Li, Z.; Guillot, R.; Blataze, J.-P.; Gandon, V.; Bour, C. Synthesis of Medium-Sized Carbocycles by Gallium-Catalysed Tandem Carbonyl–Olefin Metathesis/Transfer Hydrogenation. *Org. Lett.* **2019**, *21*, 8132–8137. (r)Wang, R.; Chen, Y.; Shu, M.; Zhao, W.; Tao, M.; Du, C.; Fu, X.; Li, A.; Lin, Z. $AuCl_3$-Catalyzed Ring-Closing Carbonyl–Olefin Metathesis. *Chem. Eur. J.* **2020**, *26*, 1941–1946. (s) Hanson, C. S.; Psaltakis, M. C.; Cortes, J. J.; Siddiqi, S. S.; Devery, J. J. Investigation of Lewis Acid-Carbonyl Solution Interactions via Infrared-Monitored Titration. *J. Org. Chem.* **2020**, *85*, 820−832.

8. For interrupted carbonyl–olefin metathesis approaches, see: Ludwig, J. R.; Watson, R. B.; Nasrallah, D. J.; Gianino, J. B.; Zimmerman, P. M.; Wiscons, R. A.; Schindler, C. S. Interrupted Carbonyl–Olefin Metathesis via Oxygen Atom Transfer. *Science* **2018**, *361*, 1363-1369.
9. For reviews on cyclopentadienes, see: (a) Hartwig, J. F. *Organotransition Metal Chemistry: From Bonding to Catalysis*.; University Science Books: Sausalito, **2009**. (b) Macomber, D. W.; Hart, W. P.; Rausch, M. D.; Functionally Substituted Cyclopentadienyl Metal Compounds. *Adv. Organomet. Chem.* **1982**, *21*, 1-55.
10. For selected examples of the synthesis of cyclopentadienes, see: (a) Xi, Z.; Song, Q.; Chen, J.; Guan, H.; Li, P. Dialkenylation of Carbonyl Groups by Alkenyllithium Compounds: Formation of Cyclopentadiene Derivatives by the Reaction of 1,4-Dilithio-1,3-dienes with Ketones and Aldehydes. *Angew. Chem. Int. Ed.* **2001**, *40*, 1913−1916. (b) Lv, Y.; Yan, X.; Yan, L.; Wang, Z.; Chen, J.; Deng, H.; Shao, M.; Zhang, H.; Cao, W. An Efficient One-Pot Three-Component Process for the Synthesis of Highly Substituted Perfluoroalkylated Cyclopentadienes. *Tetrahedron* **2013**, *69*, 4205−4210. (c) X. Cheng, X.; L. Zhu, L.; Lin, M.; Chen, J.; Huang, X. Rapid Access to Cyclopentadiene Derivatives through Gold-Catalyzed Cycloisomerization of Ynamides with Cyclopropenes by Preferential Activation of Alkenes over Alkynes. *Chem. Commun.* **2017**, *53*, 3745−3748. (d) Bankar, S. K.; Singh, B.; Tung, P.; Ramasastry, S. S. V. Palladium-Catalyzed Intramolecular Trost–Oppolzer-Type Alder–Ene Reaction of Dienyl Acetates to Cyclopentadienes. *Angew. Chem., Int. Ed.* **2018**, *57*, 1678−1682.
11. Dixon, T.; Schweibenz, A.; Hight, B.; Kang, A.; Dailey, S.; Kim, M.- Y.; Chen, Y.; Kim, S.; Neale, A.; Groth, T.; Ike, S.; Khan, B.; Lieu, D.; Stone, T.; Orellana, R.; Couch, J. Bacteria-Induced Static Batch Fungal Fermentation of the Diterpenoid Cyathin A_3, a Small-Molecule Inducer of Nerve Growth Factor. *Ind. Microbiol. Biotechnol.* **2011**, *38*, 607-615.
12. (a) Crews, P.; Klein, T. E.; Hogue, E. R.; Myers, B. L. Tricyclic Diterpenes from the Brown Marine Algae Dictyota divaricata and Dictyota linearis. *J. Org. Chem.* **1982**, *47*, 811-815. (b) Piers, E.; Friesen, R. W. Annulations Leading to Diene Systems. Total Synthesis of the Diterpenoid (±)-(14S)-Dolasta-1(15),7,9-trien-14-ol. *J. Org. Chem.* **1986**, *51*, 3405-3406. (c) Piers, E.; Friesen, R. W. Annulations Leading to Diene Systems. Total Syntheses of the Dolastane-type Diterpenoids (±)-(5S,12R,14S)-Dolasta-1(15),7,9-trien-14-ol and (±)-Amijitrienol. *Can. J. Chem.* **1992**, *70*, 1204-1220. (d) Leung, L. T.; Chiu, P. Total Synthesis of (−)-Dolastatrienol. *Chem. Asian J.* **2015**, *10*, 1042-1049.
13. (a) Sun, H. H.; McConnell, O. J.; Fenical, W. Tricyclic Diterpenoids of the Dolastane Ring System from the Marine Alga *Dictyota divaricataI. Tetrahedron* **1981**, *37*, 1237-1242. (b) Pattenden, G.; Robertson, G. M. Free Radical Reactions in Synthesis. Total Synthesis of Isoamijiol. *Tet. Lett.* **1986**, *27*, 399-402. (c) Mehta, G.; Krishnamurthy, N. An Enantioselective

Approach to Dolastane Diterpenes. Total Synthesis of Marine Natural Products (+)-Isoamijiol and (+)-Dolasta-1(15),7,9-trien-14-OL. *Tet. Lett.* **1987**, *28*, 5945-5948. (d) Tori, M.; Toyoda, N.; Sono, M. Total Synthesis of Allocyathin B2, a Metabolite of Bird's Nest Fungi. *J. Org. Chem.* **1998**, *63*, 306-313. (e) Waters, S. P.; Tian, Y.; Li, Y.- M.; Danishefsky, S. J. Total Synthesis of (−)-Scabronine G, an Inducer of Neurotrophic Factor Production. *J. Am. Chem. Soc.* **2005**, *127*, 13514-13515. (f) Kobaykawa, Y.; Makada, M. Total Syntheses of (−)-Scabronines G and A, and (−)-Episcabronine A *Angew. Chem. Int. Ed.* **2013**, *52*, 7569-7573.

Chapter 2: Ring-Opening Carbonyl–Olefin Metathesis

*Portions of this work have been published in:

Albright, H.; Vonesh, H. L.; Becker, M. R.; Alexander, B. W.; Ludwig, J. R.; Wiscons, R. A.; Schindler, C. S. $GaCl_3$–Catalyzed Ring-Opening Carbonyl–Olefin Metathesis. **2018**, *20*, 4954−4958.

2.1 Introduction

The metathesis reaction between two olefins is among the most powerful catalytic strategies for carbon-carbon bond formation to enable synthetic access to more complex olefins.[1] An important advancement in the field of olefin metathesis is ring-opening cross-metathesis (ROCM). In ROCM, cyclic olefins (**2**), in combination with a metal-alkylidene catalyst, undergo a ring-opening metathesis, followed by a cross-metathesis with another olefin to form more functionalized olefin products; including symmetrically capped (**3**) and end-differentiated (**4**) products (Figure 2.1).[2] Selectivity for end-differentiated products (**4**) depends on both the olefin substrates and metal-alkylidene catalyst employed in the ROCM. After the initial ring-opening metathesis, a subsequent cross-metathesis with another equivalent of cyclic olefin (**2**) can occur, resulting in the products.

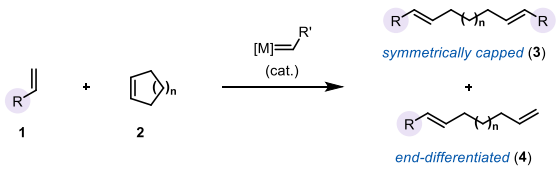

Figure 2.1: Ring-opening olefin–olefin cross-metathesis.

Analogous to olefin–olefin metathesis, carbonyl–olefin metathesis between carbonyl and olefin moieties also enables the construction of new carbon-carbon bonds to access more complex olefins.[3,4] Despite meaningful and vital progress, the currently available protocols for carbonyl–olefin metathesis remain significantly less advanced.[5-8] More recently, Lewis acid-catalyzed methodologies have been developed as complimentary alternatives to existing strategies for carbonyl–olefin metathesis.[9,10] In 2016, the Schindler lab reported that aryl ketone substrates,

together with catalytic amounts of $FeCl_3$, can undergo an intramolecular [2+2]-cycloaddition to form intermediate oxetanes.[10a,10c] These oxetanes intermediates subsequently fragment *via* a retro-[2+2]-cycloaddition, forming the desired ring-closing carbonyl–olefin metathesis products. In the last seven years, a limited number of intermolecular ring-opening and cross carbonyl–olefin metathesis reactions have been reported in the literature: catalyzed by either visible-light-induced 1,3-diol formation,[8a] solid state Lewis acids,[8b] carbocations as organic Lewis acids,[10k,10n] or molecular iodine.[10o] Due to the success of Lewis acid catalysts for ring-closing carbonyl–olefin metathesis, their use was investigated for ring-opening carbonyl–olefin metathesis.

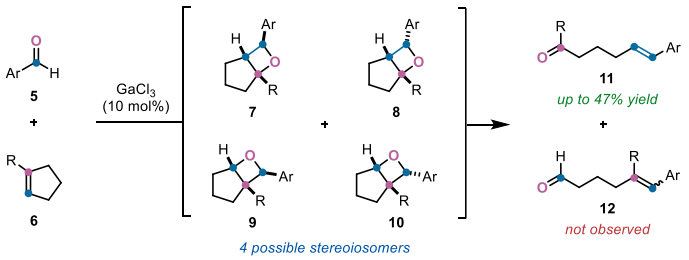

Figure 2.2: *This work:* $GaCl_3$-catalyzed ring-opening carbonyl–olefin metathesis.

This work showcases the controlling features of this transformation, with a specific emphasis on substrate scope and competing reaction pathways. Lewis acid-catalyzed ring-opening carbonyl–olefin metathesis showed the desired olefin metathesis products only yielding ~50% of the mass balance, which was initially attributed to the formation of regioisomeric oxetane intermediates **7** and **8** vs. **9** and **10** (Figure 2.2). Fragmentation of oxetane **9** and/or **10** would provide the aldehyde olefin metathesis product **12**, which could subsequent decomposition under the reaction conditions, accounting for loss in mass balance. Insights gained from this work will guide further reaction development and catalyst design, and continues to expand and improve the synthetic utility of available protocols.

2.2 Results and Discussion

Aryl aldehydes **5** and substituted cyclopentenes **6** were used as substrates for the development of a catalytic ring-opening carbonyl–olefin metathesis reaction (Figure 2.2). Cyclopentenes **6** were proposed to be ideal olefin substrates for reaction optimization due to the inherent ring strain of the proposed [3.2.0] bicyclic oxetane intermediate, which was expected to facilitate oxetane fragmentation to the metathesis products **11** and **12**. Additionally, the electronic

characteristics of 1-substituted cyclopentenes were expected to favor the formation of oxetane **7** and/or **8**; ultimately resulting in ketone **9** as the major olefin metathesis product.

Benzaldehyde **13** and 1-methylcyclopentene **14** were employed as substrates for the initial evaluation of Lewis acids (Figure 2.3). Strong Lewis acids such as $AlCl_3$ or $BF_3{\cdot}OEt_2$ were not efficient in promoting ring-opening carbonyl–olefin metathesis (entries 1 and 2, Figure 2.3). Similarly, $TiCl_4$ and $FeBr_3$ were also found to be inefficient in catalyzing the desired transformation (entries 3 and 4, Figure 2.3). Promising results were obtained with 10 mol% of $InCl_3$, which resulted in the formation of ketone **15** as the exclusive metathesis product in 25% yield (entry 5, Figure 2.3). Yields increased to 33% of **15** when using 10 mol% of $FeCl_3$ (entry 6, Figure 2.3); varying catalyst loadings of $FeCl_3$, as well as lowering the reaction concentration, did not improve the yields of the ketone metathesis product (entries 7-9, Figure 2.3).

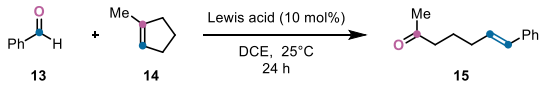

entry	Lewis acid	cat. loading (mol%)	solvent	conc. (M)	yield (%)
1	$AlCl_3$	10	DCE	0.1	0
2	$BF_3{\cdot}OEt_2$	10	DCE	0.1	2
3	$TiCl_4$	10	DCE	0.1	0
4	$FeBr_3$	10	DCE	0.1	0
5	$InCl_3$	10	DCE	0.1	25
6	$FeCl_3$	10	DCE	0.1	33
7	$FeCl_3$	5	DCE	0.1	11
8	$FeCl_3$	20	DCE	0.1	27
9	$FeCl_3$	10	DCE	0.01	11
10	**$GaCl_3$**	**10**	**DCE**	**0.1**	**47**
11	$GaCl_3$	5	DCE	0.1	34
12	$GaCl_3$	20	DCE	0.1	20
13	$GaCl_3$	10	DCE	0.01	8
14	$GaCl_3$	10	DCE	0.5	34
15	$Fe(OTf)_3$	10	DCE	0.1	4
16	$Sc(OTf)_3$	10	DCE	0.1	13
17	HCl	10	DCE	0.1	0
18	TfOH	10	DCE	0.1	2

Conditions: All reactions were performed with 0.4 mmol **13** and 0.1mmol **14** in DCE (0.1 M, 1 mL) at 25°C for 24h. Yields were determined by GC analysis.

Figure 2.3: Reaction optimization.

Continuing efforts identified $GaCl_3$ as the superior Lewis acid catalyst for ring-opening carbonyl–olefin metathesis, promoting the formation of the ketone **15** in 47% yield (entry 10, Figure 2.3). Alternative catalyst loadings of $GaCl_3$ (5 or 20 mol%) and additional reaction concentrations (0.01 M or 0.5 M) were not beneficial and diminished yields the ketone metathesis product were observed (entries 11-14, Figure 2.3). Metal triflates, such as $Fe(OTf)_3$ or $Sc(OTf)_3$, were not viable catalyst for ring-opening carbonyl–olefin metathesis (entries 15 and 16, Figure 2.3). Brønsted acids HCl and TfOH were also found to be inefficient in promoting this

transformation, which is consistent with the Schindler lab's previous observations for Lewis acid-catalyzed carbonyl–olefin metathesis (entries 15 and 16, Figure 2.3). Importantly, the unsaturated, alkyl ketone **15** was the only metathesis product isolated for all the catalysts and conditions that were evaluated. The corresponding aldehyde **12** was not observed.

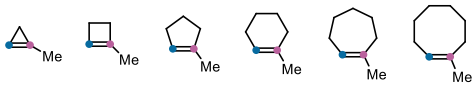

	16	**17**	**14**	**18**	**19**	**20**
RSE[a]	54.5	29.7	5.0	1.7	6.3	7.4
reactivity[b]	0%	-	47%	18%	0%	0%

[a]ring strain energy (kcal/mol)[11]; [b]**Conditions:** All reactions were performed with 4.0 equiv. **13** and 1.0 equiv. of olefin substrates with 10 mol% $GaCl_3$ in DCE (0.1 M) at 25°C for 24 h.

Figure 2.4: Ring strain of cyclic olefins.

The effect of ring strain[11] was investigated next for ring-opening carbonyl–olefin metathesis. A multitude of substituted, cyclic olefins of varying ring sizes were evaluated with benzaldehyde under the optimized reaction conditions (Figure 2.4). Interestingly, the yields obtained from these transformations do not correlate with the inherent ring strain of the cyclic olefins. Cycloheptane **19** (6.3 kcal/mol) and cyclooctene **20** (7.4 kcal/mol) do not result in the formation of the desired metathesis products, while cyclohexene **18** with a lower ring strain of 1.7 kcal/mol forms the corresponding metathesis product, albeit in a low yield of 18%.

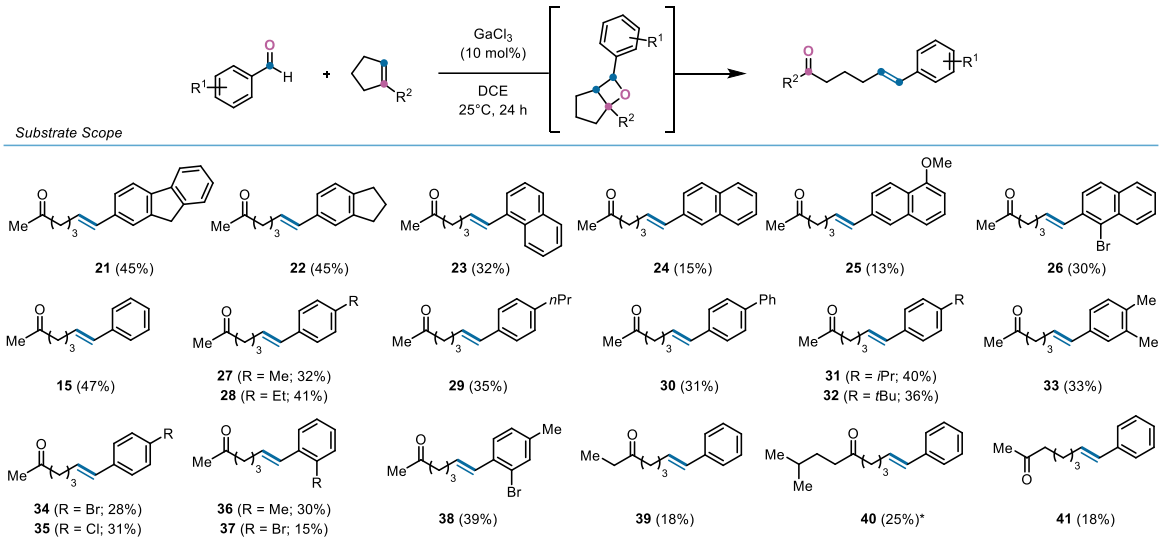

Conditions: All reactions were performed with 4.0 equivalents of aldehyde and 1.0 equivalent of olefin substrates in DCE (0.1 M) at 25°C for 24 h. *Yield obtained by GC.

Figure 2.5: Aldehyde and olefin scope for ring-opening carbonyl–olefin metathesis.

Following the exploration of ring strain, additional aldehydes and cyclic olefins were evaluated upon their ability to undergo the desired transformation (Figure 2.5). A variety of electronically and sterically differentiated aromatic aldehydes, in combination with 1-methylcyclopentene **14**, were effective and resulted in up to 47% yield of the ketone metathesis products (**21**-**38**, Figure 2.5). Aliphatic aldehydes were not productive under the optimized reaction conditions, however distinct substitution of the cyclopentene, either ethyl **39** or isopentyl **40**, were productive, albeit in lower yields of 18% and 25%, respectively. The corresponding ketone of 1-methylcyclohexene provided **41** in 18% yield as well. Importantly, the unsaturated, alkyl ketones **11** were formed as the exclusive metathesis products; no formation of the aldehyde metathesis products **12** were observed.

2.3 Mechanistic Investigations

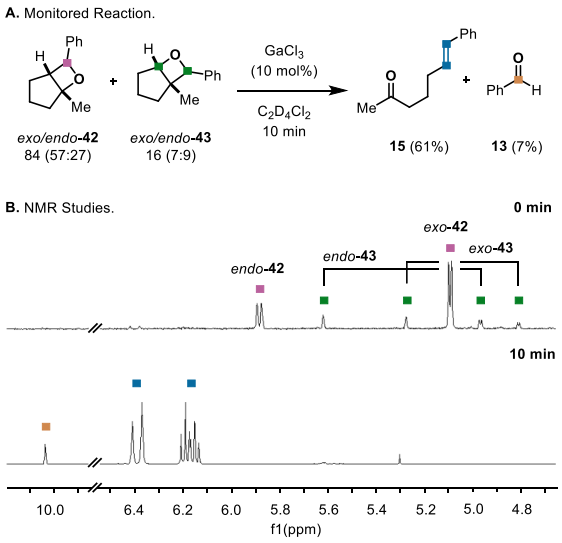

Figure 2.6: ^{1}H-NMR fragmentation studies of oxetanes **42** and **43**.

Subsequent efforts focused on elucidating the mechanism, the mass balance for ring-opening carbonyl–olefin metathesis, and why there was a maximum of 50% yield of the metathesis products. To study these inquiries, a mixture of regioisomeric oxetanes **42** and **43** were independently synthesized *via* Paterno−Büchi chemistry[12] (Figure 2.6). The oxetane mixture was enriched chromatographically to contain predominantly oxetane **42**, which corresponded to the expected major oxetane intermediate in ring-opening carbonyl–olefin metathesis of **13** and **14** (>5:1 ratio **42**:**43**). The mixture of oxetanes were subjected to the optimized reaction conditions

and monitored *via* ^{1}H-NMR (Figure 2.6B). After 10 min, clean conversion to **15** as a single olefinic product was isolated in 61% yield along with 7% yield of benzaldehyde (**13**). Notably, no significant aldehyde signals were observed that would correspond to the aldehyde metathesis product.

Oxetane *exo*-**43** was again synthesized through Paterno−Büchi chemistry,[12] isolated as a single regio- and stereoisomer, subjected to 10 mol% of $GaCl_3$ and monitored *via* ^{1}H-NMR (Figure 2.7A). Oxetane *exo*-**43** corresponded to the minor oxetane regioisomer (**9**, Figure 2.2) that could be formed during ring-opening carbonyl–olefin metathesis between **13** and **14**. However, no formation of aldehyde **44** was observed and the reaction resulted in complete decomposition of **43** (Figure 2.7A). To further determine the stability of the proposed aldehyde metathesis product **44** and the ketone metathesis product **15**, both compounds were independently synthesized and subjected to the optimized reaction conditions (Figure 2.7B). While methyl ketone **15** was stable under the reaction conditions, aldehyde **44** underwent rapid decomposition.

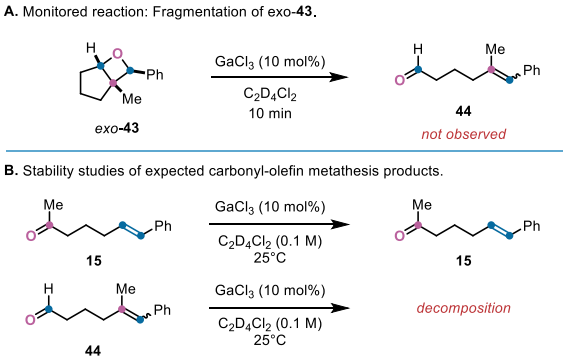

Figure 2.7: Mechanistic investigations of aldehyde **44**. **A.** Fragmentation study of oxetane *exo*-**43**. **B.** Stability investigations of the ketone and aldehyde metathesis products.

Based on the insights gained from investigating the fragmentation of the regioisomeric oxetanes and metathesis products, *in situ* ^{1}H-NMR experiments were conducted to elucidate any possible byproduct formation (Figure 2.8). Within 20 min, the exclusive formation of a single pair of olefin signals is observed which corresponded to methyl ketone **15** (blue, Figure 2.8B). However, a new set of signals at 3.4 ppm also appeared which did not correspond to ketone **15** (**A**, gold, Figure 5B). After 24 hours, signals corresponding to a second, unknown compound formed (**B**, green, Figure 5B). Importantly, no signals corresponding to oxetanes **42** or **43** were observed over the course of these ^{1}H-NMR studies.

With these results in hand, subsequent efforts were aimed at the isolation and identification of both byproducts **A** and **B**. Larger scale reactions were conducted and pure samples of both compounds **A** and **B** were isolated. Byproduct **A**, which formed within 20 min as a competing compound to the ketone metathesis product **15**, was identified as bicyclopentane **46** and was isolated in 20% yield (Figure 2.9B). Byproduct **B**, which formed in 10% yield, was characterized as pyran **47**. Both byproducts **A** and **B** are not the results of a ring-opening carbonyl–olefin metathesis pathway and do not represent products resulting from the fragmentation of intermediate oxetanes **42** and **43**, or decomposition of aldehyde **44**.

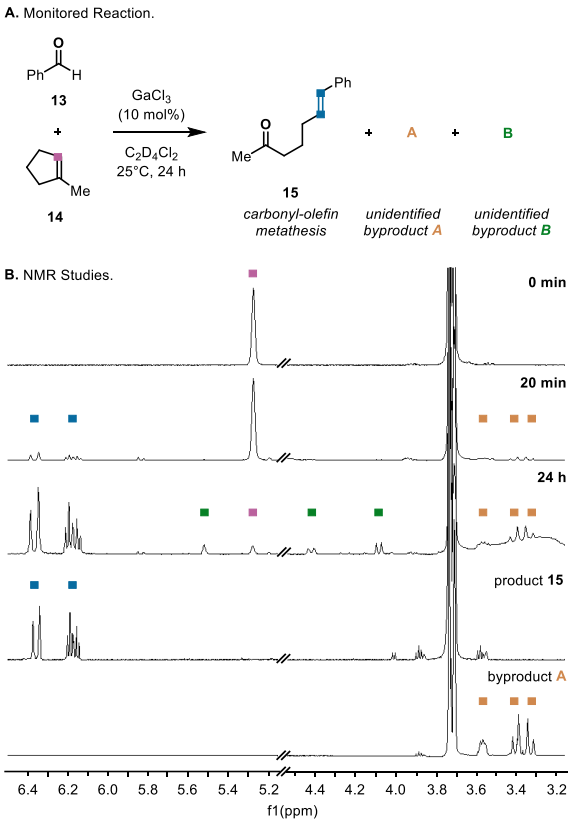

Figure 2.8: ^{1}H-NMR experiment of the $GaCl_3$-catalyzed ring-opening carbonyl–olefin metathesis reaction.

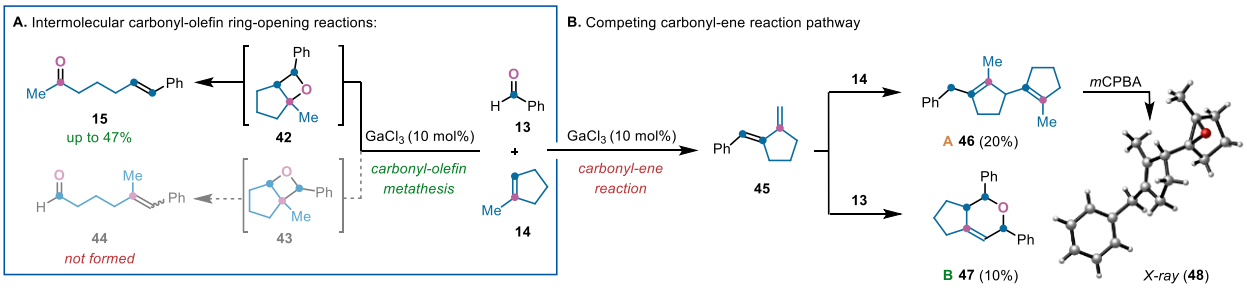

Figure 2.9: Mass balance of ring-opening carbonyl–olefin metathesis. **A.** Regioselective oxetane formation (**42**) to produce ketone metathesis products. **B.** Competing carbonyl-ene reaction pathway and the resulting byproducts.

These results are consistent with the regioselective formation of oxetane **42** as the exclusive productive intermediate in catalytic ring-opening carbonyl–olefin metathesis (Figure 2.9A). However, the formation of both bicyclopentane **46** and pyran **47** is consistent with a competing carbonyl-ene pathway resulting in diene **45** as a reactive intermediate. Diene **45** can undergoes addition with a second equivalent of 1-methylcyclopentene **14** to form bicyclopentane **46**, or a second equivalent of benzaldehyde **13** to form pyran **47** (Figure 2.9B).

2.4 Conclusions

The investigation of $GaCl_3$-catalyzed ring-opening carbonyl–olefin metathesis revealed important details of the controlling features of this reaction pathway. This transformation proceeds *via* selective formation of one regioisomeric oxetane, that subsequently fragments to result in unsaturated, alkyl ketones as the exclusive metathesis products. The low yields that are observed over the course of these studies are the direct result of competing carbonyl-ene reaction pathways that furnish two additional byproducts. Developing a catalyst system with the ability to preferentially favor one pathway over the other—ring-opening carbonyl–olefin metathesis vs. carbonyl-ene—holds great potential to create a high yielding ring-opening carbonyl–olefin metathesis of general synthetic utility.

2.5 Experimental Procedures and Supplemental Information

2.5.1 General Information

All moisture-sensitive reactions were performed under an atmosphere of nitrogen in flame-dried round bottom flasks or glass vials fitted with rubber septa and/or septa equipped screw caps. Stainless steel syringes were used to transfer air or moisture-sensitive liquids. Flash

chromatography was performed using silica gel Silia Flash® 40-63 micron (230-400 mesh) from Silicycle. All chemicals were purchased from SigmaAldrich, Alfa Aesar, Acros Organics, Oakwood, TCI America, Frontier Scientific, Matrix Scientific, Ark Pharm, and Chem Impex International, and were used as received unless otherwise stated. Tetrahydrofuran and dimethylformamide were dried by being passed through columns of activated alumina. Proton Nuclear Magnetic Resonance NMR (^{1}H NMR) spectra and carbon nuclear magnetic resonance (^{13}C NMR) spectra were recorded on a Varian Unity Plus 400, Varian MR400, Varian vnmrs 500, Varian Inova 500, Varian Mercury 500, and Varian vnmrs 700 spectrometers. Chemical shifts for protons are reported in parts per million and are references to the NMR solvent peak ($CDCl_3$: δ 7.27). Chemical shifts for carbons are reported in parts per million and are referenced to the carbon resonances of the NMR solvent ($CDCl_3$: δ 77.00). Data are represented as follows: chemical shift, integration, multiplicity (br = broad, s = singlet, d = doublet, t = triplet, q = quartet, p = pentet, dd = doublet of doublet, m = multiplet), and coupling constants in Hertz (Hz). Mass spectroscopic (MS) data was recorded at the Mass Spectrometry Facility at the Department of Chemistry of the University of Michigan in Ann Arbor, MI on an Agilent Q-TOF HPLC-MS with ESI high resolution mass spectrometer. Infrared (IR) spectra were obtained using either an Avatar 360 FT-IR or Perkin Elmer Spectrum BX FT-IR spectrometer. IR data are represented as frequency of absorption (cm^{-1}).

2.5.2 Optimization

Table 2.1: Lewis acid screen.

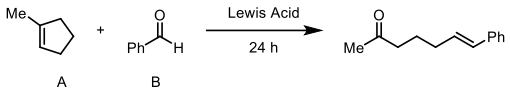

A B

Entry	A (equiv)	B (equiv)	Lewis Acid	Loading (mol%)	Temp. (C°)	Solvent	Concentration (M)	Yield (%)
1	1	4	$FeCl_3$	10	25	DCE	0.1	32.5
2	1	4	$GaCl_3$	10	25	DCE	0.1	45.6
3	1	4	$BF_3{\bullet}OEt_2$	10	25	DCE	0.1	1.5
4	1	4	$FeBr_3$	10	25	DCE	0.1	0.7
5	1	4	$TiCl_4$	10	25	DCE	0.1	0.0
6	1	4	$AlCl_3$	10	25	DCE	0.1	0.1
7	1	4	$Fe(OTf)_3$	10	25	DCE	0.1	3.8
8	1	4	$Sc(OTf)_3$	10	25	DCE	0.1	13.3
9	1	4	$InCl_3$	10	25	DCE	0.1	24.6
10	1	4	HCl	10	25	DCE	0.1	0.0
11	1	4	TfOH	10	25	DCE	0.1	2.2
12	1	4	H_2SO_4	10	25	DCE	0.1	5.8

Conditions: 0.1 mmol olefin substrate in solvent with benzaldehyde and Lewis acid. Yields were determined by GC.

Table 2.2: Solvent screen.

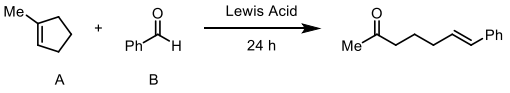

A B

Entry	A (equiv)	B (equiv)	Lewis Acid	Loading (mol%)	Temp. (C°)	Solvent	Concentration (M)	Yield (%)
1	1	4	$FeCl_3$	10	25	DCE	0.1	32.5
2	1	4	$GaCl_3$	10	25	DCE	0.1	45.6
13	1	4	$GaCl_3$	10	25	DCM	0.1	24.5
14	1	4	$GaCl_3$	10	25	THF	0.1	0.0
15	1	4	$GaCl_3$	10	25	Et_2O	0.1	0.0
16	1	4	$GaCl_3$	10	25	MeOH	0.1	0.0
17	1	4	$GaCl_3$	10	25	DMF	0.1	0.0
18	1	4	$GaCl_3$	10	25	Hexanes	0.1	13.1
19	1	4	$GaCl_3$	10	25	Toluene	0.1	4.0
20	1	4	$GaCl_3$	10	25	Benzene	0.1	4.8
21	1	4	$GaCl_3$	10	25	MeCN	0.1	0.2
22	1	4	$GaCl_3$	10	25	DMSO	0.1	0.0
23	1	4	$FeCl_3$	10	25	DCM	0.1	15.5
24	1	4	$FeCl_3$	10	25	THF	0.1	0.0
25	1	4	$FeCl_3$	10	25	Et_2O	0.1	0.2
26	1	4	$FeCl_3$	10	25	MeOH	0.1	0.0
27	1	4	$FeCl_3$	10	25	DMF	0.1	0.0
28	1	4	$FeCl_3$	10	25	Hexanes	0.1	9.6
29	1	4	$FeCl_3$	10	25	Toluene	0.1	10.3
30	1	4	$FeCl_3$	10	25	Benzene	0.1	11.4
31	1	4	$FeCl_3$	10	25	MeCN	0.1	0.1
32	1	4	$FeCl_3$	10	25	DMSO	0.1	0.0

Conditions: 0.1 mmol olefin substrate in solvent with benzaldehyde and Lewis acid. Yields were determined by GC.

Table 2.3: Substrate ratio screen.

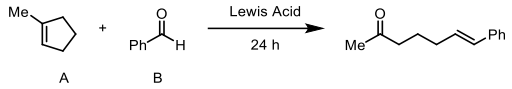

A B

Entry	A (equiv)	B (equiv)	Lewis Acid	Loading (mol%)	Temp. (C°)	Solvent	Concentration (M)	Yield (%)
1	1	4	$FeCl_3$	10	25	DCE	0.1	32.5
2	1	4	$GaCl_3$	10	25	DCE	0.1	45.6
33	1	5	$GaCl_3$	10	25	DCE	0.1	22.3
34	1	3	$GaCl_3$	10	25	DCE	0.1	33.9
35	1	2	$GaCl_3$	10	25	DCE	0.1	27.2
36	1	1	$GaCl_3$	10	25	DCE	0.1	24.9
37	2	1	$GaCl_3$	10	25	DCE	0.1	29.9
38	3	1	$GaCl_3$	10	25	DCE	0.1	26.6
39	4	1	$GaCl_3$	10	25	DCE	0.1	31.8
40	1	5	$FeCl_3$	10	25	DCE	0.1	14.4
41	1	3	$FeCl_3$	10	25	DCE	0.1	19.0
42	1	2	$FeCl_3$	10	25	DCE	0.1	13.4
43	1	1	$FeCl_3$	10	25	DCE	0.1	14.6
44	2	1	$FeCl_3$	10	25	DCE	0.1	15.5
45	3	1	$FeCl_3$	10	25	DCE	0.1	17.7
46	4	1	$FeCl_3$	10	25	DCE	0.1	21.5

Conditions: 0.1 mmol olefin substrate in solvent with benzaldehyde and Lewis acid. Yields were determined by GC.

Table 2.4: Temperature screen.

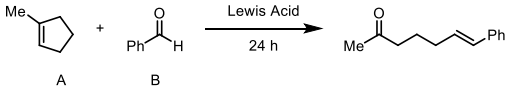

A B

Entry	A (equiv)	B (equiv)	Lewis Acid	Loading (mol%)	Temp. (C°)	Solvent	Concentration (M)	Yield (%)
1	1	4	$FeCl_3$	10	25	DCE	0.1	32.5
2	1	4	$GaCl_3$	10	25	DCE	0.1	45.6
47	1	4	$GaCl_3$	10	40	DCE	0.1	31.6
48	1	4	$GaCl_3$	10	80	DCE	0.1	12.6
49	1	4	$FeCl_3$	10	40	DCE	0.1	31.4
50	1	4	$FeCl_3$	10	80	DCE	0.1	29.2

Conditions: 0.1 mmol olefin substrate in solvent with benzaldehyde and Lewis acid. Yields were determined by GC.

Table 2.5: Catalyst loading screen.

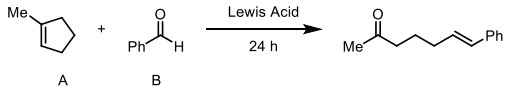

A B

Entry	A (equiv)	B (equiv)	Lewis Acid	Loading (mol%)	Temp. (C°)	Solvent	Concentration (M)	Yield (%)
1	1	4	$FeCl_3$	10	25	DCE	0.1	32.5
2	1	4	$GaCl_3$	10	25	DCE	0.1	45.6
51	1	4	$GaCl_3$	5	25	DCE	0.1	34.1
52	1	4	$GaCl_3$	20	25	DCE	0.1	19.5
53	1	4	$GaCl_3$	50	25	DCE	0.1	8.9
54	1	4	$GaCl_3$	100	25	DCE	0.1	0.6
55	1	4	$FeCl_3$	5	25	DCE	0.1	11.3
56	1	4	$FeCl_3$	20	25	DCE	0.1	26.5
57	1	4	$FeCl_3$	50	25	DCE	0.1	10.8
58	1	4	$FeCl_3$	100	25	DCE	0.1	0.0

Conditions: 0.1 mmol olefin substrate in solvent with benzaldehyde and Lewis acid. Yields were determined by GC.

Table 2.6: Concentration screen.

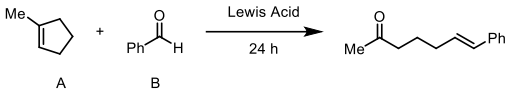

A B

Entry	A (equiv)	B (equiv)	Lewis Acid	Loading (mol%)	Temp. (C°)	Solvent	Concentration (M)	Yield (%)
1	1	4	$FeCl_3$	10	25	DCE	0.1	32.5
2	1	4	$GaCl_3$	10	25	DCE	0.1	45.6
59	1	4	$GaCl_3$	10	25	DCE	0.01	7.8
60	1	4	$GaCl_3$	10	25	DCE	0.05	18.9
61	1	4	$GaCl_3$	10	25	DCE	0.2	27.7
62	1	4	$GaCl_3$	10	25	DCE	0.3	25.5
63	1	4	$GaCl_3$	10	25	DCE	0.5	23.6
64	1	4	$GaCl_3$	10	25	DCE	1.0	22.8
65	1	4	$FeCl_3$	10	25	DCE	0.01	11.0
66	1	4	$FeCl_3$	10	25	DCE	0.05	15.3
67	1	4	$FeCl_3$	10	25	DCE	0.2	22.6
68	1	4	$FeCl_3$	10	25	DCE	0.3	25.3
69	1	4	$FeCl_3$	10	25	DCE	0.5	21.2
70	1	4	$FeCl_3$	10	25	DCE	1.0	15.6

Conditions: 0.1 mmol olefin substrate in solvent with benzaldehyde and Lewis acid. Yields were determined by GC.

Table 2.7: Time point screen.

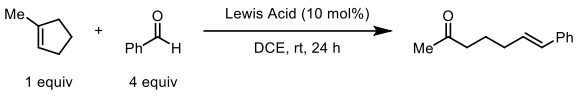

1 equiv 4 equiv

Entry	Lewis Acid	Time (h)	Yield (%)
1	$GaCl_3$	0.5	24.7
2	$GaCl_3$	1	27.4
3	$GaCl_3$	3	34.4
4	$GaCl_3$	6	37.2
5	$GaCl_3$	21	44.5
6	$GaCl_3$	24	45.6
1	$FeCl_3$	0.5	30.8
2	$FeCl_3$	1	31.3
3	$FeCl_3$	3	32.0
4	$FeCl_3$	6	31.8
5	$FeCl_3$	21	32.2
6	$FeCl_3$	24	32.5

Conditions: 0.1 mmol olefin substrate in DCE (0.1M) with 0.01mmol of Lewis acid for 24h at room temperature. Yields were determined by GC.

2.5.3 Mechanistic Investigations

Oxetane Fragmentation Experiments

Oxetane regioisomers were synthesized according to literature precedent.[12] The mixture of regiosisomers, **42** and **43** (40 mg, 0.21 mmol, 1 equiv.) shown below, was subjected to $GaCl_3$ (3.6 mg, 0.02 mmol, 0.1 equiv.) in 0.1 M DCE under N_2 gas at 25 °C for 10 minutes. The reaction mixture was quenched by passing through a silica plug and eluted with DCM into a flask and then concentrated and the crude material was characterized by NMR shown below. The ketone metathesis product **15** was produced in 61% yield (23.9 mg).

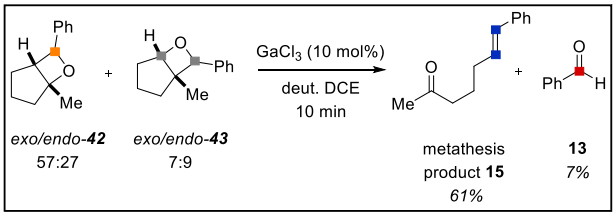

Abbreviated ^{1}H NMR Spectra

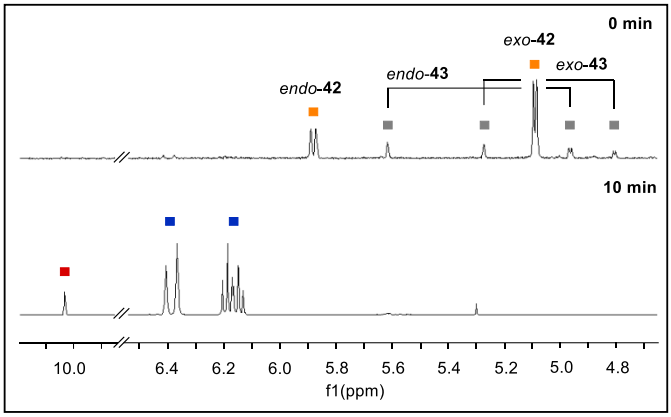

Full ^{1}H NMR Spectra

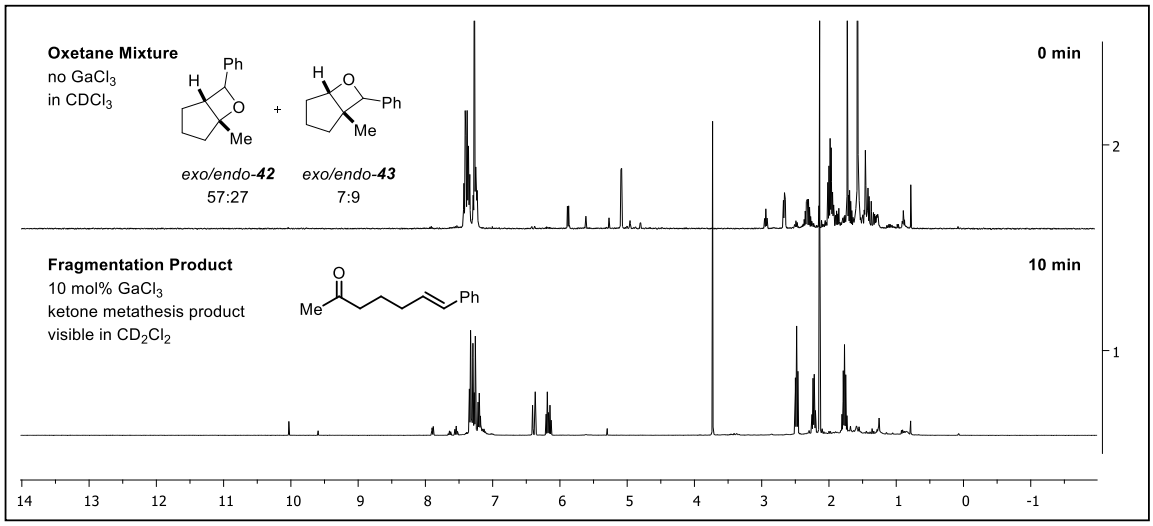

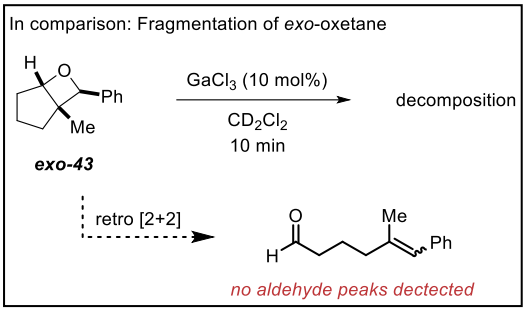

A single diastereomer of the synthesized oxetane mixture was isolated following flash column chromatography with hexanes/EtOAc (9:1) (see below for characterization in deuterated DCM, spectra match reported data).[12] This *exo*-**43** diastereomer, would provide the aldehyde metathesis product following oxetane fragmentation. In an NMR tube, the oxetane *exo*-**43** (10 mg, 0.053 mmol, 1 equiv.) was dissolved in deuterated DCE (0.1 M) and $GaCl_3$ (0.9 mg, 0.0053 mmol, 0.1 equiv.) was added. The reaction was monitored by ^1H NMR and over the course of 24 h, the oxetane decomposed and there was no identifiable products formed.

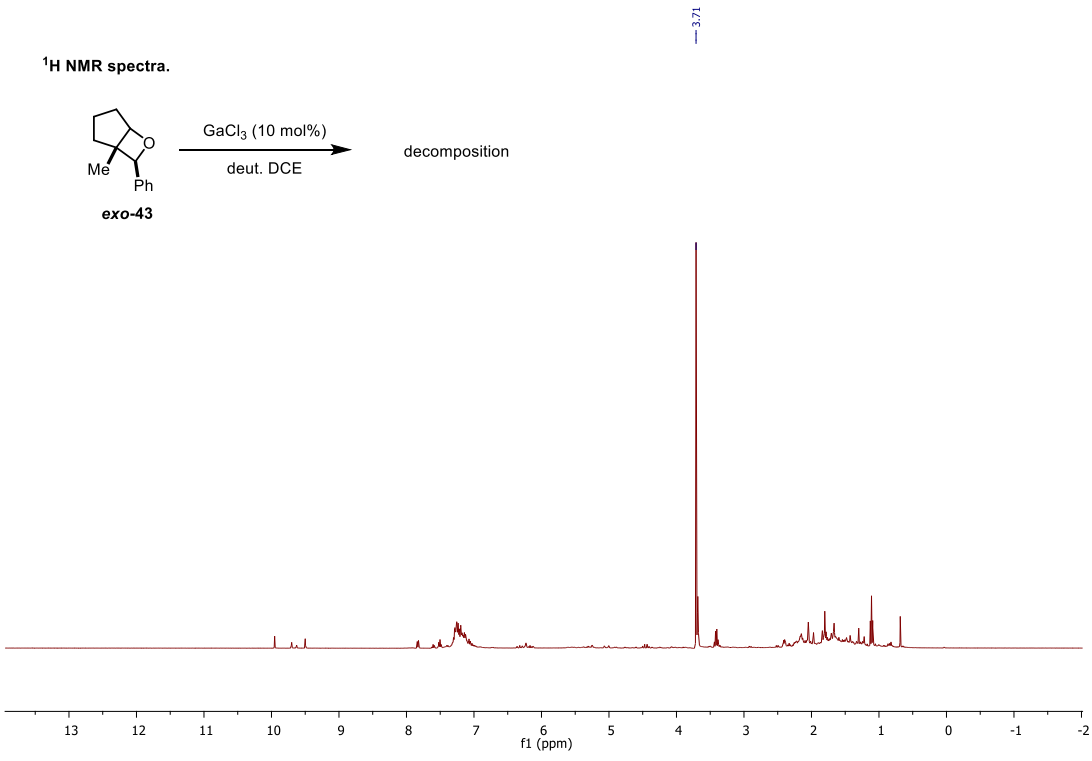

Metathesis Product Stability

Metathesis product **15** (18.8 mg, 0.10 mmol, 1 equiv.) was dissolved in deuterated DCE (0.1 M) in and NMR tube and the first NMR was taken (see below). $GaCl_3$ (1.8 mg, 0.01 mmol, 0.1 equiv.) was added to the NMR tube and the reaction as monitored over 24 hours. The resulting spectra is below displaying no decomposition.

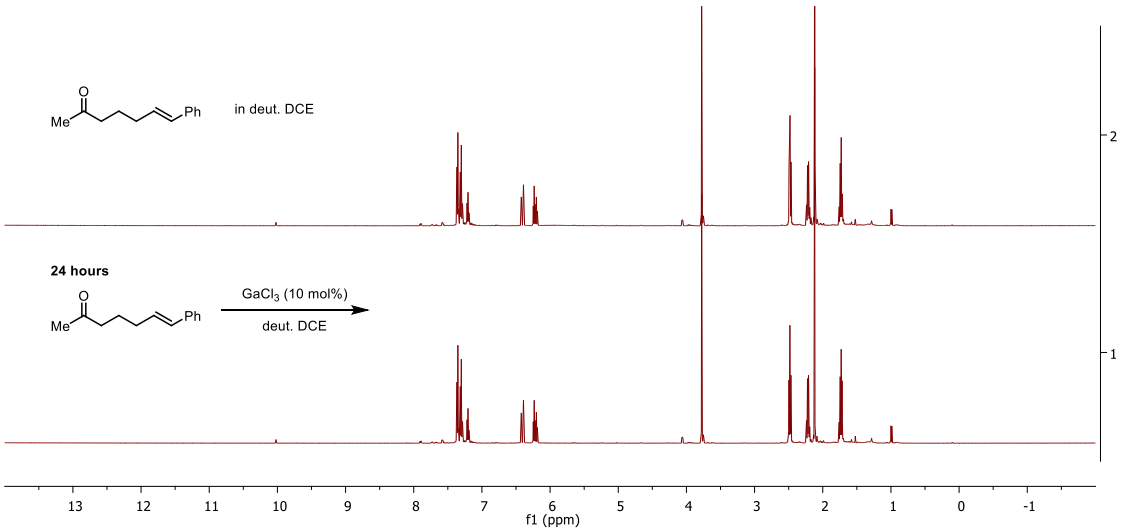

Possible metathesis product **44** (15.0 mg, 0.08 mmol, 1 equiv.) was dissolved in deuterated DCE (0.1 M) in and NMR tube and the first NMR was taken (see below). $GaCl_3$ (1.4 mg, 0.008 mmol, 0.1 equiv.) was added to the NMR tube and the reaction as monitored over 24 hours. The resulting spectra is below displaying complete decomposition.

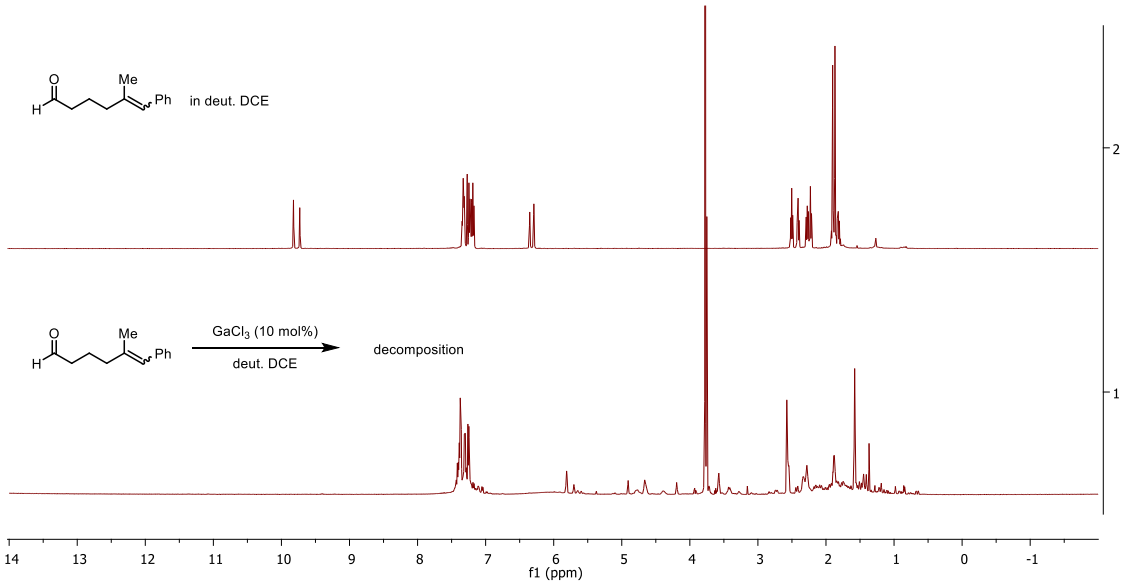

^{1}H NMR Monitored Metathesis Reaction

In an NMR tube, 1-methylcyclopentene (8.4µL, 0.08 mmol, 1 equiv.) was dissolved in deuterated DCE (0.8 mL, 0.1 M) and benzaldehyde (33 µL, 0.32 mmol, 4 equiv.) was added followed by $GaCl_3$ (1.4 mg, 0.008 mmol). The reaction was monitored with ^{1}H NMR over the course of 24 h at 25 °C.

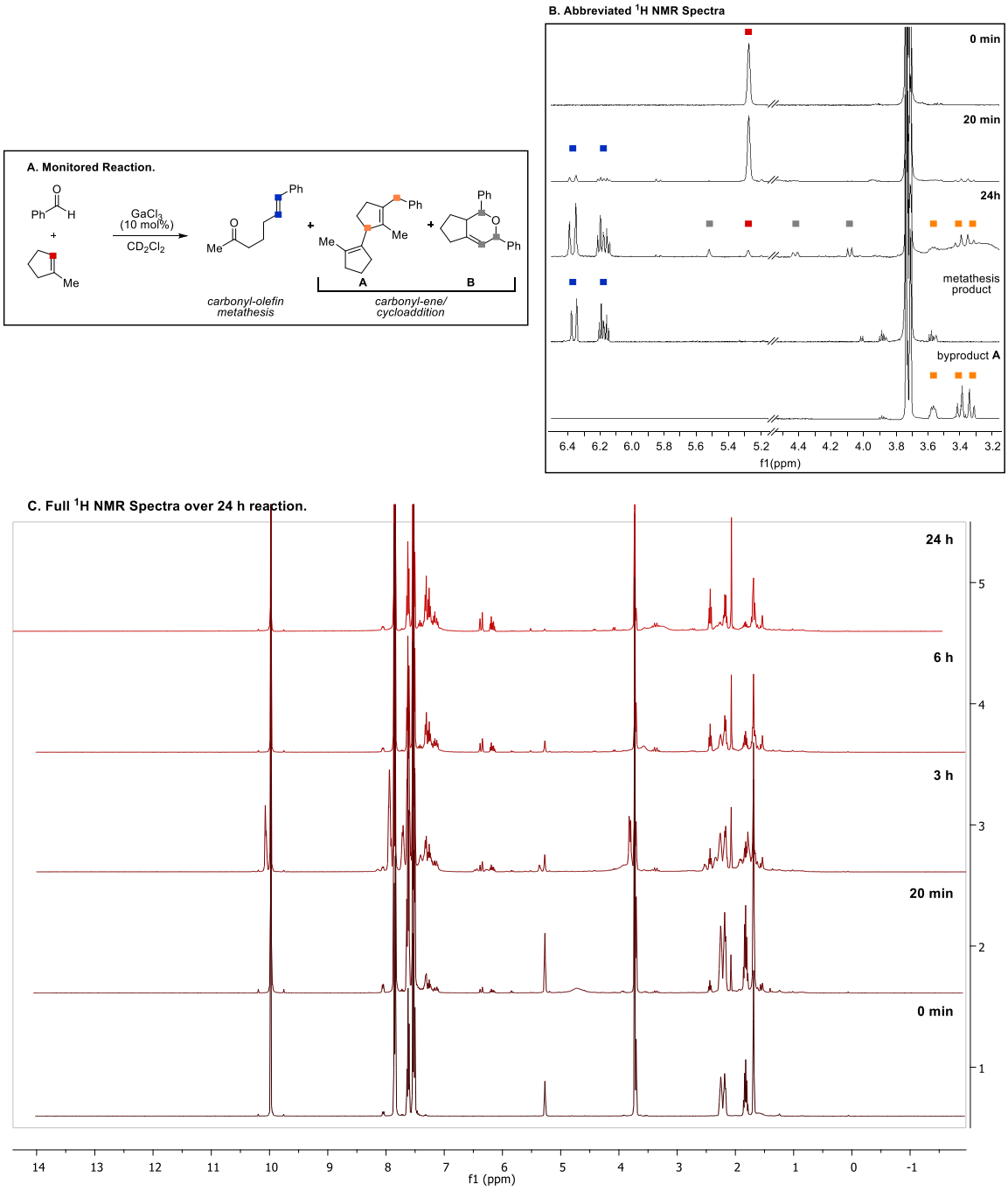

X-Ray Crystallographic Data for 48

Single-Crystal Structure Determination

Single-crystal X-ray diffraction data were collected using a Rigaku XtaLAB Synergy-S X-ray diffractometer configured in a kappa goniometer geometry. The diffractometer is equipped with a low temperature device and a PhotonJet-S microfocus Cu source (λ = 1.54187 Å) set at a rough divergence of 9.5 and operated at 50 kV and 1 mA. X-ray intensities were measured at 230(1) K with the HyPix-6000HE detector placed 32.01 mm from the sample. The data were processed with CrysAlisPro v38.46 (Rigaku Oxford Diffraction) and corrected for absorption. The structures were solved in OLEX2[13] using SHELXTL[14] and refined using SHELXL.[15] All non-hydrogen atoms were refined anisotropically with hydrogen atoms placed at idealized positions.

Table of Crystallographic Parameters

Material	exp_338
Space Group	*P*-1
a Å	7.7053(3)
b Å	9.0846(4)
c Å	12.4853(5)
α (°)	110.671(4)
β (°)	97.192(3)
γ (°)	99.545(4)
Volume (Å^3)	790.232
Temperature (K)	230(1)
ρ_{calc} (g cm^{-3})	1.128
R_1/wR_2	5.57/12.66
GOF	1.055

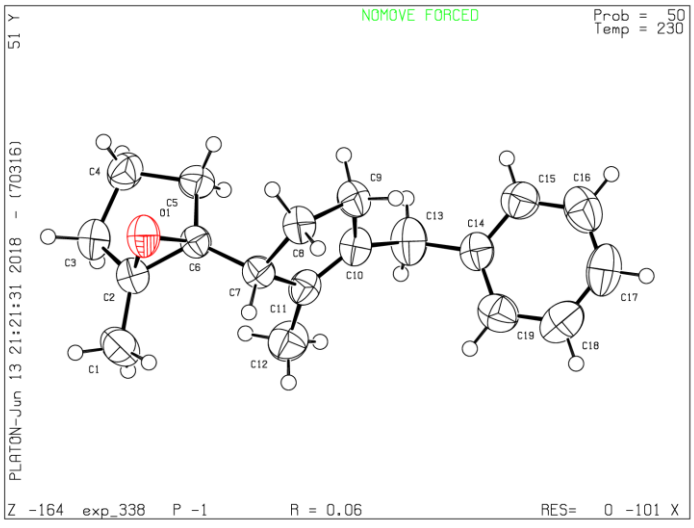

2.5.4 Experimental Procedures

Substrate Synthesis

All olefin substrates for the ring-opening carbonyl-olefin metathesis reaction were purchased from SigmaAldrich or Fisher Scientific, were synthesized according to corresponding reference to compound in the metathesis section or are reported below.

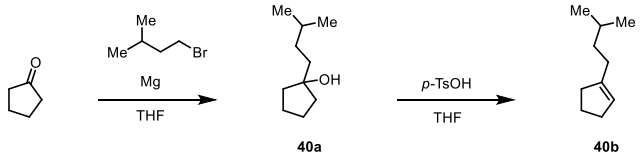

1-butylcyclopentanol (40a): To freshly grinded magnesium turnings (1084 mg, 44.6 mmol, 1.25 equiv.) was added slowly a solution of 1-bromo-3-methylbutane (5.13 mL, 42.8 mmol, 1.2 equiv.) in THF (45 mL) at 0 °C and the mixture allowed to warm up to 25 °C and stirred for 1.5 h at 25 °C. A solution of cyclopentanone (3.16 mL, 35.7 mmol, 1.0 equiv.) in THF (15 mL) was added slowly over 10 min at 0 °C and the solution gradually warmed up to 25 °C and stirred overnight. The reaction was quenched by addition of NH_4Cl (aq.) and acidified with 1 M HCl to pH 2-3 and stirred until all solids were dissolved. The aqueous layer was extracted with EtOAc (3x50 mL) and the combined organic layers were dried over $MgSO_4$, filtered and concentrated in vacuo. Purification by flash column chromatography (30% EtOAc/hexanes) afforded **40a** 2.0 g (36%) as a yellow liquid.

1-isopentylcyclopent-1-ene (40b): 40a (1.00 g, 6.4 mmol, 1.0 equiv.) was dissolved in (7 mL THF) with p-toluenesulfonic acid monohydrate (243 mg, 20 mol%) and refluxed overnight. Solvent was removed in vacuo and the residue partitioned between $NaHCO_3$ (aq.) and Et_2O. The aqueous layer was extracted with Et_2O (3x) and the combined organic layers dried over $MgSO_4$, filtered and concentrated in vacuo. Purification by flash column chromatography (100% pentane) afforded **40b** 539 mg (61%) as a colorless liquid, 8:1 mixture (*endo*:*exo* olefin isomers).

^{1}H NMR (400 MHz; $CDCl_3$) δ_H 5.32 (s, 1H), 2.30 (t, J = 6.0 Hz, 2H), 2.23 (t, J = 6.9 Hz, 2H), 2.07 (s, 1H), 1.85 (p, J = 7.5 Hz, 2H), 1.53 (dd, J = 13.2, 6.6 Hz, 1H), 1.35 – 1.30 (m, 3H), 0.90 (d, J = 6.4 Hz, 6H).

^{13}C NMR (135 MHz, $CDCl_3$) δ_C145.3, 122.7, 37.0, 35.1, 34.1, 32.4, 29.0, 23.4, 22.6, 14.1.

ν_{max} (FTIR)/cm^{-1}: 1716, 1658, 1544, 1501, 1455, 1104, 1011, 998, 802, 785.

***m/z* (ESI+) HRMS [M+H] $C_{10}H_{18}^+$:** formula found 138.1442, cald. 138.1409

Ring-Opening Carbonyl–Olefin Metathesis Reactions

General metathesis procedure: A flame-dried round bottom flask with a magnetic stir bar, was charged with $GaCl_3$ (0.1 equiv.) in DCE (0.1 M) followed by aldehyde (4.0 equiv.) and olefin (1.0 equiv.) substrates. The resulting mixture was stirred at 25 °C under N_2 for 24 hours. The reaction mixture was quenched by passing through a silica plug and eluted with DCM into a flask and then concentrated and the crude material was purified using column chromatography with indicated eluent to provide pure metathesis product.

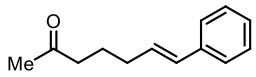

(*E*)-7-phenylhept-6-en-2-one (15): The metathesis was performed according to general procedure, by subjecting 1-methylcyclopentene (12.2 mmol, 1 equiv.) and benzaldehyde (48.7 mmol, 4 equiv.). Purification by flash column chromatography eluting with hexanes/EtOAc (9:1) provided **15** 1.07 g (47%) as a clear oil.

^{1}H NMR (400 MHz; $CDCl_3$) δ_H 7.37 – 7.29 (m,4H), 7.24 – 7.15 (m, 1H), 6.40 (d, *J* = 15.8 Hz, 1H), 6.18 (dt, *J* = 15.8, 6.9 Hz, 1H), 2.49 (t, *J* = 7.4 Hz, 2H), 2.32 – 2.19 (m, 2H), 2.22 – 2.05 (m, 3H), 1.83 – 1.69 (m, 2H).

^{13}C NMR (135 MHz, $CDCl_3$) δ_C 208.8, 137.5, 130.7, 129.8, 128.5, 127.0, 125.9, 42.9, 32.3, 30.0, 23.2.

***ν*$_{max}$ (FTIR)/cm^{-1}:** 2956, 1711, 1587, 1503, 1458, 1368, 1263, 1111, 1056, 972.

***m/z* (ESI+) HRMS [M+H] $C_{13}H_{16}O^+$:** formula found 188.1299, cald. 188.1201.

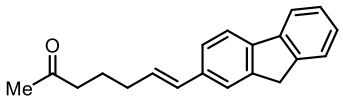

(*E*)-7-(9H-fluoren-2-yl)hept-6-en-2-one (21): The metathesis was performed according to general procedure, by subjecting 1-methylcyclopentene (0.91 mmol, 1 equiv.) and 9H-fluorene-2-carbaldehyde (3.65 mmol, 4 equiv.). Purification by flash column chromatography eluting with hexanes/EtOAc (9:1) provided **21** 114.0 mg (45%) as a pale yellow solid.

^{1}H NMR (400 MHz; $CDCl_3$) δ_H 7.76 (d, *J* = 7.5 Hz, 1H), 7.71 (d, *J* = 7.9 Hz, 1H), 7.54 (d, *J* = 8.4 Hz, 2H), 7.37 (dd, *J* = 14.0, 7.1 Hz, 2H), 7.29 (t, *J* = 7.5 Hz, 1H), 6.47 (d, *J* = 15.8 Hz, 1H), 6.27

– 6.19 (m, 1H), 3.90 (s, 2H), 2.51 (t, *J* = 7.4 Hz, 2H), 2.27 (q, *J* = 7.2 Hz, 2H), 2.16 (s, 3H), 1.80 (m, 2H).

^{13}C NMR (135 MHz, $CDCl_3$) δ_C 208.9, 143.6, 143.4, 141.5, 140.7, 136.3, 131.0, 129.3, 126.7, 126.5, 125.03, 124.97, 122.3, 119.9, 119.7, 42.9, 36.8, 32.4, 30.0, 23.3.

ν_{max} (FTIR)/cm^{-1}: 2935, 2361, 1706, 1652, 1558, 1521, 1355, 1304, 1161, 1002.

***m/z* (ESI+) HRMS [M+Na] $C_{20}H_{20}O^+$:** formula found 299.1410, cald. 299.1406.

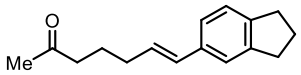

(*E*)-7-(2,3-dihydro-1H-inden-5-yl)hept-6-en-2-one (22): The metathesis was performed according to general procedure, by subjecting 1-methylcyclopentene (0.12 mmol, 1 equiv.) and indane-5-carbaldehyde (0.73 mmol, 4 equiv.). Purification by flash column chromatography eluting with hexanes/EtOAc (9:1) provided **22** 12.5 mg (45%) as a clear oil.

^{1}H NMR (400 MHz; $CDCl_3$) δ_H 7.27 (s, 16H), 7.24 (s, 4H), 7.16 (d, *J* = 7.6 Hz, 4H), 7.11 (d, *J* = 7.9 Hz, 4H), 6.37 (d, *J* = 15.8 Hz, 3H), 6.14 – 6.09 (m, 3H), 2.89 (dd, *J* = 12.7, 6.5 Hz, 15H), 2.48 (t, *J* = 7.3 Hz, 7H), 2.22 (s, 5H), 2.21 (s, 2H), 2.20 (d, *J* = 20.4 Hz, 9H), 2.21 – 1.93 (m, 28H), 1.81 – 1.62 (m, 9H).

^{13}C NMR (135 MHz, $CDCl_3$) δ_C 208.9, 144.6, 143.3, 135.7, 131.0, 128.5, 124.3, 124.2, 121.7, 42.9, 32.7, 32.6, 32.3, 30.0, 25.5, 23.3.

ν_{max} (FTIR)/cm^{-1}: 2935, 2845, 1706, 1489, 1436, 1356, 1161, 1096, 1002, 965.

***m/z* (ESI+) HRMS [M+Na] $C_{16}H_{20}O^+$:** formula found 251.1410, cald. 251.1406.

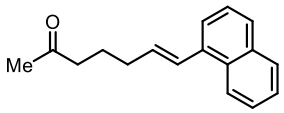

(*E*)-7-(naphthalen-1-yl)hept-6-en-2-one (23): The metathesis was performed according to general procedure, by subjecting 1-methylcyclopentene (1.22 mmol, 1 equiv.) and naphthalene-1-carbaldehyde (4.88 mmol, 4 equiv.). Purification by flash column chromatography eluting with hexanes/EtOAc (9:1) provided **23** 93.5 mg (32%) as a clear oil.

^{1}H NMR (400 MHz, $CDCl_3$) δ_H 8.13 (d, *J* = 8.7 Hz, 1H), 7.86 (d, *J* = 7.5 Hz, 1H), 7.77 (d, *J* = 8.2 Hz, 1H), 7.59 – 7.42 (m, 4H), 7.14 (d, *J* = 15.5 Hz, 1H), 6.21 (dt, *J* = 15.2, 6.9 Hz, 1H), 2.55 (t, *J* = 7.3 Hz, 2H), 2.37 (qd, *J* = 7.2, 1.5 Hz, 2H), 2.18 (s, 3H), 1.86 (p, *J* = 7.3 Hz, 2H).

^{13}C NMR (126 MHz, $CDCl_3$) δ_C 208.8, 135.3, 133.6, 133.1, 131.0, 128.5, 127.8, 127.4, 125.8, 125.6, 125.6, 123.8, 123.5, 42.9, 32.7, 30.0, 23.3.

ν_{max} (FTIR)/cm^{-1}: 2924, 1710, 1589, 1508, 1394, 1354, 1156, 966, 774, 730.

***m/z* (ESI+) HRMS [M+Na] $C_{17}H_{18}O^+$:** formula found 261.1250, cald. 261.1256.

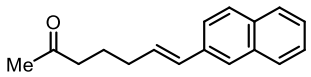

(*E*)-7-(naphthalen-2-yl)hept-6-en-2-one (24): The metathesis was performed according to general procedure, by subjecting 1-methylcyclopentene (1.83 mmol, 1 equiv.) and 2-naphthaldehyde (7.30 mmol, 4 equiv.). Purification by flash column chromatography eluting with hexanes/EtOAc (9:1) provided **24** 67.0 mg (15%) as a clear oil.

^{1}H NMR (400 MHz; $CDCl_3$) δ_H 7.83 – 7.75 (m, 3H), 7.68 (s, 1H), 7.58 (d, *J* = 8.2 Hz, 1H), 7.48 – 7.41 (m, 2H), 6.56 (d, *J* = 15.5 Hz, 1H), 6.31 (dt, *J* = 14.3, 7.2 Hz, 1H), 2.52 (t, *J* = 7.4 Hz, 2H), 2.30 (d, *J* = 7.1 Hz, 2H), 2.16 (s, 3H), 1.86 – 1.80 (m, 2H).

^{13}C NMR (135 MHz, $CDCl_3$) δ_C 208.8, 135.0, 133.7, 132.7, 130.8, 130.3, 128.1, 127.8, 127.6, 126.2, 125.54, 125.47, 123.5, 42.9m 32.4, 30.0, 23.3.

ν_{max} (FTIR)/cm^{-1}: 2965, 2854, 1719, 1709, 1442, 1376, 1144, 1100, 942, 809.

***m/z* (ESI+) HRMS [M+Na] $C_{17}H_{18}O^+$:** formula found 261.1252, cald. 261.1250.

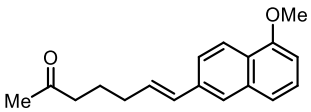

(*E*)-7-(5-methoxynaphthalen-2-yl)hept-6-en-2-one (25): The metathesis was performed according to general procedure, by subjecting 1-methylcyclopentene (1.8 mmol, 1 equiv.) and 5-methoxy-2-napthaldehyde (7.3 mmol, 4 equiv.). Purification by flash column chromatography eluting with hexanes/EtOAc (7:1) provided **25** 63 mg (13%) as a yellow solid.

^{1}H NMR (700 MHz; $CDCl_3$) δ_H 7.67 (dd, *J* = 14.1, 8.7 Hz, 2H), 7.61 (s, 1H), 7.53 (d, *J* = 8.6 Hz, 1H), 7.13 – 7.09 (m, 2H), 6.51 (d, *J* = 15.7 Hz, 1H), 6.27 – 6.21 (m, 1H), 3.92 (s, 3H), 2.51 (t, *J* = 7.4 Hz, 2H), 2.27 (q, *J* = 7.2 Hz, 2H), 2.15 (s, 3H), 1.80 (p, *J* = 7.4 Hz, 2H).

^{13}C NMR (175 MHz; $CDCl_3$) δ_C 209.1, 157.7, 134.0, 133.1, 131.0, 129.5, 129.4, 129.2, 127.1, 125.5, 124.2, 119.0, 106.0, 55.5, 43.1, 32.6, 30.2, 23.5.

ν_{max} (FTIR)/cm^{-1}: 2939, 2836, 1706, 1599, 1483, 1353, 1161, 1121, 1028, 967.

***m/z* (ESI+) HRMS [M+Na] $C_{18}H_{20}O_2^+$:** formula found 291.1359, cald. 291.1356.

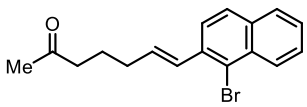

(*E*)-7-(1-bromonaphthalen-2-yl)hept-6-en-2-one (26): The metathesis was performed according to general procedure, by subjecting 1-methylcyclopentene (0.61 mmol, 1 equiv.) and 1-bromonaphthalene-2-carbaldehyde (2.44 mmol, 4 equiv.). Purification by flash column chromatography eluting with hexanes/EtOAc (9:1) provided **26** 57.9 mg (30%) as a clear oil.

^{1}H NMR (400 MHz, $CDCl_3$) δ_H 8.34 (d, *J* = 8.5 Hz, 1H), 7.79 (d, *J* = 8.1 Hz, 1H), 7.74 (d, *J* = 8.6 Hz, 1H), 7.63 – 7.56 (m, 2H), 7.49 (t, *J* = 7.4 Hz, 1H), 7.06 (d, *J* = 15.7 Hz, 1H), 6.26 (dt, *J* = 15.8, 7.0 Hz, 1H), 2.54 (t, *J* = 7.3 Hz, 2H), 2.35 (qd, *J* = 7.2, 1.4 Hz, 2H), 2.17 (s, 3H), 1.85 (p, *J* = 7.3 Hz, 2H).

^{13}C NMR (126 MHz, $CDCl_3$) δ_C 208.8, 134.9, 133.8, 133.6, 132.6, 130.7, 128.0, 127.61, 127.58, 127.5, 126.2, 124.3, 122.8, 42.8, 32.6, 30.1, 23.0.

ν_{max} (FTIR)/cm^{-1}: 3054, 2927, 1955, 1710, 1353, 1153, 964, 809, 743, 653.

***m/z* (ESI+) HRMS [M+Na] $C_{17}H_{17}BrO^+$:** formula found 339.0357, cald. 339.0361.

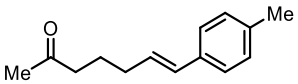

(*E*)-7-(p-tolyl)hept-6-en-2-one (27): The metathesis was performed according to general procedure, by subjecting 1-methylcyclopentene (1.22 mmol, 1 equiv.) and 4-methylbenzaldehyde (4.88 mmol, 4 equiv.). Purification by flash column chromatography eluting with hexanes/EtOAc (9:1) provided **27** 78.9 mg (32%) as an orange solid.

^{1}H NMR (400 MHz, $CDCl_3$) δ_H 7.24 (d, *J* = 7.9 Hz, 2H), 7.11 (d, *J* = 7.8 Hz, 2H), 6.36 (d, *J* = 15.8 Hz, 1H), 6.12 (dt, *J* = 15.7, 7.0 Hz, 1H), 2.48 (t, *J* = 7.4 Hz, 2H), 2.34 (s, 3H), 2.26 – 2.19 (m, 2H), 2.14 (s, 3H), 1.77 (p, *J* = 7.4 Hz, 2H).

^{13}C NMR (126 MHz, $CDCl_3$) δ_C 208.9, 136.7, 134.7, 130.5, 129.2, 128.8, 125.8, 42.9, 32.3, 30.0, 23.3, 21.1.

ν_{max} (FTIR)/cm^{-1}: 2940, 1710, 1512, 1367, 1353, 1158, 983, 813, 788, 722.

***m/z* (ESI+) HRMS [M+Na] $C_{14}H_{18}O^+$:** formula found 225.1241, cald. 225.1256.

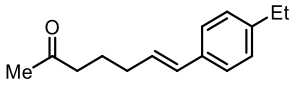

(*E*)-7-(4-ethylphenyl)hept-6-en-2-one (28): The metathesis was performed according to general procedure, by subjecting 1-methylcyclopentene (1.22 mmol, 1 equiv.) and 4-ethylbenzaldehyde (4.88 mmol, 4 equiv.). Purification by flash column chromatography eluting with hexanes/EtOAc (9:1) provided **28** 109.0 mg (41%) as a clear oil.

^{1}H NMR (400 MHz, $CDCl_3$) δ_H 7.27 (d, *J* = 7.8 Hz, 2H), 7.14 (d, *J* = 7.8 Hz, 2H), 6.37 (d, *J* = 15.8 Hz, 1H), 6.12 (dt, *J* = 15.7, 7.0 Hz, 1H), 2.63 (q, *J* = 7.6 Hz, 2H), 2.48 (t, *J* = 7.4 Hz, 2H), 2.22 (q, *J* = 7.2 Hz, 2H), 2.14 (s, 3H), 1.77 (p, *J* = 7.3 Hz, 2H), 1.23 (t, *J* = 7.6 Hz, 3H).

^{13}C NMR (126 MHz, $CDCl_3$) δ_C 208.9, 143.2, 135.0, 130.5, 128.8, 128.0, 125.9, 42.9, 32.3, 30.0, 28.5, 23.3, 15.6.

***ν*$_{max}$ (FTIR)/cm^{-1}:** 3020, 2962, 2931, 1712, 1511, 1355, 1154, 966, 850, 813.

***m/z* (ESI+) HRMS [M+Na] $C_{15}H_{20}O^+$:** formula found 239.1409, cald. 239.1412.

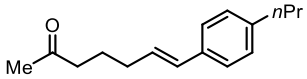

(*E*)-7-(4-propylphenyl)hept-6-en-2-one (29): The metathesis was performed according to general procedure, by subjecting 1-methylcyclopentene (0.84 mmol, 1 equiv.) and 4-propylbenzaldehyde (3.4 mmol, 4 equiv.). Purification by flash column chromatography eluting with hexanes/EtOAc (9:1) provided **29** 68.0 mg (35%) as a clear oil.

^{1}H NMR (500 MHz; $CDCl_3$) δ_H 7.25 (d, *J* = 7.9 Hz, 2H), 7.10 (d, *J* = 7.9 Hz, 2H), 6.36 (d, *J* = 15.8 Hz, 1H), 6.15 – 6.07 (m, 1H), 2.56 (t, *J* = 7.6 Hz, 2H), 2.47 (t, *J* = 7.4 Hz, 2H), 2.21 (q, *J* = 7.1 Hz, 2H), 2.13 (s, 3H), 1.76 (p, *J* = 7.3 Hz, 2H), 1.62 (q, *J* = 7.5 Hz, 2H), 0.93 (t, *J* = 7.3 Hz, 3H).

^{13}C NMR (125 MHz; $CDCl_3$) δ_C 209.1, 141.8, 135.2, 130.7, 128.9, 128.8, 126.0, 37.9, 32.4, 30.2, 24.7, 23.4, 14.0.

***ν*$_{max}$ (FTIR)/cm^{-1}:** 3021, 2956, 2930, 2871, 1714, 1511, 1356, 1154, 966, 788.

***m/z* (ESI+) HRMS [M+Na] $C_{16}H_{22}O^+$:** formula found 253.1573, cald. 253.1563.

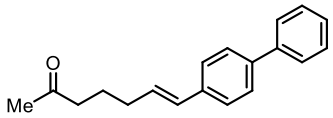

(*E*)-7-([1,1'-biphenyl]-4-yl)hept-6-en-2-one (30): The metathesis was performed according to general procedure, by subjecting 1-methylcyclopentene (1.8 mmol, 1 equiv.) and biphenyl-4-carboxaldehyde (7.3 mmol, 4 equiv.). Purification by flash column chromatography eluting with hexanes/EtOAc (9:1) provided **30** 150.2 mg (31%) as a white solid.

^{1}H NMR (500 MHz; $CDCl_3$) δ_H 7.59 (d, *J* = 8.0 Hz, 2H), 7.54 (d, *J* = 8.1 Hz, 2H), 7.43 (q, *J* = 7.7 Hz, 4H), 7.33 (t, *J* = 7.4 Hz, 1H), 6.43 (d, *J* = 15.8 Hz, 1H), 6.27 – 6.18 (m, 1H), 2.50 (t, *J* = 7.3 Hz, 2H), 2.25 (q, *J* = 7.1 Hz, 2H), 2.15 (s, 3H), 1.79 (p, *J* = 7.3 Hz, 2H).

^{13}C NMR (125 MHz; $CDCl_3$) δ_C 209.0, 140.9, 139.9, 136.8, 130.4, 130.2, 128.9, 127.4, 127.0, 126.5, 43.0, 32.5, 30.2, 23.4.

ν_{max} (FTIR)/cm^{-1}: 2937, 2890, 1706, 1486, 1406, 1372, 1360, 1159, 966, 758.

***m/z* (ESI+) HRMS [M+Na] $C_{19}H_{20}O^+$:** formula found 287.1408, cald. 287.1406.

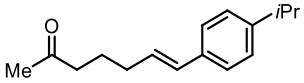

(*E*)-7-(4-isopropylphenyl)hept-6-en-2-one (31): The metathesis was performed according to general procedure, by subjecting 1-methylcyclopentene (1.22 mmol, 1 equiv.) and 4-isopropylbenzaldehyde (4.88 mmol, 4 equiv.). Purification by flash column chromatography eluting with hexanes/EtOAc (9:1) provided **31** 112.0 mg (40%) as a yellow solid.

^{1}H NMR (400 MHz, $CDCl_3$) δ_H 7.28 (d, *J* = 7.9 Hz, 2H), 7.17 (d, *J* = 7.9 Hz, 2H), 6.37 (d, *J* = 15.8 Hz, 1H), 6.12 (dt, *J* = 15.5, 6.9 Hz, 1H), 2.89 (hept, *J* = 7.0 Hz, 1H), 2.48 (t, *J* = 7.4 Hz, 2H), 2.22 (q, *J* = 7.2 Hz, 2H), 2.14 (s, 3H), 1.77 (p, *J* = 7.3 Hz, 2H), 1.25 (d, *J* = 6.9 Hz, 6H).

^{13}C NMR (126 MHz, $CDCl_3$) δ_C 208.9, 147.8, 135.2, 130.5, 128.9, 126.5, 125.9, 42.9, 33.8, 32.3, 30.0, 23.9, 23.3.

ν_{max} (FTIR)/cm^{-1}: 3022, 2956, 2867, 1706, 1512, 1358, 1161, 1051, 976, 817.

***m/z* (ESI+) HRMS [M+Na] $C_{16}H_{22}O^+$:** formula found 253.1567, cald. 253.1569.

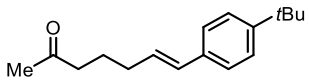

(*E*)-7-(4-(*tert*-butyl)phenyl)hept-6-en-2-one (32): The metathesis was performed according to general procedure, by subjecting 1-methylcyclopentene (1.8 mmol, 1 equiv.) and 4-tert-butylbenzaldehyde (7.3 mmol, 4 equiv.). Purification by flash column chromatography eluting with hexanes/EtOAc (9:1) provided **32** 160.2 mg (36%) as a clear oil.

^{1}H NMR (500 MHz; $CDCl_3$) δ_H 7.33 (d, *J* = 8.3 Hz, 2H), 7.28 (d, *J* = 8.3 Hz, 2H), 6.37 (d, *J* = 15.8 Hz, 1H), 6.16 – 6.08 (m, 1H), 2.47 (t, *J* = 7.4 Hz, 2H), 2.22 (q, *J* = 7.1 Hz, 2H), 2.13 (s, 3H), 1.76 (p, *J* = 7.3 Hz, 2H), 1.31 (s, 9H).

^{13}C NMR (125 MHz; $CDCl_3$) δ_C 209.1, 150.2, 134.9, 130.6, 129.2, 125.8, 125.6, 77.4, 77.2, 76.9, 43.0, 34.6, 32.4, 31.4, 30.2, 23.4.

ν_{max} (FTIR)/cm^{-1}: 2959, 2904, 2866, 1714, 1411, 1363, 1269, 1154, 966, 813.

***m/z* (ESI+) HRMS [M+Na] $C_{17}H_{24}O^+$:** formula found 267.1727, cald. 267.1719.

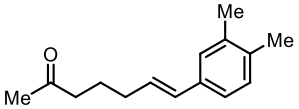

(*E*)-7-(3,4-dimethylphenyl)hept-6-en-2-one (33): The metathesis was performed according to general procedure, by subjecting 1-methylcyclopentene (1.22 mmol, 1 equiv.) and 3,4-dimethylbenzaldehyde (4.88 mmol, 4 equiv.). Purification by flash column chromatography eluting with hexanes/EtOAc (9:1) provided **33** 86.4 mg (33%) as a clear oil.

^{1}H NMR (400 MHz, $CDCl_3$) δ_H 7.13 (s, 1H), 7.07 (t, *J* = 5.7 Hz, 2H), 6.34 (d, *J* = 15.8 Hz, 1H), 6.11 (dt, *J* = 15.5, 6.9 Hz, 1H), 2.48 (t, *J* = 7.4 Hz, 2H), 2.25 (d, *J* = 5.7 Hz, 6H), 2.22 (q, *J* = 7.2, 6.8 Hz, 2H), 2.14 (s, 3H), 1.77 (p, *J* = 7.4 Hz, 2H).

^{13}C NMR (126 MHz, $CDCl_3$) δ_C 208.9, 136.6, 135.4, 135.2, 130.6, 129.8, 128.5, 127.2, 123.4, 42.9, 32.3, 30.0, 23.3, 19.8, 19.5.

ν_{max} (FTIR)/cm^{-1}: 3012, 2921, 1712, 1501, 1448, 1354, 1154, 965, 883, 799.

***m/z* (ESI+) HRMS [M+Na] $C_{15}H_{20}O^+$:** formula found 239.1411, cald. 239.1412.

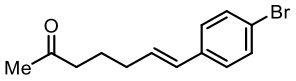

(*E*)-7-(4-bromophenyl)hept-6-en-2-one (34): The metathesis was performed according to general procedure, by subjecting 1-methylcyclopentene (3.7 mmol, 1 equiv.) and 4-bromo-benzaldehyde (14.6 mmol, 4 equiv.). Purification by flash column chromatography eluting with hexanes/EtOAc (9:1) provided **34** 269.2 mg (28%) as an off-white solid.

^{1}H NMR (700 MHz; $CDCl_3$) δ_H 7.41 (d, *J* = 8.4 Hz, 2H), 7.19 (d, *J* = 8.4 Hz, 2H), 6.32 (d, *J* = 15.9 Hz, 1H), 6.19 – 6.13 (m, 1H), 2.47 (t, *J* = 7.3 Hz, 2H), 2.21 (q, *J* = 7.2 Hz, 2H), 2.14 (s, 3H), 1.76 (p, *J* = 7.3 Hz, 2H).

^{13}C NMR (175 MHz; $CDCl_3$) δ_C 208.9, 136.7, 131.7, 130.9, 129.7, 127.7, 120.8, 43.0, 32.4, 30.2, 23.2.

***ν*$_{max}$ (FTIR)/cm^{-1}:** 2939, 2882, 2835, 1707, 1489, 1354, 1160, 1071, 979, 815.

***m/z* (ESI+) HRMS [M+Na] $C_{13}H_{15}BrO^+$:** formula found 289.0207, cald. 289.0198.

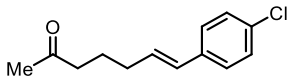

(*E*)-7-(4-chlorophenyl)hept-6-en-2-one (35): The metathesis was performed according to general procedure, by subjecting 1-methylcyclopentene (3.7 mmol, 1 equiv.) and 4-chlorobenzaldehyde (14.6 mmol, 4 equiv.). Purification by flash column chromatography eluting with hexanes/EtOAc (9:1) provided **35** 250.0 mg (31%) as a clear oil.

^{1}H NMR (700 MHz; $CDCl_3$) δ_H 7.26 (m, 4H), 6.34 (d, *J* = 15.8 Hz, 1H), 6.18 – 6.12 (m, 1H), 2.48 (t, *J* = 7.3 Hz, 2H), 2.22 (q, *J* = 7.2 Hz, 2H), 2.15 (s, 3H), 1.77 (p, *J* = 7.3 Hz, 2H).

^{13}C NMR (175 MHz; $CDCl_3$) δ_C 208.9, 136.2, 132.7, 130.7, 129.6, 128.8, 127.3, 43.0, 32.4, 30.2, 23.3.

***ν*$_{max}$ (FTIR)/cm^{-1}:** 2939, 2882, 2833, 1708, 1493, 1354, 1159, 1089, 979, 817.

***m/z* (ESI+) HRMS [M+Na] $C_{13}H_{15}ClO^+$:** formula found 245.0707, cald. 245.0704.

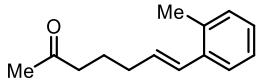

(*E*)-7-(o-tolyl)hept-6-en-2-one (36): The metathesis was performed according to general procedure, by subjecting 1-methylcyclopentene (1.22 mmol, 1 equiv.) and 2-methylbenzaldehyde

(4.88 mmol, 4 equiv.). Purification by flash column chromatography eluting with hexanes/EtOAc (9:1) provided **36** 75.5 mg (30%) as a clear oil.

^{1}H NMR (400 MHz, $CDCl_3$) δ_H 7.43 – 7.39 (m, 1H), 7.18 – 7.12 (m, 3H), 6.59 (dt, *J* = 15.7, 1.6 Hz, 1H), 6.04 (dt, *J* = 15.6, 7.0 Hz, 1H), 2.50 (t, *J* = 7.4 Hz, 2H), 2.34 (s, 3H), 2.26 (qd, *J* = 7.2, 1.5 Hz, 2H), 2.16 (s, 3H), 1.79 (p, *J* = 7.3 Hz, 2H).

^{13}C NMR (126 MHz, $CDCl_3$) δ_C 208.9, 136.7, 134.9, 131.2, 130.2, 128.5, 126.9, 126.0, 125.4, 42.9, 32.6, 30.0, 23.3, 19.8.

***ν*max (FTIR)/cm^{-1}:** 3018, 2934, 1712, 1597, 1459, 1335, 1155, 1108, 965, 746.

***m/z* (ESI+) HRMS [M+Na] $C_{14}H_{18}O^+$:** formula found 225.1244, cald. 225.1256.

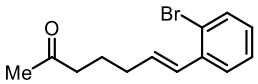

(*E*)-7-(2-bromophenyl)hept-6-en-2-one (37): The metathesis was performed according to general procedure, by subjecting 1-methylcyclopentene (1.22 mmol, 1 equiv.) and 2-bromobenzaldehyde (4.88 mmol, 4 equiv.). Purification by flash column chromatography eluting with hexanes/EtOAc (9:1) provided **37** 50.0 mg (15%) as a clear oil.

^{1}H NMR (400 MHz, $CDCl_3$) δ_H 7.51 (dd, *J* = 27.2, 7.9 Hz, 2H), 7.25 (t, *J* = 7.7 Hz, 1H), 7.08 (t, *J* = 7.7 Hz, 1H), 6.72 (d, *J* = 15.7 Hz, 1H), 6.15 – 6.07 (m, 1H), 2.51 (t, *J* = 7.3 Hz, 2H), 2.28 (q, *J* = 7.2 Hz, 2H), 2.16 (s, 3H), 1.80 (p, *J* = 7.2 Hz, 2H).

^{13}C NMR (126 MHz, $CDCl_3$) δ_C 208.7, 137.4, 133.0, 132.9, 132.9, 132.8, 132.8, 129.6, 129.5, 128.3, 127.4, 123.1, 42.7, 32.4, 30.1, 30.0, 22.9.

***ν*max (FTIR)/cm^{-1}:** 2932, 1711, 1465, 1435, 1355, 1155, 1020, 964, 747, 667.

***m/z* (ESI+) HRMS [M+Na] $C_{13}H_{15}BrO^+$:** formula found 289.0198, cald. 289.0204.

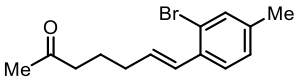

(*E*)-7-(2-bromo-4-methylphenyl)hept-6-en-2-one (38): The metathesis was performed according to general procedure, by subjecting 1-methylcyclopentene (0.61 mmol, 1 equiv.) and 2-bromo-4-methyl-benzaldehyde (2.67 mmol, 4 equiv.). Purification by flash column chromatography eluting with hexanes/EtOAc (9:1) provided **38** 66.6 mg mg (39%) as a pale yellow solid.

^{1}H NMR (400 MHz; $CDCl_3$) δ_H 7.36 (d, *J* = 4.4 Hz, 2H), 7.06 (d, *J* = 7.9 Hz, 1H), 6.68 (d, *J* = 15.8 Hz, 1H), 6.06 (dt, *J* = 14.4, 7.1 Hz, 1H), 2.50 (t, *J* = 7.3 Hz, 2H), 2.31 (s, 3H), 2.26 (q, *J* = 7.2 Hz, 2H), 2.16 (s, 3H), 1.79 (p, *J* = 7.2 Hz, 2H).

^{13}C NMR (135 MHz, $CDCl_3$) δ_C 208.8, 138.5, 134.5, 133.2, 132.0, 129.4, 128.3, 126.5, 122.9, 42.8, 32.4, 30.1, 23.1, 20.7.

***ν*max (FTIR)/cm^{-1}:** 2921, 2361, 2336, 1714, 1652, 1602, 1521, 1357, 1238, 988.

***m/z* (ESI+) HRMS [M+Na] $C_{14}H_{17}BrO^+$:** formula found 303.0355, cald. 303.0355.

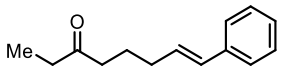

(*E*)-8-phenyloct-7-en-3-one (39): The metathesis was performed according to general procedure, by subjecting 1-ethylcyclopentene.[16] (0.83 mmol, 1 equiv.) and benzaldehyde (3.33 mmol, 4 equiv.). Purification by flash column chromatography eluting with hexanes/EtOAc (9:1) provided **39** 30.0 mg (18%) as a clear liquid.

^{1}H NMR (400 MHz; $CDCl_3$) δ_H 7.44 – 7.28 (m, 4H), 7.21 (t, *J* = 7.2 Hz, 1H), 6.39 (d, *J* = 15.8 Hz, 1H), 6.24 – 6.11 (m, 1H), 2.55 – 2.38 (m, 4H), 2.23 (q, *J* = 7.1 Hz, 2H), 1.79 (p, *J* = 7.3 Hz, 2H), 1.14 – 0.94 (m, 3H).

^{13}C NMR (135 MHz, $CDCl_3$) δ_C 211.5, 137.6, 130.6, 129.9, 128.5, 127.0, 125.9, 41.5, 36.0, 23.4, 23.3, 7.8.

***ν*max (FTIR)/cm^{-1}:** 2935, 1710, 1597, 1493, 1448, 1374, 1203, 1071, 1026, 964.

***m/z* (ESI+) HRMS [M+Na] $C_{14}H_{18}O^+$:** formula found 225.1250, cald. 225.1254.

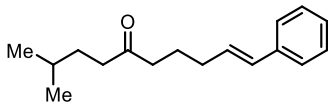

(*E*)-2-methyl-10-phenyldec-9-en-5-one (40): The metathesis was performed according to general procedure, by subjecting **40b** (0.1 mmol, 1 equiv.) and benzaldehyde (0.4 mmol, 4 equiv.). Purification by flash column chromatography eluting with hexanes/EtOAc (9:1) provided **40** 5.2 mg (21%) as a clear liquid.

^{1}H NMR (400 MHz; $CDCl_3$) δ_H 7.35 (dd, J = 6.9, 1.8 Hz, 2H), 7.33 – 7.29 (m, 2H), 7.23 – 7.19 (m, 1H), 6.39 (dd, J = 15.8, 1.9 Hz, 1H), 6.22 – 6.14 (m, 1H), 2.47 (td, J = 7.4, 1.8 Hz, 2H), 2.40

(td, J = 7.9, 1.8 Hz, 2H), 2.23 (q, J = 7.0 Hz, 2H), 1.78 (pd, J = 7.8, 1.7 Hz, 2H), 1.53 (dtd, J = 13.4, 6.7, 1.7 Hz, 1H), 1.49 – 1.43 (m, 2H), 0.88 (dd, J = 6.6, 1.4 Hz, 6H).

^{13}C NMR (135 MHz, $CDCl_3$) δ_C 211.4, 137.5, 130.6, 129.9, 128.5, 127.0, 125.9, 41.9, 41.0, 32.6, 32.4, 27.7, 23.3, 22.3.

***ν*max (FTIR)/cm^{-1}:** 2995, 1698, 1596, 1454, 1309, 1202, 1166, 826, 742, 686.

***m/z* (ESI+) HRMS [M+] $C_{17}H_{24}O^+$:** formula found 244.1800, cald. 244.1827.

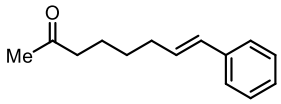

(*E*)-8-phenyloct-7-en-2-one (41): The metathesis was performed according to general procedure, by subjecting 1-methylcyclohexene (0.83 mmol, 1 equiv.) and benzaldehyde (3.33 mmol, 4 equiv.). Purification by flash column chromatography eluting with hexanes/EtOAc (9:1) provided **41** 23.2 mg (18%) as a clear liquid.

^{1}H NMR (400 MHz; $CDCl_3$) δ_H 7.34 (d, *J* = 7.6 Hz, 2H), 7.30 (t, *J* = 7.6 Hz, 2H), 7.21 (d, *J* = 7.2 Hz, 1H), 6.39 (d, *J* = 15.8 Hz, 1H), 6.21 (m, 1H), 2.47 (t, *J* = 7.4 Hz, 2H), 2.23 (q, *J* = 7.2 Hz, 2H), 2.15 (s, 3H), 1.68 – 1.60 (m, 2H), 1.49 (dt, *J* = 14.9, 7.5 Hz, 2H).

^{13}C NMR (135 MHz, $CDCl_3$) δ_C 209.0, 137.7, 130.4, 130.2, 128.5, 126.9, 125.9, 43.6, 32.8, 29.9, 28.9, 23.4.

***ν*max (FTIR)/cm^{-1}:** 2927, 2361, 1844, 1792, 1772, 1562, 1533, 1436, 1419, 1033.

***m/z* (ESI+) HRMS [M+Na] $C_{14}H_{18}O^+$:** formula found 225.1257, cald. 224.1250.

Aldehyde Synthesis

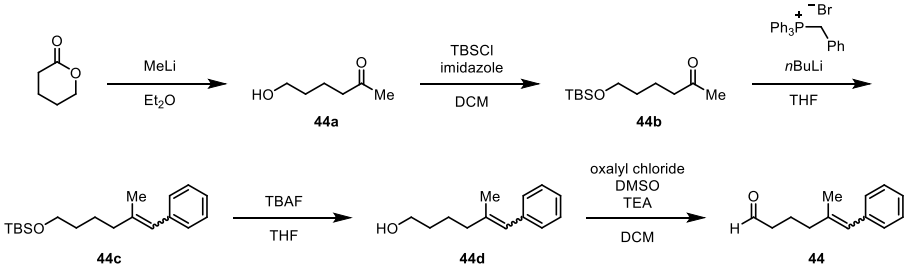

6-hydroxyhexan-2-one (44a): δ-veralactone (29.97 mmol, 1 equiv.) was dissolved in Et_2O (0.3 M) under N_2 and cooled to -78 °C. A solution of MeLi (32.96 mmol, 1.1 equiv., 1.6 M in Et_2O) was added dropwise via syringe and the solution was stirred for 1 hour. The reaction was quenched

with saturated aqueous NH_4Cl and brought to 25 °C. The organic layer was removed and the aqueous phase was washed with EtOAc. The combined organic layers were washed with brine and dried over Na_2SO_4. The product was concentrated under reduced pressure to give **44a** 3.10 g (89%) as an oil, which was carried through crude to the next step.

6-((*tert*-butyldimethylsilyl)oxy)hexan-2-one (44b): A solution of the crude alcohol **44a** was prepared in DCM (0.5 M) at 0 °C. TBSCl (14.20 mmol, 1.1 equiv.) and imidazole (13.56 mmol, 1.05 equiv.) were added and the solution was warmed to 25 °C. Once at 25 °C, the reaction mixture stirred for 12 hours before being diluted with DCM and quenched with water. The layers were separated and the aqueous phase was washed with DCM. The combined organic layers were washed with brine and the mixture was dried over Na_2SO_4. The product was concentrated under reduced pressure and purified by column chromatography eluting with hexanes/EtOAc (9:1) to give **44b** 2.01 g (68%) as a clear oil, which was carried through crude to the next step.

T*ert*-butyldimethyl((5-methyl-6-phenylhex-5-en-1-yl)oxy)silane (44c): Benzyltriphenylphosphine bromide (8.68 mmol, 2 equiv.) was dissolved in THF (0.6 M) and cooled to -78 °C. nBuLi (8.68 mmol, 2 equiv., 2.5 M in hexanes) was added dropwise via syringe and the solution was allowed to stir for 15 minutes at that temperature before being allowed to warm to 25 °C over 30 minutes. The reaction mixture was cooled to 0 °C and a solution of **44b** in THF (0.8 M) was added via addition funnel over 10 minutes. The solution was heated to reflux and stirred overnight. The mixture was cooled to 0 °C prior to quench with saturated aqueous NH_4Cl. The organic layer was separated and the aqueous phase was washed with Et_2O. The combined organic layers were washed with brine, the off-white solid was filtered off, and the eluent was dried with Na_2SO_4. The product was concentrated under reduced pressure to a clear oil and purified by column chromatography eluting with hexanes/EtOAc (19:1) to give **44c** 1.02 g (77%) as a mixture of inseparable *E*/*Z* isomers, which was carried through crude to the next step.

5-methyl-6-phenylhex-5-en-1-ol (44d): A solution of TBAF (1.97 mmol, 1.2 equiv.) in THF (1 M) was added to a solution of **44c** in THF (0.3 M) at 0 °C. The reaction was allowed to warm to 25 °C and stirred overnight. The reaction was quenched with saturated aqueous NH_4Cl. The organic layer was separated and the aqueous phase was washed with EtOAc. The combined organic layers were washed with brine and the mixture was dried over Na_2SO_4. The product was concentrated under reduced pressure and purified by column chromatography eluting with

hexanes/EtOAc (7:3) to give **44d** 241.0 mg (77%) as a mixture of *E*/*Z* isomers, which was carried through crude to the next step.

5-methyl-6-phenylhex-5-enal (44): Oxalyl chloride (3.47 mmol, 3 equiv.) was added to DCM (0.1 M) at -78 °C. DMSO (6.94 mmol, 6 equiv.) was added and the solution was stirred for 15 minutes. **44d** dissolved in DCM was added slowly via syringe and the mixture was stirred for 1 hour at -78 °C. TEA (11.56 mmol, 10 equiv.) was added and the reaction was allowed to warm to 25 °C. After 4 hours, the reaction was quenched with a minimal amount of 10% aqueous NH_4Cl. The organic layer was removed and the aqueous phase was washed with DCM. The combined organic layers were washed with brine and the mixture was dried over Na_2SO_4. The product was concentrated under reduced pressure and purified by column chromatography eluting with hexanes/EtOAc (9:1) to give **44** 132.3 mg (61%) as a mixture of *E/Z* isomers.

(*E*) isomer: ^{1}H NMR (400 MHz; $CDCl_3$) δ_H ^{1}H NMR (500 MHz, cdcl$_3$) δ 9.73 (s, 5H), 7.33 (m, 2H), 7.25 – 7.12 (m, 3H), 6.29 (s, 1H), 2.50 (t, *J* = 7.2 Hz, 1H), 2.41 (t, *J* = 7.2 Hz, 1H), 2.30 – 2.26 (m, 1H), 2.23 (t, *J* = 7.5 Hz, 1H), 1.91 – 1.86 (m, 1H), 1.84 – 1.79 (m, 4H).

^{13}C NMR (135 MHz, $CDCl_3$) δ_C 202.2, 137.7, 128.5, 128.0, 126.1, 125.9, 43.2, 31.6, 23.7, 20.3.

(*Z*) isomer: ^{1}H NMR (400 MHz; $CDCl_3$) δ_H 9.82 (s, 1H), 7.33 (m, 2H), 7.25 – 7.12 (m, 3H), 6.35 (s, 6H), 2.50 (t, *J* = 7.2 Hz, 1H), 2.41 (t, *J* = 7.2 Hz, 1H), 2.30 – 2.26 (m, 1H), 2.23 (t, *J* = 7.5 Hz, 1H), 1.91 – 1.86 (m, 51H), 1.84 – 1.79 (m, 1H).

^{13}C NMR (135 MHz, $CDCl_3$) δ_C 202.4, 138.2, 128.8, 128.1, 126.6, 126.0, 43.5, 39.8, 23.7, 17.5.

***ν*$_{max}$ (FTIR)/cm^{-1}:** 3022, 2934, 2719, 1722, 1598, 1492, 1441, 1073, 742, 698.

***m/z* (ESI+) HRMS [M+Na] $C_{13}H_{16}O^+$:** formula found 211.1086, cald. 211.1093.

Metathesis Byproduct Characterization

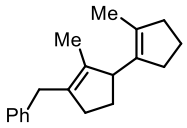

3'-benzyl-2,2'-dimethyl-[1,1'-bi(cyclopentane)]-1,2'-diene (46): The metathesis was performed according to general procedure, by subjecting 1-methylcyclopentene (12.2 mmol, 1 equiv.) and benzaldehyde (48.7 mmol, 4 equiv.). Purification by flash column chromatography eluting with hexanes/EtOAc (9:1) provided **46** 324 mg (20%) as a clear liquid.

^{1}H NMR (400 MHz; $CDCl_3$) δ_H 7.04 (s, 2H), 6.98 – 6.90 (m, 3H), 3.37 (s, 1H), 3.21 (d, *J* = 14.6 Hz, 1H), 3.14 (d, *J* = 14.7 Hz, 1H), 2.10 (dt, *J* = 26.1, 6.8 Hz, 2H), 2.04 – 1.94 (m, 3H), 1.85 – 1.78 (m, 1H), 1.68 (ddd, *J* = 14.2, 9.1, 5.5 Hz, 1H), 1.53 (dt, *J* = 30.3, 11.8 Hz, 3H), 1.46 (s, 3H), 1.39 – 1.32 (m, 4H).

^{13}C NMR (135 MHz, $CDCl_3$) δ_C 140.7, 137.6, 134.6, 134.5, 131.7, 128.5, 128.2, 125.6, 48.6, 38.6, 35.1, 35.0, 31.9, 27.0, 21.8, 13.8, 12.4.

***ν*$_{max}$ (FTIR)/cm^{-1}:** 2922, 2839, 1601, 1493, 1452, 1377, 1189, 1077, 1029, 908.

***m/z* (ESI+) HRMS [M+] $C_{19}H_{24}^+$:** formula found 252.1884, cald. 252.1878.

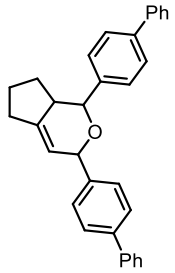

1,3-di([1,1'-biphenyl]-4-yl)-1,3,5,6,7,7a-hexahydrocyclopenta[c]pyran (S47): The metathesis was performed according to general procedure, by subjecting 1-methylcyclopentene (12.2 mmol, 1 equiv) and benzaldehyde (48.7 mmol, 4 equiv). Purification by flash column chromatography eluting with hexanes/EtOAc (9:1) provided **S47** 52 mg (10%) as a clear liquid.

^{1}H NMR (400 MHz; $CDCl_3$) δ_H 7.60 (dd, *J* = 13.9, 5.4 Hz, 8H), 7.55 (t, *J* = 8.6 Hz, 4H), 7.44 (dd, *J* = 13.0, 7.5 Hz, 4H), 7.36 – 7.33 (m, 2H), 5.58 (s, 1H), 4.55 (dd, *J* = 11.4, 2.3 Hz, 1H), 4.21 (d, *J* = 10.0 Hz, 1H), 2.87 (d, *J* = 8.8 Hz, 1H), 2.82 (dd, *J* = 13.8, 2.5 Hz, 1H), 2.43 (dd, *J* = 25.0, 10.9 Hz, 2H), 1.97 – 1.93 (m, 1H), 1.62 – 1.58 (m, 1H), 1.27 – 1.19 (m, 1H).

^{13}C NMR (135 MHz, $CDCl_3$) δ_C 141.70, 141.67, 141.1, 140.59, 140.56, 140.4, 138.7, 128.6, 127.4, 127.3, 127.2, 127.1, 127.0, 126.91, 126.88, 126.8, 126.4, 123.0, 87.4, 79.8, 51.1, 37.5, 31.4, 26.2;

***ν*$_{max}$ (FTIR)/cm^{-1}:** 2902, 2839, 1701, 1593, 1462, 1377, 1229, 1177, 1129, 1008.

***m/z* (ESI+) HRMS [M+] $C_{32}H_{28}^+$:** formula found 428.5700, cald. 428.5750.

Note: **S45** was isolated and fully characterized above, while **47** could not be isolated, but characteristic ^{1}H NMR and ^{13}C NMR shifts match **S47.**

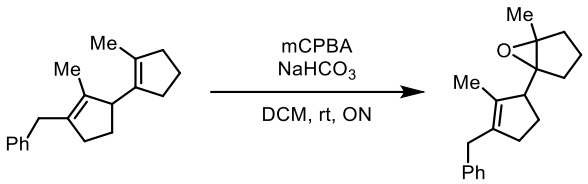

1-(3-benzyl-2-methylcyclopent-2-en-1-yl)-5-methyl-6-oxabicyclo[3.1.0]hexane (48): The epoxidation was performed by subjecting 3'-benzyl-2,2'-dimethyl-[1,1'-bi(cyclopentane)]-1,2'-diene (0.18 mmol, 1 equiv.) to mCPBA (0.23 mmol, 1.3 equiv.) and $NaHCO_3$ (0.32 mmol, 1.6 equiv.) in DCM at 25 °C for 12 hours. The reaction mixture was quenched by the addition of water (10 mL) and then extraction with DCM (3 x 20 mL) and dried with Na_2SO_4 and concentrated. Purification by flash column chromatography eluting with hexanes/EtOAc (9:1) provided **48** 20.0 mg (41.8%) as a clear liquid.

^{1}H NMR (400 MHz; $CDCl_3$) δ_H 7.28 (dd, *J* = 10.0, 3.7 Hz, 2H), 7.19 (t, *J* = 7.4 Hz, 1H), 7.14 (d, *J* = 7.1 Hz, 2H), 3.47 – 3.34 (m, 2H), 2.66 (s, 1H), 2.33 – 2.16 (m, 2H), 2.09 – 1.83 (m, 3H), 1.79 (dd, *J* = 12.8, 7.8 Hz, 1H), 1.65 (s, 3H), 1.64 – 1.59 (m, 1H), 1.48 – 1.42 (m, 4H), 1.42 – 1.26 (m, 3H).

^{13}C NMR (135 MHz, $CDCl_3$) δ_C 140.2, 137.3, 131.2, 128.4, 128.3, 125.8, 50.5, 34.93, 34.88, 33.1, 26.1, 25.2, 18.1, 16.3, 12.8.

***ν_{max}* (FTIR)/cm^{-1}:** 2922, 2839, 2041, 1493, 1452, 1264, 1188, 1077, 926, 854.

***m/z* (ESI+) HRMS [M+Na] $C_{19}H_{24}O^+$:** formula found 291.1726, cald. 291.1719.

2.5.5 NMR Spectra

Substrates

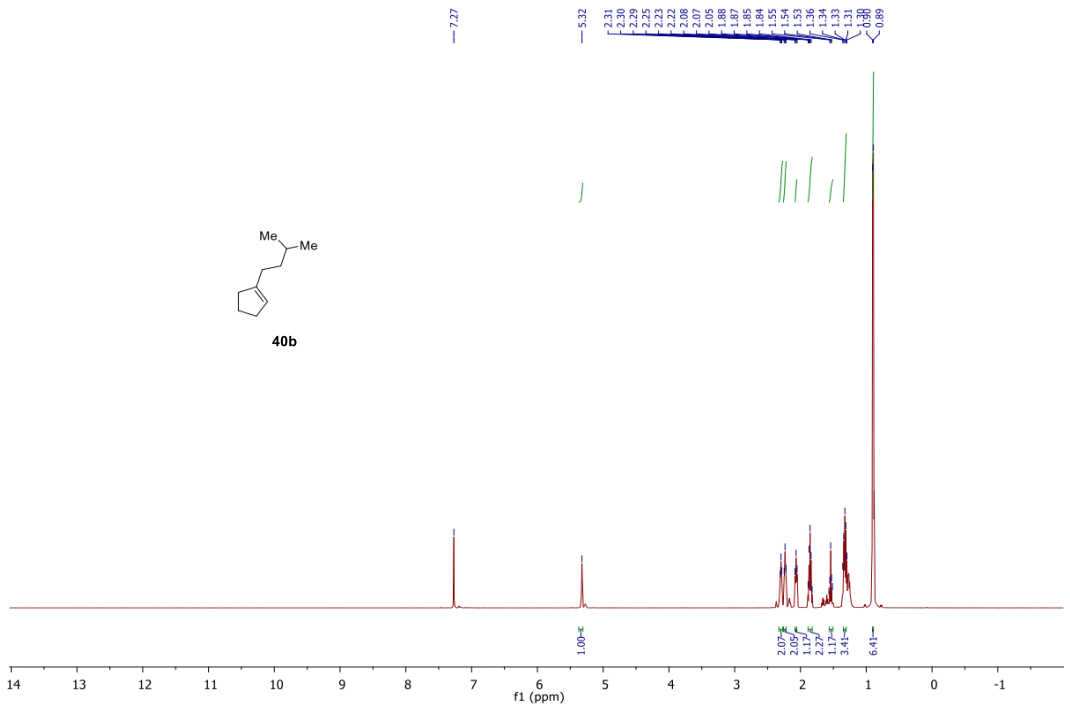

40b

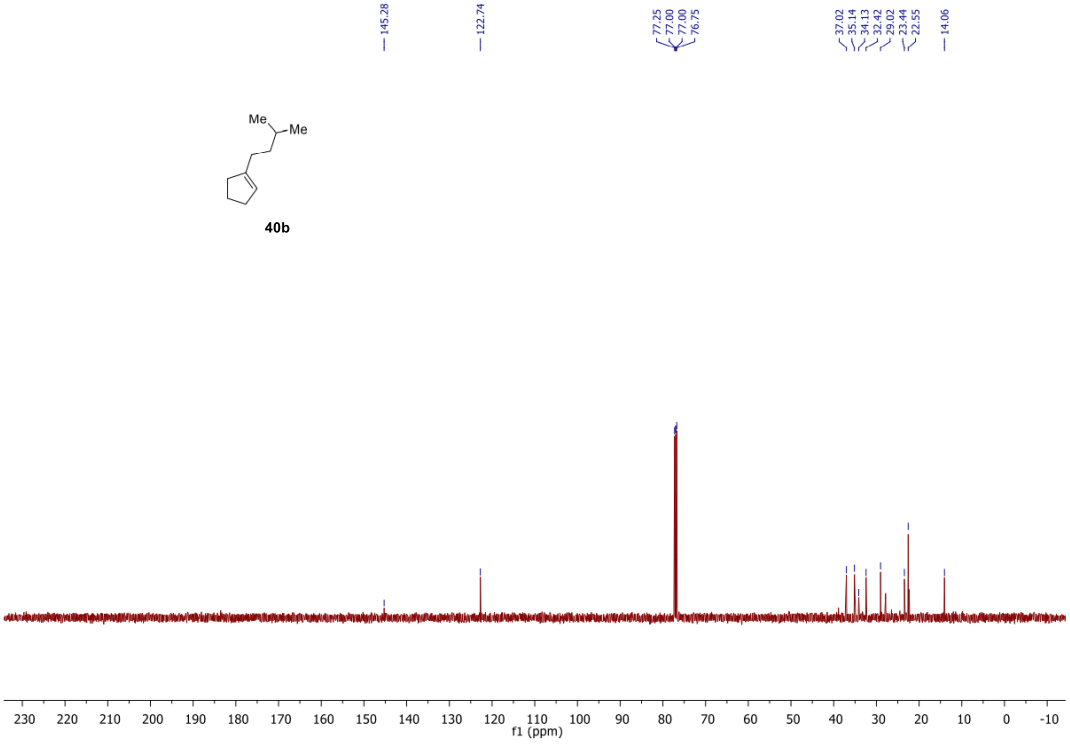

40b

Metathesis Products

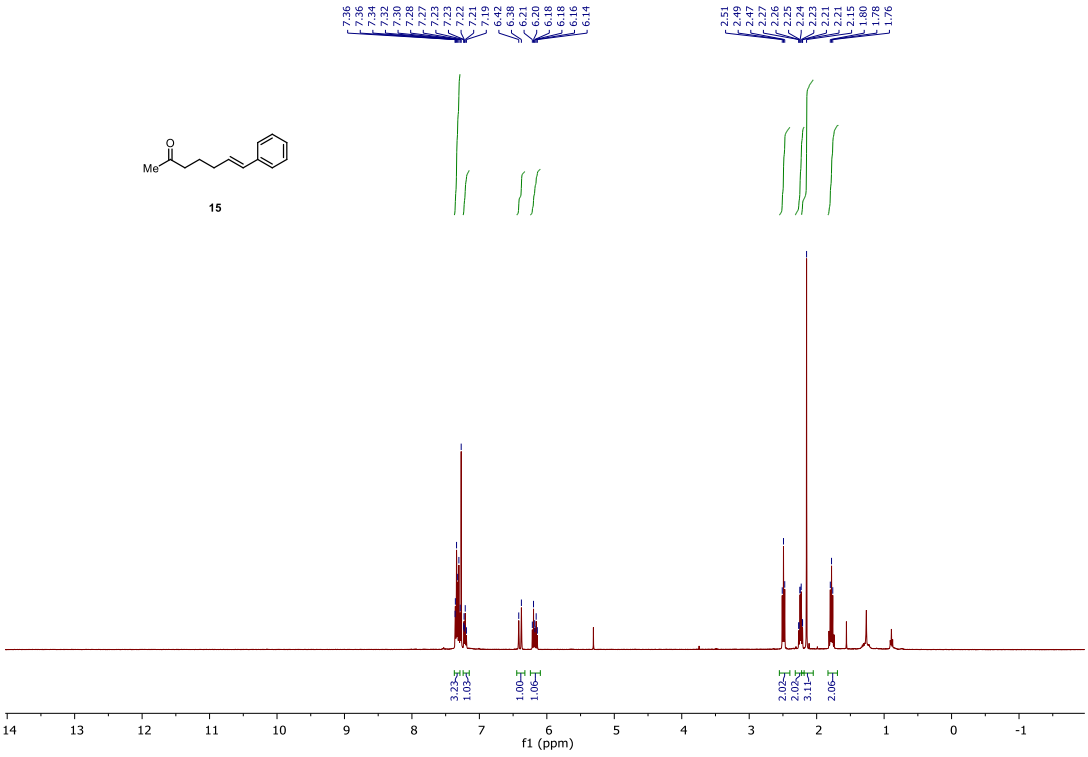

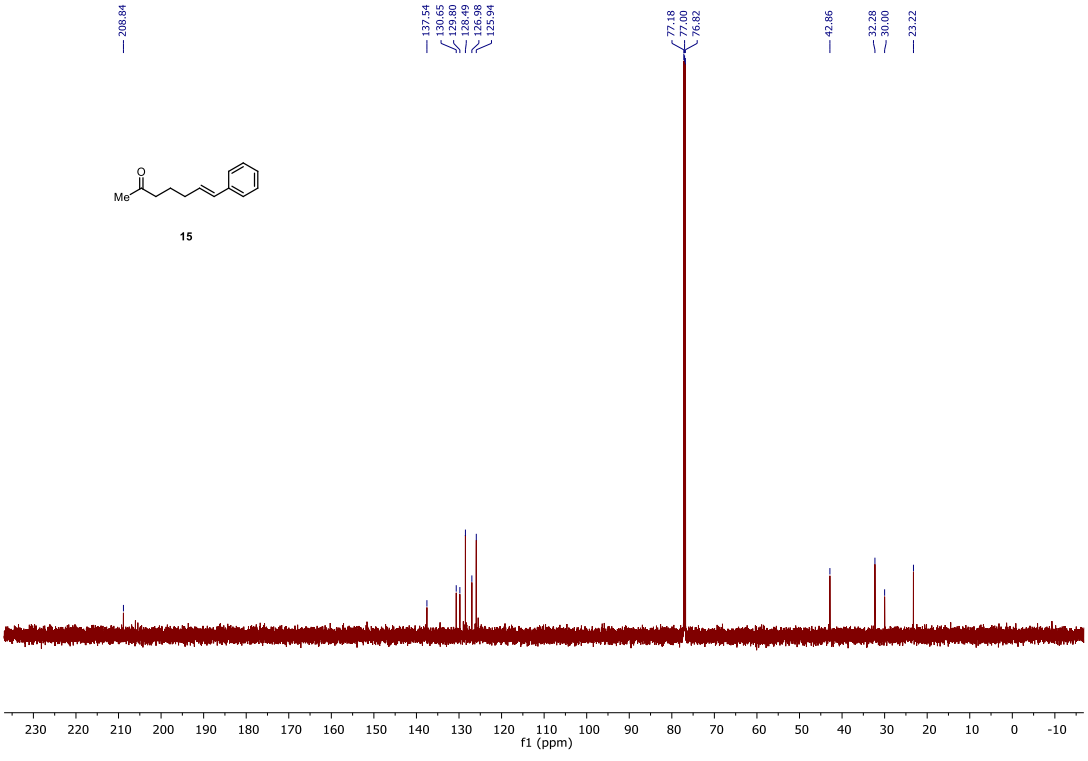

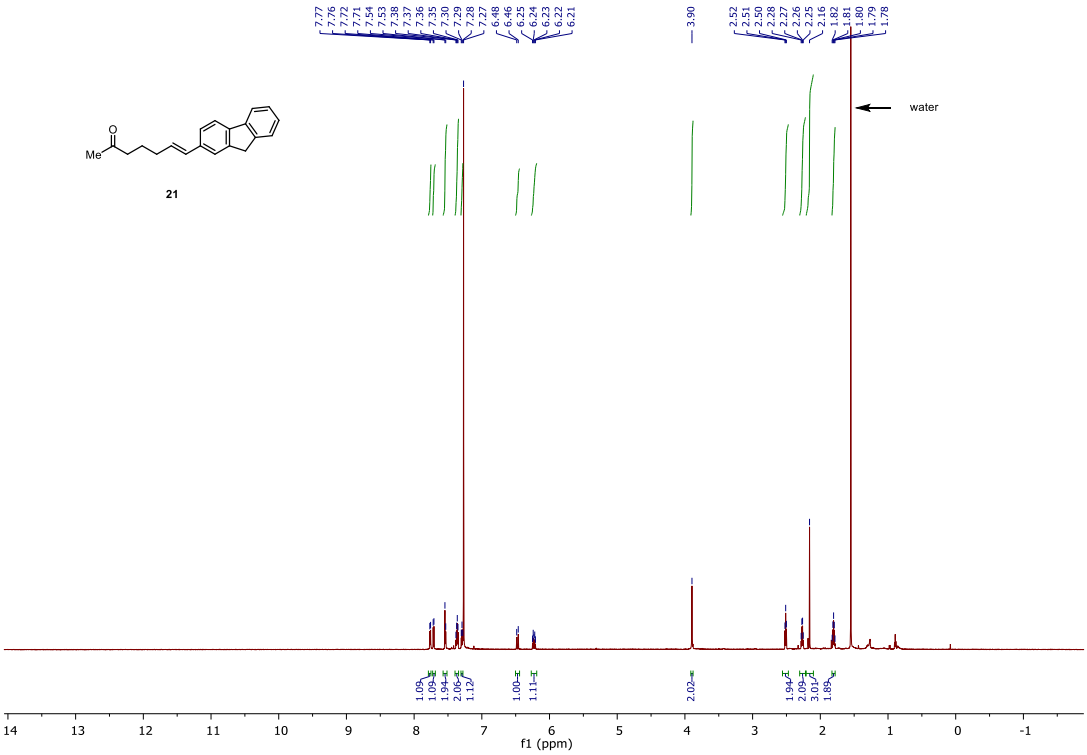
7.77
7.76
7.72
7.71
7.54
7.53
7.38
7.37
7.36
7.35
7.30
7.29
7.28
7.27
6.48
6.46
6.25
6.24
6.23
6.22
6.21
3.90
2.52
2.51
2.50
2.28
2.27
2.26
2.25
2.16
1.82
1.81
1.80
1.79
1.78
water
Me
O
21
1.09
1.09
1.94
2.06
1.12
1.00
1.11
2.02
1.94
2.09
3.01
1.85
14 13 12 11 10 9 8 7 6 5 4 3 2 1 0 -1
f1 (ppm)

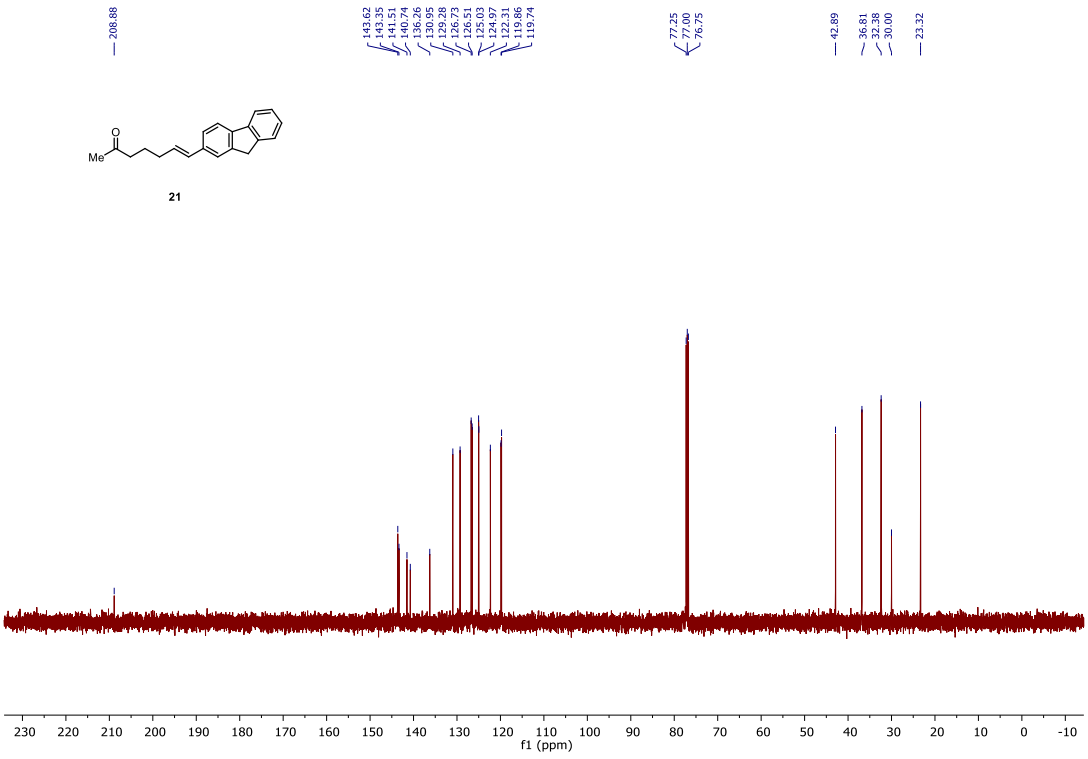
208.88
143.62
143.35
141.51
140.74
136.26
130.95
129.28
128.73
126.51
125.03
124.97
122.31
119.86
119.74
77.25
77.00
76.75
42.89
36.81
23.38
30.00
23.32
Me
O
21
230 220 210 200 190 180 170 160 150 140 130 120 110 100 90 80 70 60 50 40 30 20 10 0 -10
f1 (ppm)

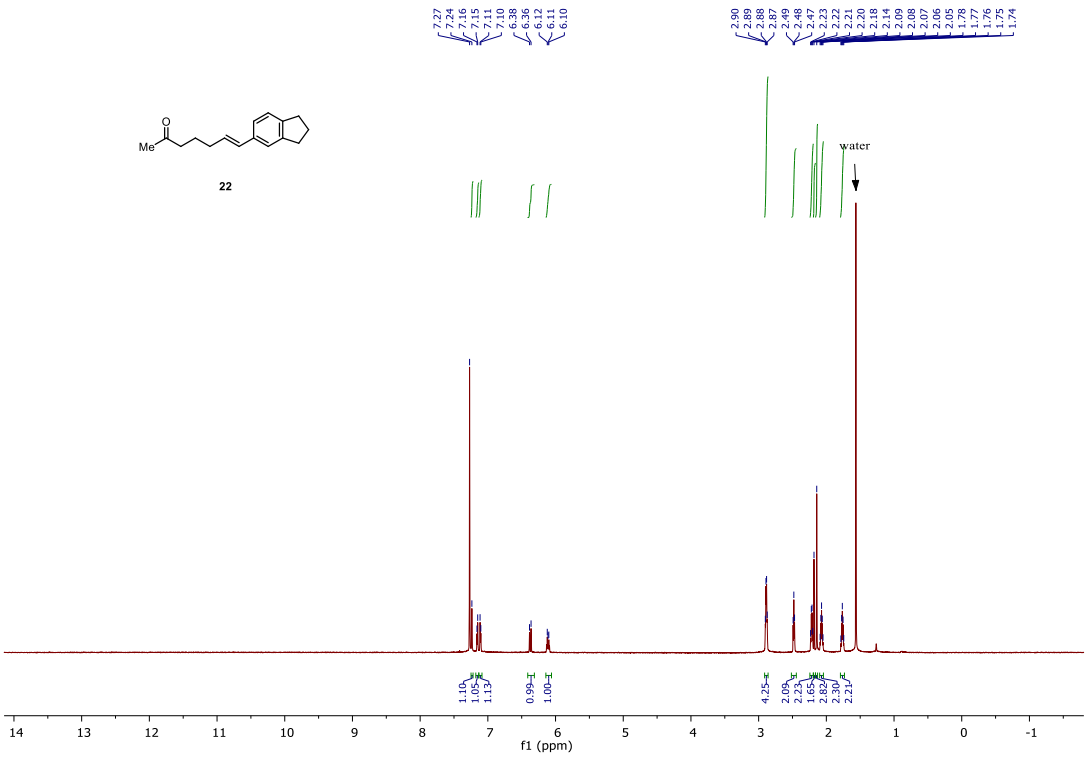
7.27
7.24
7.16
7.15
7.11
7.10
6.38
6.36
6.12
6.11
6.10
2.90
2.89
2.88
2.87
2.49
2.48
2.47
2.23
2.22
2.21
2.20
2.18
2.14
2.09
2.08
2.07
2.06
2.05
1.78
1.77
1.76
1.75
1.74
Me
O
22
water
1.10
1.05
1.13
0.99
1.00
4.25
2.05
2.23
1.65
2.82
2.30
2.21
14 13 12 11 10 9 8 7 6 5 4 3 2 1 0 -1
f1 (ppm)

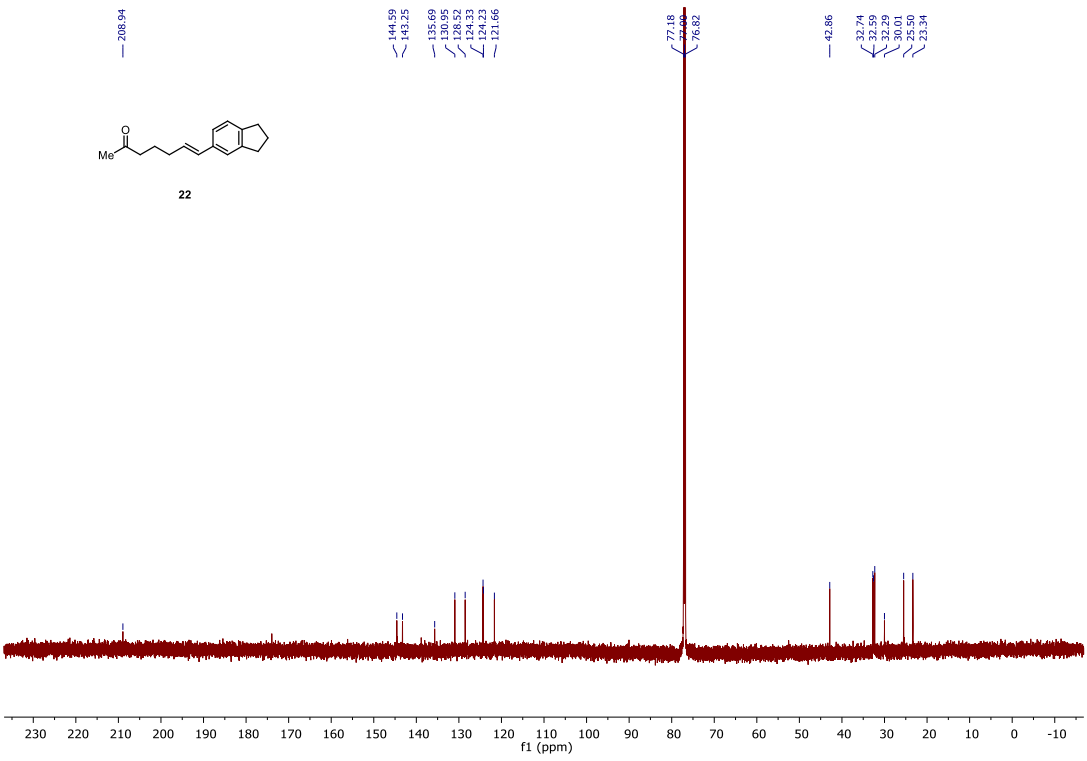
208.94
144.59
143.25
135.69
130.95
128.52
124.33
124.23
121.66
77.18
77.00
76.82
42.86
32.74
32.59
32.29
30.01
25.50
23.34
Me
O
22
230 220 210 200 190 180 170 160 150 140 130 120 110 100 90 80 70 60 50 40 30 20 10 0 -10
f1 (ppm)

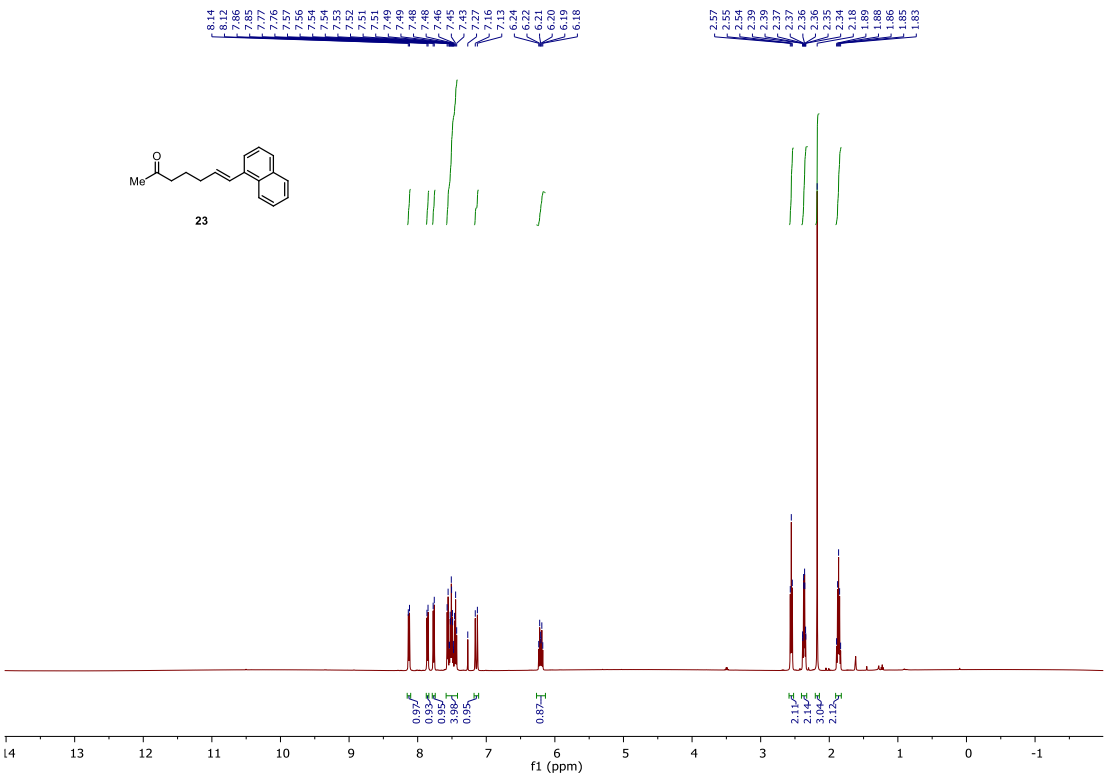
8.14
8.12
7.86
7.85
7.77
7.76
7.57
7.56
7.54
7.54
7.53
7.52
7.51
7.51
7.49
7.49
7.48
7.48
7.46
7.45
7.43
7.27
7.16
7.13
6.24
6.22
6.21
6.20
6.19
6.18
2.57
2.55
2.54
2.39
2.39
2.37
2.37
2.36
2.36
2.35
2.34
2.18
1.89
1.88
1.86
1.85
1.83
Me
O
23
0.97
0.93
0.95
0.98
0.95
0.87
2.11
2.14
3.04
2.12
f1 (ppm)

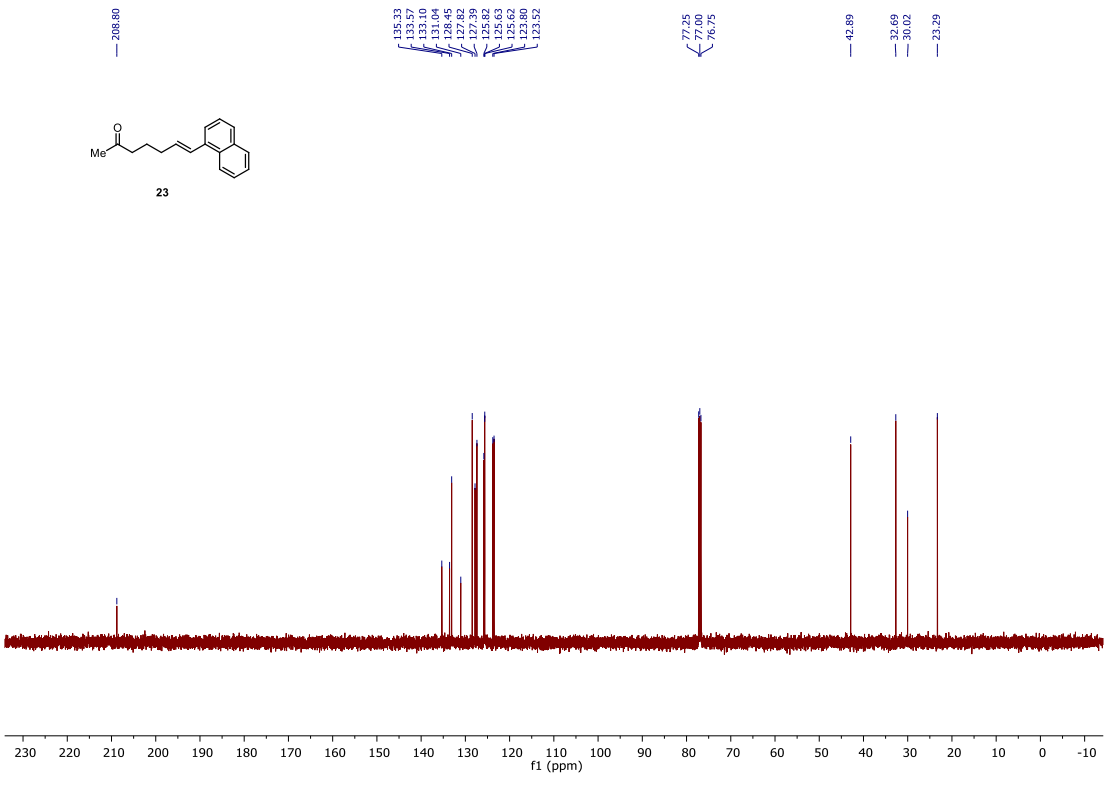
208.80
135.33
133.57
133.10
131.04
128.45
127.82
127.39
125.82
125.63
125.62
123.80
123.52
77.25
77.00
76.75
42.89
32.69
30.02
23.29
Me
O
23
f1 (ppm)

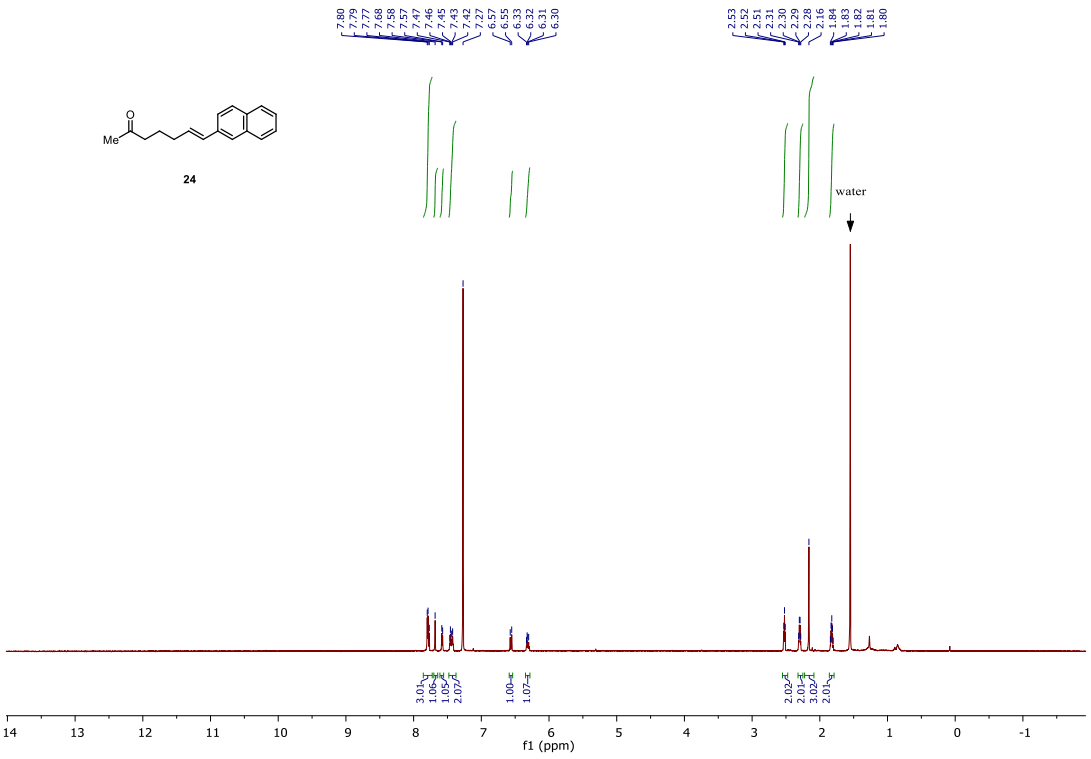
7.80
7.79
7.77
7.68
7.58
7.57
7.47
7.46
7.45
7.43
7.42
7.27
6.57
6.55
6.33
6.32
6.31
6.30
2.53
2.52
2.51
2.31
2.30
2.29
2.28
2.16
1.84
1.83
1.82
1.81
1.80
water
Me
O
24
3.01
1.06
1.05
2.07
1.00
1.07
2.02
2.01
3.02
2.01
f1 (ppm)

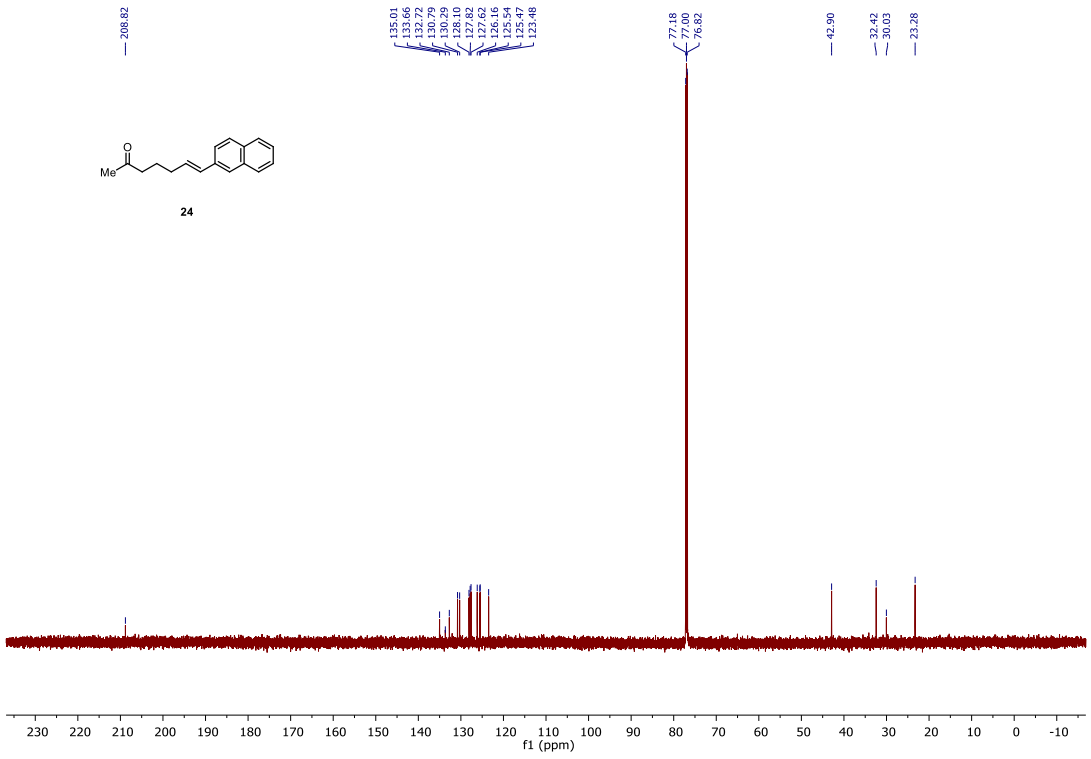
208.82
135.01
133.66
132.72
130.79
130.29
128.10
127.82
127.62
126.16
125.54
125.47
123.48
77.18
77.00
76.82
42.90
32.42
30.03
23.28
Me
O
24
f1 (ppm)

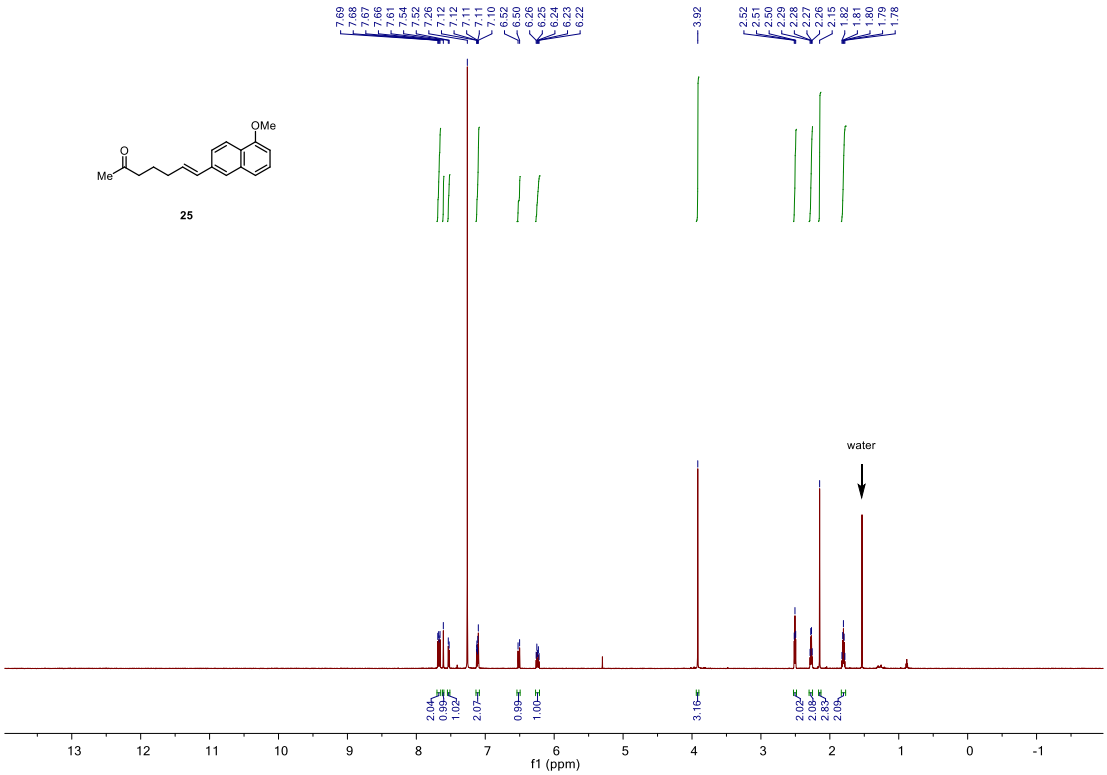
7.69
7.68
7.67
7.66
7.61
7.54
7.52
7.26
7.12
7.12
7.11
7.11
7.10
6.52
6.50
6.26
6.25
6.24
6.23
6.22
3.92
2.52
2.51
2.50
2.29
2.28
2.27
2.26
2.15
1.82
1.81
1.80
1.79
1.78
OMe
O
Me
25
water
2.04
0.99
1.02
2.07
0.99
1.00
3.16
2.02
2.08
2.83
2.09
13 12 11 10 9 8 7 6 5 4 3 2 1 0 -1
f1 (ppm)

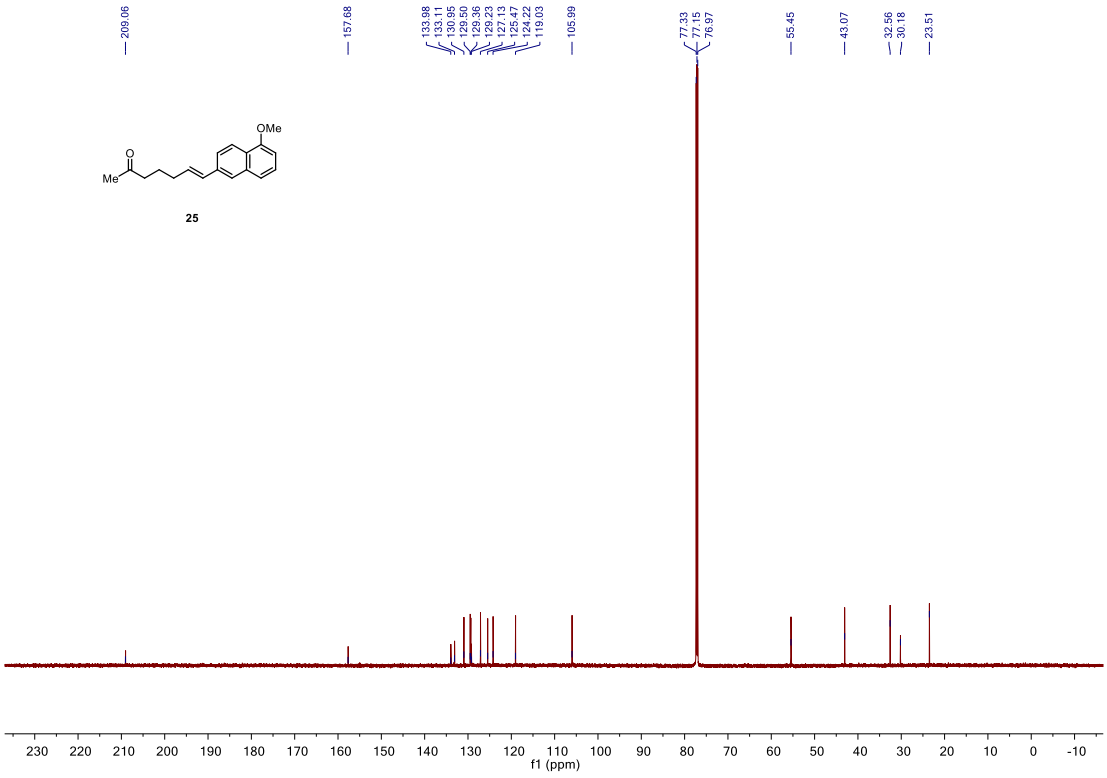
209.06
157.68
133.98
133.11
130.95
129.50
129.36
129.23
127.13
125.47
124.22
119.03
105.99
77.33
77.15
76.97
55.45
43.07
32.56
30.18
23.51
OMe
O
Me
25
230 220 210 200 190 180 170 160 150 140 130 120 110 100 90 80 70 60 50 40 30 20 10 0 -10
f1 (ppm)

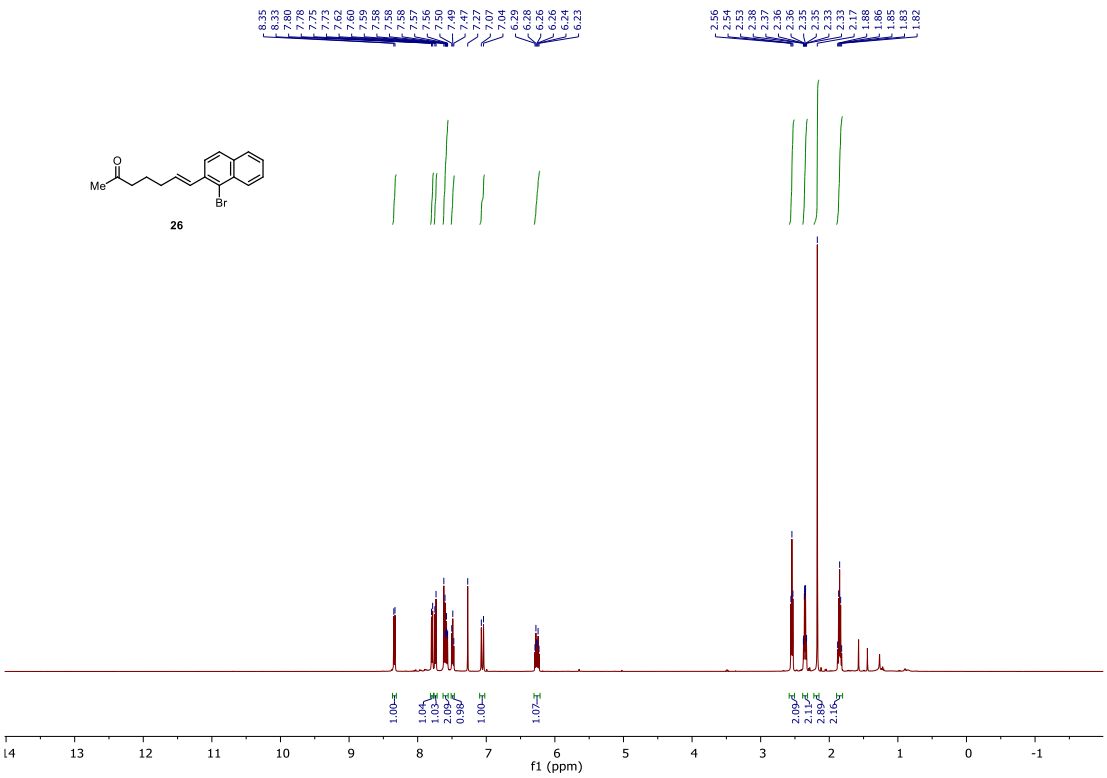
8.35
8.33
7.80
7.78
7.75
7.73
7.62
7.60
7.59
7.58
7.58
7.58
7.57
7.56
7.50
7.49
7.47
7.27
7.07
7.04
6.29
6.28
6.26
6.26
6.24
6.23
2.56
2.54
2.53
2.38
2.37
2.36
2.36
2.35
2.35
2.33
2.17
1.88
1.86
1.85
1.83
1.82
O
Me
Br
26
1.00
1.04
1.03
2.09
0.98
1.00
1.07
2.09
2.11
2.89
2.16
f1 (ppm)

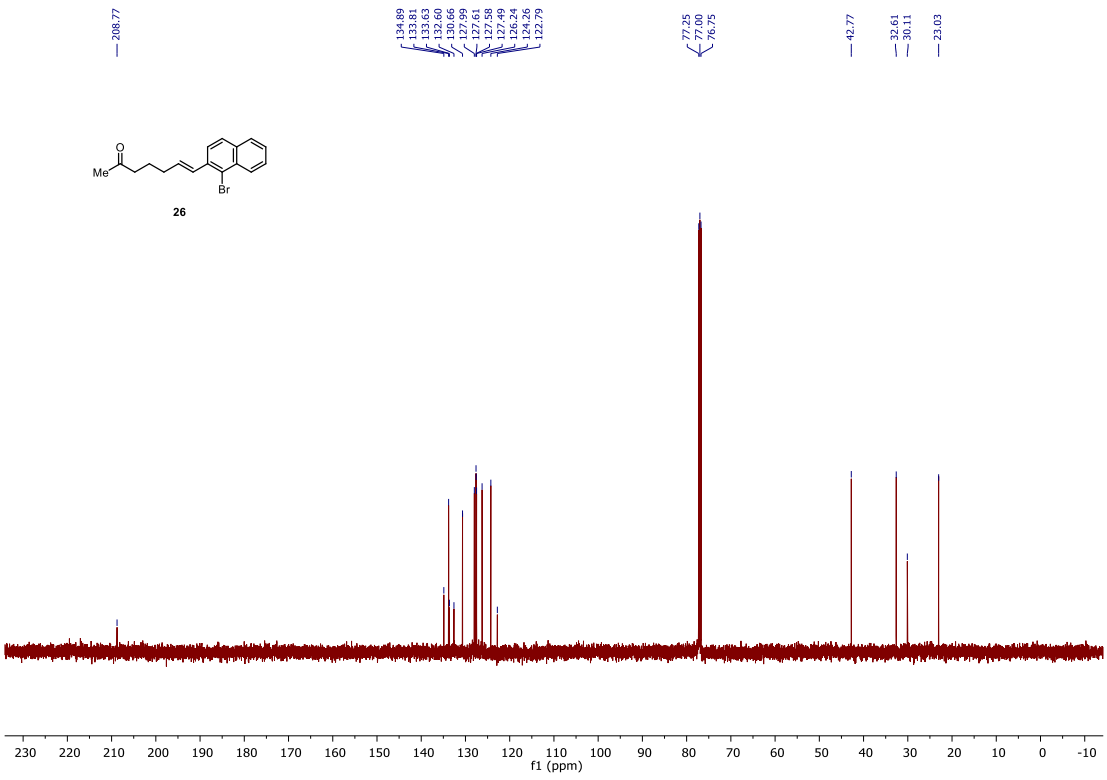
208.77
134.89
133.81
133.63
132.60
130.66
127.99
127.61
127.58
127.49
126.24
124.26
122.79
77.25
77.00
76.75
42.77
32.61
30.11
23.03
O
Me
Br
26
f1 (ppm)

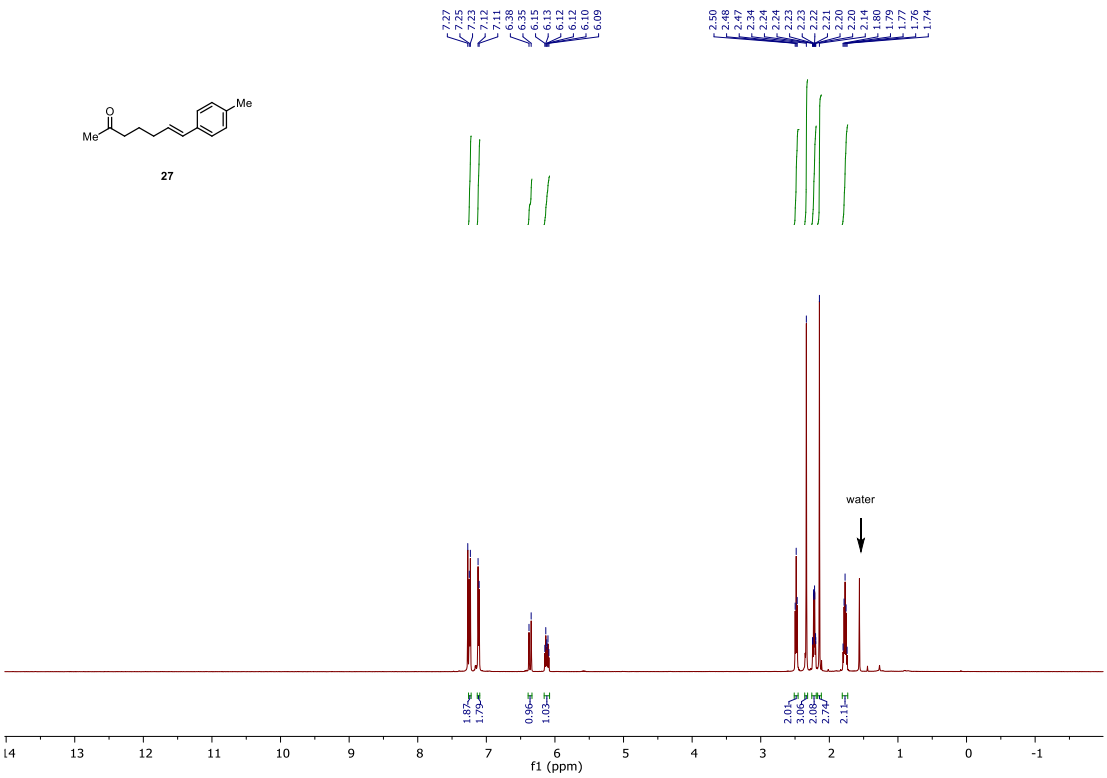
7.27
7.25
7.23
7.12
7.11
6.38
6.35
6.15
6.13
6.12
6.12
6.10
6.09
2.50
2.48
2.47
2.34
2.24
2.24
2.23
2.23
2.22
2.21
2.20
2.20
2.14
1.80
1.79
1.77
1.76
1.74
Me
Me
O
27
water
1.87
1.79
0.96
1.03
2.01
3.06
2.08
2.74
2.11
f1 (ppm)

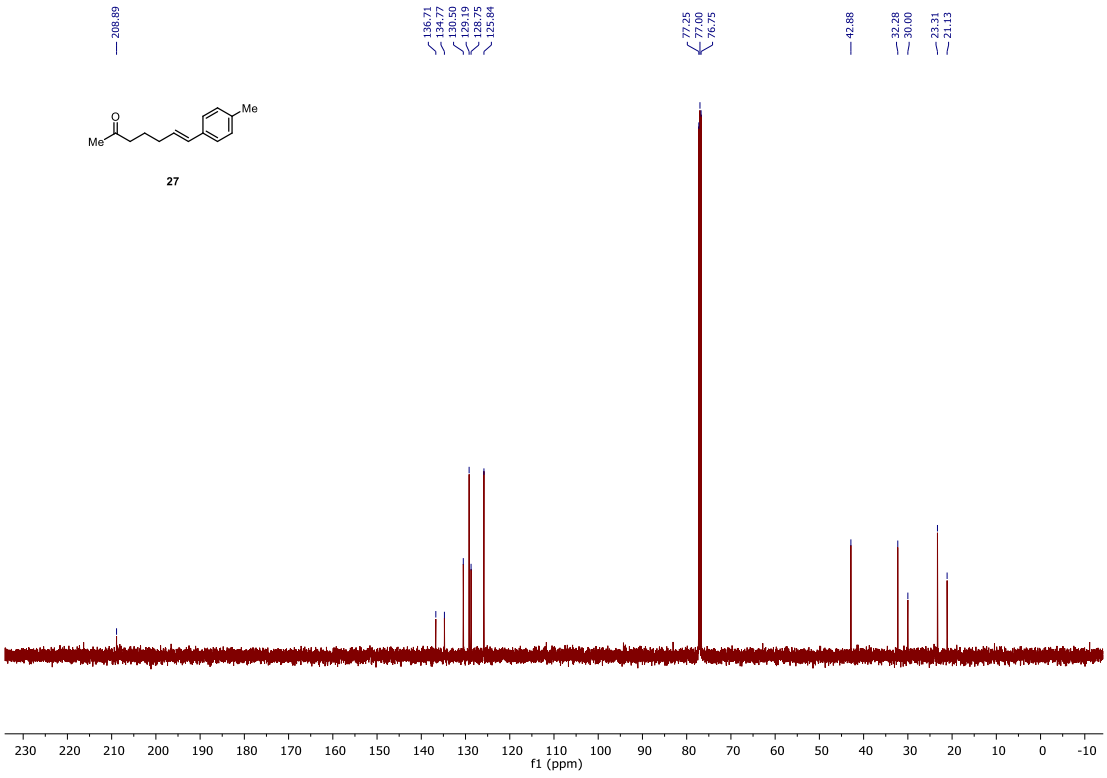
208.89
136.71
134.77
130.50
129.19
128.75
125.84
77.25
77.00
76.75
42.88
32.28
30.00
23.31
21.13
Me
Me
O
27
f1 (ppm)

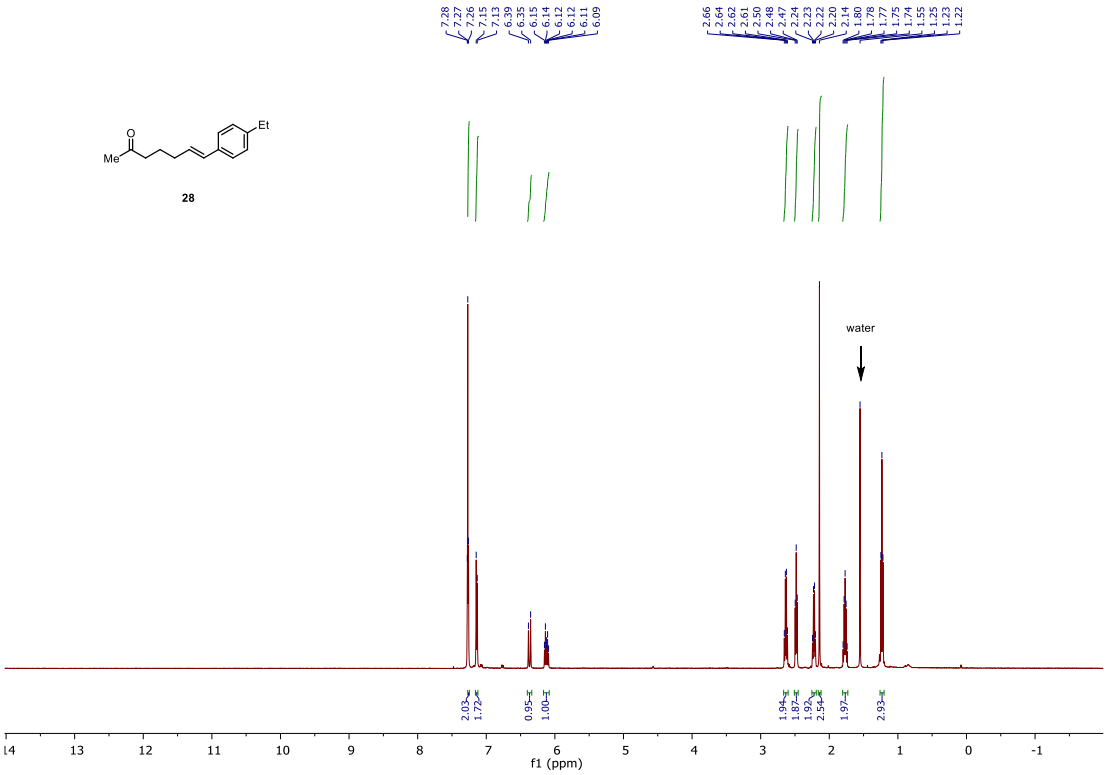
7.28
7.27
7.26
7.15
7.13
6.39
6.35
6.15
6.14
6.12
6.12
6.11
6.09
2.66
2.64
2.62
2.61
2.50
2.48
2.47
2.24
2.23
2.22
2.20
2.14
1.98
1.78
1.77
1.75
1.74
1.55
1.25
1.23
1.22
water
O
Me
Et
28
2.03
1.72
0.95
1.00
1.94
1.87
1.92
2.54
1.97
2.93
f1 (ppm)

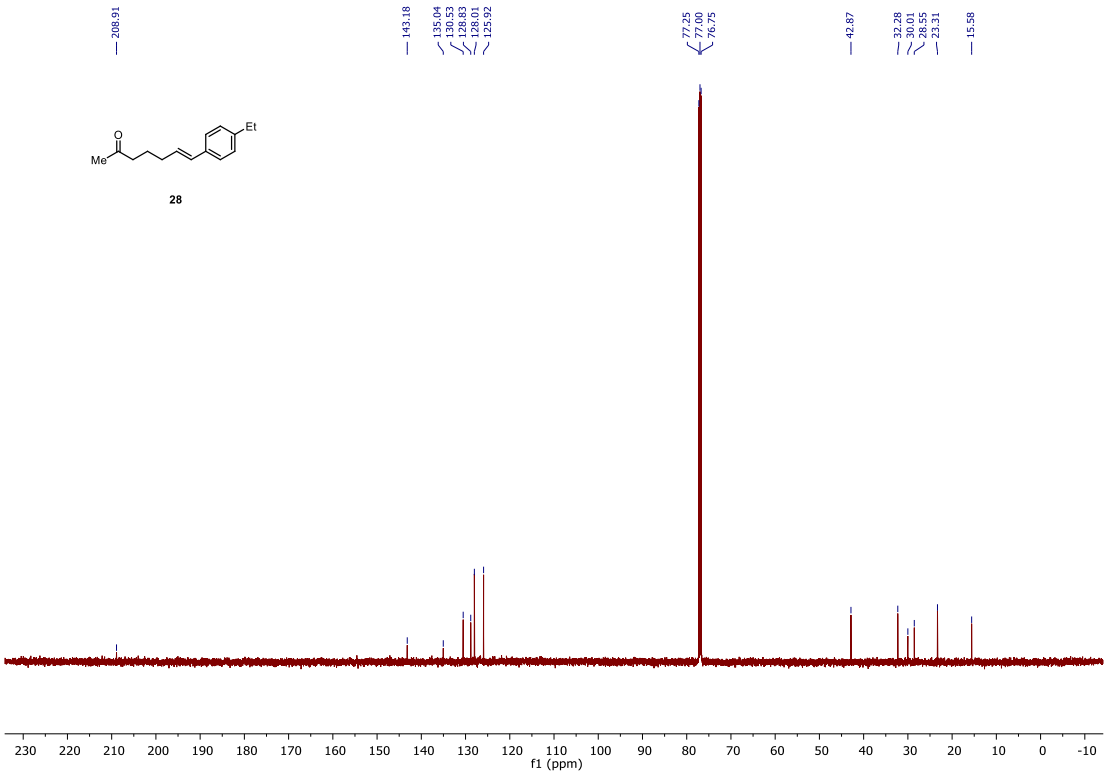
208.91
143.18
135.04
130.53
128.83
128.01
125.92
77.25
77.00
76.75
42.87
32.28
30.01
28.55
23.31
15.58
O
Me
Et
28
f1 (ppm)

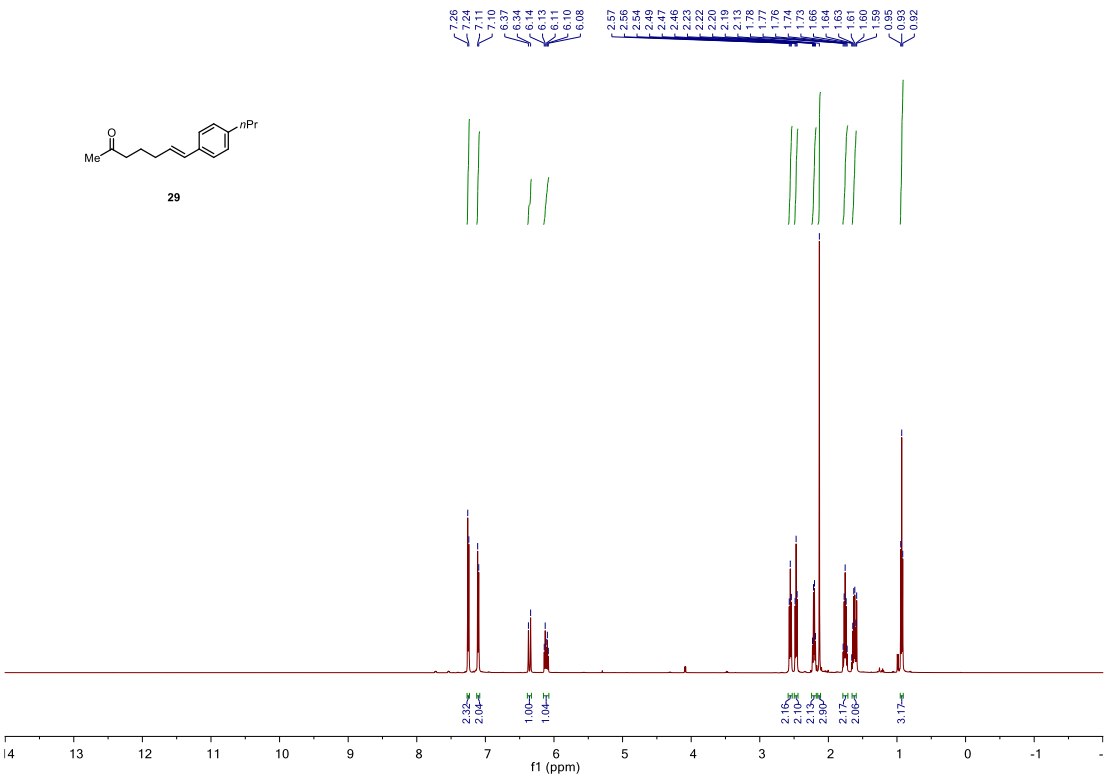
7.26
7.24
7.11
7.10
6.37
6.34
6.14
6.13
6.11
6.10
6.08
2.57
2.56
2.54
2.49
2.47
2.46
2.23
2.22
2.20
2.19
2.13
1.78
1.77
1.76
1.74
1.73
1.66
1.64
1.63
1.61
1.60
1.59
0.95
0.93
0.92
O
Me
nPr
29
2.32
2.04
1.00
1.04
2.16
2.10
2.13
2.90
2.17
2.06
3.17
f1 (ppm)

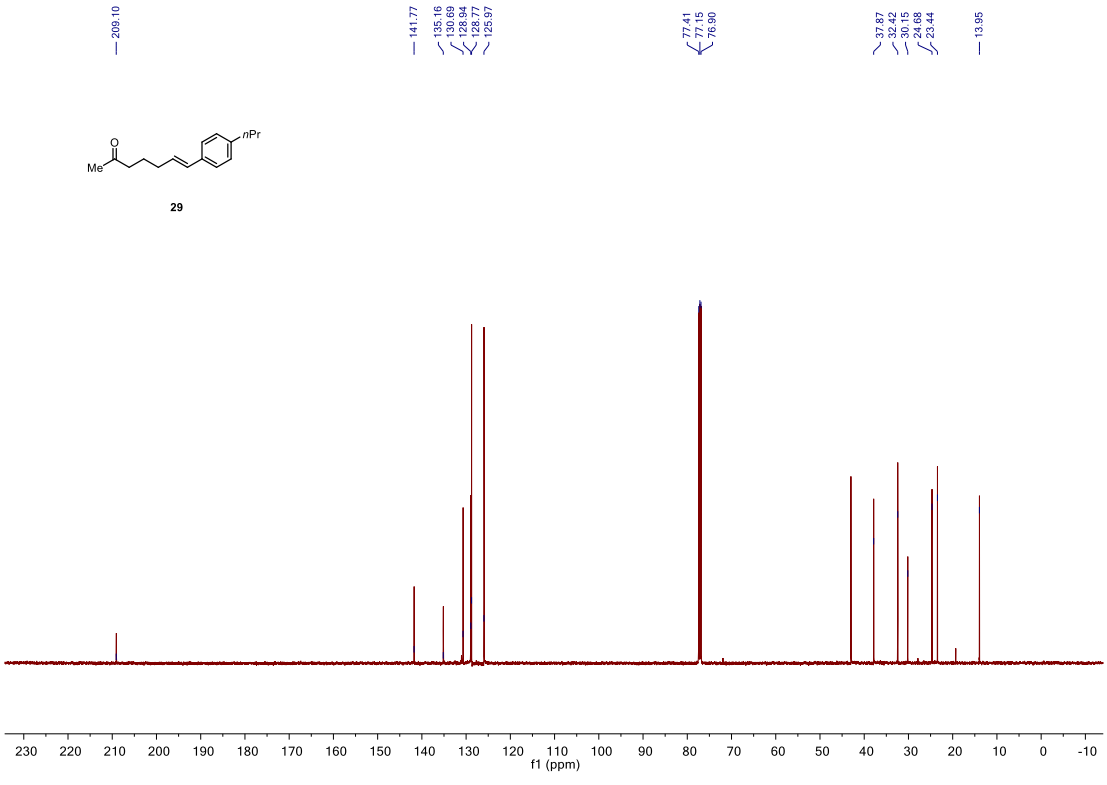
209.10
141.77
135.16
130.69
128.94
128.77
125.97
77.41
77.15
76.90
37.87
32.42
30.15
24.68
23.44
13.95
O
Me
nPr
29
f1 (ppm)

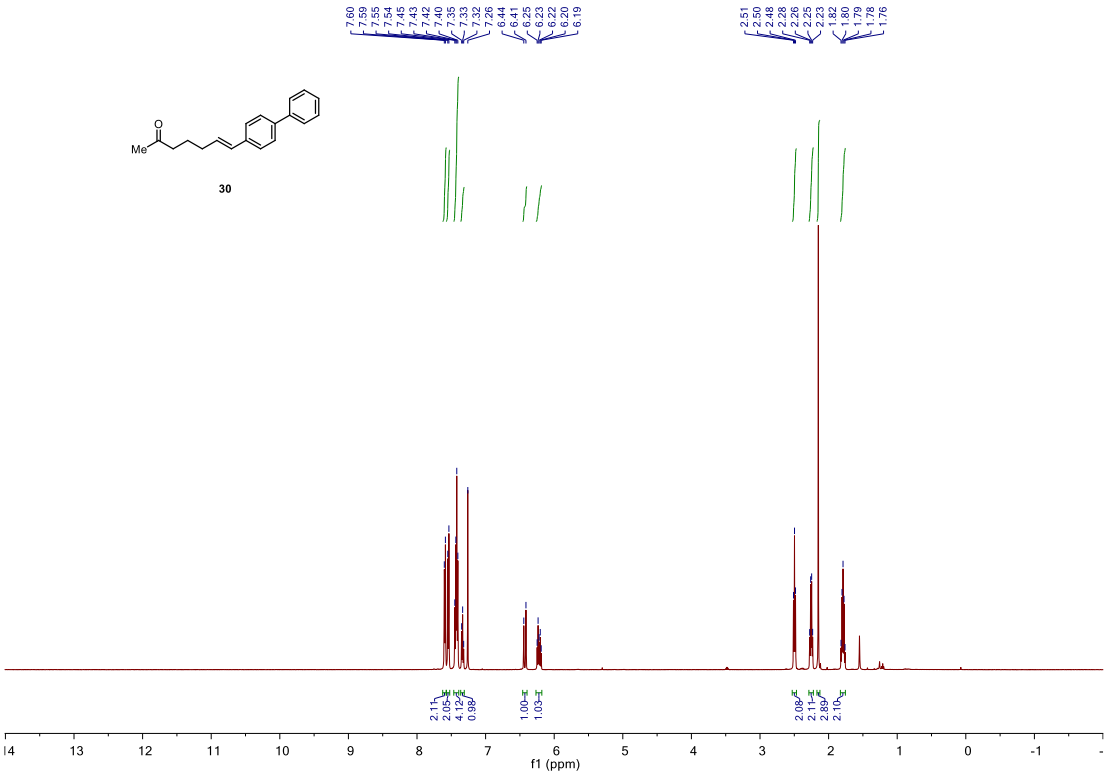
7.60
7.59
7.55
7.54
7.45
7.43
7.42
7.40
7.35
7.33
7.32
7.26
6.44
6.41
6.25
6.23
6.22
6.20
6.19
2.51
2.50
2.48
2.28
2.26
2.25
2.23
1.82
1.80
1.79
1.78
1.76
Me
O
30
2.11
2.05
4.12
0.98
1.00
1.03
2.08
2.11
2.89
2.10
f1 (ppm)

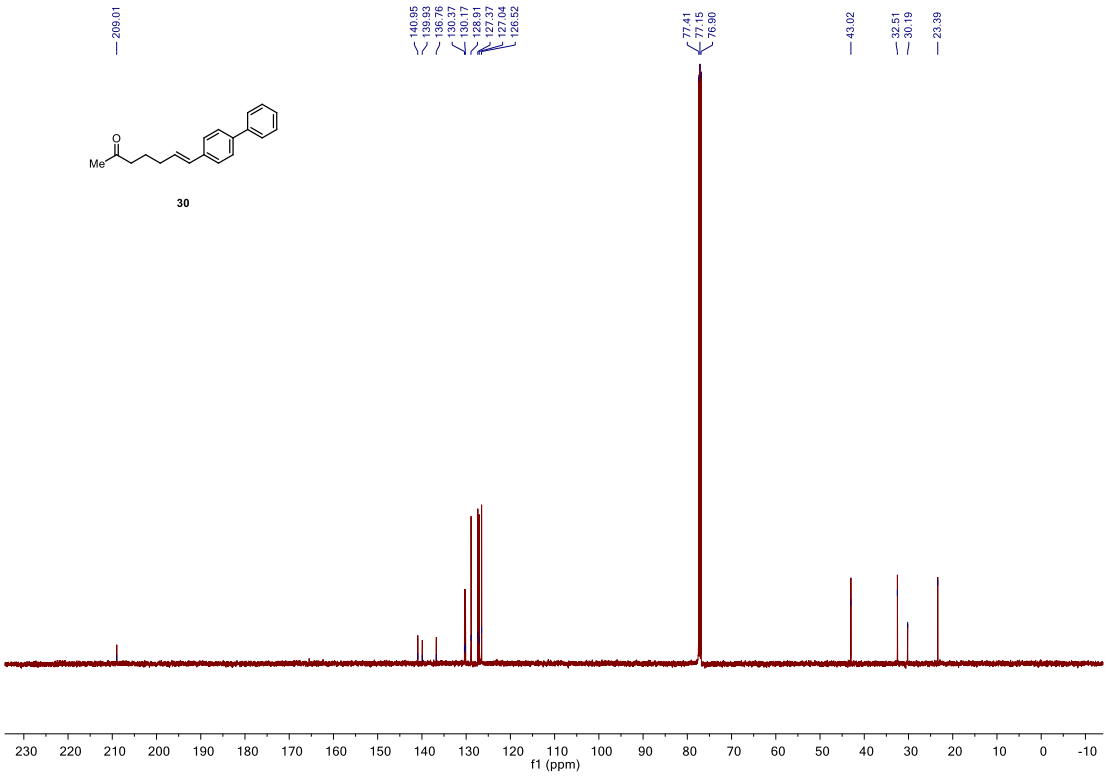
209.01
140.95
139.93
136.76
130.37
130.17
128.91
127.37
127.04
126.52
77.41
77.15
76.90
43.02
32.51
30.19
23.39
Me
O
30
f1 (ppm)

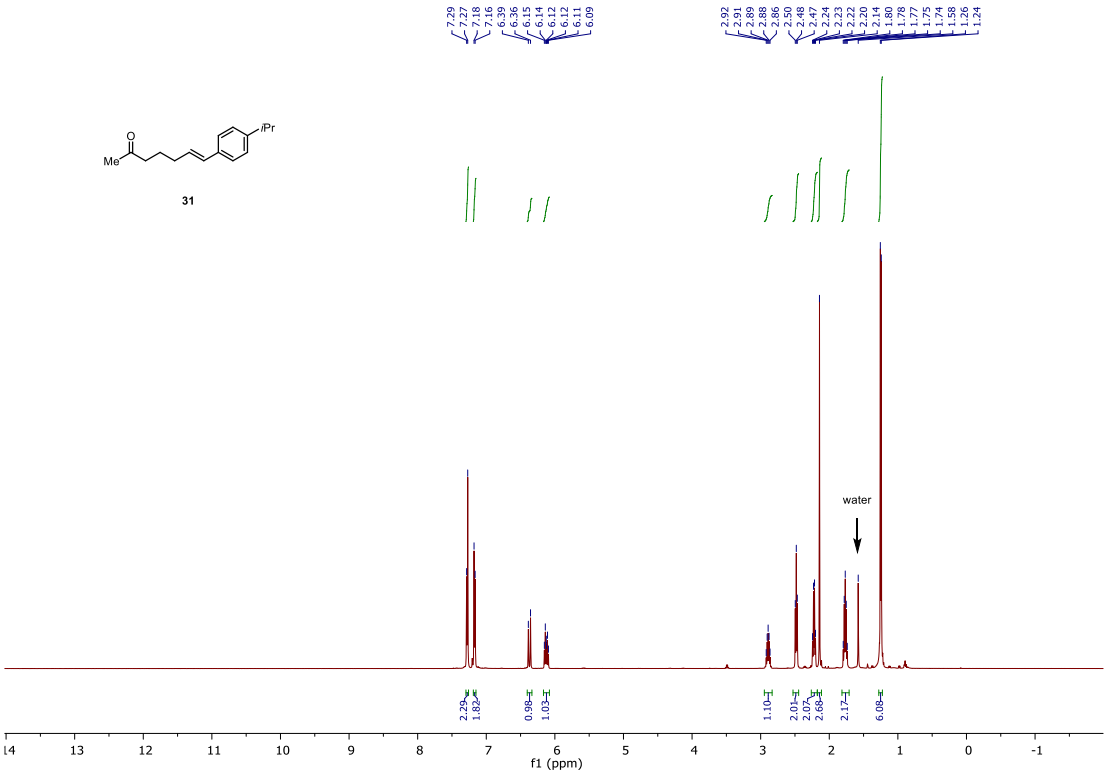
7.29
7.27
7.18
7.16
6.39
6.36
6.15
6.14
6.12
6.12
6.11
6.09
2.92
2.91
2.89
2.88
2.86
2.50
2.48
2.47
2.24
2.23
2.22
2.20
2.14
1.80
1.78
1.77
1.75
1.74
1.58
1.26
1.24
Me
O
iPr
31
water
2.29
1.82
0.98
1.03
1.10
2.01
2.07
2.68
2.17
6.08
f1 (ppm)

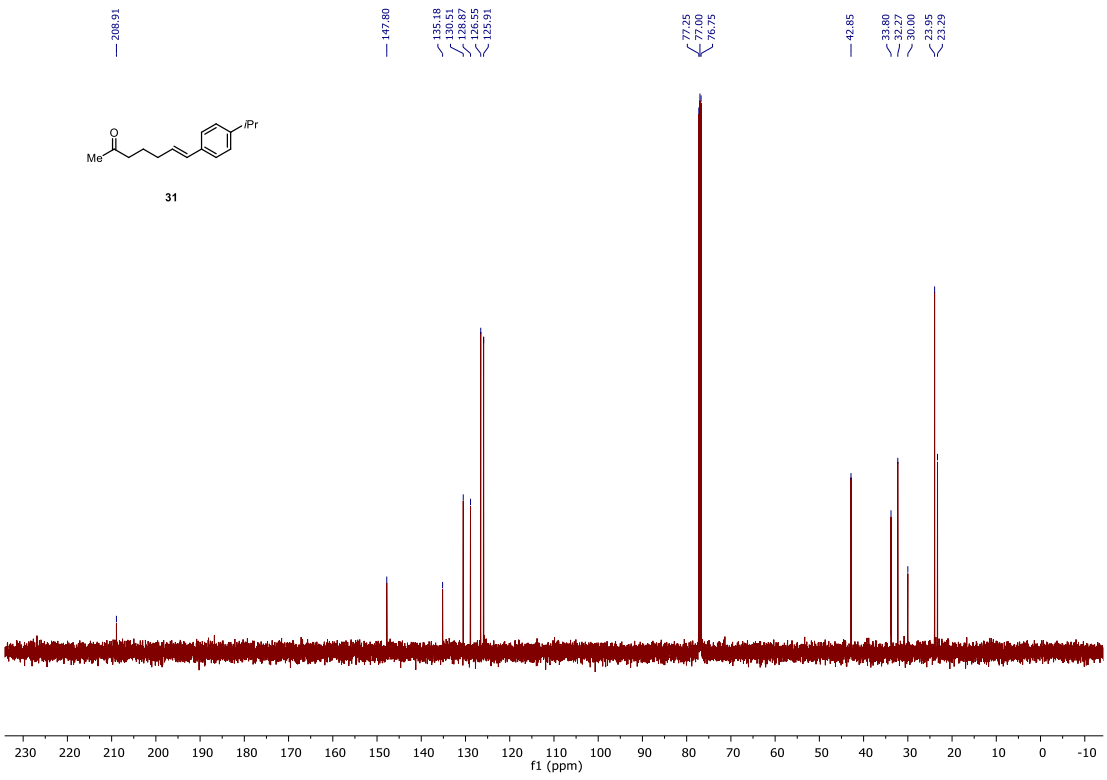
208.91
147.80
135.18
130.51
128.87
126.55
125.91
77.25
77.00
76.75
42.85
33.80
32.27
30.00
23.95
23.29
Me
O
iPr
31
f1 (ppm)

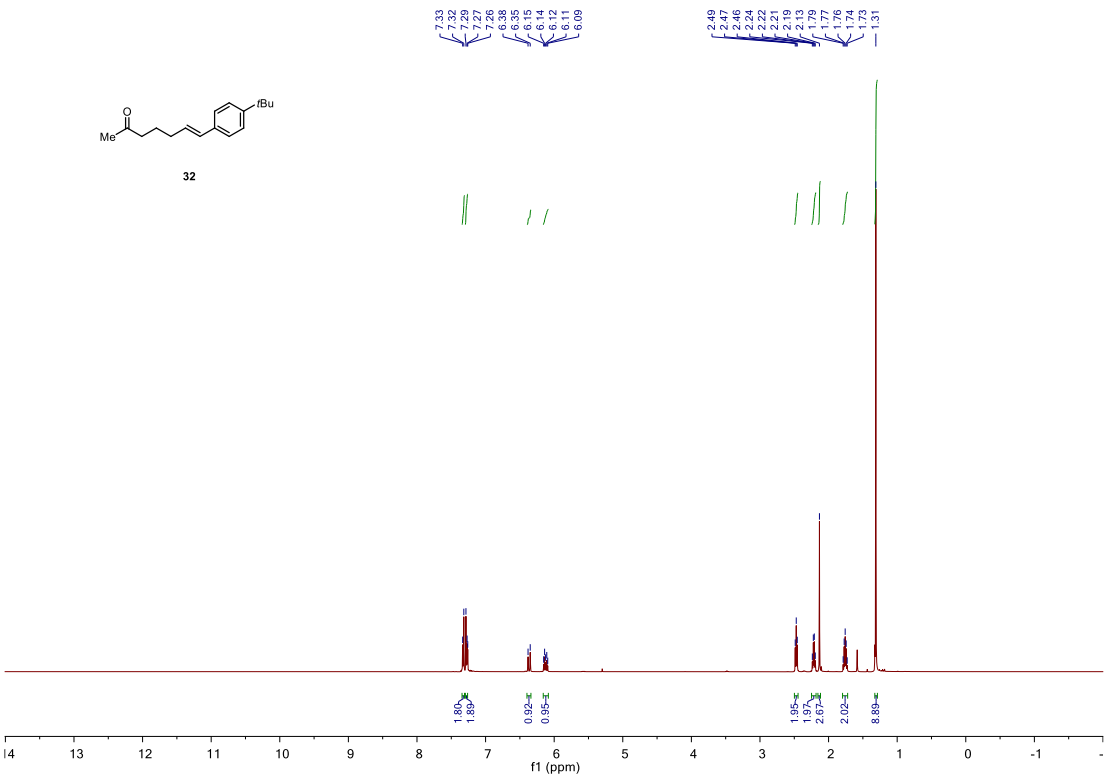
7.33
7.32
7.29
7.27
7.26
6.38
6.35
6.15
6.14
6.12
6.11
6.09
2.49
2.47
2.46
2.24
2.22
2.21
2.19
2.13
1.79
1.77
1.76
1.74
1.73
1.31
O
Me
tBu
32
1.80
1.89
0.92
0.95
1.95
1.97
2.67
2.02
8.89
f1 (ppm)

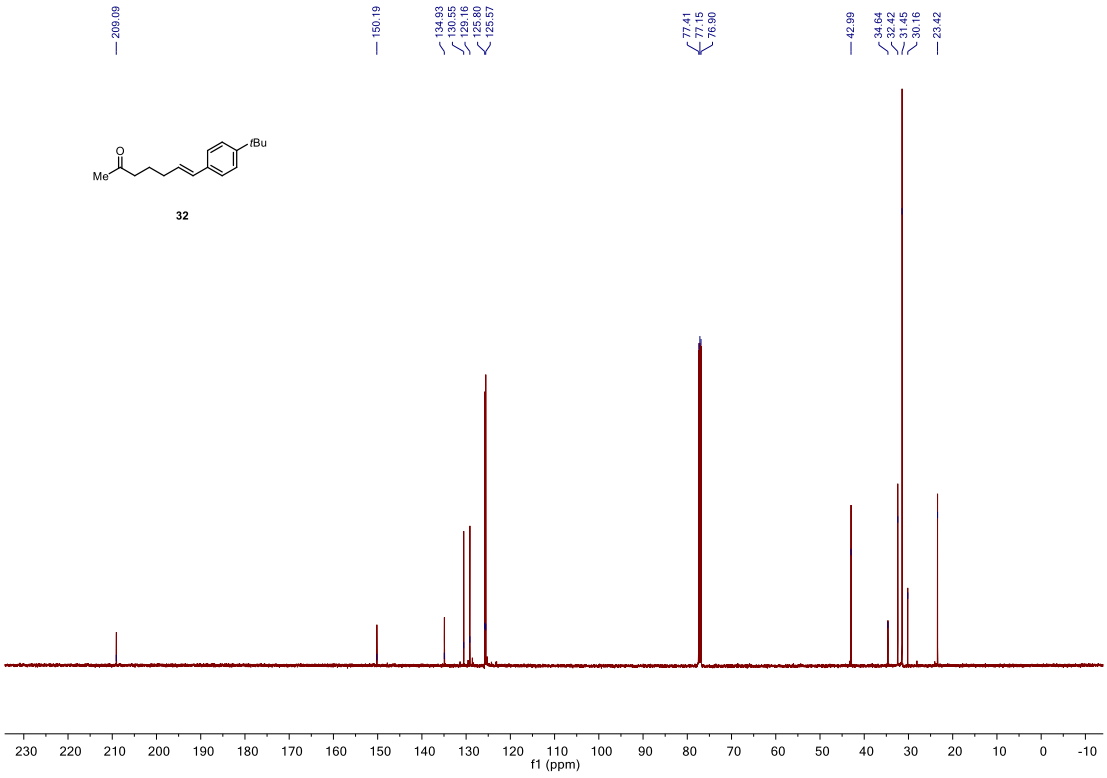
209.09
150.19
134.93
133.55
129.16
125.80
125.57
77.41
77.15
76.90
42.99
34.64
32.42
31.45
30.16
23.42
O
Me
tBu
32
f1 (ppm)

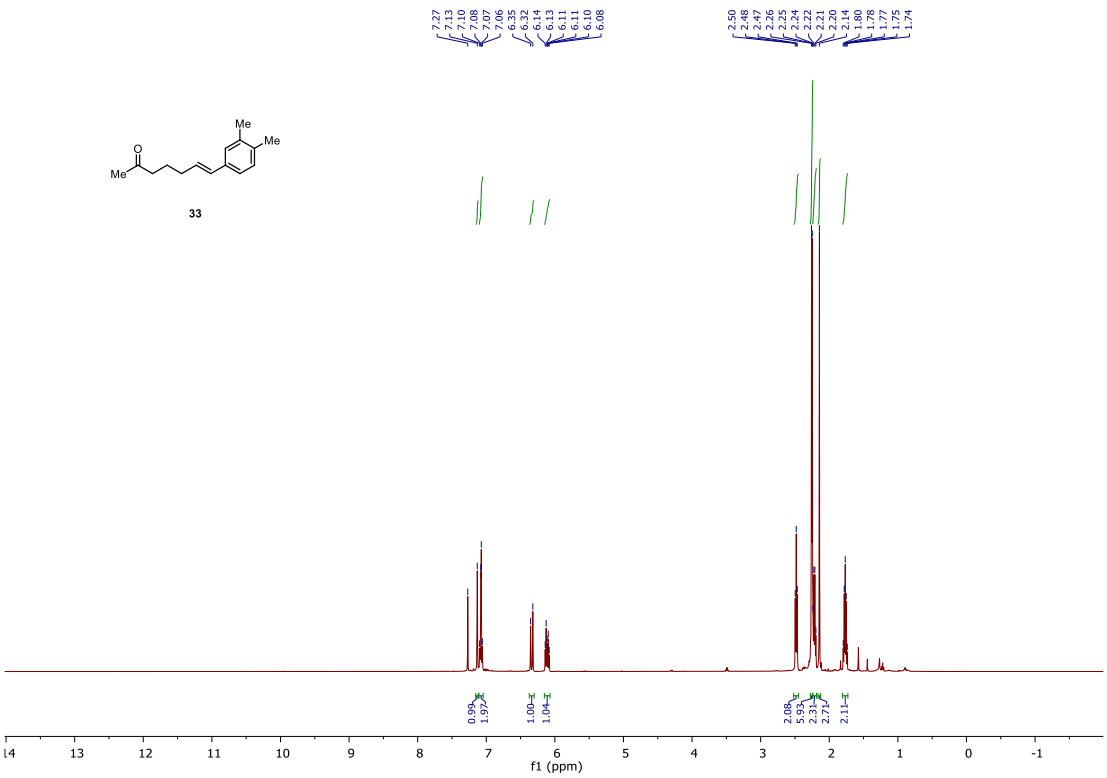
7.27
7.13
7.10
7.08
7.07
7.06
6.35
6.32
6.14
6.13
6.11
6.11
6.10
6.08
2.50
2.48
2.47
2.26
2.25
2.24
2.22
2.21
2.20
2.14
1.80
1.78
1.77
1.75
1.74
Me
Me
O
Me
33
0.99
1.97
1.00
1.04
2.08
5.95
2.31
2.71
2.11
f1 (ppm)

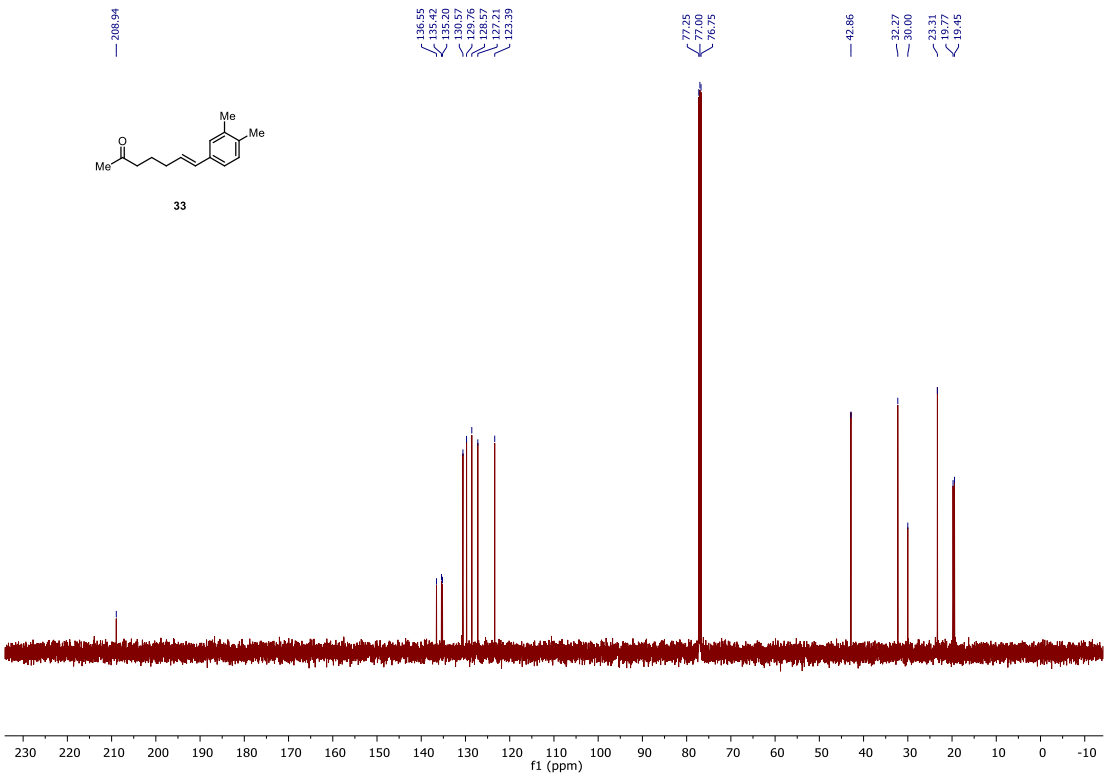
208.94
136.55
135.42
135.20
130.57
129.76
128.57
127.21
123.39
77.25
77.00
76.75
42.86
32.27
30.00
23.31
19.77
19.45
Me
Me
O
Me
33
f1 (ppm)

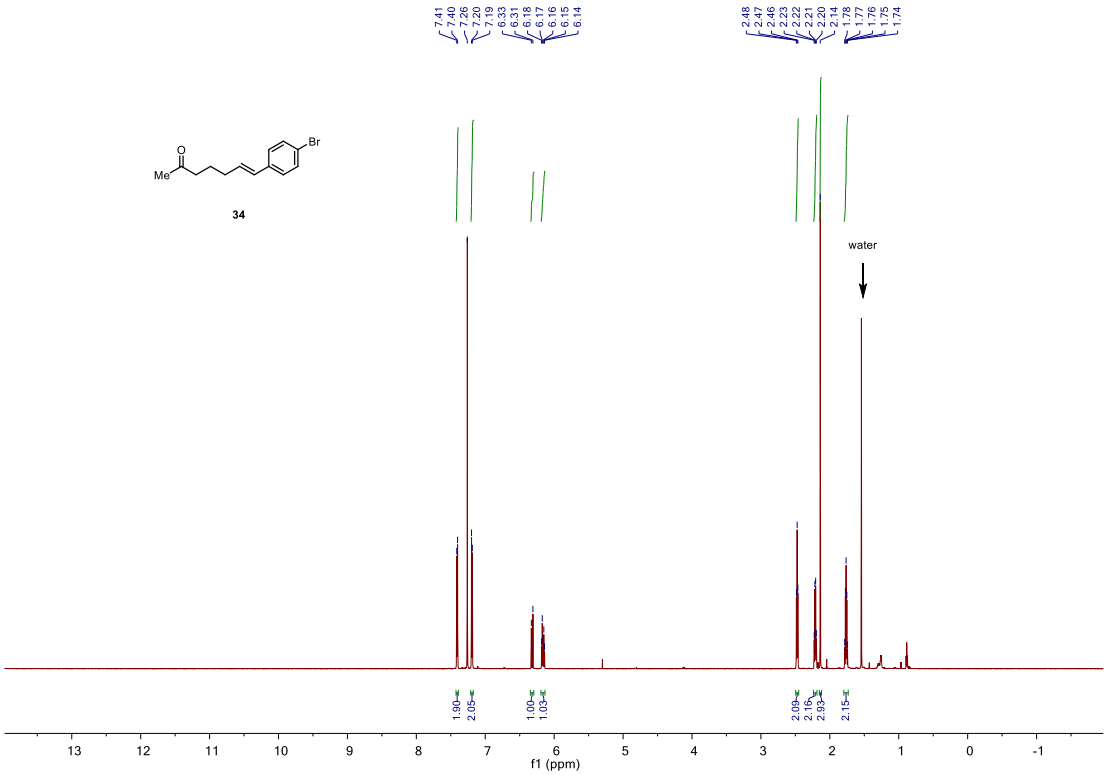
7.41
7.40
7.26
7.20
7.19
6.33
6.31
6.18
6.17
6.16
6.15
6.14
2.48
2.47
2.46
2.23
2.22
2.21
2.20
2.14
1.78
1.77
1.76
1.75
1.74
Br
O
Me
34
water
1.90
2.05
1.00
1.03
2.09
2.16
2.93
2.15
13 12 11 10 9 8 7 6 5 4 3 2 1 0 -1
f1 (ppm)

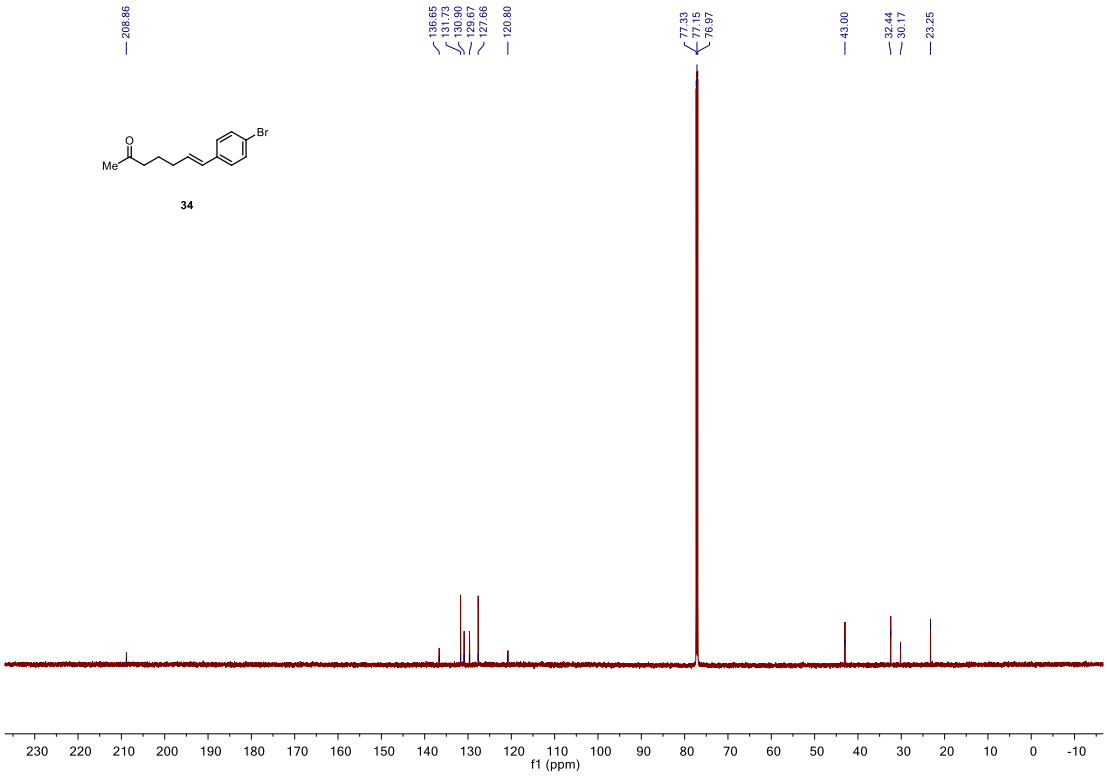
208.86
136.65
131.73
130.90
129.67
127.66
120.80
77.33
77.15
76.97
43.00
32.44
30.17
23.25
Br
O
Me
34
230 220 210 200 190 180 170 160 150 140 130 120 110 100 90 80 70 60 50 40 30 20 10 0 -10
f1 (ppm)

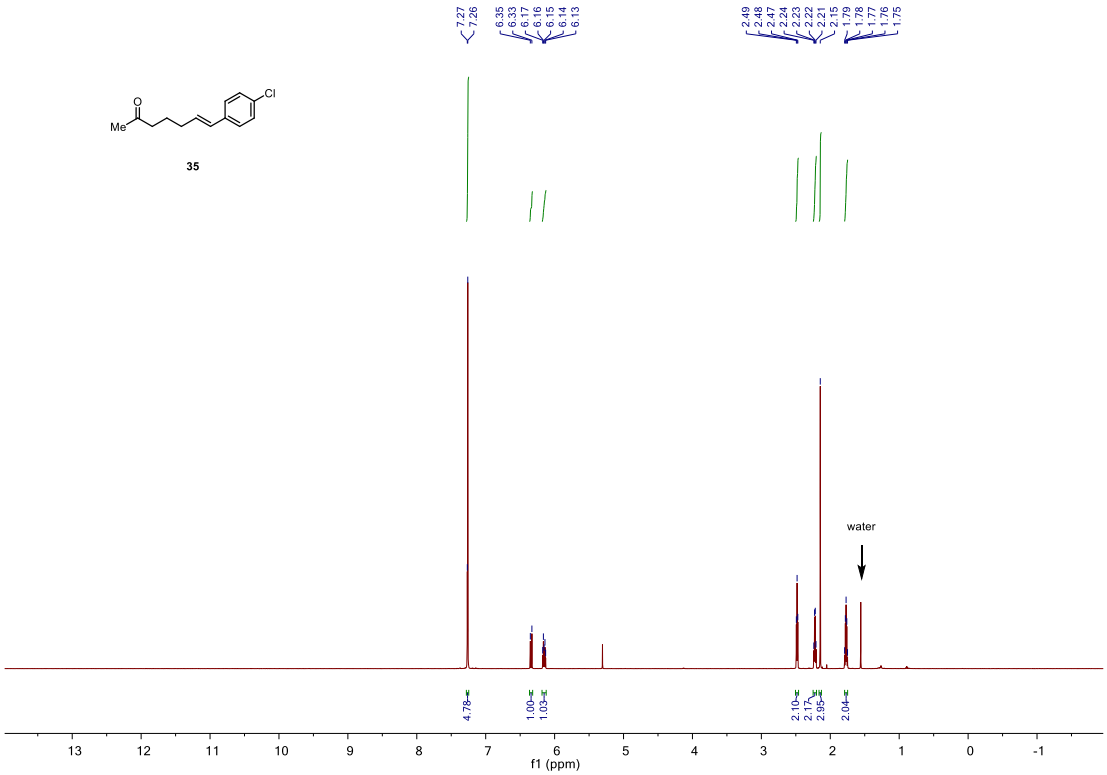
7.27
7.26
6.35
6.33
6.17
6.16
6.15
6.14
6.13
2.49
2.48
2.47
2.24
2.23
2.22
2.21
2.15
1.79
1.78
1.77
1.76
1.75
Cl
O
Me
35
water
4.78
1.00
1.03
2.10
2.17
2.95
2.04
13 12 11 10 9 8 7 6 5 4 3 2 1 0 -1
f1 (ppm)

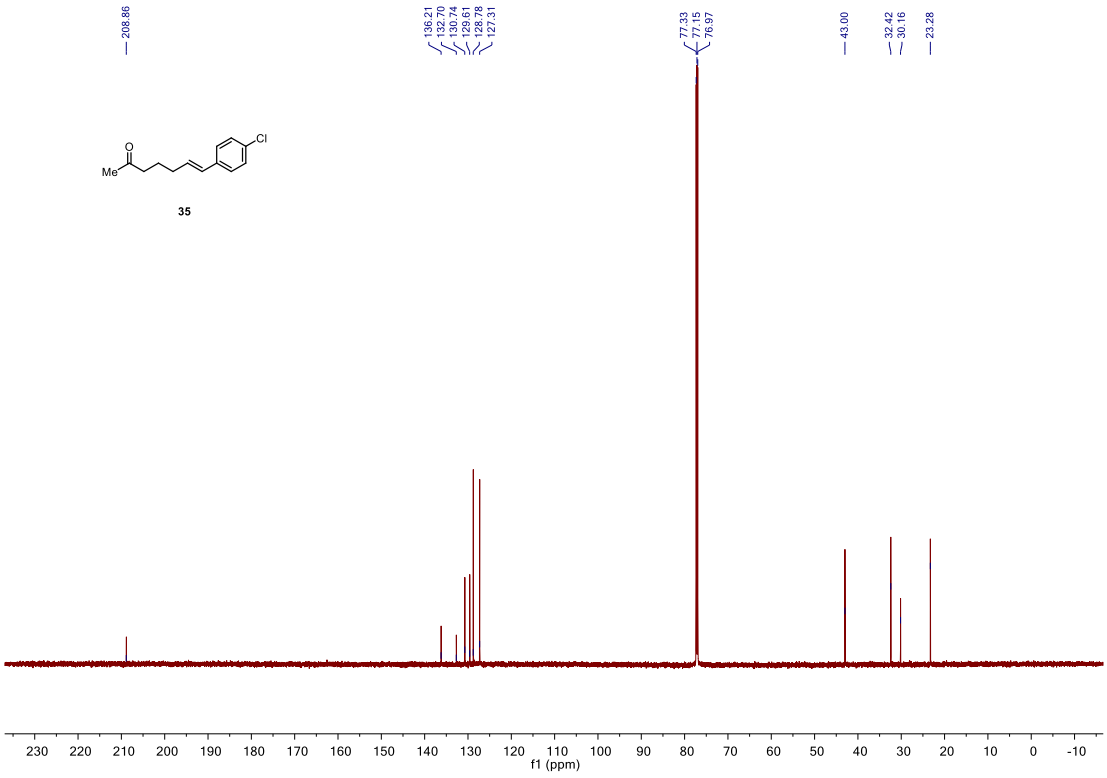
208.86
136.21
132.70
130.74
129.61
128.78
127.31
77.33
77.15
76.97
43.00
32.42
30.16
23.28
Cl
O
Me
35
230 220 210 200 190 180 170 160 150 140 130 120 110 100 90 80 70 60 50 40 30 20 10 0 -10
f1 (ppm)

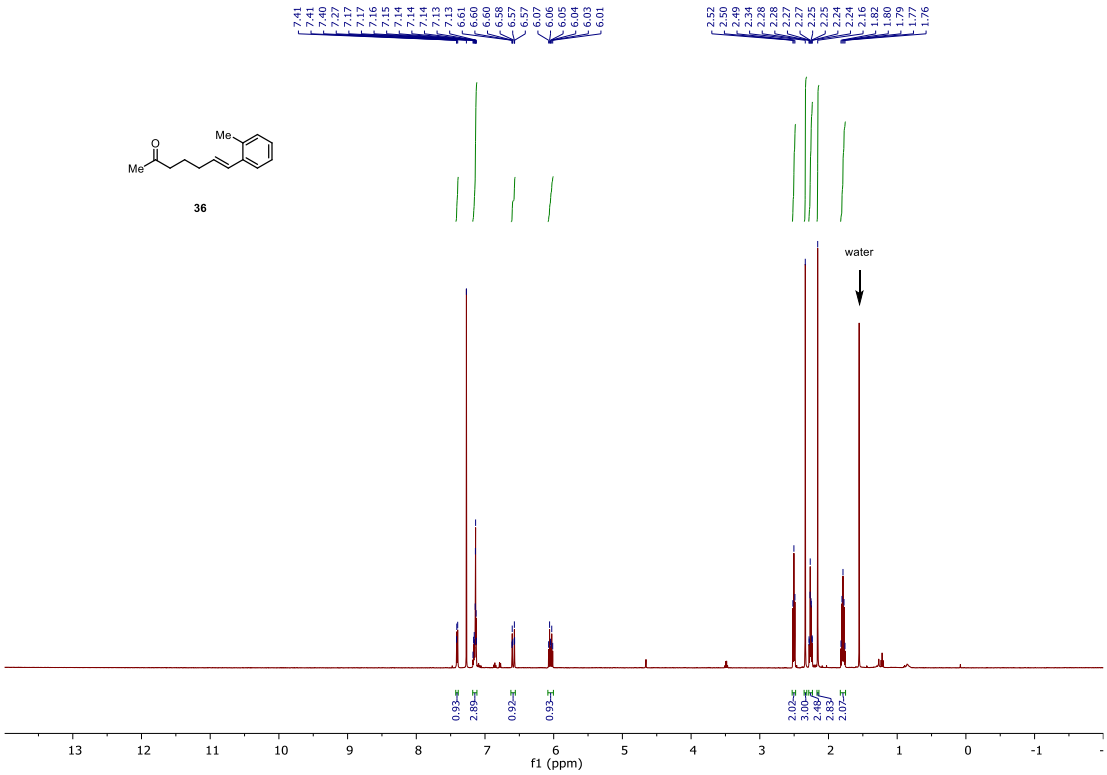
7.41
7.41
7.40
7.27
7.17
7.17
7.16
7.15
7.14
7.14
7.14
7.13
6.61
6.60
6.60
6.58
6.57
6.57
6.07
6.06
6.05
6.04
6.03
6.01
2.52
2.50
2.49
2.34
2.28
2.28
2.27
2.27
2.25
2.25
2.24
2.24
2.16
1.82
1.80
1.79
1.77
1.76
Me
O
Me
36
water
0.93
2.89
0.92
0.93
2.02
3.00
2.48
2.07
f1 (ppm)

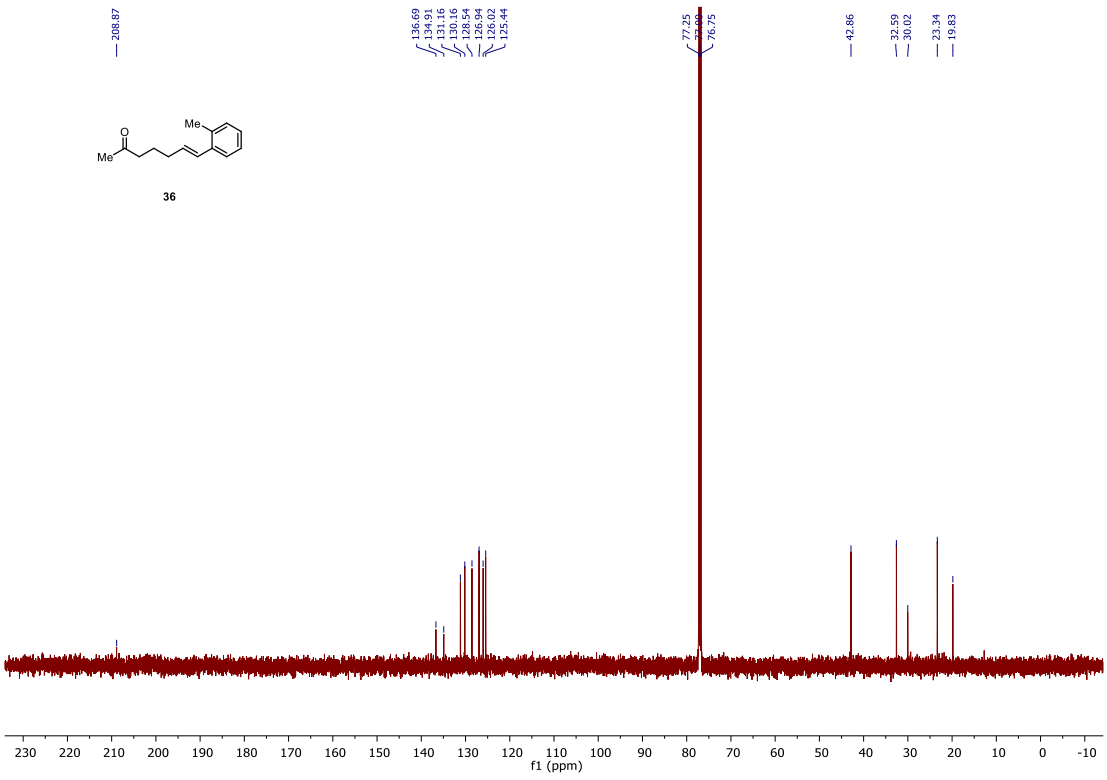
208.87
136.69
134.91
131.16
130.16
128.54
126.94
126.02
125.44
77.25
77.00
76.75
42.86
32.59
30.02
23.34
19.83
Me
O
Me
36
f1 (ppm)

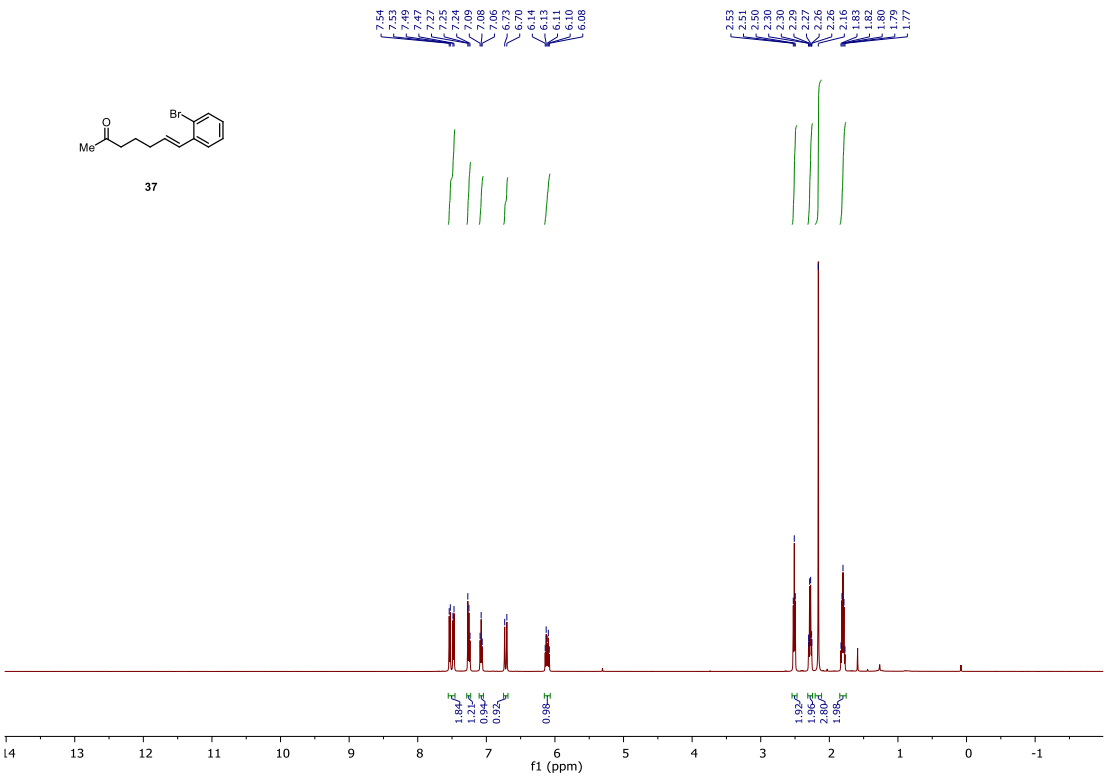
7.54
7.53
7.49
7.47
7.27
7.25
7.24
7.09
7.08
7.06
6.73
6.70
6.14
6.13
6.11
6.10
6.08
2.53
2.51
2.50
2.30
2.29
2.27
2.26
2.26
2.16
1.83
1.82
1.80
1.79
1.77
Br
O
Me
37
1.84
1.21
0.94
0.92
0.98
1.92
1.96
2.80
1.98
f1 (ppm)

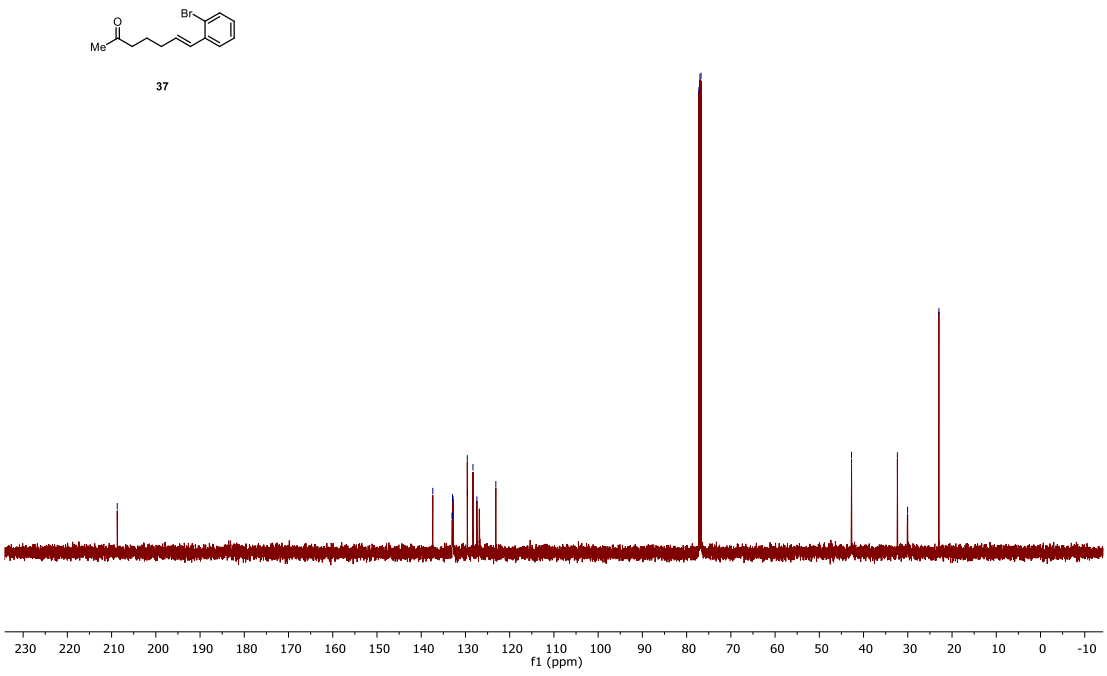
208.72
137.39
133.01
132.99
132.92
132.82
132.76
129.58
129.55
128.30
127.41
123.13
77.25
76.99
76.74
42.72
32.35
30.09
30.05
22.97
Br
O
Me
37
f1 (ppm)

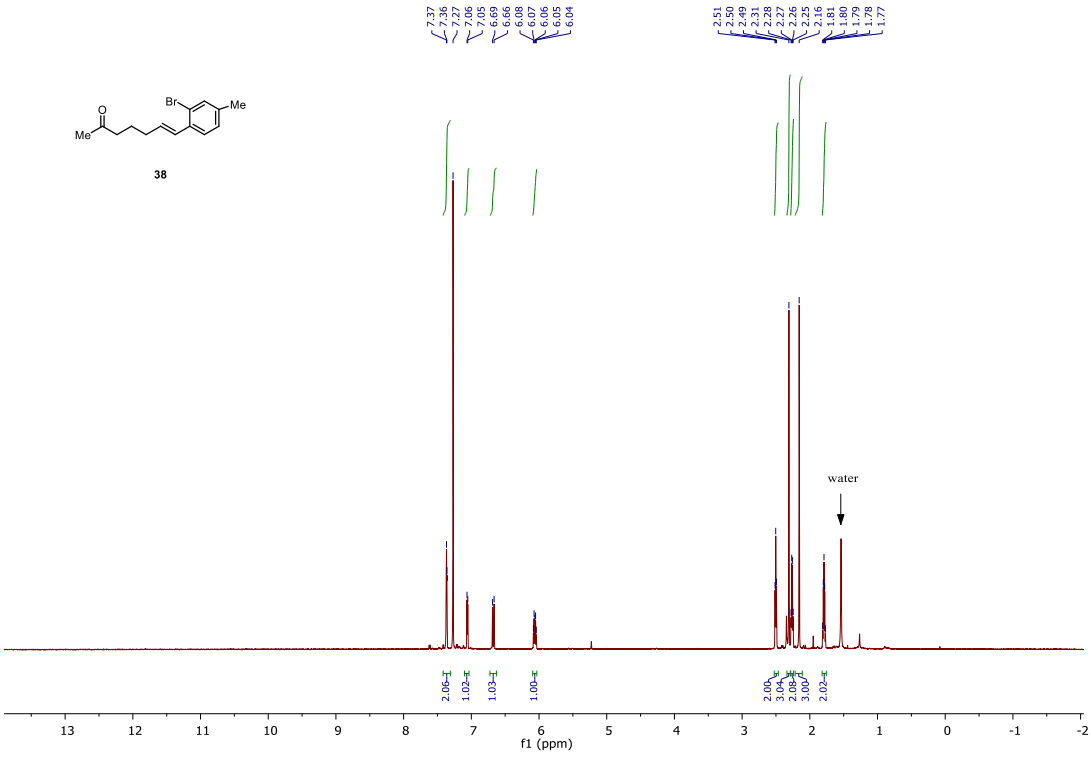
7.37
7.36
7.27
7.06
7.05
6.69
6.66
6.08
6.07
6.06
6.05
6.04
2.51
2.50
2.49
2.31
2.28
2.27
2.26
2.25
2.16
1.81
1.80
1.79
1.78
1.77
Br
Me
O
Me
38
water
2.06
1.02
1.03
1.00
2.00
3.04
2.08
3.00
2.02
13 12 11 10 9 8 7 6 5 4 3 2 1 0 -1 -2
f1 (ppm)

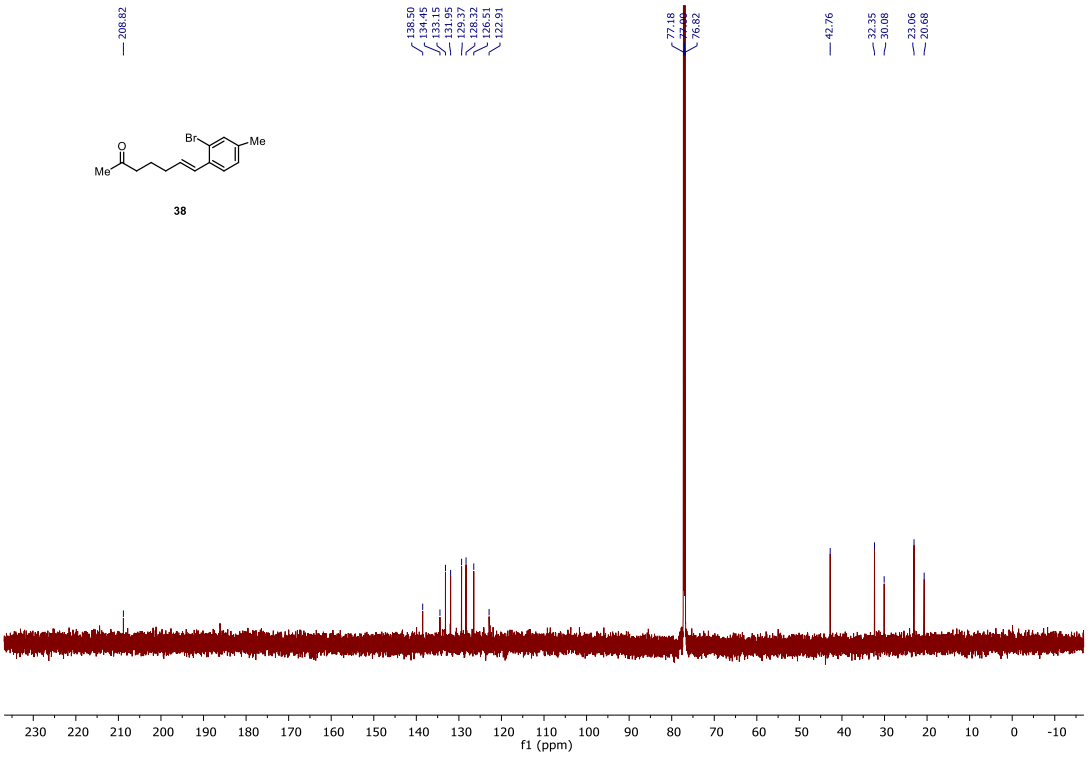
208.82
138.50
134.45
133.15
131.95
129.37
128.32
126.51
122.91
77.18
77.00
76.82
42.76
32.35
30.08
23.06
20.68
Br
Me
O
Me
38
230 220 210 200 190 180 170 160 150 140 130 120 110 100 90 80 70 60 50 40 30 20 10 0 -10
f1 (ppm)

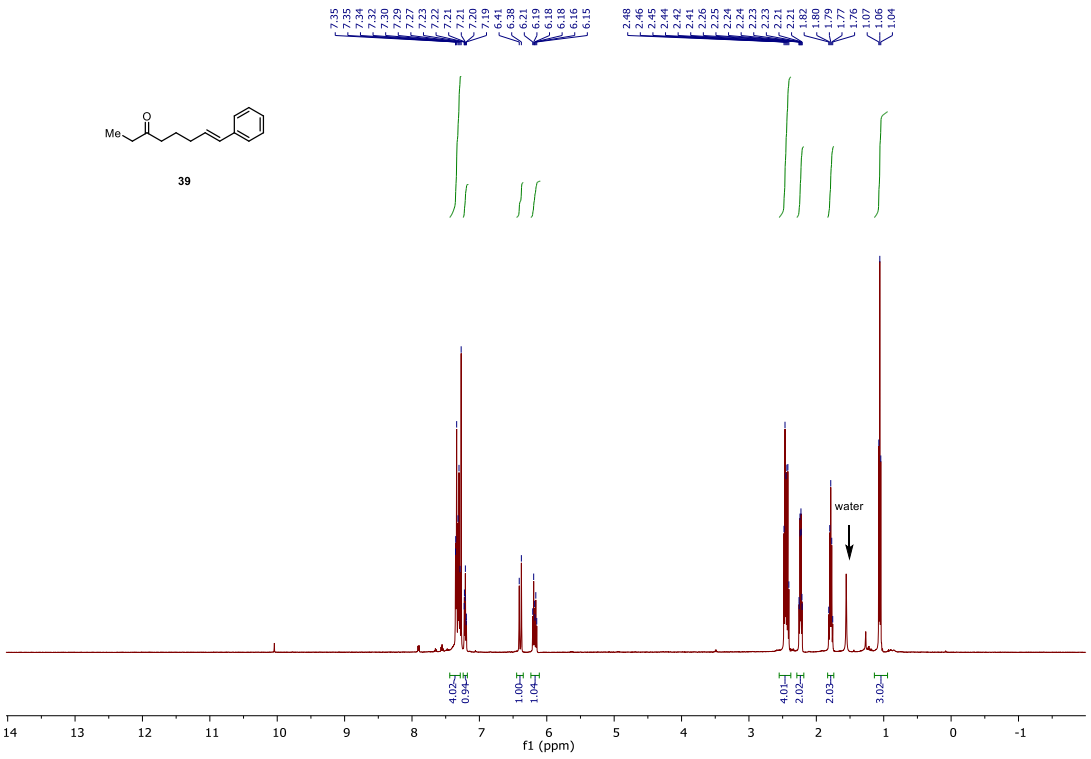
Me
O
39
water
f1 (ppm)

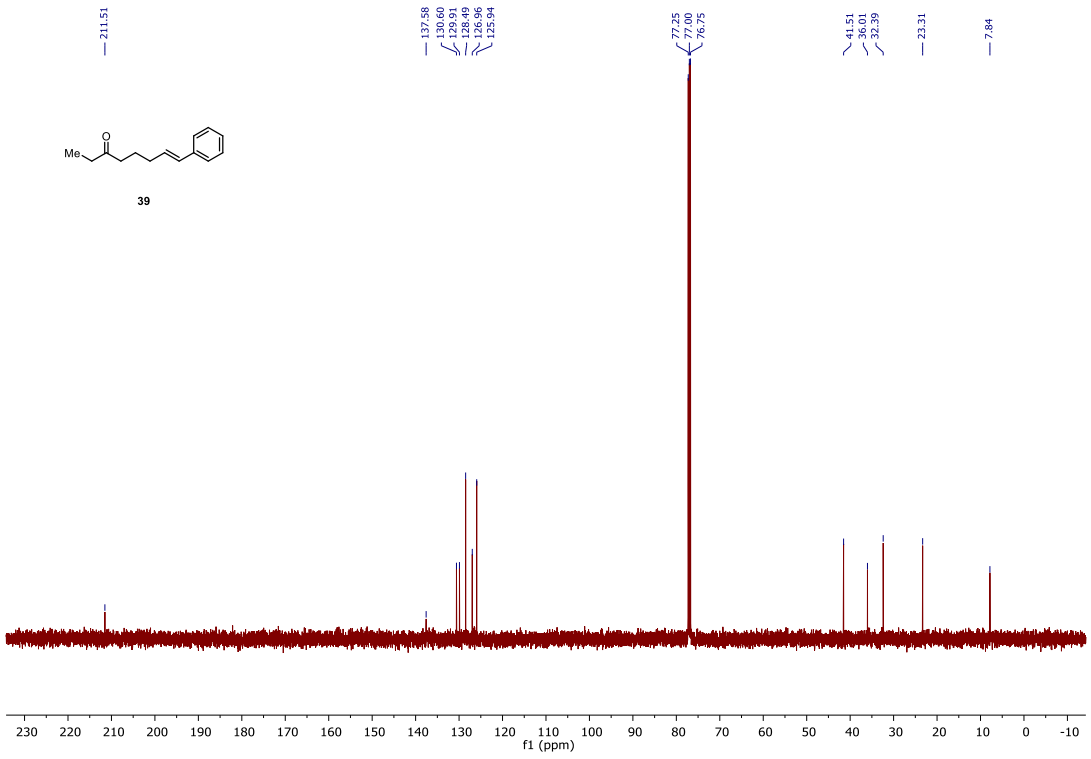
Me
O
39
f1 (ppm)

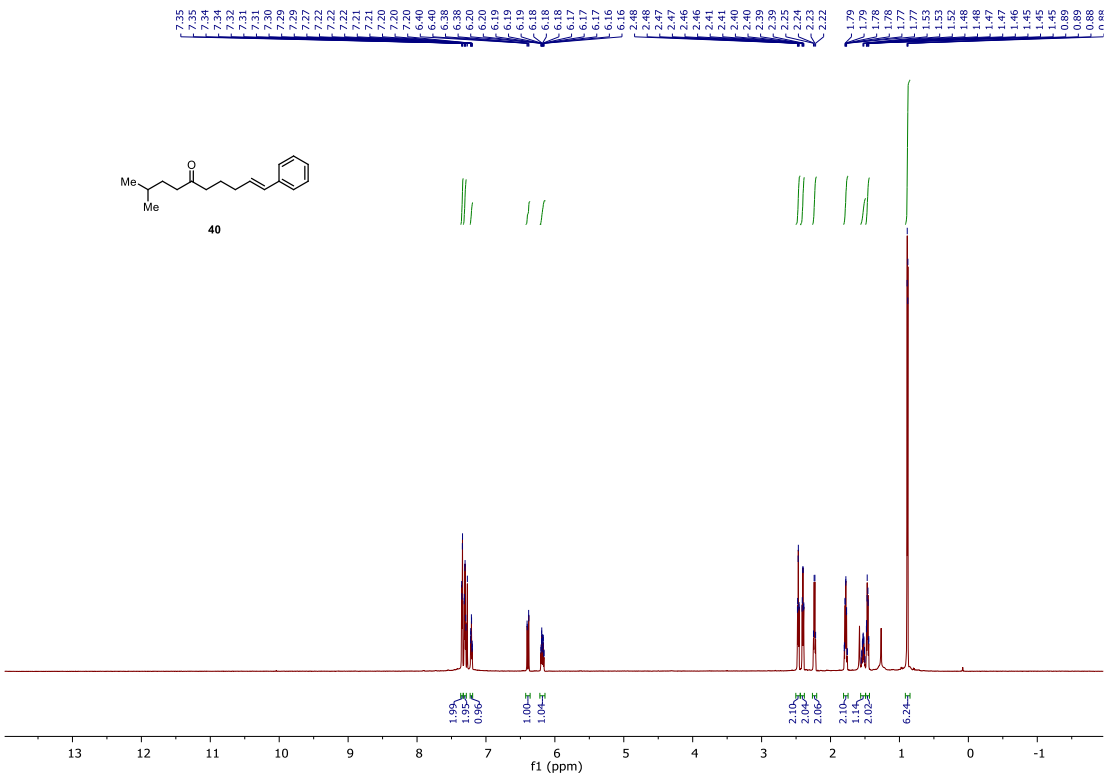
Me
Me
O
40
f1 (ppm)

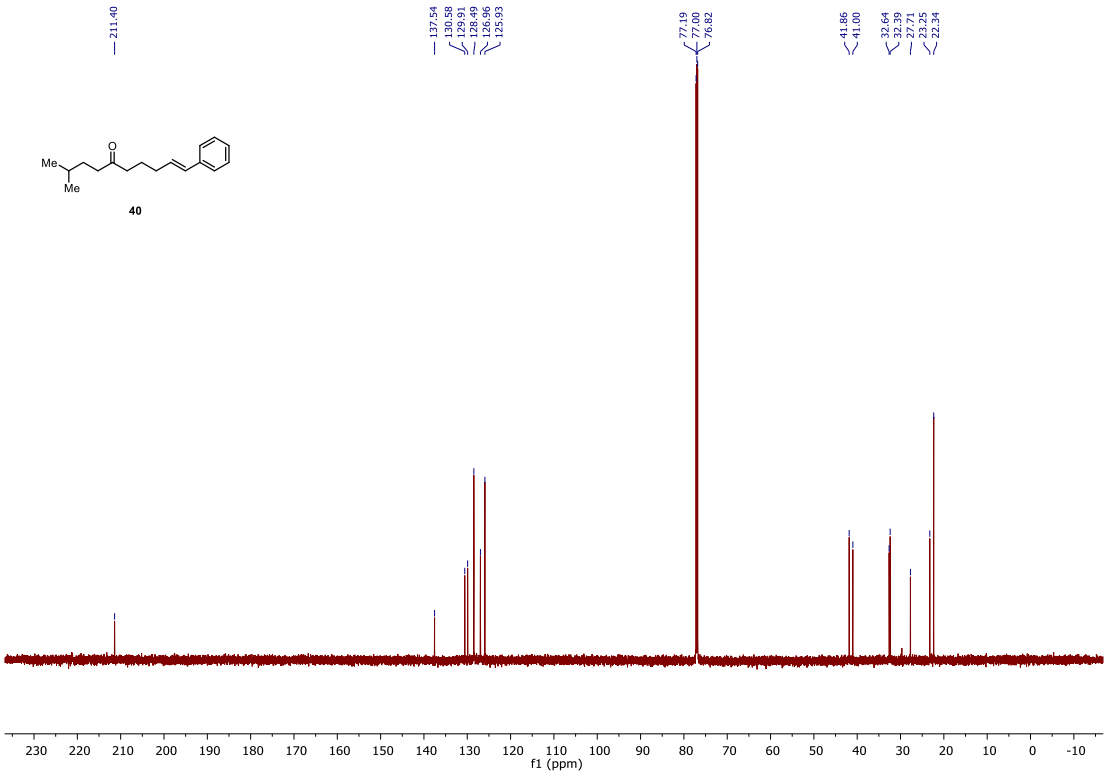
Me
Me
O
40
f1 (ppm)

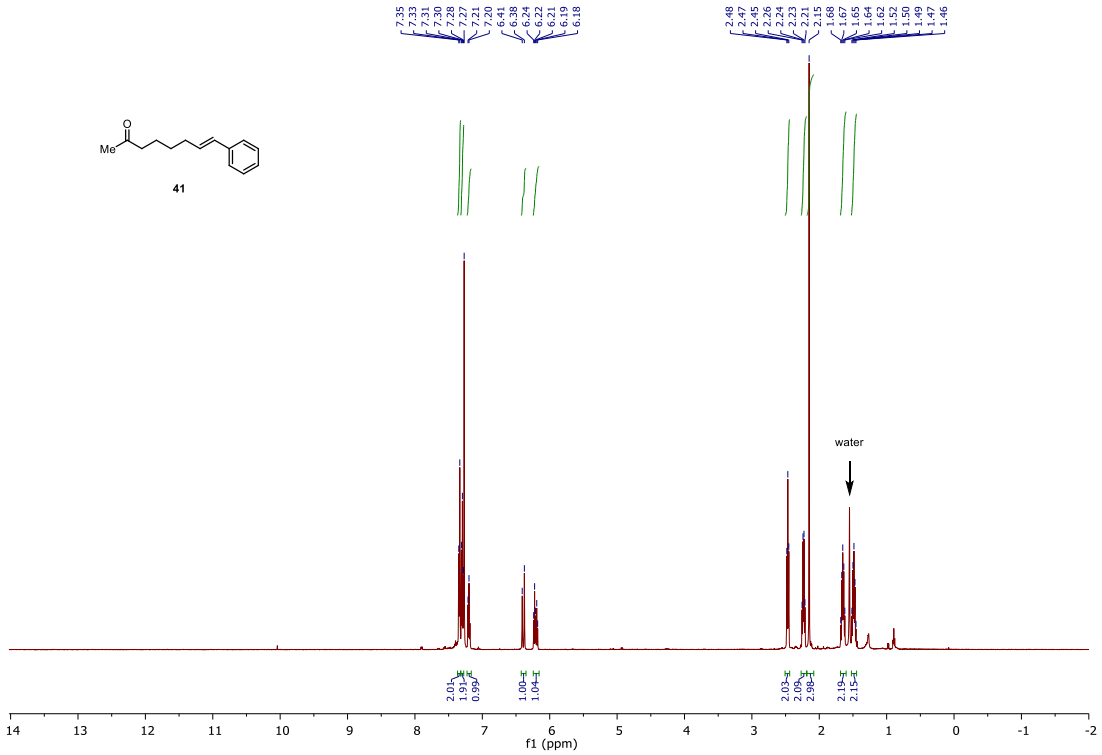
7.35
7.33
7.31
7.30
7.28
7.27
7.21
7.20
6.41
6.38
6.24
6.22
6.21
6.19
6.18
2.48
2.47
2.45
2.26
2.24
2.23
2.21
2.15
1.68
1.67
1.65
1.64
1.62
1.52
1.50
1.49
1.47
1.46
O
Me
41
water
2.01
1.93
0.99
1.00
1.04
2.03
2.09
2.98
2.19
2.15
14 13 12 11 10 9 8 7 6 5 4 3 2 1 0 -1 -2
f1 (ppm)

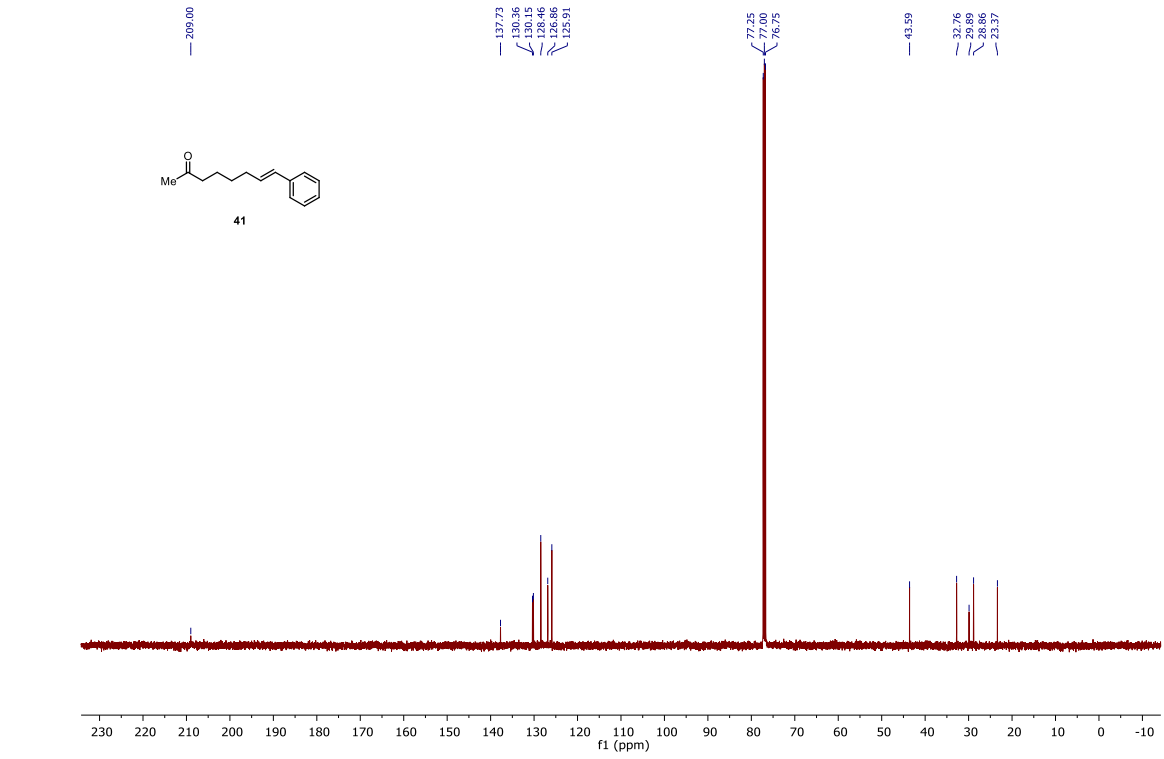
209.00
137.73
130.36
130.15
128.46
126.86
125.91
77.25
77.00
76.75
43.59
32.76
29.89
28.86
23.37
O
Me
41
230 220 210 200 190 180 170 160 150 140 130 120 110 100 90 80 70 60 50 40 30 20 10 0 -10
f1 (ppm)

Oxetane

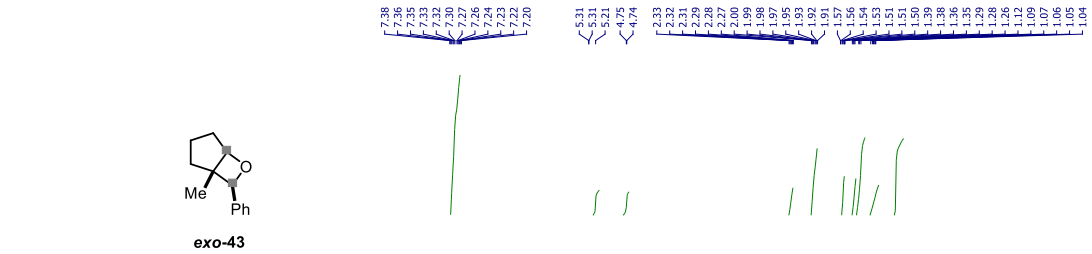

***exo*-43**

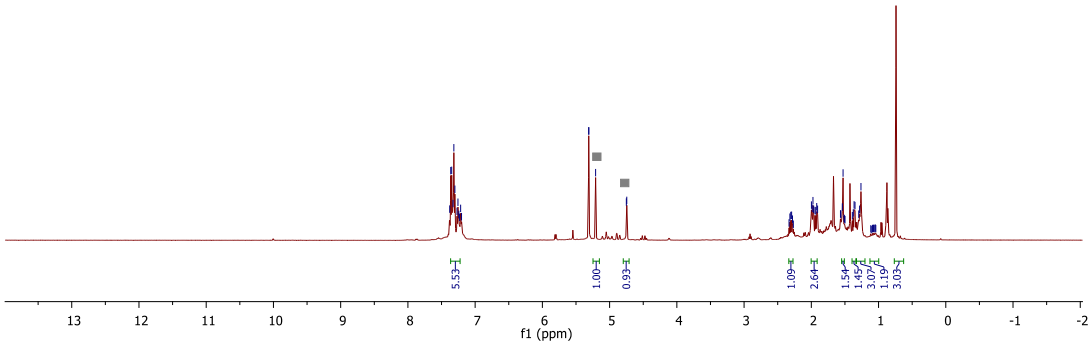

***exo*-43**

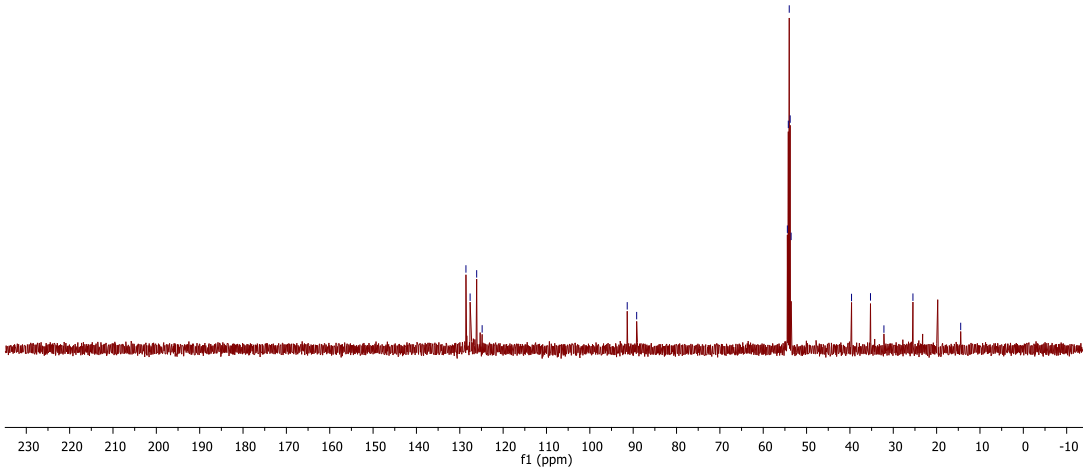

Aldehyde

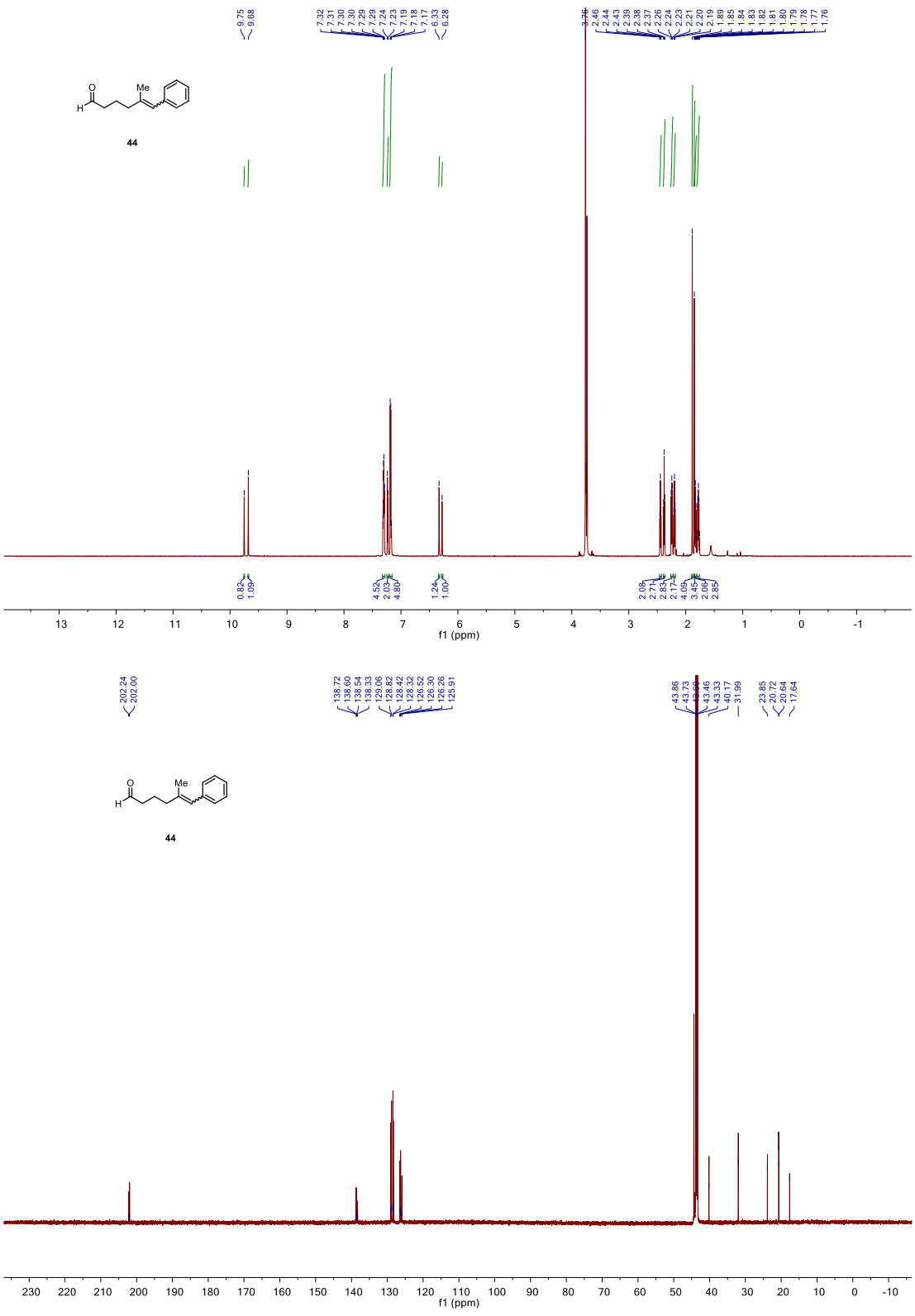

Carbonyl-Ene Byproducts

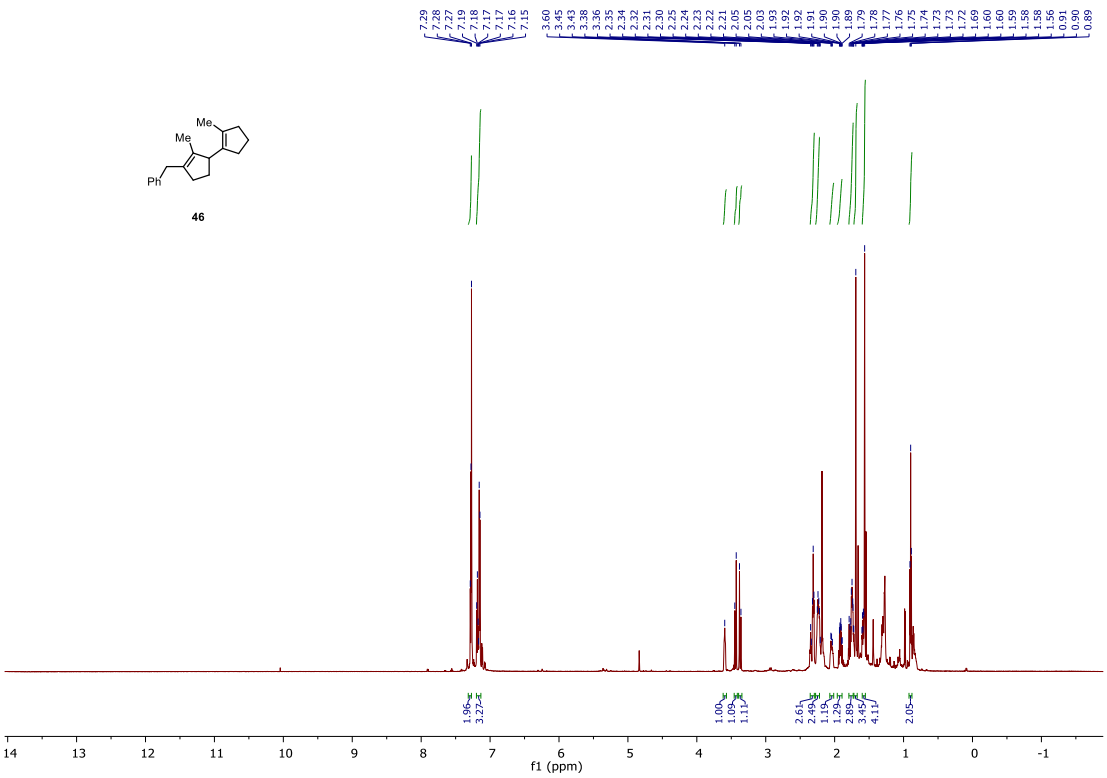
Me
Me
Ph
46
f1 (ppm)

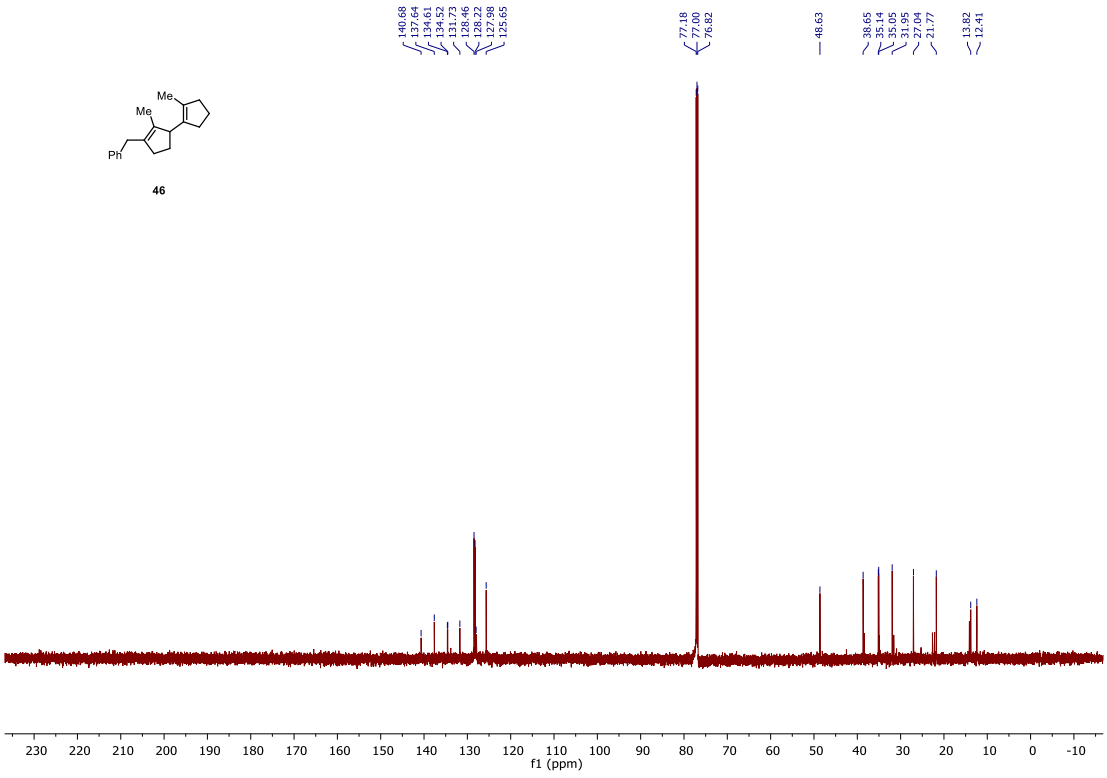
Me
Me
Ph
46
f1 (ppm)

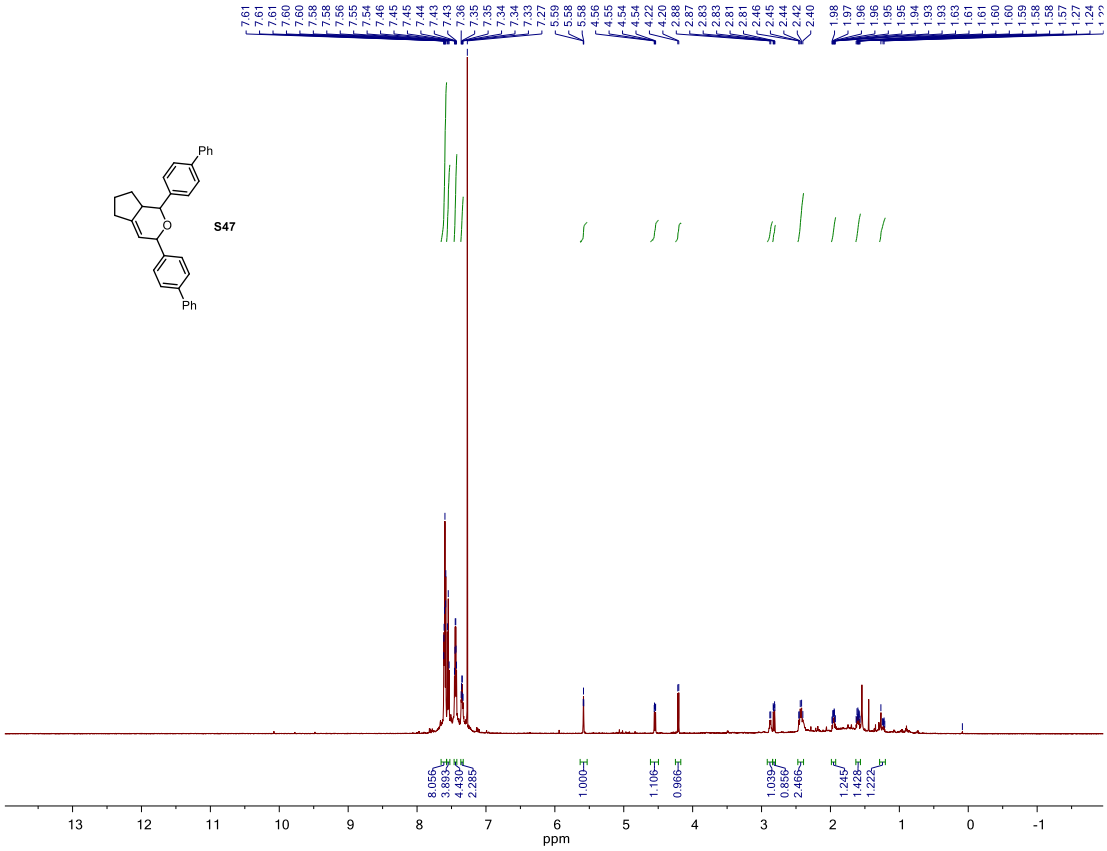
S47
Ph
Ph
ppm

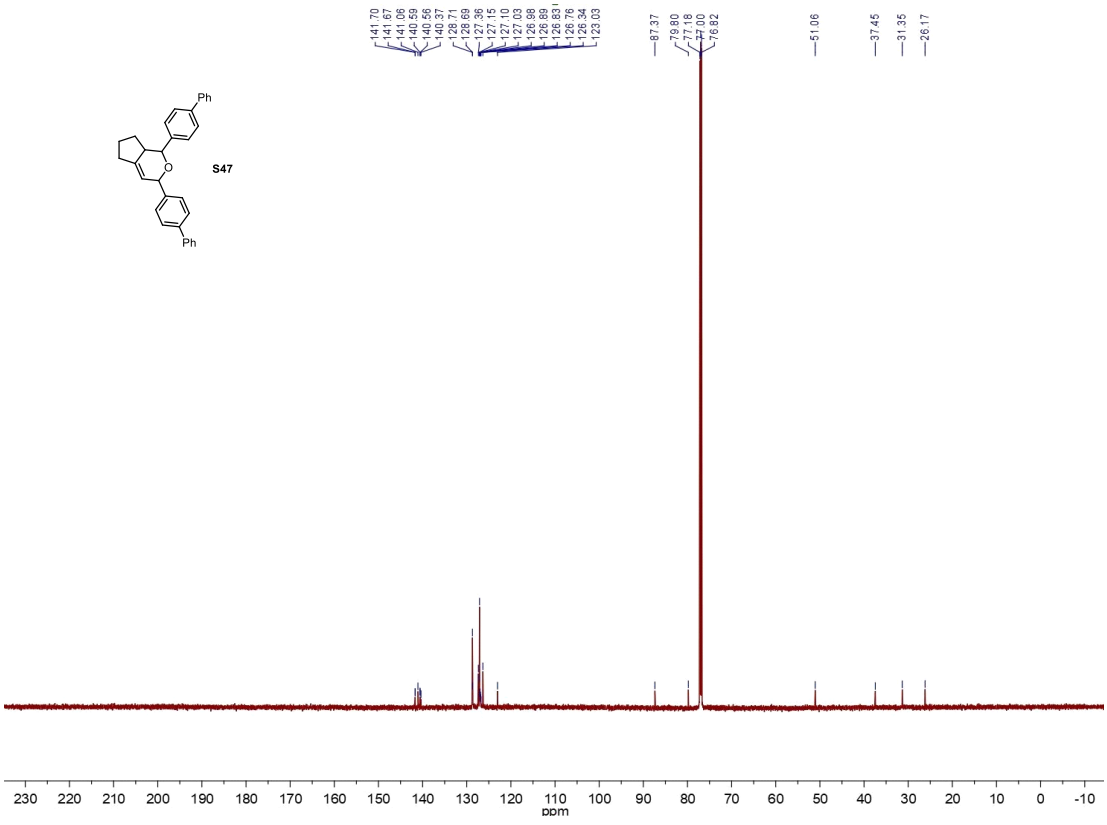
S47
Ph
Ph
ppm

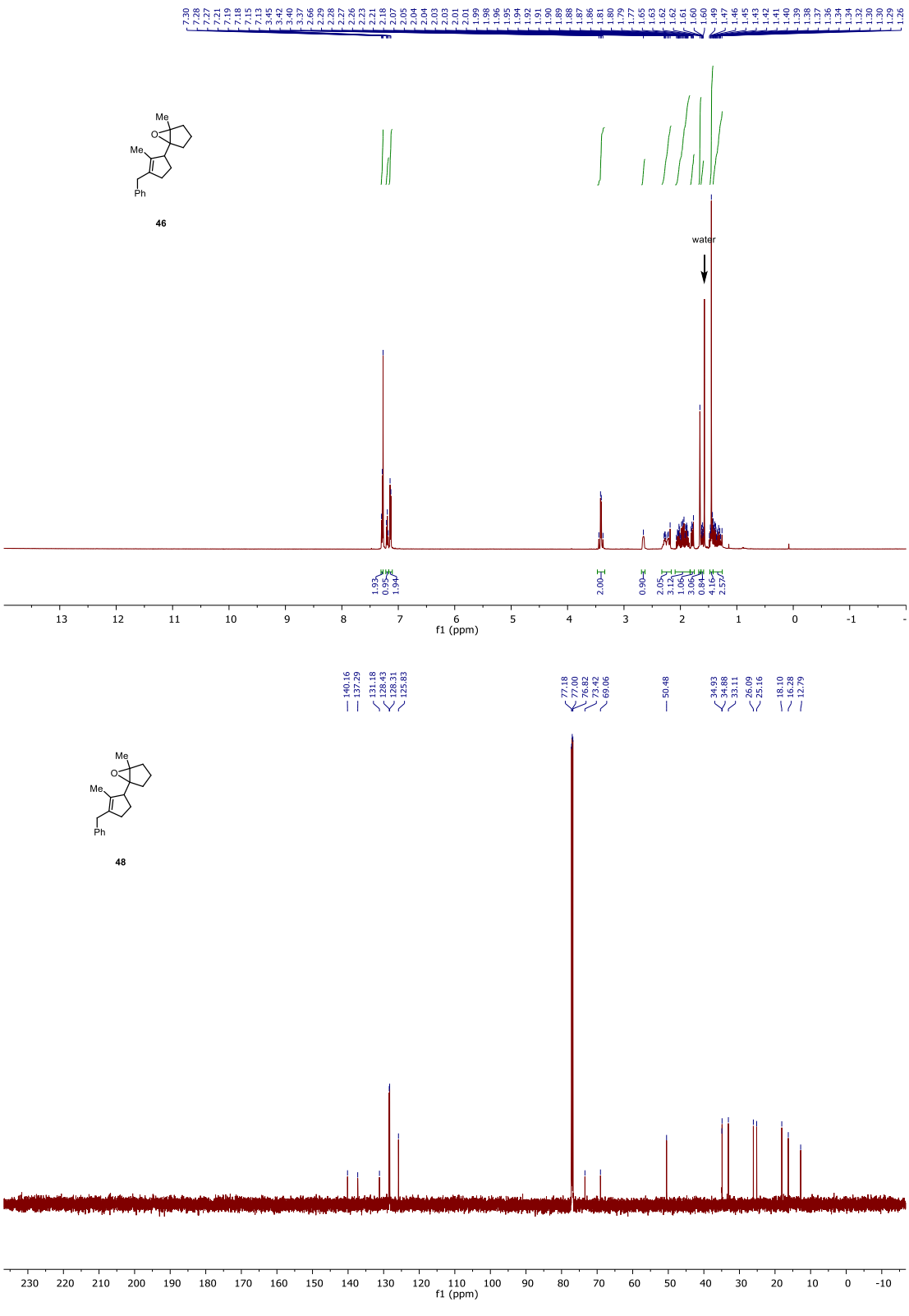

Adapted with permission from *Org. Lett.* **2018**, *20*, 4954−4958.
Copyright 2022 American Chemical Society.

2.6 References

1. *Handbook of Metathesis*, 2nd ed.; Grubbs, R. H., Wenzel, A. G., O'Leary, D. J., Khosravi, E., Eds.; Wiley-VCH: Weinheim, Germany, 2015; Vols. 1−3.
2. For selected examples of ring-opening cross-metathesis, see: (a) Snapper, M. L.; Tallarico, J. A.; Randall, M. L. Regio- and Stereoselective Ring-Opening Cross-Metathesis. Rapid Entry into Functionalized Bicyclo[6.3.0] Ring Systems. *J. Am. Chem. Soc.* **1997**, *119*, 1478−1479. (b) Tallarico, J. A.; Randall, M. L.; Snapper, M. L. Selectivity in Ring-Opening Metatheses. *Tetrahedron* **1997**, *53*, 16511−16520. (c) Cuny, G. D.; Cao, J.; Hauske, J. R. Ring Opening Cross-Metathesis on Solid Support. *Tetrahedron Lett.* **1997**, *38*, 5237−5240. (d) Michaut, M.; Parrain, J.-L.; Santelli, M. Selective Ring Opening Cross Metathesis of Cyclopropenone Ketal: A One Step Synthesis of Protected Divinyl Ketones. *Chem. Commun.* **1998**, *0*, 2567−2568. (e) Arjona, O.; Csáky, A. G.; Plumet, J. Regiochemical Aspects in the Ring Opening-Cross Metathesis of Bicyclic Alkenes. *Synthesis* **2000**, *2000*, 857−861. (f) Katayama, H.; Urushima, H.; Nishioka, T.; Wada, C.; Nagao, M.; Ozawa, F. Highly Selective Ring-Opening/Cross-Metathesis Reactions of Norbornene Derivatives Using Selenocarbene Complexes as Catalysts. *Angew. Chem., Int. Ed.* **2000**, *39*, 4513−4515. (g) Garber, S. B.; Kingsbury, J. S.; Gray, B. L.; Hoveyda, A. H. Efficient and Recyclable Monomeric and Dendritic Ru-Based Metathesis Catalysts. J. *Am. Chem. Soc.* **2000**, *122*, 8168−8170. (h) Arjona, O.; Csáky, A. G.; Murcia, C.; Plumet, J.; Mula, M. B. Regio- and Stereoselective Ring-Opening Dimerization–Cross-Coupling Metathesis of 7-Oxanorbornene Derivatives. *J. Organomet. Chem.* **2001**, *627*, 105−108. (i) Morgan, J. P.; Morrill, C.; Grubbs, R. H. Selective Ring Opening Cross Metathesis of Cyclooctadiene and Trisubstituted Cycloolefins. *Org. Lett.* **2002**, *4*, 67−70. (j) Weeresakare, G. M.; Liu, Z.; Rainier, J. D. Highly Regioselective Ring-Opening/Cross-Metathesis Reactions of 2-Sulfonylnorbornene Derivatives. *Org. Lett.* **2004**, *6*, 1625−1627.
3. For carbonyl−olefin metathesis reactions proceeding via oxetane photoadducts, see: (a) Jones, G., II; Schwartz, S. B.; Marton, M. T. 374 Regiospecific Thermal Cleavage of Some Oxetan Photoadducts: Carbonyl–Olefin Metathesis in Sequential Photochemical and Thermal Steps. *J. Chem. Soc., Chem. Commun.* **1973**, *11*, 374−375. (b) Jones, G., II; Acquadro, M. A.; Carmody, M. A. Long-Chain Enals via Carbonyl–Olefin Metathesis. An Application in Pheromone Synthesis. *J. Chem. Soc., Chem. Commun.* **1975**, 206−207. (c) Carless, H. A. J.; Trivedi, H. S. New Ring Expansion Reaction of 2-tButyloxetans. *J. Chem. Soc., Chem. Commun.* **1979**, *8*, 382−383. (d) Pérez-Ruiz, R.; Gil, S.; Miranda, M. A. Stereodifferentiation in the Photochemical Cycloreversion of Diastereomeric Methoxynaphthalene-Oxetane Dyads. *J. Org. Chem.* **2005**, *70*, 1376−1381. (e) Pérez-Ruiz, R.; Miranda, M. A.; Alle, R.; Meerholz, K.; Griesbeck, A. G. An Efficient Carbonyl-Alkene Metathesis of Bicyclic Oxetanes: Photoinduced Electron Transfer Reduction of the Paternò−Büchi Adducts from 2,3-Dihydrofuran and Aromatic Aldehydes. *Photochem. Photobiol. Sci.* **2006**, *5*, 51−55. (f) Valiulin, R. A.; Kutateladze, A. G. Harvesting the Strain Installed by a Paternò−Büchi Step in a Synthetically Useful Way: High-Yielding Photoprotolytic Oxametathesis in Polycyclic Systems. *Org. Lett.* **2009**, *11*, 3886−3889. (g) D'Auria, M.; Racioppi, R.; Viggiani, L. Paternò−Büchi Reaction Between Furan and Heterocyclic Aldehydes: Oxetane Formation vs. Metathesis. *Photochem. Photobiol. Sci.* **2010**, *9*, 1134−1138. (h) Valiulin, R. A.; Arisco, T. M.; Kutateladze, A. G. Double-Tandem $[4_\pi+2_\pi]\cdot[2_\pi+2_\pi]\cdot[4_\pi+2_\pi]\cdot[2_\pi+2_\pi]$ Synthetic Sequence with Photoprotolytic Oxametathesis and Photoepoxidation in the Chromone Series. *J. Org. Chem.* **2011**, *76*, 1319−1332. (i) Valiulin, R. A.; Arisco, T. M.; Kutateladze, A. G. Photoinduced Intramolecular Cyclopentanation vs Photoprotolytic Oxametathesis in

Polycyclic Alkenes Outfitted with Conformationally Constrained Aroylmethyl Chromophores. *J. Org. Chem.* **2013**, *78*, 2012−2025.

4. For Brønsted and Lewis acid-mediated carbonyl−olefin metathesis reactions, see: (a) Schopov, I.; Jossifov, C. A Carbonyl–Olefin Exchange Reaction – New Route to Polyconjugated Polymers, 1. A New Synthesis of Polyphenylacetylene. *Makromol. Chem., Rapid Commun.* **1983**, *4*, 659−662. (b) Jackson, A. C.; Goldman, B. E.; Snider, B. B. Intramolecular and Intermolecular Lewis Acid Catalyzed Ene Reactions Using Ketones as Enophiles. *J. Org. Chem.* **1984**, *49*, 3988–3994. (c) van Schiak, H.-P.; Vijn, R.-J.; Bickelhaupt, F. Acid-Catalyzed Olefination of Benzaldehyde. *Angew. Chem. Int. Ed.* **1994**, *33*, 1611–1612. (d) Jossifov, C.; Kalinova, R.; Demonceau, A. Carbonyl Olefin Metathesis. *Chim. Oggi* **2009**, *40*, 85−87. (e) Soicke, A.; Slavov, N.; Neudörfl, J.-M.; Schmalz, H.-G. Metal-Free Intramolecular Carbonyl–Olefin Metathesis of *ortho*-Prenylaryl Ketones. *Synlett* **2011**, *2011*, 2487−2490.
5. For a stoichiometric approach relying on molybdenum alkylidenes, see: Fu, G. C.; Grubbs, R. H. Synthesis of Cycloalkenes via Alkylidene-Mediated Olefin Metathesis and Carbonyl Olefination. *J. Am. Chem. Soc.* **1993**, *115*, 3800−3801.
6. For organocatalytic approaches, see: (a) Griffith, A. K.; Vanos, C. M.; Lambert, T. H. Organocatalytic Carbonyl–Olefin Metathesis. *J. Am. Chem. Soc.* **2012**, *134*, 18581−18584. (b) Hong, X.; Liang, Y.; Griffith, A. K.; Lambert, T. H.; Houk, K. N. Distortion-Accelerated Cycloadditions and Strain-Release-Promoted Cycloreversions in the Organocatalytic Carbonyl–Olefin Metathesis. *Chem. Sci.* **2014**, *5*, 471−475. (c) Zhang, Y.; Jermaks, J.; MacMillan, S. N.; Lambert, T. H. Synthesis of 2H Chromenes via Hydrazine-Catalyzed Ring-Closing Carbonyl–Olefin Metathesis. *ACS Catal.* **2019**, *9*, 9259−9264. (d) Lambert, T. H. Development of a Hydrazine-Catalyzed Carbonyl–Olefin Metathesis Reaction. *Synlett* **2019**, *30*, 1954−1965. (e) Jermaks, J.; Quach, P. K.; Seibel, Z. M.; Pomarole, J.; Lambert, T. H. Ring-Opening Carbonyl–Olefin Metathesis of Norbornenes. *Chem. Sci.*, **2020**, *11*, 7884-7895.
7. For Brønsted acid-catalyzed approaches, see: (a) Catti, L.; Tiefenbacher, K. Brønsted Acid-Catalyzed Carbonyl–Olefin Metathesis Inside a Self-Assembled Supramolecular Host. *Angew. Chem., Int. Ed.* **2018**, *57*, 14589−14592. (b) To, T. A.; Pei, C.; Koenigs, R.; Nguyen, T. V. Hydrogen Bonding Networks Enable Brønsted Acid-Catalyzed Carbonyl–Olefin Metathesis. *Preprint at* https://chemrxiv.org/engage/chemrxiv/article-details/615d8156f718df1626d54e8c.
8. For other approaches, see: (a) Pitzer, L.; Sandfort, F.; Strieth-Kalthoff, F.; Glorius, F. Carbonyl–Olefin Cross-Metathesis Through a Visible-Light-Induced 1,3-Diol Formation and Fragmentation Sequence. *Angew. Chem., Int. Ed.* **2018**, *57*, 16219−16223. (b) Rivero-Crespo, M.A.; Tejeda Serrano, M.; Perez-Sanchez, H.; Ceron-Carrasco, J. P.; Leyva-Perez, A. Intermolecular Carbonyl–Olefin Metathesis with Vinyl Ethers Catalyzed by Homogeneous and Solid Acids in Flow. *Angew. Chem., Int. Ed.* **2020**, 59, 3846−3849.
9. For a review on Lewis acid-catalyzed carbonyl–olefin metathesis reactions, see: [‡]Albright, H.; [‡]Davis, A. J.; [‡]Gomez-Lopez, J. L.; [‡]Vonesh, H. L.; Quach, P; Lambert, T. H.; Schindler, C. S. Carbonyl–Olefin Metathesis Reactions. *Chem. Rev.* **2021**, *121*, 9359–9406. [‡]Authors contributed equally.
10. For Lewis acid-catalyzed approaches, see: (a) Ludwig, J. R.; Zimmerman, P. M.; Gianino, J. B.; Schindler, C. S. Iron(III)-Catalysed Carbonyl–Olefin Metathesis. *Nature* **2016**, *533*, 374−379. (b) McAtee, C. M.; Riehl, P. S.; Schindler, C. S. Polycyclic Aromatic Hydrocarbons via Iron(III)-Catalyzed Carbonyl–Olefin Metathesis. *J. Am. Chem. Soc.* **2017**, *139*, 2960−2963. (c) Ludwig, J. R.; Phan, S.; McAtee, C. M.; Zimmerman, P. M.; Devery, J. J.; Schindler, C. S.

Mechanistic Investigations of the Iron(III)-Catalyzed Carbonyl–Olefin Metathesis Reaction. *J. Am. Chem. Soc.* **2017**, *139*, 10832−10842. (d) Groso, E. J.; Golonka, A. N.; Harding, R. A.; Alexander, B. W.; Sodano, T. M.; Schindler, C. S. 3-Aryl-2,5-Dihydropyrroles via Catalytic Carbonyl–Olefin Metathesis. *ACS Catal.* **2018**, *8*, 2006−2011. (e) Albright, H.; Vonesh, H. L.; Becker, M. R.; Alexander, B. W.; Ludwig, J. L.; Wiscons, R. A.; Schindler, C. S. $GaCl_3$-Catalyzed Ring-Opening Carbonyl–Olefin Metathesis. *Org. Lett.* **2018**, *20*, 4954−4958. (f) Albright, H.; Riehl, P. S.; McAtee, C. M.; Reid, J. P.; Ludwig, J. R.; Karp, L. A.; Zimmerman, P. M.; Sigman, M. S.; Schindler, C. S. Catalytic Carbonyl–Olefin Metathesis of Aliphatic Ketones: Iron(III) Homo-Dimers as Lewis Acidic Superelectrophiles. *J. Am. Chem. Soc.* **2019**, *141*, 1690−1700. (g) Riehl, P. S.; Nasrallah, D. J.; Schindler, C. S. Catalytic Transannular Carbonyl–Olefin Metathesis Reactions. *Chem. Sci.* **2019**, *10*, 10267−10274. (h) Rykaczewski, K. A.; Groso, E. J.; Vonesh, H. L.; Gaviria, M. A.; Richardson, A. D.; Zehnder, T. E.; Schindler, C. S. Tetrahydropyridines via $FeCl_3$-Catalyzed Carbonyl−Olefin Metathesis. *Org. Lett.* **2020**, *22*, 7, 2844−2848. (i) Albright, H.; Vonesh, H. L.; Schindler, C. S. Superelectrophilic Fe(III)-Ion Pairs as Stronger Lewis Acid Catalysts for (*E*)-Selective Intermolecular Carbonyl−Olefin Metathesis. *Org. Lett.* **2020**, *22*, 3155−3160. (j) Davis, A. J.; Watson, R. B.; Nasrallah, D. J.; Gomez-Lopez, J. L.; Schindler, C. S. *Nat. Catal.* **2020**, *3*, 787−796. (k) Naidu, V. R.; Bah, J.; Franzén, J. Direct Organocatalytic Oxo-Metathesis, a *trans*-Selective Carbocation-Catalyzed Olefination of Aldehydes. *Eur. J. Org. Chem.* **2015**, *2015*, 1834−1839. (l) Ma, L.; Li, W.; Xi, H.; Bai, X.; Ma, E.; Yan, X.; Li, Z. $FeCl_3$-Catalyzed Ring-Closing Carbonyl–Olefin Metathesis. *Angew. Chem., Int. Ed.* **2016**, *55*, 10410−10413. (m) Ni, S.; Franzén, J. Carbocation Catalysed Ring Closing Aldehyde-Olefin Metathesis. *Chem. Commun.* **2018**, *54*, 12982−12985. (n) Tran, U. P. N.; Oss, G.; Pace, D. P.; Ho, J.; Nguyen, T. V. Tropylium-Promoted Carbonyl–Olefin Metathesis Reactions. *Chem. Sci.* **2018**, *9*, 5145−5151. (o) Tran, U. P. M.; Oss, G.; Breugst, M.; Detmar, E.; Pace, D. P.; Liyanto, K.; Nguyen, T. V. Carbonyl–Olefin Metathesis Catalyzed by Molecular Iodine. *ACS Catal.* **2019**, *9*, 912−919. (p) Hanson, C. S.; Psaltakis, M. C.; Cortes, J. J.; Devery, J. J. Catalyst Behavior in Metal-Catalyzed Carbonyl–Olefin Metathesis. *J. Am. Chem. Soc.* **2019**, *141*, 11870−11880. (q) Djurovic, A.; Vayer, M.; Li, Z.; Guillot, R.; Blataze, J.-P.; Gandon, V.; Bour, C. Synthesis of Medium-Sized Carbocycles by Gallium-Catalysed Tandem Carbonyl–Olefin Metathesis/Transfer Hydrogenation. *Org. Lett.* **2019**, *21*, 8132–8137. (r) Wang, R.; Chen, Y.; Shu, M.; Zhao, W.; Tao, M.; Du, C.; Fu, X.; Li, A.; Lin, Z. $AuCl_3$-Catalyzed Ring-Closing Carbonyl–Olefin Metathesis. *Chem. Eur. J.* **2020**, *26*, 1941–1946. (s) Hanson, C. S.; Psaltakis, M. C.; Cortes, J. J.; Siddiqi, S. S.; Devery, J. J. Investigation of Lewis Acid-Carbonyl Solution Interactions via Infrared-Monitored Titration. *J. Org. Chem.* **2020**, *85*, 820−832.

11. Schleyer, P. V. R.; Williams, J. E.; Blanchard, K. R. Evaluation of Strain in Hydrocarbons. The Strain in Adamantane and its Origin. *J. Am. Chem. Soc.* **1970**, *92*, 2377−2386.
12. Griesback, A. G.; Stadtmueller, S. Electronic Control of Stereoselectivity in Photocycloaddition Reactions. 4. Effects of Methyl Substituents at the Donor Olefin. *J. Am. Chem. Soc.* **1991**, *113*, 6923−6928.
13. Dolomanov, O. V., Bourhis, L. J., Gildea, R. J., Howard, J. A. K., Puschmann, H. *OLEX2*: A Complete Structure Solution, Refinement and Analysis Program. *J. Appl. Cryst.* **2009**, *42*, 339−341.
14. Sheldrick, G. M. *SHELXT* – Integrated Space-Group and Crystal-Structure Determination. *Acta Cryst. A* **2015**, *71*, 3−8.
15. Sheldrick, G. M. Crystal Structure Refinement with *SHELXL*. *Acta Cryst. C* **2015**, *71*, 3−8.

16. Ryan, J., Šiaučiulis, M., Gomm, A., Maciá, B., O'Reilly, E., Caprio, V. Transaminase Triggered Aza-Michael Approach for the Enantioselective Synthesis of Piperidine Scaffolds. *J. Am. Chem. Soc.* **2016,** *138,* 15798−15800.

Chapter 3: Intermolecular Cross Carbonyl–Olefin Metathesis

*Portions of this work have been published in:

Albright, H.;‡ Vonesh, H. L.;‡ Schindler, C. S. Superelectrophilic Fe(III)-Ion Pairs as Stronger Lewis Acid Catalysts for *(E)*-Selective Intermolecular Carbonyl–Olefin Metathesis. *Org. Lett.* **2020**, *22*, 3155−3160. ‡Authors contributed equally.

3.1 Introduction

Olefin–olefin cross-metathesis reactions are among the most prevalent and fundamental tools for direct carbon-carbon bond formation and allow access to more complex olefins from simple olefin precursors.[1] In traditional olefin–olefin cross-metathesis, a metal alkylidene catalyst reacts with olefins **1** and **2**, which are converted to the corresponding heterodimerization product **3** or homodimerization products **4** and **5** (Figure 3.1).[2] The selectivity between these products can be controlled and depends on the choice of substrates, the ratio of the two olefin starting materials, and the type of metal alkylidene catalyst employed.[3,4] *(E)*-olefins are the thermodynamically favored products, however a mixture of both diastereomers is generally observed.[2]

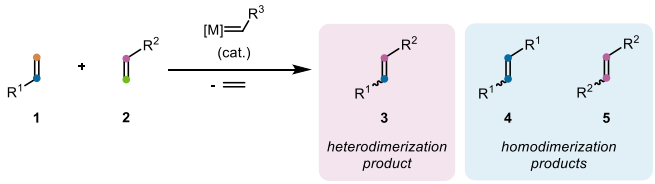

Figure 3.1: Traditional olefin–olefin cross metathesis.

More recently, there has been an increased interest in carbonyl–olefin metathesis due the ability to directly form carbon-carbon bonds between carbonyl and olefin functionalities.[5-10] In an effort to discover new and more efficient carbonyl–olefin metathesis protocols, several Lewis acid-catalyzed approaches have been developed.[11-12] These Lewis acid-catalyzed reactions form intermediate oxetanes through either stepwise or concerted [2+2]-cycloaddition pathways, followed by a subsequent stepwise fragmentation or retro-[2+2]-cycloaddition to yield the corresponding carbonyl–olefin metathesis products. Based on this design principle, a number of

protocols have been developed for ring-closing, ring-opening, and transannular carbonyl–olefin metathesis that proceed through oxetane intermediates.[11] Additional approaches for intermolecular cross carbonyl–olefin metathesis exist relying on either visible-light-induced 1,3-diol formation,[9a] solid state Lewis acids,[9b] carbocations as organic Lewis acids,[12k,12n] or molecular iodine[12o] (Figure 3.2). In comparison to olefin–olefin cross-metathesis, the currently available protocols for cross carbonyl–olefin metathesis remain limited in scope, yield, and are significantly underdeveloped.

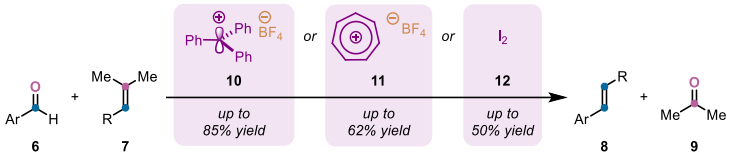

Figure 3.2: Recent reports of Lewis acid-catalyzed intermolecular cross carbonyl–olefin metathesis.

Detailed mechanic investigations of iron(III)-catalyzed carbonyl–olefin metathesis determined that the $FeCl_3$ activates aryl carbonyls in a monomeric fashion, and kinetic experiments determined the rate order to be 1 (**13**, Figure 3.3).[12c] Continued studies for aliphatic ketone substrates, which are notoriously more difficult to engage under Lewis acid catalysis, were also performed and surprisingly, a rate order of 2 was measured for $FeCl_3$ (**14**, Figure 3.3).[12f]

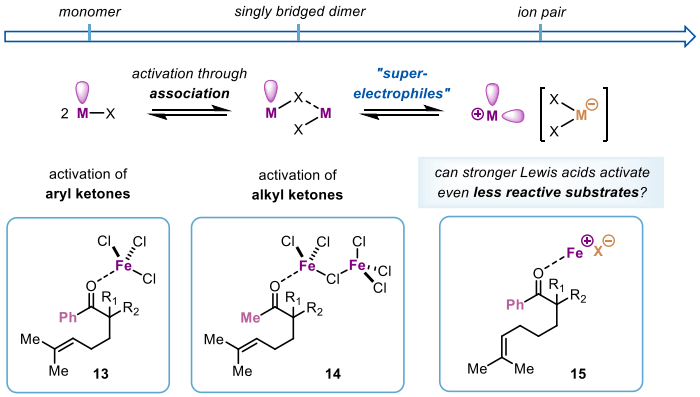

Figure 3.3: Activation of less reactive carbonyl substrates by stronger Lewis acids.

This new finding suggests that stronger Lewis acids are formed by dimerization through Lewis acid/Lewis base interactions of the $FeCl_3$. Stronger Lewis acid catalysts are created *via* dimerization and subsequent ionization can potentially activate unreactive substrates (such as **15**, Figure 3.3). The notion of utilizing stronger Lewis acids was applied to engage previously unreactive, substituted aryl ketone substrates for ring-closing carbonyl–olefin metathesis to form medium-sized rings.[12j] $AlCl_3$ in combination with $AgSbF_6$ promotes chloride abstraction, which

forms an ion pair, $[AlCl_2]^+[SbF_6]$, that acts as the active Lewis acid catalyst; ultimately providing metathesis products for 26 examples in up to 99% yield (**17** and **18**, Figure 3.4).

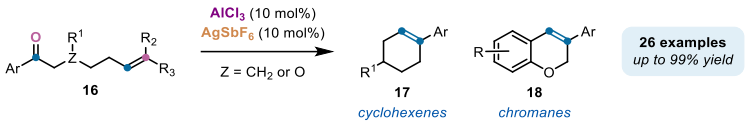

Figure 3.4: 6-membered ring formation via a superelectrophilic aluminum/silver ion pair catalyst.

The aluminum/silver ion pair catalyst promotes a concerted carbonyl-ene/hydroalkoxylation pathway, forming the key oxetane intermediate, for carbonyl–olefin metathesis. Ion pair catalyst's ability to form oxetane intermediates was the foundation of this approach for a more selective intermolecular cross carbonyl–olefin metathesis protocol. Previous reports are not generally selective for *(E)*- or *(Z)*-olefins, and more recent reports suffer from lower yields and continued lack of selectivity. The proposed application of a more reactive Lewis acid dimer or ion pair would aim to selectively form one of the four possible regio- and diastereomeric oxetane intermediates, followed by subsequent fragment, to provide one of the three possible metathesis products.

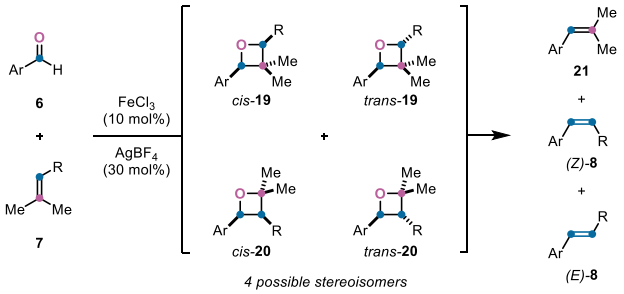

Figure 3.5: *This work:* Intermolecular cross carbonyl–olefin metathesis promoted via an iron/silver ion pair catalyst.

This work showcases the detailed mechanistic investigations into the controlling features of Lewis acid-catalyzed intermolecular cross carbonyl–olefin metathesis, specifically focusing on the substrate scope and competing reaction pathways. The study also investigates a multitude of Lewis acids, Lewis acid dimers, and ion pairs that could be applied for a more general reaction protocol. The intermolecular cross carbonyl–olefin metathesis between aromatic aldehydes **6** and olefins **7**—relying on superelectrophilic Fe(III)-ion pairs[12j,12q] as stronger Lewis acid catalysts—could result in four possible diastereomers (*cis*- and *trans*-**19** and **20**) that would lead to three distinct metathesis products (**21**, *(Z)*-**8**, and *(E)*-**8**; Figure 3.5). The potential to selectively generate

one diastereomer or regioisomer would increase the efficiency of intermolecular cross carbonyl–olefin metathesis. The mechanistic studies conducted are consistent with regiospecific oxetane formation (*cis*- and *trans*-**20**) and subsequent stereospecific oxetane fragmentation (*trans*-**20**), which accounts for the high selectivity in products seen over the course of these investigations. Insights gained from this will guide further reaction development and catalyst design and continues to expand and improve the synthetic utility of available protocols.

3.2 Results and Discussion

Benzaldehyde (**22**) and 2-methyl-2-butene (**23**) were utilized as the initial aryl aldehyde and olefin substrates for optimization of intermolecular cross carbonyl–olefin metathesis (Figure 3.6). Early efforts identified a 5:1 ratio of **22**:**23** as optimal for the transformation (see 3.5.2 , Table 3.10). In their report, Franzén and co-workers achieved 60% yield of **24** otherwise identical conditions to entry 1, Figure 3.6, with $TrBF^{\neg 4}$ (20 mol%) acting as a cationic catalyst.[12k] In comparison, traditional Lewis acids, such as $BF_3{\cdot}OEt_2$ and $FeCl_3$ promoted the desired transformation in 28% and 19% yield, respectively (entries 1 and 2, Figure 3.6).

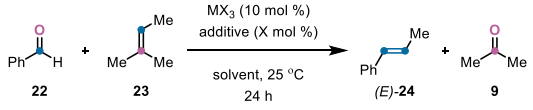

entry	Lewis acid	additive	mol %	solvent	yield (%)
1[a]	$BF_3{\cdot}Et_2O$	-	-	DCM	28
2[a]	$FeCl_3$	-	-	DCM	19
3[a]	$FeCl_3$	-	-	DCE	16
4[a]	$FeCl_3$	-	-	toluene	2
5[a]	$GaCl_3$	-	-	DCM	17
6[a]	$AlCl_3$	-	-	DCM	0
7[a]	$Fe(OTf)_3$	-	-	DCM	30
8[a]	$Sc(OTf)_3$	-	-	DCM	26
9[b]	$FeCl_3$	AgOTs	30	DCM	0
10[b]	$FeCl_3$	$AgAsF_6$	30	DCM	31
11[b]	$FeCl_3$	$AgSbF_6$	30	DCM	24
12[b]	$FeCl_3$	$AgPF_6$	30	DCM	36
13[c]	**$FeCl_3$**	**$AgBF_4$**	**30**	**DCM**	**51**
14[b]	$FeCl_3$	$AgBF_4$	100	DCM	28
15[b]	$FeCl_3$	$AgBF_4$	20	DCM	27
16[b]	$FeCl_3$	$AgBF_4$	10	DCM	20
17[b]	$GaCl_3$	$AgBF_4$	30	DCM	35
18[d]	$FeCl_3$	$AgBF_4$	30	DCM	27
19[e]	$FeCl_3$	$AgBF_4$	30	DCM	19

Conditions: All reactions were performed using 5.0 equivalents of the substrate **22** and 1 equivalent of **23** in DCM (0.3 M) at 25 °C for 24 h. Yields are reported based on NMR analysis[a], GC analysis[b], or isolated yield[c]. [d]2.0 equivalents of **22** were used. [e]1.0 equivalent of **22** was used.

Figure 3.6: Reaction optimization.

Evaluating different solvents including dichloroethane and toluene, under otherwise identical reaction conditions lead to decreased yields of **24** (entries 3 and 4, Figure 3.6). $GaCl_3$ was analogous to $FeCl_3$ and resulted in 17% yield of the desired metathesis product (entry 5, Figure 3.6), while stronger Lewis acids, such as $AlCl_3$, were unsuccessful in promoting the desired carbonyl–olefin metathesis (entry 6, Figure 3.6). Promising results were also obtained with catalytic amounts of metal triflates, $Fe(OTf)_3$ and $Sc(OTf)_3$, resulting in the formation of *(E)*-olefin **24** in increased yields of 30% and 26%, respectively (entries 7 and 8, Figure 3.6).

Recently, the Schindler group showed that heterobimetallic ion pairs[12j] function as Lewis acidic superelectrophiles and are able to promote catalytic carbonyl–olefin metathesis.[12j,12q] These heterobimetallic ion pair catalyst are formed through halide abstraction from neutral metal salts (MX_n) with silver salts (AgX).[13] Employing the same hypothesis, catalytic amounts of silver salts were combined with $FeCl_3$ as the Lewis acid and resulted in increased yields of the desired carbonyl–olefin metathesis product **24** (entries 9-13, Figure 3.6). Specifically, $AgBF_4$ (30 mol%) was identified as the optimal silver salt, and together with $FeCl_3$, provided **24** in 51% yield (entry 13, Figure 3.6). Increasing or decreasing the amount of $AgBF_4$ under otherwise identical conditions resulted in diminished yields of **24** (entries 14, 15, and 16, Figure 3.6). $GaCl_3$—which had similar yields to $FeCl_3$—was also evaluated in combination with 30 mol% of $AgBF_4$, however, this combination was unproductive, yielding only 35% (entry 17, Figure 3.6). Importantly, *(E)*-olefin **24** was observed as the exclusive carbonyl–olefin metathesis product for all Lewis acids and reaction conditions evaluated; the *(Z)*-olefin metathesis product was not observed.

Subsequent efforts focused on gaining experimental support for heterobimetallic ion pairs active as the active catalyst species under the optimal reaction conditions. Several Lewis acidic species could potentially operate as the active catalyst: $FeCl_3$ (**A**), $AgBF_4$ (**B**), heterobimetallic ion pairs $[FeCl_2]^+[BF_4]^-$ (**C**) and/or $[Fe]^{3+}3[BF_4]^-$ (**D**) resulting from chloride abstraction, or $FeCl_2F$ (**E**), FeF_3 (**F**), and BF_3 (**G**), formed *via* fluoride transfer or decomposition of **C** and **D** (Figure 3.7). As previously demonstrated, $FeCl_3$, alone, only formed the metathesis product **24** in 19% yield, while the sole use of $AgBF_4$ failed to promote the desired transformation all together; eliminating **A** and **B** as active catalyst (entries 1 and 2, Figure 3.7). Equimolar loadings of 10 mol% $FeCl_3$ and $AgBF_4$ were able to catalyze the reaction in equally low yields of 20% (entry 3, Figure 3.7). In comparison, the optimal reaction conditions relying on $FeCl_3$ (10 mol%) and $AgBF_4$ (30 mol%)

provided **24** in 51% yield (entry 4, Figure 3.7). Quantitative formation of AgCl, as a white solid, is observed over the course of this transformation (see 3.5.2, Table 3.4).

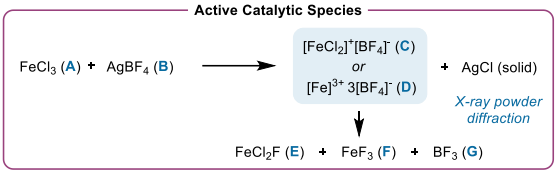

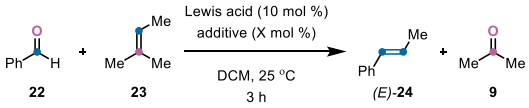

entry	species	Lewis acid	additive	X mol %	yield (%)
1[a]	A	$FeCl_3$	-	-	19
2[b]	B	-	$AgBF_4$	30	0
3[c,d]	C	$FeCl_3$	$AgBF_4$	10	20
4[b,d]	**D**	**$FeCl_3$**	**$AgBF_4$**	**30**	**51**
5[b]	E	$FeCl_3$	AgF	10	4
6[b]	F	$FeCl_3$	AgF	30	9
7[a]	F	FeF_3	-	-	0
8[a]	G	$BF_3{\cdot}Et_2O$	-	-	28

Conditions: All reactions were performed using 5.0 equivalents of **22** and 1.0 equivalent of **23** in DCM (0.3 M) at 25 °C for 3 h. Yields were determined *via* NMR[a] with $PhMe_3Si$ an an internal standard, based on isolated[b] yield, or by GC.[c] The formation of AgCl was observed.[d]

Figure 3.7: Evaluation of active catalytic species.

To evaluate **E**, $FeCl_3$ and AgF (both in 10 mol%) were combined and resulted in the formation of product. This result suggests that $FeCl_2F$ may be formed under these conditions albeit, **24** was observed in only 4% yield, making **E** unlikely as the operating catalyst (entry 5, Figure 3.7). $FeCl_3$ and AgF (in 10 and 30 mol%, respectively) provided only 9% yield of the desired metathesis product whereas FeF_3 resulted in 0% yield of **24** (entries 6 and 7, Figure 3.7). Together, these results eliminated **F** as an active catalyst for this transformation and confirmed that FeF_3 it is not forming from fluoride transfer in the presence of F^- ions from the $AgBF_4$ additive. Furthermore, when the reaction was conducted with $BF_3{\cdot}Et_2O$ (10 mol%), the **24** was observed in diminished yields of 28% (entry 8, Figure 3.7). Collectively, these results suggest the formation of $[FeCl_2]^+[BF_4]^-$, and most likely $[Fe]^{3+}3[BF_4]^-$ (due to the quantitative formation of AgCl), as heterobimetallic ion pairs which serve as the active catalytic species under the optimal conditions for intermolecular cross carbonyl–olefin metathesis.

The olefin substrate scope for intermolecular cross carbonyl–olefin metathesis was investigated next (Figure 3.8). Substitution of longer aliphatic chains for the olefin moiety—including ethyl, isobutyl, and *n*-heptyl—were viable and formed the respective metathesis products

in up to 40% yield (**28**-**30**, Figure 3.8). 2-ethyl-2-pentene (**31**) was also found to be reactive and provided 23% yield of the metathesis product, while styrene derivative **32**, as well as other styrene derivatives, were unreactive under the optimized reaction conditions. Importantly, the corresponding *(E)*-olefins were the exclusive metathesis products observed over the course of these transformations.

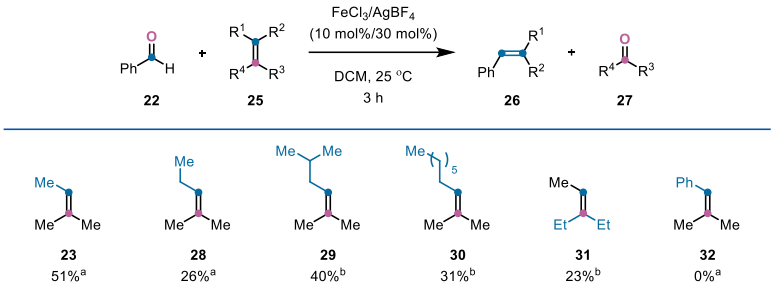

Conditions: All reactions were performed with 5.0 equiv. aldehyde and 1.0 equiv. of olefin substrates with 10 mol% $FeCl_3$ and 30 mol% $AgBF_4$ in DCM (0.3 M) at 25 °C for 3 h.[a]benzaldehyde as aldehyde. [b]4-chlorobenzaldehyde as aldehyde.

Figure 3.8: Evaluation of the olefin substrate scope.

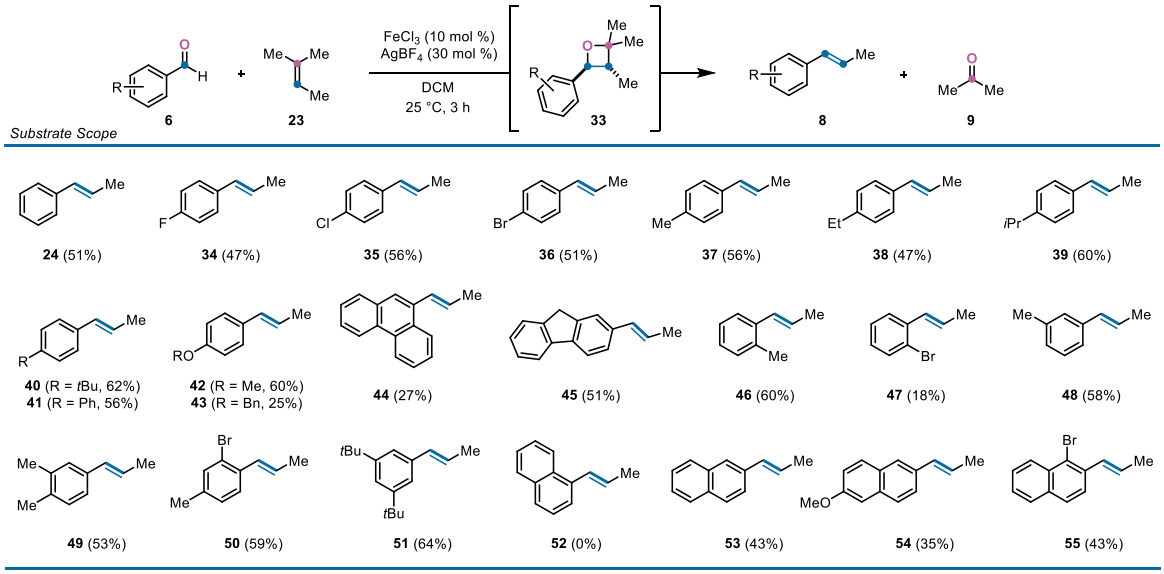

Conditions: All reactions were performed with 5.0 equivalents of aldehyde and 1.0 equivalent of olefin substrate, $FeCl_3$ (10 mol %), and $AgBF_4$ (30 mol %) in dichloromethane (0.3 M) at 25 °C for 3 h.

Figure 3.9: Aldehyde scope for intermolecular cross carbonyl–olefin metathesis.

Following the exploration of the olefin scope, aldehyde substrates were investigated (Figure 3.9). *Para*-substituted aryl aldehydes with both electron-withdrawing and electron-donating groups were viable under the optimized reaction conditions, resulting in up to 62% yield of the metathesis products (**34**-**43**, Figure 3.9). Polyaromatic substrates including phenanthrene-

and fluorene-derived aryl aldehydes promoted the desired metathesis transformation in low to moderate yields of 27% and 51%, respectively (**44** and **45**, Figure 3.9). *Ortho*-, *meta*-, *para*-, and multi-substituted aldehydes were also compatible for intermolecular cross carbonyl–olefin metathesis and formed the desired products in yields of up to 64% (**46**-**51**, Figure 3.9). Furthermore, 2-naphthaldehyde substrates provided moderate yields in up to 43% (**53**-**55**, Figure 3.9). In accordance with the previous observations made while studying the controlling features of this transformation, only *(E)*-olefin metathesis products were observed.

3.3 Mechanistic Investigations

The inherent reactivity of carbonyls and olefins are thoroughly discussed in various chapters (Chapters 1 and 4), and carbonyl-ene and Prins reaction pathways could be operative under the reaction conditions for intermolecular cross carbonyl–olefin metathesis. An aldehyde and olefin could undergo a Lewis acid-catalyzed carbonyl-ene reaction to form a reactive intermediate that could subsequently eliminate water, forming the observed metathesis product. To investigate the viability of this postulation, carbonyl-ene products **56** and 5**7** were independently prepared and subjected to the optimized reaction conditions (Figure 3.10). Both carbonyl-ene intermediates were not reactive, indicating that this is not the operative mechanistic pathway for this transformation.

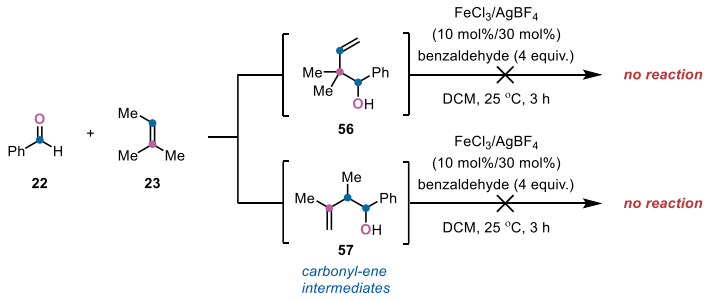

Figure 3.10: Evaluation of a carbonyl-ene pathway.

Subsequent efforts aimed to determine the origin of the exclusive *(E)*-selectivity observed in this transformation. Upon addition of aryl aldehydes **6** and olefins **7**, four distinct oxetane stereoisomers could form (Figure 3.11). *Trans*- and *cis*-oxetanes **19** are predicted to be the minor products formed, whereas *trans*- and *cis*-oxetanes **20** would be expected as the major isomers due to the carbonyl oxygen atom adding to the more electrophilic carbon of the olefin. Fragmentation of these oxetane intermediates could result in three distinct metathesis products: *(E)*-**8** formed upon

fragmentation of *trans*-**20**, *(Z)*-**8** resulting from *cis*-**20**, and trisubstituted alkene **20** as the product obtained from both, *cis*- and *trans*-**19**.

Trans-**58**[14] was synthesized independently *via* Paternò–Büchi chemistry and then subjected to the optimized reaction conditions (Figure 3.11, I). The only product observed was trisubstituted olefin **32**, which was stable under reaction conditions. Olefin **32** is not observed under the optimized reaction for intermolecular cross carbonyl–olefin metathesis. This result suggests that regioisomeric oxetanes *cis*- and/or *trans*-**19** are not formed as reactive intermediates in this transformation, confirming the observed lack of olefin product **21**.

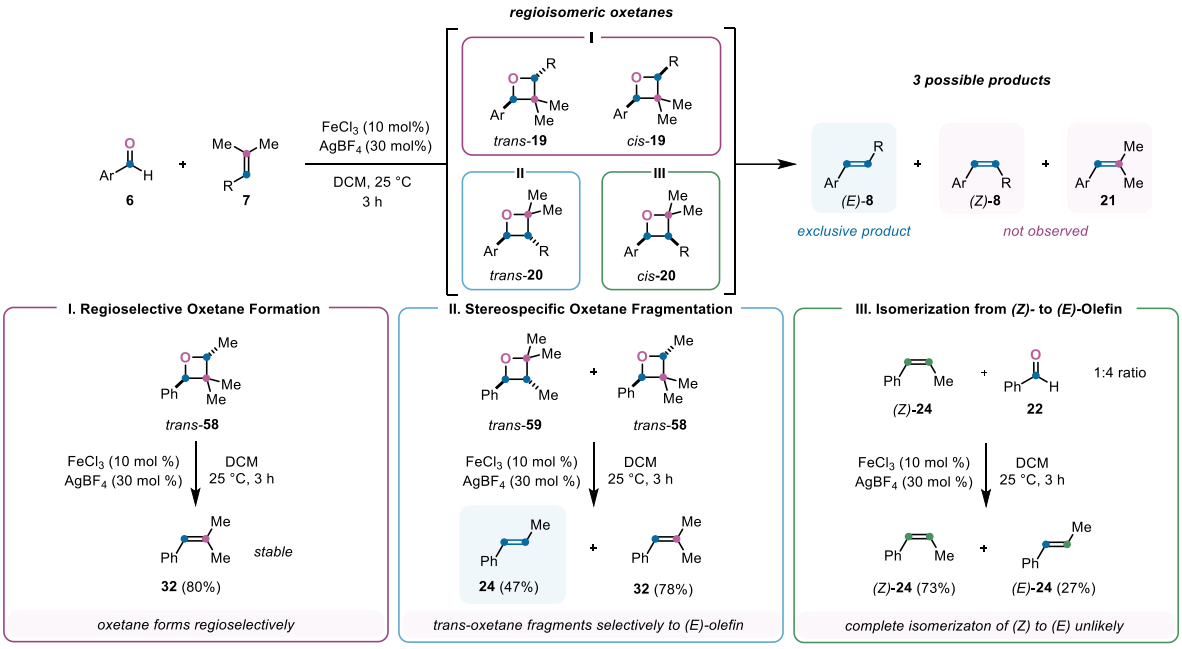

Figure 3.11: Mechanistic investigations for intermolecular cross carbonyl–olefin metathesis. Experiments in support of **I.** regioselective oxetane formation, **II.** stereospecific oxetane fragmentation, and lack of **III**. (*E*)-olefin product isomerization.

To investigate whether oxetane *trans*-**20** fragments stereospecifically, *trans*-**59**[14] was synthesized *via* Paternò–Büchi chemistry as a mixture of isomers (with *trans*-**58**, Figure 3.11, II). *Trans*-**59**, together with *trans*-**58**, were characterized as a mixture of oxetanes (in a 2.6:1 ratio, *trans*-**58**:*trans*-**59**) and subjected to the optimal reaction conditions (Figure 3.11, II and Figure 3.12). The expected olefin metathesis products *(E)*-**24** and **32** were observed in 47% and 78% yield, resulting from the fragmentation of *trans*-**59** and *trans*-**58**, respectively. This result confirmed the stereospecific oxetane fragmentation *trans*-**58**. The corresponding stereoisomer *(Z)*-**8** was not observed over the course of any of these transformations.

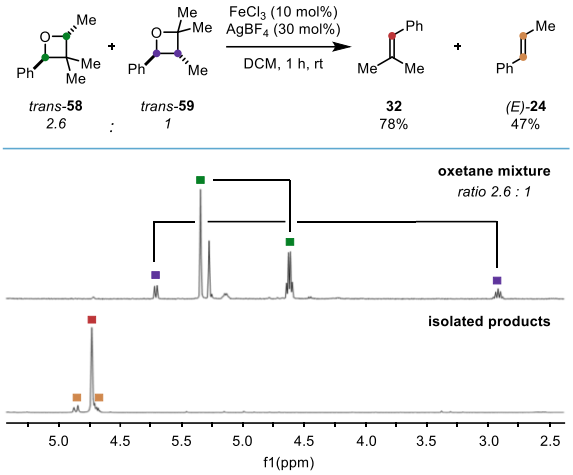

Figure 3.12: ^{1}H-NMRs of oxetanes *trans*-**58** and *trans*-**59** and their subsequent fragmentation.

Another possible reaction pathway that could be operative under the optimized reaction conditions was the isomerization of *(Z)*-**8**, which could proceed rapidly under the optimized reaction conditions. To test this notion, *(Z)*-**24** was combing with benzaldehyde (**22**) in a 1:4 ratio, to mimic optimal reaction conditions (Figure 11, III). Isomerization from *(Z)*-**24** to *(E)*-**24** was observed, however, in only 23% yield over the course of the transformation.

These combined results suggest that under the optimized reaction conditions for intermolecular cross carbonyl–olefin metathesis, aldehydes **6** and olefin **7** regioselectively form *trans*- and *cis*-**20**, and *trans*-**20** fragments stereospecificly, resulting in the exclusive formation of *(E)*-olefin products **8**. Additionally, intermolecular cross carbonyl–olefin metathesis of benzaldehyde **22** and trisubstituted olefin **23** was monitored via ^{1}H-NMR (see 3.5.3). The formation of the *(E)*-olefin metathesis product, *(E)*-**8**, is observed within the five minutes and, ultimately, becomes the major product in solution over the course of reaction. The diminished yields are hypothesized to be the result of competing decomposition pathways during either oxetane formation or fragmentation (Figure 3.11, II and Figure 3.12).

3.4 Conclusions

Mechanistic investigation into supereletrophilic iron(III)-ion pair-catalyzed intermolecular cross carbonyl–olefin metathesis have revealed significant insights into the reaction pathway. Of the four possible oxetane intermediates, experimental evidence suggests that the metathesis reaction proceeds *via* one distinct regioisomer and results in the selective formation of the *(E)*-olefin metathesis products. The diminished yields observed throughout this method are most likely

due to competing decomposition pathways during either oxetane formation and/or subsequent oxetane fragmentation. The observations reported herein are expected aid in the development of more efficient catalyst systems to not only improve the yields of this transformation, but also develop this reaction design into a platform for general synthetic utility.

3.5 Experimental Procedures and Supplemental Information

3.5.1 General Information

All moisture-sensitive reactions were performed under an atmosphere of nitrogen in flame-dried round bottom flasks or glass vials fitted with rubber septa and/or septa equipped screw caps. Stainless steel syringes were used to transfer air or moisture-sensitive liquids. Flash chromatography was performed using silica gel Silia Flash® 40-63 micron (230-400 mesh) from Silicycle. All chemicals were purchased from SigmaAldrich, Alfa Aesar, Acros Organics, Oakwood, TCI America, Frontier Scientific, Matrix Scientific, Ark Pharm, and Chem Impex International, and were used as received unless otherwise stated. Tetrahydrofuran and dimethylformamide were dried by being passed through columns of activated alumina. Proton Nuclear Magnetic Resonance NMR (^{1}H NMR) spectra and carbon nuclear magnetic resonance (^{13}C NMR) spectra were recorded on a Varian Unity Plus 400, Varian MR400, Varian vnmrs 500, Varian Inova 500, Varian Mercury 500, and Varian vnmrs 700 spectrometers. Chemical shifts for protons are reported in parts per million and are references to the NMR solvent peak ($CDCl_3$: δ 7.27). Chemical shifts for carbons are reported in parts per million and are referenced to the carbon resonances of the NMR solvent ($CDCl_3$: δ 77.00). Data are represented as follows: chemical shift, integration, multiplicity (br = broad, s = singlet, d = doublet, t = triplet, q = quartet, p = pentet, dd = doublet of doublet, m = multiplet), and coupling constants in Hertz (Hz). Mass spectroscopic (MS) data was recorded at the Mass Spectrometry Facility at the Department of Chemistry of the University of Michigan in Ann Arbor, MI on an Agilent Q-TOF HPLC-MS with ESI high resolution mass spectrometer. Infrared (IR) spectra were obtained using either an Avatar 360 FT-IR or Perkin Elmer Spectrum BX FT-IR spectrometer. IR data are represented as frequency of absorption (cm^{-1}).

3.5.2 Optimization

Table 3.1: Lewis acid screen.

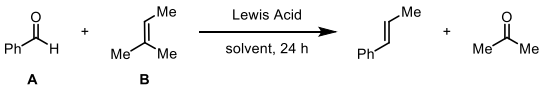

Entry	Lewis Acid	Loading (mol%)	A	B	Solvent	Yield
1	$FeCl_3$	10	5	1	DCM	19
2	$GaCl_3$	10	5	1	DCM	17
3	$AlCl_3$	10	5	1	DCM	0
4	$Fe(OTf)_3$	10	5	1	DCM	30
5	$Sc(OTf)_3$	10	5	1	DCM	26
6	$SnCl_4$	10	5	1	DCM	10
7	BF_3•OEt_2	10	5	1	DCM	28
8	$TiCl_4$	10	5	1	DCM	0
9	$FeCl_2$	10	5	1	DCM	0
10	$FeBr_3$	10	5	1	DCM	25
11	FeF_3	10	5	1	DCM	0
12	BCl_3	10	5	1	DCM	0
13	$Fe(acac)_3$	10	5	1	DCM	0
14	$ZnBr_2$	10	5	1	DCM	0
15	$ZnCl_2$	10	5	1	DCM	0
16	$SbCl_3$	10	5	1	DCM	0
17	Et_2AlCl	10	5	1	DCM	0
18	$EtAlCl_2$	10	5	1	DCM	0
19	$GaBr_3$	10	5	1	DCM	15
20	$AlBr_3$	10	5	1	DCM	0
21	$InBr_3$	10	5	1	DCM	1
22	$ScCl_3$	10	5	1	DCM	0
23	$Sn(OTf)_2$	10	5	1	DCM	3
24	$RuCl_3$	10	5	1	DCM	1
25	$InCl_3$	10	5	1	DCM	0
26	pTsOH•H_2O	10	5	1	DCM	0
27	H_2SO_4	10	5	1	DCM	22
28	HCl	10	5	1	DCM	0
29	TfOH	10	5	1	DCM	16

Conditions: Olefin and benzaldehyde were subjected to metathesis in solvent (0.3M) at room temperature for 24 h. Yields were determined via NMR with $PhMe_3Si$ as internal standard.

Table 3.2: Lewis acid screen with Ag salt.

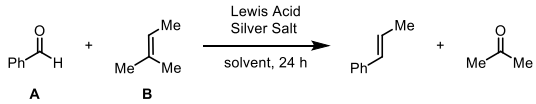

Entry	Lewis Acid	Loading (mol%)	A	B	Ag Salt	Solvent	Yield
1	$FeCl_3$	10	5	1	$AgBF_4$ (30 mol%)	DCM	43
2	$GaCl_3$	10	5	1	$AgBF_4$ (30 mol%)	DCM	35
3	$Fe(OTf)_3$	10	5	1	$AgBF_4$ (30 mol%)	DCM	25
4	$Sc(OTf)_3$	10	5	1	$AgBF_4$ (30 mol%)	DCM	32
5	$SnCl_4$	10	5	1	$AgBF_4$ (30 mol%)	DCM	31
6	BF_3•OEt_2	10	5	1	$AgBF_4$ (30 mol%)	DCM	23
7	$FeBr_3$	10	5	1	$AgBF_4$ (30 mol%)	DCM	41
8	$AlCl_3$	10	5	1	$AgBF_4$ (30 mol%)	DCM	35

Conditions: Olefin and benzaldehyde were subjected to metathesis in solvent (0.3M) at room temperature for 3 h. Yields were determined via GC with dodecane as internal standard.

Table 3.3: Ag salt screen.

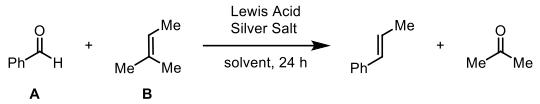

Entry	Lewis Acid	Loading (mol%)	**A**	**B**	Ag Salt	Solvent	Yield
1	$FeCl_3$	10	5	1	$AgSbF_6$ (30 mol%)	DCM	24
2	$FeCl_3$	10	5	1	$AgCOOCF_3$ (30 mol%)	DCM	0
3	$FeCl_3$	10	5	1	$AgPF_6$ (30 mol%)	DCM	36
4	$FeCl_3$	10	5	1	$AgNO_3$ (30 mol%)	DCM	6
5	$FeCl_3$	10	5	1	$AgBF_4$ (30 mol%)	DCM	43
6	$FeCl_3$	10	5	1	Ag*p*OTs (30 mol%)	DCM	0
7	$FeCl_3$	10	5	1	$AgAsF_6$ (30 mol%)	DCM	31
8	$FeCl_3$	10	5	1	$AgNTf_2$ (30 mol%)	DCM	30
9	$FeCl_3$	10	5	1	Ag_2O (30 mol%)	DCM	0

Conditions: Olefin and benzaldehyde were subjected to metathesis in solvent (0.3M) at room temperature for 3 h. Yields were determined via GC with dodecane as internal standard.

Table 3.4: AgCl recovery.

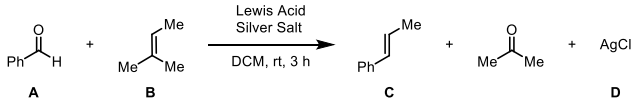

Entry	Lewis Acid	Loading (mol%)	**A**	**B**	Ag Salt	Yield **C**	Yield **D**
1	$FeCl_3$	10	5	1	$AgBF_4$ (30 mol%)	40	95

Conditions: Olefin (0.214 mmol) and benzaldehyde (1.07 mmol) were subjected to metathesis in DCM (0.3M) at room temperature for 3 h. Yield for **C** were determined via NMR with $PhMe_3Si$ as internal standard. Yield for **D** was determined via isolation (8.7 mg).

Table 3.5: Lewis acid and Ag salt loading screen.

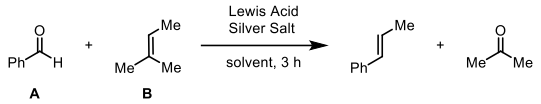

Entry	Lewis Acid	Loading (mol%)	A	B	Ag Salt	Solvent	Yield
1	$FeCl_3$	1	5	1	$AgBF_4$ (30 mol%)	DCM	8
2	$FeCl_3$	5	5	1	$AgBF_4$ (30 mol%)	DCM	33
3	$FeCl_3$	10	5	1	$AgBF_4$ (30 mol%)	DCM	43
4	$FeCl_3$	30	5	1	$AgBF_4$ (30 mol%)	DCM	27
5	$FeCl_3$	50	5	1	$AgBF_4$ (30 mol%)	DCM	20
6	$FeCl_3$	100	5	1	$AgBF_4$ (30 mol%)	DCM	6
7	$FeCl_3$	10	5	1	$AgBF_4$ (5 mol%)	DCM	16
8	$FeCl_3$	10	5	1	$AgBF_4$ (10 mol%)	DCM	20
9	$FeCl_3$	10	5	1	$AgBF_4$ (20 mol%)	DCM	27
10	$FeCl_3$	10	5	1	$AgBF_4$ (30 mol%)	DCM	43
11	$FeCl_3$	10	5	1	$AgBF_4$ (50 mol%)	DCM	30
12	$FeCl_3$	10	5	1	$AgBF_4$ (100 mol%)	DCM	28
13	$FeCl_3$	1	5	1	$AgBF_4$ (3 mol%)	DCM	22
14	$FeCl_3$	5	5	1	$AgBF_4$ (15 mol%)	DCM	22
15	$FeCl_3$	10	5	1	$AgBF_4$ (30 mol%)	DCM	43
16	$FeCl_3$	30	5	1	$AgBF_4$ (30 mol%)	DCM	27
17	$FeCl_3$	50	5	1	$AgBF_4$ (150 mol%)	DCM	26
18	$FeCl_3$	100	5	1	$AgBF_4$ (300 mol%)	DCM	24

Conditions: Olefin and benzaldehyde were subjected to metathesis in solvent (0.3M) at room temperature for 3 h. Yields were determined via GC with dodecane as internal standard.

Table 3.6: Solvent screen.

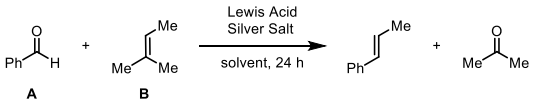

Entry	Lewis Acid	Loading (mol%)	A	B	Ag Salt	Solvent	Yield
1	$FeCl_3$	10	5	1	none	DCE	16
2	$FeCl_3$	10	5	1	$AgSbF_6$ (30 mol%)	DCE	22
3	$FeCl_3$	10	5	1	none	hexanes	<5
4	$FeCl_3$	10	5	1	none	DMF	0
5	$FeCl_3$	10	5	1	none	DMSO	0
6	$FeCl_3$	10	5	1	none	Et_2O	0
7	$FeCl_3$	10	5	1	none	benzene	<5
8	$FeCl_3$	10	5	1	none	toluene	<5
9	$FeCl_3$	10	5	1	none	CF_3-toluene	<5
10	$FeCl_3$	10	5	1	none	MeCN	0
11	$FeCl_3$	10	5	1	none	THF	0

Conditions: Olefin and benzaldehyde were subjected to metathesis in solvent (0.3M) at room temperature for 24 h. Yields were determined via NMR with $PhMe_3Si$ as internal standard.

Table 3.7: Time point screen.

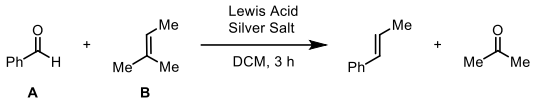

Entry	Lewis Acid	Loading (mol%)	A	B	Ag Salt	Time (h)	Yield
1	$FeCl_3$	10	5	1	$AgBF_4$ (30 mol%)	1	32
2	$FeCl_3$	10	5	1	$AgBF_4$ (30 mol%)	2	36
3	$FeCl_3$	10	5	1	$AgBF_4$ (30 mol%)	3	36
4	$FeCl_3$	10	5	1	$AgBF_4$ (30 mol%)	6	37
5	$FeCl_3$	10	5	1	$AgBF_4$ (30 mol%)	12	31
6	$FeCl_3$	10	5	1	$AgBF_4$ (30 mol%)	24	37

Conditions: Olefin and benzaldehyde were subjected to metathesis in solvent (0.3M)for 3 h. Yields were determined via GC with dodecane as internal standard.

Table 3.8: Solvent concentration screen.

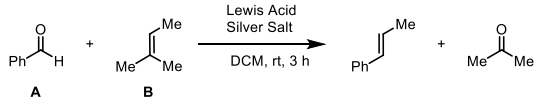

Entry	Lewis Acid	Loading (mol%)	A	B	Ag Salt	Conc. (M)	Yield
1	$FeCl_3$	10	5	1	$AgBF_4$ (30 mol%)	1.0	22
2	$FeCl_3$	10	5	1	$AgBF_4$ (30 mol%)	0.5	31
3	$FeCl_3$	10	5	1	$AgBF_4$ (30 mol%)	0.3	43
4	$FeCl_3$	10	5	1	$AgBF_4$ (30 mol%)	0.1	17
5	$FeCl_3$	10	5	1	$AgBF_4$ (30 mol%)	0.05	7
6	$FeCl_3$	10	5	1	$AgBF_4$ (30 mol%)	0.01	0

Conditions: Olefin and benzaldehyde were subjected to metathesis in solvent (0.3M) at room temperature for 3 h. Yields were determined via GC with dodecane as internal standard.

Table 3.9: Temperature screen.

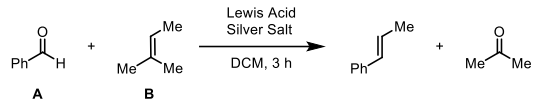

Entry	Lewis Acid	Loading (mol%)	A	B	Ag Salt	Temp (°C)	Yield
1	$FeCl_3$	10	5	1	$AgBF_4$ (30 mol%)	-78	0
2	$FeCl_3$	10	5	1	$AgBF_4$ (30 mol%)	-10	3
3	$FeCl_3$	10	5	1	$AgBF_4$ (30 mol%)	0	12
4	$FeCl_3$	10	5	1	$AgBF_4$ (30 mol%)	25	43
5	$FeCl_3$	10	5	1	$AgBF_4$ (30 mol%)	30	26
6	$FeCl_3$	10	5	1	$AgBF_4$ (30 mol%)	40	12

Conditions: Olefin and benzaldehyde were subjected to metathesis in solvent (0.3M) for 3 h. Yields were determined via GC with dodecane as internal standard.

Table 3.10: Starting material ratio screen.

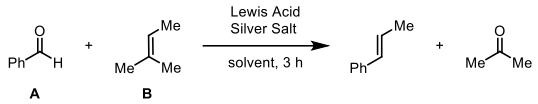

Entry	Lewis Acid	Loading (mol%)	A	B	Ag Salt	Solvent	Yield
1	$FeCl_3$	10	6	1	$AgBF_4$ (30 mol%)	DCM	31
2	$FeCl_3$	10	5	1	$AgBF_4$ (30 mol%)	DCM	31
3	$FeCl_3$	10	4	1	$AgBF_4$ (30 mol%)	DCM	29
4	$FeCl_3$	10	3	1	$AgBF_4$ (30 mol%)	DCM	28
5	$FeCl_3$	10	2	1	$AgBF_4$ (30 mol%)	DCM	27
6	$FeCl_3$	10	1	1	$AgBF_4$ (30 mol%)	DCM	19
7	$FeCl_3$	10	1	2	$AgBF_4$ (30 mol%)	DCM	7
8	$FeCl_3$	10	1	3	$AgBF_4$ (30 mol%)	DCM	1
9	$FeCl_3$	10	1	4	$AgBF_4$ (30 mol%)	DCM	0
10	$FeCl_3$	10	1	5	$AgBF_4$ (30 mol%)	DCM	0
11	$FeCl_3$	10	1	6	$AgBF_4$ (30 mol%)	DCM	0

Conditions: Olefin and benzaldehyde were subjected to metathesis in solvent (0.3M)for 3 h. Yields were determined via GC with dodecane as internal standard.

3.5.3 Mechanistic Investigations

Carbonyl-Ene Pathway Experiments

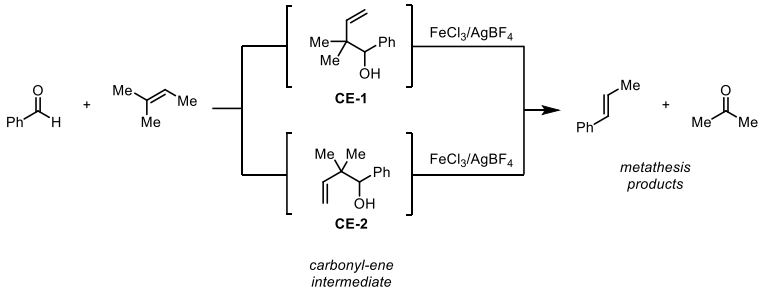

Carbonyl-ene intermediate **CE-1** and **CE-2** were synthesized according to literature precedent[15,16] and were subsequently subjected to the optimized reaction conditions to determine if the reaction proceeds via a carbonyl-ene pathway.

A flame-dried 4 dram vial with a magnetic stir bar, was charged with $FeCl_3$ (2.76 mg, 0.017 mmol, 0.1 equiv.) and $AgBF_4$ (9.94 mg, 0.051 mmol, 0.3 equiv.) in DCM (0.55 mL, 0.3 M) followed by carbonyl-ene intermediate **CE-1** (30.0 mg, 0.170 mmol, 1.0 equiv.). The resulting mixture was stirred at room temperature for 3 hours. The reaction mixture was quenched by passing through a

silica plug and eluted with DCM into a flask and then concentrated and the crude material was investigated via NMR spectroscopy to show decomposition of starting material with not products identified following chromatography.

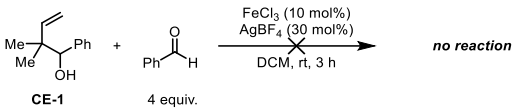

A flame-dried 4 dram vial with a magnetic stir bar, was charged with $FeCl_3$ (2.76 mg, 0.017 mmol, 0.1 equiv.) and $AgBF_4$ (9.94 mg, 0.051 mmol, 0.3 equiv.) in DCM (0.55 mL, 0.3 M) followed by benzaldehyde (72.3 mg, 0.681 mmol, 4.0 equiv.) and carbonyl-ene intermediate **CE-1** (30.0 mg, 0.170 mmol, 1.0 equiv.). The resulting mixture was stirred at room temperature for 3 hours. The reaction mixture was quenched by passing through a silica plug and eluted with DCM into a flask and then concentrated and the crude material was investigated via NMR spectroscopy to show no reaction and recovery of starting material.

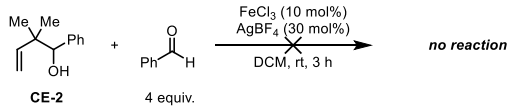

A flame-dried 4 dram vial with a magnetic stir bar, was charged with $FeCl_3$ (2.76 mg, 0.017 mmol, 0.1 equiv.) and $AgBF_4$ (9.94 mg, 0.051 mmol, 0.3 equiv) in DCM (0.55 mL, 0.3M) followed by benzaldehyde (72.3 mg, 0.681 mmol, 4.0 equiv.) and carbonyl-ene intermediate **CE-2** (30.0 mg, 0.170 mmol, 1.0 equiv.). The resulting mixture was stirred at room temperature for 3 hours. The reaction mixture was quenched by passing through a silica plug and eluted with DCM into a flask and then concentrated and the crude material was investigated via NMR spectroscopy to show no reaction and recovery of starting material.

Oxetane Pathway Experiments

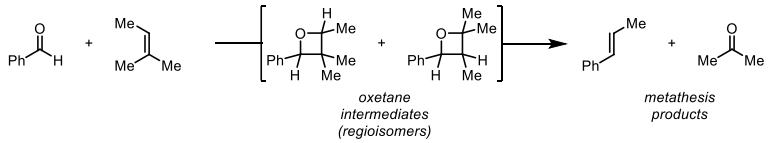

Oxetane intermediates were synthesized according to the procedure described below to determine their ability to fragment to desired metathesis products under optimized reaction conditions to support a reaction pathway incorporating oxetane intermediates.

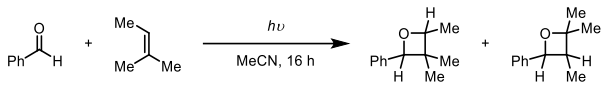

A 4 dram vial was charged with a stir bar and then benzaldehyde (800 mg, 7.54 mmol, 1.0 equiv.) and 2-methyl-2-butene (925 mg, 13.2 mmol, 1.75 equiv.) were dissolved in MeCN (9.5 mL, 1.0 M). The reaction mixture was subjected to UVA light in a Luzchem photoreactor for 16 hours. The reaction mixture was then concentrated and subjected to column chromatography (1:10 EtOAc:hexanes) to isolate a mixture of regio- and diastereomers (*trans*-**58** and *trans*-**59**). 2D NMR techniques were utilized to determined separate spectroscopic data of mixture: COSY, HMBC, HSQC, DEPT, NOESY. Significant and characteristic correlations are included below for each diastereomer.

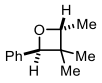

trans-**58**

trans-**58** characterization:

^{1}H NMR (400 MHz; CD_2Cl_2) δ_H 7.33 (t, *J* = 7.6 Hz, 9H), 7.25 (d, *J* = 7.8 Hz, 13H), 5.38 (s, 4H), 4.65 (q, *J* = 6.3 Hz, 4H), 1.30 (s, 15H), 1.23 (d, *J* = 6.4 Hz, 14H), 0.60 (s, 14H).

^{13}C NMR (135 MHz, CD_2Cl_2) δ_C 141.0, 128.5, 127.6, 125.7, 89.0, 84.5, 43.4, 27.2, 17.5, 17.4.

ν_{max} (FTIR)/cm^{-1}: 1701 1453, 1394, 1178, 1095, 966, 953, 834, 728, 705.

HRMS (ESI) m/z: $[M+H]^+$ Calcd for $C_{12}H_{17}O^+$: 177.1264; Found 177.1261.

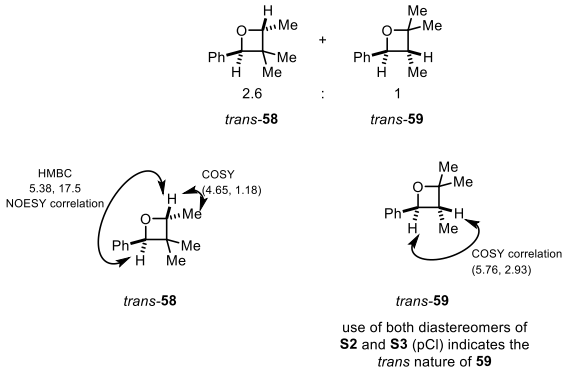

Purification by flash column chromatography eluting with pentane/Et_2O (10:1) provided *trans*-**58** and *trans*-**59** in a 2.6:1 ratio as a clear oil.

59 characterization:

^{1}H NMR (400 MHz; CD_2Cl_2) δ_H 7.87 (d, *J* = 7.2 Hz, 1H), 7.65 (t, *J* = 7.5 Hz, 1H), 7.54 (t, *J* = 7.4 Hz, 1H), 7.39 – 7.22 (m, 2H), 5.75 (d, *J* = 8.2 Hz, 1H), 2.93 (dt, *J* = 15.0, 7.5 Hz, 1H), 1.55 (s, 153), 1.26 (s, 3H), 0.63 (d, *J* = 7.5 Hz, 3H).

^{13}C NMR (135 MHz, CD_2Cl_2) δ_C 134.9, 130.1, 129.6, 127.3, 126.2, 83.8, 79.2, 42.4, 30.6, 24.5, 11.2.

ν_{max} (FTIR)/cm^{-1}: 1701 1453, 1394, 1178, 1095, 966, 953, 834, 728, 705.

HRMS (ESI) m/z: $[M+H]^+$ Calcd for $C_{12}H_{17}O^+$: 177.1264; Found 177.1261.

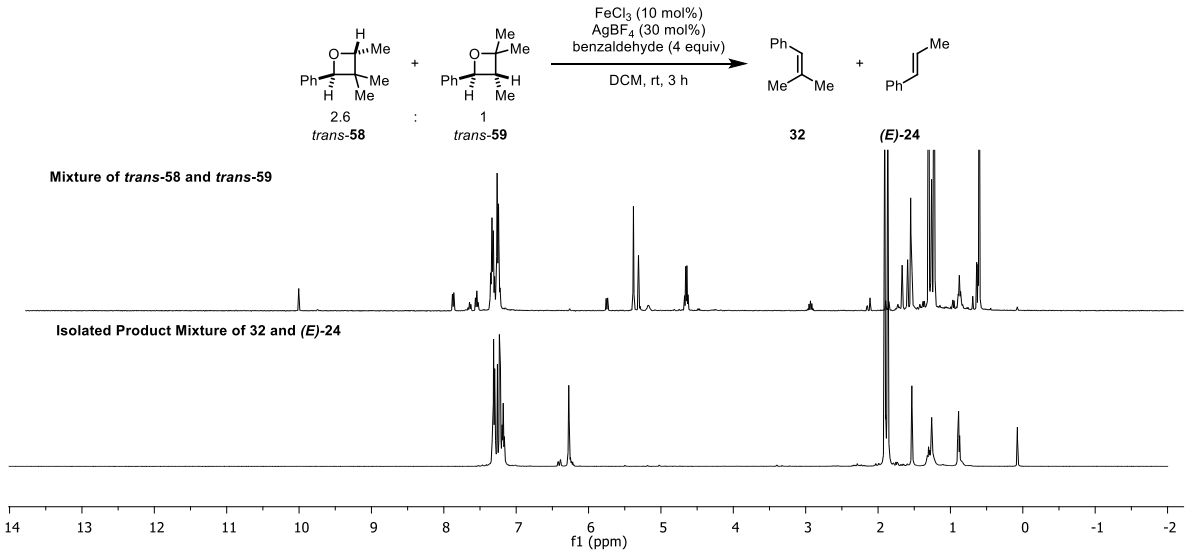

Following further chromatography, a 2.6:1 mixture of *trans*-**58**:*trans*-**59** was subjected to optimized reaction conditions. A 4 dram, flame-dried vial was charged with a stir bar and $FeCl_3$ (7.36 mg, 0.045 mmol, 0.10 equiv.) and $AgBF_4$ (26.5 mg, 0.136 mmol, 0.30 equiv.) followed by

DCM (1.5 mL, 0.3M) and benzaldehyde (193 mg, 1.82 mmol, 4.0 equiv). The oxetane mixture (80.0 mg, 0.454 mmol, 1.0 equiv) was then added and the reaction was then run at room temperature for 3 hours. The reaction was quenched by passing through a silica plug with DCM as the eluent and then concentrated and isolated with column chromatography (1:10 Et_2O:pentane) to provide metathesis products **32** and *(E)*-**24** as a nonpolar mixture with yields of 78% (33.7 mg) **32** and 47% (7.0 mg) *(E)*-**24**, 40.7 mg total of two isomers (shown above).

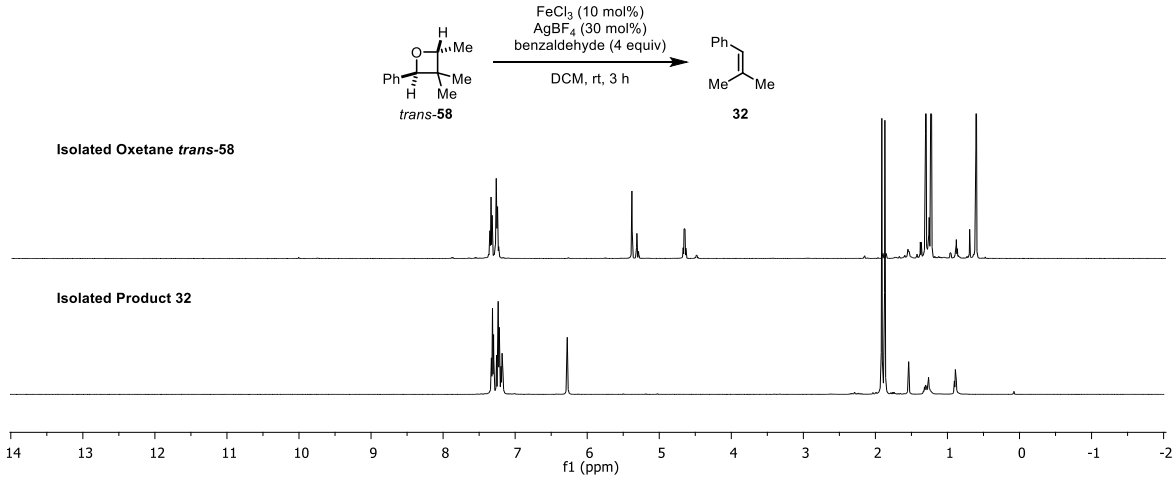

Following further chromatography, diastereomer *trans*-**58** was isolated and subjected to optimized reaction conditions. A 4 dram, flame-dried vial was charged with a stir bar and $FeCl_3$ (4.60 mg, 0.028 mmol, 0.10 equiv.) and $AgBF_4$ (16.6 mg, 0.085 mmol, 0.30 equiv.) followed by DCM (1.0 mL, 0.3 M) and benzaldehyde (120 mg, 1.13 mmol, 4.0 equiv.). The oxetane *trans*-**58** (50.0 mg, 0.284 mmol, 1.0 equiv.) was then added and the reaction was then run at room temperature for 3 hours. The reaction was quenched by passing through a silica plug with DCM as the eluent and then concentrated and isolated with column chromatography (1:10 Et_2O:pentane) to provide metathesis product **32**, 30 mg, 80%. Spectroscopic data of **32** matches commercial standard (shown above).

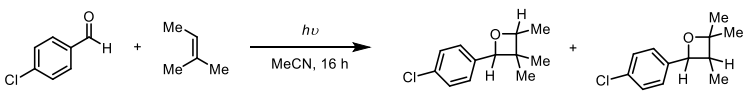

A 4 dram vial was charged with a stir bar and then 4-chlorobenzaldehyde (662 mg, 4.71 mmol, 1.0 equiv) and 2-methyl-2-butene (578 mg, 8.25 mmol, 1.75 equiv) were dissolved in MeCN (9.5 mL, 1.0 M). The reaction mixture was subjected to UVA light in a Luzchem photoreactor for 16 hours.

The reaction mixture was then concentrated and subjected to column chromatography (1:10 EtOAc:hexanes) to isolate a mixture of regio- and diastereomers.

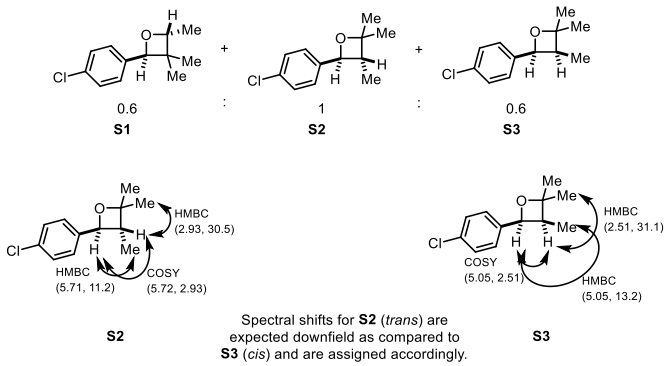

Purification by flash column chromatography eluting with pentane/Et_2O (10:1) provided **S1, S2** and **S3** in a 0.6:1.0:0.6 ratio as a clear oil. 2D NMR techniques were utilized to determined separate spectroscopic data of mixture: COSY, HMBC, HSQC, DEPT, NOESY. Significant and characteristic correlations are included below for each diastereomer.

S1 characterization:

^{1}H NMR (400 MHz; CD_2Cl_2) δ_H 7.30 (m, 2H), 7.25 (d, *J* = 8.4 Hz, 2H), 5.35 (s, 1H), 4.65 (q, *J* = 6.4 Hz, 1H), 1.29 (s, 3H), 1.22 (d, *J* = 6.4 Hz, 3H), 0.30 (s, 3H).

^{13}C NMR (135 MHz, CD_2Cl_2) δ_C 139.7, 133.1, 128.9, 127.2, 88.4, 84.7, 43.4, 27.2, 17.5, 17.4.

S2 characterization:

^{1}H NMR (400 MHz; CD_2Cl_2) δ_H 7.30 (m, 2H), 7.25 (d, *J* = 8.4 Hz, 2H), 5.71 (d, *J* = 8.3 Hz, 1H), 2.93 (p, *J* = 7.6 Hz, 1H), 1.54 (s, 3H), 1.25 (s, 3H), 0.63 (d, *J* = 7.5 Hz, 3H).

^{13}C NMR (135 MHz, CD_2Cl_2) δ_C 140.1, 132.9, 128.6, 127.7, 84.07, 78, 42.4, 30.5, 24.5, 11.2.

S3 characterization:

^{1}H NMR (400 MHz; CD_2Cl_2) δ_H 7.25 (d, *J* = 8.4 Hz, 2H), 7.21 (d, *J* = 8.4 Hz, 2H), 5.05 (d, *J* = 7.7 Hz, 1H), 2.51 (p, *J* = 7.2 Hz, 1H), 1.40 (s, 3H), 1.39 (s, 3H), 1.13 (d, *J* = 7.1 Hz, 3H)

^{13}C NMR (135 MHz, CD_2Cl_2) δ_C 142.8, 133.4, 128.62, 127.23, 84.09, 83.2, 49.0, 31.1, 23.1, 13.2.

ν_{max} (FTIR)/cm^{-1}: 1715, 1612, 1455, 1384, 1278, 1195, 943, 933, 824, 720.

HRMS (ESI) m/z: $[M]^+$ Calcd for $C_{12}H_{15}ClO^+$: 210.0811; Found 210.0810.

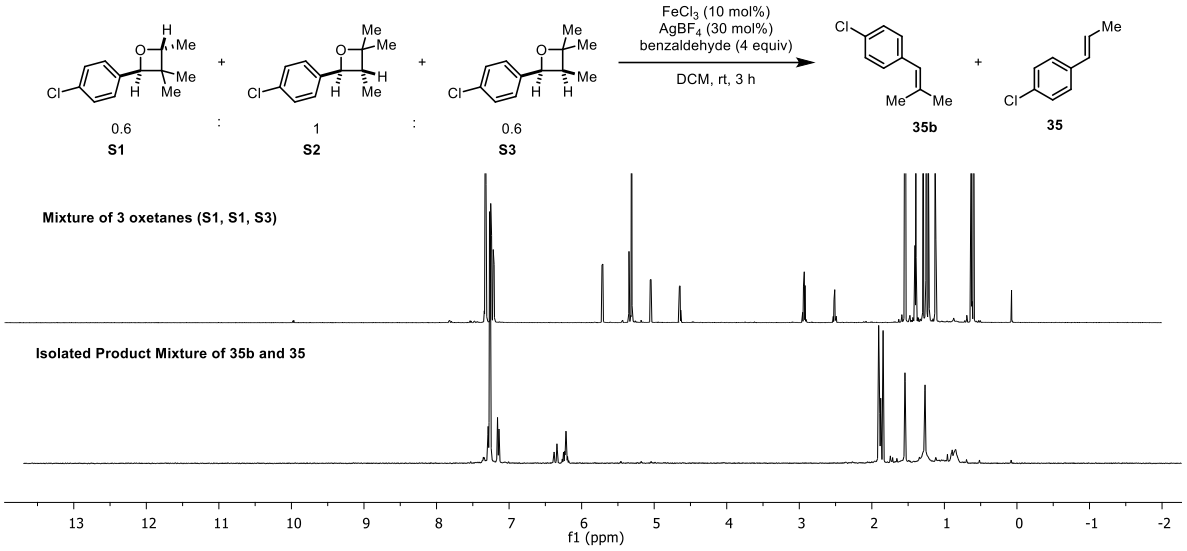

S1:**S2**:**S3** was subjected to optimized reaction conditions. A 4 dram, flame-dried vial was charged with a stir bar and $FeCl_3$ (1.15 mg, 0.007 mmol, 0.10 equiv.) and $AgBF_4$ (4.16 mg, 0.021 mmol, 0.30 equiv.) followed by DCM (0.3 mL, 0.3 M) and 4-chlorobenzaldehyde (40.0 mg, 0.285 mmol, 4.0 equiv.). The oxetane mixture (15.0 mg, 0.071 mmol, 1.0 equiv.) was then added and the reaction was then run at room temperature for 3 hours. The reaction was quenched by passing through a silica plug with DCM as the eluent and then concentrated and isolated with column chromatography (1:10 Et_2O:pentane) to provide metathesis products **35b** and **35** as a nonpolar mixture with yields of 26% (3.10 mg) of **35b** and 36% (3.90 mg) **35**, 7.0 mg total of two isomers (shown above).

Reaction Progress Investigation

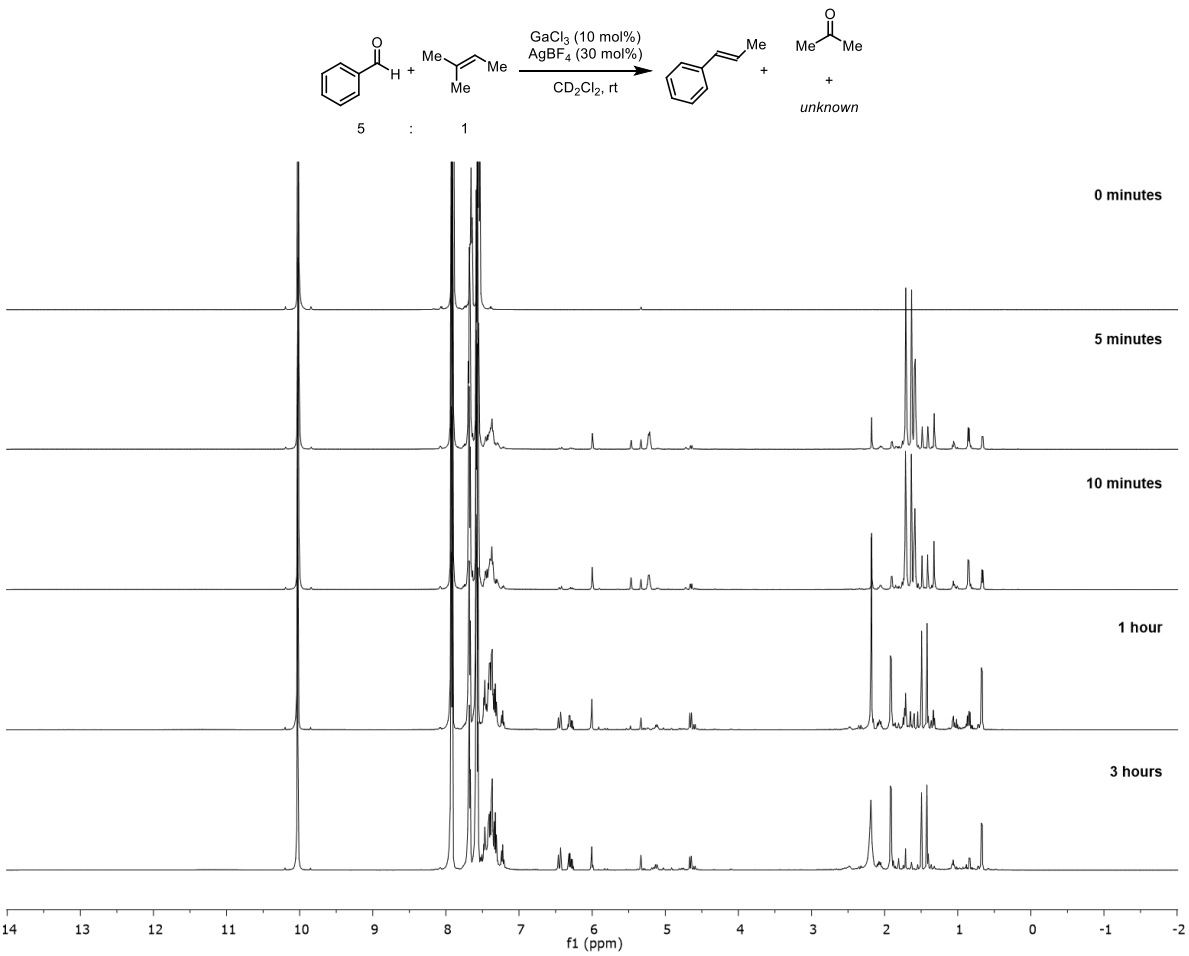

A NMR tube was charged with $GaCl_3$ (0.1 equiv.) and $AgBF_4$ (0.3 equiv.) in CD_2Cl_2 (0.3M) followed by benzaldehyde (5.0 equiv.). A ^{1}H-NMR spectrum was taken as a 0 minute time point. Then 2-methyl-2-butene (1.0 equiv.) was added and spectra were taken at 5 minutes, 10 minutes, 1 hour and 3 hours (shown above).

Decomposition and Isomerization Studies

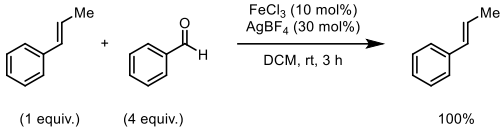

A flame-dried 4 dram vial with a magnetic stir bar, was charged with $FeCl_3$ (4.12 mg, 0.0254 mmol, 0.1 equiv.) and $AgBF_4$ (14.8 mg, 0.0762 mmol, 0.3 equiv.) in DCM (0.8 mL, 0.3 M) followed by benzaldehyde (108.0 mg, 1.02 mmol, 4 equiv.) and [(*E*)-prop-1-enyl]benzene (30.0 mg, 0.254 mmol, 1.0 equiv.). The resulting mixture was stirred at room temperature for 3 hours. The reaction mixture was quenched by passing through a silica plug and eluted with DCM into a flask and then concentrated. Purification by flash column chromatography eluting with pentane/Et_2O (9:1) provided a mixture of products as a clear oil. The mixture was investigated via NMR spectroscopy to show recovery of the starting material.

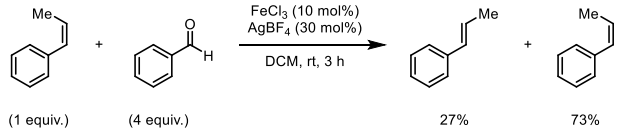

A flame-dried 4 dram vial with a magnetic stir bar, was charged with $FeCl_3$ (4.12 mg, 0.0254 mmol, 0.1 equiv.) and $AgBF_4$ (14.8 mg, 0.0762 mmol, 0.3 equiv.) in DCM (0.8 mL, 0.3 M) followed by benzaldehyde (108.0 mg, 1.02 mmol, 4 equiv.) and [(*Z*)-prop-1-enyl]benzene (30.0 mg, 0.254 mmol, 1.0 equiv.). The resulting mixture was stirred at room temperature for 3 hours. The reaction mixture was quenched by passing through a silica plug and eluted with DCM into a flask and then concentrated. Purification by flash column chromatography eluting with pentane/Et_2O (9:1) provided a mixture of products as a clear oil. The mixture was investigated via NMR spectroscopy to show isomerization of the resulting products.

3.5.4 Experimental Procedures

Substrate Synthesis

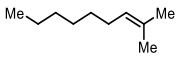

2-methylnon-2-ene (30): To a cold (0°C) stirred slurry of methyltrihenylphosphonium iodide (17.5 mmol, 2.0 equiv.) in THF (0.1 M) under a nitrogen atmosphere was added *n*-BuLi (17.5 mmol, 2.0 equiv.), and the resulting mixture was stirred for 15 min. Heptanal (8.76 mmol, 1.0 equiv.) dissolved in 1-2 mL of THF was then added to the slurry, the ice bath was removed, and the reaction was allowed to proceed for 18 h. The mixture was poured into an equal volume of water and extracted with diethyl ether (3x25 mL). The ether extracts were washed with brine (1x25 mL), dried with Na_2SO_4, filed and then concentrated. Purification by flash column chromatography eluting with pentanes/Et_2O (9:1) provided **30** 990 mg (81%) as a clear oil.

^{1}H NMR (500 MHz; $CDCl_3$) δ_H 5.18 – 5.06 (m, 1H), 1.97 (q, J = 6.9 Hz, 2H), 1.70 (s, 3H), 1.61 (s, 3H), 1.36 – 1.23 (m, 8H), 0.89 (t, J = 6.9 Hz, 3H).

^{13}C NMR (135 MHz, $CDCl_3$) δ_C 131.1, 124.9, 31.8, 29.9, 29.0, 28.0, 25.7, 22.7, 17.7, 14.1. Spectroscopic data matches literature report.[17]

Intermolecular Cross Carbonyl–Olefin Metathesis Reactions

General metathesis procedure: A flame-dried 4 dram vial with a magnetic stir bar, was charged with $FeCl_3$ (0.1 equiv.) and $AgBF_4$ (0.3 equiv.) in DCM (0.3 M) followed by aldehyde (5.0 equiv.) and olefin (1.0 equiv.) substrates. The resulting mixture was stirred at room temperature for 3 hours. The reaction mixture was quenched by passing through a silica plug and eluted with DCM into a flask and then concentrated and the crude material was purified using column chromatography with indicated eluent to provide pure metathesis product.

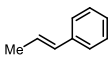

***(E)*-prop-1-en-1-ylbenzene (24):** The metathesis was performed according to general procedure, by subjecting 2-methyl-2-butene (1.20 mmol, 1 equiv.) and benzaldehyde (6.00 mmol, 5 equiv.). Purification by flash column chromatography eluting with pentane/Et_2O (9:1) provided **24** 72.5 mg (51%) as a clear oil.

^{1}H NMR (400 MHz, $CDCl_3$) δ_H 7.32 (dt, J = 15.0, 7.2 Hz, 5H), 7.20 (t, J = 7.2 Hz, 1H), 6.42 (dd, J = 15.7, 1.9 Hz, 1H), 6.25 (dq, J = 15.9, 6.5 Hz, 1H), 1.90 (d, J = 6.5 Hz, 3H).

^{13}C NMR (135 MHz, $CDCl_3$) δ_C 137.9, 131.0, 128.4, 126.7, 125.8, 125.7, 18.5.

Spectroscopic data matches literature report.[18]

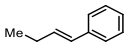

***(E)*-but-1-en-1-ylbenzene (28p):** The metathesis was performed according to general procedure, by subjecting 2-methylpent-2-ene (0.475mmol, 1 equiv.) and benzaldehyde (2.38 mmol, 5 equiv.). Purification by flash column chromatography eluting with pentane/Et_2O (9:1) provided **28p** 16.5 mg (26%) as a clear oil.

^{1}H NMR (400 MHz, $CDCl_3$) δ_H 7.35 (m, 1H), 7.25 (m, 2H), 7.15 (m, 2H), 6.37 (d, 1H, J = 15Hz), 6.25 (dt, 1H, J = 6.6Hz), 2.20 (m, 2H), 1.08 (t, 3H, J = 7.5 Hz).

^{13}C NMR (135 MHz, $CDCl_3$) δ_C 138.0, 132.4, 128.4, 126.9, 125.6, 26.0, 13.6.

Spectroscopic data matches literature report.[19]

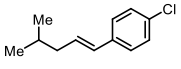

***(E)*-1-chloro-4-(4-methylpent-1-en-1-yl)benzene (29p):** The metathesis was performed according to general procedure, by subjecting 2,5-dimethylhex-2-ene (0.45 mmol, 1 equiv.) and 4-chlorobenzaldehyde (2.23 mmol, 5 equiv.). Purification by flash column chromatography eluting with pentane/Et_2O (9:1) provided **29p** 26.0 mg (40%) as a clear oil.

^{1}H NMR (500 MHz, $CDCl_3$) δ_H 7.39 – 7.24 (m, 6H), 6.33 (d, *J* = 15.8 Hz, 1H), 6.26 – 6.13 (m, 1H), 2.14 – 2.03 (m, 2H), 1.79 – 1.66 (m, 1H), 0.95 (d, *J* = 6.7 Hz, 6H).

^{13}C NMR (126 MHz, $CDCl_3$) δ_C 136.4, 132.3, 130.6, 129.6, 128.6, 127.1, 42.4, 28.5, 22.4.

***ν*$_{max}$ (FTIR)/cm^{-1}:** 2954, 2924, 1490, 1383, 1241, 1173, 1090, 1087, 965, 825.

HRMS (ESI) m/z: $[M]^+$ Calcd for $C_{12}H_{15}Cl^+$: 194.0862; Found 194.0871.

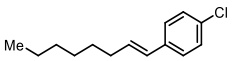

***(E)*-1-chloro-4-(oct-1-en-1-yl)benzene (30p):** The metathesis was performed according to general procedure, by subjecting 2-methylnon-2-ene (1.00 mmol, 1 equiv.) and 4-

chlorobenzaldehyde (5.00 mmol, 5 equiv.). Purification by flash column chromatography eluting with pentane/Et_2O (9:1) provided **30p** 68.1 mg (31%) as a clear oil.

^{1}H NMR (500 MHz, $CDCl_3$) δ_H 7.26 (s, 4H), 6.33 (d, J = 15.9 Hz, 1H), 6.21 (dt, J = 15.7, 6.8 Hz, 1H), 2.25 – 2.16 (m, 2H), 1.47 (h, J = 6.8 Hz, 2H), 1.37 – 1.28 (m, 6H), 0.90 (t, J = 6.6 Hz, 3H).

^{13}C NMR (126 MHz, $CDCl_3$) δ_C 136.4, 132.2, 132.0, 128.6, 128.5, 127.1, 33.0, 31.7, 29.3, 28.9, 22.6, 14.1.

ν_{max} (FTIR)/cm^{-1}: 2955, 2924, 2853, 1490, 1465, 1177, 1090, 1012, 962, 833.

HRMS (ESI) m/z: $[M]^+$ Calcd for $C_{14}H_{19}Cl^+$: 222.1178; Found 222.1175.

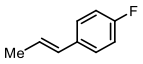

***(E)*-1-fluoro-4-(prop-1-en-1-yl)benzene (34):** The metathesis was performed according to general procedure, by subjecting 2-methyl-2-butene (1.00 mmol, 1 equiv.) and 4-fluorobenzaldehyde (5.00 mmol, 5 equiv.). Purification by flash column chromatography eluting with pentane/Et_2O (9:1) provided **34** 64.1 mg (47%) as a clear oil.

^{1}H NMR (500 MHz, $CDCl_3$) δ_H 7.29 (dd, J = 8.7, 5.7 Hz, 2H), 6.98 (t, J = 8.7 Hz, 2H), 6.37 (d, J = 15.7 Hz, 1H), 6.16 (dq, J = 15.7, 6.6 Hz, 1H), 1.88 (d, J = 6.7 Hz, 3H).

^{13}C NMR (126 MHz, $CDCl_3$) δ_C 161.8 (d, J = 245.4 Hz), 129.8, 127.2, 127.1, 125.4 (d, J = 1.9 Hz), 115.3 (d, J = 21.6 Hz), 18.4.

Spectroscopic data matches literature report.[18]

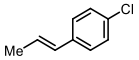

***(E)*-1-chloro-4-(prop-1-en-1-yl)benzene (35):** The metathesis was performed according to general procedure, by subjecting 2-methyl-2-butene (1.00 mmol, 1 equiv.) and 4-chlorobenzaldehyde (5.00 mmol, 5 equiv.). Purification by flash column chromatography eluting with pentane/Et_2O (9:1) provided **35** 84.0 mg (56%) as a clear oil.

^{1}H NMR (500 MHz, $CDCl_3$) δ_H 7.26 (s, 4H), 6.36 (d, *J* = 15.8 Hz, 1H), 6.23 (dq, *J* = 15.7, 6.6 Hz, 1H), 1.89 (d, *J* = 6.7 Hz, 3H).

^{13}C NMR (126 MHz, $CDCl_3$) δ_C 136.4, 132.2, 129.8, 128.6, 127.0, 126.5, 18.5.

Spectroscopic data matches literature report.[18]

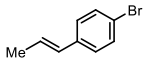

***(E)*-1-bromo-4-(prop-1-en-1-yl)benzene (36):** The metathesis was performed according to general procedure, by subjecting 2-methyl-2-butene (1.00 mmol, 1 equiv.) and 4-bromobenzaldehyde (5.00 mmol, 5 equiv.). Purification by flash column chromatography eluting with pentane/Et_2O (9:1) provided **36** 101.0 mg (51%) as a clear oil.

^{1}H NMR (500 MHz, $CDCl_3$) δ_H 7.41 (d, *J* = 8.2 Hz, 2H), 7.20 (d, *J* = 8.2 Hz, 2H), 6.34 (dd, *J* = 15.8, 1.7 Hz, 1H), 6.24 (dq, *J* = 15.8, 6.5 Hz, 1H), 1.88 (dd, *J* = 6.5, 1.5 Hz, 3H).

^{13}C NMR (126 MHz, $CDCl_3$) δ_C 136.8, 131.5, 129.9, 127.3, 126.6, 120.3, 18.5.

Spectroscopic data matches literature report.[18]

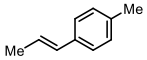

***(E)*-1-methyl-4-(prop-1-en-1-yl)benzene (37):** The metathesis was performed according to general procedure, by subjecting 2-methyl-2-butene (1.00 mmol, 1 equiv.) and 4-phenylbenzaldehyde (5.00 mmol, 5 equiv.). Purification by flash column chromatography eluting with pentane/Et_2O (9:1) provided **37** 109 mg (56%) as a white solid.

^{1}H NMR (500 MHz, $CDCl_3$) δ_H 7.24 (dd, *J* = 8.0, 2.8 Hz, 2H), 7.11 (dd, *J* = 8.1, 2.8 Hz, 2H), 6.38 (d, *J* = 13.8 Hz, 1H), 6.20 (dqd, *J* = 16.0, 6.6, 2.9 Hz, 1H), 2.34 (s, 3H), 1.88 (dd, *J* = 6.6, 2.3 Hz, 3H).

^{13}C NMR (126 MHz, $CDCl_3$) δ_C 136.4, 134.9, 130.6, 129.1, 125.6, 124.7, 21.2, 18.6. Spectroscopic data matches literature report.[20]

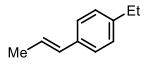

***(E)*-1-ethyl-4-(prop-1-en-1-yl)benzene (38):** The metathesis was performed according to general procedure, by subjecting 2-methyl-2-butene (1.00 mmol, 1 equiv.) and 4-ethylbenzaldehyde (5.00 mmol, 5 equiv.). Purification by flash column chromatography eluting with pentane/Et_2O (9:1) provided **38** 69.0 mg (47%) as a clear oil.

^{1}H NMR (400 MHz, $CDCl_3$) δ_H 7.28 (d, *J* = 6.7 Hz, 2H), 7.15 (d, *J* = 7.9 Hz, 2H), 6.40 (d, *J* = 15.8 Hz, 1H), 6.21 (td, *J* = 13.2, 6.5 Hz, 1H), 2.67 – 2.57 (m, 2H), 1.95 – 1.85 (m, 3H), 1.25 (t, *J* = 7.6 Hz, 3H).

^{13}C NMR (135 MHz, $CDCl_3$) δ_C 142.8, 135.4, 130.8, 127.9, 125.7, 124.7, 28.5, 18.5, 15.6.

ν_{max} (FTIR)/cm^{-1}: 2962, 2728, 1700, 1605, 1453, 1304, 1212, 1166, 964, 825.

HRMS (ESI) m/z: $[M]^+$ Calcd for $C_{11}H_{14}^+$: 146.1096; Found 146.1098.

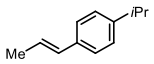

***(E)*-1-isopropyl-4-(prop-1-en-1-yl)benzene (39):** The metathesis was performed according to general procedure, by subjecting 2-methyl-2-butene (1.00 mmol, 1 equiv.) and 4-isopropylbenzaldehyde (5.00 mmol, 5 equiv.). Purification by flash column chromatography eluting with pentane/Et_2O (9:1) provided **39** 96.3 mg (60%) as a clear oil.

^{1}H NMR (500 MHz, $CDCl_3$) δ_H 7.29 – 7.24 (m, 2H), 7.16 (d, *J* = 7.9 Hz, 2H), 6.39 (dd, *J* = 15.9, 1.9 Hz, 1H), 6.20 (dq, *J* = 15.8, 6.6 Hz, 1H), 2.89 (hept, *J* = 6.8 Hz, 1H), 1.88 (dd, *J* = 6.6, 1.7 Hz, 3H), 1.25 (d, *J* = 6.9 Hz, 6H).

^{13}C NMR (126 MHz, $CDCl_3$) δ_C 147.4, 135.6, 130.8, 126.5, 125.7, 124.7, 33.8, 24.0, 18.5.

ν_{max} (FTIR)/cm^{-1}: 3021, 2958, 2928, 2869, 1511, 1053, 962, 843, 787, 724.

HRMS (ESI) m/z: $[M]^+$ Calcd for $C_{12}H_{16}^+$: 160.1252; Found 160.1250.

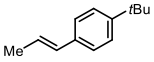

***(E)*-1-(tert-butyl)-4-(prop-1-en-1-yl)benzene (40):** The metathesis was performed according to general procedure, by subjecting 2-methyl-2-butene (1.00 mmol, 1 equiv.) and 4-tert-butylbenzaldehyde (5.00 mmol, 5 equiv.). Purification by flash column chromatography eluting with pentane/Et_2O (9:1) provided **40** 109.0 mg (62%) as a clear oil.

^{1}H NMR (500 MHz, $CDCl_3$) δ_H 7.33 (d, *J* = 8.3 Hz, 2H), 7.28 (d, *J* = 8.5 Hz, 2H), 6.39 (dd, *J* = 15.8, 1.9 Hz, 1H), 6.21 (dq, *J* = 15.6, 6.6 Hz, 1H), 1.88 (dd, *J* = 6.6, 1.6 Hz, 3H), 1.32 (s, 9H).

^{13}C NMR (126 MHz, $CDCl_3$) δ_C 149.7, 135.2, 130.7, 125.5, 125.4, 124.9, 34.5, 31.3, 18.5.

ν_{max} (FTIR)/cm^{-1}: 3024, 2960, 2866, 1513, 1362, 1268, 1110, 962, 842, 788.

HRMS (ESI) m/z: $[M]^+$ Calcd for $C_{13}H_{18}^+$: 174.1409; Found 174.1413.

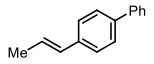

***(E)*-4-(prop-1-en-1-yl)-1,1'-biphenyl (41):** The metathesis was performed according to general procedure, by subjecting 2-methyl-2-butene (1.00 mmol, 1 equiv) and 4-phenylbenzaldehyde (5.00

mmol, 5 equiv). Purification by flash column chromatography eluting with pentane/Et_2O (9:1) provided **41** 109 mg (56%) as a white solid.

^{1}H NMR (500 MHz, $CDCl_3$) δ_H 7.64 – 7.58 (m, 2H), 7.55 (d, *J* = 8.2 Hz, 2H), 7.48 – 7.38 (m, 4H), 7.34 (t, *J* = 7.3 Hz, 1H), 6.45 (dd, *J* = 15.8, 1.9 Hz, 1H), 6.30 (dq, *J* = 15.6, 6.6 Hz, 1H), 1.92 (dd, *J* = 6.6, 1.6 Hz, 3H).

^{13}C NMR (126 MHz, $CDCl_3$) δ_C 140.9, 139.5, 137.0, 130.6, 128.7, 127.2, 127.1, 126.9, 126.2, 125.9, 18.6.

Spectroscopic data matches literature report.[19]

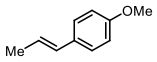

***(E)*-1-methoxy-4-(prop-1-en-1-yl)benzene (42):** The metathesis was performed according to general procedure, by subjecting 2-methyl-2-butene (1.00 mmol, 1 equiv.) and 4-methoxylbenzaldehyde (5.00 mmol, 5 equiv.). Purification by flash column chromatography eluting with pentane/Et_2O (9:1) provided **42** 89.0 mg (60%) as a clear oil.

^{1}H NMR (400 MHz, $CDCl_3$) δ_H 7.37 – 7.23 (m, 2H), 6.81 (dd, *J* = 17.3, 9.8 Hz, 2H), 6.34 (d, *J* = 15.7 Hz, 1H), 6.09 (dq, *J* = 15.6, 6.6 Hz, 1H), 3.79 (d, *J* = 8.0 Hz, 3H), 1.89 – 1.75 (m, 3H).

^{13}C NMR (135 MHz, $CDCl_3$) δ_C 158.5, 130.8, 130.3, 126.8, 123.5, 113.9, 55.3, 18.4.

Spectroscopic data matches literature report.[21]

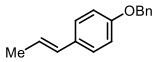

***(E)*-1-(benzyloxy)-4-(prop-1-en-1-yl)benzene (43):** The metathesis was performed according to general procedure, by subjecting 2-methyl-2-butene (0.71 mmol, 1 equiv.) and 4-benzyloxybenzaldehyde (3.56 mmol, 5 equiv.). Purification by flash column chromatography eluting with pentane/Et_2O (9:1) provided **43** 40.0 mg (25%) as a clear oil.

^{1}H NMR (500 MHz, $CDCl_3$) δ_H 7.44 (d, *J* = 7.2 Hz, 3H), 7.39 (t, *J* = 7.6 Hz, 3H), 7.37 – 7.30 (m, 2H), 6.91 (d, *J* = 8.7 Hz, 2H), 6.38 – 6.32 (m, 1H), 6.15 – 6.06 (m, 1H), 5.07 (s, 2H), 1.86 (dd, *J* = 6.6, 1.6 Hz, 3H).

^{13}C NMR (126 MHz, $CDCl_3$) δ_C 157.8, 145.4, 137.1, 130.3, 128.6, 127.9, 127.5, 126.9, 123.6, 114.9, 70.0, 18.4.

ν_{max} (FTIR)/cm^{-1}: 3033, 2906, 2904, 1608, 1508, 1450, 1237, 1036, 973, 838.

HRMS (ESI) m/z: $[M]^+$ Calcd for $C_{16}H_{16}O^+$: 225.1235; Found 225.1231.

Spectroscopic data matches literature report.[22]

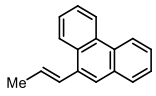

***(E)*-9-(prop-1-en-1-yl)phenanthrene (44):** The metathesis was performed according to general procedure, by subjecting 2-methyl-2-butene (0.64 mmol, 1 equiv.) and phenanthrene-9-carbaldehyde (3.21 mmol, 5 equiv.). Purification by flash column chromatography eluting with pentane/Et_2O (9:1) provided **44** 38.3 mg (27%) as a white solid.

^{1}H NMR (500 MHz, $CDCl_3$) δ_H 8.73 (d, *J* = 8.0 Hz, 1H), 8.67 (d, *J* = 8.0 Hz, 1H), 8.19 (d, *J* = 7.9 Hz, 1H), 7.88 (d, *J* = 7.7 Hz, 1H), 7.78 (s, 1H), 7.71 – 7.55 (m, 4H), 7.14 (d, *J* = 15.4 Hz, 1H), 6.41 – 6.29 (m, 1H), 2.05 (dd, *J* = 6.6, 1.5 Hz, 3H).

^{13}C NMR (126 MHz, $CDCl_3$) δ_C 134.6, 132.0, 130.8, 130.3, 129.9, 129.3, 128.7, 128.5, 126.4, 124.8, 124.3, 123.0, 122.5, 18.9.

ν_{max} (FTIR)/cm^{-1}: 2956, 2922, 2851, 1432, 1243, 1144, 964, 886, 745, 719.

HRMS (ESI) m/z: $[M]^+$ Calcd for $C_{17}H_{14}^+$: 218.1096; Found 218.1095.

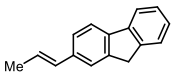

***(E)*-2-(prop-1-en-1-yl)-9H-fluorene (45):** The metathesis was performed according to general procedure, by subjecting 2-methyl-2-butene (1.00 mmol, 1 equiv.) and 9H-fluorene-2-carbaldehyde (5.00 mmol, 5 equiv.). Purification by flash column chromatography eluting with pentane/Et_2O (9:1) provided **45** 105 mg (51%) as a white solid.

^{1}H NMR (400 MHz, $CDCl_3$) δ_H 7.75 (t, *J* = 9.5 Hz, 1H), 7.71 (d, *J* = 7.9 Hz, 1H), 7.54 (d, *J* = 4.7 Hz, 2H), 7.38 – 7.33 (m, 2H), 7.29 (t, *J* = 6.3 Hz, 1H), 6.49 (d, *J* = 15.8 Hz, 1H), 6.35 – 6.24 (m, 1H), 3.89 (s, 2H), 1.92 (d, *J* = 6.6 Hz, 3H).

^{13}C NMR (135 MHz, $CDCl_3$) δ_C 143.6, 143.3, 141.6, 140.5, 136.7, 131.3, 126.7, 126.4, 125.2, 125.0, 124.8, 122.2, 119.8, 119.7, 36.8, 18.6.

ν_{max} (FTIR)/cm^{-1}: 3015, 2907, 1453, 1394, 1178, 1095, 966, 953, 834, 728.

HRMS (ESI) m/z: $[M]^+$ Calcd for $C_{16}H_{14}^+$: 206.1096; Found 206.1091.

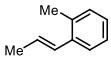

***(E)*-1-methyl-2-(prop-1-en-1-yl)benzene (46):** The metathesis was performed according to general procedure, by subjecting 2-methyl-2-butene (1.00 mmol, 1 equiv.) and 2-methylbenzaldehyde (5.00 mmol, 5 equiv.). Purification by flash column chromatography eluting with pentane/Et_2O (9:1) provided **46** 79 mg (60%) as a clear oil.

^{1}H NMR (400 MHz, $CDCl_3$) δ_H 7.55 (d, *J* = 7.4 Hz, 1H), 7.32 – 7.04 (m, 3H), 6.75 (d, *J* = 15.6 Hz, 1H), 6.26 (dt, *J* = 15.6, 6.6 Hz, 1H), 2.48 (s, 3H), 2.06 (dd, *J* = 6.6, 1.5 Hz, 3H).

^{13}C NMR (135 MHz, $CDCl_3$) δ_C 137.0, 134.8, 130.1, 128.8, 126.9, 126.7, 126.0, 125.4, 19.8, 18.8. Spectroscopic data matches literature report.[23]

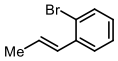

***(E)*-1-bromo-2-(prop-1-en-1-yl)benzene (47):** The metathesis was performed according to general procedure, by subjecting 2-methyl-2-butene (1.00 mmol, 1 equiv.) and 2-bromobenzaldehyde (5.00 mmol, 5 equiv.). Purification by flash column chromatography eluting with pentane/Et_2O (9:1) provided **47** 35.0 mg (18%) as a clear oil.

^{1}H NMR (500 MHz; $CDCl_3$) δ_H 7.53 (d, *J* = 8.0 Hz, 1H), 7.48 (dd, *J* = 7.8, 1.6 Hz, 1H), 7.25 (t, *J* = 7.5 Hz, 1H), 7.06 (td, *J* = 7.7, 1.6 Hz, 1H), 6.74 (dd, *J* = 15.8, 1.9 Hz, 1H), 6.20 (dq, *J* = 15.5, 6.6 Hz, 1H), 1.94 (dd, *J* = 6.7, 1.7 Hz, 3H).

^{13}C NMR (126 MHz, $CDCl_3$) δ_C 137.7, 132.8, 129.9, 128.8, 128.1, 127.4, 126.8, 123.0, 18.7.

ν_{max} (FTIR)/cm^{-1}: 2912, 1697, 1587, 1465, 1434, 1263, 1019, 960, 822, 743.

HRMS (ESI) m/z: $[M]^+$ Calcd for $C_9H_9Br^+$: 195.9888; Found 195.9891.

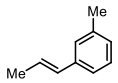

***(E)*-1-methyl-3-(prop-1-en-1-yl)benzene (48):** The metathesis was performed according to general procedure, by subjecting 2-methyl-2-butene (1.00 mmol, 1 equiv.) and 3-methylbenzaldehyde (5.00 mmol, 5 equiv.). Purification by flash column chromatography eluting with pentane/Et_2O (9:1) provided **48** 76.0 mg (58%) as a clear oil.

^{1}H NMR (500 MHz, $CDCl_3$) δ_H 7.21 – 7.12 (m, 3H), 7.02 (d, *J* = 7.3 Hz, 1H), 6.38 (dq, *J* = 15.6, 1.7 Hz, 1H), 6.23 (dq, *J* = 15.7, 6.5 Hz, 1H), 2.34 (s, 3H), 1.89 (dd, *J* = 6.5, 1.6 Hz, 3H).

^{13}C NMR (126 MHz, $CDCl_3$) δ_C 137.9, 137.9, 131.0, 128.3, 127.5, 126.6, 125.5, 122.9, 21.4, 18.5.

ν_{max} (FTIR)/cm^{-1}: 3021, 2913, 2851, 1603, 1487, 1445, 1376, 959, 760, 689.

HRMS (ESI) m/z: $[M]^+$ Calcd for $C_{10}H_{12}^+$: 132.0930; Found 132.0943.

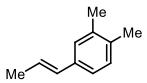

***(E)*-1,2-dimethyl-4-(prop-1-en-1-yl)benzene (49):** The metathesis was performed according to general procedure, by subjecting 2-methyl-2-butene (0.56 mmol, 1 equiv.) and 3,4-dimethylbenzaldehyde (2.78 mmol, 5 equiv.). Purification by flash column chromatography eluting with pentane/Et_2O (9:1) provided **49** 77.1 mg (53%) as a clear oil.

^{1}H NMR (500 MHz, $CDCl_3$) δ_H 7.12 (s, 1H), 7.10 – 7.04 (m, 2H), 6.40 – 6.32 (m, 1H), 6.19 (dq, *J* = 15.5, 6.5 Hz, 1H), 2.25 (d, *J* = 5.6 Hz, 6H), 1.88 (dt, *J* = 6.7, 1.3 Hz, 3H).

^{13}C NMR (126 MHz, $CDCl_3$) δ_C 136.5, 135.6, 135.1, 130.9, 129.7, 127.1, 124.4, 123.2, 19.8, 19.4, 18.4.

ν_{max} (FTIR)/cm^{-1}: 3016, 2914, 2852, 1499, 1445, 1375, 961, 880, 824, 781.

HRMS (ESI) m/z: $[M]^+$ Calcd for $C_{11}H_{14}^+$: 146.1096; Found 146.1093.

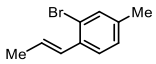

***(E)*-2-bromo-4-methyl-1-(prop-1-en-1-yl)benzene (50):** The metathesis was performed according to general procedure, by subjecting 2-methyl-2-butene (0.36 mmol, 1 equiv.) and 2-bromo-4-methyl-benzaldehyde (1.78 mmol, 5 equiv.). Purification by flash column chromatography eluting with pentane/Et_2O (9:1) provided **50** 44.0 mg (59%) as a clear oil.

^{1}H NMR (500 MHz, $CDCl_3$) δ_H 7.39 – 7.34 (m, 2H), 7.08 – 7.03 (m, 1H), 6.70 (dq, *J* = 15.6, 1.8 Hz, 1H), 6.15 (dq, *J* = 15.7, 6.7 Hz, 1H), 2.31 (s, 3H), 1.92 (dd, *J* = 6.7, 1.8 Hz, 3H).

^{13}C NMR (126 MHz, $CDCl_3$) δ_C 138.2, 134.8, 133.1, 129.6, 128.3, 127.8, 126.4, 122.7, 20.7, 18.6.

ν_{max} (FTIR)/cm^{-1}: 3028, 2911, 2851, 1604, 1484, 1443, 1037, 960, 825, 787.

HRMS (ESI) m/z: $[M]^+$ Calcd for $C_{10}H_{11}Br^+$: 210.0044; Found 210.0046.

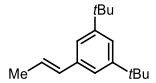

***(E)*-1,3-di-tert-butyl-5-(prop-1-en-1-yl)benzene (51):** The metathesis was performed according to general procedure, by subjecting 2-methyl-2-butene (0.56 mmol, 1 equiv.) and 3,5-ditert-

butylbenzaldehyde (2.78 mmol, 5 equiv.). Purification by flash column chromatography eluting with pentane/Et_2O (9:1) provided **51** 82.5 mg (64%) as a clear oil.

^{1}H NMR (500 MHz, $CDCl_3$) δ_H 7.30 (dd, *J* = 11.1, 1.4 Hz, 1H), 7.22 (s, 2H), 6.51 – 6.41 (m, 1H), 6.26 (dq, *J* = 15.5, 6.6 Hz, 1H), 1.91 (dd, *J* = 6.6, 1.6 Hz, 3H), 1.36 (s, 18H).

^{13}C NMR (126 MHz, $CDCl_3$) δ_C 150.7, 137.1, 131.8, 125.0, 121.0, 120.1, 34.8, 31.4, 18.5.

***ν*$_{max}$ (FTIR)/cm^{-1}:** 2961, 2866, 1593, 1476, 1361, 1247, 1201, 960, 873, 705.

HRMS (ESI) m/z: $[M]^+$ Calcd for $C_{17}H_{26}^+$: 230. 2035; Found 230.2046.

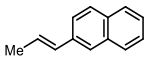

***(E)*-2-(prop-1-en-1-yl)naphthalene (53):** The metathesis was performed according to general procedure, by subjecting 2-methyl-2-butene (1.00 mmol, 1 equiv.) and naphthalene-2-carbaldehyde (5.00 mmol, 5 equiv.). Purification by flash column chromatography eluting with pentane/Et_2O (9:1) provided **53** 72.0 mg (43%) as a white solid.

^{1}H NMR (500 MHz, $CDCl_3$) δ_H 7.82 – 7.74 (m, 3H), 7.67 (s, 1H), 7.58 (dd, *J* = 8.6, 1.7 Hz, 1H), 7.44 (dtd, *J* = 17.7, 7.0, 1.4 Hz, 2H), 6.58 (dd, *J* = 15.8, 1.8 Hz, 1H), 6.39 (dq, *J* = 15.8, 6.6 Hz, 1H), 1.96 (dd, *J* = 6.6, 1.6 Hz, 3H).

^{13}C NMR (126 MHz, $CDCl_3$) δ_C 135.4, 133.7, 132.6, 131.1, 128.0, 127.8, 127.6, 126.2, 126.1, 125.4, 125.1, 123.5, 18.6.

Spectroscopic data matches literature report.[19]

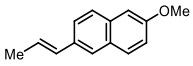

***(E)*-2-methoxy-6-(prop-1-en-1-yl)naphthalene (54):** The metathesis was performed according to general procedure, by subjecting 2-methyl-2-butene (1.00 mmol, 1 equiv.) and 6-methoxynaphthalene-2-carbaldehyde (5.00 mmol, 5 equiv.). Purification by flash column chromatography eluting with pentane/Et_2O (9:1) provided **54** 69.0 mg (35%) as a white solid.

^{1}H NMR (500 MHz, $CDCl_3$) δ_H 7.68 (dd, *J* = 11.7, 8.6 Hz, 2H), 7.61 (s, 1H), 7.54 (dd, *J* = 8.5, 2.0 Hz, 1H), 7.15 – 7.08 (m, 2H), 6.54 (dd, *J* = 15.7, 2.2 Hz, 1H), 6.38 – 6.28 (m, 1H), 3.92 (s, 3H), 1.94 (dd, *J* = 6.5, 1.8 Hz, 3H).

^{13}C NMR (126 MHz, $CDCl_3$) δ_C 157.4, 133.6, 133.3, 131.1, 129.3, 129.1, 126.9, 125.1, 125.0, 124.1, 118.8, 105.8, 55.3; 18.6.

ν_{max} (FTIR)/cm^{-1}: 3005, 2959, 2909, 2849, 1599, 1482, 1261, 1030, 968, 859.

HRMS (ESI) m/z: $[M+H]^+$ Calcd for $C_{14}H_{14}OH^+$: 199.1123; Found 199.1117.

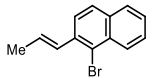

***(E)*-1-bromo-2-(prop-1-en-1-yl)naphthalene (55):** The metathesis was performed according to general procedure, by subjecting 2-methyl-2-butene (0.43 mmol, 1 equiv.) and 1-bromonaphthalene-2-carbaldehyde (2.14 mmol, 5 equiv.). Purification by flash column chromatography eluting with pentane/Et_2O (9:1) provided **55** 45.4 mg (43%) as a clear oil.

^{1}H NMR (500 MHz; $CDCl_3$) δ_H 8.34 (d, *J* = 8.5 Hz, 1H), 7.78 (d, *J* = 8.1 Hz, 1H), 7.73 (d, *J* = 8.6 Hz, 1H), 7.62 (d, *J* = 8.6 Hz, 1H), 7.57 (t, *J* = 7.7 Hz, 1H), 7.48 (t, *J* = 7.5 Hz, 1H), 7.08 (dd, *J* = 15.7, 2.0 Hz, 1H), 6.35 (dq, *J* = 16.0, 6.6 Hz, 1H), 2.01 (dd, *J* = 6.8, 1.6 Hz, 3H).

^{13}C NMR (126 MHz, $CDCl_3$) δ_C 135.2, 133.5, 132.7, 131.0, 129.7, 128.0, 127.6, 127.5, 127.4, 126.1, 124.3, 122.5, 18.9.

ν_{max} (FTIR)/cm^{-1}: 3053, 2910, 2848, 1327, 947, 819, 791, 763, 738, 653.

HRMS (ESI) m/z: $[M]^+$ Calcd for $C_{13}H_{11}Br^+$: 264.0044; Found 264.0054.

3.5.5 NMR Spectra
Substrates

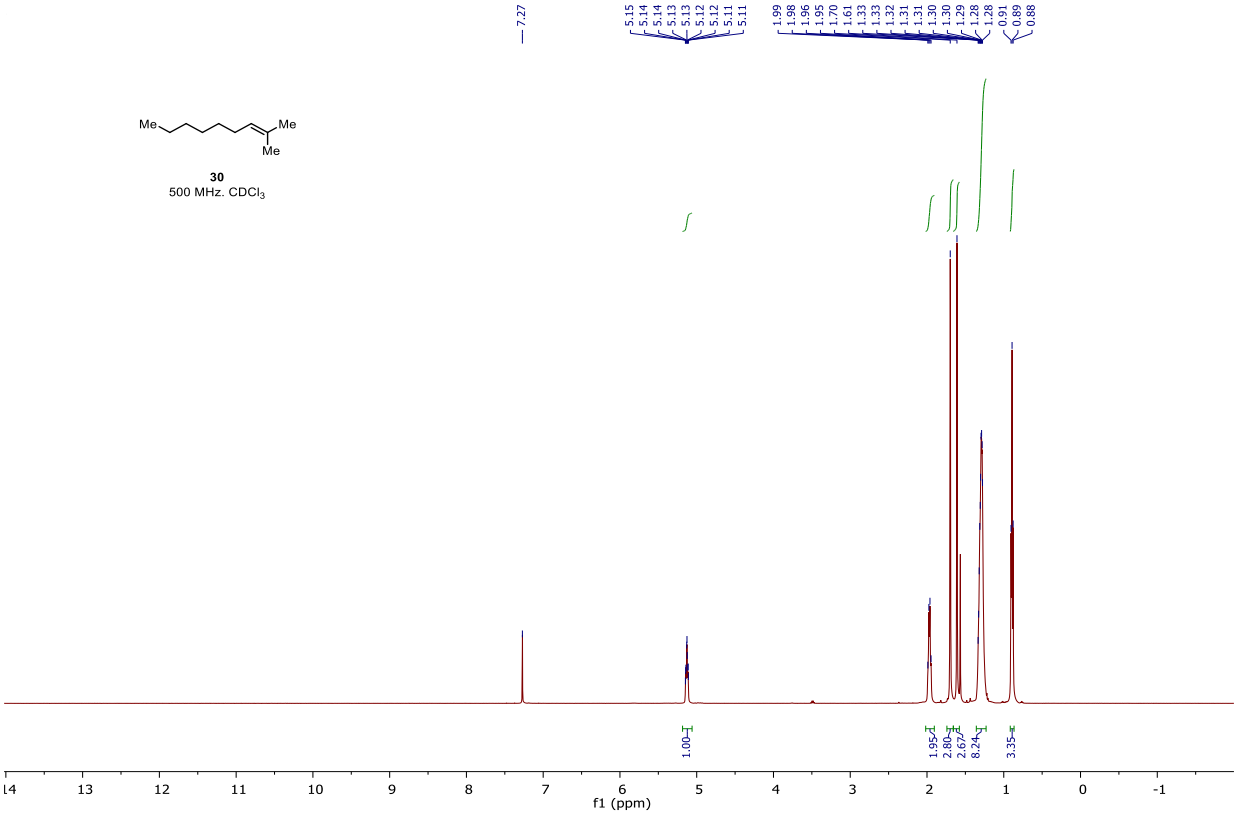

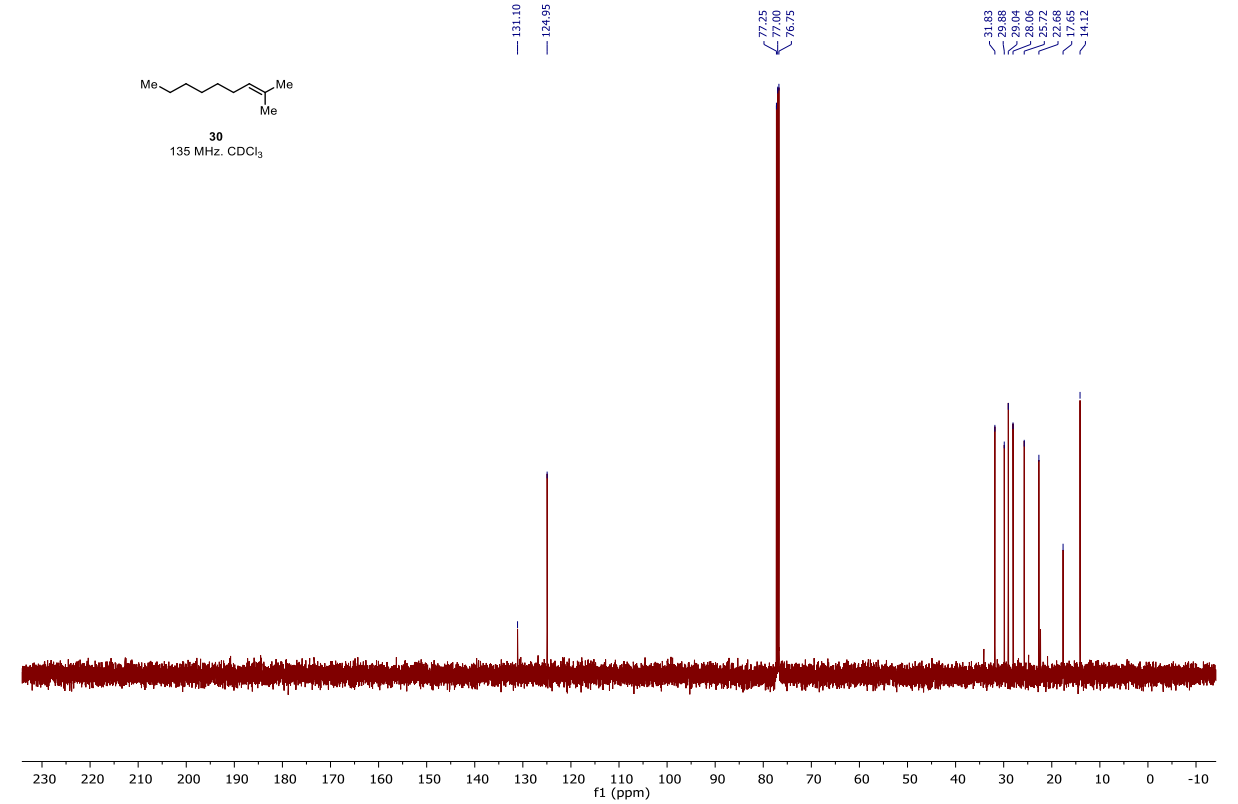

* Due to the high volatility and non-polar nature of the compounds, some NMRs contain residual pentanes from column chromatography

Metathesis Products

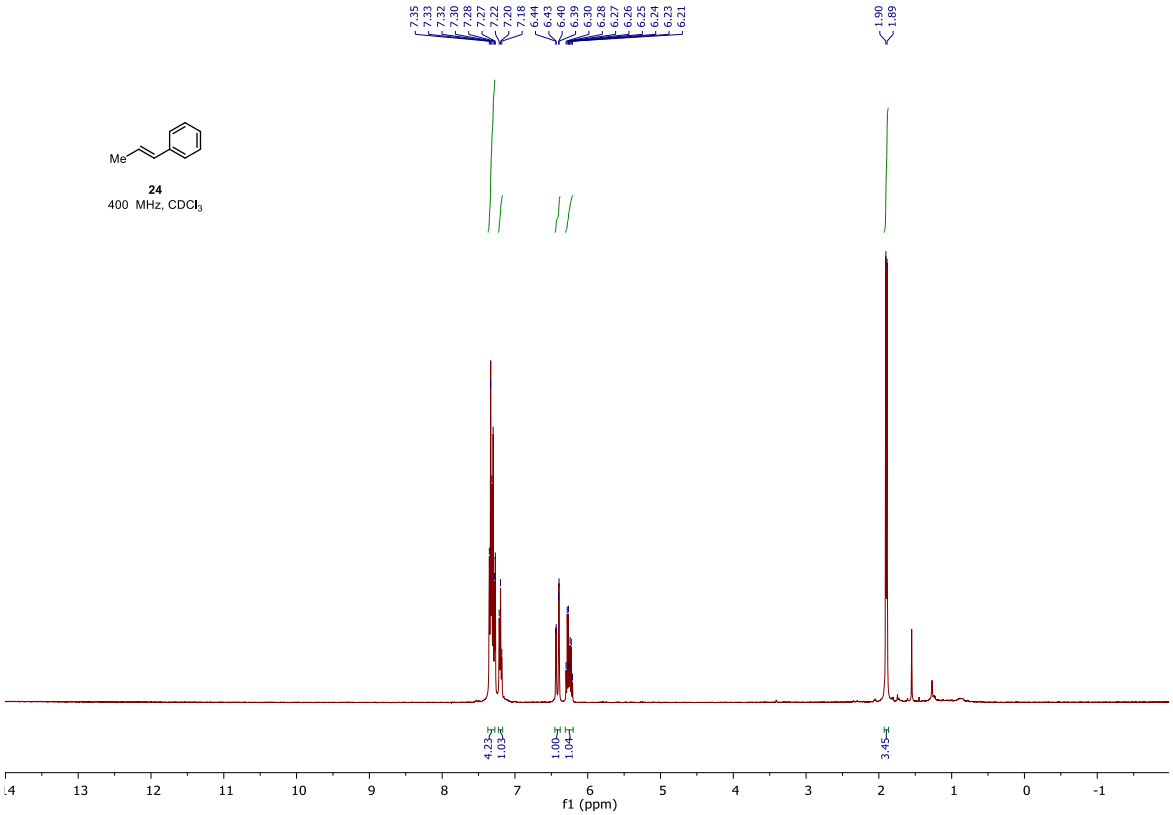

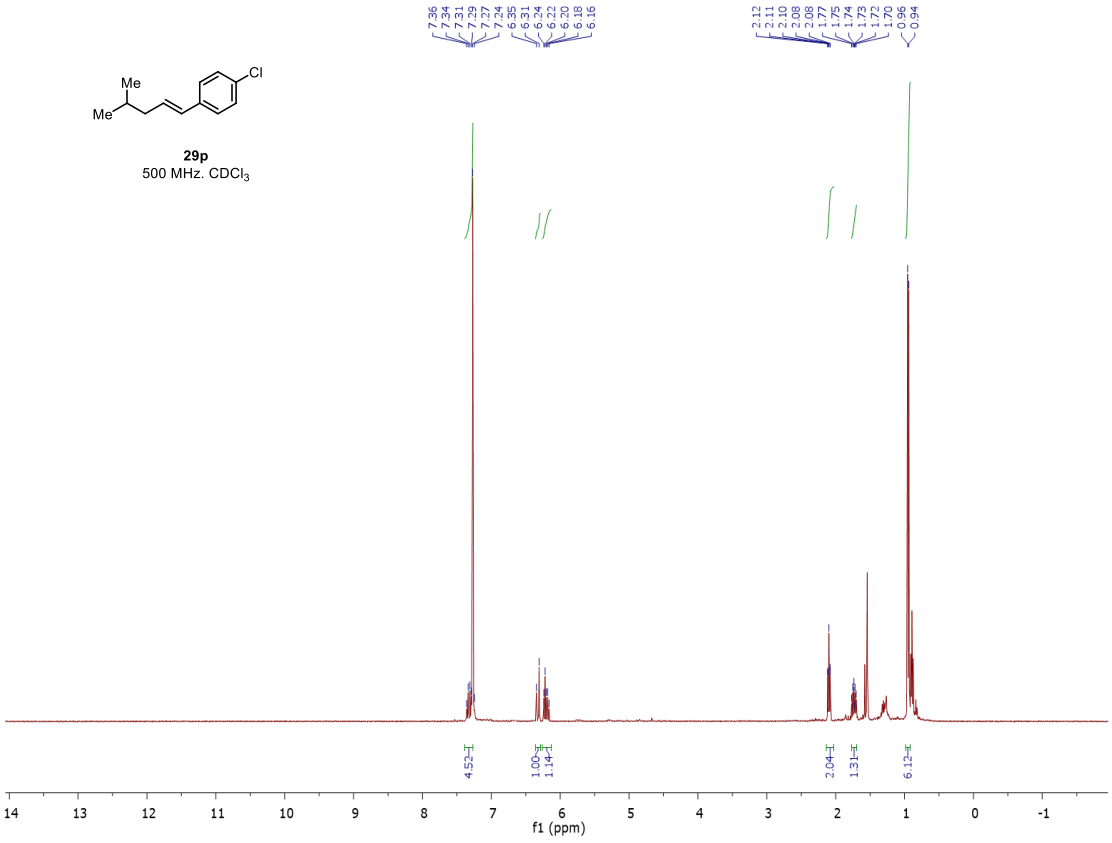

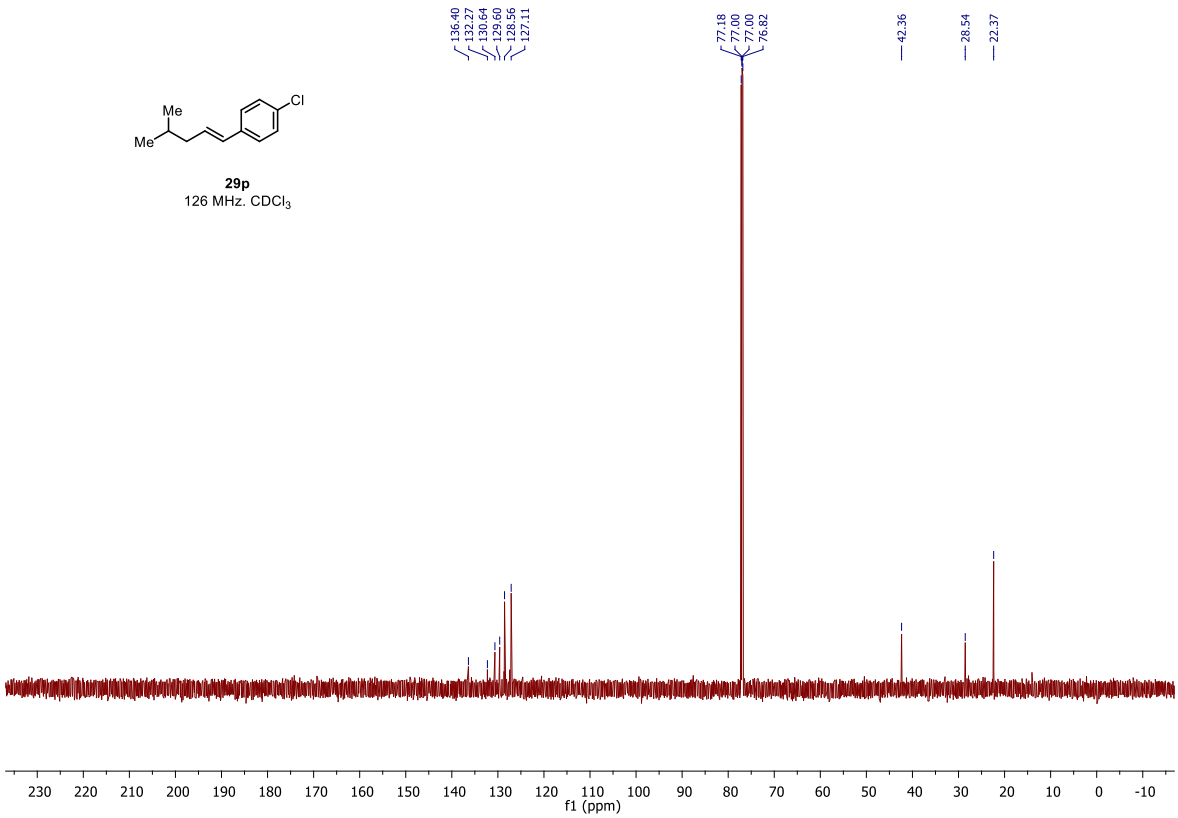
136.40
132.27
130.64
129.60
128.56
127.11
77.18
77.00
77.00
76.82
42.36
28.54
22.37
Me
Me
Cl
29p
126 MHz. CDCl3
f1 (ppm)

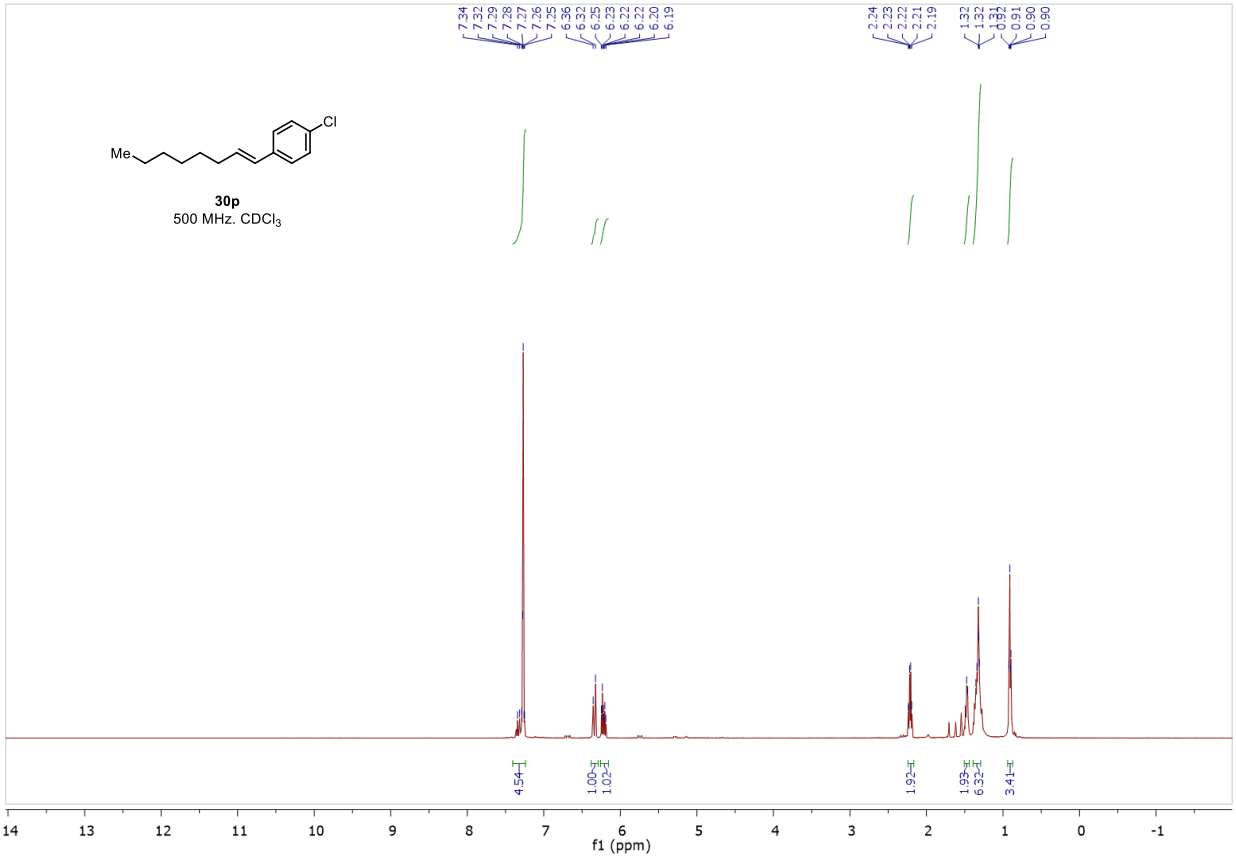
7.34
7.32
7.29
7.28
7.27
7.26
7.25
6.36
6.32
6.25
6.23
6.22
6.22
6.20
6.19
2.24
2.23
2.22
2.21
2.19
1.32
1.32
1.31
0.91
0.90
0.90
Me
Cl
30p
500 MHz. CDCl3
4.54
1.00
1.02
1.92
1.93
6.32
3.41
f1 (ppm)

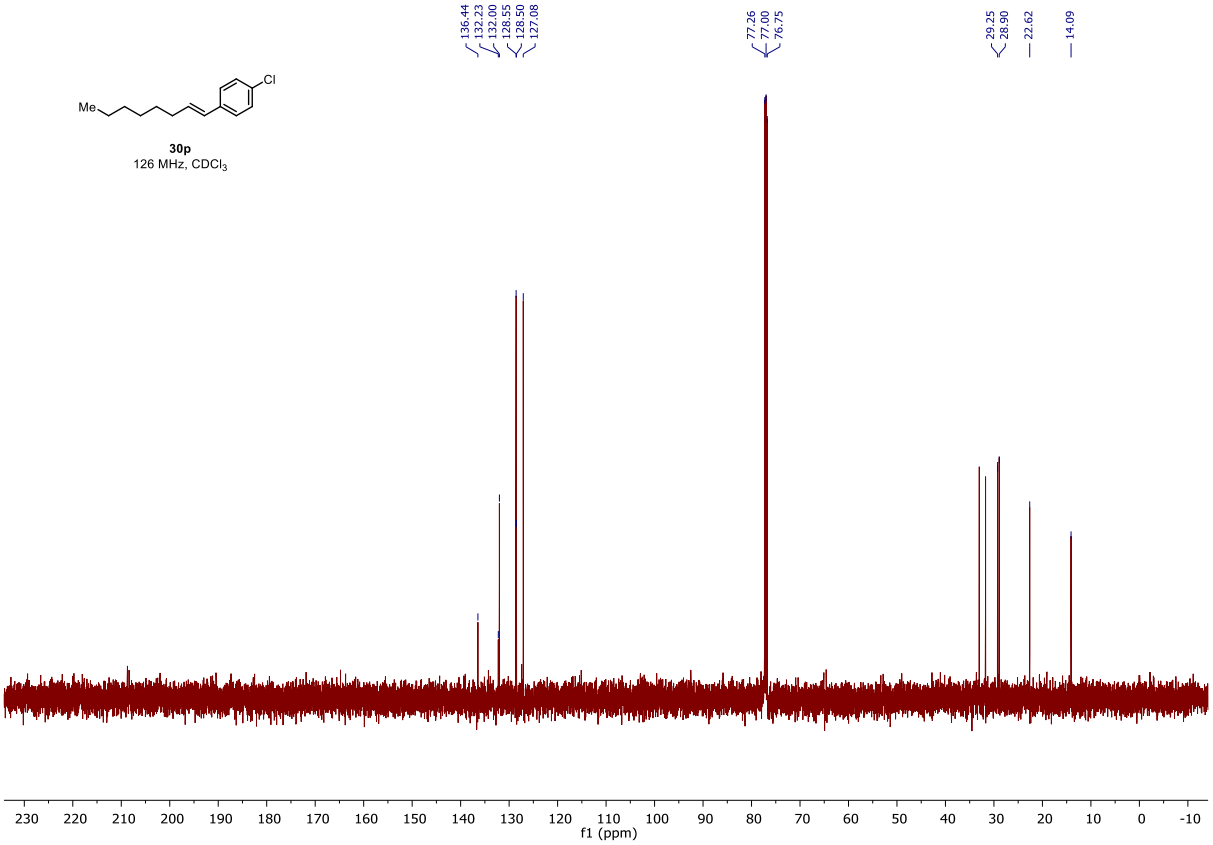

30p
126 MHz, $CDCl_3$

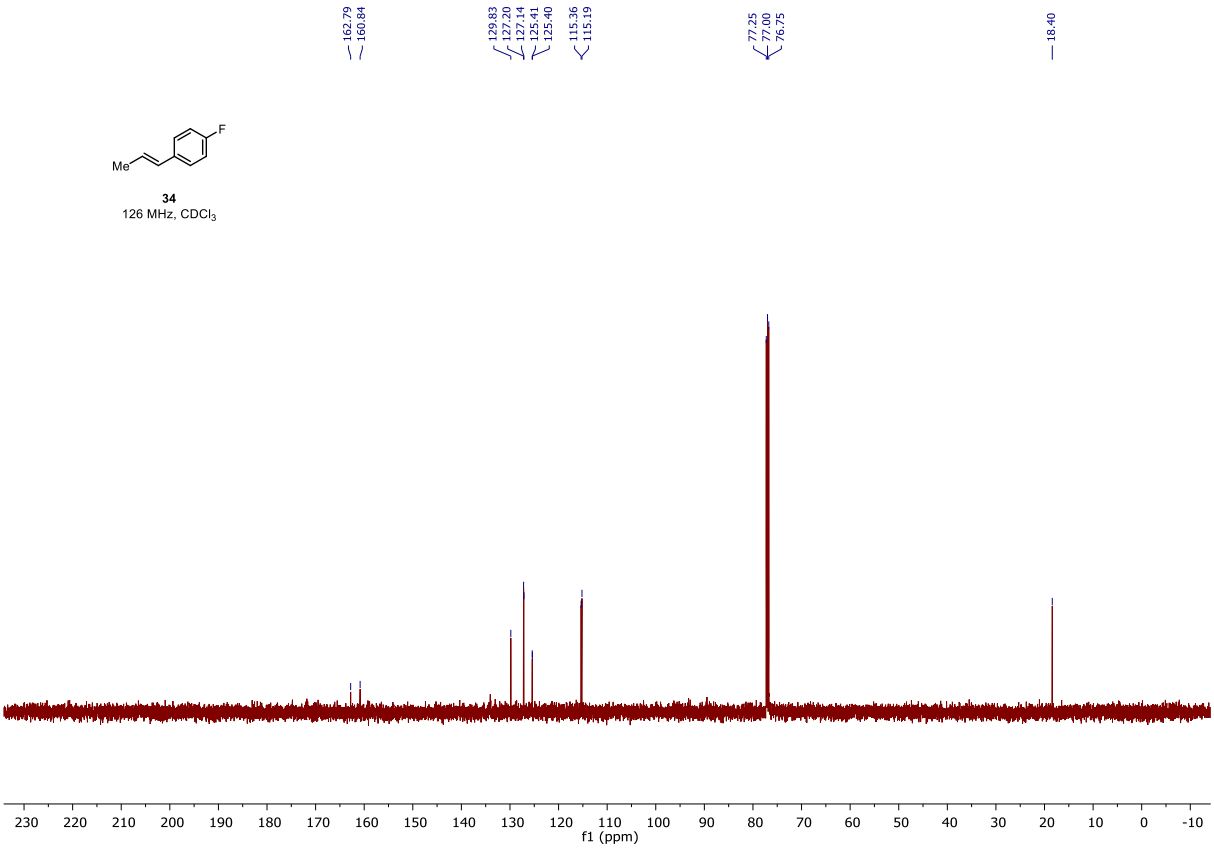

34
126 MHz, $CDCl_3$

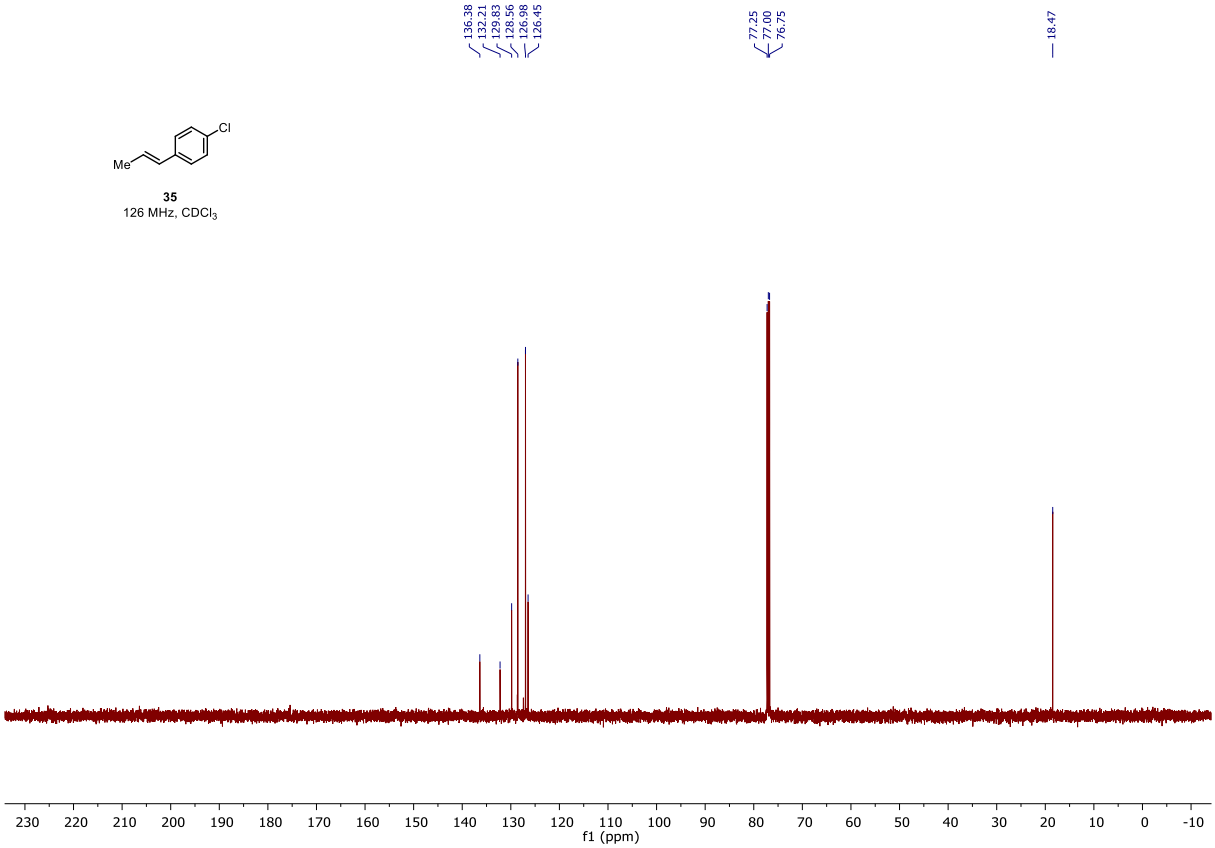

35
126 MHz, $CDCl_3$

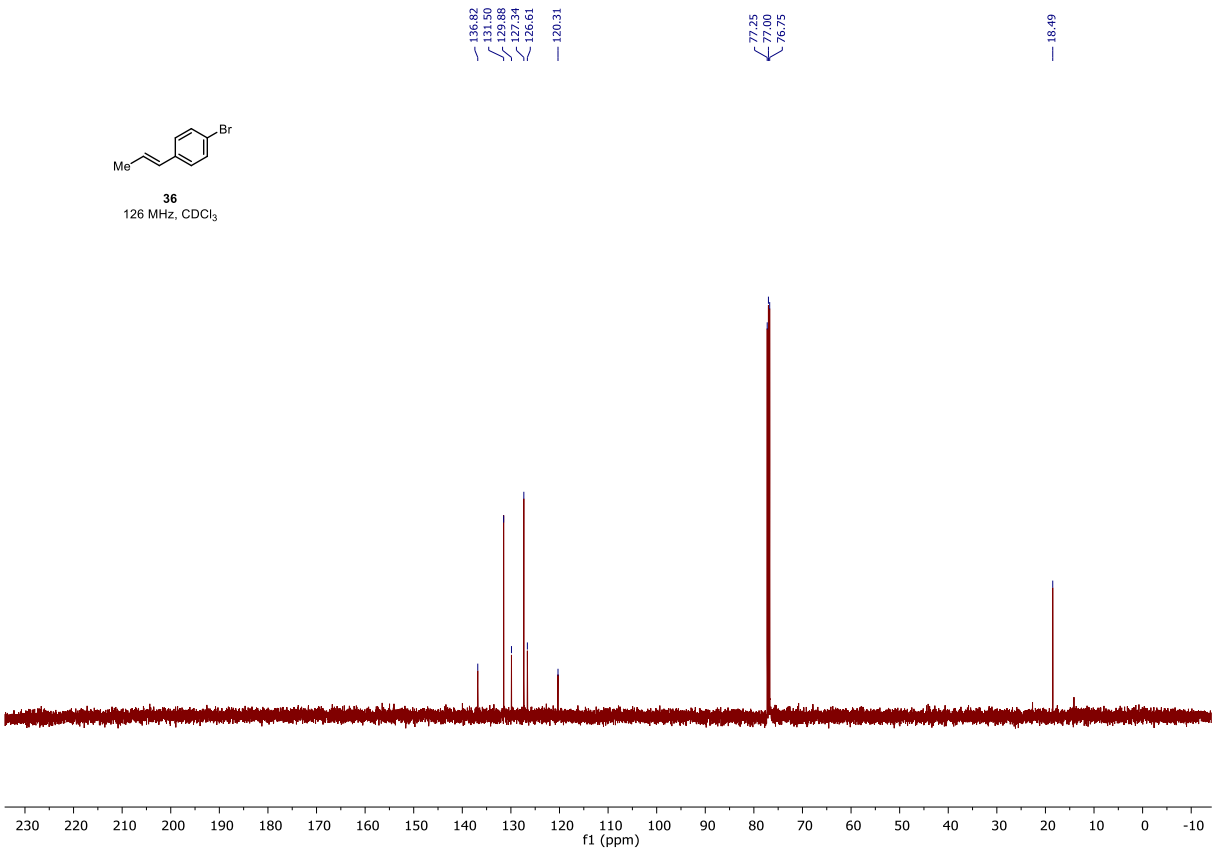

36
126 MHz, $CDCl_3$

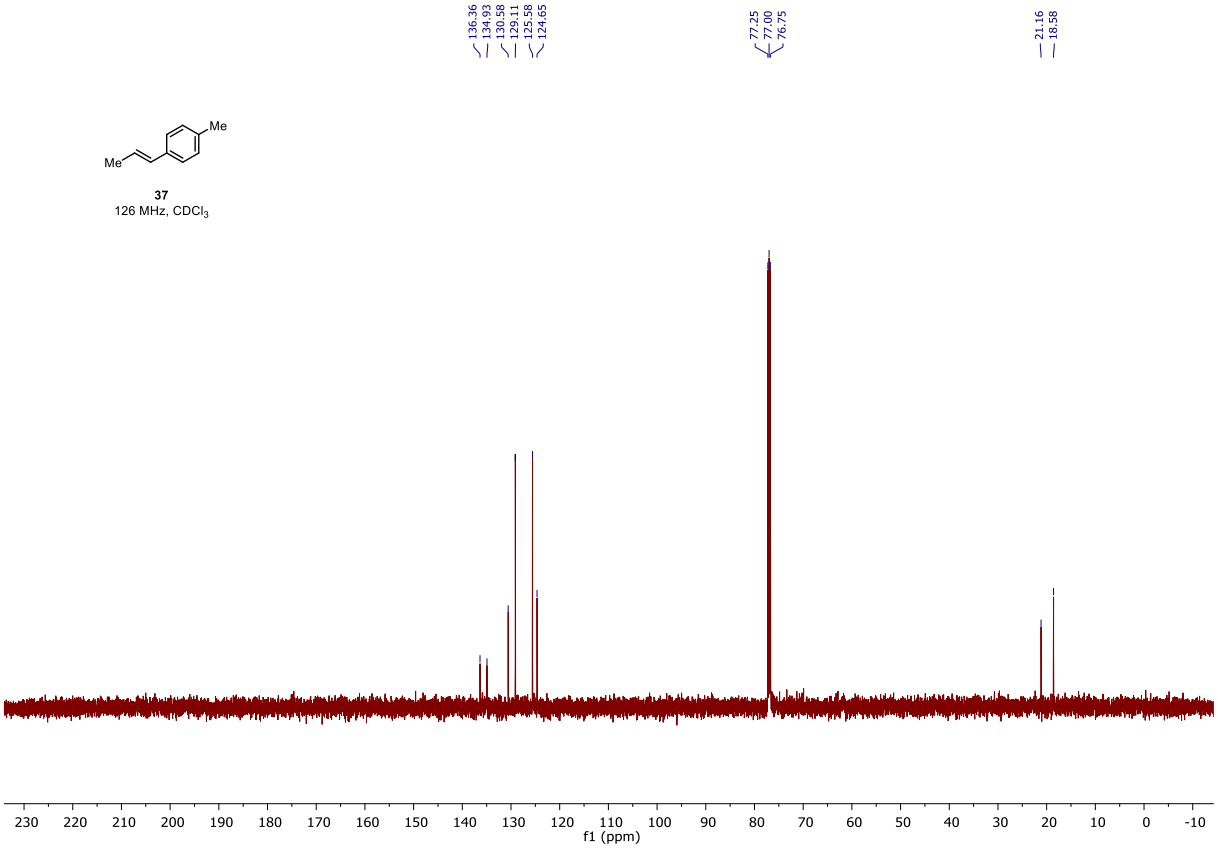
136.36
134.93
130.58
129.11
125.58
124.65
77.25
77.00
76.75
21.16
18.58
Me
Me
37
126 MHz, CDCl3
f1 (ppm)

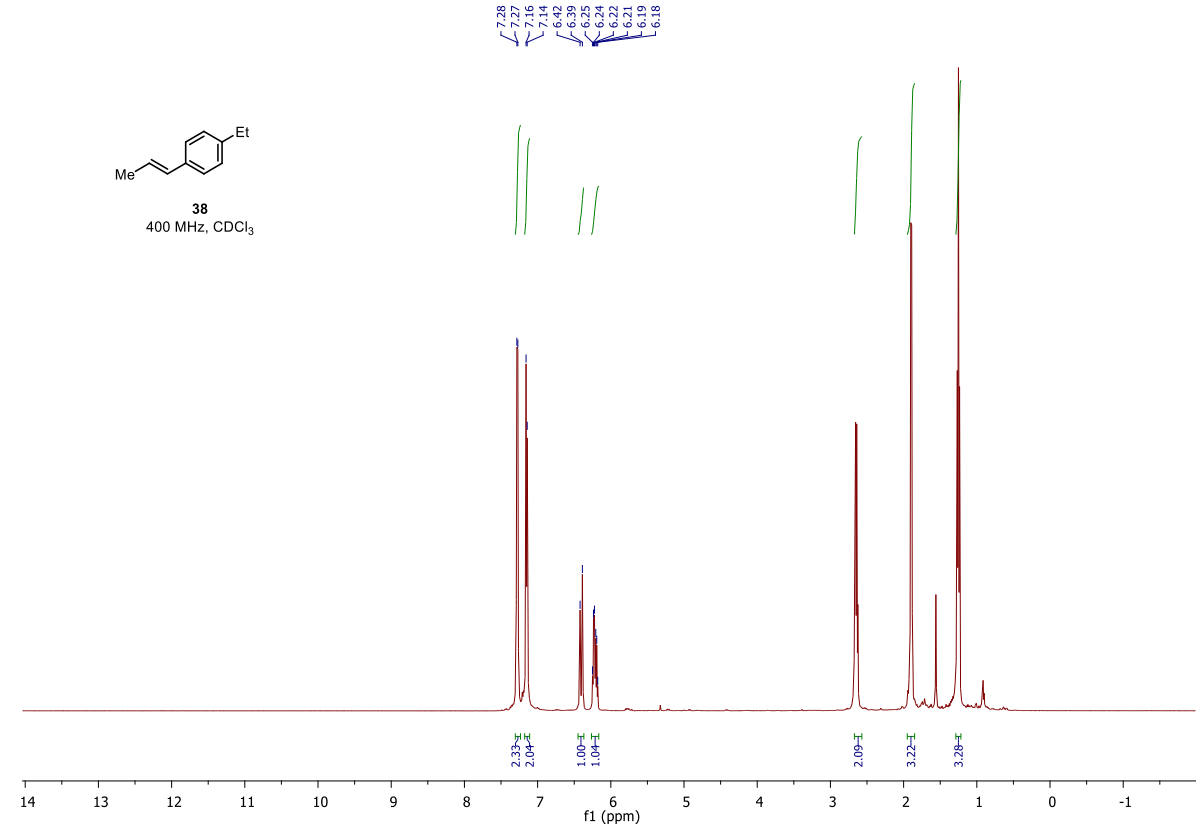
7.28
7.27
7.16
7.14
6.42
6.39
6.25
6.24
6.22
6.21
6.19
6.18
Et
Me
38
400 MHz, CDCl3
2.33
2.04
1.00
1.04
2.09
3.22
3.28
f1 (ppm)

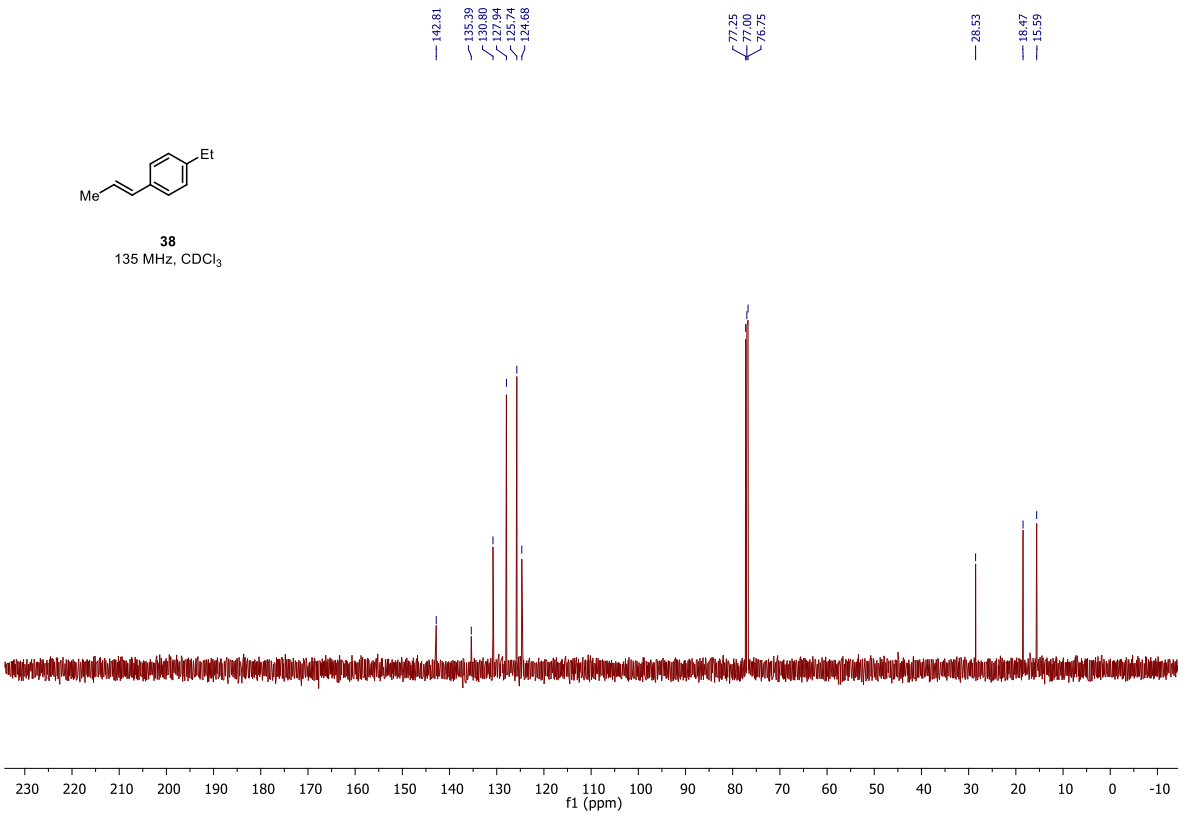
142.81
135.39
130.80
127.94
125.74
124.68
77.25
77.00
76.75
28.53
18.47
15.59
Et
Me
38
135 MHz, CDCl3
f1 (ppm)

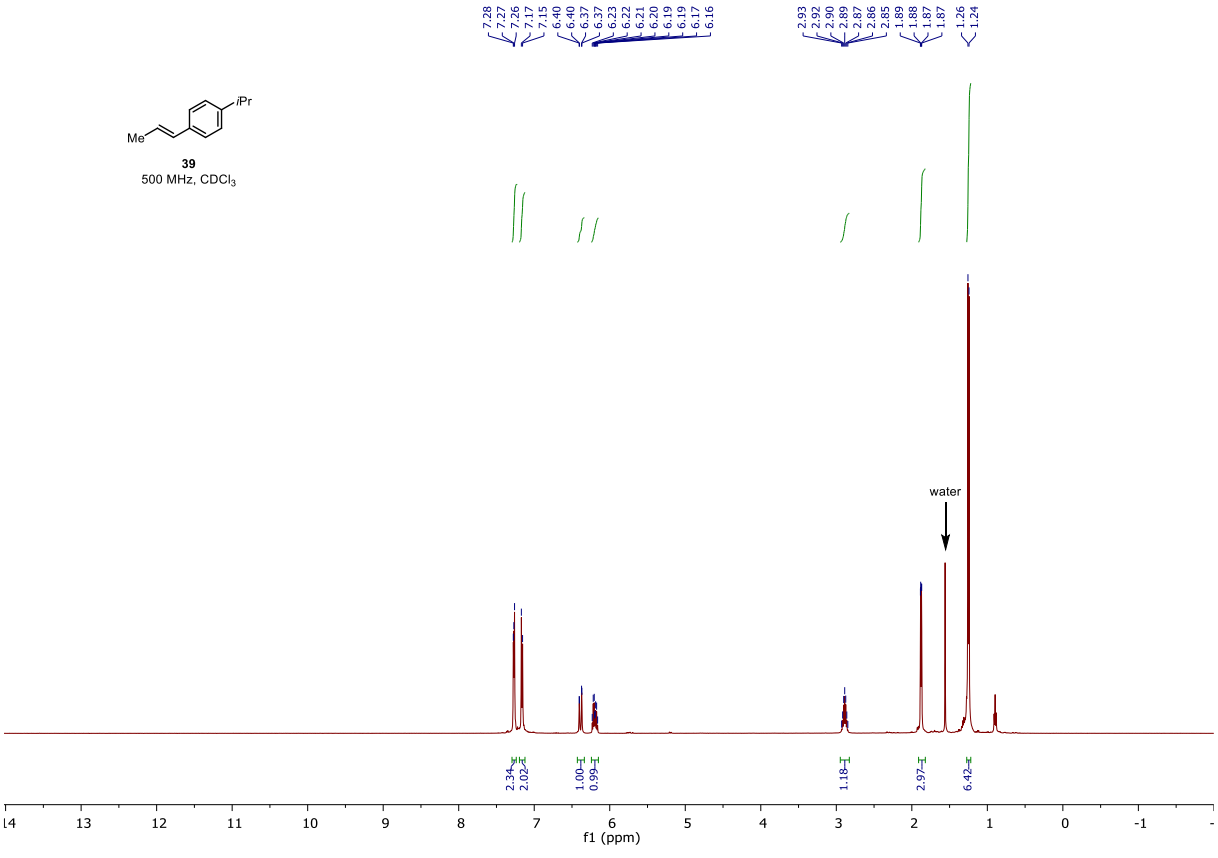
7.28
7.27
7.26
7.17
7.15
6.40
6.37
6.23
6.22
6.21
6.20
6.19
6.17
6.16
2.93
2.92
2.90
2.89
2.87
2.86
2.85
1.89
1.88
1.87
1.26
1.24
iPr
Me
39
500 MHz, CDCl3
water
2.34
2.02
1.00
0.99
1.18
2.97
6.42
f1 (ppm)

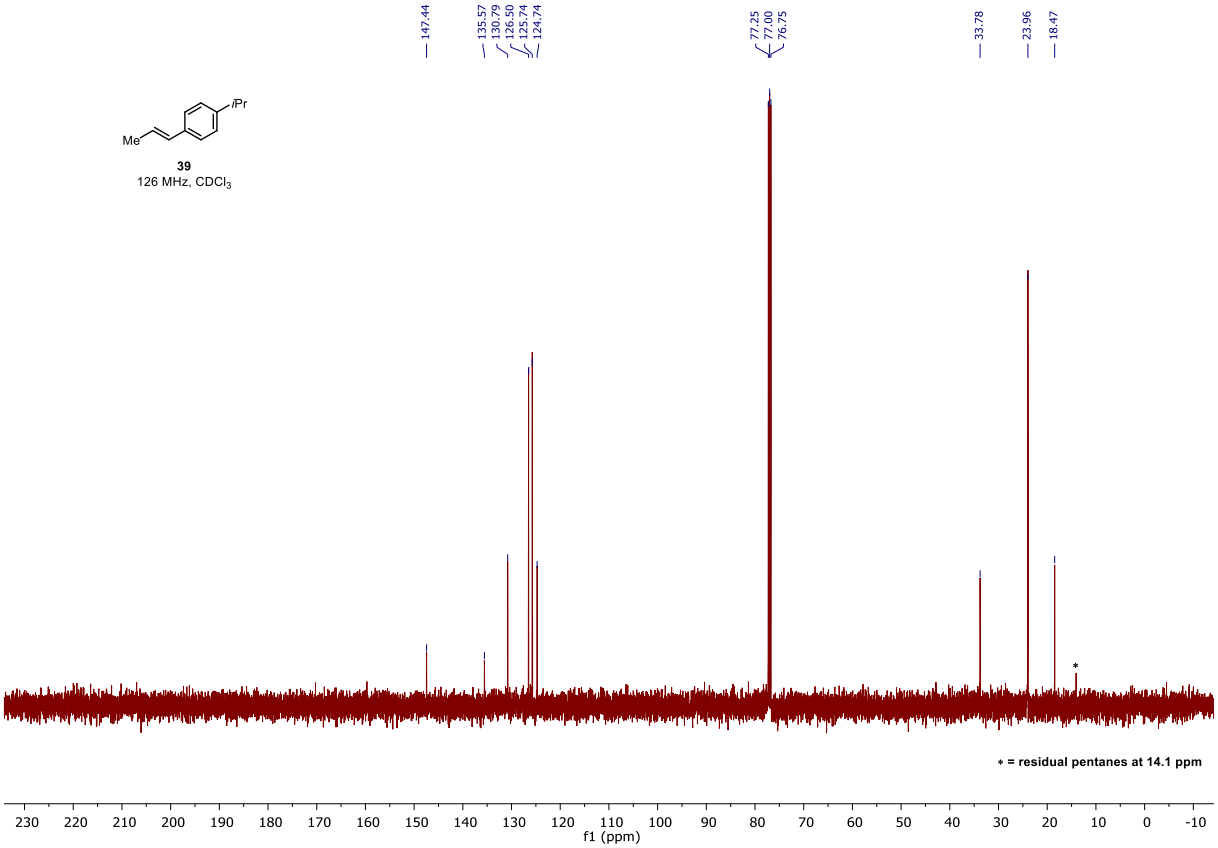
147.44
135.57
130.79
126.50
125.74
124.74
77.25
77.00
76.75
33.78
23.96
18.47
iPr
Me
39
126 MHz, CDCl3
* = residual pentanes at 14.1 ppm
f1 (ppm)

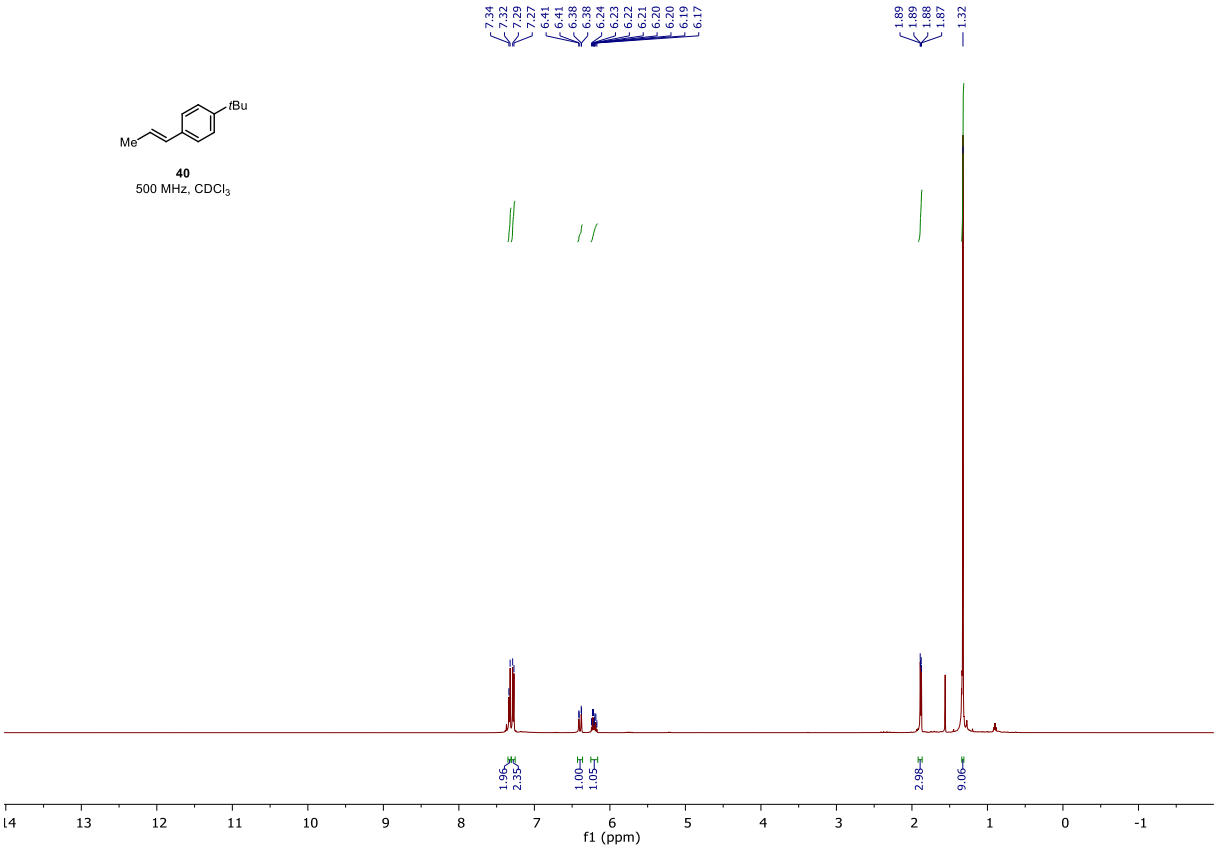
7.34
7.32
7.29
7.27
6.41
6.41
6.38
6.38
6.24
6.23
6.22
6.21
6.20
6.20
6.19
6.17
1.89
1.89
1.88
1.87
1.32
tBu
Me
40
500 MHz, CDCl3
1.96
2.35
1.00
1.05
2.98
9.06
f1 (ppm)

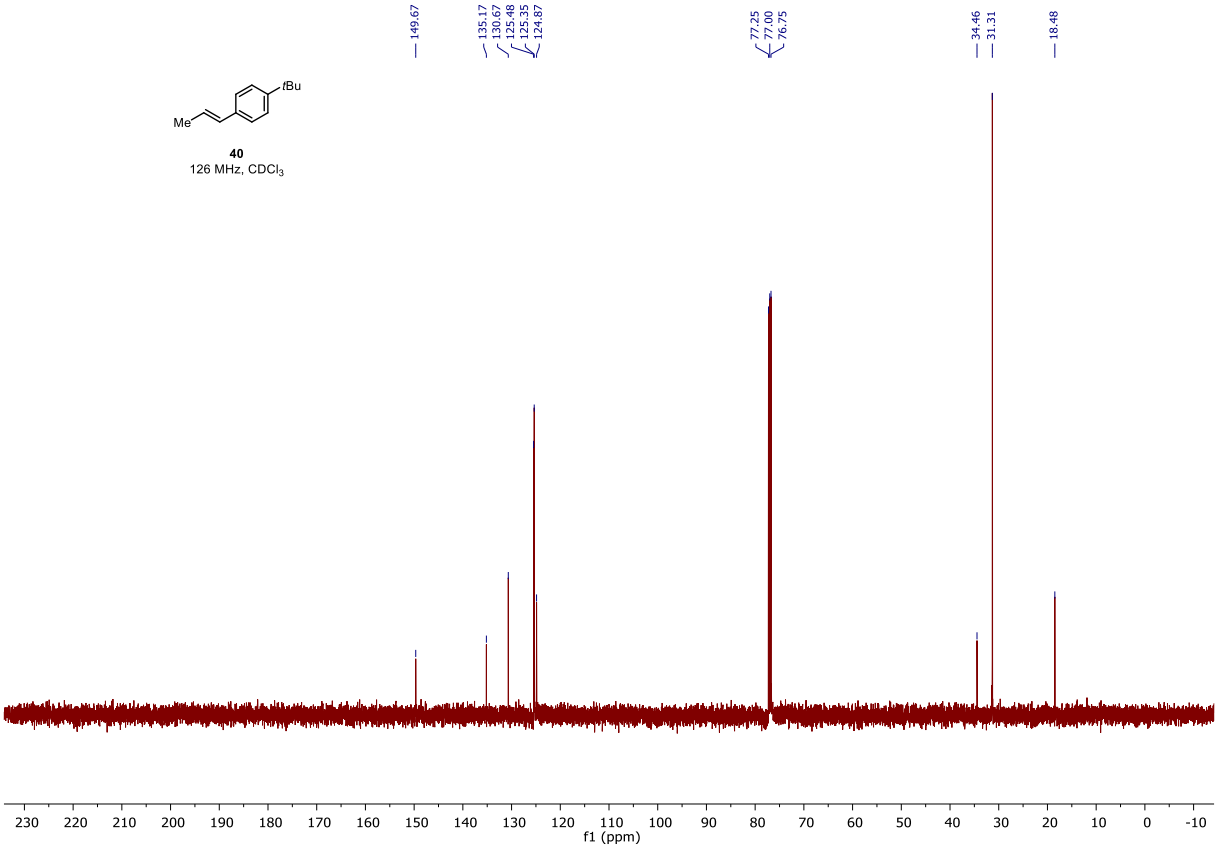

40
126 MHz, $CDCl_3$

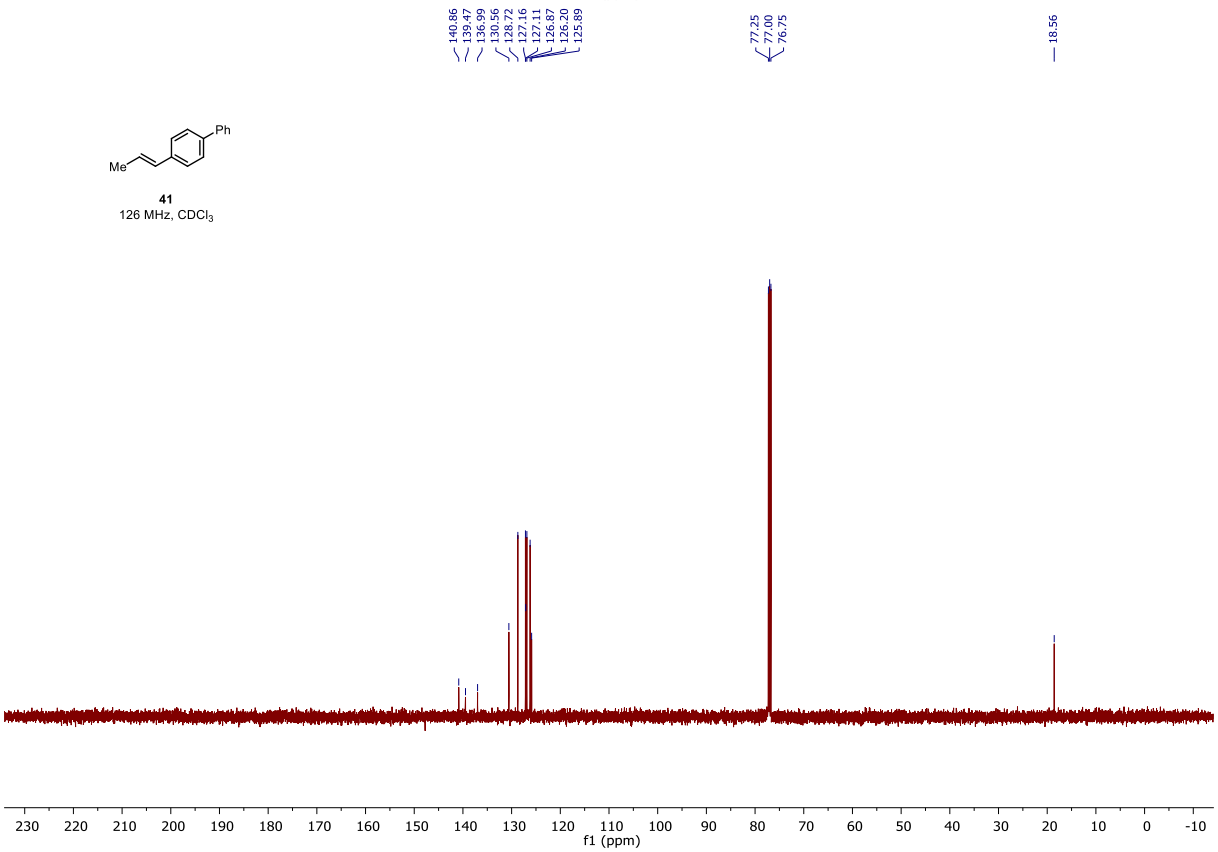

41
126 MHz, $CDCl_3$

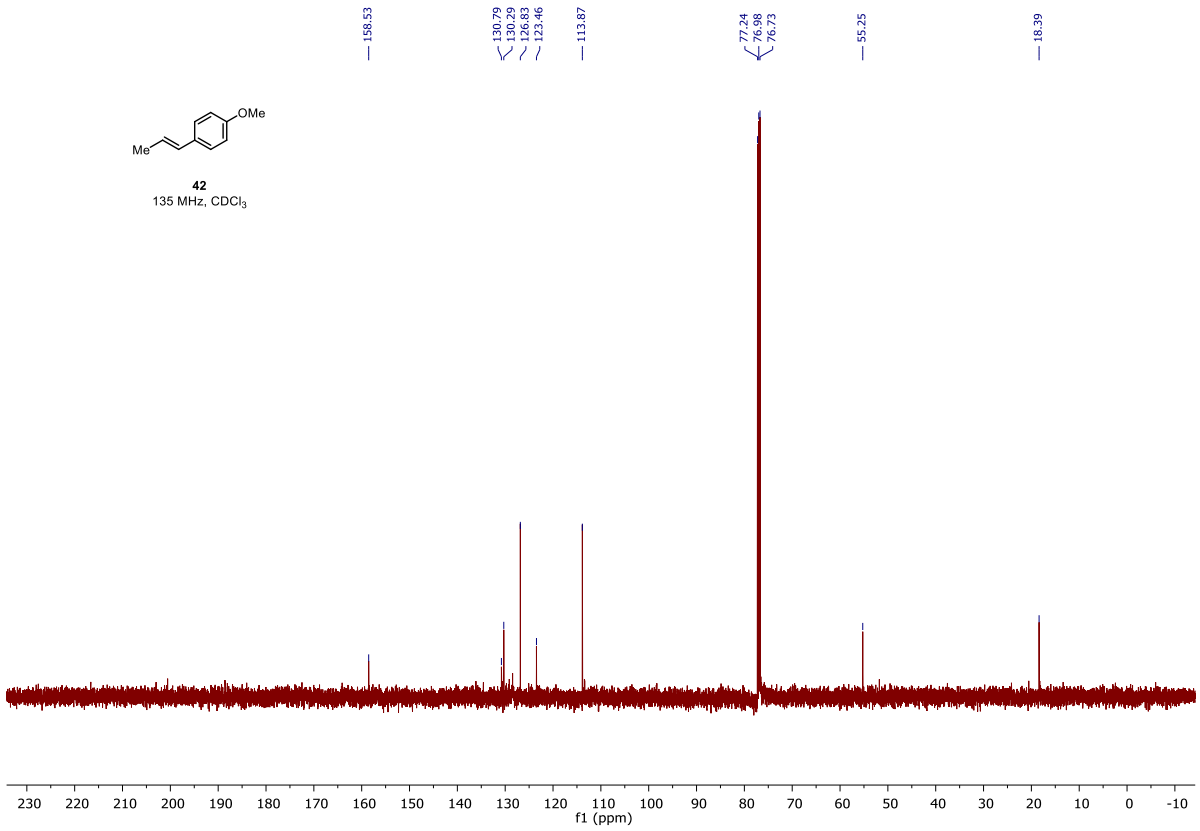
158.53
130.79
130.29
126.83
123.46
113.87
77.24
76.98
76.73
55.25
18.39
OMe
Me
42
135 MHz, CDCl3
230 220 210 200 190 180 170 160 150 140 130 120 110 100 90 80 70 60 50 40 30 20 10 0 -10
f1 (ppm)

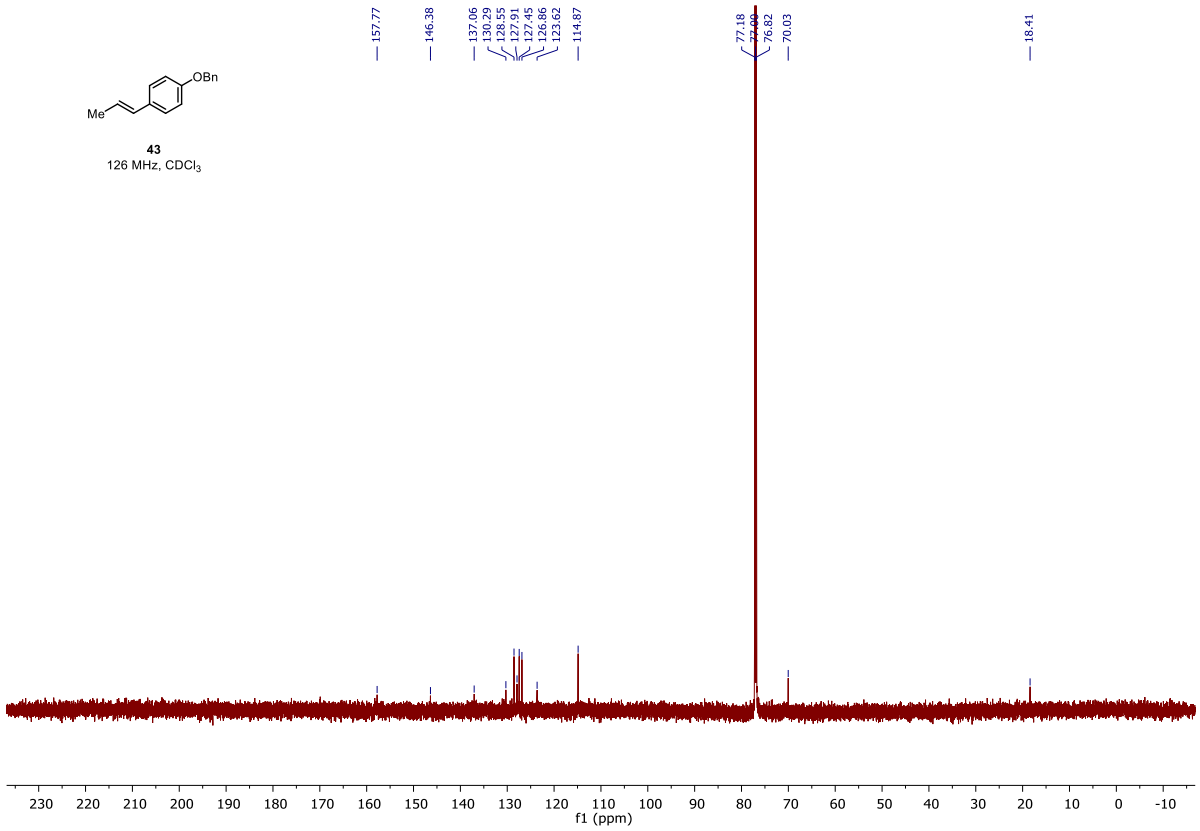
157.77
146.38
137.06
130.29
128.55
127.91
127.45
126.86
123.62
114.87
77.18
76.82
70.03
18.41
OBn
Me
43
126 MHz, CDCl3
230 220 210 200 190 180 170 160 150 140 130 120 110 100 90 80 70 60 50 40 30 20 10 0 -10
f1 (ppm)

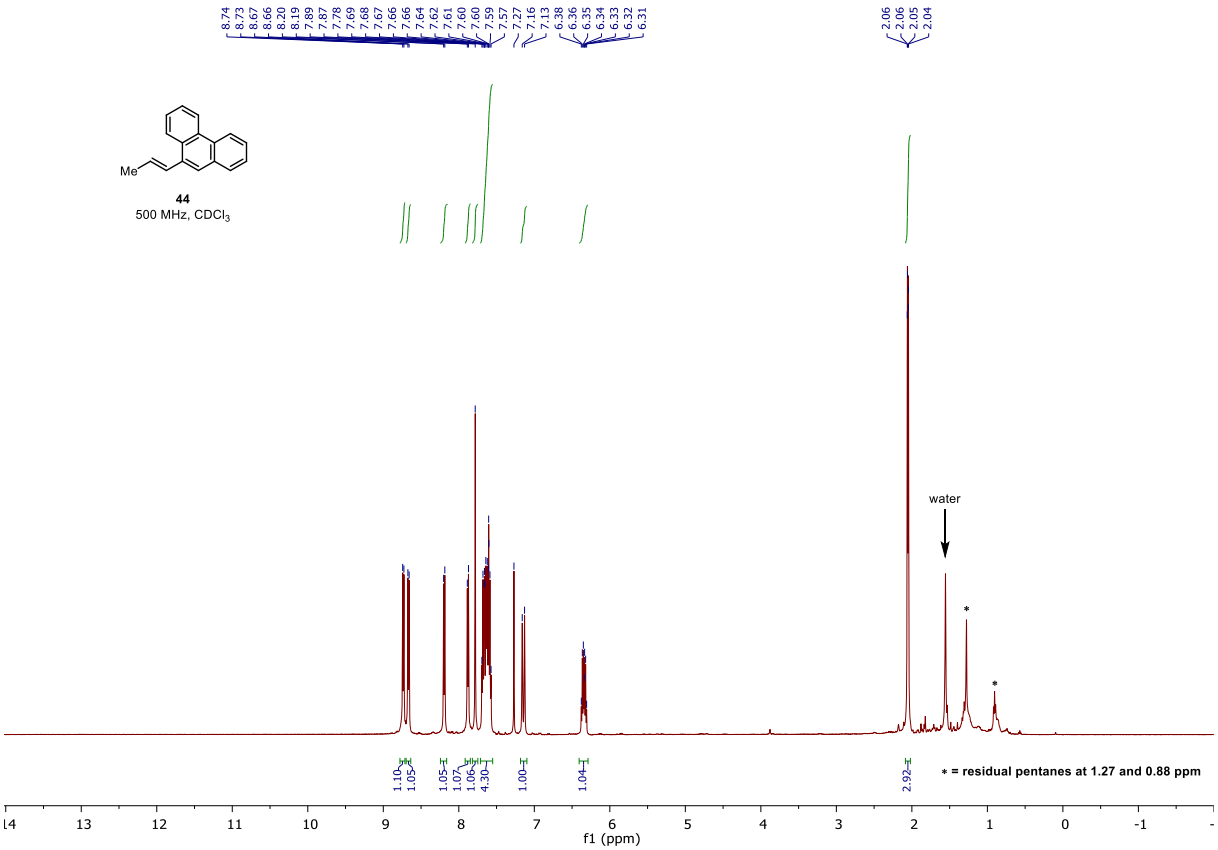
8.74
8.73
8.67
8.66
8.20
8.19
7.89
7.87
7.78
7.69
7.68
7.67
7.66
7.66
7.64
7.62
7.61
7.60
7.60
7.59
7.57
7.27
7.16
7.13
6.38
6.36
6.35
6.34
6.33
6.32
6.31
2.06
2.06
2.05
2.04
Me
44
500 MHz, CDCl3
water
*
*
1.10
1.05
1.05
1.07
1.06
4.30
1.00
1.04
2.92
* = residual pentanes at 1.27 and 0.88 ppm
f1 (ppm)

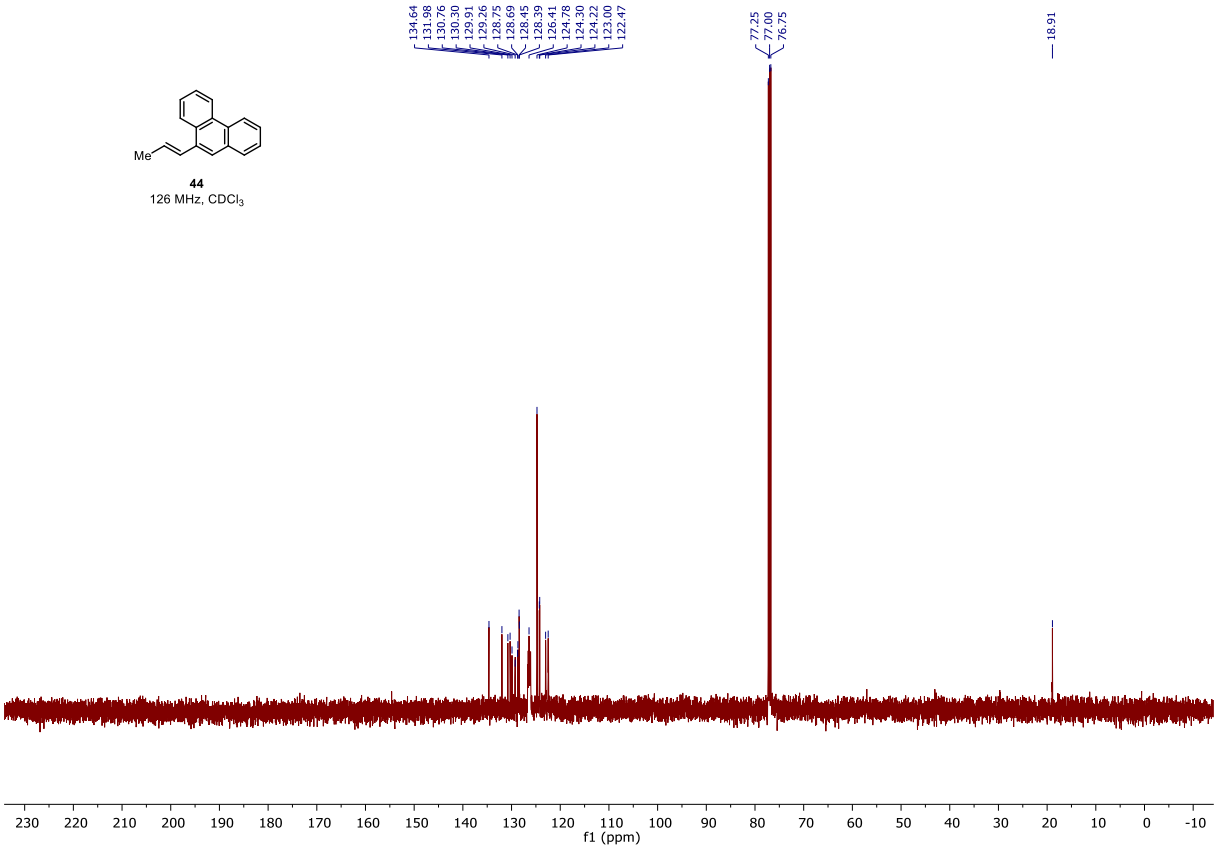
134.64
131.98
130.76
130.30
129.91
129.26
128.75
128.69
128.45
128.39
126.41
124.78
124.30
124.22
123.00
122.47
77.25
77.00
76.75
18.91
Me
44
126 MHz, CDCl3
f1 (ppm)

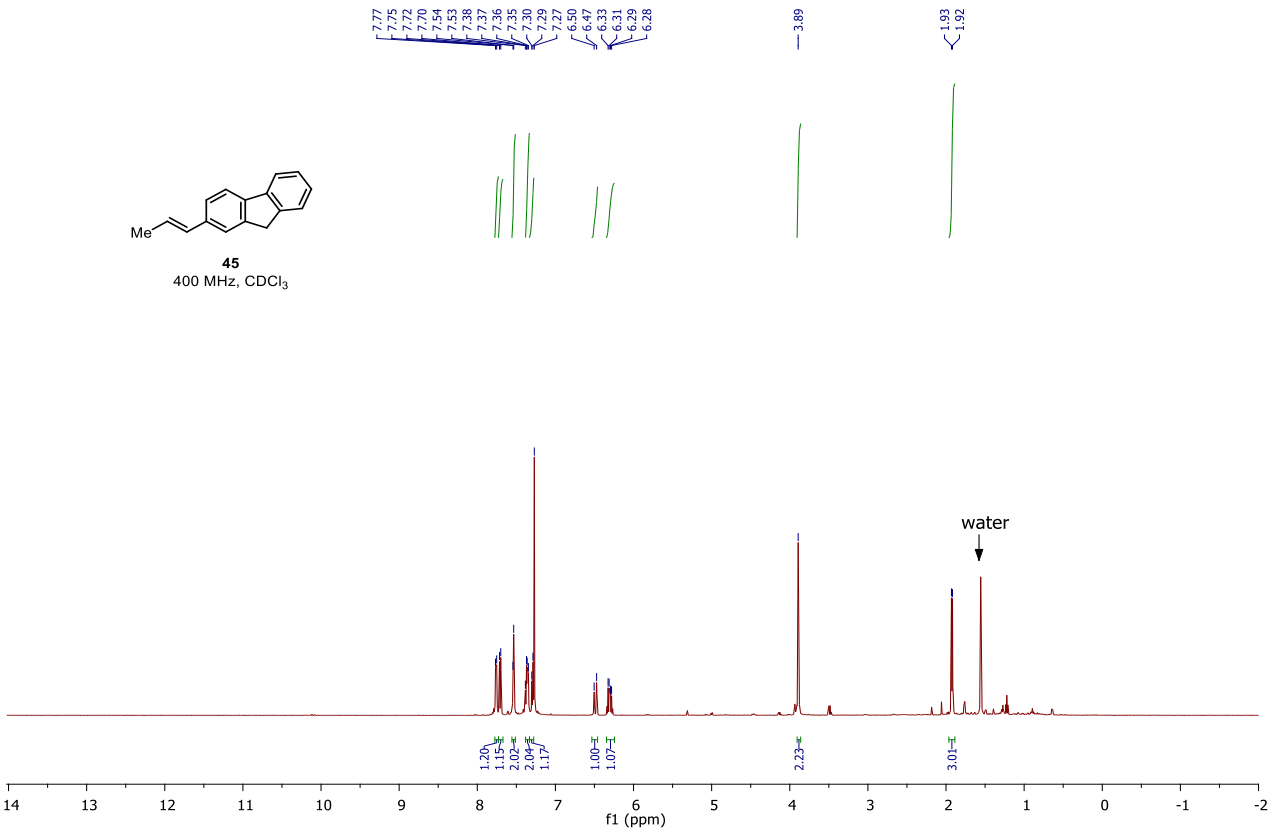

45
400 MHz, $CDCl_3$

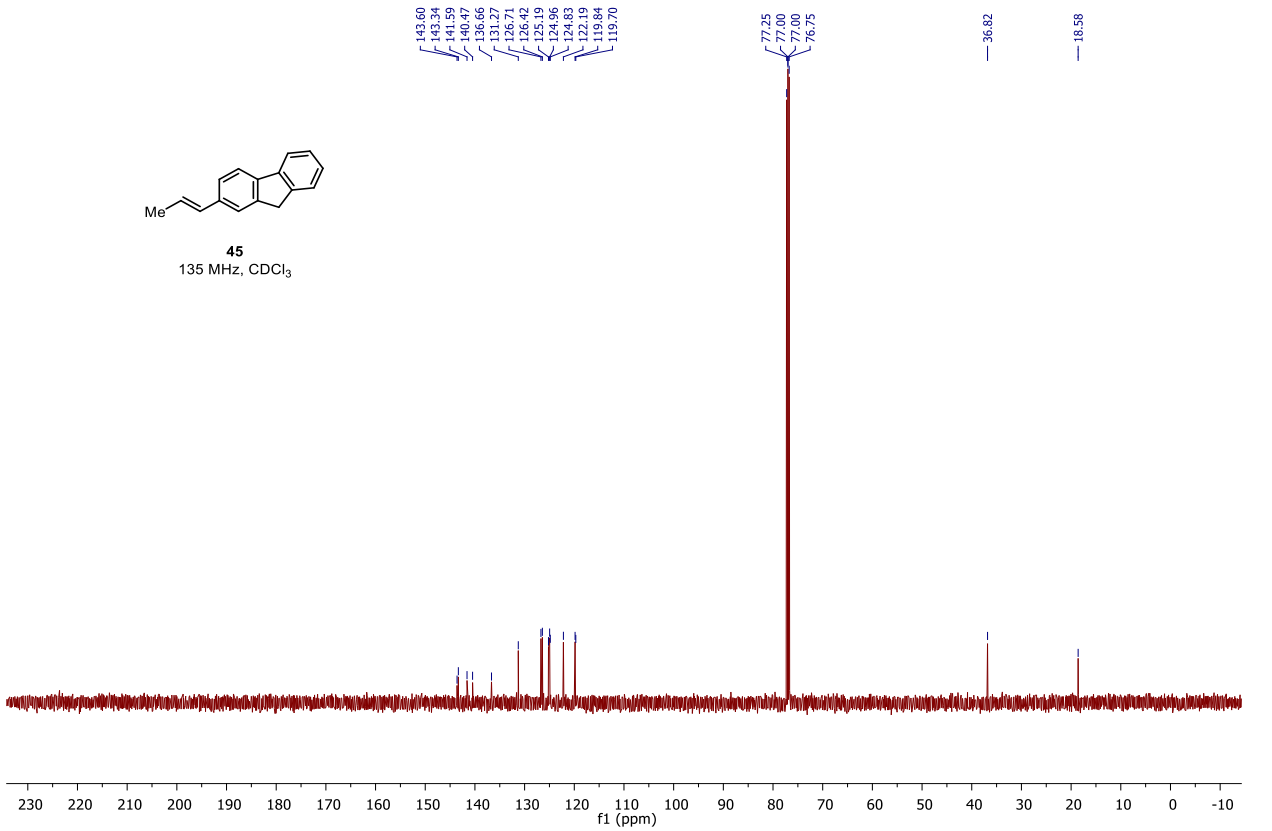

45
135 MHz, $CDCl_3$

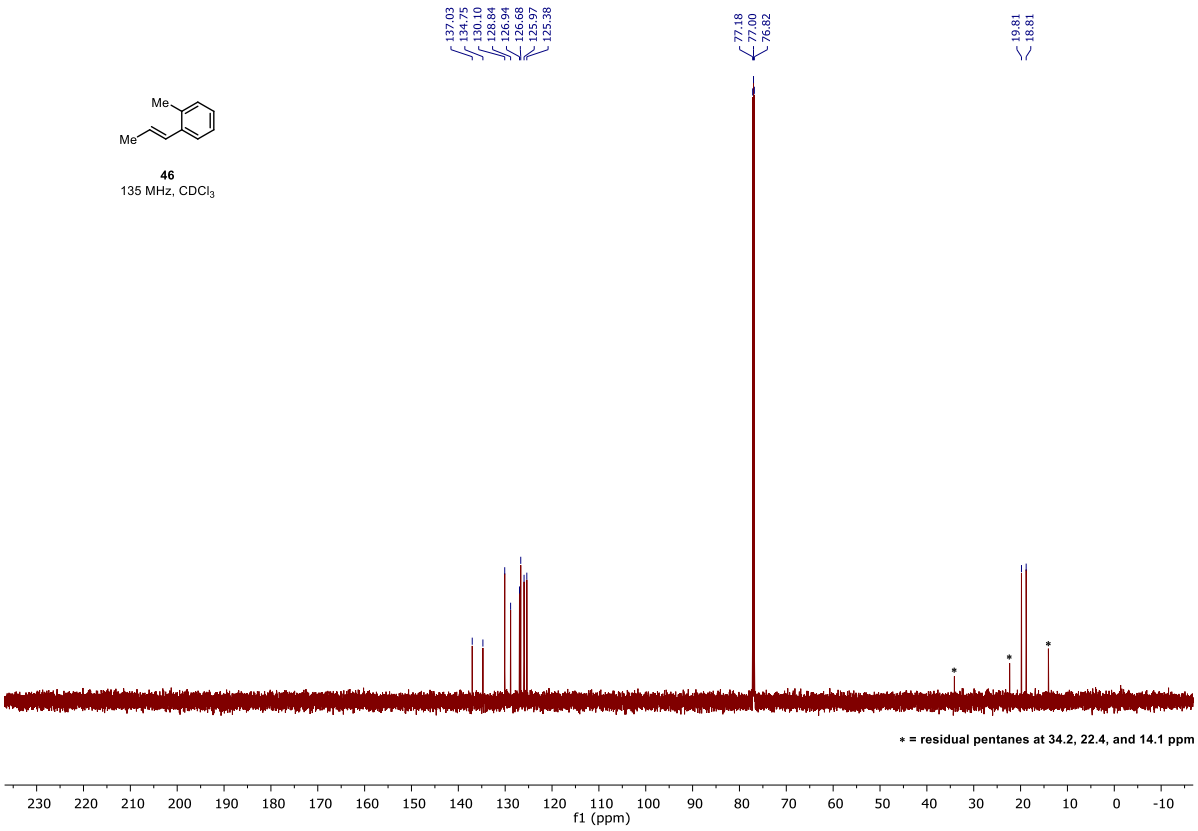
137.03
134.75
130.10
128.84
126.94
126.68
125.97
125.38
77.18
77.00
76.82
19.81
18.81
Me
Me
46
135 MHz, CDCl3
* = residual pentanes at 34.2, 22.4, and 14.1 ppm
f1 (ppm)

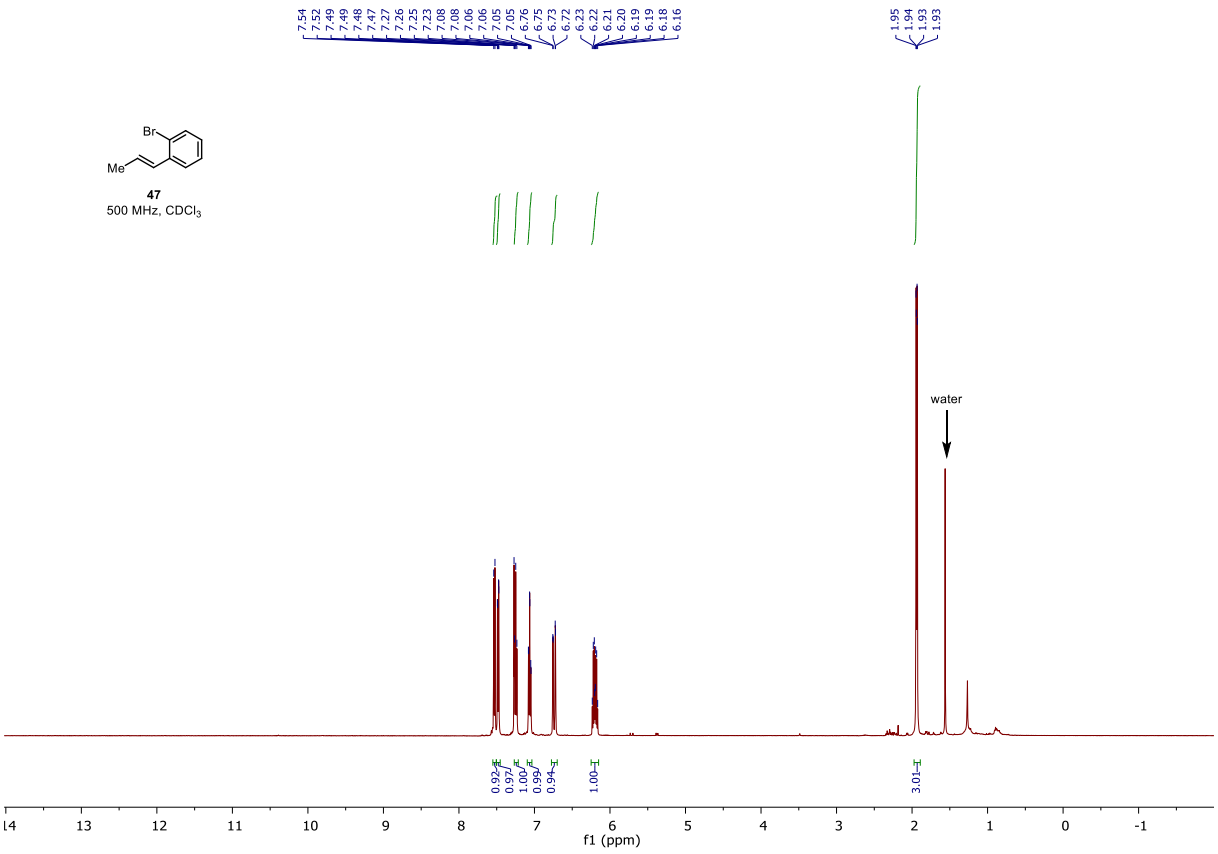
7.54
7.52
7.49
7.49
7.48
7.47
7.27
7.26
7.25
7.23
7.08
7.08
7.06
7.06
7.05
7.05
6.76
6.75
6.73
6.72
6.23
6.22
6.21
6.20
6.19
6.19
6.18
6.16
1.95
1.94
1.93
1.93
Br
Me
47
500 MHz, CDCl3
water
0.92
0.97
1.00
0.99
0.94
1.00
3.01
f1 (ppm)

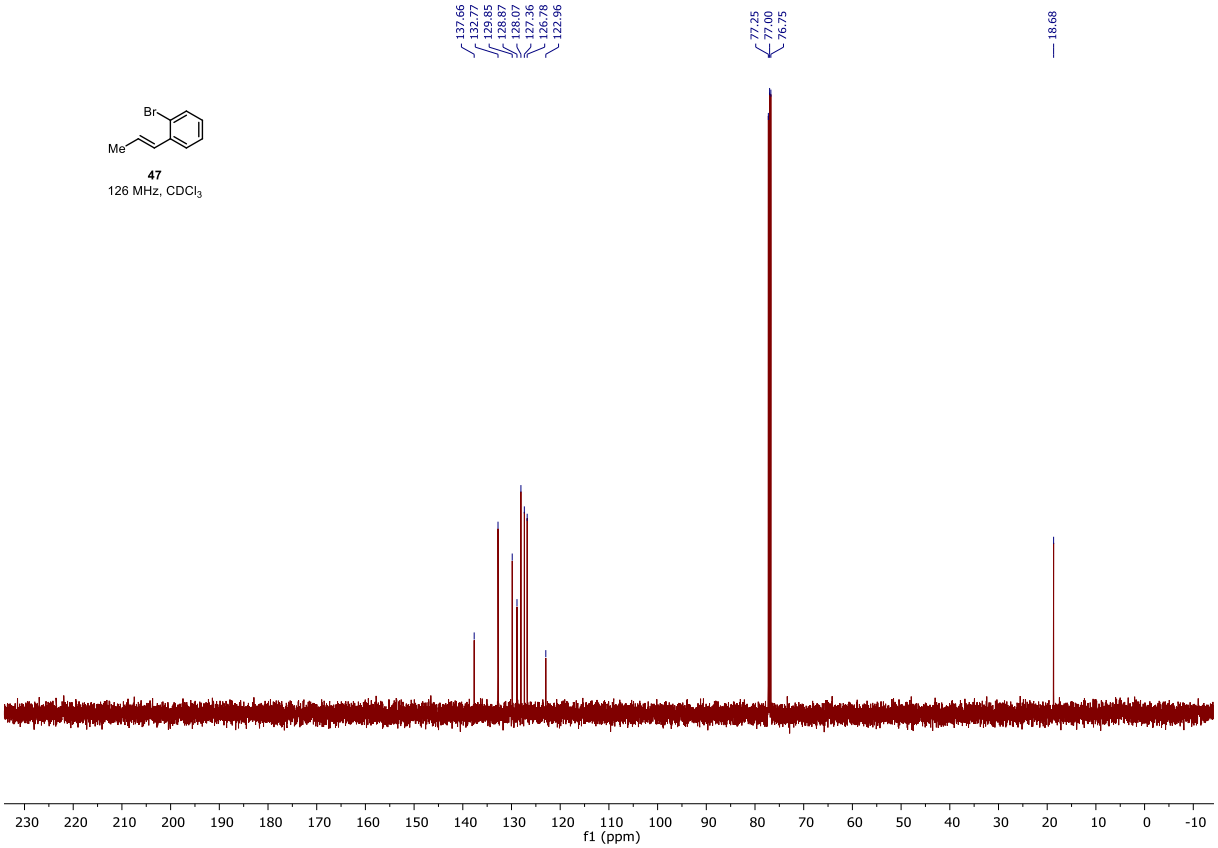
137.66
132.77
129.85
128.87
128.07
127.36
126.78
122.96
77.25
77.00
76.75
18.68
Br
Me
47
126 MHz, CDCl3
f1 (ppm)

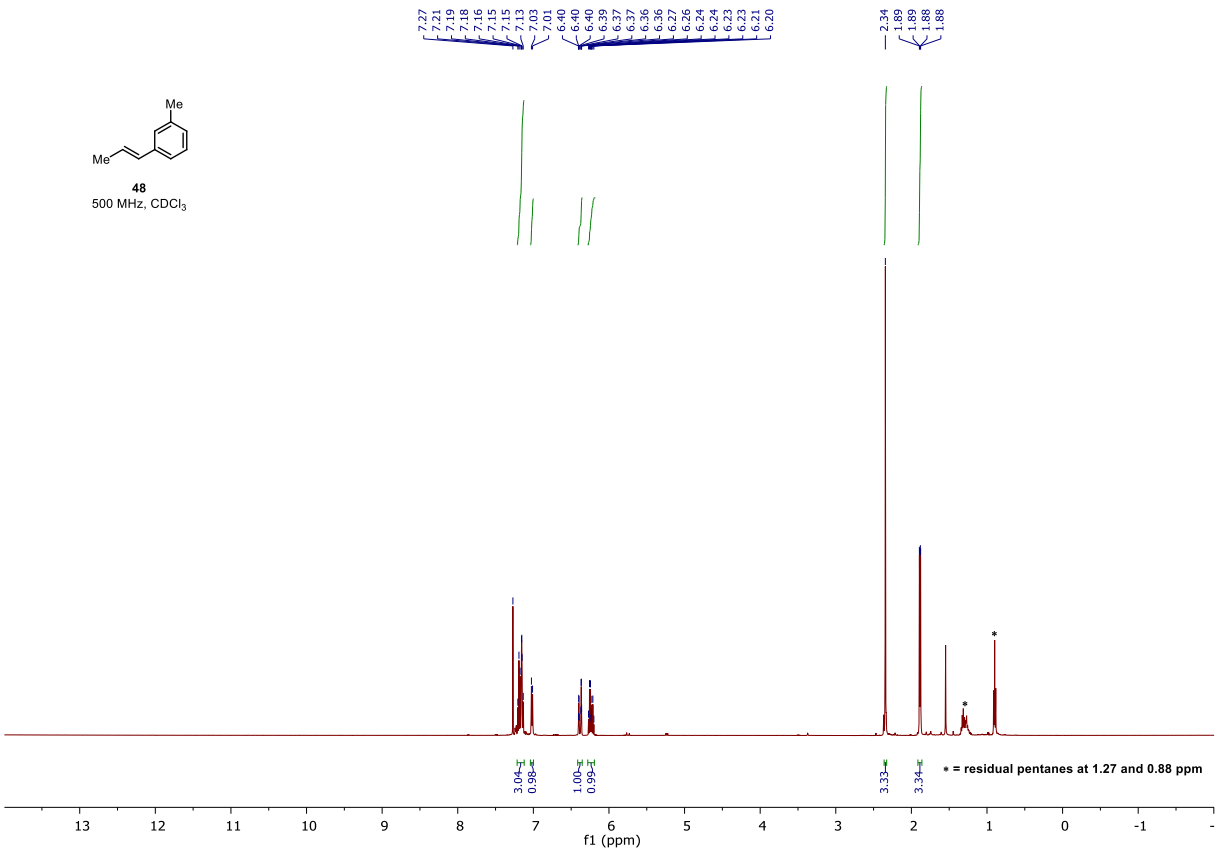
7.27
7.21
7.19
7.18
7.16
7.15
7.15
7.13
7.03
7.01
6.40
6.40
6.39
6.37
6.37
6.36
6.36
6.27
6.26
6.24
6.24
6.23
6.23
6.21
6.20
2.34
1.89
1.89
1.88
1.88
Me
Me
48
500 MHz, CDCl3
3.04
0.98
1.00
0.99
3.33
3.34
* = residual pentanes at 1.27 and 0.88 ppm
f1 (ppm)

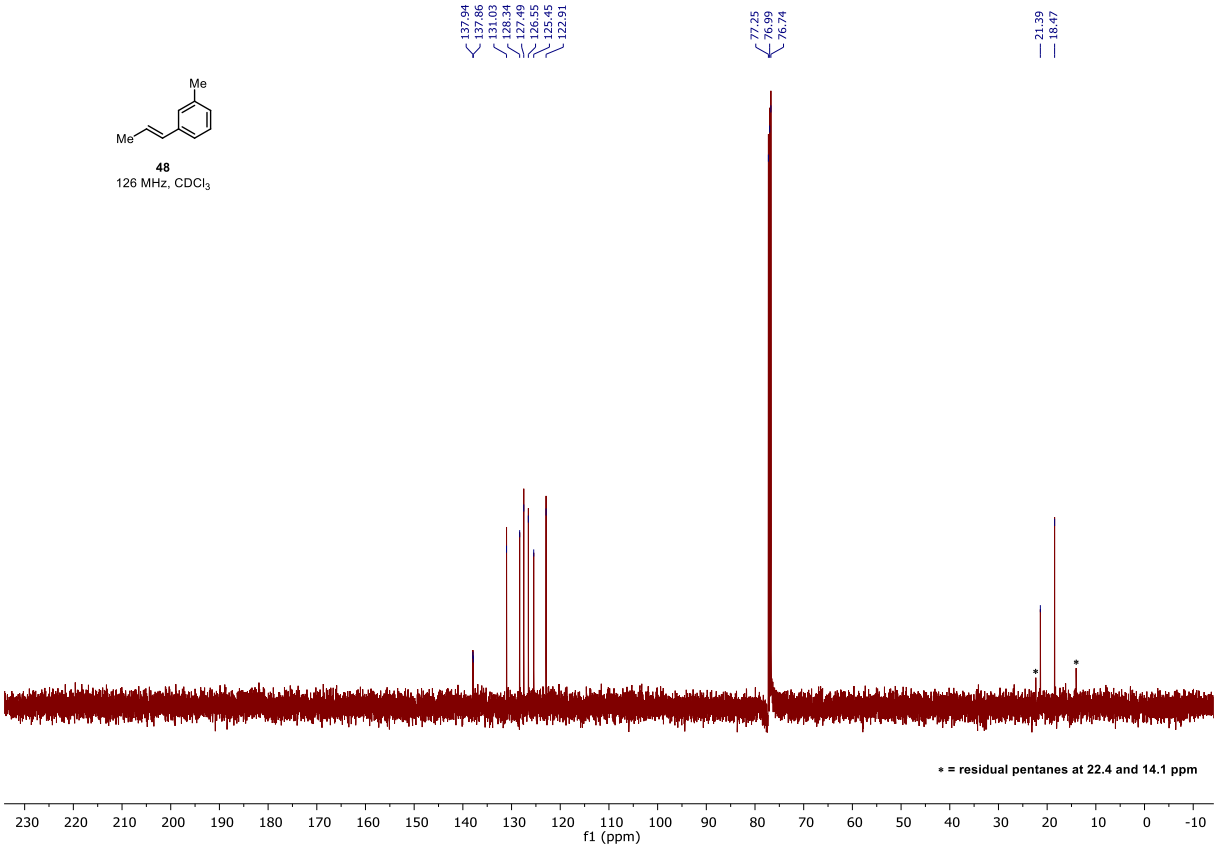
137.94
137.66
131.03
128.34
127.49
126.55
125.45
122.91
77.25
76.99
76.74
21.39
18.47
Me
Me
48
126 MHz, CDCl3
* = residual pentanes at 22.4 and 14.1 ppm
f1 (ppm)

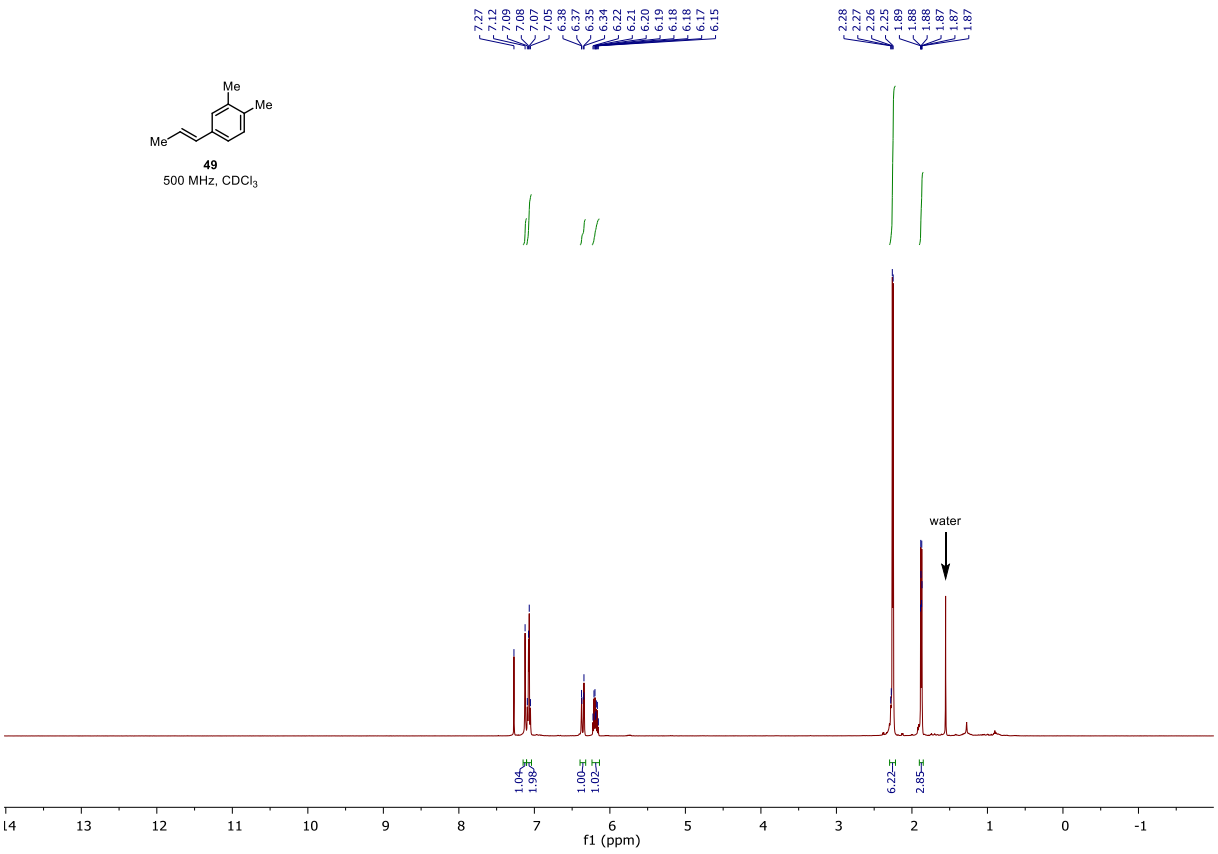
7.27
7.12
7.09
7.08
7.07
7.05
6.38
6.37
6.35
6.34
6.22
6.21
6.20
6.19
6.18
6.18
6.17
6.15
2.28
2.27
2.27
2.26
2.25
1.88
1.88
1.87
1.87
1.87
Me
Me
Me
49
500 MHz, CDCl3
water
1.04
1.98
1.00
1.02
6.22
2.85
f1 (ppm)

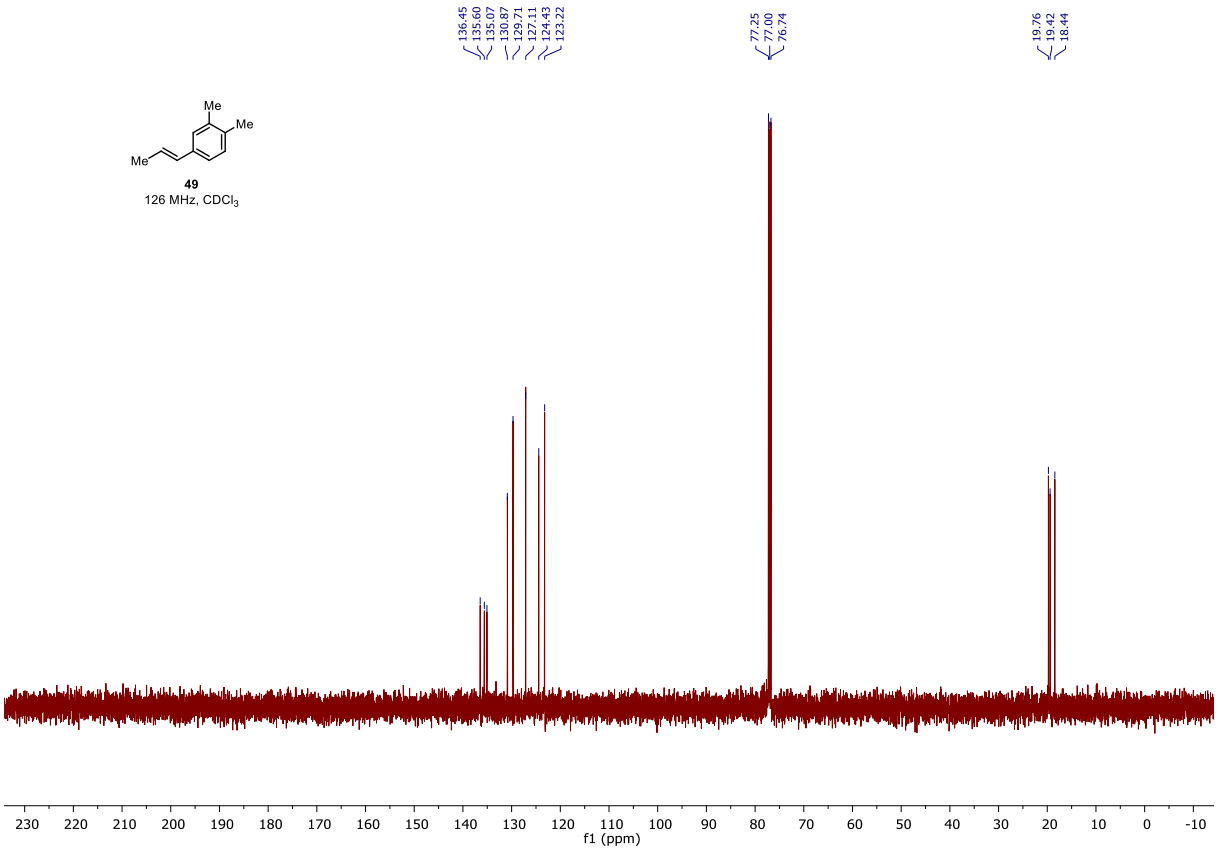
136.45
135.60
135.07
130.87
129.71
127.11
124.43
123.22
77.25
77.00
76.74
19.76
19.42
18.44
Me
Me
Me
49
126 MHz, CDCl3
230 220 210 200 190 180 170 160 150 140 130 120 110 100 90 80 70 60 50 40 30 20 10 0 -10
f1 (ppm)

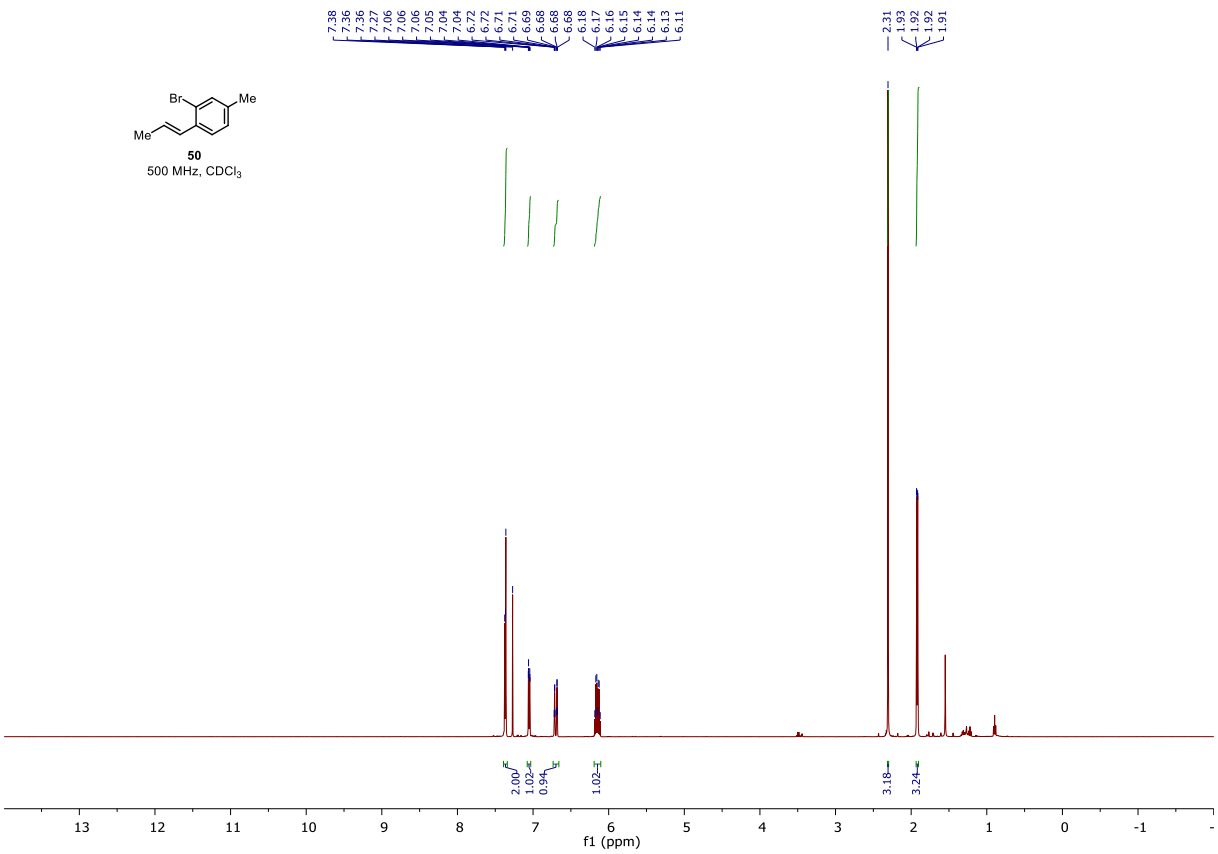
7.38
7.36
7.36
7.27
7.06
7.06
7.06
7.05
7.04
7.04
6.72
6.72
6.71
6.71
6.69
6.68
6.68
6.68
6.18
6.17
6.16
6.15
6.14
6.14
6.13
6.11
2.31
1.93
1.92
1.92
1.91
Br
Me
Me
50
500 MHz, CDCl3
2.00
1.02
0.94
1.02
3.18
3.24
13
12
11
10
9
8
7
6
5
4
3
2
1
0
-1
f1 (ppm)

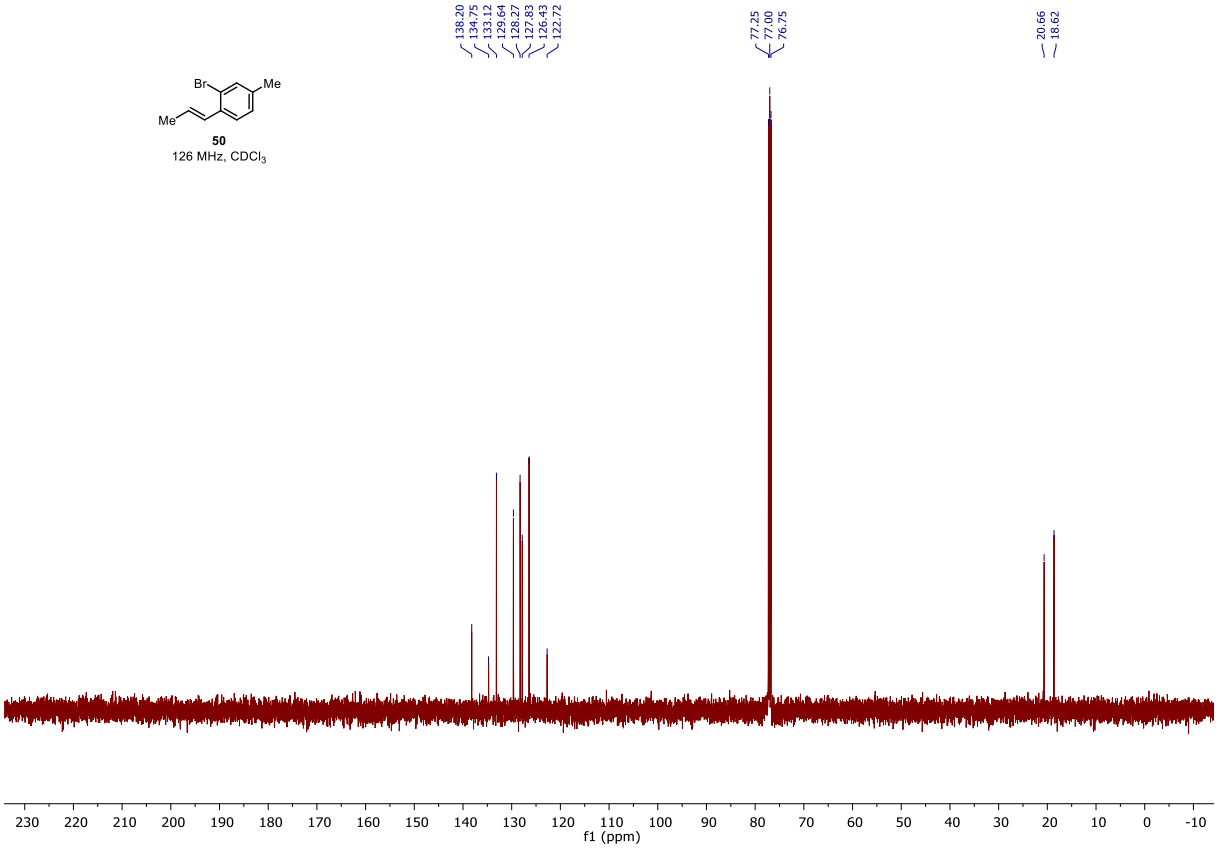
138.20
134.75
133.12
129.64
128.27
127.83
126.43
122.72
77.25
77.00
76.75
20.66
18.62
Br
Me
Me
50
126 MHz, CDCl3
f1 (ppm)

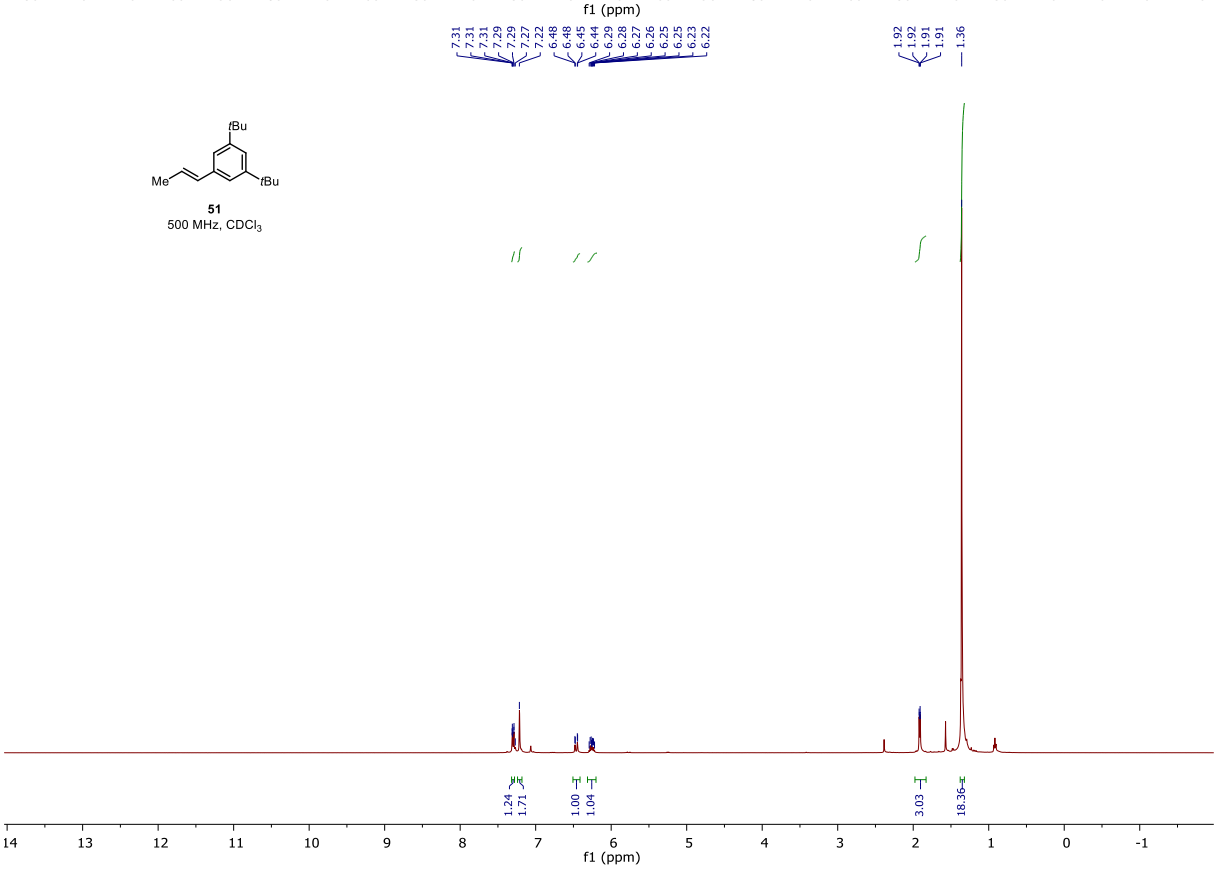
7.31
7.31
7.31
7.29
7.29
7.27
7.22
6.48
6.48
6.45
6.44
6.29
6.28
6.27
6.26
6.25
6.25
6.23
6.22
1.92
1.92
1.91
1.91
1.36
tBu
Me
tBu
51
500 MHz, CDCl3
1.24
1.71
1.00
1.04
3.03
18.36
f1 (ppm)

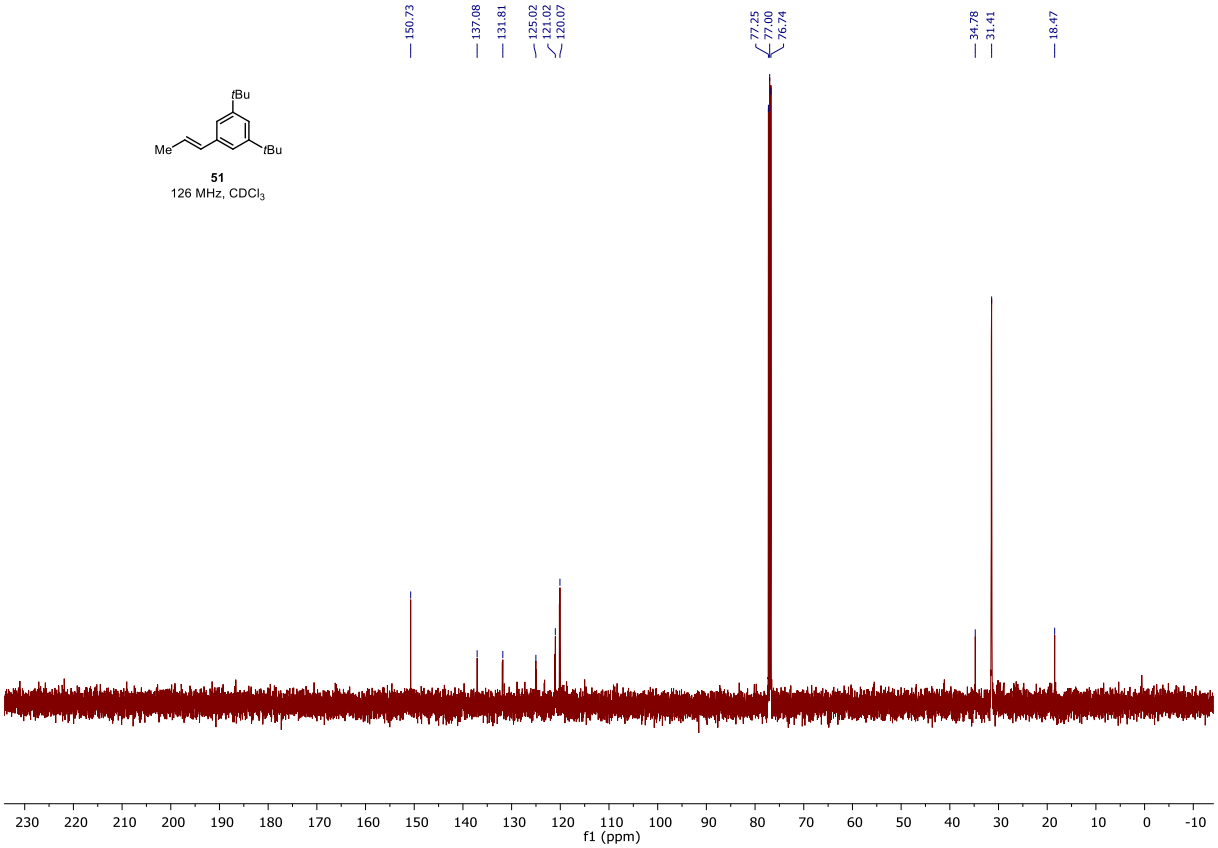

51
126 MHz, $CDCl_3$

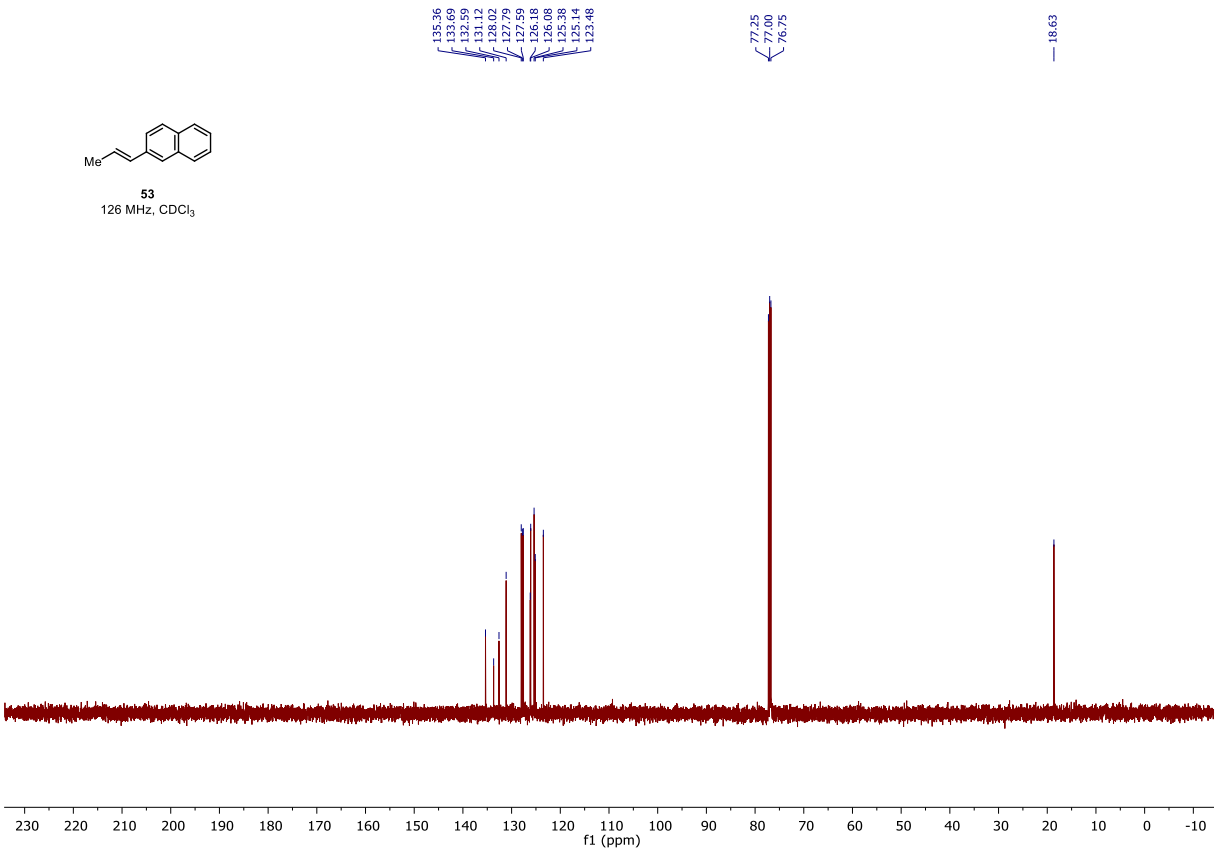

53
126 MHz, $CDCl_3$

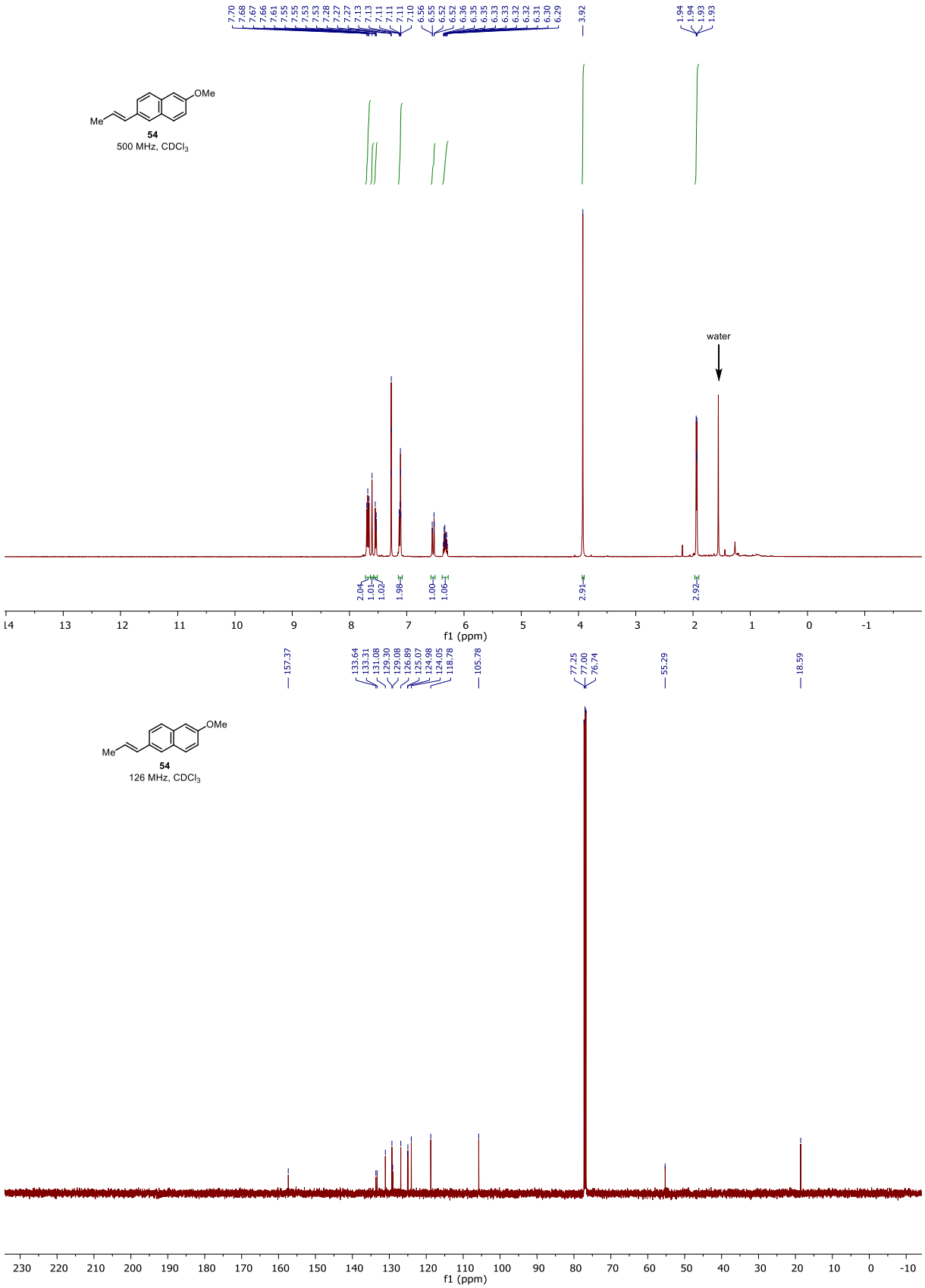
OMe
Me
54
500 MHz, CDCl3
water
f1 (ppm)
OMe
Me
54
126 MHz, CDCl3
f1 (ppm)

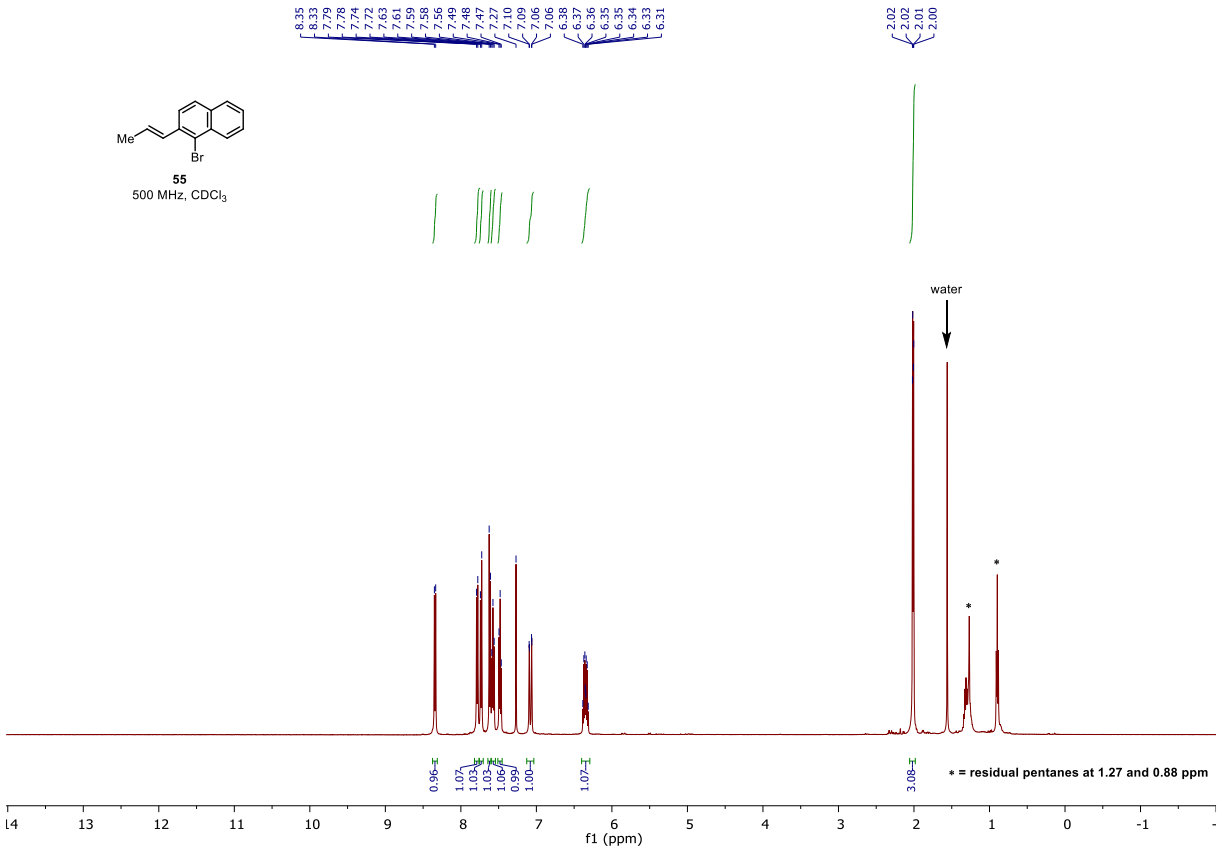
Me
Br
55
500 MHz, CDCl3
water
* = residual pentanes at 1.27 and 0.88 ppm
f1 (ppm)

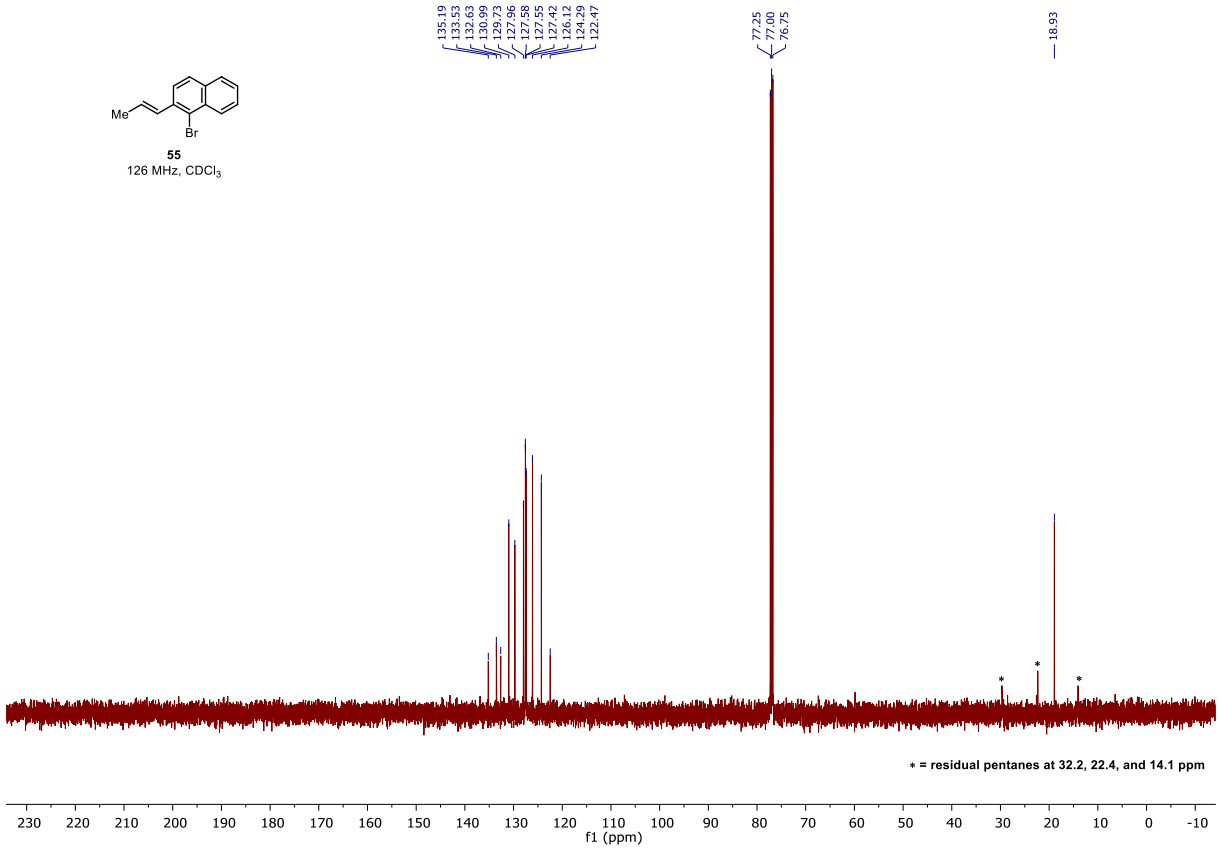
Me
Br
55
126 MHz, CDCl3
* = residual pentanes at 32.2, 22.4, and 14.1 ppm
f1 (ppm)

Oxetanes

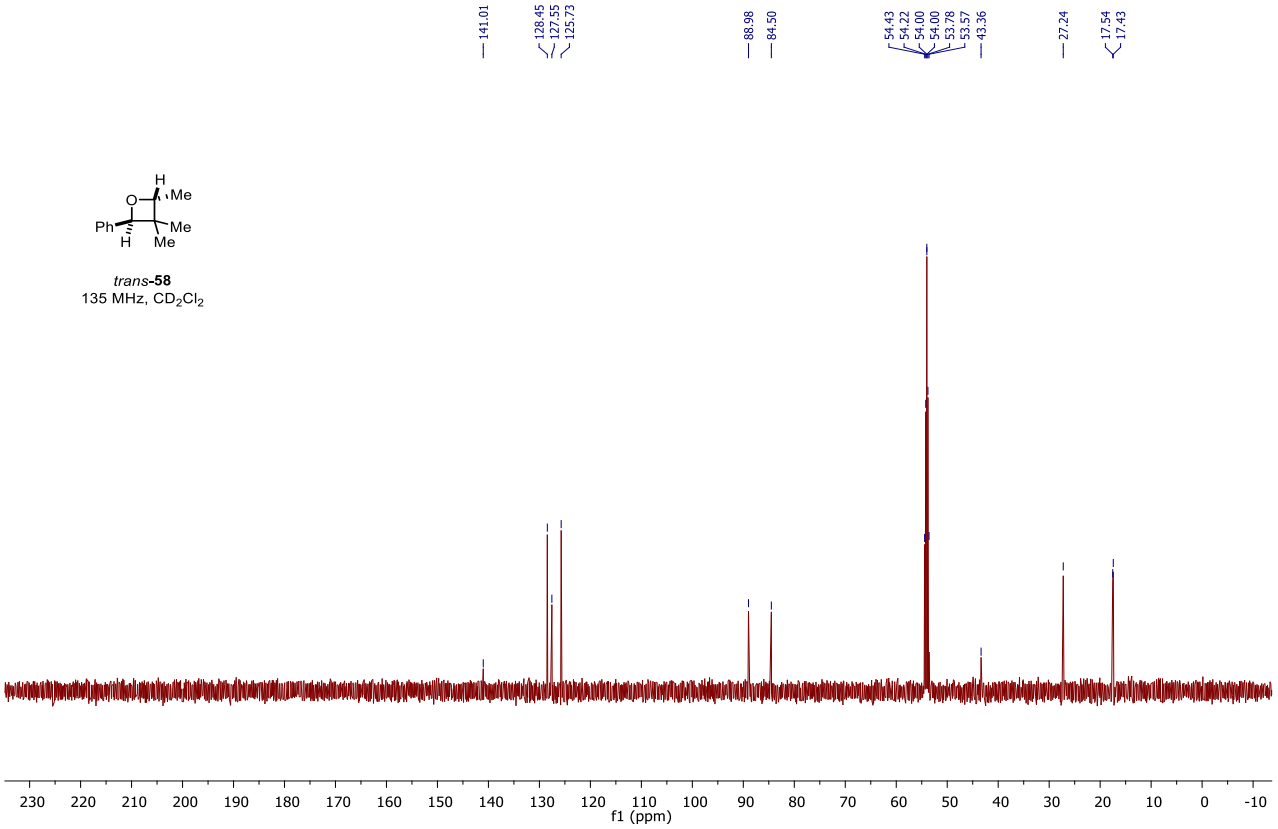
141.01
128.45
127.55
125.73
88.98
84.50
54.43
54.22
54.00
54.00
53.78
53.57
43.36
27.24
17.54
17.43
trans-58
135 MHz, CD2Cl2
f1 (ppm)

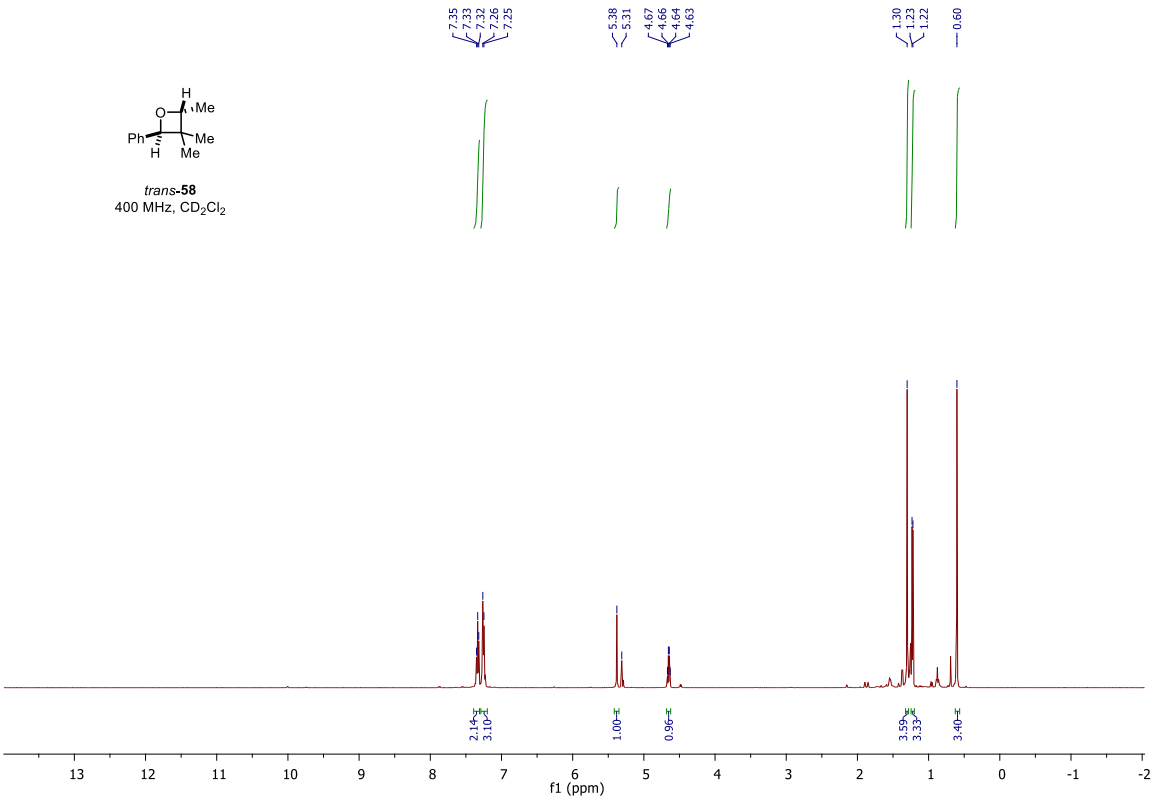
7.35
7.33
7.32
7.26
7.25
5.38
5.31
4.67
4.66
4.64
4.63
1.30
1.23
1.22
0.60
trans-58
400 MHz, CD2Cl2
2.14
3.10
1.00
0.96
3.59
3.33
3.40
f1 (ppm)

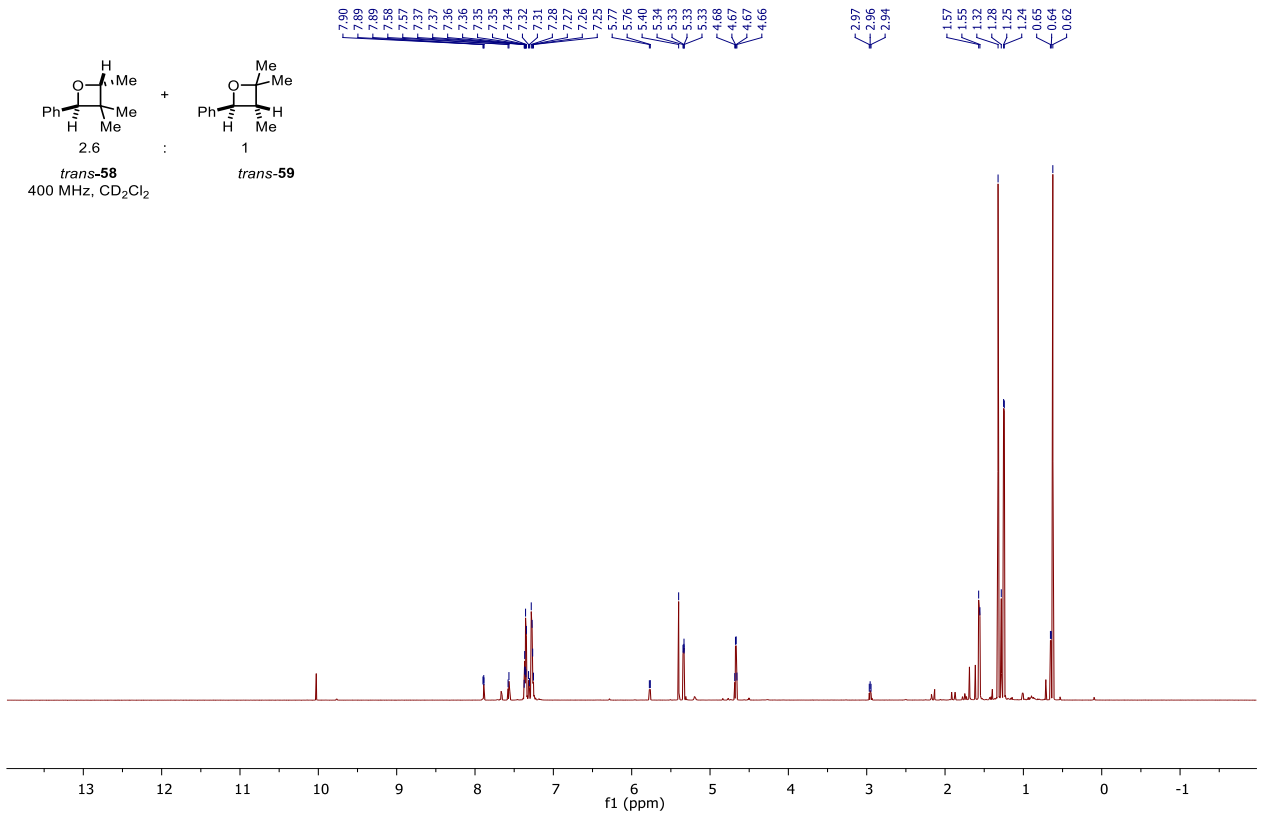
7.90
7.89
7.89
7.89
7.58
7.57
7.37
7.37
7.36
7.36
7.35
7.35
7.34
7.32
7.31
7.28
7.27
7.26
7.25
5.77
5.76
5.40
5.34
5.33
5.33
5.33
4.68
4.67
4.67
4.66
2.97
2.96
2.94
1.57
1.55
1.32
1.28
1.25
1.24
0.65
0.64
0.62
2.6 : 1
trans-58
400 MHz, CD2Cl2
trans-59
13 12 11 10 9 8 7 6 5 4 3 2 1 0 -1
f1 (ppm)

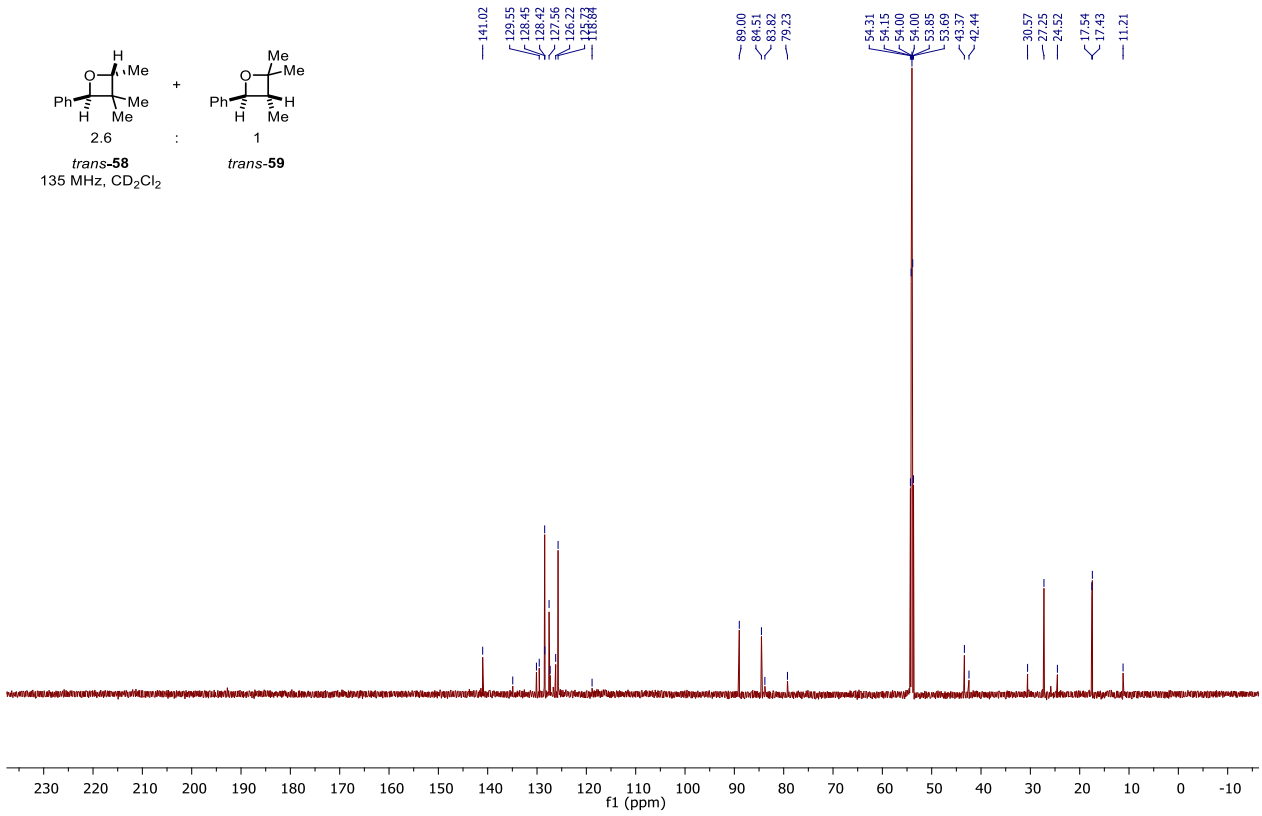
141.02
129.55
128.45
128.42
127.56
126.22
89.00
84.51
83.82
79.23
54.31
54.15
54.00
54.00
53.85
53.69
43.37
42.44
30.57
27.25
24.52
17.54
17.43
11.21
2.6 : 1
trans-58
135 MHz, CD2Cl2
trans-59
230 220 210 200 190 180 170 160 150 140 130 120 110 100 90 80 70 60 50 40 30 20 10 0 -10
f1 (ppm)

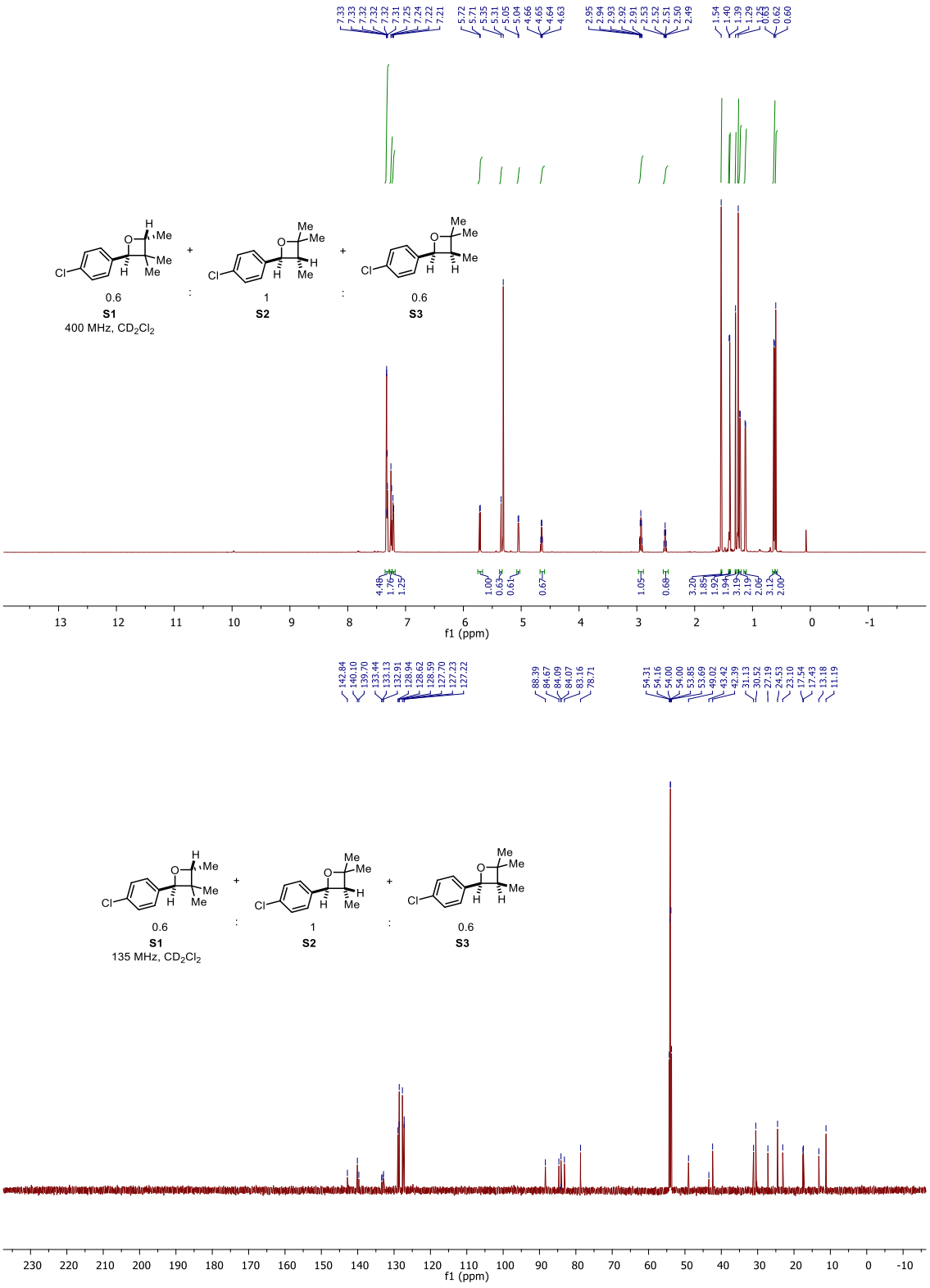

Adapted with permission from *Org. Lett.* **2020**, *22*, 3155-3160.
Copyright 2022 American Chemical Society.

3.6 References

1. *Handbook of Metathesis*, 2nd ed.; Grubbs, R. H., Wenzel, A. G., O'Leary, D. J., Khosravi, E., Eds.; Wiley-VCH: Weinheim, Germany, 2015; Vols. 1−3.
2. Grela, K. *Olefin Metathesis: Theory and Practice*; Wiley-VCH: Weinheim, Germany, 2014.
3. Blackwell, H. E.; O'Leary, D. J.; Chatterjee, A. K.; Washenfelder, R. A.; Bussmann, D. A.; Grubbs, R. H. New Approaches to Olefin Cross-Metathesis. *J. Am. Chem. Soc.* **2000**, *122*, 58−71.
4. Chatterjee, A. K.; Choi, T.-L.; Sanders, D. P.; Grubbs, R. H. A General Model for Selectivity in Olefin Cross Metathesis. *J. Am. Chem. Soc.* **2003**, *125*, 11360−11370.
5. For a stoichiometric approach relying on molybdenum alkylidenes, see: Fu, G. C.; Grubbs, R. H. Synthesis of Cycloalkenes via Alkylidene-Mediated Olefin Metathesis and Carbonyl Olefination. *J. Am. Chem. Soc.* **1993**, *115*, 3800−3801.
6. For carbonyl−olefin metathesis reactions proceeding via oxetane photoadducts, see: (a) Jones, G., II; Schwartz, S. B.; Marton, M. T. 374 Regiospecific Thermal Cleavage of Some Oxetan Photoadducts: Carbonyl–Olefin Metathesis in Sequential Photochemical and Thermal Steps. *J. Chem. Soc., Chem. Commun.* **1973**, *11*, 374−375. (b) Jones, G., II; Acquadro, M. A.; Carmody, M. A. Long-Chain Enals via Carbonyl–Olefin Metathesis. An Application in Pheromone Synthesis. *J. Chem. Soc., Chem. Commun.* **1975**, 206−207. (c) Carless, H. A. J.; Trivedi, H. S. New Ring Expansion Reaction of 2-tButyloxetans. *J. Chem. Soc., Chem. Commun.* **1979**, *8*, 382−383. (d) Pérez-Ruiz, R.; Gil, S.; Miranda, M. A. Stereodifferentiation in the Photochemical Cycloreversion of Diastereomeric Methoxynaphthalene-Oxetane Dyads. *J. Org. Chem.* **2005**, *70*, 1376−1381. (e) Pérez-Ruiz, R.; Miranda, M. A.; Alle, R.; Meerholz, K.; Griesbeck, A. G. An Efficient Carbonyl-Alkene Metathesis of Bicyclic Oxetanes: Photoinduced Electron Transfer Reduction of the Paternò−Büchi Adducts from 2,3-Dihydrofuran and Aromatic Aldehydes. *Photochem. Photobiol. Sci.* **2006**, *5*, 51−55. (f) Valiulin, R. A.; Kutateladze, A. G. Harvesting the Strain Installed by a Paternò−Büchi Step in a Synthetically Useful Way: High-Yielding Photoprotolytic Oxametathesis in Polycyclic Systems. *Org. Lett.* **2009**, *11*, 3886−3889. (g) D'Auria, M.; Racioppi, R.; Viggiani, L. Paternò−Büchi Reaction Between Furan and Heterocyclic Aldehydes: Oxetane Formation vs. Metathesis. *Photochem. Photobiol. Sci.* **2010**, *9*, 1134−1138. (h) Valiulin, R. A.; Arisco, T. M.; Kutateladze, A. G. Double-Tandem $[4_\pi+2_\pi]\cdot[2_\pi+2_\pi]\cdot[4_\pi+2_\pi]\cdot[2_\pi+2_\pi]$ Synthetic Sequence with Photoprotolytic Oxametathesis and Photoepoxidation in the Chromone Series. *J. Org. Chem.* **2011**, *76*, 1319−1332. (i) Valiulin, R. A.; Arisco, T. M.; Kutateladze, A. G. Photoinduced Intramolecular Cyclopentanation vs Photoprotolytic Oxametathesis in Polycyclic Alkenes Outfitted with Conformationally Constrained Aroylmethyl Chromophores. *J. Org. Chem.* **2013**, *78*, 2012−2025.
7. For Brønsted and Lewis acid-mediated carbonyl−olefin metathesis reactions, see: (a) Schopov, I.; Jossifov, C. A Carbonyl–Olefin Exchange Reaction – New Route to Polyconjugated Polymers, 1. A New Synthesis of Polyphenylacetylene. *Makromol. Chem., Rapid Commun.* **1983**, *4*, 659−662. (b) Jackson, A. C.; Goldman, B. E.; Snider, B. B. Intramolecular and Intermolecular Lewis Acid Catalyzed Ene Reactions Using Ketones as Enophiles. *J. Org. Chem.* **1984**, *49*, 3988–3994. (c) van Schiak, H.-P.; Vijn, R.-J.; Bickelhaupt, F. Acid-Catalyzed Olefination of Benzaldehyde. *Angew. Chem. Int. Ed.* **1994**, *33*, 1611–1612. (d) Jossifov, C.; Kalinova, R.; Demonceau, A. Carbonyl Olefin Metathesis. *Chim. Oggi* **2009**, *40*, 85−87. (e) Soicke, A.; Slavov, N.; Neudörfl, J.-M.; Schmalz, H.-G. Metal-Free Intramolecular Carbonyl–Olefin Metathesis of *ortho*-Prenylaryl Ketones. *Synlett* **2011**, *2011*, 2487−2490.

8. For organocatalytic approaches, see: (a) Griffith, A. K.; Vanos, C. M.; Lambert, T. H. Organocatalytic Carbonyl–Olefin Metathesis. *J. Am. Chem. Soc.* **2012**, *134*, 18581−18584. (b) Hong, X.; Liang, Y.; Griffith, A. K.; Lambert, T. H.; Houk, K. N. Distortion-Accelerated Cycloadditions and Strain-Release-Promoted Cycloreversions in the Organocatalytic Carbonyl–Olefin Metathesis. *Chem. Sci.* **2014**, *5*, 471−475. (c) Zhang, Y.; Jermaks, J.; MacMillan, S. N.; Lambert, T. H. Synthesis of 2H Chromenes via Hydrazine-Catalyzed Ring-Closing Carbonyl–Olefin Metathesis. *ACS Catal.* **2019**, *9*, 9259−9264. (d) Lambert, T. H. Development of a Hydrazine-Catalyzed Carbonyl–Olefin Metathesis Reaction. *Synlett* **2019**, *30*, 1954−1965. (e) Jermaks, J.; Quach, P. K.; Seibel, Z. M.; Pomarole, J.; Lambert, T. H. Ring-Opening Carbonyl–Olefin Metathesis of Norbornenes. *Chem. Sci.*, **2020**, *11*, 7884-7895.
9. For other approaches, see: (a) Pitzer, L.; Sandfort, F.; Strieth-Kalthoff, F.; Glorius, F. Carbonyl–Olefin Cross-Metathesis Through a Visible-Light-Induced 1,3-Diol Formation and Fragmentation Sequence. *Angew. Chem., Int. Ed.* **2018**, *57*, 16219−16223. (b) Rivero-Crespo, M.A.; Tejeda Serrano, M.; Perez-Sanchez, H.; Ceron-Carrasco, J. P.; Leyva-Perez, A. Intermolecular Carbonyl–Olefin Metathesis with Vinyl Ethers Catalyzed by Homogeneous and Solid Acids in Flow. *Angew. Chem., Int. Ed.* **2020**, 59, 3846−3849.
10. For Brønsted acid-catalyzed approaches, see: (a) Catti, L.; Tiefenbacher, K. Brønsted Acid-Catalyzed Carbonyl–Olefin Metathesis Inside a Self-Assembled Supramolecular Host. *Angew. Chem., Int. Ed.* **2018**, *57*, 14589−14592. (b) To, T. A.; Pei, C.; Koenigs, R.; Nguyen, T. V. Hydrogen Bonding Networks Enable Brønsted Acid-Catalyzed Carbonyl–Olefin Metathesis. *Preprint at* https://chemrxiv.org/engage/chemrxiv/article-details/615d8156f718df1626d54e8c.
11. For a review on Lewis acid-catalyzed carbonyl–olefin metathesis reactions, see: [‡]Albright, H.; [‡]Davis, A. J.; [‡]Gomez-Lopez, J. L.; [‡]Vonesh, H. L.; Quach, P; Lambert, T. H.; Schindler, C. S. Carbonyl–Olefin Metathesis Reactions. *Chem. Rev.* **2021**, *121*, 9359–9406. [‡]Authors contributed equally.
12. For Lewis acid-catalyzed approaches, see: (a) Ludwig, J. R.; Zimmerman, P. M.; Gianino, J. B.; Schindler, C. S. Iron(III)-Catalysed Carbonyl–Olefin Metathesis. *Nature* **2016**, *533*, 374−379. (b) McAtee, C. M.; Riehl, P. S.; Schindler, C. S. Polycyclic Aromatic Hydrocarbons via Iron(III)-Catalyzed Carbonyl–Olefin Metathesis. *J. Am. Chem. Soc.* **2017**, *139*, 2960−2963. (c) Ludwig, J. R.; Phan, S.; McAtee, C. M.; Zimmerman, P. M.; Devery, J. J.; Schindler, C. S. Mechanistic Investigations of the Iron(III)-Catalyzed Carbonyl–Olefin Metathesis Reaction. *J. Am. Chem. Soc.* **2017**, *139*, 10832−10842. (d) Groso, E. J.; Golonka, A. N.; Harding, R. A.; Alexander, B. W.; Sodano, T. M.; Schindler, C. S. 3-Aryl-2,5-Dihydropyrroles via Catalytic Carbonyl–Olefin Metathesis. *ACS Catal.* **2018**, *8*, 2006−2011. (e) Albright, H.; Vonesh, H. L.; Becker, M. R.; Alexander, B. W.; Ludwig, J. L.; Wiscons, R. A.; Schindler, C. S. $GaCl_3$-Catalyzed Ring-Opening Carbonyl–Olefin Metathesis. *Org. Lett.* **2018**, *20*, 4954−4958. (f) Albright, H.; Riehl, P. S.; McAtee, C. M.; Reid, J. P.; Ludwig, J. R.; Karp, L. A.; Zimmerman, P. M.; Sigman, M. S.; Schindler, C. S. Catalytic Carbonyl–Olefin Metathesis of Aliphatic Ketones: Iron(III) Homo-Dimers as Lewis Acidic Superelectrophiles. *J. Am. Chem. Soc.* **2019**, *141*, 1690−1700. (g) Riehl, P. S.; Nasrallah, D. J.; Schindler, C. S. Catalytic Transannular Carbonyl–Olefin Metathesis Reactions. *Chem. Sci.* **2019**, *10*, 10267−10274. (h) Rykaczewski, K. A.; Groso, E. J.; Vonesh, H. L.; Gaviria, M. A.; Richardson, A. D.; Zehnder, T. E.; Schindler, C. S. Tetrahydropyridines via $FeCl_3$-Catalyzed Carbonyl−Olefin Metathesis. *Org. Lett.* **2020**, *22*, 7, 2844−2848. (i) Albright, H.; Vonesh, H. L.; Schindler, C. S. Superelectrophilic Fe(III)-Ion Pairs as Stronger Lewis Acid Catalysts for (*E*)-Selective

Intermolecular Carbonyl−Olefin Metathesis. *Org. Lett.* **2020**, *22*, 3155−3160. (j) Davis, A. J.; Watson, R. B.; Nasrallah, D. J.; Gomez-Lopez, J. L.; Schindler, C. S. *Nat. Catal.* **2020**, *3*, 787−796. (k) Naidu, V. R.; Bah, J.; Franzén, J. Direct Organocatalytic Oxo-Metathesis, a *trans*-Selective Carbocation-Catalyzed Olefination of Aldehydes. *Eur. J. Org. Chem.* **2015**, *2015*, 1834−1839. (l) Ma, L.; Li, W.; Xi, H.; Bai, X.; Ma, E.; Yan, X.; Li, Z. $FeCl_3$-Catalyzed Ring-Closing Carbonyl–Olefin Metathesis. *Angew. Chem., Int. Ed.* **2016**, *55*, 10410−10413. (m) Ni, S.; Franzén, J. Carbocation Catalysed Ring Closing Aldehyde-Olefin Metathesis. *Chem. Commun.* **2018**, *54*, 12982−12985. (n) Tran, U. P. N.; Oss, G.; Pace, D. P.; Ho, J.; Nguyen, T. V. Tropylium-Promoted Carbonyl–Olefin Metathesis Reactions. *Chem. Sci.* **2018**, *9*, 5145−5151. (o) Tran, U. P. M.; Oss, G.; Breugst, M.; Detmar, E.; Pace, D. P.; Liyanto, K.; Nguyen, T. V. Carbonyl–Olefin Metathesis Catalyzed by Molecular Iodine. *ACS Catal.* **2019**, *9*, 912−919. (p) Hanson, C. S.; Psaltakis, M. C.; Cortes, J. J.; Devery, J. J. Catalyst Behavior in Metal-Catalyzed Carbonyl–Olefin Metathesis. *J. Am. Chem. Soc.* **2019**, *141*, 11870−11880. (q) Djurovic, A.; Vayer, M.; Li, Z.; Guillot, R.; Blataze, J.-P.; Gandon, V.; Bour, C. Synthesis of Medium-Sized Carbocycles by Gallium-Catalysed Tandem Carbonyl–Olefin Metathesis/Transfer Hydrogenation. *Org. Lett.* **2019**, *21*, 8132–8137. (r) Wang, R.; Chen, Y.; Shu, M.; Zhao, W.; Tao, M.; Du, C.; Fu, X.; Li, A.; Lin, Z. $AuCl_3$-Catalyzed Ring-Closing Carbonyl–Olefin Metathesis. *Chem. Eur. J.* **2020**, *26*, 1941–1946. (s) Hanson, C. S.; Psaltakis, M. C.; Cortes, J. J.; Siddiqi, S. S.; Devery, J. J. Investigation of Lewis Acid-Carbonyl Solution Interactions via Infrared-Monitored Titration. *J. Org. Chem.* **2020**, *85*, 820−832.

13. (a) Olah, G.A. Superelectrophiles. *Angew. Chem., Int. Ed. Engl.* **1993**, *32*, 767−788. (b) Olah, G.A.; Klumpp, D.A. *Superelectrophiles and Their Chemistry*; Wiley-VCH Verlag GmbH & Co. KGaA, 2007.
14. Carless, H.A.J.; Maitra, A.K.; Trivedi, H.S. Photochemical Cycloaddition of Aldehydes to Styrenes. *J. Chem. Soc., Chem. Commun.* **1979**, *0*, 984−985.
15. Fleury, L.M.; Kosal, A.D.; Masters, J.T.; Ashfeld, B.L. Cooperative Titanocene and Phosphine Catalysis: Accelerated C–X Activation for the Generation of Reactive Organometallics. *J. Org. Chem.* **2013**, *78*, 253–269.
16. Hayashi, N.; Honda, H.; Yasuda, M.; Shibata, I.; Baba, A. Generation of Allylic Indium by Hydroindation of 1,3-Dienes and One-Pot Reaction with Carbonyl Compounds. *Org. Lett.* **2006**, *8*, 4553–4556.
17. Vyvyan, J.R.; Brown, R.C.; Woods, B.P. Alkylation of 2-Substituted (6-Methyl-2-pyridyl)methyllithium Species with Epoxides. *J. Org. Chem.* **2009**, *74*, 1374–1376.
18. Al-Masum, M.; Alam, S. Remarkable Regioselectivity in Microwave-enhanced Palladium-catalyzed Allylation Reaction Involving Allyltrifluoroborates and Aryl Halides. *Tetrahedron Lett*. **2009**, *50*, 5201–5204.
19. Sakai, N.; Moriya, T.; Konakahara, T. An Efficient One-Pot Synthesis of Unsymmetrical Ethers: A Directly Reductive Deoxygenation of Esters Using an $InBr_3/Et_3SiH$ Catalytic System. *J. Org. Chem.* **2007**, *72*, 5920–5922.
20. Rauf, W.; Brown, J.M. Catalytic Amide-Mediated Methyl Transfer from Silanes to Alkenes in Fujiwara–Moritani Oxidative Coupling. *Angew. Chem. Int. Ed.* **2008**, *47*, 4228 –4230.
21. Kumar, R.; Sharma, A.; Sharma, N.; Kumar, V; Sinha, A.K. Neutral Ionic Liquid [hmim]Br as a Green Reagent and Solvent for the Mild and Efficient Dehydration of Benzyl Alcohols into *(E)*-Arylalkenes Under Microwave Irradiation. *Eur. J. Org. Chem.* **2008**, *33*, 5577–5582.
22. Ischay, M.A.; Ament, M.S.; Yoon, T.P. Crossed Intermolecular [2 + 2] Cycloaddition of Styrenes by Visible Light Photocatalysis. *Chem. Sci.* **2012**, *3*, 2807–2811.

23. Tiecco, M.; Tingoli, M. Regiochemistry and Stereochemistry of Nickel-Promoted, Carbon-Carbon Bond-Forming Reactions of Cyclic Sulfur Compounds. *J. Org. Chem.* **1985**, *50*, 3828–3831.

Chapter 4: Interrupted Carbonyl–Olefin Metathesis of Cyclic, Aliphatic Ketones

4.1 Introduction

Carbonyls and olefins undergo important carbon-carbon bond forming transformations under Lewis or Brønsted acid catalysis (Figure 4.1A). Depending on the choice of Lewis or Brønsted acid, these functional groups typically react *via* carbonyl-ene[1] or Prins[2] reaction pathways. The carbonyl-ene reaction proceeds in either a stepwise or concerted fashion, often going through transition state **2**, to provide homoallylic alcohols **4**. Alternatively, the Prins reaction follows a stepwise mechanism; forming a carbocation intermediate that is quenched by an exogenous nucleophile to yield the corresponding alcohols **5**.

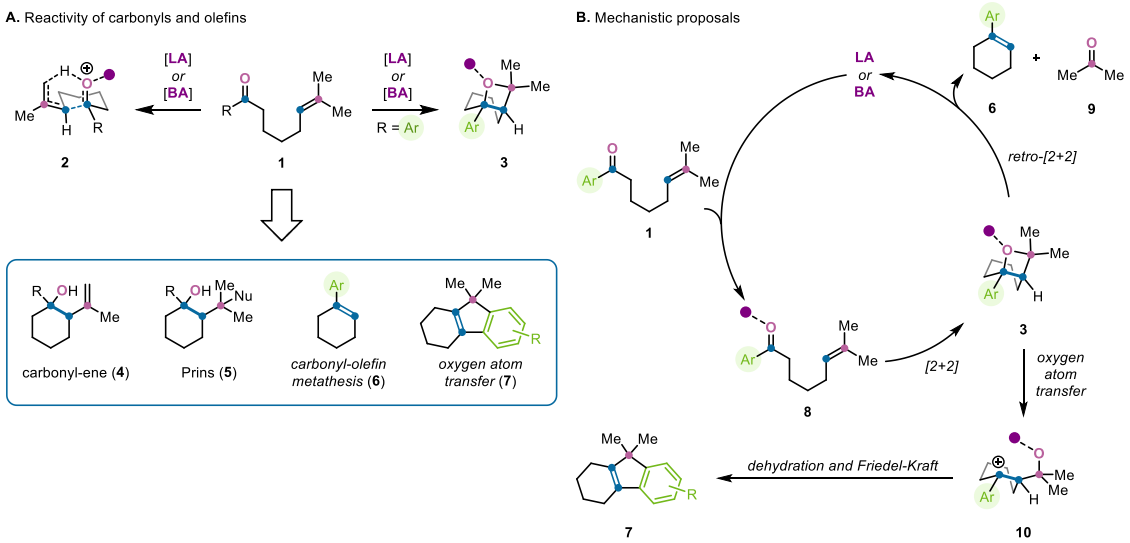

Figure 4.1: Synopsis of the reactivity between carbonyls and olefins. **A.** Inherent reactivity of carbonyls and olefins. **B.** Mechanistic proposals for Lewis acid-catalyzed carbonyl–olefin metathesis and Brønsted acid-catalyzed interrupted carbonyl–olefin metathesis.

Another well-established reaction between carbonyls and olefins is carbonyl–olefin metathesis.[3-10] In 2016, the Schindler lab had their first report on Lewis acid-catalyzed ring-closing carbonyl–olefin metathesis[10a] and have continued to extensively investigate Lewis acid-catalyzed transformations. A detailed exploration of the 2016 supported their original mechanistic hypothesis: (a) first, the Lewis acid coordinates to the carbonyl **1**, (b) the activated carbonyl then

undergoes a concerted, asynchronous [2+2]-cycloaddition (**8**), (c) forming oxetane intermediate **3**, (d) that subsequently fragments *via* a retro-[2+2]-cycloaddition to yield the cyclic olefin metathesis product and a carbonyl byproduct (**6** and **9**, respectively, Figure 4.1B).[10a,10c] Recently, a fourth mode of reactivity has been reported—interrupted carbonyl–olefin metathesis—in which aryl ketone substrates (**1**) are converted into tetrahydrofluorene products (**7**, Figure 4.1B).[11] Under the optimized reaction conditions, Brønsted acid catalyzes the formation of the same oxetane intermediate **3**; however, **3** fragments through an oxygen atom transfer mechanism to form a carbocation. Then the resulting stabilized benzylic carbocation **10** undergoes a dehydration and Friedel-Kraft type reaction to provide **7**.

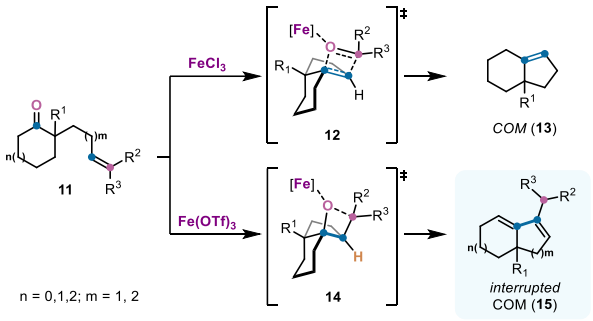

Figure 4.2: *This work:* Iron-catalyzed carbonyl–olefin metathesis and interrupted carbonyl–olefin metathesis of cyclic, aliphatic ketones.

General methodologies have been developed for both carbonyl–olefin metathesis[9] and interrupted carbonyl–olefin metathesis of aryl carbonyls,[11] but the reactivity of less activated aliphatic carbonyls remained elusive. In 2019, the Schindler group found that aliphatic ketones (**11**) undergo divergent reactivity depending on the choice of Lewis acid catalyst (Figure 4.2).[10f] While catalytic amounts of $FeCl_3$ promote the expected carbonyl–olefin metathesis product (**13**), conversion of **11** with $Fe(OTf)_3$ exclusively results in the formation of functionalized pentalenes, indenes, naphthalenes, and azulenes as interrupted carbonyl–olefin metathesis products (**15**). Compared to aryl ketones, mechanistic studies of **11** suggest a distinct interrupted carbonyl–olefin metathesis pathway. After formation of oxetane intermediate **14**, fragmentation occurs through C–O bond cleavage and subsequent elimination of the α-proton to form the olefin.

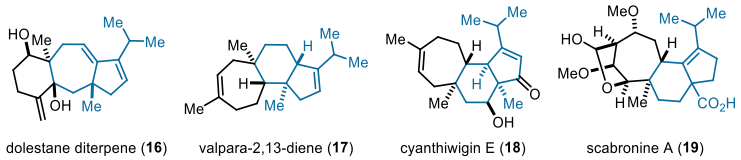

Figure 4.3: Representative natural products incorporating **15**.

Development of this novel methodology allows for access to a variety of bicyclic frameworks that are found in biologically active natural products, including the dolestane diterpene[12] (**16**), valpara-2,13-diene[13] (**17**) and cyanthiwigin E[14] (**18**), and scabronine A[15] (**19**) (Figure 4.3). Dolastane diterpenes and 7-6-5 tricyclic diterpenes have been extracted from fungi, plants, and an assortment of marine organisms.[16] These scaffolds demonstration biological activity for potential antibiotics, antifungals, antitumor agents, and nerve growth factors for applications as therapeutic agents to treat neurodegenerative diseases such as Alzheimer's and Parkinson's.[17]

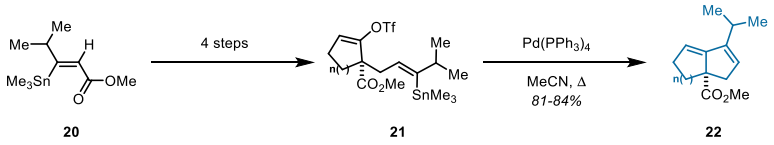

Figure 4.4: Piers and co-workers' synthetic route to isopropyl bicyclic scaffolds.

Several of these compounds have been synthesized[12-13,18] and yet, there is still no direct or general methodology for the formation of the characteristic cyclopentene ring with the pendant isopropyl moiety. In 1986, the Piers group synthesized these bicyclic frameworks over several steps with the key carbon-carbon bond forming step being a harsh palladium-catalyzed cross-coupling of stannyl substrates (Figure 4.4).[12b] Rapid access to these bicyclic cyclopentene cores, similar to the dolastane diterpenes, can be readily achieved by employing the divergent reactivity that has been discovered for cyclic, aliphatic ketones.

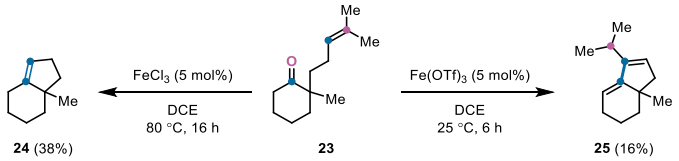

Figure 4.5: Divergent reactivity of cyclic ketone **23** with distinct iron(III) sources.

Initially, efforts were focused on developing the carbonyl–olefin metathesis for aliphatic ketone **23** (Figure 4.5).[10f] The divergent reactivity was discovered during while evaluating

different Lewis acids, particularly two different iron(III)-sources, $FeCl_3$ and $Fe(OTf)_3$. Subjecting **23** to catalytic amounts of $FeCl_3$ resulted in the expected carbonyl–olefin metathesis product **24** in 38% yield. However, when $Fe(OTf)_3$ was used as the catalyst, a new compound was isolated as the exclusive product in 16% yield. The new compound, potentially resulting from a carbonyl-ene or Prins reaction, did not correlate with either of the expected products and was instead determined to be indene **25**. Interested in the newfound reactivity of **23**, reaction conditions were investigated to improve the efficiency of the desire transformation.

4.2 Results and Discussion

Initial investigations of this new interrupted carbonyl–olefin metathesis focused on determining the optimal Lewis or Brønsted acid catalyst, as well as solvent, reaction time, temperature, and concentration. Conversion of easily synthesized *β*-ketoester **26** with 5 mol% $Fe(OTf)_3$ in DCE at ambient temperature led to the formation of tetrahydropentalene **27** in 40% yield (entry 1, Figure 4.6). Increasing the temperature to 80 °C was beneficial, yielding 60% of the desired metathesis product; however, other metal triflates, such as $Bi(OTf)_3$, $Dy(OTf)_3$, and $In(OTf)_3$, gave little to no conversion (entries 2-5, Figure 4.6).

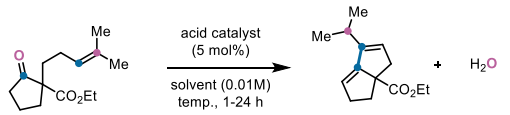

26 **27**

entry	Lewis acid	solvent	T (°C)	yield **27** (%)	conversion **26** (%)
1	$Fe(OTf)_3$	DCE	23	40	50
2	$Fe(OTf)_3$	DCE	80	60	100
3	$Bi(OTf)_3$	DCE	80	0	0
4	$Dy(OTf)_3$	DCE	80	0	0
5	$In(OTf)_3$	DCE	80	30	47
6	$Fe(OTf)_3$	DCM	80	58	100
7	$Fe(OTf)_3$	chlorobenzene	80	54	75
8	$Fe(OTf)_3$	toluene	80	82	100
9	**$Fe(OTf)_3$**	**benzene**	**80**	**99**	**100**
10	$In(OTf)_3$	benzene	80	57	100
11	$Fe(OTf)_3$	benzene	23	21	23
12	$Fe(OTf)_3$	benzene	40	22	77
13	$AlCl_3$	benzene	80	0	0
14	Me_2AlCl^a	benzene	80	0	0
15	$SnCl_4$	benzene	80	0	81
16	$TiCl_4$	benzene	80	0	34
17	$GaCl_3$	benzene	80	0	100
18	TfOH	DCE	80	35	100
19	TfOH	benzene	80	35	100

Conditions: All reactions were performed with 0.25 mmol of **26** and 5 mol% acid catalyst in solvent (0.01 M) for 1-24h.[a]100 mol%.

Figure 4.6: Reaction optimization.

Continued optimization efforts focused on evaluating different reaction solvents with $Fe(OTf)_3$ and $In(OTf)_3$ as catalysts. Catalytic amounts of $Fe(OTf)_3$ with DCM or chlorobenzene provided similar yields to DCE with 58% and 54%, respectively (entries 6 and 7, Figure 4.6). Toluene and benzene proved to be superior solvents, with increased yields of up to 99% (entries 8 and 9, Figure 4.6). Lowering the reaction temperature to either ambient temperatures or slightly elevated temperatures (40 ºC), in benzene, resulted in decreased yields of **27** (entries 11 and 12, Figure 4.6). Additional Lewis acids, including $AlCl_3$, Me_2AlCl, $SnCl_4$, $TiCl_4$, and $GaCl_3$, failed to promote the desired transformation under otherwise identical reaction conditions (entries 13-17, Figure 4.6). Based on these results, it was postulated that the presence of residual triflic acid in $Fe(OTf)_3$ could function as the active catalyst. However, converting *β*-ketoester **26** with catalytic amounts of triflic acid resulted in only 35% yield of tetrahydropentalene **27** in both, DCE and benzene (entries 18 and 19, Figure 4.6).

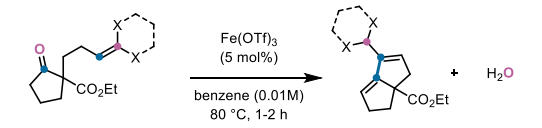

entry	olefin		yield (%)	entry	olefin		yield (%)
1		**26**	99	5		**31**	94
2		**28**	86[a]	6		**32**	71
3		**29**	n.r.	7		**33**	95
4		**30**	n.r.	8 9		**34:** R = Me **35:** R = H	n.r. n.r.

Conditions: All reactions were performed 5 mol% of $Fe(OTf)_3$ in benzene (0.01M) at 80 °C for 1-24 h.[a]Includes olefin isomer in yield.

Figure 4.7: Evaluation of the olefin scope.

With optimized reaction conditions in hand, the substrate's olefin scope was evaluated next (Figure 4.7). Prenyl fragments (**26**), as well as longer aliphatic substituents (**28**), were productive under reaction conditions resulting in 99% and 86% (entries 1 and 2, Figure 4.7). Styrene substrates **29** and **30** resulted in exclusive re-isolation of the substrates, while trisubstituted olefins cyclohexylidene **31** and cycloheptylidene **32**, formed the corresponding tetrahydropentalene products in 94% and 71% yield (entries 3-6, Figure 4.7). 1,1-disubsituted analog **33** was a suitable

substrate, resulting in 95% yield of the desired product; terminal olefins of this type presumably isomerize to trisubstituted prenyl olefin under reaction conditions (entry 7, Figure 4.7). Both crotylated substrate **34** and mono-substituted olefin **35** were unproductive, demonstrating that nucleophilic olefins are integral for reaction success (entries 8 and 9, Figure 4.7).

Continuing efforts centered around the examination of cyclic ketones upon their ability to undergo the desired transformation (Figure 4.8). Importantly, this protocol readily provided access to bicyclic scaffolds of varying ring sizes: including 5-5-fused tetrahydropentalenes (**27**), 5-6-fused tetrahydroindenes (**36** and **37**), 6-6-fused hexahydronaphthalene (**38**), and 5-7-fused hexahydroazulene (**39**) analogs. Model substrate, cyclopentanone **26** cyclized quantitatively, forming **27**, while the analogous cyclohexanone substrate afforded **36** in reduced yields of 40%. The addition of a methylene subunit to the olefin alkyl chain was beneficial for the transformation, which resulted in increased yields of tetrahydroindene **37** and hexahydronaphthalene **38** in 72% and 82% yield, respectively. In comparison to **36**, the cycloheptanone homolog formed tetrahydroazulene **39** in increased yields of 59%.

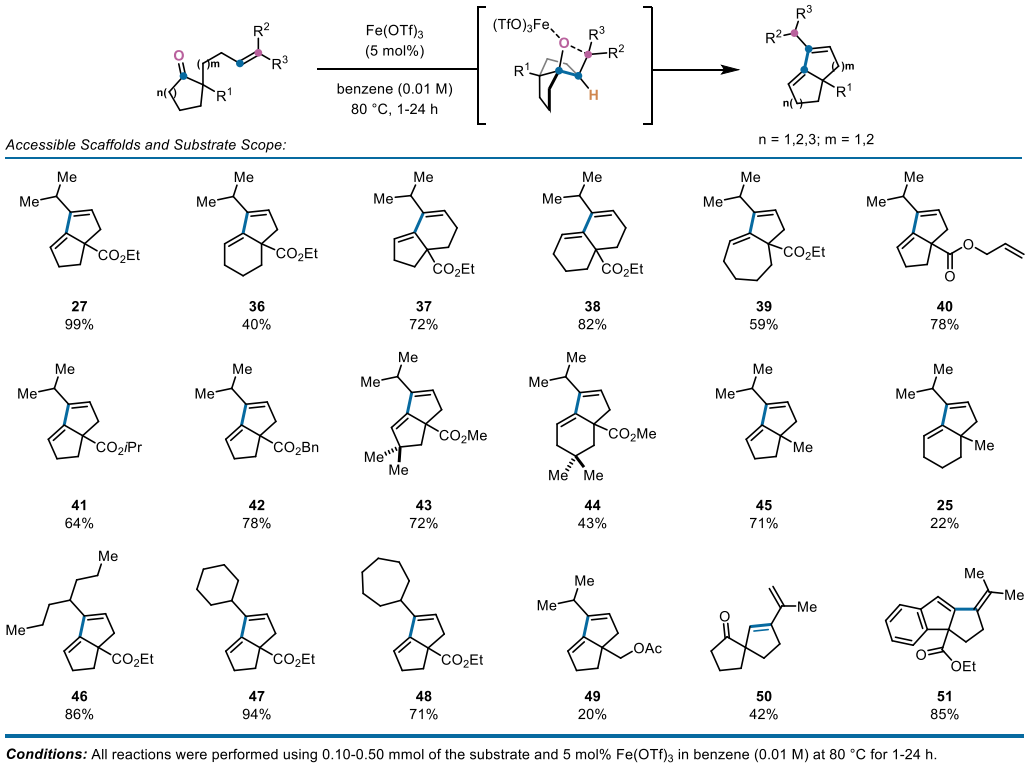

Figure 4.8: Substrate scope for cyclic, aliphatic ketones for the interrupted carbonyl–olefin metathesis reaction.

Substitution of the ester moiety was well tolerated and provided 78% yield of allyl ester **40**, 64% yield of isopropyl ester **41**, and 78% yield of benzyl ester **42**. Additional substituents on cyclopentanone and cyclohexanone substrates resulted in the corresponding tetrahydropentalene (**43**) and tetrahydroindene (**44**) products in 72% and 43% yield, respectively. As seen with the formation of pentalene **45** and tetrahydroindene **25**; the β-ketoester functionality is not necessary for the transformation. However, the ester seems to be advantageous, since the yields of the **45** and **25** were about 20% lower compared to the homologous ester-containing products **27** and **36**. Substitution of the olefin subunit was also compatible under the optimized reaction conditions and tetrahydropentalenes **46**-**48** were obtained in up to 94% yield, whereas acetate **49** was formed in only 20% overall yield. Aldehydes were found to be more reactive than ketones, affording an interesting spirocyclic carbonyl-ene reaction product **50** in 42%. Meanwhile, pentaindene **51** resulted from the cyclization of an indanone substrate in 85% yield, although the product incorporates a tetrasubstituted alkene moiety.

4.3 Mechanistic Investigations

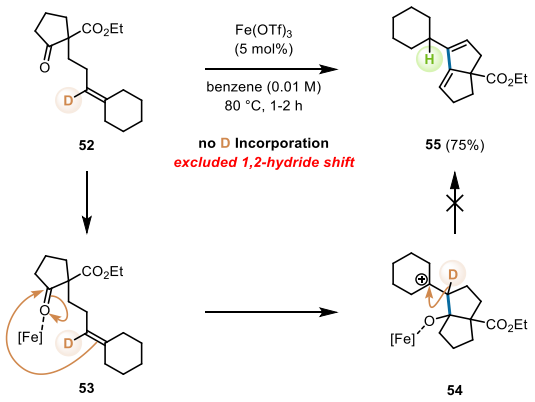

Figure 4.9: Deuterium labeling studies to evaluate a possible 1,2-hydride shift mechanism.

Subsequent efforts were focused on investigating the divergent reactivity of interrupted carbonyl–olefin metathesis and gaining valuable insight into the controlling features of this transformation. The hydride shift mechanistic pathway is active in the biosynthesis of cyathane diterpenoid natural products, analogous to **16**-**19** (Figure 4.3).[19] To evaluate this mechanistic hypothesis, deuterium labeling studies were conducted on cyclopentanone **52** (Figure 4.9). If a 1,2-hydride shift pathway was operative, $Fe(OTf)_3$ would coordinate **52**, resulting in the formation of intermediate **53**. Nucleophilic attack of the olefin onto the electrophilic carbon of the ketone would

forge the new C–C bond (highlighted in blue) and result in the formation of a tertiary carbocation (**54**). A 1,2-hydride shift of the deuterium (highlighted in gold) would incorporate the deuterium into the structure and create a new tertiary carbocation; subsequent eliminations and a dehydration would result in the deuterium labeled **55**. However, under optimized reaction conditions, no deuterium incorporation of tetrahydropentalene **55** was of observed and eliminated the possibility of a 1,2-hydride shift operating under these conditions.

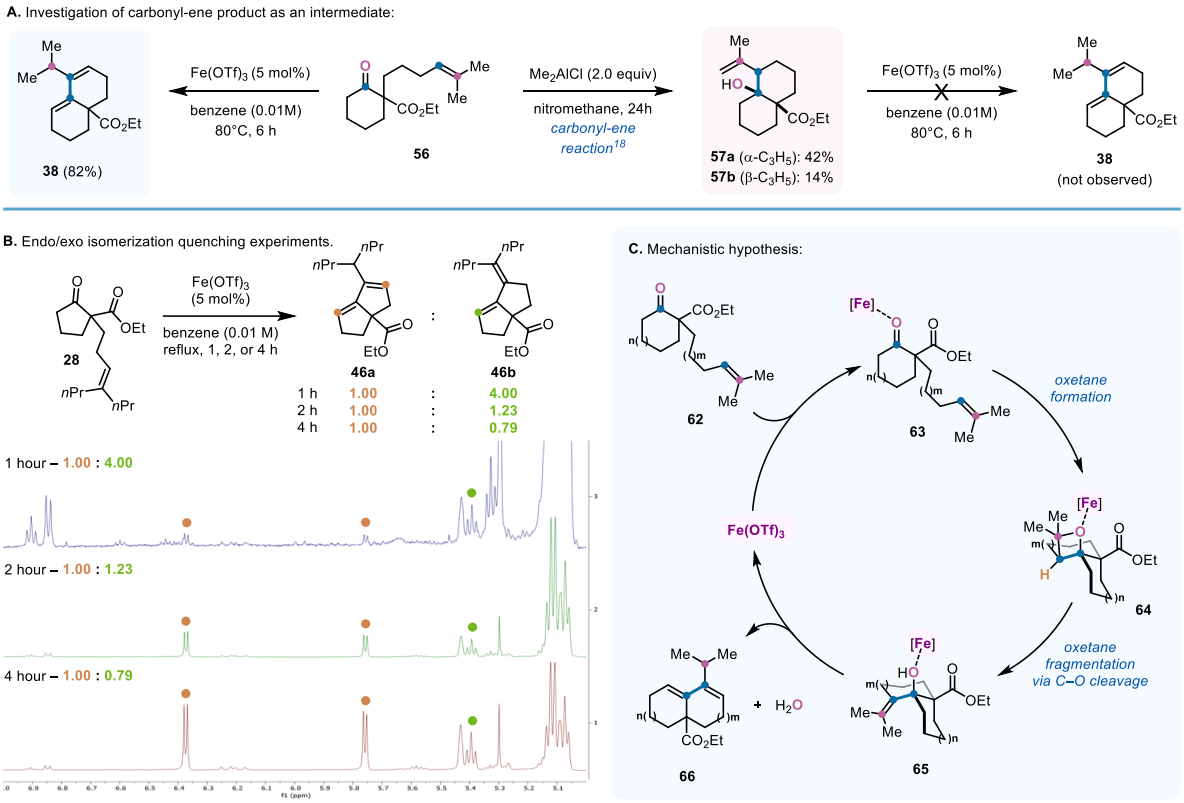

Figure 4.10: Mechanistic evidence for the proposed interrupted carbonyl–olefin metathesis reaction pathway. **A.** Investigation of carbonyl-ene pathway. **B.** *Endo/exo* isomerization experiments. **C.** Proposed mechanism.

Another possible reaction pathway that could be operative under the optimized reaction conditions was a Lewis acid catalyzed carbonyl-ene reaction. To investigate the viability of this postulation, cyclohexanone **56**, which is reported to undergo a carbonyl-ene reaction[20] with superstoichiometric amounts of Me_2AlCl, formed the corresponding cyclization products **57a** and **57b** in 56% yield (3:1 ratio; Figure 4.10A). Carbonyl-ene adducts **57a** and **57b** were exposed to $Fe(OTf)_3$ and under the optimized reaction conditions, no formation of tetrahydronaphthalene **38** was observed. Instead, the reaction resulted in the re-isolation of the starting materials, **57a** and

57b, as well as cyclohexanone **56**, eliminating the possibility of a carbonyl-ene reaction under the optimized conditions.

Isomerization studies were also conducted to offer additional experimental evidence for the observed *endo*-isomer products (Figure 4.10B). Using substrate **28**, which provided both *endo* (**46a**, shown in orange) and *exo* (**46b**, shown in green) isomers, reactions were quenched at varying timepoints to compare the ratio of the isomers. **46b**, the kinetic isomer, is initially formed in greater quantities. However, over the course of the reaction **46b** converts to the more stable, thermodynamic isomer **46a**; confirming the observed *endo* isomer products are favored. Lastly, to provide support to our observed experimental results, computational studies (B3LYP-D3/cc-pVTZ(-f)//LACVP** (SCRF, ε=2.284 for benzene) were then conducted (see 4.5.4 for more details). The calculated transition state energy for the $Fe(OTf)_3$-catalyzed pathway proceeding through a carbonyl-ene reaction is ~7.2 kcal/mol higher in energy than the corresponding oxetane pathway. These results correlate with the experimental carbonyl-ene studies and further support oxetane formation is the preferred reaction pathway.

Both experimental and computational results for the interrupted carbonyl–olefin metathesis of cyclic, aliphatic ketones led to a distinct mechanistic proposal in comparison to the previously reported mechanism for aryl ketones (**1**).[11] Lewis acid coordination of $Fe(OTf)_3$ to the substrate **62** results in activated intermediate **63** (Figure 4.10C). **63** undergo a [2+2]-cycloaddition to form oxetane **64**, analogous to carbonyl–olefin metathesis. However, the traditional carbonyl–olefin metathesis reaction pathway is interrupted and fragmentation of **64** occurs through a newly proposed oxetane fragmentation pathway via C–O cleavage. A tertiary carbocation is formed on the isopropyl moiety and elimination of the adjacent α-proton in oxetane **64** (highlighted in orange) yields the tetrasubstituted olefin and activated alcohol in intermediate **65**. Subsequent isomerization of the olefin and elimination of water results in the synthesis of the observed pentalene, indene, naphthalene, or azulene products.

4.4 Conclusions

The method described herein represents a new iron(III)-catalyzed reaction pathway for the synthesis of pentalene, indene, naphthalene, or azulene products that proceeds through a distinct interrupted carbonyl–olefin metathesis. This transformation differs from the previously reported oxygen atom transfer interrupted carbonyl–olefin metathesis pathway. Mechanistic elucidation,

from both experiments and computations, supports that after oxetane formation, fragmentation occurs *via* C–O bond cleavage and subsequent elimination of the α-proton to form an olefin; isomerizations and dehydration leads to the observed products. This method broadens the scope of aliphatic carbonyls, which are less reactive substrates in Lewis acid catalysis, and provides an additional mode of reactivity between carbonyl and olefin moieties that compliments the existing carbonyl-ene, Prins, and carbonyl–olefin metathesis reactions.

4.5 Experimental Procedures and Supplemental Information

4.5.1 General Information

All moisture-sensitive reactions were performed under an atmosphere of nitrogen in flame-dried round bottom flasks or glass vials fitted with rubber septa and/or septa equipped screw caps. Stainless steel syringes were used to transfer air or moisture-sensitive liquids. Flash chromatography was performed using silica gel Silia Flash® 40-63 micron (230-400 mesh) from Silicycle. All chemicals were purchased from SigmaAldrich, Alfa Aesar, Acros Organics, Oakwood, TCI America, Frontier Scientific, Matrix Scientific, Ark Pharm, and Chem Impex International, and were used as received unless otherwise stated. Tetrahydrofuran and dimethylformamide were dried by being passed through columns of activated alumina. Proton Nuclear Magnetic Resonance NMR (^{1}H NMR) spectra and carbon nuclear magnetic resonance (^{13}C NMR) spectra were recorded on a Varian Unity Plus 400, Varian MR400, Varian vnmrs 500, Varian Inova 500, Varian Mercury 500, and Varian vnmrs 700 spectrometers. Chemical shifts for protons are reported in parts per million and are references to the NMR solvent peak ($CDCl_3$: δ 7.27). Chemical shifts for carbons are reported in parts per million and are referenced to the carbon resonances of the NMR solvent ($CDCl_3$: δ 77.00). Data are represented as follows: chemical shift, integration, multiplicity (br = broad, s = singlet, d = doublet, t = triplet, q = quartet, p = pentet, dd = doublet of doublet, m = multiplet), and coupling constants in Hertz (Hz). Mass spectroscopic (MS) data was recorded at the Mass Spectrometry Facility at the Department of Chemistry of the University of Michigan in Ann Arbor, MI on an Agilent Q-TOF HPLC-MS with ESI high resolution mass spectrometer. Infrared (IR) spectra were obtained using either an Avatar 360 FT-IR or Perkin Elmer Spectrum BX FT-IR spectrometer. IR data are represented as frequency of absorption (cm^{-1}).

4.5.2 Optimization

Table 4.1: Preliminary Lewis acid screen.

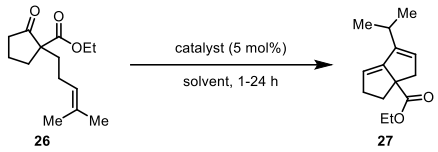

26 **27**

Entry	Lewis Acid	Solvent	cat. loading (mol%)	Temp. (°C)	Conc. (M)	Yield (%)	Conversion (%)
1	TfOH	DCE	5	80	0.01	35.4	100.0
2	$Fe(OTf)_3$	DCE	5	80	0.01	60.3	100.0
3	$Bi(OTf)_3$	DCE	5	80	0.01	0.0	0.0
4	$Sc(OTf)_3$	DCE	5	80	0.01	69.9	100.0
5	$Mg(OTf)_2$	DCE	5	80	0.01	0.0	0.0
6	$Dy(OTf)_3$	DCE	5	80	0.01	0.0	0.0
7	$In(OTf)_3$	DCE	5	80	0.01	30.1	47.3
8	$FeCl_3$	DCE	5	80	0.01	0.0	0.0

Conditions: All reactions were run on a 0.247 mmol scale of **26** and yields were determined following isolation of **27.**

Table 4.2: Extensive Lewis acid screen.

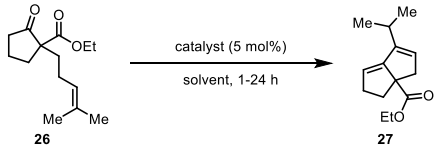

26 **27**

Entry	Lewis Acid	Solvent	cat. loading (mol%)	Temp. (°C)	Conc. (M)	Yield (%)	Conversion (%)
1	$Dy(OTf)_3$	PhH	5	80	0.01	0.0	0.0
2	$FeCl_3$	PhH	5	80	0.01	0.0	0.0
3	$In(OTf)_3$	PhH	5	80	0.01	57.0	100.0
4	$Bi(OTf)_3$	PhH	5	80	0.01	77.0	0.0
5	$Mg(OTf)_2$	PhH	5	80	0.01	0.0	0.0
6	$Sc(OTf)_3$	PhH	5	80	0.01	<2	39.0
7	TfOH	PhH	5	80	0.01	35.4	100.0
8	$Fe(OTf)_3$	PhH	5	80	0.01	99.0	100.0
9	$AlCl_3$	PhH	5	80	0.01	0.0	0.0
10	$Zn(OTf)_3$	PhH	5	80	0.01	0.0	0.0
11	$GaCl_3$	PhH	5	80	0.01	<5	100.0
12	$TiCl_4$	PhH	5	80	0.01	0.0	33.9
13	$SnCl_4$	PhH	5	80	0.01	0.0	80.5

Conditions: All reactions were run on a 0.247 mmol scale of **26** and yields were determined following isolation of **27.**

Table 4.3: Solvent screen.

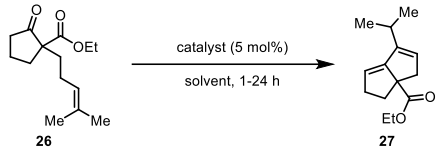

Entry	Lewis Acid	Solvent	cat. loading (mol%)	Temp. (°C)	Conc. (M)	Yield (%)	Conversion (%)
1	$Fe(OTf)_3$	PhH	5	80	0.01	99.0[a]	100.0
2	$Fe(OTf)_3$	$PhCH_3$	5	80	0.01	82.0	100.0
3	$Fe(OTf)_3$	DCM	5	80	0.01	57.9	100.0
4	$Fe(OTf)_3$	THF	5	80	0.01	0.0	33.0
5	$Fe(OTf)_3$	PhCl	5	80	0.01	54.0	75.0
6	$Fe(OTf)_3$	DMF	5	80	0.01	0.0	0.0

Conditions: All reactions were ran on a 0.247 mmol scale of **26** and yields were determined by NMR using $SiMe_3Ph$ standard.
[a]Isolated yields.

Table 4.4: Catalyst loading screen.

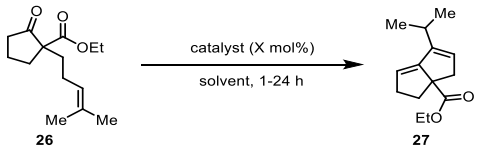

Entry	Lewis Acid	Solvent	cat. loading (mol%)	Temp. (°C)	Conc. (M)	Yield (%)	Conversion (%)
1	$Fe(OTf)_3$	PhH	1	80	0.01	0.0	33
2	$Fe(OTf)_3$	PhH	5	80	0.01	99.0[a]	100.0
3	$Fe(OTf)_3$	PhH	20	80	0.01	69.5[a]	100.0
4	$Fe(OTf)_3$	PhH	50	80	0.01	84.0	84.0
5	$Fe(OTf)_3$	PhH	100	80	0.01	63.0	100.0

Conditions: All reactions were ran on a 0.247 mmol scale of **26** and yields were determined by NMR using $SiMe_3Ph$ standard.
[a]Isolated yields.

Table 4.5: Temperature screen.

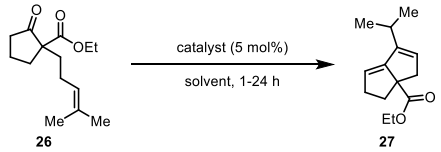

Entry	Lewis Acid	Solvent	cat. loading (mol%)	Temp. (°C)	Conc. (M)	Yield (%)	Conversion (%)
1	$Fe(OTf)_3$	PhH	5	15	0.01	15.0	26.0
2	$Fe(OTf)_3$	PhH	5	20	0.01	21.0	23.0
3	$Fe(OTf)_3$	PhH	5	40	0.01	22.0	77.0
4	$Fe(OTf)_3$	PhH	5	80	0.01	99.0[a]	100.0

Conditions: All reactions were ran on a 0.247 mmol scale of **26** and yields were determined by NMR using $SiMe_3Ph$ standard.
[a]Isolated yields.

Table 4.6: Solvent concentration screen.

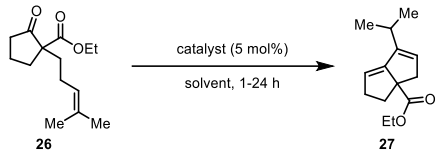

Entry	Lewis Acid	Solvent	cat. loading (mol%)	Temp. (°C)	Conc. (M)	Yield (%)	Conversion (%)
1	$Fe(OTf)_3$	PhH	5	80	0.01	99.0[a]	100.0
2	$Fe(OTf)_3$	PhH	5	80	0.025	71.0	100.0
3	$Fe(OTf)_3$	PhH	5	80	0.05	60.0	100.0
4	$Fe(OTf)_3$	PhH	5	80	0.1	49.0	100.0
5	$Fe(OTf)_3$	PhH	5	80	1.0	26.0[b]	100.0

Conditions: All reactions were ran on a 0.247 mmol scale of **26** and yields were determined by NMR using $SiMe_3Ph$ standard.
[a]Isolated yields. [b] 2.48mmol scale.

4.5.3 Mechanistic Investigations

Carbonyl-ene Studies

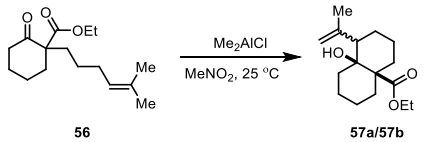

57a/57b diastereomeric mixture was synthesized according to reported procedure by Snider[20] and spectroscopic data of mixture matched reported spectra for an isolated yield of 56% (42% α-C_3H_5 and 14% β-C_3H_5).

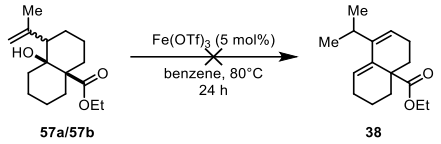

A flame-dried round bottom flask was charged with **57a/57b** (0.11 mmol, 1.0 equiv) at room temperature. To the flask was added $Fe(OTf)_3$ (0.005 mmol, 0.05 equiv) in benzene (10.6 mL, 0.01M), and the resulting mixture was stirred in the presences of N_2 for 24 hours at 80 °C with a reflux condenser. After 24 hours, the reaction mixture was passed through a short silica plug eluting with DCM. The filtrate was concentrated under reduced pressure and the crude material analyzed with NMR. **57a/57b** mixture was recovered 22.3 mg, 79% and **56** was also recovered 5.2 mg, 18%.

Deuterium Labeling Study

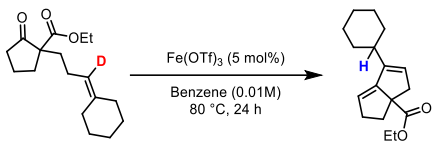

52 55

A flame-dried round bottom flask was charged with **52** (0.11 mmol, 1.0 equiv) at room temperature. To the flask was added $Fe(OTf)_3$ (0.005 mmol, 0.05 equiv) in benzene (10.7 mL, 0.01M), and the resulting mixture was stirred in the presences of N_2 for 24 hours at 80°C with a reflux condenser. Upon completion, the reaction mixture was passed through a short silica plug eluting with DCM. The filtrate was concentrated under reduced pressure and the crude material was purified using column chromatography with indicated eluent to provide 28.1 mg, (75%) of **55** with no deuterium incorporation.

Isomerization Studies

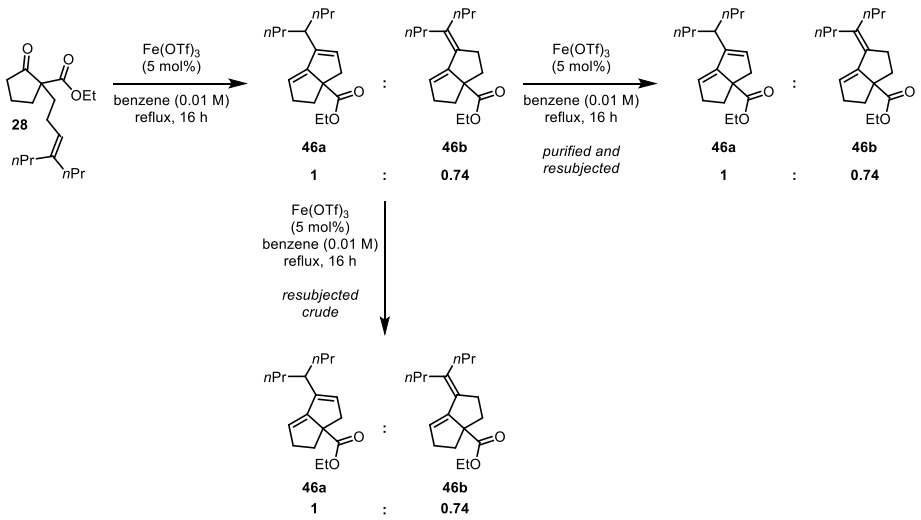

A flame-dried round bottom flask was charged with **28** (200 mg, 1.00 equiv., 0.679 mmol) at room temperature. To the flask was added $Fe(OTf)_3$ (17.1 mg, 0.05 equiv., 34.0 µmol) in benzene (68 mL, 0.01 M), and the resulting mixture was stirred in the presences of N_2 for 16 hours at 80 °C with a reflux condenser. Upon completion, the reaction mixture was passed through a short silica plug eluting with DCM. The filtrate was concentrated under reduced pressure and half of the crude material was kept and the other half of the crude material was purified using column chromatography (9:1, EtOAc:hexanes) to provide **46a** and **46b** (1:0.74) as an inseparable mixture.

Crude Resubjection

A flame-dried round bottom flask was charged with **46a** and **46b** (50.0 mg, 1.00 equiv) at room temperature. To the flask was added $Fe(OTf)_3$ (4.27 mg, 0.05 Eq, 8.49 µmol) in benzene (17 mL, 0.01 M), and the resulting mixture was stirred in the presences of N_2 for 16 hours at 80 °C with a reflux condenser. Upon completion, the reaction mixture was passed through a short silica plug eluting with DCM. The filtrate was concentrated under reduced pressure and the crude material analyzed with $PhMe_3Si$ as an internal standard *via* 1H-NMR to determine the ratio **46a** and **46b** (1:0.74).

Purified Resubjection

A flame-dried round bottom flask was charged with **46a** and **46b** (50.0 mg, 1.00 equiv) at room temperature. To the flask was added $Fe(OTf)_3$ (4.27 mg, 0.05 Eq, 8.49 µmol) in benzene (17 mL, 0.01 M), and the resulting mixture was stirred in the presences of N_2 for 16 hours at 80 °C with a

reflux condenser. Upon completion, the reaction mixture was passed through a short silica plug eluting with DCM. The filtrate was concentrated under reduced pressure and the crude material analyzed with $PhMe_3Si$ as an internal standard *via* 1H-NMR to determine the ratio **46a** and **46b** (1:0.74).

Quenching Studies

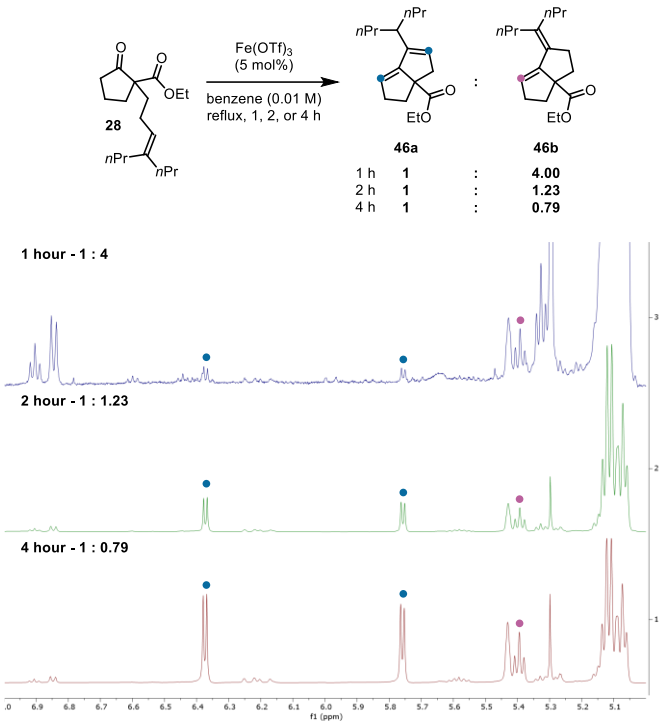

Three reactions were set up in triplicate. A flame-dried round bottom flask was charged with **28** (30.0 mg) at room temperature. To the flask was added $Fe(OTf)_3$ (2.56 mg, 0.05 Eq, 5.09 µmol) in benzene (9.0 mL, 0.01 M), and the resulting mixture was stirred in the presences of N_2 for either 1, 2, or 4 hours at 80 °C with a reflux condenser. Upon completion, the reaction mixture was passed through a short silica plug eluting with DCM. The filtrate was concentrated under reduced pressure and the crude material analyzed with $PhMe_3Si$ as an internal standard *via* 1H-NMR to determine the ratio **46a** and **46b**.

4.5.4 Computational Data

Computational experiments are ongoing, the most recent reaction coordinate diagram is shown below (B3LYP-D3/cc-pVTZ(-f)//LACVP** (SCRF, ε=2.284 for benzene)).

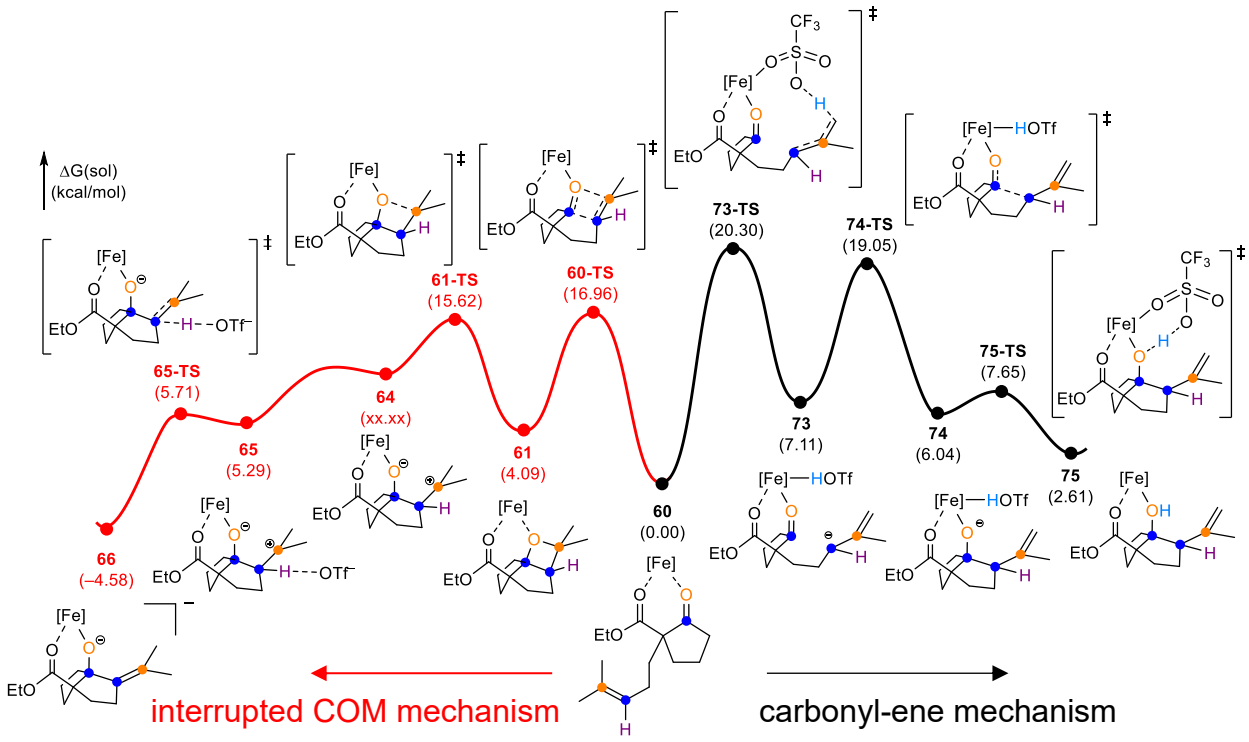

4.5.5 Experimental Procedures

Substrate Synthesis

General Alkylation Procedure: A flame dried flask equipped with a stir bar and reflux condenser was charged with sodium hydride (1.2 equiv., 60% dispersion) and dry DMF (0.12 M) and cooled to 0 °C under nitrogen. Ketone (1.0 equiv.) was added to the solution dropwise via syringe. The reaction was left stirring at 0°C for 30 min. and was then heated to 150 °C. The alkyl iodide (1.2 equiv.) was added dropwise via syringe. The reaction was monitored by TLC until completion. The organic layer was extracted with ethyl acetate 3 times and washed with water (3 times), sat. aq. NH_4Cl, aq. $NaHCO_3$, and brine. The organic layer was dried with Na_2SO_4 and concentrated under reduced pressure. Purification flash column chromatography eluting with hexanes/EtOAc (7:2) provided alkylated product.

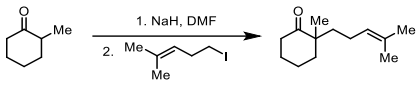

2-methyl-2-(4-methylpent-3-en-1-yl)cyclohexan-1-one (23): The general alkylation procedure was followed employing 2-methylcyclohexanone (2.23 mmol) and 5-iodo-2-methylpent-2-ene[21] (2.67 mmol). Following purification, **23** was produced in 172 mg (40%).

^{1}H NMR (400 MHz; $CDCl_3$) δ_H 5.08 (t, *J* = 6.4 Hz, 1H), 2.44 (ddd, *J*= 14.3, 10.6, 5.9), 2.33 (dt, *J* = 14.2, 5.2 Hz, 1H), 2.01-1.89 (m, 2H), 1.89-1.62 (m, 9H), 1.60 (m, 4H), 1.46-1.36 (m, 1H), 1.06 (s, 3H).

^{13}C NMR (135 MHz, $CDCl_3$) δ_C 216.0, 131.9, 124.1, 48.6, 39.5, 38.8, 37.7, 27.6, 25.7, 22.48, 22.45, 21.1, 17.6.

***ν*max (FTIR)/cm^{-1}:** 2930, 2903, 1703, 1700, 1448, 1375, 1122, 986, 827, 742.

***m/z* (ESI+) HRMS [M+H] $C_{13}H_{22}O^+$:** formula found 195.1725, cald. 195.1743.

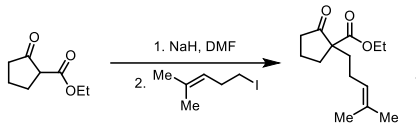

ethyl 1-(4-methylpent-3-en-1-yl)-2-oxocyclopentane-1-carboxylate (26): The general alkylation procedure was followed employing ethyl 2-oxocyclopentane-1-carboxylate (4.2 mmol) and 5-iodo-2-methylpent-2-ene[21] (5.0 mmol). Following purification, **26** was produced in 700 mg (70%).

^{1}H NMR (400 MHz; $CDCl_3$) δ_H 5.11-5.04 (m, 1H), 4.22-4.12 (m, 2H), 2.60-2.50 (m, 1H), 2.45-2.36 (m, 1H), 2.30-2.20 (m, 1H), 2.03-1.88 (m, 6H), 1.68 (s, 3H), 1.60 (s, 3H), 1.58-1.55 (m, 1H), 1.26 (t, *J* = 7.1 Hz, 3H).

^{13}C NMR (135 MHz, $CDCl_3$) δ_C 214.8, 170.9, 132.5, 123.3, 61.3, 60.4, 37.9, 33.9, 32.7, 25.6, 23.6, 19.6, 17.6, 14.1.

***ν*max (FTIR)/cm^{-1}:** 2969, 1747, 1716, 1445, 1365, 1219, 1205, 1141, 1031, 826.

***m/z* (ESI+) HRMS [M+H] $C_{14}H_{22}O_3^+$:** formula found 239.1641, cald. 239.1642.

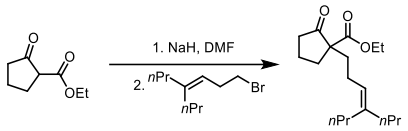

ethyl 2-oxo-1-(4-propylhept-3-en-1-yl)cyclopentane-1-carboxylate (28): The general alkylation procedure was followed employing ethyl 2-oxocyclopentane-1-carboxylate (2.24 mmol) and 1-bromo-4-propylhept-3-ene[22] (2.69 mmol). Following purification, **28** was produced in 320 mg (49%).

^{1}H NMR (400 MHz; $CDCl_3$) δ_H 5.07 (t, *J* = 6.6 Hz, 1H), 4.18 (qd, *J* = 7.1, 2.8 Hz), 2.56 (dd, *J* = 12.5, 5.2 Hz, 1H), 2.46-2.36 (m, 1H), 2.27 (dd, *J* = 17.7, 9.1 Hz, 1H), 2.15-1.80 (m, 9H), 1.65-1.49 (m, 2H), 1.37 (dt, *J* = 14.4, 7.2 Hz, 4H), 1.27 (t, *J* = 7.1 Hz, 3H), 0.88 (dt, *J* = 11.5, 7.3 Hz, 6H).

^{13}C NMR (135 MHz, $CDCl_3$) δ_C 214.8, 170.9, 140.3, 123.4, 61.4, 60.5, 38.9, 37.9, 34.3, 32.7, 32.0, 23.3, 21.5, 21.2, 19.6, 14.2, 14.1, 13.9.

***ν*$_{max}$ (FTIR)/cm^{-1}:** 2957, 2870, 175, 1718, 1454, 1257, 1141, 1026, 855, 818, 741.

***m/z* (ESI+) HRMS [M+H] $C_{18}H_{30}O_3^+$:** formula found 295.2274, cald. 295.2268.

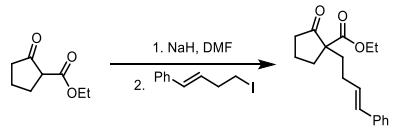

ethyl (E)-2-oxo-1-(4-phenylbut-3-en-1-yl)cyclopentane-1-carboxylate (29): The general alkylation procedure was followed employing ethyl 2-oxocyclopentane-1-carboxylate (1.92 mmol) and (E)-(4-iodobut-1-en-1-yl)benzene[23] (2.30 mmol). Following purification, **29** was produced in 310 mg (56%).

^{1}H NMR (400 MHz; $CDCl_3$) δ_H 7.34-7.16 (m, 5H), 6.35 (d, *J*= 15.8 Hz, 1H), 6.15-6.09 (m, 1H), 4.18-4.09 (m, 2H), 2.56-2.50 (m, 1H), 2.42-2.36 (m, 1H), 2.28-2.19 (m, 2H), 2.16-2.06 (m, 2H), 2.00-1.88 (m, 3H), 1.75-1.68 (m, 1H), 1.21 (t, *J* = 7.0 Hz, 3H).

^{13}C NMR (135 MHz, $CDCl_3$) δ_C 214.7, 137.5, 130.5, 129.5, 128.5, 127.0, 126.0, 61.4, 37.9, 33.4, 32.9, 28.5, 19.6, 14.1.

***ν*$_{max}$ (FTIR)/cm^{-1}:** 29970, 2854, 1729, 1716, 1445, 1229, 1145, 1141, 1025, 910.

***m/z* (ESI+) HRMS [M+H] $C_{18}H_{22}O_3^+$:** formula found 287.1642, cald. 287.1642.

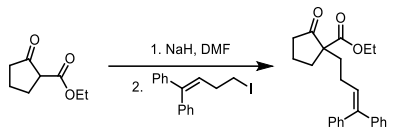

ethyl 1-(4,4-diphenylbut-3-en-1-yl)-2-oxocyclopentane-1-carboxylate (30): The general alkylation procedure was followed employing ethyl 2-oxocyclopentane-1-carboxylate (1.28 mmol) and (4-iodobut-1-ene-1,1-diyl)dibenzene[21] (1.54 mmol). Following purification, **30** was produced in 93 mg (20%).

^{1}H NMR (400 MHz; $CDCl_3$) δ_H 7.41-7.30 (m, 2H), 7.27-7.09 (m, 6H), 6.03 (dd, *J* = 14.2, 7.0 Hz, 1H), 4.16-4.11 (m, 2H), 2.50-2.34 (m, 2H), 2.23-2.03 (m, 3H), 2.00-1.82 (m, 2H), 1.80-1.65 (m, 3H), 1.26 (m, 3H).

^{13}C NMR (135 MHz, $CDCl_3$) δ_C 214.7, 173.4, 142.3, 139.8, 129.8, 129.7, 128.3, 128.2, 128.1, 127.2, 127.04, 126.97, 61.4, 60.3, 37.8, 34.0, 31.6, 24.4, 19.5, 14.2.

***ν*max (FTIR)/cm^{-1}:** 2966, 2855, 1726, 1658, 1446, 1256, 1155, 1027, 940, 708.

***m/z* (ESI+) HRMS [M+H] $C_{24}H_{26}O_3^+$:** formula found 363.1953, cald. 363.1955.

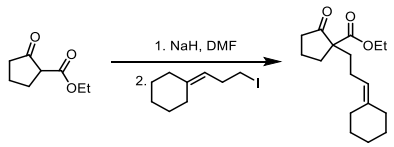

ethyl 1-(3-cyclohexylidenepropyl)-2-oxocyclopentane-1-carboxylate (31): The general alkylation procedure was followed employing ethyl 2-oxocyclopentane-1-carboxylate (1.92 mmol) and (3-iodopropylidene)cyclohexane[22] (2.31 mmol). Following purification, **31** was produced in 281 mg (53%).

^{1}H NMR (400 MHz; $CDCl_3$) δ_H 5.03 (t, *J* = 6.6 Hz, 1H) 4.25-4.08 (m, 2H), 2.60-2.50 (m, 1H), 2.46-2.36 (m, 1H), 2.32-2.24 (m, 2H), 2.12-2.08 (m, 1H), 2.06-2.03 (m, 1H), 1.98-1.88 (m, 8H), 1.64-1.58 (m, 1H), 1.55-1.47 (m, 4H), 1.46-1.40 (m, 1H), 1.26 (t, *J* = 3.5 Hz, 3H).

^{13}C NMR (135 MHz, $CDCl_3$) δ_C 215.1, 175.5, 137.0, 121.3, 67.9, 61.3, 38.2, 38.0, 33.5, 32.8, 28.2, 25.2, 23.0, 22.8, 22.6, 19.6, 14.1.

***ν*max (FTIR)/cm^{-1}:** 2924, 2853, 1731, 1720, 1444, 1366, 1188, 1143, 1027, 916.

***m/z* (ESI+) HRMS [M+Na] $C_{17}H_{26}O_3^+$:** formula found 301.1779, cald. 301.1774.

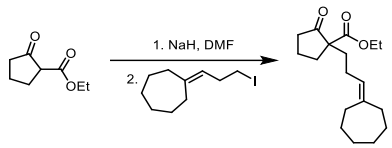

ethyl 1-(3-cycloheptylidenepropyl)-2-oxocyclopentane-1-carboxylate (32): The general alkylation procedure was followed employing ethyl 2-oxocyclopentane-1-carboxylate (4.8 mmol) and (3-iodopropylidene)cycloheptane[22] (5.7 mmol). Following purification, **32** was produced in 450 mg (32%).

^{1}H NMR (400 MHz; $CDCl_3$) δ_H 5.08 (t, II = 6.98 Hz, 1H), 4.21-4.12 (m, 2H), 2.60-2.49 (m, 1H), 2.47-2.38 (m, 1H), 2.29-2.20 (m, 2H), 2.19-2.12 (m, 4H), 2.07-1.85 (m, 6H), 1.61-1.50 (m, 8H), 1.27 (t, *J* = 5.5 Hz, 3H).

^{13}C NMR (135 MHz, $CDCl_3$) δ_C 214.8, 170.9, 142.2, 123.6, 61.3, 60.5, 38.0, 37.8, 33.9, 32.7, 29.9, 29.3, 29.1, 27.1, 23.2, 19.6, 14.1.

***ν_{max}* (FTIR)/cm^{-1}:** 2919, 2848, 1735, 1717, 1442, 1256, 1190, 1141, 1111, 1026.

***m/z* (ESI+) HRMS [M+H] $C_{18}H_{28}O_3^+$:** formula found 293.2116, cald. 293.2111.

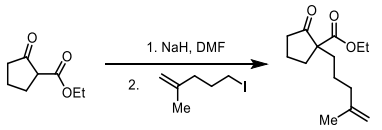

ethyl 1-(4-methylpent-4-en-1-yl)-2-oxocyclopentane-1-carboxylate (33): The general alkylation procedure was followed employing ethyl 2-oxocyclopentane-1-carboxylate (0.96 mmol) and 5-iodo-2-methylpent-1-ene[24] (1.15 mmol). Following purification, **33** was produced in 238 mg (20%).

^{1}H NMR (400 MHz; $CDCl_3$) δ_H 4.70 (s, 1H), 1.66 (s, 1H), 4.15-4.11 (m, 2H), 2.43-2.25 (m, 3H), 2.03-1.98 (m, 1H), 1.69 (s, 3H), 1.65-1.55 (m, 3H), 1.54-1.36 (m, 4H), 1.26 (td, *J* = 7.5, 5.0 Hz, 5H).

^{13}C NMR (135 MHz, $CDCl_3$) δ_C 214.9, 171.0, 145.0, 110.3, 61.3, 60.4, 37.9, 37.8, 33.4, 32.8, 22.6, 22.2, 19.6, 14.1.

***ν_{max}* (FTIR)/cm^{-1}:** 2922, 2852, 1730, 1449, 1373, 1244, 1149, 1129, 1025, 885.

***m/z* (ESI+) HRMS [M+H] $C_{14}H_{22}O_3^+$:** formula found 239.1638, cald. 239.1642.

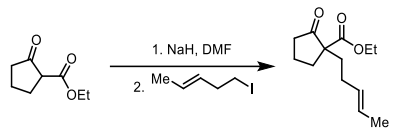

ethyl (E)-2-oxo-1-(pent-3-en-1-yl)cyclopentane-1-carboxylate (34): The general alkylation procedure was followed employing ethyl 2-oxocyclopentane-1-carboxylate (0.64 mmol) and (E)-5-iodopent-2-ene[23] (0.77 mmol). Following purification, **34** was produced in 55 mg (38%).

^{1}H NMR (400 MHz; $CDCl_3$) δ_H 5.49-5.42 (m, 1H), 5.41-5.34 (m, 1H), 4.21-4.12 (m, 2H), 2.57-2.51 (m, 1H), 2.45-2.37 (m, 1H), 2.30-2.21 (m, 1H), 2.13-1.80 (m, 7H), 1.63 (d, *J* = 6.2 hz, 3H), 1.26 (t, *J* = 7.1 Hz, 3H).

^{13}C NMR (135 MHz, $CDCl_3$) δ_C 214.8, 170.9, 130.1, 125.7, 61.3, 60.3, 37.9, 33.7, 32.7, 28.0, 19.6, 17.9, 14.1.

***ν*max (FTIR)/cm^{-1}:** 2960, 1747, 1716, 1447, 1226, 1159, 1146, 1026, 965, 917.

***m/z* (ESI+) HRMS [M+H] $C_{13}H_{20}O_3^+$:** formula found 225.1488, cald. 225.1485.

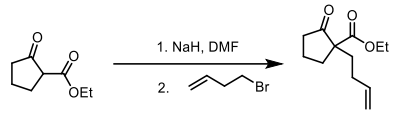

ethyl 1-(but-3-en-1-yl)-2-oxocyclopentane-1-carboxylate (35): The general alkylation procedure was followed employing ethyl 2-oxocyclopentane-1-carboxylate (0.80 mmol) and 4-bromobut-1-ene (0.96 mmol). Following purification, **35** was produced in 76 mg (45%).

^{1}H NMR (400 MHz; $CDCl_3$) δ_H 5.78 (dd, *J* = 16.9, 10.4 Hz, 1H), 5.06-4.93 (m, 2H), 4.21-4.14 (m, 2H), 2.60-2.50 (m, 1H), 2.46-2.37 (m, 1H), 2.31-2.22 (m, 1H), 2.12-1.91 (m, 6H), 1.70-1.64 (m, 1H), 1.26 (t, *J* = 7.1 Hz, 3H).

^{13}C NMR (135 MHz, $CDCl_3$) δ_C 214.7, 170.9, 137.7, 115.1, 61.4, 60.2, 37.9, 33.0, 32.8, 29.1, 19.6, 14.1.

***ν*max (FTIR)/cm^{-1}:** 2975, 1750, 1720, 1424, 1446, 1369, 1254, 1188, 1023, 913.

***m/z* (ESI+) HRMS [M+H] $C_{12}H_{18}O_3^+$:** formula found 211.1330, cald. 211.1329.

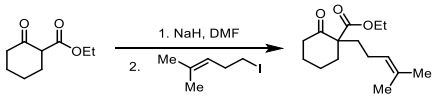

ethyl 1-(4-methylpent-3-en-1-yl)-2-oxocyclohexane-1-carboxylate (36s): The general alkylation procedure was followed employing ethyl 2-oxocyclohexane-1-carboxylate (4.19 mmol)

and 5-iodo-2-methylpent-2-ene[21] (5.03 mmol). Following purification, **36s** was produced in 423 mg (40%).

^{1}H NMR (400 MHz; $CDCl_3$) δ_H 5.09 (s, 1H), 4.21 (q, *J* = 7.1 Hz, 2H), 2.57-2.44 (m, 3H), 2.08-1.69 (m, 7H), 1.70-1.65 (m, 4H), 1.60 (s, 3H), 1.49-1.43 (m, 1H), 1.28 (t *J* = 7.1 Hz, 3H).

^{13}C NMR (135 MHz, $CDCl_3$) δ_C 208.1, 172.0, 132.2, 123.6, 61.1, 60.7, 41.1, 36.1, 34.7, 27.7, 25.7, 23.0, 22.6, 17.6, 14.2.

***ν*max (FTIR)/cm^{-1}:** 2932, 1710, 1449, 1365, 1205, 1131, 1093, 1058, 1022, 909.

***m/z* (ESI+) HRMS [M+H] $C_{15}H_{24}O_3^+$:** formula found 253.1796, cald. 253.1798.

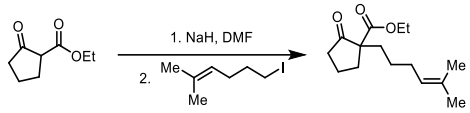

ethyl 1-(5-methylhex-4-en-1-yl)-2-oxocyclopentane-1-carboxylate (37s): The general alkylation procedure was followed employing ethyl 2-oxocyclopentane-1-carboxylate (2.56 mmol) and 6-iodo-2-methylhex-2-ene[25] (3.07 mmol). Following purification, **37s** was produced in 215 mg (33%).

^{1}H NMR (400 MHz; $CDCl_3$) δ_H 5.09 (t, *J*= 6.8 Hz, 1H), 4.22-4.07 (m, 2H), 2.53 (dd, *J*= 13.2, 6.0 Hz, 1H), 2.44-2.36 (m, 3H), 2.27-2.18 (m, 1H), 2.03-1.83 (m, 6H), 1.69 (s, 3H), 1.59-1.50 (m, 4H), 1.39-1.31 (m, 1H), 1.26 (t, *J*= 7.2 Hz, 1H).

^{13}C NMR (135 MHz, $CDCl_3$) δ_C 215.0, 171.1, 132.0, 123.9, 61.3, 60.6, 38.0, 35.6, 32.7, 28.2, 25.7, 25.1, 19.6, 17.7, 14.1.

***ν*max (FTIR)/cm^{-1}:** 2961, 2857, 1749, 1716, 1446, 1376, 1226, 1142, 1026, 856.

***m/z* (ESI+) HRMS [M+H] $C_{15}H_{24}O_3^+$:** formula found 253.1799, cald. 253.1798.

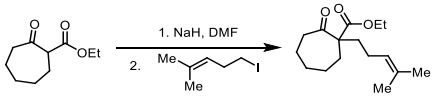

ethyl 1-(4-methylpent-3-en-1-yl)-2-oxocycloheptane-1-carboxylate (39s): The general alkylation procedure was followed employing ethyl 2-oxocycloheptane-1-carboxylate (2.71 mmol) and 5-iodo-2-methylpent-2-ene[21] (3.25 mmol). Following purification, **39s** was produced in 577 mg (80%).

^{1}H NMR (400 MHz; $CDCl_3$) δ_H 5.09 (t, *J*= 6.8 Hz, 1H), 4.20 (q, *J* = 7.1 Hz, 2H), 2.66-2.60 (m, 1H), 2.52-2.46 (m, 1H), 2.20-2.13 (m, 1H), 2.02-1.90 (m, 3H), 1.78-1.73 (m, 2H), 1.71-1.54 (m, 11H) 1.49-1.43 (m, 1H), 1.27 (t, *J* = 7.1 Hz, 3H).

^{13}C NMR (135 MHz, $CDCl_3$) δ_C 209.6, 172.5, 132.2, 123.6, 62.7, 61.0, 42.0, 35.4, 32.8, 29.9, 25.64, 25.61, 24.9, 23.3, 17.6, 14.1.

***ν*max (FTIR)/cm^{-1}:** 2929, 1724, 1709, 1444, 1365, 1219, 1148, 1111, 1022, 840.

***m/z* (ESI+) HRMS [M+H] $C_{16}H_{26}O_3^+$:** formula found 267.1957, cald. 267.1955.

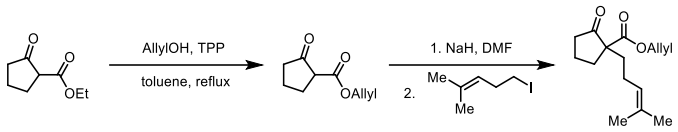

allyl 1-(4-methylpent-3-en-1-yl)-2-oxocyclopentane-1-carboxylate (40s): allyl 2-oxocyclopentane-1-carboxylate was synthesized via transesterification reaction based on reported procedure.[26] Following purification, the general alkylation procedure was followed employing ethyl 2-oxocycloheptane-1-carboxylate (1.93 mmol) and 5-iodo-2-methylpent-2-ene[21] (2.31 mmol). Following purification, **40s** was produced in 300 mg (62%).

^{1}H NMR (400 MHz; $CDCl_3$) δ_H 5.96-5.82 (m, 5H), 5.32 (d, *J* = 172 Hz, 1H), 5.24 (d, *J* = 10.5 Hz, 1H), 5.07 (t, *J* = 6.9 Hz, 1H), 4.61 (d, *J* = 5.6 Hz, 2H), 2.662-2.52 (m, 1H), 2.45-2.38 (m, 1H), 2.32-2.25 (m, 1H), 2.18-1.77 (m, 7H), 1.67 (s, 3H), 1.60 (s, 3H).

^{13}C NMR (135 MHz, $CDCl_3$) δ_C 214.6, 170.6, 132.6, 131.7, 1232, 118.5, 65.8, 60.5, 37.9, 33.9, 32.7, 25.6, 23.6, 19.6, 17.6.

***ν*max (FTIR)/cm^{-1}:** 2966, 2914, 1749, 1718, 1445, 1216, 1139, 983, 926, 830.

***m/z* (ESI+) HRMS [M+H] $C_{15}H_{22}O_3^+$:** formula found 251.1647, cald. 251.1642.

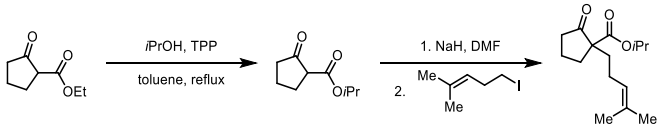

isopropyl 1-(4-methylpent-3-en-1-yl)-2-oxocyclopentane-1-carboxylate (41s): isopropyl 2-oxocyclopentane-1-carboxylate was synthesized via transesterification reaction based on reported procedure.[26] Following purification, the general alkylation procedure was followed employing ethyl 2-oxocycloheptane-1-carboxylate (2.35 mmol) and 5-iodo-2-methylpent-2-ene[21] (2.82 mmol). Following purification, **41s** was produced in 253 mg (43%).

^{1}H NMR (400 MHz; $CDCl_3$) δ_H 5.08 (t, *J*= 6.8 Hz, 1H), 5.02 (dt, *J* = 12.5, 6.2 Hz), 2.55-2.50 (m, 1H), 2.43-2.39 (m, 1H), 2.27-2.22 (m, 1H), 2.07-1.89 (m, 6H), 1.67 (s, 3H), 1.60 (s, 3H), 1.57-1.53 (m, aH), 1.24 (d, *J* = 6.2 Hz, 6H).

^{13}C NMR (135 MHz, $CDCl_3$) δ_C 214.9, 170.5, 132.4, 123.4, 68.8, 60.4, 37.9, 33.8, 32.8, 25.6, 23.5, 21.7, 21.6, 19.6, 17.6.

***ν*max (FTIR)/cm^{-1}:** 2967, 2914, 1747, 1712, 1450, 1373, 1221, 1142, 1102, 934.

***m/z* (ESI+) HRMS [M+H] $C_{15}H_{24}O_3^+$:** formula found 253.1801, cald. 253.1798.

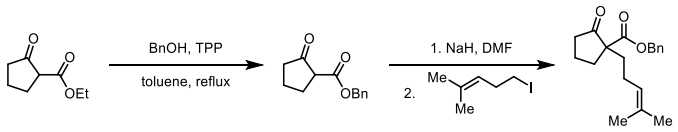

benzyl 1-(4-methylpent-3-en-1-yl)-2-oxocyclopentane-1-carboxylate (42s): benzyl 2-oxocyclopentane-1-carboxylate was synthesized via transesterification reaction based on reported procedure.[26] Following purification, the general alkylation procedure was followed employing ethyl 2-oxocycloheptane-1-carboxylate (2.29 mmol) and 5-iodo-2-methylpent-2-ene[21] (2.75 mmol). Following purification, **42s** was produced in 323 mg (47%).

^{1}H NMR (400 MHz; $CDCl_3$) δ_H 7.40-7.28 (m, 5H), 5.15 (s, 2H), 5.04 (t, *J* = 7.0 Hz, 1H), 2.58-2.52 (m, 1H), 2.45-2.34 (m, 1H), 2.31-2.21 (m, 1H), 2.07-1.85 (m, 8H), 1.66 (s, 3H), 1.54 (s, 3H).

^{13}C NMR (135 MHz, $CDCl_3$) δ_C 214.5, 170.8, 135.7, 132.5, 128.5, 128.2, 127.9, 123.2, 66.9, 60.5, 37.9, 33.9, 32.7, 25.6, 23.5, 19.6, 17.6.

***ν*max (FTIR)/cm^{-1}:** 2966, 1732, 1718, 1454, 1375, 1229, 1216, 1142, 1027, 761.

***m/z* (ESI+) HRMS [M+Na] $C_{19}H_{24}O_3^+$:** formula found 323.1619, cald. 323.1618.

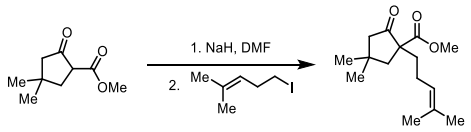

methyl 4,4-dimethyl-1-(4-methylpent-3-en-1-yl)-2-oxocyclopentane-1-carboxylate (43s): The general alkylation procedure was followed employing methyl 4,4-dimethyl-2-oxocyclopentane-1-carboxylate (2.14 mmol) and 5-iodo-2-methylpent-2-ene[21] (2.57 mmol). Following purification, **43s** was produced in 50 mg (9%).

^{1}H NMR (400 MHz; $CDCl_3$) δ_H 5.05 (t, *J* = 6.9 Hz, 1H), 3.73 (s, 3H), 2.61 (d, *J* = 13.5 Hz, 1H), 2.32-2.28 (m, 1H), 2.19 (d, *J* = 17.6 Hz, 1H), 2.06-1.98 (m 2H), 1.94-1.87 (m, 1H), 1.79 (d, *J* = 13.7 Hz, 1H), 1.67 (s, 3H), 1.59 (s, 3H), 1.16 (s, 3H), 1.09 (s, 3H).

^{13}C NMR (135 MHz, $CDCl_3$) δ_C 214.0, 171.8, 132.7, 123.0, 61.4, 53.1, 52.7, 46.2, 37.3, 33.4, 30.3, 29.2, 25.7, 23.8, 17.6.

ν_{max} (FTIR)/cm^{-1}: 2953.5, 2866.2, 1734.7, 1724.1, 1433.4, 1369.7, 1231.8, 1166.3, 971.5, 831.7.

***m/z* (ESI+) HRMS [M+] $C_{15}H_{24}O_3^+$:** formula found 253.1799, cald. 253.1798.

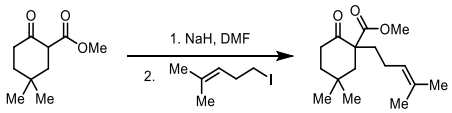

methyl 5,5-dimethyl-1-(4-methylpent-3-en-1-yl)-2-oxocyclohexane-1-carboxylate (44s): The general alkylation procedure was followed employing methyl 5,5-dimethyl-2-oxocyclohexane-1-carboxylate (4.0 mmol) and 5-iodo-2-methylpent-2-ene[21] (4.8 mmol). Following purification, **44s** was produced in 502 mg (45%).

^{1}H NMR (400 MHz; $CDCl_3$) δ_H 5.07 (t, *J* = 5.9 Hz, 1H), 3.73 (s, 3H), 2.82 (td, *J* = 14.1, 5.9 Hz, 1H), 2.35-2.28 (m, 2H), 2.17-2.10 (m, 1H), 1.78-1.70 (m, 3H), 1.67 (s, 3), 1.65-1.57 (m, 4H), 1.52-1.46 (m, 2H), 1.06 (s, 3H), 0.99 (s, 3H).

^{13}C NMR (135 MHz, $CDCl_3$) δ_C 209.1, 173.8, 132.2, 123.7, 57.7, 52.1, 49.1, 40.1, 37.6, 36.6, 32.0, 30.9, 25.6, 25.3, 23.4, 17.6.

ν_{max} (FTIR)/cm^{-1}: 2951, 2853, 1712, 1430, 1368, 1217, 1140, 1137, 1123, 998.

***m/z* (ESI+) HRMS [M+H] $C_{16}H_{26}O_3^+$:** formula found 267.1950, cald. 267.1955.

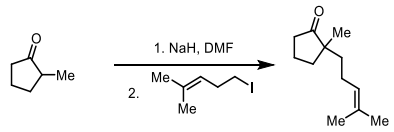

2-methyl-2-(4-methylpent-3-en-1-yl)cyclopentan-1-one (45s): The general alkylation procedure was followed employing 2-methyl cyclopentanone (10.2 mmol) and 5-iodo-2-methylpent-2-ene[21] (12.2 mmol). Following purification, **45s** was produced in 600 mg (33%).

^{1}H NMR (400 MHz; $CDCl_3$) δ_H 5.07 (t, *J* = 6.7 Hz, 1H), 2.32-2.16 (m, 2H), 2.01-1.83 (m, 5H), 1.75-1.70 (m, 1H), 1.69 (s, 3H), 1.60 (s, 3H), 1.46-1.37 (m, 2H), 1.02 (s, 3H).

^{13}C NMR (135 MHz, $CDCl_3$) δ_C 223.5, 131.8, 124.1, 48.2, 37.7, 36.6, 35.6, 25.7, 23.0, 21.8, 18.7, 17.6.

ν_{max} (FTIR)/cm^{-1}: 2958, 2952, 1733, 1452, 1373, 1174, 1159, 1102, 1066, 829.

***m/z* (ESI+) HRMS [M+] $C_{12}H_{20}O^+$:** formula found 180.1512, cald. 180.1514.

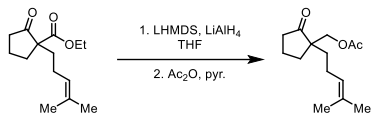

(1-(4-methylpent-3-en-1-yl)-2-oxocyclopentyl)methyl acetate (49s): LiHMDS (2.52 mmol, 1.0 equiv.) was added to a solution of **26** (2.52 mmol, 1.0 equiv.) in 2 mL anhydrous THF at 0 °C. After stirring at this temperature for 30 min, $LiAlH_4$ (5.04 mmol, 2.0 equiv.) was added and stirring was continued for 30 minutes. The reaction mixture was then quenched with cold water and the resulting suspension was filtered through Celite®. The filtrate was then dried using Na_2SO_4 and evaporated. The crude, intermediate alcohol (1.23 mmol) was then added to 1 mL of pyridine and acetic anhydride (2.47 mmol, 2.00 equiv.) and allowed to stir for 5 hours. Following purification, **49s** was produced in 200 mg (68%).

^{1}H NMR (400 MHz; $CDCl_3$) δ_H 5.03 (s, 1H), 4.08 (dd, J = 28.8, 10.9 Hz, 2H), 2.34 – 2.23 (m, 2H), 2.09 – 1.80 (m, 9H), 1.67 (s, 3H), 1.59 (s, 3H), 1.46 (dt, J = 18.7, 9.3 Hz, 2H).

^{13}C NMR (135 MHz, $CDCl_3$) δ_C 220.4, 170.8, 132.4, 123.4, 67.2, 51.5, 38.4, 33.4, 31.0, 25.6, 22.7, 20.8, 18.9, 17.6.

***ν*max (FTIR)/cm^{-1}:** 2954, 2858, 1735, 1454, 1373, 1230, 1153, 1037, 902, 821; ***m/z* (ESI+) HRMS [M+H] $C_{14}H_{22}O_3^+$:** formula found 221.1531, cald. 221.1536.

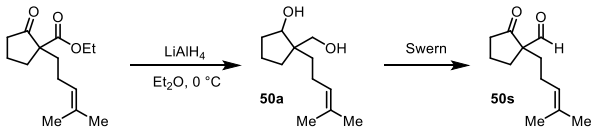

1-(4-methylpent-3-en-1-yl)-2-oxocyclopentane-1-carbaldehyde (50s): A flame-dried flask was charged with a stir bar under N_2 and $LiAlH_4$ (6.00 mmol, 2.0 equiv.) was added in diethyl ether (50 mL) and cooled to 0 °C with an ice bath. **26** (3.00 mmol, 1.0 equiv.) was added slowly via syringe and the reaction was allowed to warm to room temperature and stir overnight. The reaction was quenched with the portion wise addition of $Na_2SO_4 \cdot 10H_2O$ until bubbling ceased. The slurry was filtered through Celite® and eluted with additional diethyl ether before it was concentrated and used crude in the following step. In a flame-dried flask, oxalyl chloride (3.78 mmol, 3.0 equiv.) was added to DCM (50 mL, 0.025 M) and cooled to -78 °C with a dry ice/acetone bath. DMSO (7.56 mmol, 6.0 equiv.) was added slowly via syringe and the reaction mixture was allowed to stir

for 15 minutes at -78°C. **50a** (1.26 mmol, 1.0 equiv.) was added slowly to reaction mixture and stirred at -78 °C for 1 hour. Triethylamine (1.76 mL, 12.6 mmol, 10.0 equiv.) was added and the reaction was allowed to warm to room temperature before it was quenched with 10% aq. NH_4Cl (10 mL) and extracted with DCM (3 x 30 mL) and washed with brine (30 mL) and then dried with Na_2SO_4 and concentrated. Purification flash column chromatography eluting with hexanes/EtOAc (7:2) provided product **50s** 122 mg (50%).

^{1}H NMR (400 MHz; $CDCl_3$) δ_H 9.41 (s, 1H) 5.03 (t, *J* = 6.4 Hz, 1H), 2.63-2.57 (m, 1H), 2.34-2.21 (m, 2H), 2.06-2.00 (m, 1H), 1.99-1.85 (m, 4H), 1.83-1.78 (m, 1H), 1.74-1.63 (m, 4H), 1.57 (s, 3H).

^{13}C NMR (135 MHz, $CDCl_3$) δ_C 215.1, 198.7, 133.5, 122.7, 67.6, 38.5, 33.1, 27.8, 25.6, 23.3, 19.3, 17.7.

***ν*max (FTIR)/cm^{-1}:** 2965, 2854, 1719, 1709, 1442, 1376, 1144, 1100, 942, 809.

***m/z* (ESI+) HRMS [M+H] $C_{12}H_{18}O_2^+$:** formula found 195.1372, cald. 195.1380.

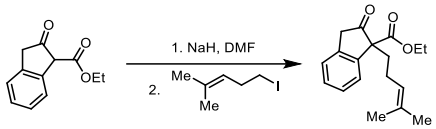

ethyl 1-(4-methylpent-3-en-1-yl)-2-oxo-2,3-dihydro-1H-indene-1-carboxylate (51s): The general alkylation procedure was followed employing methyl ethyl 2-oxo-2,3-dihydro-1H-indene-1-carboxylate[27] (2.45 mmol) and 5-iodo-2-methylpent-2-ene (2.94 mmol). Following purification, **51s** was produced in 200 mg (29%).

^{1}H NMR (400 MHz; $CDCl_3$) δ_H 7.38-7.31 (m, 4H), 4.93 (t, *J* = 7.1 Hz, 1H), 4.14-4.02 (m, 2H), 3.77 (d, *J* = 22.4 Hz, 1H), 3.46 (d, *J* = 22.4 Hz, 1H), 2.35-2.30 (m, 1H), 2.25-2.21 (m, 1H), 1.72-1.66 (m, 2H), 1.59 (s, 3H), 1.30 (s, 3H), 1.14 (t, *J*= 7.1 Hz, 3H).

^{13}C NMR (135 MHz, $CDCl_3$) δ_C 212.7, 170.3, 140.6, 137.5, 132.6, 128.4, 127.8, 124.9, 124.3, 123.4, 65.2, 61.6, 43.6, 33.8, 25.6, 23.0, 17.3, 13.9.

***ν*max (FTIR)/cm^{-1}:** 2943, 2832, 1658, 1641, 1452, 1450, 1407, 1225, 1112, 1013.

***m/z* (ESI+) HRMS [M+H] $C_{18}H_{22}O_3^+$:** formula found 287.1635, cald. 287.1642.

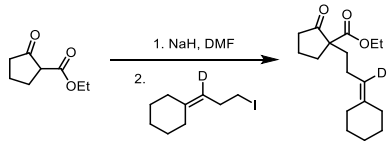

ethyl 1-(3-cyclohexylidenepropyl)-2-oxocyclopentane-1-carboxylate (52): The general alkylation procedure was followed employing ethyl 2-oxocyclopentane-1-carboxylate (1.09 mmol) and (3-iodopropylidene-1-d)cyclohexane[22] (1.31 mmol). Following purification, **52** was produced in 150 mg (49%).

^{1}H NMR (400 MHz; $CDCl_3$) δ_H 4.24 – 4.12 (m, 2H), 2.55 (dd, *J* = 12.9, 5.2 Hz, 1H), 2.44 – 2.36 (m, 1H), 2.30 – 2.23 (m, 1H), 2.12 – 1.88 (m, 9H), 1.60 – 1.47 (m, 8H), 1.27 (t, *J* = 7.1 Hz, 3H).

^{13}C NMR (135 MHz, $CDCl_3$) δ_C 214.8, 170.9, 140.6, 119.9, 61.3, 60.5, 37.9, 37.0, 34.3, 32.7, 28.6, 28.5, 27.8, 26.7, 22.6, 19.6, 14.1.

***ν*$_{max}$ (FTIR)/cm^{-1}:** 2921, 2851, 1748, 1716, 1444, 1434, 1230, 1145, 1025, 854.

***m/z* (ESI+) HRMS [M+] $C_{17}H_{25}DO_3^+$:** formula found 280.2019, cald. 280.2017.

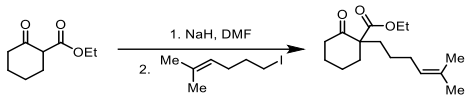

ethyl 1-(5-methylhex-4-en-1-yl)-2-oxocyclohexane-1-carboxylate (56): The general alkylation procedure was followed employing ethyl 2-oxocyclohexane-1-carboxylate (2.35 mmol) and 6-iodo-2-methylhex-2-ene[25] (2.82 mmol). Following purification, **56** was produced in 300 mg (48%).

^{1}H NMR (400 MHz; $CDCl_3$) δ_H 5.09 (t, *J* = 7.1 Hz, 1H), 4.20 (q, *J*= 7.1 Hz, 2H), 2.54-2.49 (m, 1H), 2.47/2.42 (m, 2H), 2.02-1.95 (m, 3H), 1.90-1.84 (m, 1H), 1.79-1.68 (m, 5H), 1.63-1.50 (m, 5H), 1.47-1.41 (m, 1H), 1.29-1.23 (m, 5H).

^{13}C NMR (135 MHz, $CDCl_3$) δ_C 208.1, 172.1, 131.8, 124.1, 61.1, 60.1, 41.1, 36.0, 34.3, 28.3, 27.6, 25.7, 24.5, 22.6, 17.7, 14.2.

***ν*$_{max}$ (FTIR)/cm^{-1}:** 2930, 2860, 1711, 1447, 1297, 1201, 1174, 1091, 1022, 822.

***m/z* (ESI+) HRMS [M+H] $C_{16}H_{26}O_3^+$:** formula found 267.1961, cald. 267.1955.

Carbocyclization Reactions

Optimized carbocyclization conditions: A flame-dried round bottom flask was charged with substrate (1.0 equiv) at room temperature. To the flask was added $Fe(OTf)_3$ (0.05 equiv.) in benzene (0.01 M), and the resulting mixture was stirred in the presences of N_2 for 1-24 hours at 80 °C with a reflux condenser. Upon completion (as determined by TLC analysis), the reaction mixture was passed through a short silica plug eluting with DCM. The filtrate was concentrated

under reduced pressure and the crude material was purified using column chromatography with indicated eluent to provide pure carbocyclization products.

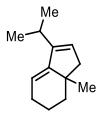

3-isopropyl-7a-methyl-5,6,7,7a-tetrahydro-1H-indene (25): The cyclization of **23** (0.25 mmol) was performed according to general procedure for carbocyclization and purification by flash column chromatography eluting with pentane/Et_2O (6:1) provided **25** 9.7 mg (22%) as a clear oil.
^{1}H NMR (400 MHz; $CDCl_3$) δ_H 6.29 (d, *J* – 9.7 Hz, 1H), 5.69-5.64 (m, 1H), 2.84-2.76 (m, 1H), 2.45-2.35 (m, 1H), 2.32-2.09 (m, 4H), 1.75-1.70 (m, 2H), 1.44-1.38 (m, 2H), 1.02 (d, *J* = 6.9 Hz, 3H), 0.98 (d, *J* = 6.8 Hz, 3H), 0.92 (s, 3H).
^{13}C NMR (135 MHz, $CDCl_3$) δ_C 140.8, 136.4, 127.0, 120.9, 44.7, 39.2, 36.1, 28.0, 26.4, 24.0, 21.6, 21.4, 21.3.
***ν*$_{max}$ (FTIR)/cm^{-1}:** 2916, 1459, 1367, 1210, 1201, 1100, 1028, 861, 786, 740.
***m/z* (ESI+) HRMS [M+H] $C_{13}H_{20}^+$:** formula found 191.1439, cald. 191.1794.

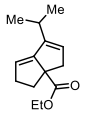

ethyl 6-isopropyl-2,4-dihydropentalene-3a(3H)-carboxylate (27): The cyclization of **26** (0.42 mmol) was performed according to general procedure for carbocyclization and purification by flash column chromatography eluting with hexanes/EtOAc (8:2) provided **27** 90 mg (99%) as a clear oil.
^{1}H NMR (400 MHz; $CDCl_3$) δ_H 6.36 (d, *J* = 5.6 Hz, 1H), 5.75 (d, *J* = 5.6 Hz, 1H), 4.19-4.10 (m, 2H), 3.44 (d, *J* = 8.3 Hz, 1H), 2.01-1.93 (m, 5H), 1.74 (d, *J* = 9.5 Hz, 7H), 1.69-1.62 (m, 1H), 1.59-1.51 (m, 2H), 1.49-1.40 (m, 1H), 1.25 (t, *J* = 7.1 Hz, 3H).
^{13}C NMR (135 MHz, $CDCl_3$) δ_C 176.5, 143.2, 135.0, 131.9, 123.3, 66.1, 30.6, 49.1, 37.4, 34.6, 25.3, 21.3, 21.0, 14.3.
***ν*$_{max}$ (FTIR)/cm^{-1}:** 2959, 2853, 1723, 1446, 1365, 1226, 1156, 1110, 1026, 878.
***m/z* (ESI+) HRMS [M+H] $C_{14}H_{20}O_2^+$:** formula found 221.1527, cald. 221.1536.

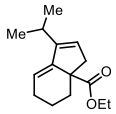

ethyl 1-isopropyl-3,4,5,6-tetrahydro-3aH-indene-3a-carboxylate (36): The cyclization of **36s** (0.25 mmol) was performed according to general procedure for carbocyclization and purification by flash column chromatography eluting with hexanes/EtOAc (8:2) provided **36s** 23.4 mg (40%) as a clear oil.

^{1}H NMR (400 MHz; $CDCl_3$) δ_H 6.37 (d, *J* = 9.9 Hz, 1H), 5.69 (s, 1H), 4.15-4.05 (m, 2H), 2.93-2.86 (m, 1H), 2.44 (dd, *J* = 12.6, 5.2 Hz, 2H), 2.32-2.22 (m, 3H), 2.17-2.10 (m, 1H), 1.66-1.58 (m, 1H), 1.48-1.21 (m, 1H), 1.21 (t, *J* = 7.1 Hz, 3H), 1.04 (t, *J* = 7.4 Hz, 6H).

^{13}C NMR (135 MHz, $CDCl_3$) δ_C 176.4, 145.4, 130.7, 127.5, 121.2, 60.2, 56.6, 36.7, 32.6, 29.4, 26.7, 24.6, 21.3, 21.0, 14.2.

***ν*max (FTIR)/cm^{-1}:** 2960, 2853, 1721, 1446, 1636, 1179, 1091, 1022, 860, 733.

***m/z* (ESI+) HRMS [M+H] $C_{15}H_{22}O_3^+$:** formula found 235.1694, cald. 235.1693.

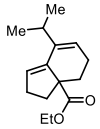

ethyl 7-isopropyl-2,3,4,5-tetrahydro-3aH-indene-3a-carboxylate (37): The cyclization of **37s** (0.20 mmol) was performed according to general procedure for carbocyclization and purification by flash column chromatography eluting with hexanes/EtOAc (8:2) provided **37** 33.5 mg (72%) as a clear oil.

^{1}H NMR (400 MHz; $CDCl_3$) δ_H 5.77 (s, 1H), 5.49 (s, 1H), 4.13-4.06 (m, 2H), 2.65 – 2.58 (m, 1H), 2.55-2.49 (m, 1H), 2.44 (dd, *J* = 12.7, 5.4 Hz, 1H), 2.36 (dd, *J* = 16.6, 9.1 Hz, 1H), 2.31 (dd, *J* = 13.0, 7.5 Hz, 1H), 2.24 (d, *J* = 13.0 Hz, 1H), 2.17 (dd, *J* = 14.8, 9.3 Hz, 1H), 1.83-1.74 (m, 2H), 1.47 (td, *J* = 12.3, 5.9 Hz, 1H), 1.34 – 1.21 (m, 1H), 1.23 – 1.17 (m, 3H), 1.10 (d, *J* = 6.8 Hz, 3H), 1.07 (d, *J* = 6.8 Hz, 3H).

^{13}C NMR (135 MHz, $CDCl_3$) δ_C 176.1, 141.4, 123.8, 121.3, 60.2, 56.4, 37.8, 33.0, 30.8, 29.8, 24.6, 22.5, 21.3, 14.2.

***ν*max (FTIR)/cm^{-1}:** 3027, 2918, 1723, 1495, 1453, 1379, 1179, 1081, 1029, 726.

***m/z* (ESI+) HRMS [M+H] $C_{16}H_{20}O_2^+$:** formula found 235.1691, cald. 235.1693.

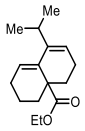

ethyl 8-isopropyl-3,4,5,6-tetrahydronaphthalene-4a(2H)-carboxylate (38): The cyclization of **56** (0.19 mmol) was performed according to general procedure for carbocyclization and purification by flash column chromatography eluting with hexanes/EtOAc (8:2) provided **38** 38 mg (82%) as a clear oil.

^{1}H NMR (400 MHz; $CDCl_3$) δ_H 5.88 (s, 1H), 5.48 (s, 1H), 4.13 – 4.06 (m, 2H), 2.72-2.66 (m, 1H), 2.29 – 2.10 (m, 6H), 1.68 – 1.64 (m, 1H), 1.53-1.42 (m, 3H), 1.20 (t, *J* = 7.2 Hz, 3H), 1.07 (dd, *J* = 24.6, 6.8 Hz, 6H).

^{13}C NMR (135 MHz, $CDCl_3$) δ_C 176.3, 142.5, 134.5, 121.3, 119.7, 60.4, 46.6, 35.7, 34.2, 28.2, 26.1, 23.5, 22.7, 22.1, 19.2, 14.3.

***ν*max (FTIR)/cm^{-1}:** 2928, 2867, 1717, 1446, 1290, 1232, 1152, 1089, 1030, 969.

***m/z* (ESI+) HRMS [M+H] $C_{16}H_{24}O_2^+$:** formula found 249.1853, cald. 249.1849.

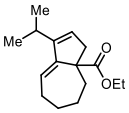

ethyl 1-isopropyl-4,5,6,7-tetrahydroazulene-3a(3H)-carboxylate (39): The cyclization of **39s** (0.38 mmol) was performed according to general procedure for carbocyclization and purification by flash column chromatography eluting with hexanes/EtOAc (8:2) provided **39** 55 mg (59%) as a clear oil.

^{1}H NMR (400 MHz; $CDCl_3$) δ_H 5.80 (dd, *J* = 8.6, 4.9 Hz, 1H), 5.53 (s, 1H), 4.17 (q, *J* = 7.1 Hz, 2H), 2.76 (d, *J* = 17.5, 2.4 Hz, 1H), 2.46-2.39 (m, 1H), 2.24-2.16 (m, 2H), 1.90-1.83 (m, 1H), 1.77-1.67 (m, 3H), 1.56-1.53 (m, 1H), 1.37-1.31 (m, 1H), 1.27-1.19 (m, 4H), 1.10 (dd, *J* = 16.0, 6.8 Hz, 6H).

^{13}C NMR (135 MHz, $CDCl_3$) δ_C 175.7, 151.3, 150.1, 124.1, 120.4, 60.4, 56.8, 46.2, 37.4, 29.0, 28.5, 28.2, 25.5, 22.0, 21.8, 14.2.

***ν*max (FTIR)/cm^{-1}:** 2919, 2847, 1719, 1631, 1443, 1233, 1154, 1140, 1025, 833.

***m/z* (ESI+) HRMS [M+H] $C_{16}H_{24}O_2^+$:** formula found 249.1854, cald. 249.1849.

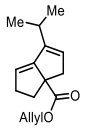

allyl 6-isopropyl-2,4-dihydropentalene-3a(3H)-carboxylate (40): The cyclization of **40s** (0.20 mmol) was performed according to general procedure for carbocyclization and purification by flash column chromatography eluting with hexanes/EtOAc (8:2) provided **40** 36 mg (78%) as a clear oil.

^{1}H NMR (400 MHz; $CDCl_3$) δ_H 6.39 (d, *J* = 5.4 Hz, 1H), 5.97 – 5.85 (m, 1H), 5.77 (d, *J* = 4.8 Hz, 1H), 5.40 – 5.18 (m, 2H), 4.64 – 4.52 (m, 2H), 3.48 (d, *J* = 8.1 Hz, 1H), 2.07-1.95 (m, 2H), 1.75 (d, J = 10.3 Hz, 6H), 1.70-1.62 (m, 1H), 1.60-1.52 (m, 2H), 1.54 – 1.41 (m, 1H).

^{13}C NMR (135 MHz, $CDCl_3$) δ_C 176.1, 143.1, 134.7, 132.4, 132.1, 117.6, 65.2, 49.2, 37.3, 34.6, 25.3, 21.3, 21.0.

***ν*max (FTIR)/cm^{-1}:** 2931, 2855, 1724, 1444, 1227, 1221, 1147, 1048, 989, 913.

***m/z* (ESI+) HRMS [M+H] $C_{15}H_{20}O_2^+$:** formula found 233.1538, cald. 233.1536.

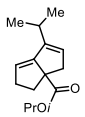

isopropyl 6-isopropyl-2,4-dihydropentalene-3a(3H)-carboxylate (41): The cyclization of **41s** (0.20 mmol) was performed according to general procedure for carbocyclization and purification by flash column chromatography eluting with hexanes/EtOAc (8:2) provided **41** 30 mg (64%) as a clear oil.

^{1}H NMR (400 MHz; $CDCl_3$) δ_H 6.36 (d, *J* = 5.6 Hz, 1H), 5.76 (d, *J* = 5.5 Hz, 1H), 4.99 (dt, *J* = 12.4, 6.2 Hz, 1H), 3.45 (d, *J* = 8.7 Hz, 1H), 2.02-1.94 (m, 2H), 6.24 (d, *J* = 11.0 Hz, 6H), 1.68-1.63 (m, 1H), 1.59-1.53 (m, 2H), 1.51-1.41 (m, 1H), 1.28-1.20 (m, 6H).

^{13}C NMR (135 MHz, $CDCl_3$) δ_C 175.9, 143.3, 135.1, 131.7, 123.2, 67.6, 66.3, 48.7, 37.5, 34.6, 25.3, 21.8, 21.7, 21.3, 21.0.

***ν*max (FTIR)/cm^{-1}:** 2975, 2849, 1716, 1445, 1372, 1252, 1176, 1106, 1067, 913.

***m/z* (ESI+) HRMS [M+H] $C_{15}H_{22}O_2^+$:** formula found 235.1692, cald. 235.1693.

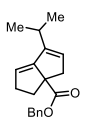

benzyl 6-isopropyl-2,4-dihydropentalene-3a(3H)-carboxylate (42): The cyclization of **42s** (0.20 mmol) was performed according to general procedure for carbocyclization and purification by flash column chromatography eluting with hexanes/EtOAc (8:2) provided **42** 44 mg (78%) as a clear oil.

^{1}H NMR (400 MHz; $CDCl_3$) δ_H 7.53-7.28 (m, 5H), 6.39 (d, *J* = 5.5 Hz, 1H), 5.78 (d, *J* = 5.2 Hz, 1H), 5.14 (s, 2H), 4.15 (dd, *J* = 14.2, 7.0 Hz, 1H), 3.48 (dd, *J* = 25.9, 8.2 Hz, 1H), 2.04-1.95 (m, 2H), 1.76 (d, *J* = 15.5 Hz, 8H), 1.69-1.64 (m, 1H), 1.60-1.54 (m, 1H), 1.52-1.43 (m, 1H), 1.29-1.22 (m, 1H).

^{13}C NMR (135 MHz, $CDCl_3$) δ_C 176.2, 143.1, 136.4, 134.6, 132.1, 128.5, 127.7, 123.5, 66.2, 49.1, 37.3, 34.5, 29.7, 25.3, 21.3, 21.0.

***ν*max (FTIR)/cm^{-1}:** 2951, 2857, 2360, 1724, 1558, 1456, 1219, 1146, 1047, 755.

***m/z* (ESI+) HRMS [M+H] $C_{19}H_{22}O_2^+$:** formula found 283.1692, cald. 283.1693.

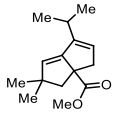

methyl 6-isopropyl-2,2-dimethyl-2,4-dihydropentalene-3a(3H)-carboxylate (43): The cyclization of **43s** (0.13 mmol) was performed according to general procedure for carbocyclization and purification by flash column chromatography eluting with hexanes/EtOAc (8:2) provided **43** 21.5 mg (72%) as a clear oil.

^{1}H NMR (400 MHz; $CDCl_3$) δ_H 6.25 (d, *J* = 5.4 Hz, 1H), 5.83 (d, *J* = 5.3 Hz, 1H), 3.68 (s, 3H), 2.17 (d, *J* = 13.1 Hz, 1H), 2.02-1.97 (m, 1H), 1.77 (d, *J* = 2.6 Hz, 6H), 1.55 (s, 2H) 1.25-1.20 (m, 1H), 1.00 (d, *J* = 8.2 Hz, 6H).

^{13}C NMR (135 MHz, $CDCl_3$) δ_C 176.9, 142.6, 136.4, 129.5, 123.8, 52.2, 50.4, 49.1, 48.2, 40.9, 28.9, 27.8, 21.5, 21.0.

***ν*max (FTIR)/cm^{-1}:** 2948, 2853, 2309, 1729, 1658, 1596, 1442, 1366, 1222, 1159.

***m/z* (ESI+) HRMS [M+H] $C_{15}H_{22}O_2^+$:** formula found 235.1689, cald. 235.1693.

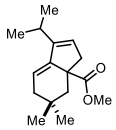

methyl 1-isopropyl-5,5-dimethyl-3,4,5,6-tetrahydro-3aH-indene-3a-carboxylate (44): The cyclization of **44s** (0.21 mmol) was performed according to general procedure for carbocyclization and purification by flash column chromatography eluting with hexanes/EtOAc (8:2) provided **44** 21.8 mg (43%) as a clear oil.

^{1}H NMR (400 MHz; $CDCl_3$) δ_H 6.29 (d, *J* = 10.0 Hz, 1H), 5.43 (d, *J* = 10.0 Hz, 1H), 3.64 (s, 3H), 2.95-2.87 (m, 1), 2.43 (dd, *J* = 13.2, 0.9 Hz, 1H) 2.30-2.20 (m, 2H), 1.68-1.58 (m, 1H), 1.13 (dd, *J* = 13.1, 4.9 Hz, 1H), 1.05-1.00 (m, 9H), 0.89 (s, 3H).

^{13}C NMR (135 MHz, $CDCl_3$) δ_C 177.7, 145.5, 137.6, 130.3, 118.4, 56.1, 51.6, 47.3, 38.9, 33.9, 32.2, 28.9, 28.2, 26.8, 21.3, 21.0.

***ν*max (FTIR)/cm^{-1}:** 2955, 2849, 1729, 1456, 1361, 1221, 1162, 1119, 1019, 775.

***m/z* (ESI+) HRMS [M+H] $C_{16}H_{24}O_2^+$:** formula found 249.1949, cald. 249.1849.

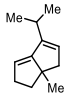

4-isopropyl-6a-methyl-1,2,6,6a-tetrahydropentalene (45): The cyclization of **45s** (0.28 mmol) was performed according to general procedure for carbocyclization and purification by flash column chromatography eluting with pentane/Et_2O (6:1) provided **45** 32 mg (71%) as a clear oil.

^{1}H NMR (400 MHz; $CDCl_3$) δ_H 6.22(d, *J* = 5.5 Hz, 1H), 5.62 (d, *J* = 5.5 Hz, 1H), 2.62 (d, *J* = 8.8 Hz, 1H), 1.99-1.78 (m, 2H), 1.76 (s, 3H), 1.72 (s, 1H), 1.60-1.52 (m, 2H), 1.49-1.40 (m, 3H), 1.17 (s, 3H).

^{13}C NMR (135 MHz, $CDCl_3$) δ_C 145.1, 142.9, 128.7, 121.4, 56.4, 51.9, 39.8, 34.7, 27.1, 25.6, 21.2, 20.8.

***ν*max (FTIR)/cm^{-1}:** 2935, 2864, 1696, 1450, 1373, 1233, 1146, 1002, 949, 871.

***m/z* (ESI+) HRMS [M+H] $C_{12}H_{18}^+$:** formula found 163.1440, cald. 163.1442.

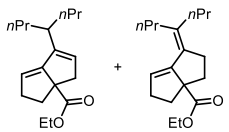

46a **46b**

ethyl 6-(heptan-4-yl)-2,4-dihydropentalene-3a(3H)-carboxylate (46a) + ethyl 1-(heptan-4-ylidene)-2,3,4,5-tetrahydropentalene-3a(1H)-carboxylate (46b): The cyclization of **28** (0.17

mmol) was performed according to general procedure for carbocyclization and purification by flash column chromatography eluting with hexanes/EtOAc (8:2) provided **46a** and **46b** (as an inseparable mixture) 40.5 mg (86%) as a clear oil.

Endo-isomer **46a**:

^{1}H NMR (400 MHz; $CDCl_3$) δ_H 6.36 (d, *J* = 5.6 Hz, 1H), 5.75 (d, *J* = 5.4 Hz, 1H), 4.28-3.97 (m, 2H), 3.59 (d, *J* = 8.8 Hz, 1H), 2.19 (dt, *J* = 12.7, 7.4 Hz, 2H), 1.96-1.86 (m, 1H), 1.73 (ddd, *J* = 25.9, 19.5, 1.02 Hz, 1H), 1.56 (dd, *J* = 12.3, 5.1 Hz, 1H), 1.45-1.33 (m, 5H), 1.31-1.28 (m, 1H), 1.29-1.16 (m, 3H), 0.97-0.71 (m, 6H); ^{13}C NMR (135 MHz, $CDCl_3$) δ_C 176.4, 145.8, 135.1, 132.1, 131.8, 65.9, 60.4, 54.9, 37.1, 33.6, 32.9, 30.5, 25.4, 22.2, 21.5, 14.3, 14.2, 14.0.

Exo-isomer **46b**:

^{1}H NMR (400 MHz; $CDCl_3$) δ_H 5.39 (dd, *J* = 16.5, 9.3 Hz, 1H), 4.28-3.97 (m, 2H), 3.46 (dd, *J* = 9.0, 2.7 Hz, 1H), 3.06 (d, *J* = 17.8 Hz, 1H), 2.36 (d, *J* = 18.2 Hz, 1H), 2.14-2.07 (m, 4H), 2.06-1.97 (m, 3H), 1.70-1.58 (m, 3H), 1.52-1.47 (m, 2H), 1.29-1.16 (m, 3H), 0.99 (t, *J* = 7.5 Hz, 2H), 0.97-0.71 (m, 4H).

^{13}C NMR (135 MHz, $CDCl_3$) δ_C 178.3, 144.1, 134.4, 130.8, 121.4, 60.5, 58.2, 48.8, 44.2, 40.0, 35.3, 34.7, 26.0, 22.6, 21.4, 14.4, 14.2, 14.0.

***ν*max (FTIR)/cm^{-1}:** 2959, 2868, 1726, 1446, 1364, 1221, 1151, 1055, 917, 731.

***m/z* (ESI+) HRMS [M+H] $C_{18}H_{28}O_2^+$:** formula found 277.2166, cald. 277.2162.

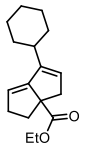

ethyl 6-cyclohexyl-2,4-dihydropentalene-3a(3H)-carboxylatecarboxylate (47): The cyclization of **31** (0.18 mmol) was performed according to general procedure for carbocyclization and purification by flash column chromatography eluting with hexanes/EtOAc (8:2) provided **47** 43.9 mg (94%) as a clear oil.

^{1}H NMR (400 MHz; $CDCl_3$) δ_H 5.72 (s, 1H), 5.42 (s, 1H), 4.17-4.09 (m, 2H), 3.60 (d, *J* = 8.8 Hz, 1H), 3.07 (d, *J* = 18.0 Hz, 1H), 2.35 (d, *J* = 18.0 Hz, 1H), 2.31-2.05 (m, 6H), 1.98-1.90 (m, 1H), 1.70-1.56 (m, 7H), 1.26 (t, *J* = 7.1 Hz, 3H).

^{13}C NMR (135 MHz, $CDCl_3$) δ_C 178.3, 146.2, 132.3, 125.4, 120.6, 60.5, 58.4, 54.8, 44.2, 39.8, 33.1, 26.2, 26.1, 25.8, 22.8, 22.4, 14.3.

***ν*max (FTIR)/cm^{-1}:** 2928, 2859, 1724, 1445, 1272, 1216, 1177, 1152, 1031, 915. ***m/z* (ESI+) HRMS [M+H] $C_{17}H_{24}O_2^+$:** formula found 261.1850, cald. 261.1849.

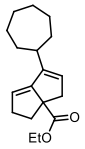

ethyl 6-cycloheptyl-2,4-dihydropentalene-3a(3H)-carboxylate (48): The cyclization of **32** (0.17 mmol) was performed according to general procedure for carbocyclization and purification by flash column chromatography eluting with hexanes/EtOAc (8:2) provided **48** 33.5 mg (71%) as a clear oil.

^{1}H NMR (400 MHz; $CDCl_3$) δ_H 5.85 (t, *J* = 6.9 Hz, 1H), 5.45 (s, 1H), 4.16-4.13 (m, 2H), 3.58 (d, *J* = 8.7 Hz, 1H), 3.07 (d, *J* = 17.1 Hz, 1H), 2.38-2.31 (m, 4H), 2.24-2.21 (m, 2H), 2.16-2.11 (m, 1H), 2.03-1.91 (m, 2H), 1.78-1.73 (m, 2H), 1.68-1.62 (m, 3H), 1.51-1.48 (m, 3H), 1.26 (t, *J* = 7.0 Hz, 3H).

^{13}C NMR (135 MHz, $CDCl_3$) δ_C 173.2, 146.8, 129.9, 123.6, 121.1, 60.5, 54.9, 44.1, 40.0, 37.4, 33.0, 32.5, 30.0, 28.4, 26.9, 26.4, 26.1, 14.3.

***ν*max (FTIR)/cm^{-1}:** 2917, 2848, 1723, 1445, 1232, 1221, 1151, 1026, 912, 730.

***m/z* (ESI+) HRMS [M+H] $C_{18}H_{26}O_2^+$:** formula found 275.2007, cald. 275.2006.

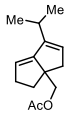

(6-isopropyl-2,4-dihydropentalen-3a(3H)-yl)methyl acetate (49): The cyclization of **49s** (0.10 mmol) was performed according to general procedure for carbocyclization and purification by flash column chromatography eluting with hexanes/EtOAc (8:2) provided **49** 44 mg (20%) as a clear oil.

^{1}H NMR (400 MHz; $CDCl_3$) δ_H 6.34 (d, *J* = 5.5 Hz, 1H), 5.63 (d, *J* = 5.4 Hz, 1H), 4.06 (d, *J* = 10.6 Hz, 1H), 3.99 (d, *J* = 10.7 Hz, 1H), 2.82 (d, *J* = 8.6 Hz, 1H), 2.06 (s, 3H), 1.92 – 1.87 (m, 1H), 1.76 (s, 3H), 1.72 (s, 3H), 1.61 – 1.55 (m, 3H), 1.49 (t, *J* = 10.5 Hz, 2H).

^{13}C NMR (135 MHz, $CDCl_3$) δ_C 171.2, 137.0, 131.5, 122.5, 69.9, 65.7, 60.2, 47.8, 34.8, 34.1, 25.0, 21.0, 20.8, 20.7.

***ν*max (FTIR)/cm^{-1}:** 2945, 2879, 1738, 1444, 1376, 1333, 1227, 1031, 907, 776.

***m/z* (ESI+) HRMS [M+H] $C_{14}H_{20}O_2^+$:** formula found 221.1531, cald. 221.1536.

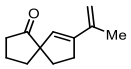

7-(prop-1-en-2-yl)spiro[4.4]non-6-en-1-one (50): The cyclization of **50s** (0.26 mmol) was performed according to general procedure for carbocyclization and purification by flash column chromatography eluting with hexanes/EtOAc (8:2) provided **50** 19.2 mg (42%) as a clear oil.

^{1}H NMR (400 MHz; $CDCl_3$) δ_H 5.48 (s, 1H), 4.96 (s, 2H), 2.74 – 2.63 (m, 1H), 2.62-2.54 (m, 1H), 2.31 (t, *J* = 6.9 Hz, 2H), 2.23 – 2.16 (m, 1H), 2.04-1.97 (m, 2H), 1.96 – 1.90 (m, 5H), 1.82 – 1.77 (m, 1H).

^{13}C NMR (135 MHz, $CDCl_3$) δ_C 222.0, 147.2, 139.4, 128.2, 114.0, 63.7, 37.3, 37.1, 34.1, 31.7, 20.5, 19.9.

***ν*$_{max}$ (FTIR)/cm^{-1}:** 2965, 2365, 2160, 1733, 1665, 1402, 1260, 1154, 1098, 1035.

***m/z* (ESI+) HRMS [M+H] $C_{12}H_{16}O^+$:** formula found 177.1250, cald. 177.1235.

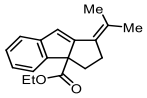

ethyl 1-(propan-2-ylidene)-2,3-dihydrocyclopenta[a]indene-3a(1H)-carboxylate (51): The cyclization of **51s** (0.37 mmol) was performed according to general procedure for carbocyclization and purification by flash column chromatography eluting with hexanes/EtOAc (8:2) provided **51** 84 mg (85%) as a clear oil.

^{1}H NMR (400 MHz; $CDCl_3$) δ_H 7.39 (d, *J* = 7.4 Hz, 1H), 7.27 – 7.21 (m, 2H), 7.13 – 7.01 (m, 1H), 6.58 (s, 1H), 4.12 – 3.98 (m, 2H), 2.83 (d, *J* = 9.2 Hz, 2H), 2.75 (ddd, *J* = 11.8, 4.8, 2.5 Hz, 1H), 2.04 (s, 3H), 1.80 (s, 3H), 1.47 – 1.40 (m, 1H), 1.11 (t, *J* = 7.1 Hz, 3H).

^{13}C NMR (135 MHz, $CDCl_3$) δ_C 172.9, 157.8, 148.4, 144.4, 129.9, 127.8, 127.1, 124.4, 123.1, 123.0, 121.4, 61.1, 35.6, 30.3, 22.4, 22.0, 13.9.

***ν*$_{max}$ (FTIR)/cm^{-1}:** 2977, 2931, 1720, 1456, 1364, 1218, 1149, 1016, 856, 733.

***m/z* (ESI+) HRMS [M+H] $C_{18}H_{20}O_2^+$:** formula found 269.1221, cald. 269.1497.

4.5.6 NMR Spectra

Substrates

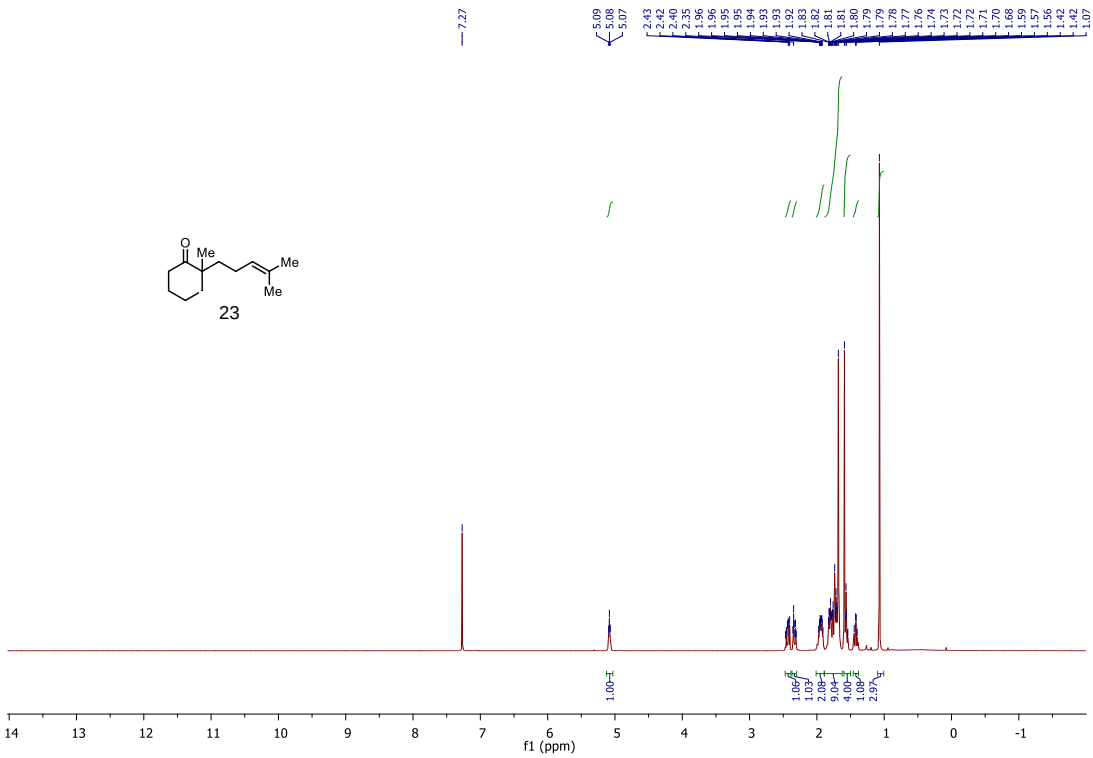

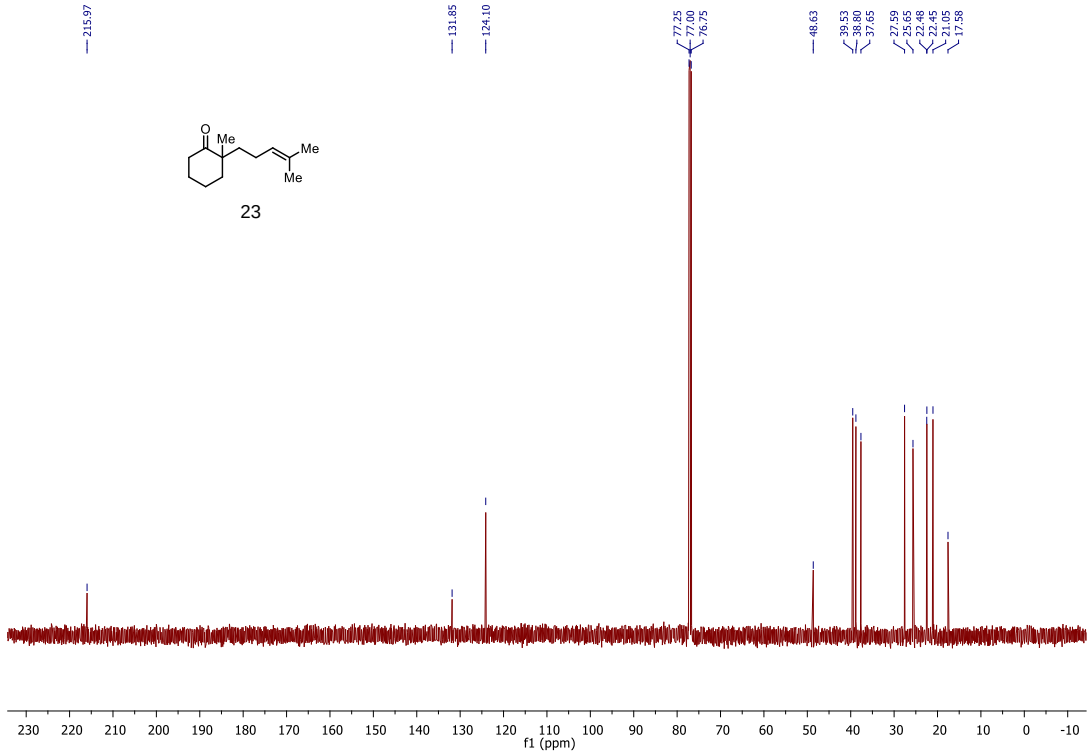

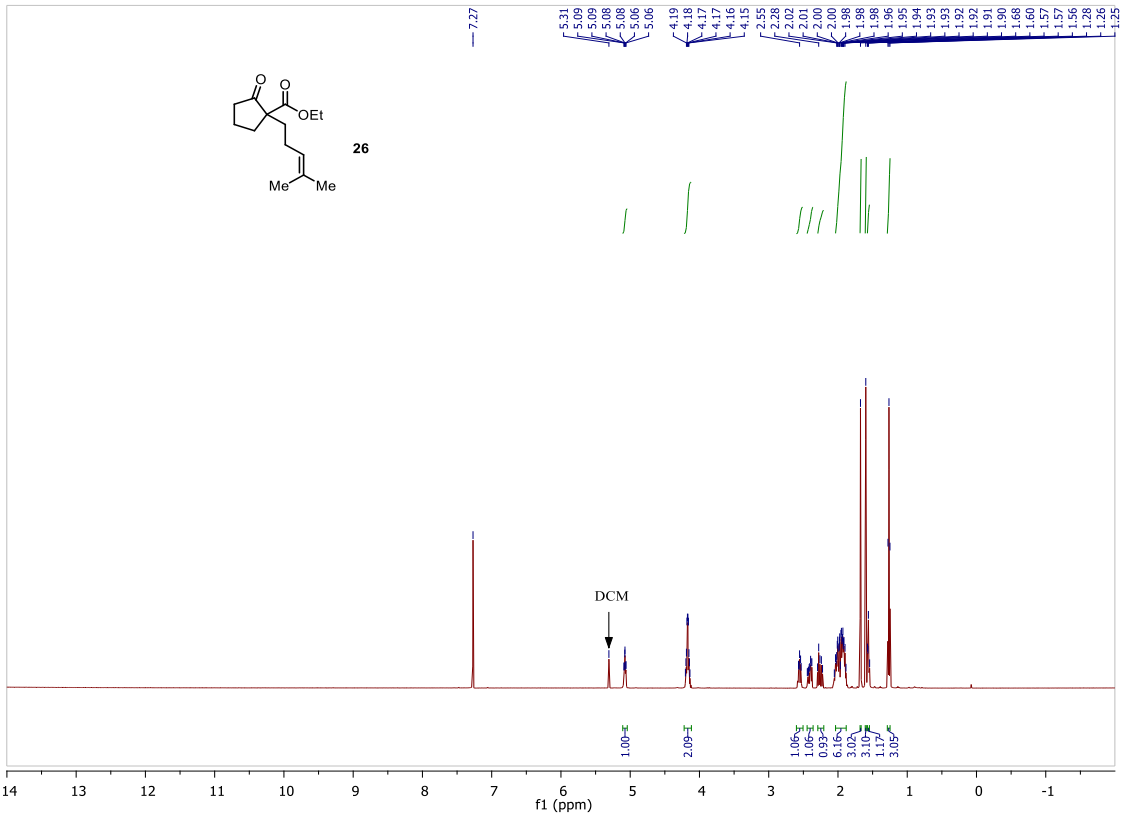
7.27
5.31
5.09
5.09
5.08
5.08
5.06
5.06
4.19
4.18
4.17
4.17
4.16
4.15
2.55
2.28
2.02
2.01
2.00
2.00
1.98
1.98
1.98
1.96
1.95
1.94
1.93
1.93
1.92
1.92
1.91
1.90
1.68
1.60
1.57
1.57
1.56
1.28
1.26
1.25
O
O
OEt
Me
Me
26
DCM
1.00
2.09
1.06
1.06
0.93
6.16
3.02
3.10
1.17
3.05
14
13
12
11
10
9
8
7
6
5
4
3
2
1
0
-1
f1 (ppm)

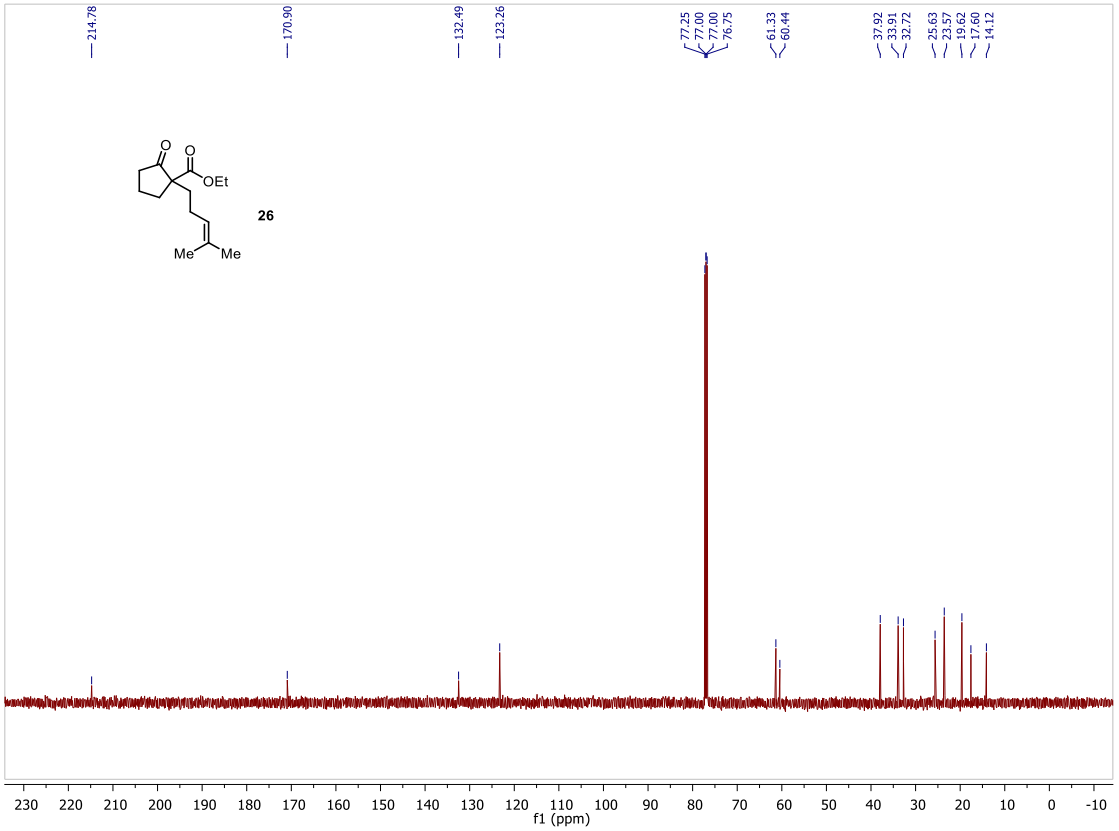
214.78
170.90
132.49
123.26
77.25
77.00
77.00
76.75
61.33
60.44
37.92
33.91
32.72
25.63
23.57
19.62
17.60
14.12
O
O
OEt
Me
Me
26
230
220
210
200
190
180
170
160
150
140
130
120
110
100
90
80
70
60
50
40
30
20
10
0
-10
f1 (ppm)

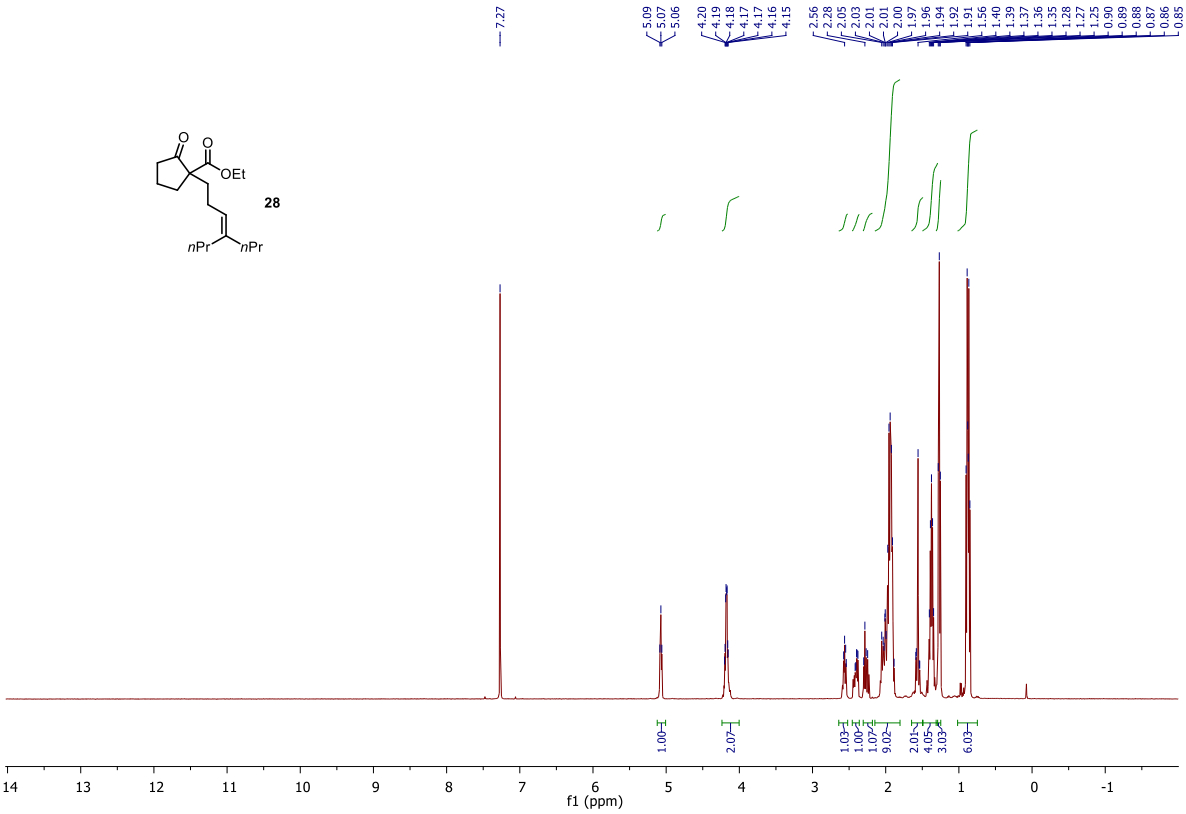
7.27
5.09
5.07
5.06
4.20
4.19
4.18
4.17
4.17
4.16
4.15
2.56
2.28
2.05
2.03
2.01
2.01
2.00
1.97
1.96
1.94
1.92
1.91
1.56
1.40
1.39
1.37
1.36
1.35
1.28
1.27
1.25
0.90
0.89
0.88
0.87
0.86
0.85
O
O
OEt
28
nPr
nPr
1.00
2.07
1.03
1.00
1.07
9.02
2.01
4.05
3.03
6.03
14
13
12
11
10
9
8
7
6
5
4
3
2
1
0
-1
f1 (ppm)

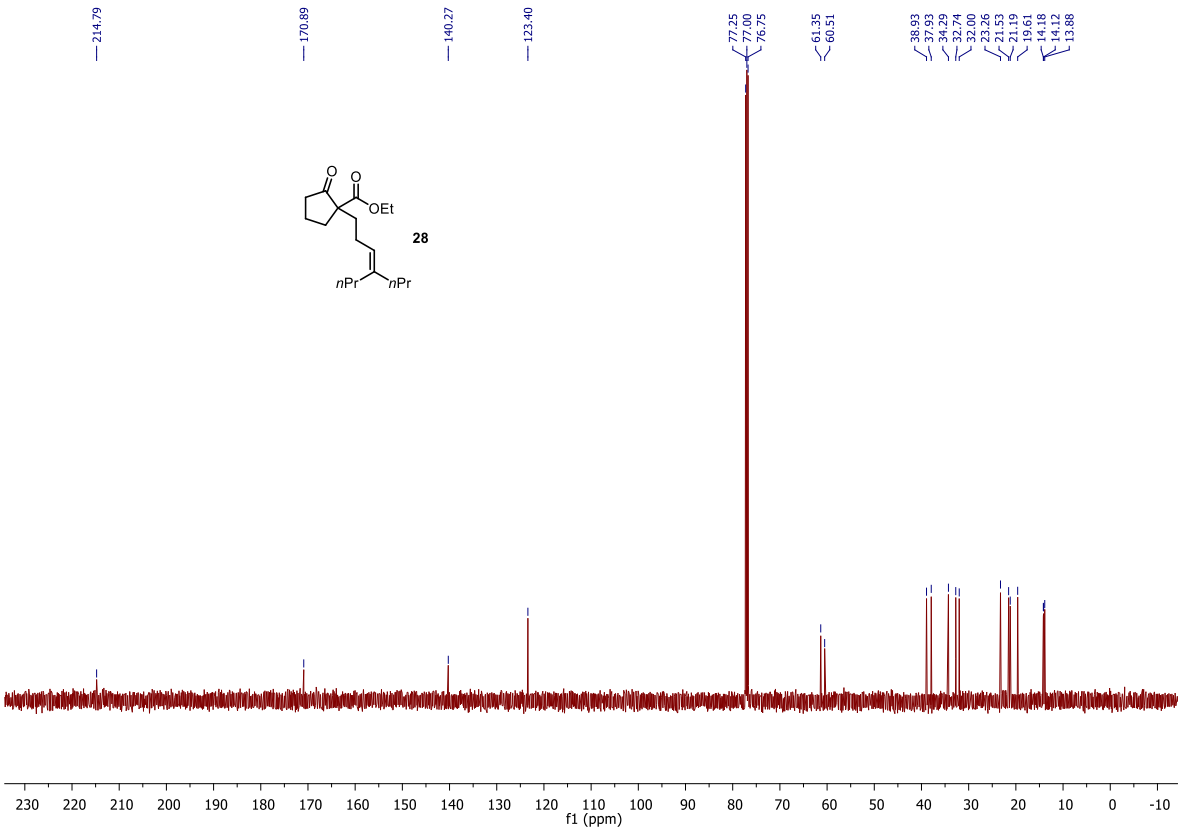
214.79
170.89
140.27
123.40
77.25
77.00
76.75
61.35
60.51
38.93
37.93
34.29
32.74
32.00
23.26
21.53
21.19
19.61
14.18
14.12
13.88
O
O
OEt
28
nPr
nPr
230
220
210
200
190
180
170
160
150
140
130
120
110
100
90
80
70
60
50
40
30
20
10
0
-10
f1 (ppm)

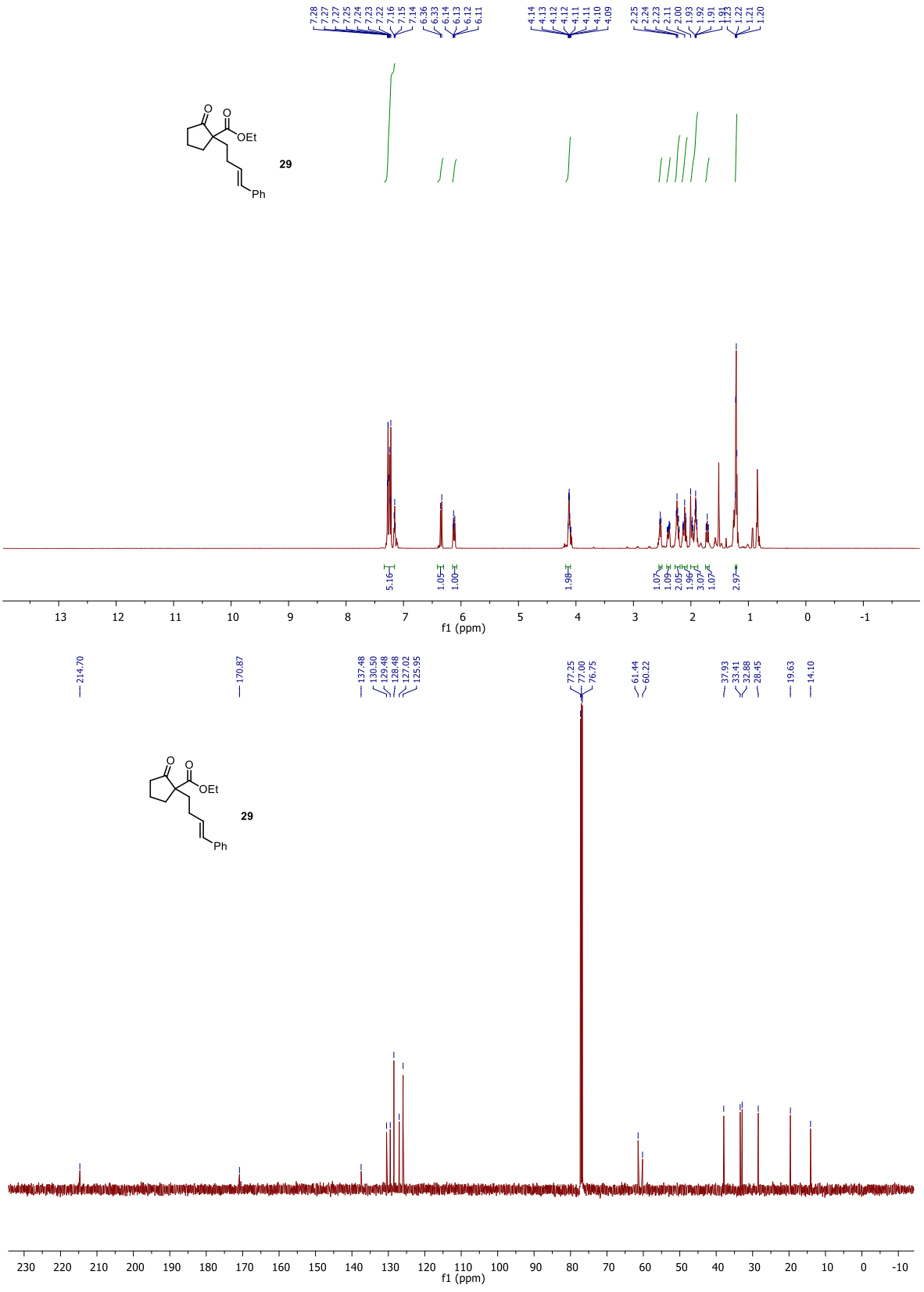
7.28
7.27
7.27
7.25
7.24
7.23
7.22
7.16
7.15
7.14
6.36
6.33
6.14
6.13
6.12
6.11
4.14
4.13
4.12
4.12
4.11
4.11
4.10
4.09
2.25
2.24
2.23
2.11
2.00
1.93
1.92
1.91
1.22
1.21
1.20
O
O
OEt
Ph
29
5.16
1.05
1.00
1.98
1.07
1.09
2.05
1.96
3.07
1.07
2.97
13
12
11
10
9
8
7
6
5
4
3
2
1
0
-1
f1 (ppm)
214.70
170.87
137.48
130.50
129.48
128.48
127.02
125.95
77.25
77.00
76.75
61.44
60.22
37.93
33.41
32.88
28.45
19.63
14.10
O
O
OEt
Ph
29
230
220
210
200
190
180
170
160
150
140
130
120
110
100
90
80
70
60
50
40
30
20
10
0
-10
f1 (ppm)

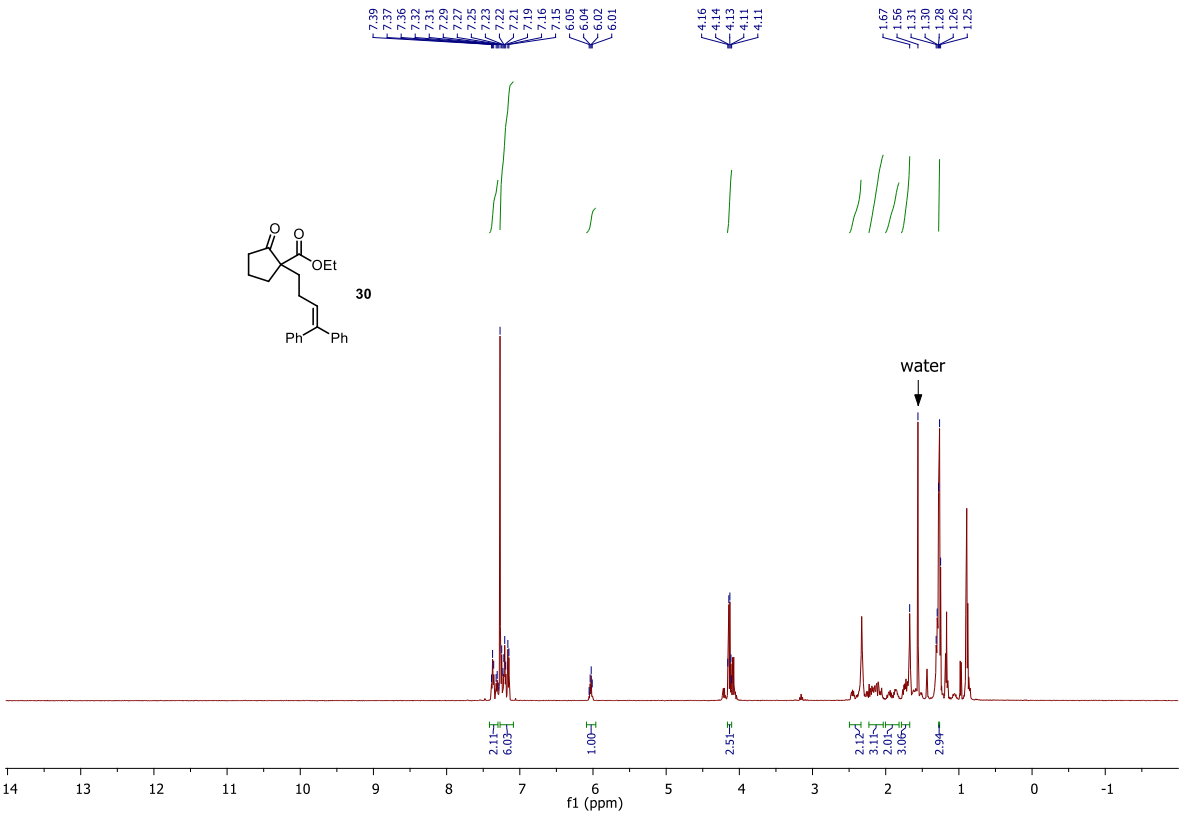
7.39
7.37
7.36
7.32
7.31
7.29
7.27
7.25
7.23
7.22
7.21
7.19
7.16
7.15
6.05
6.04
6.02
6.01
4.16
4.14
4.13
4.11
4.11
1.67
1.56
1.31
1.30
1.28
1.26
1.25
O
O
OEt
30
Ph
Ph
water
2.11
6.03
1.00
2.51
2.12
3.11
2.01
3.06
2.94
14
13
12
11
10
9
8
7
6
5
4
3
2
1
0
-1
f1 (ppm)

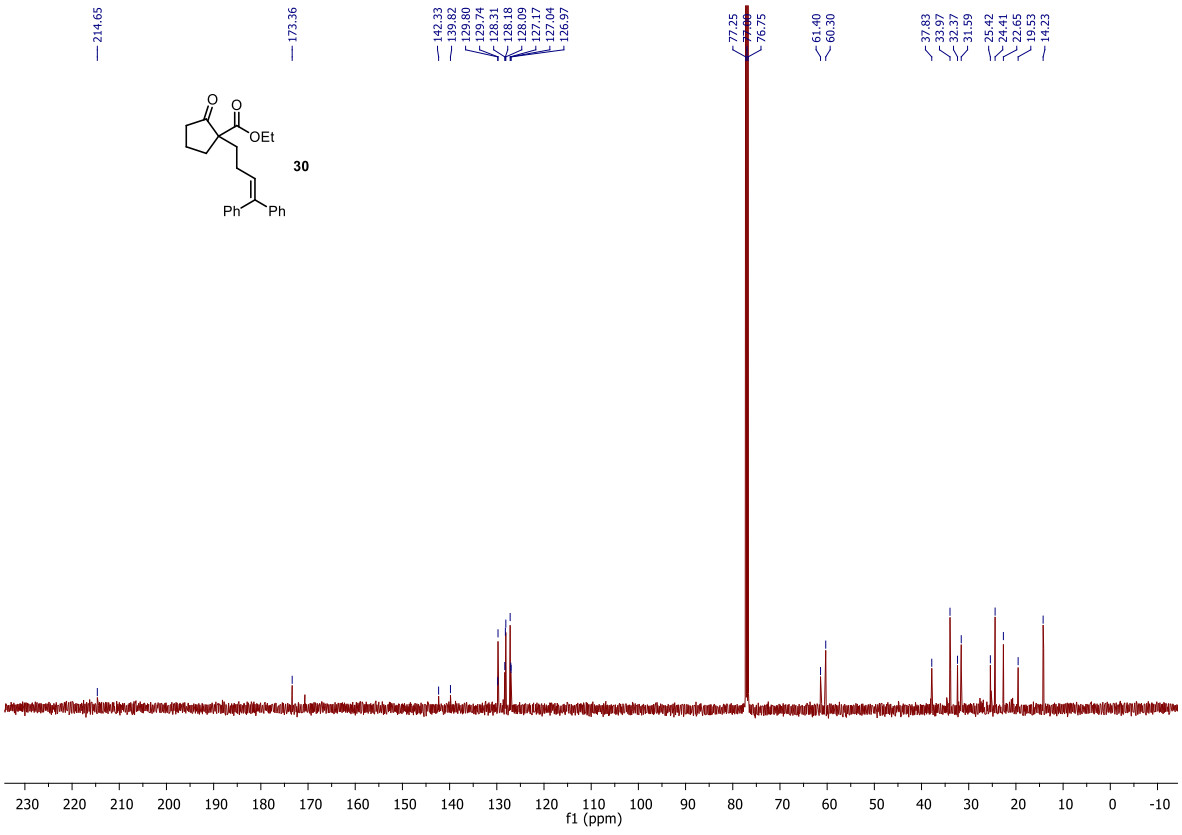
214.65
173.36
142.33
139.82
129.80
129.74
128.31
128.18
128.09
127.17
127.04
126.97
77.25
77.00
76.75
61.40
60.30
37.83
33.97
32.37
31.59
25.42
24.41
22.65
19.53
14.23
O
O
OEt
30
Ph
Ph
230
220
210
200
190
180
170
160
150
140
130
120
110
100
90
80
70
60
50
40
30
20
10
0
-10
f1 (ppm)

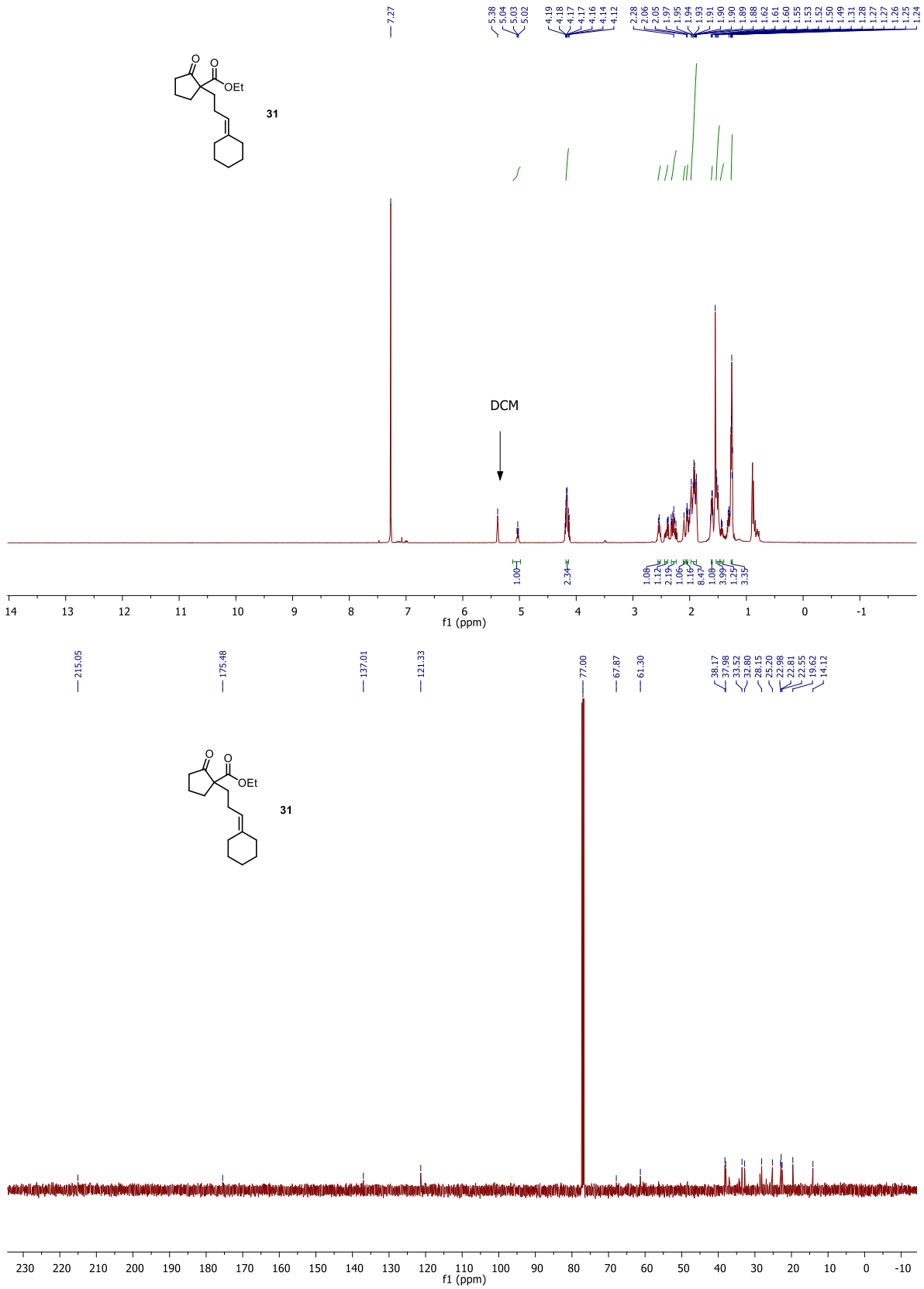
7.27
5.38
5.04
5.03
5.02
4.19
4.18
4.17
4.17
4.16
4.14
4.12
2.28
2.06
2.05
1.97
1.95
1.94
1.93
1.91
1.90
1.90
1.89
1.88
1.62
1.61
1.60
1.55
1.53
1.52
1.50
1.49
1.31
1.28
1.27
1.27
1.26
1.25
1.24
OEt
31
DCM
1.00
2.34
1.08
1.12
2.15
1.06
1.16
8.47
1.08
3.99
1.25
3.35
f1 (ppm)
215.05
175.48
137.01
121.33
77.00
67.87
61.30
38.17
37.98
33.52
32.80
28.15
25.20
22.98
22.81
22.55
19.62
14.12
OEt
31
f1 (ppm)

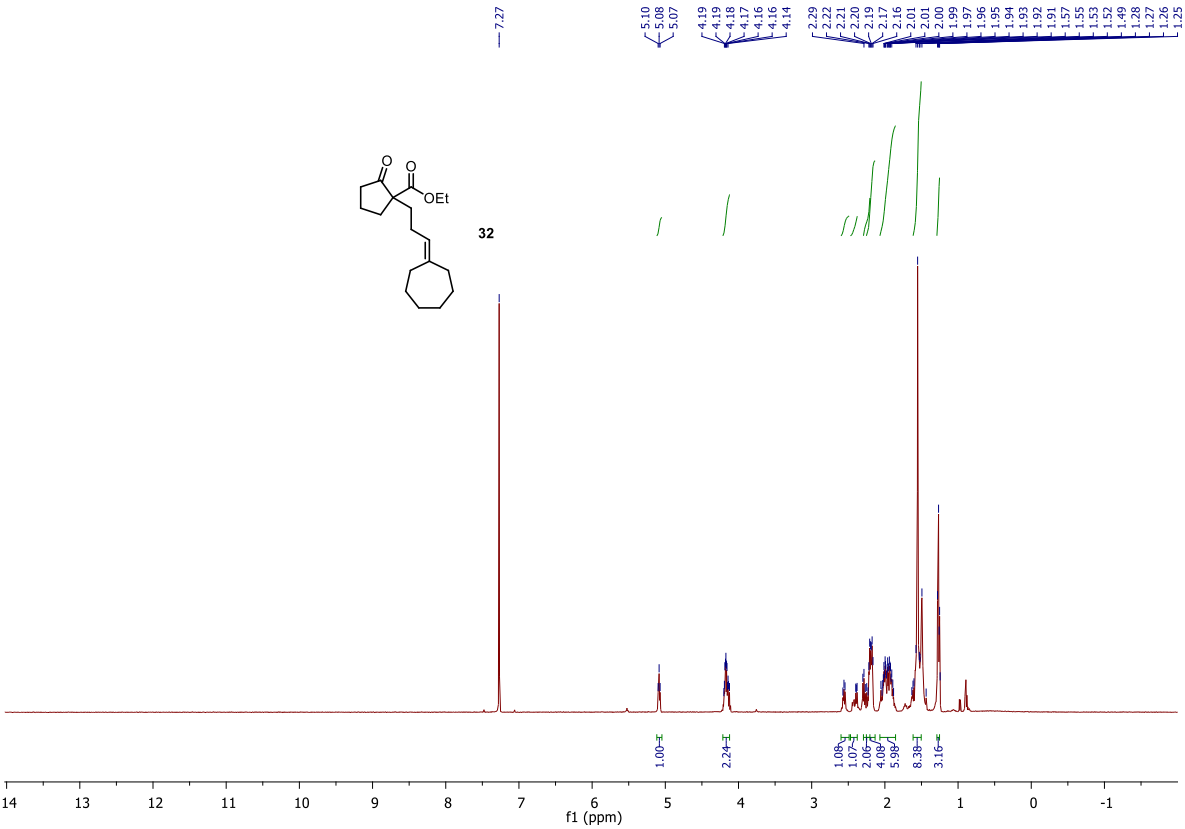
7.27
5.10
5.08
5.07
4.19
4.19
4.18
4.17
4.16
4.16
4.14
2.29
2.22
2.21
2.20
2.19
2.17
2.16
2.01
2.01
2.00
1.99
1.97
1.96
1.95
1.94
1.93
1.92
1.91
1.57
1.55
1.53
1.52
1.49
1.28
1.27
1.26
1.25
O
O
OEt
32
1.00
2.24
1.08
1.07
2.06
4.08
5.98
8.38
3.16
14
13
12
11
10
9
8
7
6
5
4
3
2
1
0
-1
f1 (ppm)

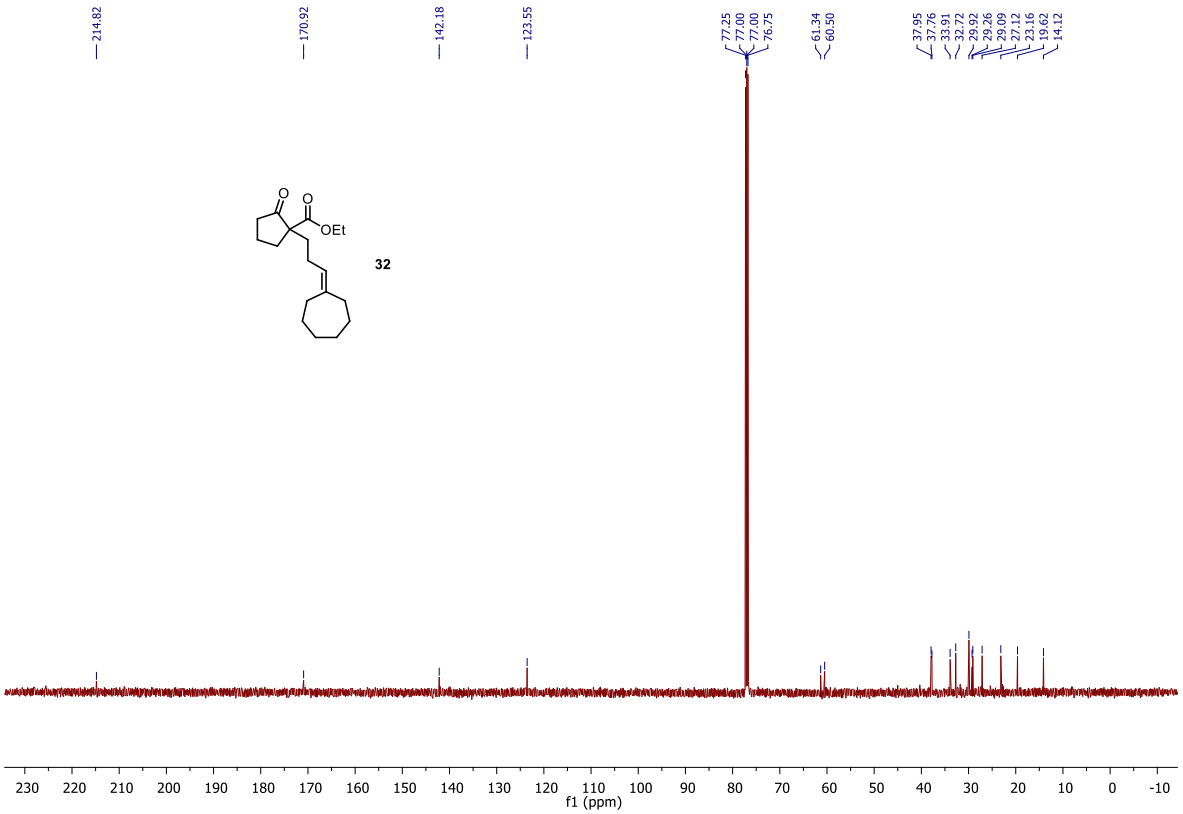
214.82
170.92
142.18
123.55
77.25
77.00
77.00
76.75
61.34
60.50
37.95
37.76
33.91
32.72
29.92
29.26
29.09
27.12
23.16
19.62
14.12
O
O
OEt
32
230
220
210
200
190
180
170
160
150
140
130
120
110
100
90
80
70
60
50
40
30
20
10
0
-10
f1 (ppm)

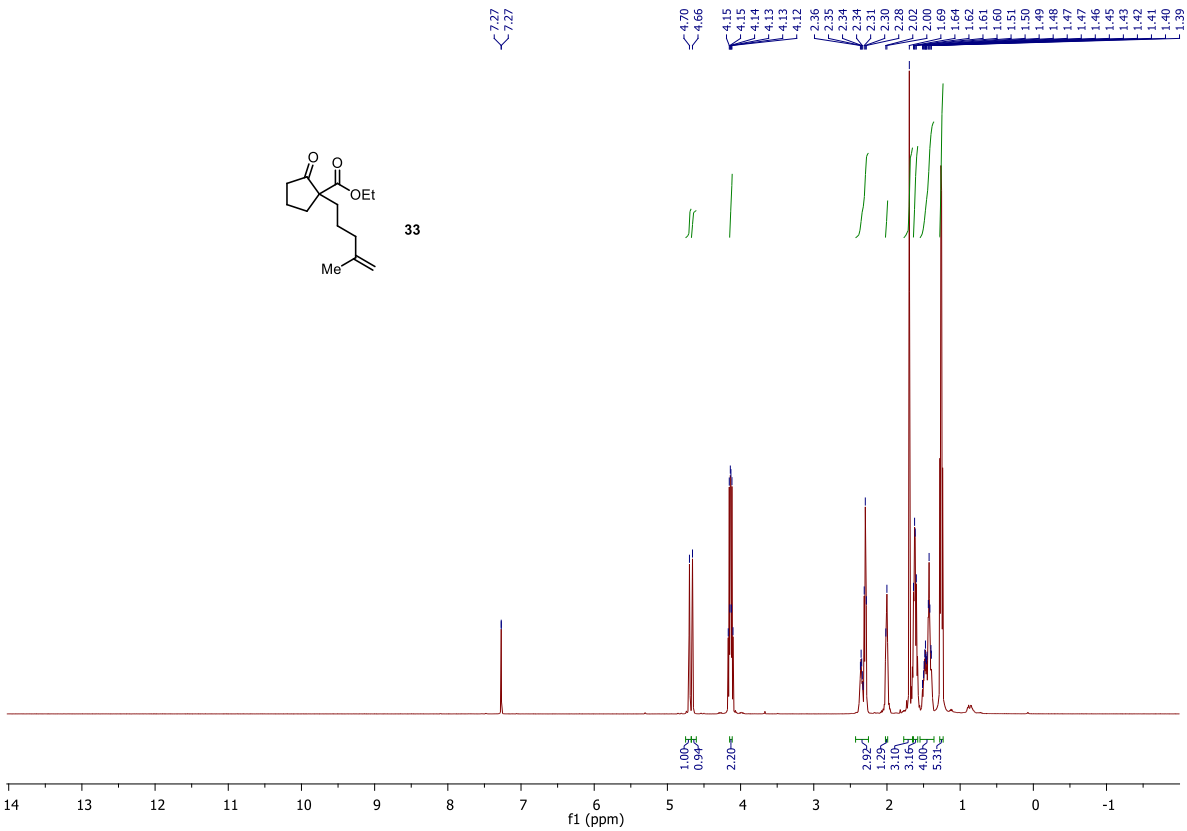
7.27
7.27
4.70
4.66
4.15
4.15
4.14
4.13
4.13
4.12
2.36
2.35
2.34
2.34
2.31
2.30
2.28
2.02
2.00
1.69
1.64
1.62
1.61
1.60
1.51
1.50
1.49
1.48
1.47
1.47
1.46
1.45
1.43
1.42
1.41
1.40
1.39
O
O
OEt
Me
33
1.00
0.94
2.20
2.92
1.29
3.10
3.16
4.06
5.31
14
13
12
11
10
9
8
7
6
5
4
3
2
1
0
-1
f1 (ppm)

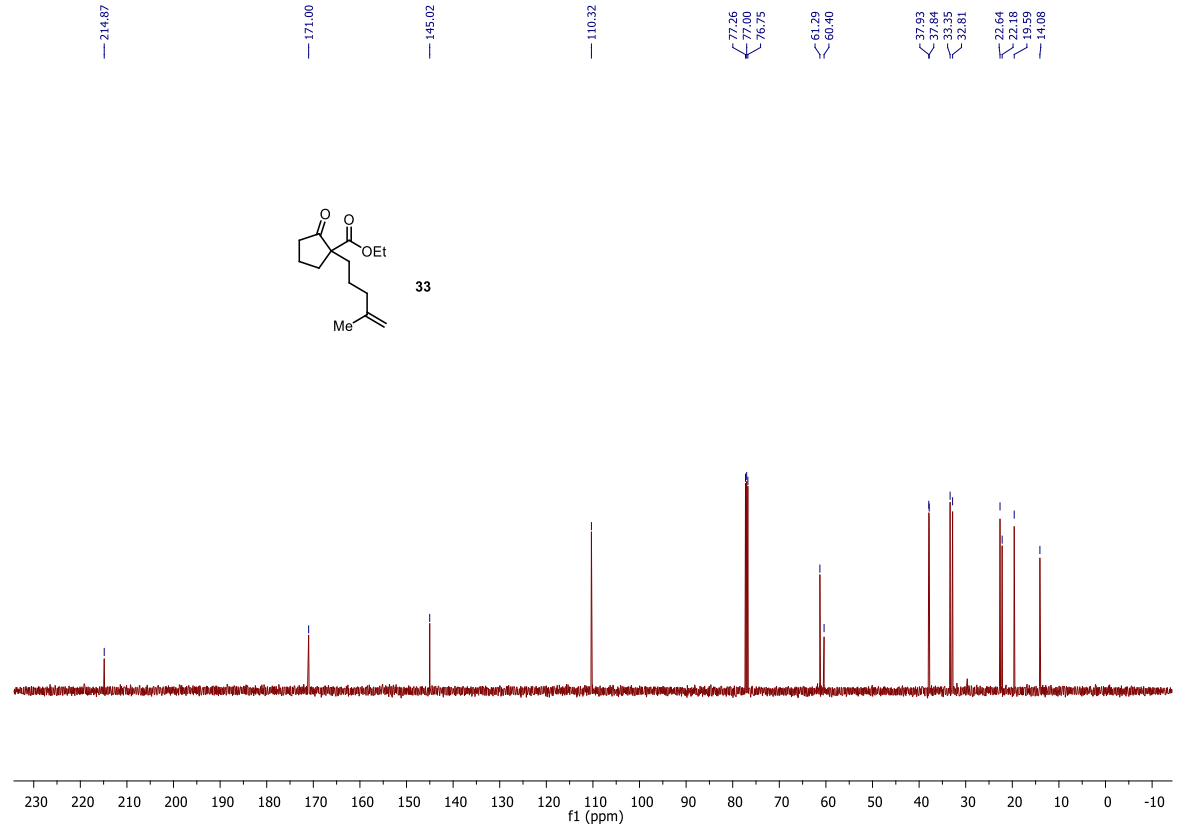
214.87
171.00
145.02
110.32
77.26
77.00
76.75
61.29
60.40
37.93
37.84
33.35
32.81
22.64
22.18
19.59
14.08
O
O
OEt
Me
33
230
220
210
200
190
180
170
160
150
140
130
120
110
100
90
80
70
60
50
40
30
20
10
0
-10
f1 (ppm)

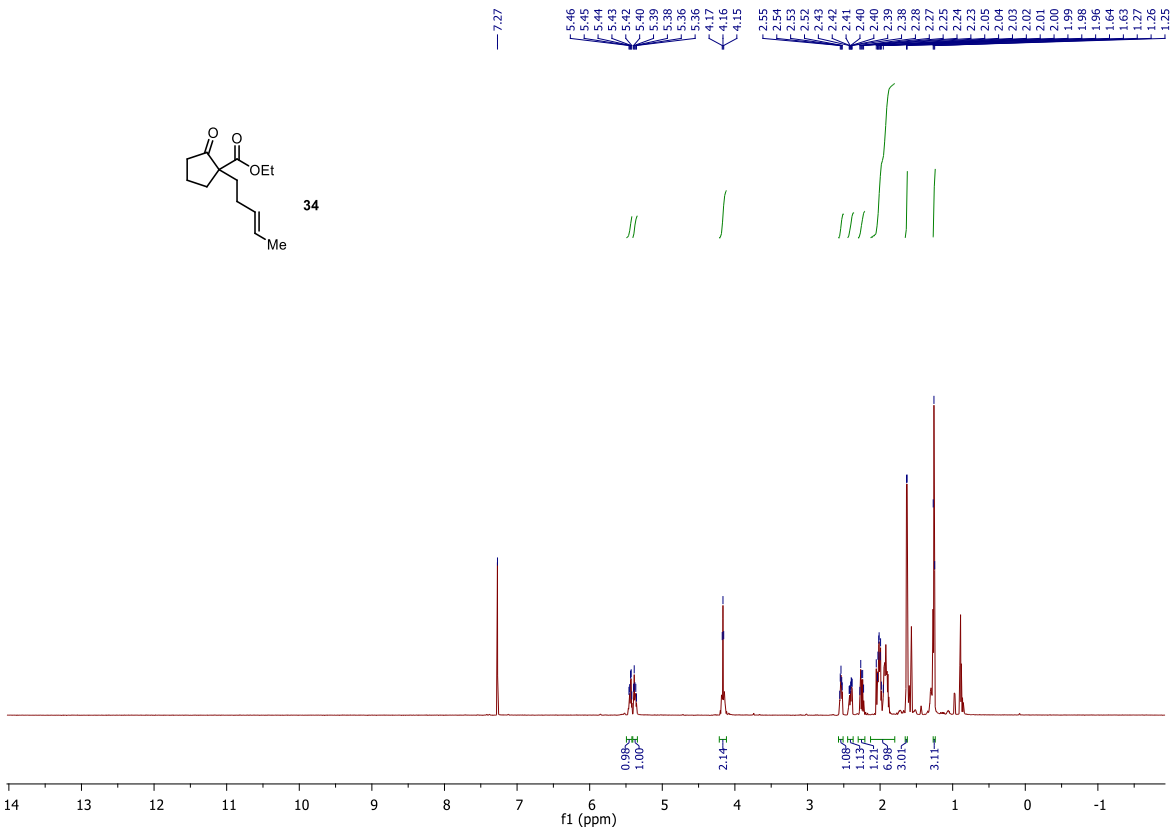
7.27
5.46 5.45 5.44 5.43 5.42 5.40 5.39 5.38 5.36 5.36
4.17 4.16 4.15
2.55 2.54 2.53 2.52 2.43 2.42 2.41 2.40 2.40 2.39 2.38 2.28 2.27 2.25 2.24 2.23 2.05 2.04 2.03 2.02 2.01 2.00 1.99 1.98 1.96 1.64 1.63 1.27 1.26 1.25
O
O
OEt
Me
34
0.98
1.00
2.14
1.08
1.13
1.21
6.98
3.01
3.11
14 13 12 11 10 9 8 7 6 5 4 3 2 1 0 -1
f1 (ppm)

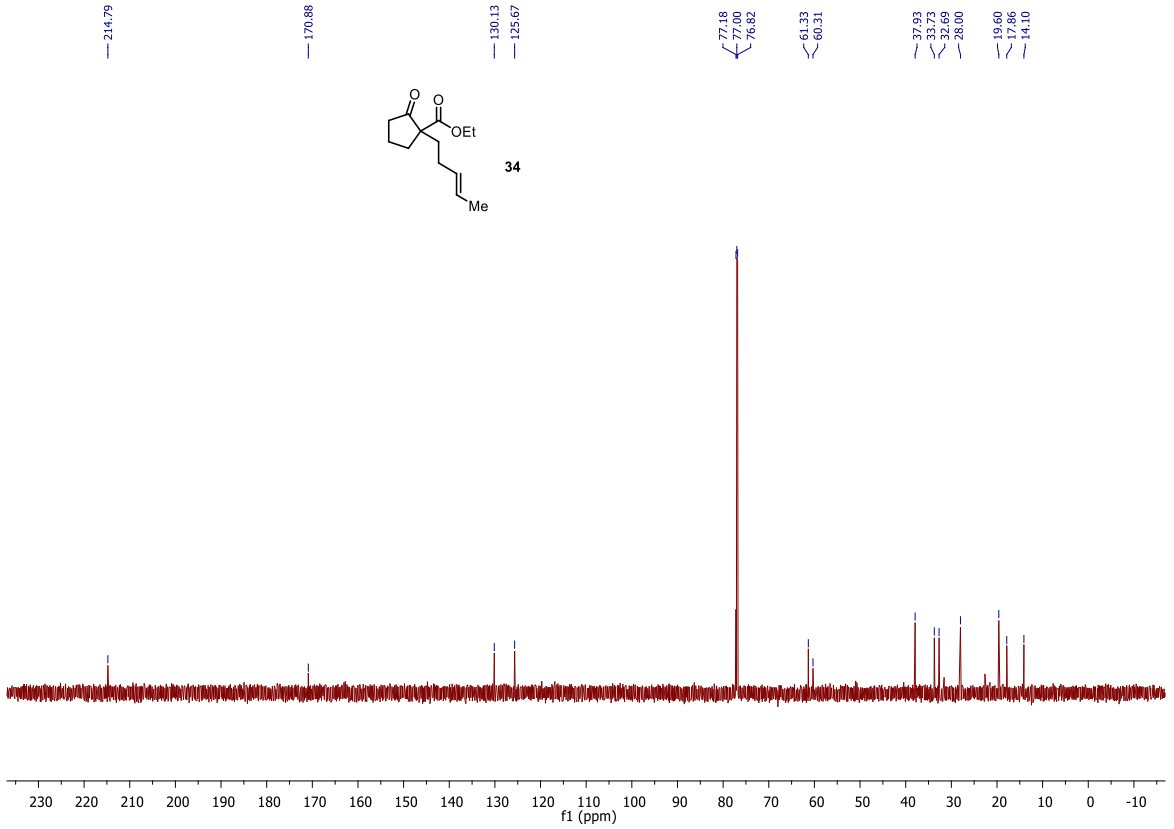
214.79
170.88
130.13
125.67
77.18
77.00
76.82
61.33
60.31
37.93
33.73
32.69
28.00
19.60
17.86
14.10
O
O
OEt
Me
34
230 220 210 200 190 180 170 160 150 140 130 120 110 100 90 80 70 60 50 40 30 20 10 0 -10
f1 (ppm)

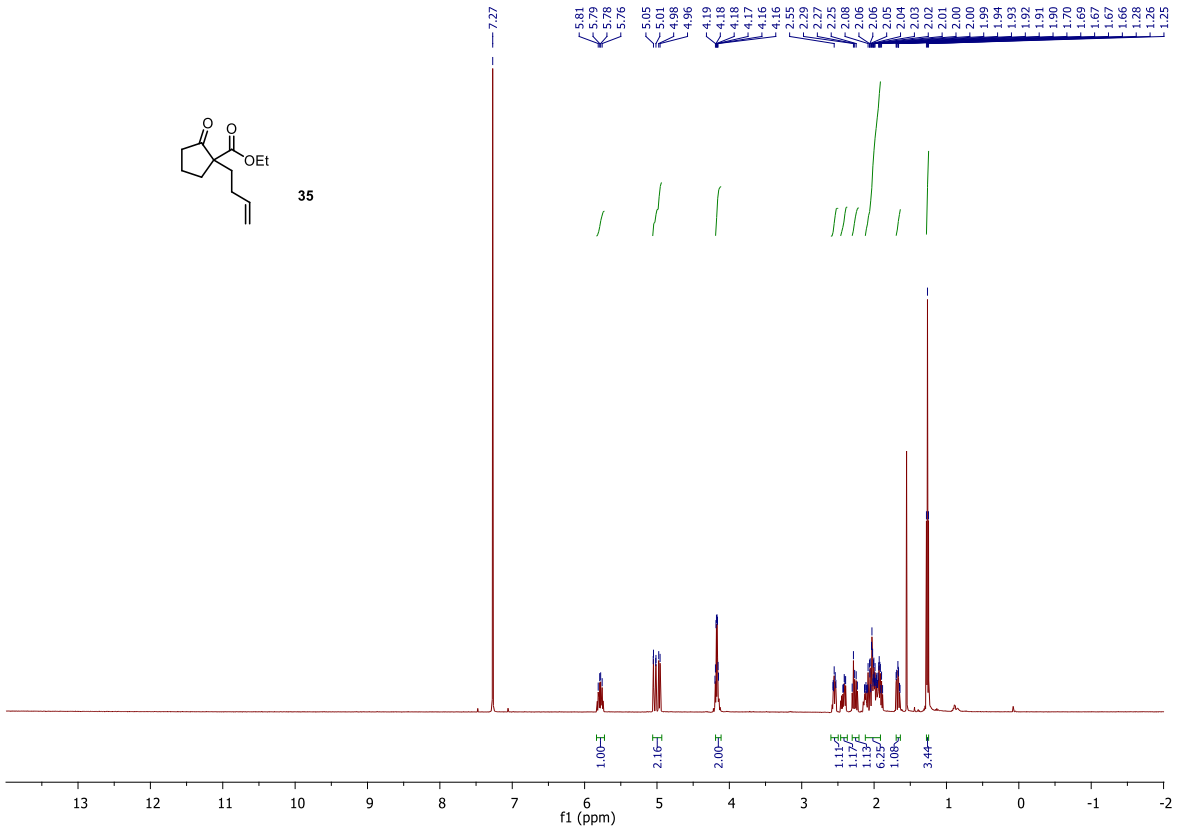
35
7.27
5.81
5.79
5.78
5.76
5.05
5.01
4.98
4.96
4.19
4.18
4.17
4.16
2.55
2.29
2.27
2.25
2.08
2.06
2.06
2.05
2.04
2.03
2.02
2.01
2.00
2.00
1.99
1.94
1.93
1.92
1.91
1.90
1.70
1.69
1.67
1.67
1.66
1.28
1.26
1.25
1.00
2.16
2.00
1.11
1.17
1.13
6.25
1.08
3.44
f1 (ppm)

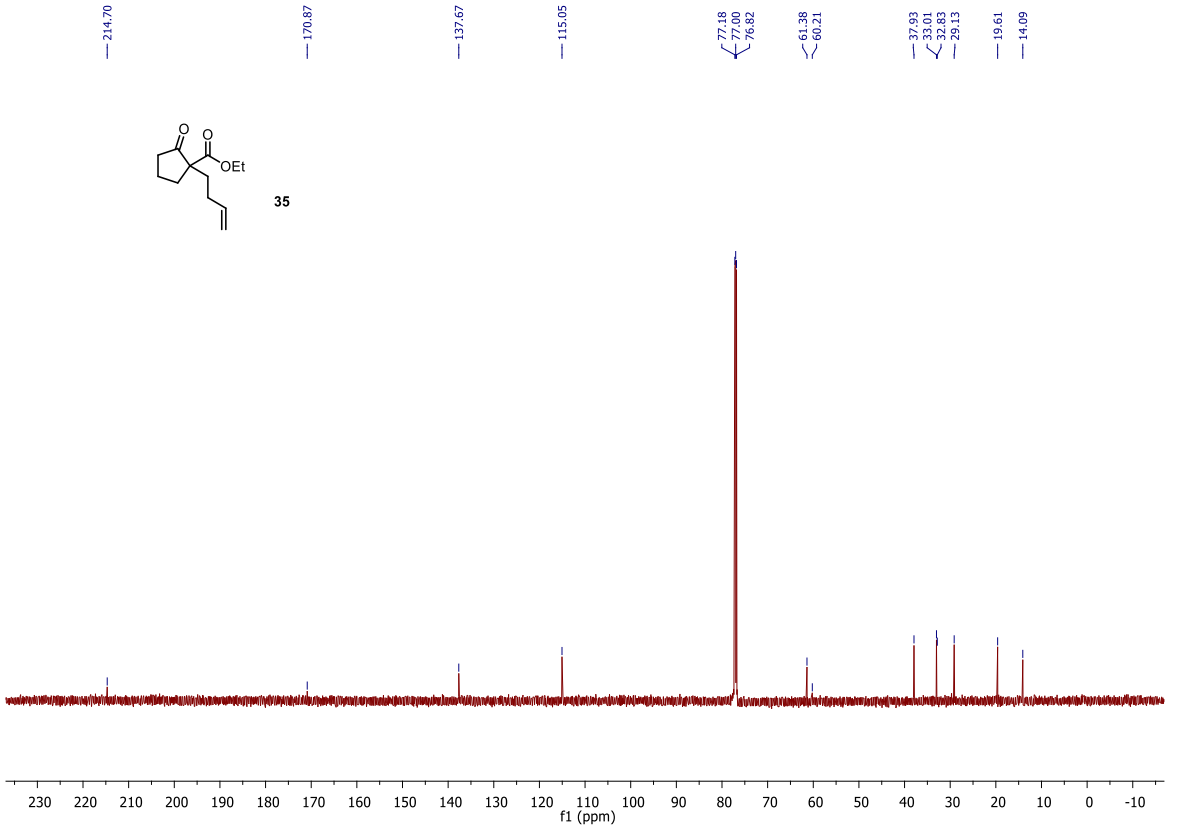
214.70
170.87
137.67
115.05
77.18
77.00
76.82
61.38
60.21
37.93
33.01
32.83
29.13
19.61
14.09
35
f1 (ppm)

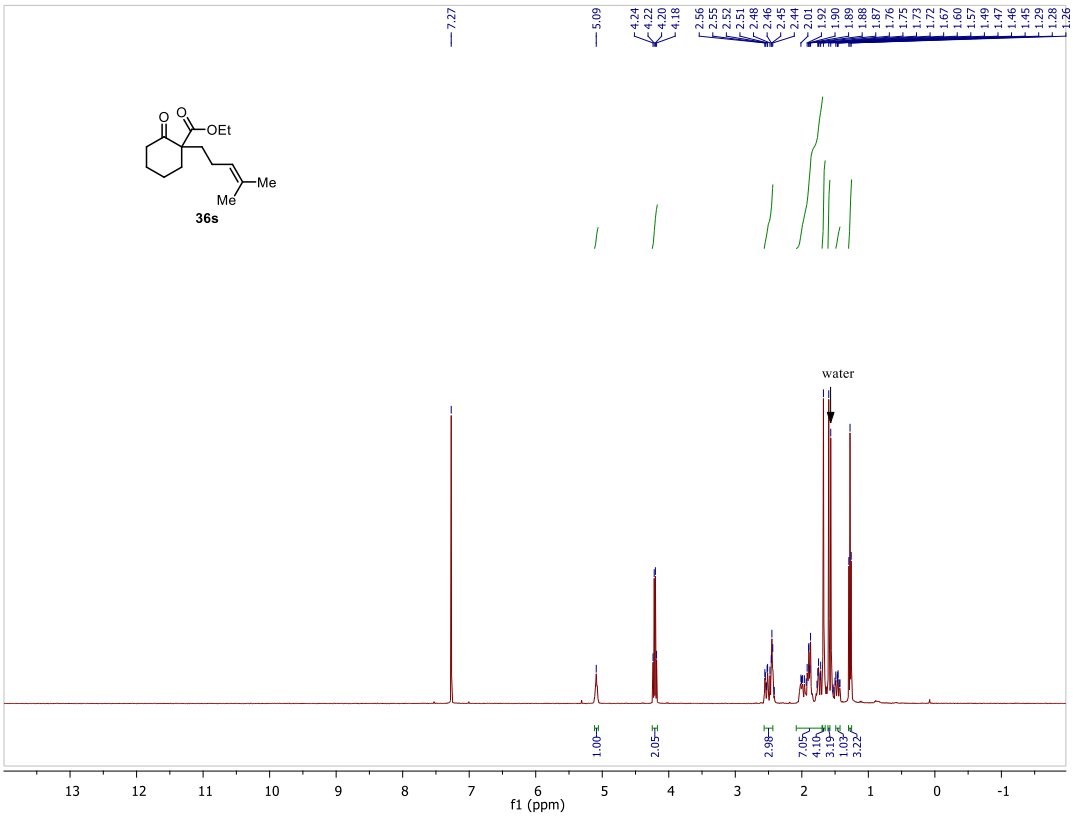
7.27
5.09
4.24
4.22
4.20
4.18
2.56
2.55
2.52
2.51
2.48
2.46
2.45
2.44
2.01
1.92
1.90
1.89
1.88
1.87
1.76
1.75
1.73
1.72
1.67
1.60
1.57
1.49
1.47
1.46
1.45
1.29
1.28
1.26
O
O
OEt
Me
Me
36s
water
1.00
2.05
2.98
7.05
4.10
3.19
1.03
3.22
13
12
11
10
9
8
7
6
5
4
3
2
1
0
-1
f1 (ppm)

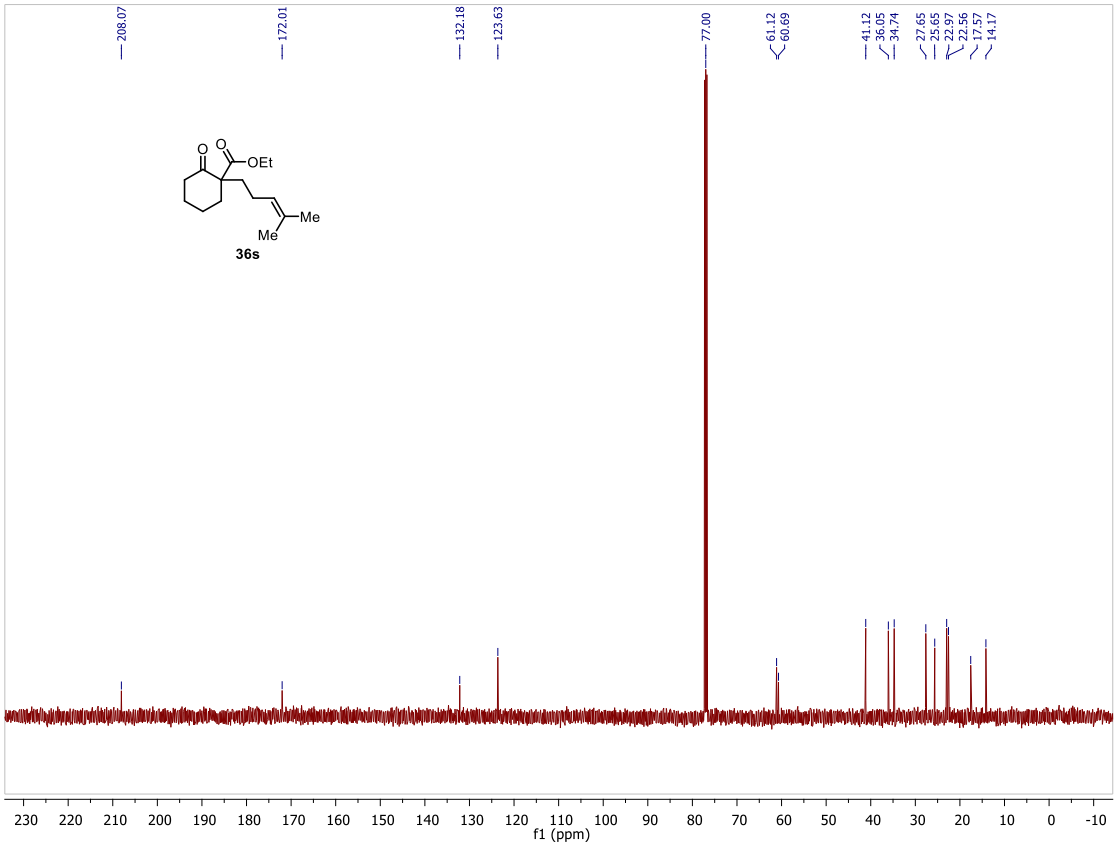
208.07
172.01
132.18
123.63
77.00
61.12
60.69
41.12
36.05
34.74
27.65
25.65
22.97
22.56
17.57
14.17
O
O
OEt
Me
Me
36s
230
220
210
200
190
180
170
160
150
140
130
120
110
100
90
80
70
60
50
40
30
20
10
0
-10
f1 (ppm)

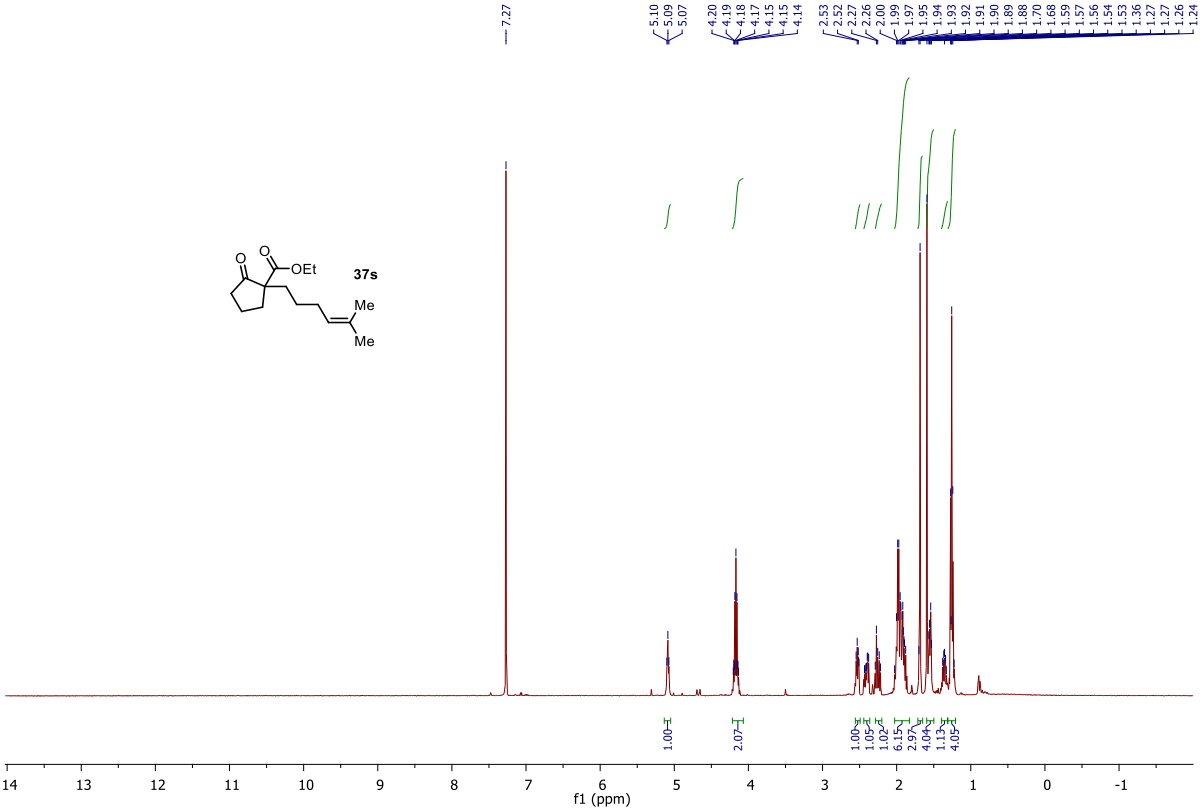
7.27
5.10
5.09
5.07
4.20
4.19
4.18
4.17
4.15
4.15
4.14
2.53
2.52
2.27
2.26
2.00
1.99
1.97
1.95
1.94
1.93
1.92
1.91
1.90
1.89
1.88
1.70
1.68
1.59
1.57
1.56
1.54
1.53
1.36
1.27
1.27
1.26
1.24
O
O
OEt
37s
Me
Me
1.00
2.07
1.00
1.05
1.02
6.15
2.97
4.04
1.13
4.05
14
13
12
11
10
9
8
7
6
5
4
3
2
1
0
-1
f1 (ppm)

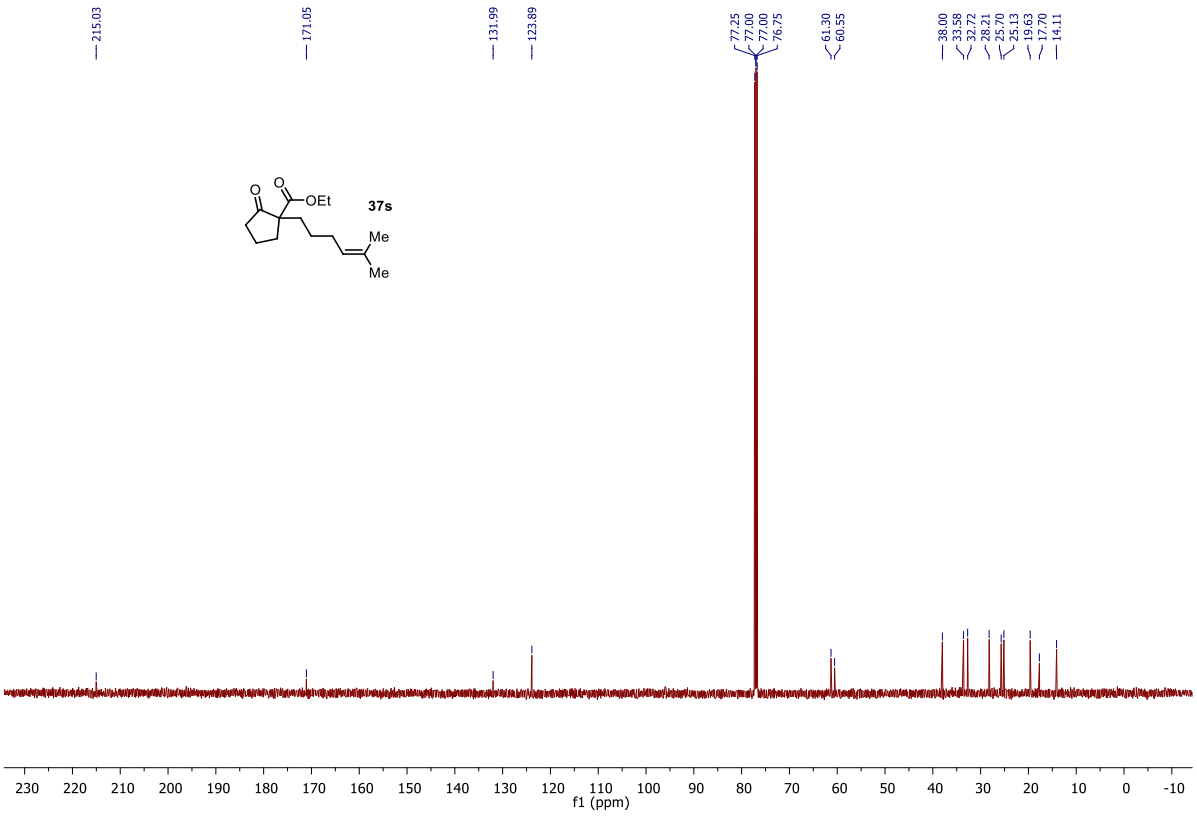
215.03
171.05
131.99
123.89
77.25
77.00
77.00
76.75
61.30
60.55
38.00
33.58
32.72
28.21
25.70
25.13
19.63
17.70
14.11
O
O
OEt
37s
Me
Me
230
220
210
200
190
180
170
160
150
140
130
120
110
100
90
80
70
60
50
40
30
20
10
0
-10
f1 (ppm)

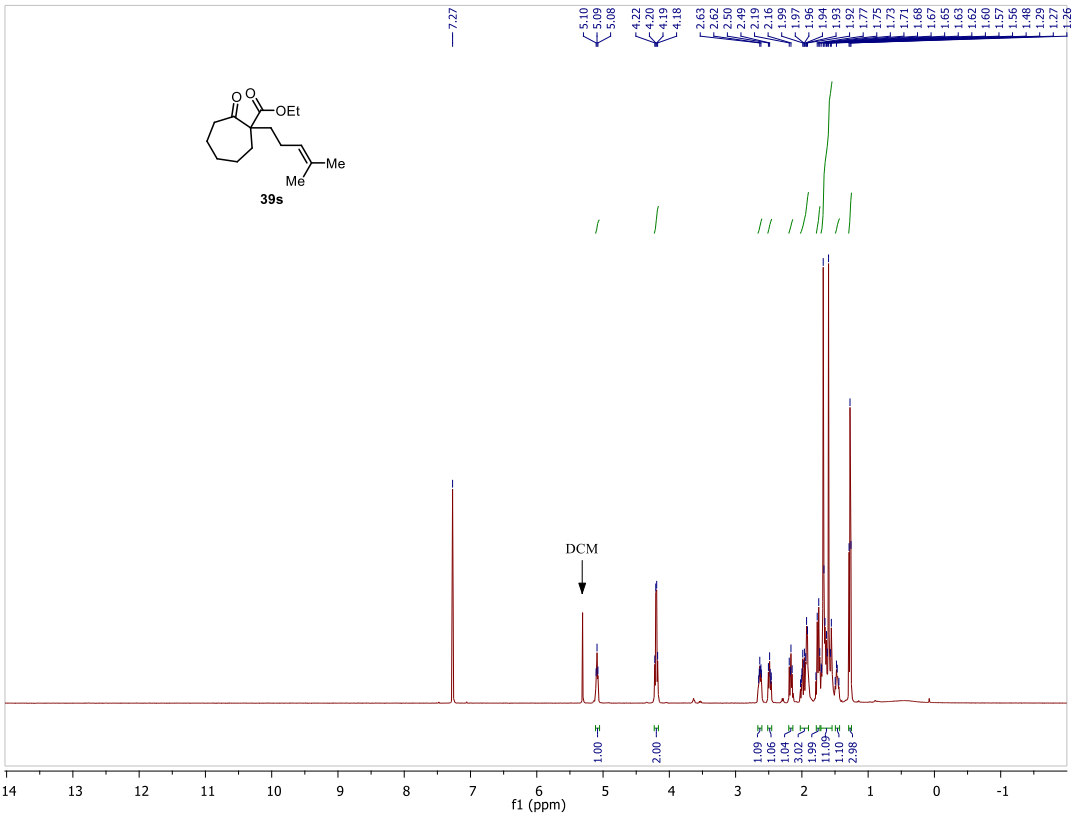
7.27
5.10
5.09
5.08
4.22
4.20
4.19
4.18
2.63
2.62
2.50
2.49
2.19
2.16
1.99
1.97
1.96
1.94
1.93
1.92
1.77
1.75
1.73
1.71
1.68
1.67
1.65
1.63
1.62
1.60
1.57
1.56
1.48
1.29
1.27
1.26
O
O
OEt
Me
Me
39s
DCM
1.00
2.00
1.09
1.06
1.04
3.02
1.99
1.94
1.10
2.98
14
13
12
11
10
9
8
7
6
5
4
3
2
1
0
-1
f1 (ppm)

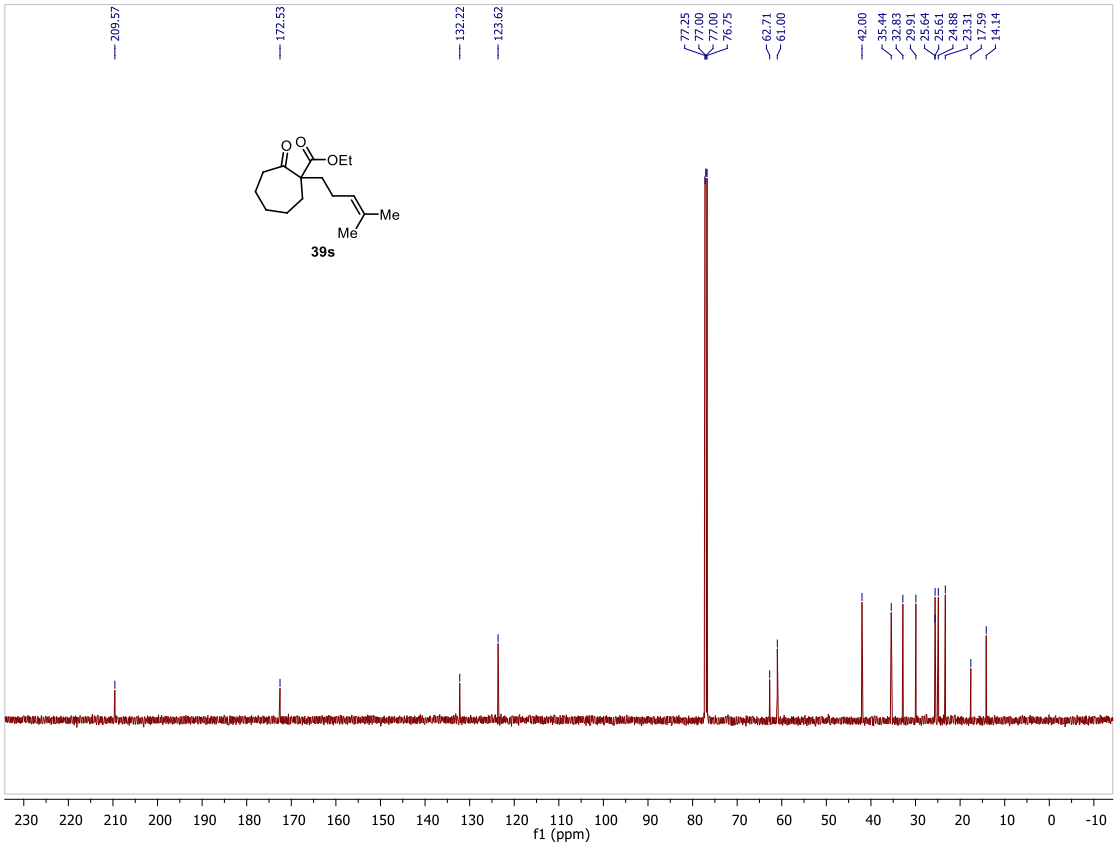
209.57
172.53
132.22
123.62
77.25
77.00
77.00
76.75
62.71
61.00
42.00
35.44
32.83
29.91
25.64
25.61
24.88
23.31
17.59
14.14
O
O
OEt
Me
Me
39s
230
220
210
200
190
180
170
160
150
140
130
120
110
100
90
80
70
60
50
40
30
20
10
0
-10
f1 (ppm)

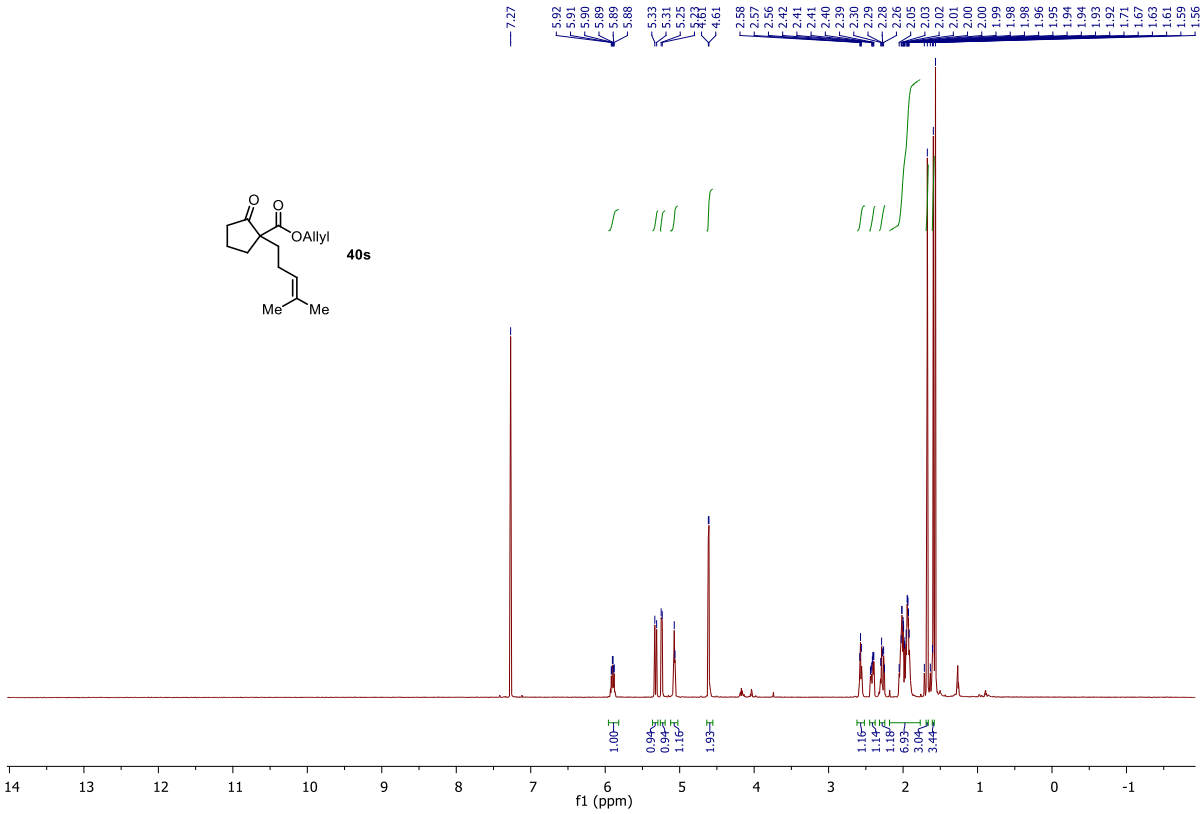
7.27
5.92
5.91
5.90
5.89
5.89
5.88
5.33
5.31
5.25
5.23
4.61
2.58
2.57
2.56
2.42
2.41
2.41
2.40
2.39
2.30
2.29
2.28
2.26
2.05
2.03
2.02
2.01
2.00
2.00
1.99
1.98
1.98
1.96
1.95
1.94
1.94
1.93
1.92
1.71
1.67
1.63
1.61
1.59
1.56
O
O
OAllyl
Me
Me
40s
1.00
0.94
0.94
1.16
1.93
1.16
1.14
1.18
6.93
3.04
3.44
14
13
12
11
10
9
8
7
6
5
4
3
2
1
0
-1
f1 (ppm)

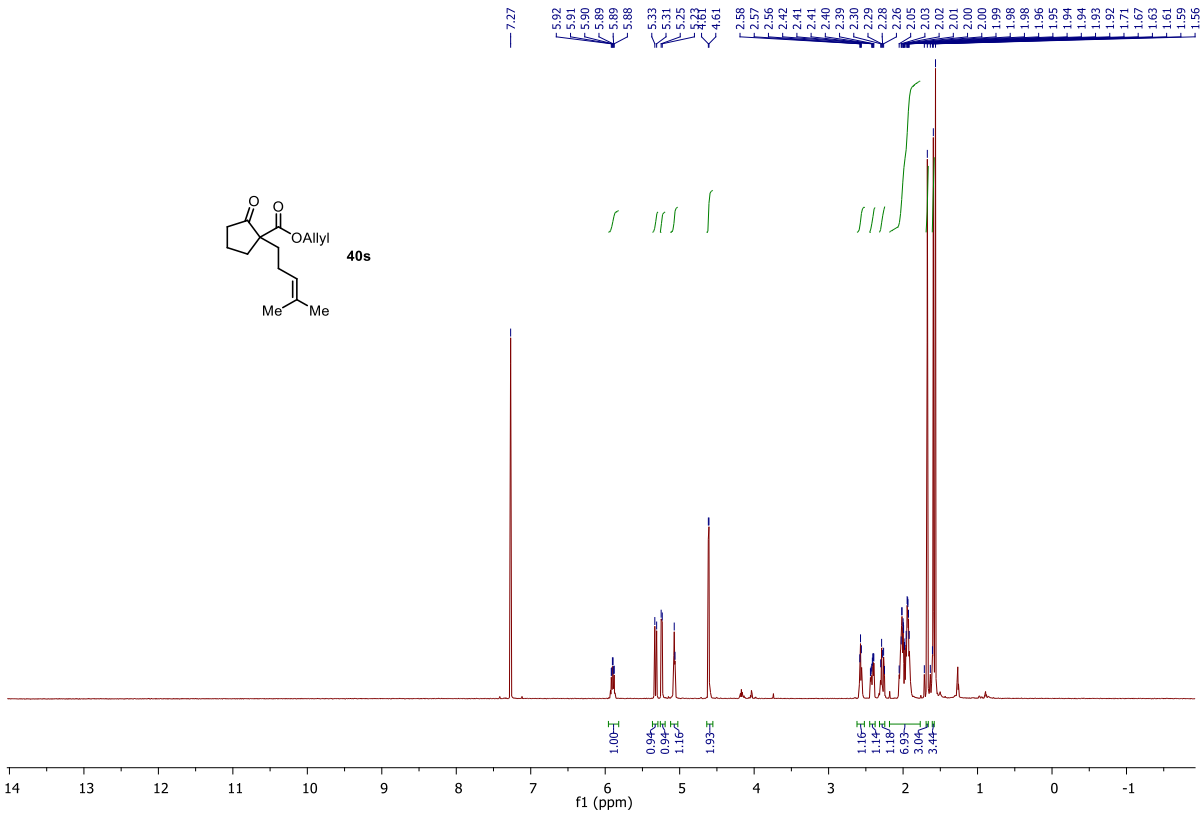
7.27
5.92
5.91
5.90
5.89
5.89
5.88
5.33
5.31
5.25
5.23
4.61
2.58
2.57
2.56
2.42
2.41
2.41
2.40
2.39
2.30
2.29
2.28
2.26
2.05
2.03
2.02
2.01
2.00
2.00
1.99
1.98
1.98
1.96
1.95
1.94
1.94
1.93
1.92
1.71
1.67
1.63
1.61
1.59
1.56
O
O
OAllyl
Me
Me
40s
1.00
0.94
0.94
1.16
1.93
1.16
1.14
1.18
6.93
3.04
3.44
14
13
12
11
10
9
8
7
6
5
4
3
2
1
0
-1
f1 (ppm)

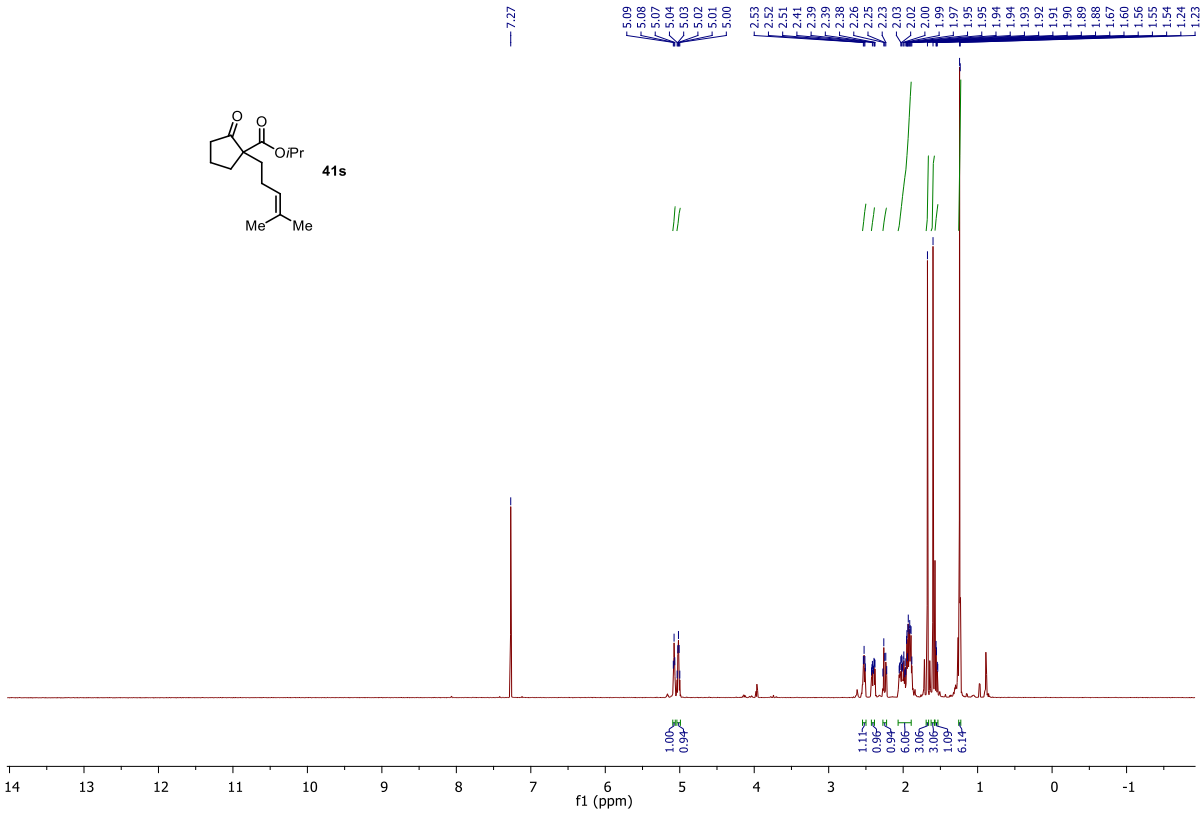
7.27
5.09
5.08
5.07
5.04
5.03
5.02
5.01
5.00
2.53
2.52
2.51
2.41
2.39
2.39
2.38
2.26
2.25
2.23
2.03
2.02
2.00
1.99
1.97
1.95
1.95
1.94
1.94
1.93
1.92
1.91
1.90
1.89
1.88
1.67
1.60
1.56
1.55
1.54
1.24
1.23
O
O
OiPr
41s
Me
Me
1.00
0.94
1.11
0.96
0.94
6.06
3.06
3.06
1.09
6.14
14 13 12 11 10 9 8 7 6 5 4 3 2 1 0 -1
f1 (ppm)

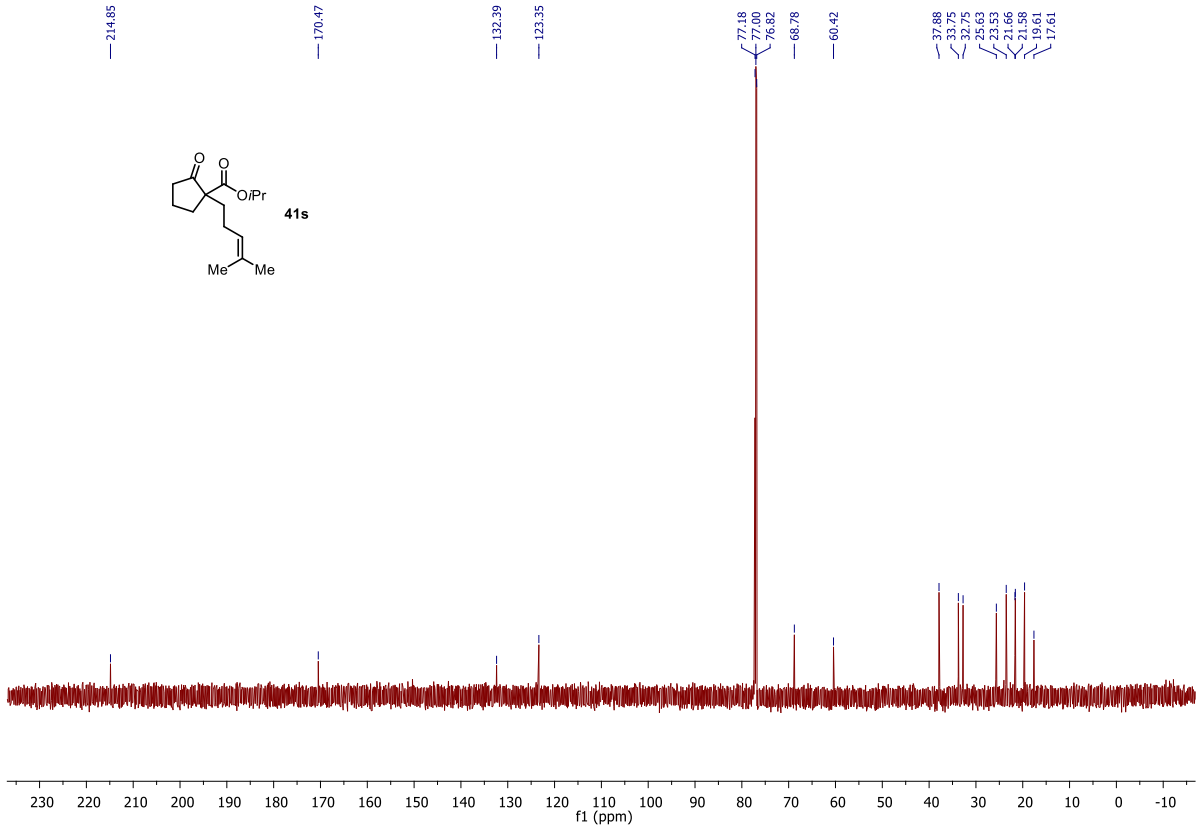
214.85
170.47
132.39
123.35
77.18
77.00
76.82
68.78
60.42
37.88
33.75
32.75
25.63
23.53
21.66
21.58
19.61
17.61
O
O
OiPr
41s
Me
Me
230 220 210 200 190 180 170 160 150 140 130 120 110 100 90 80 70 60 50 40 30 20 10 0 -10
f1 (ppm)

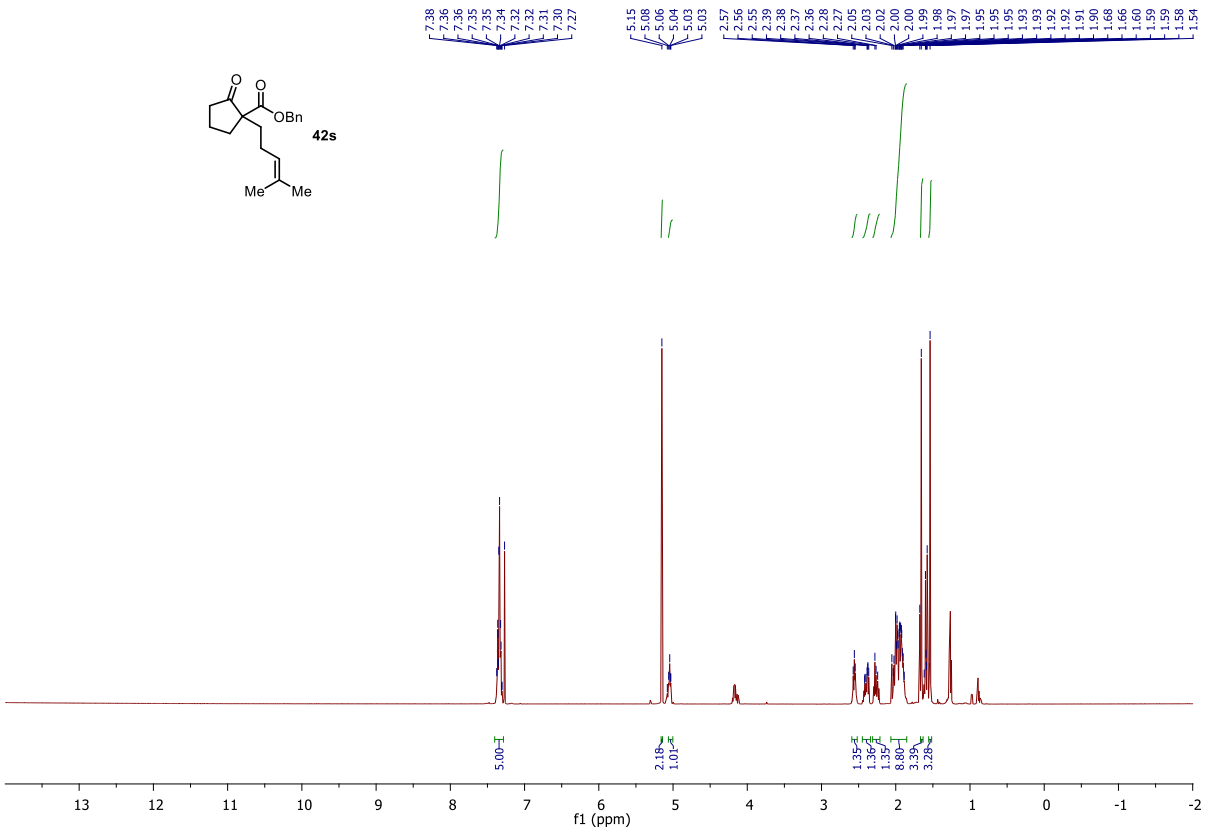
7.38 7.36 7.36 7.35 7.35 7.34 7.32 7.32 7.31 7.30 7.27
5.15 5.08 5.06 5.04 5.03 5.03
2.57 2.56 2.55 2.39 2.38 2.37 2.36 2.28 2.27 2.05 2.03 2.02 2.00 2.00 1.99 1.98 1.97 1.97 1.95 1.95 1.95 1.93 1.93 1.92 1.92 1.91 1.90 1.68 1.66 1.60 1.59 1.59 1.58 1.54
O
O
OBn
42s
Me
Me
5.00
2.18
1.01
1.35
1.36
1.35
8.80
3.39
3.26
13 12 11 10 9 8 7 6 5 4 3 2 1 0 -1 -2
f1 (ppm)

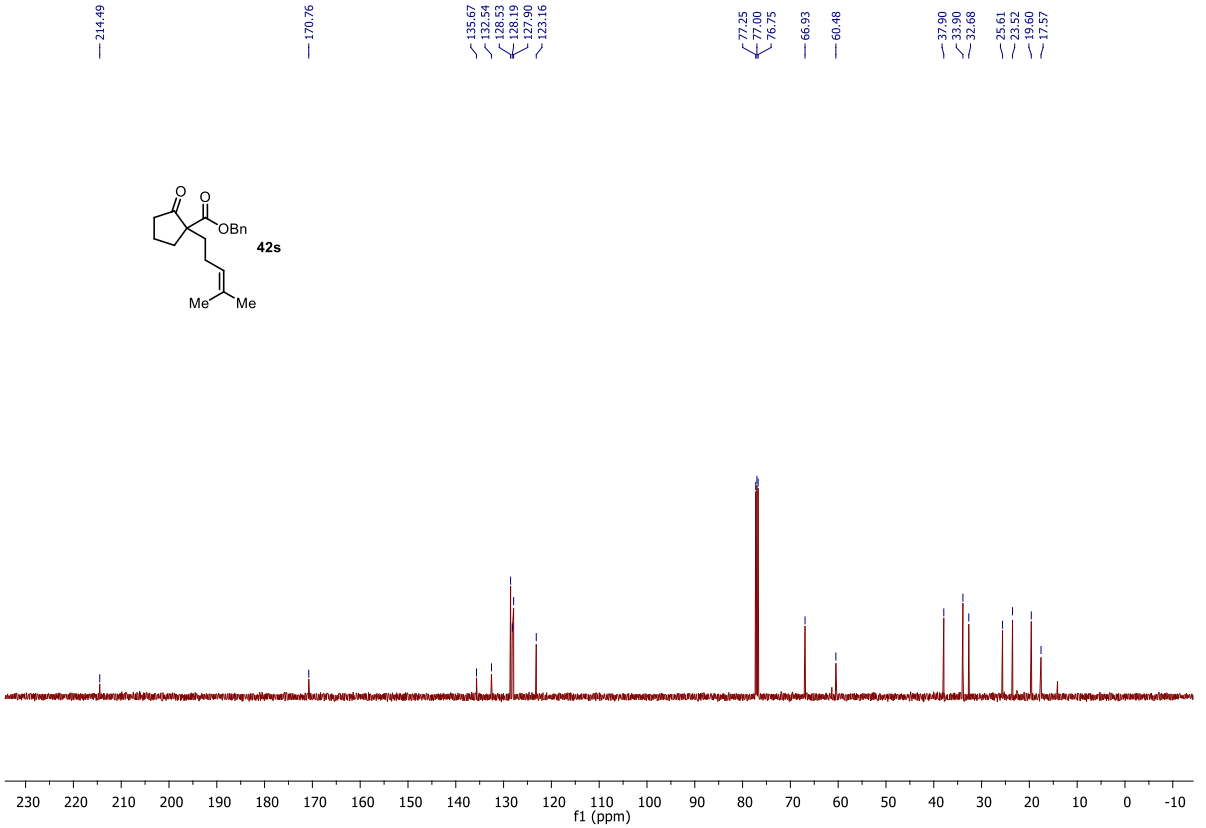
214.49
170.76
135.67
132.54
128.53
128.19
127.90
123.16
77.25
77.00
76.75
66.93
60.48
37.90
33.90
32.68
25.61
23.52
19.60
17.57
O
O
OBn
42s
Me
Me
230 220 210 200 190 180 170 160 150 140 130 120 110 100 90 80 70 60 50 40 30 20 10 0 -10
f1 (ppm)

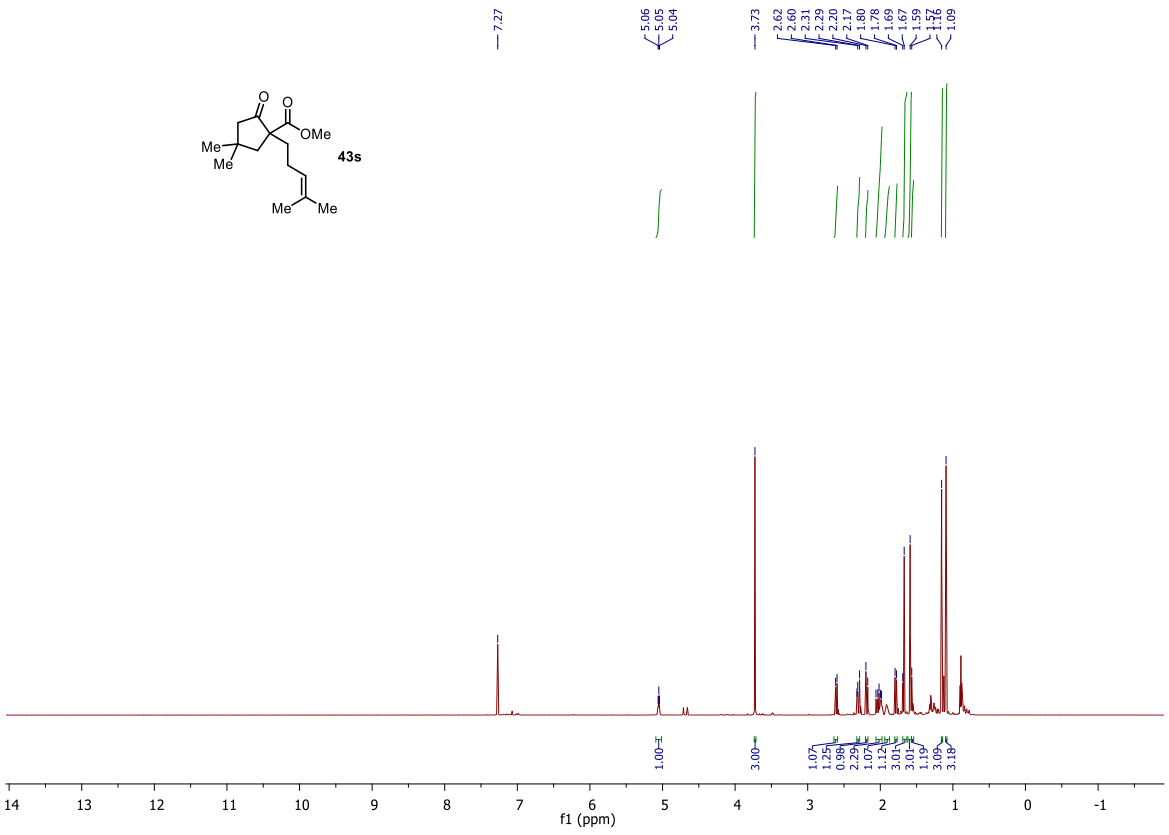
7.27
5.06
5.05
5.04
3.73
2.62
2.60
2.31
2.29
2.20
2.17
1.80
1.78
1.69
1.67
1.59
1.57
1.16
1.09
O
O
OMe
Me
Me
43s
Me
Me
1.00
3.00
1.07
1.25
0.98
2.29
1.07
1.12
3.01
3.01
1.19
3.09
3.18
14
13
12
11
10
9
8
7
6
5
4
3
2
1
0
-1
f1 (ppm)

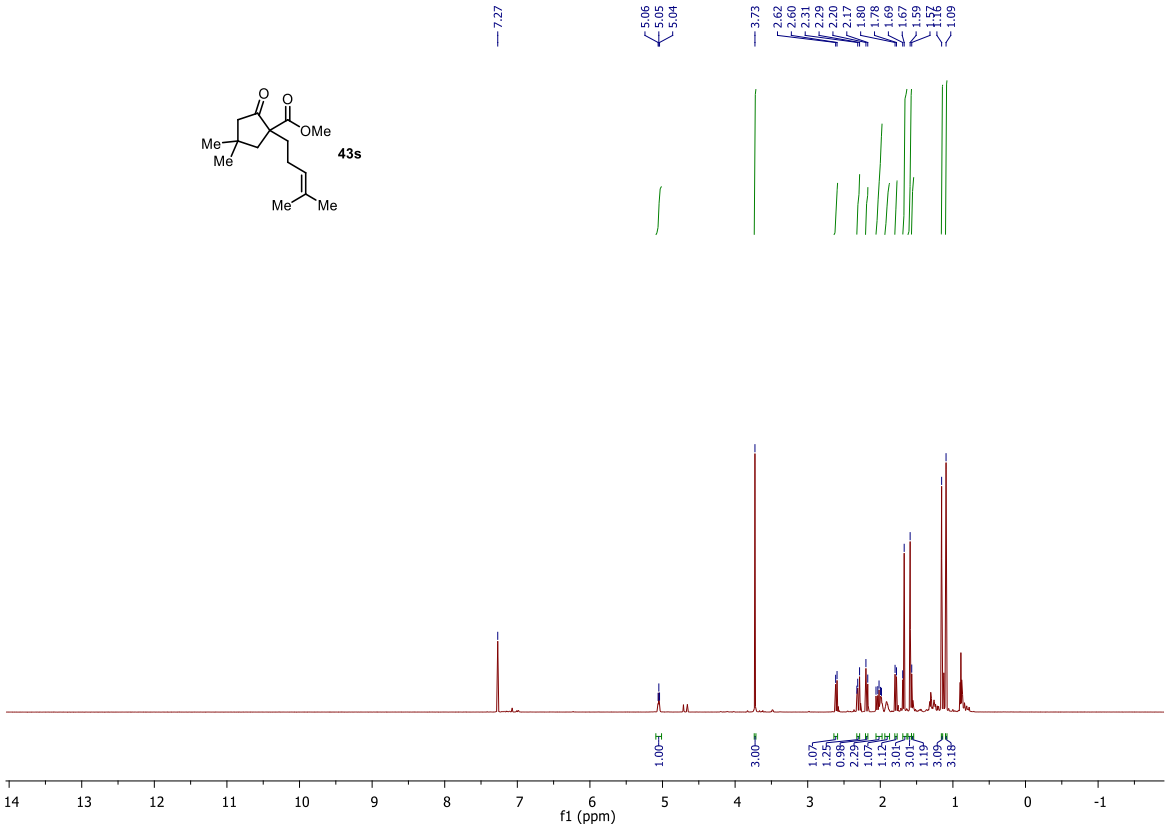
7.27
5.06
5.05
5.04
3.73
2.62
2.60
2.31
2.29
2.20
2.17
1.80
1.78
1.69
1.67
1.59
1.57
1.16
1.09
O
O
OMe
Me
Me
43s
Me
Me
1.00
3.00
1.07
1.25
0.98
2.29
1.07
1.12
3.01
3.01
1.19
3.09
3.18
14
13
12
11
10
9
8
7
6
5
4
3
2
1
0
-1
f1 (ppm)

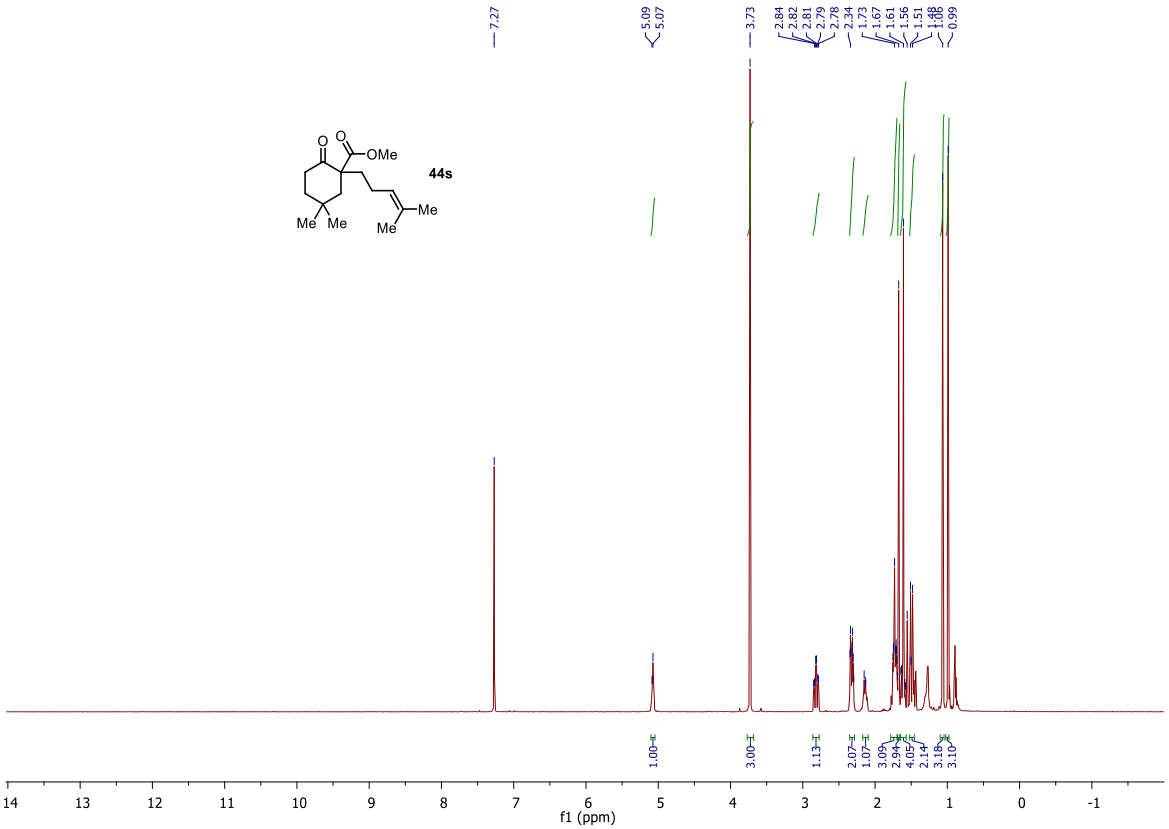
7.27
5.09
5.07
3.73
2.84
2.82
2.81
2.79
2.78
2.34
1.73
1.67
1.61
1.56
1.51
1.08
0.99
OMe
44s
Me
Me
Me
1.00
3.00
1.13
2.07
1.07
3.09
2.94
4.05
2.14
3.18
3.10
f1 (ppm)

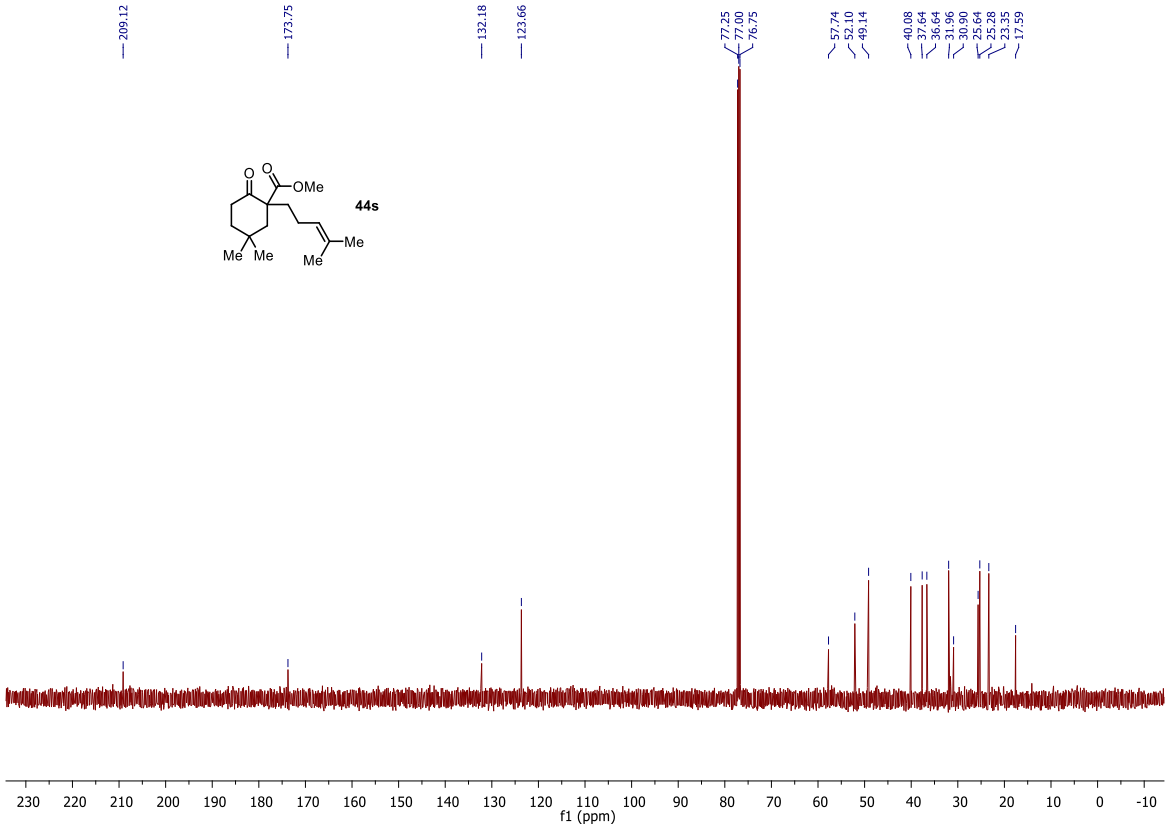
209.12
173.75
132.18
123.66
77.25
77.00
76.75
57.74
52.10
49.14
40.08
37.64
36.64
31.96
30.90
25.64
25.28
23.35
17.59
OMe
44s
Me
Me
Me
f1 (ppm)

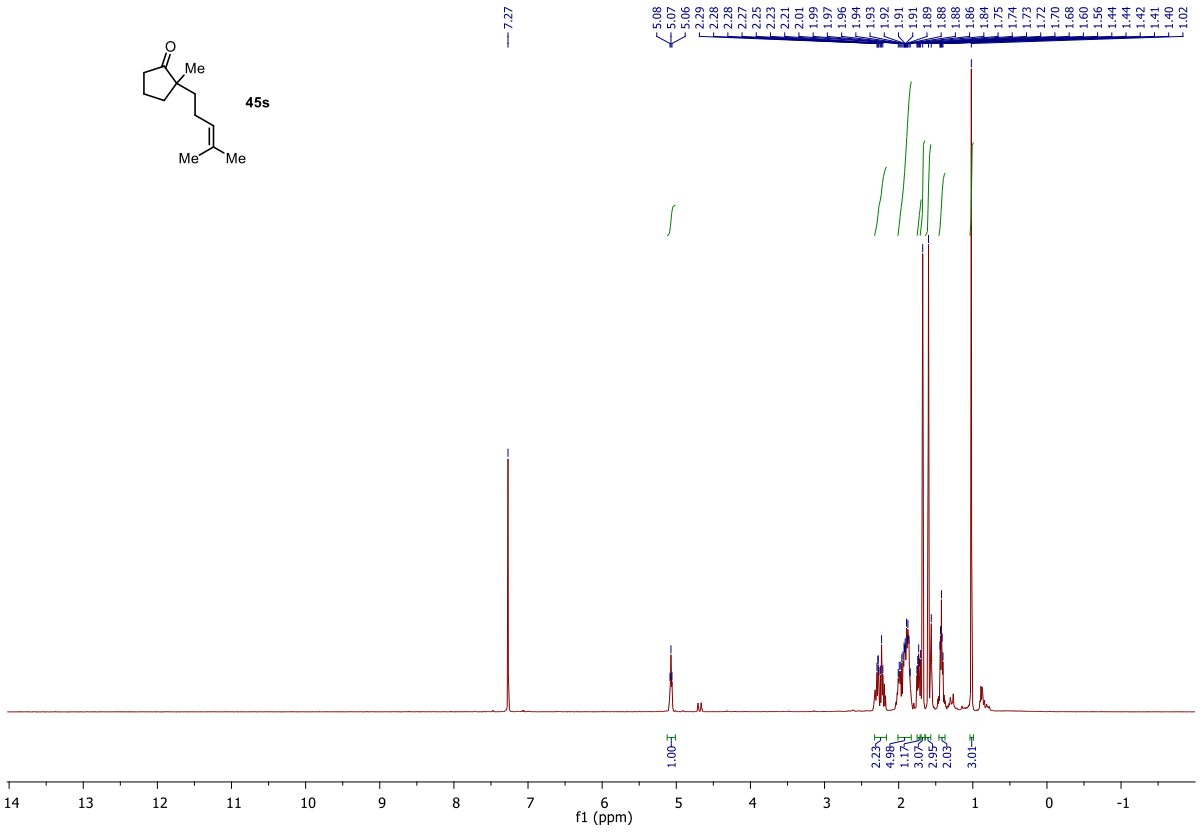
45s
7.27
5.08
5.07
5.06
2.29
2.28
2.28
2.27
2.25
2.23
2.21
2.01
1.99
1.97
1.96
1.94
1.93
1.92
1.91
1.91
1.89
1.88
1.88
1.86
1.84
1.75
1.74
1.73
1.72
1.70
1.68
1.60
1.56
1.44
1.44
1.42
1.41
1.40
1.02
1.00
2.23
4.98
1.17
3.07
2.95
2.03
3.01
f1 (ppm)

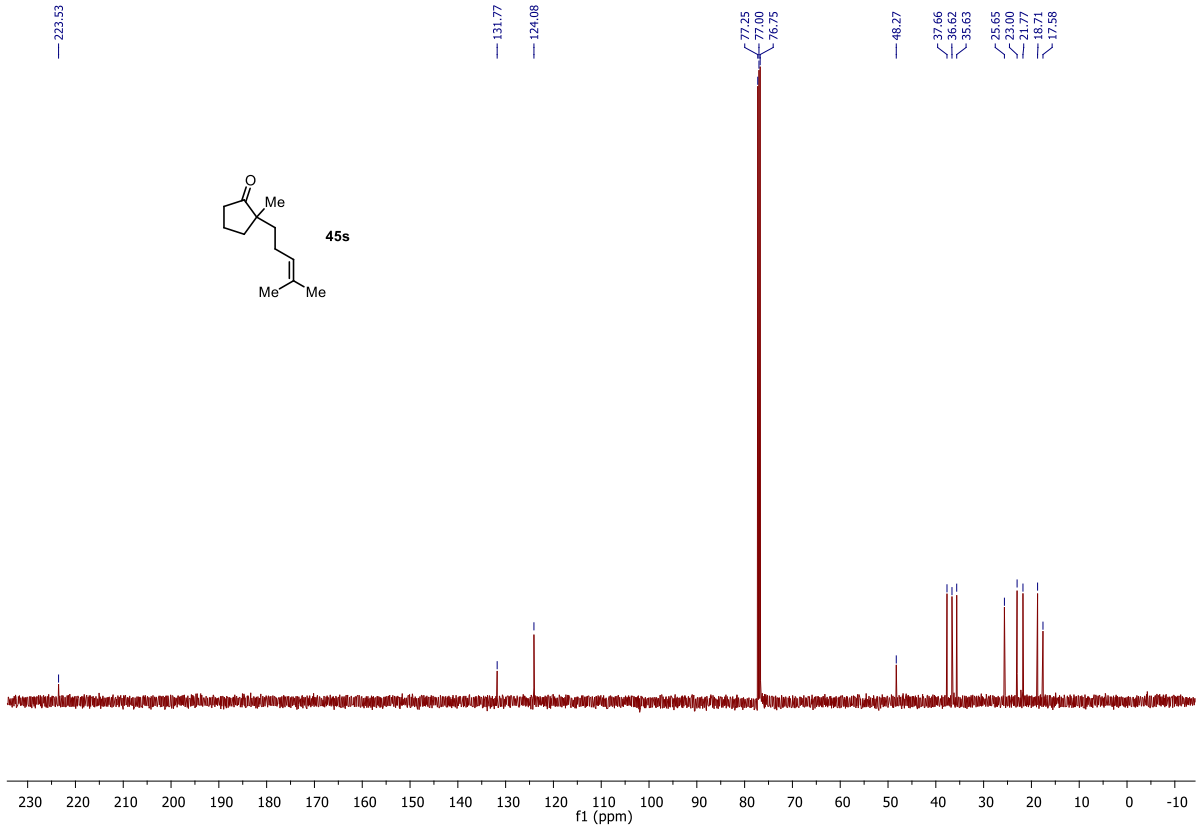
45s
223.53
131.77
124.08
77.25
77.00
76.75
48.27
37.66
36.62
35.63
25.65
23.00
21.77
18.71
17.58
f1 (ppm)

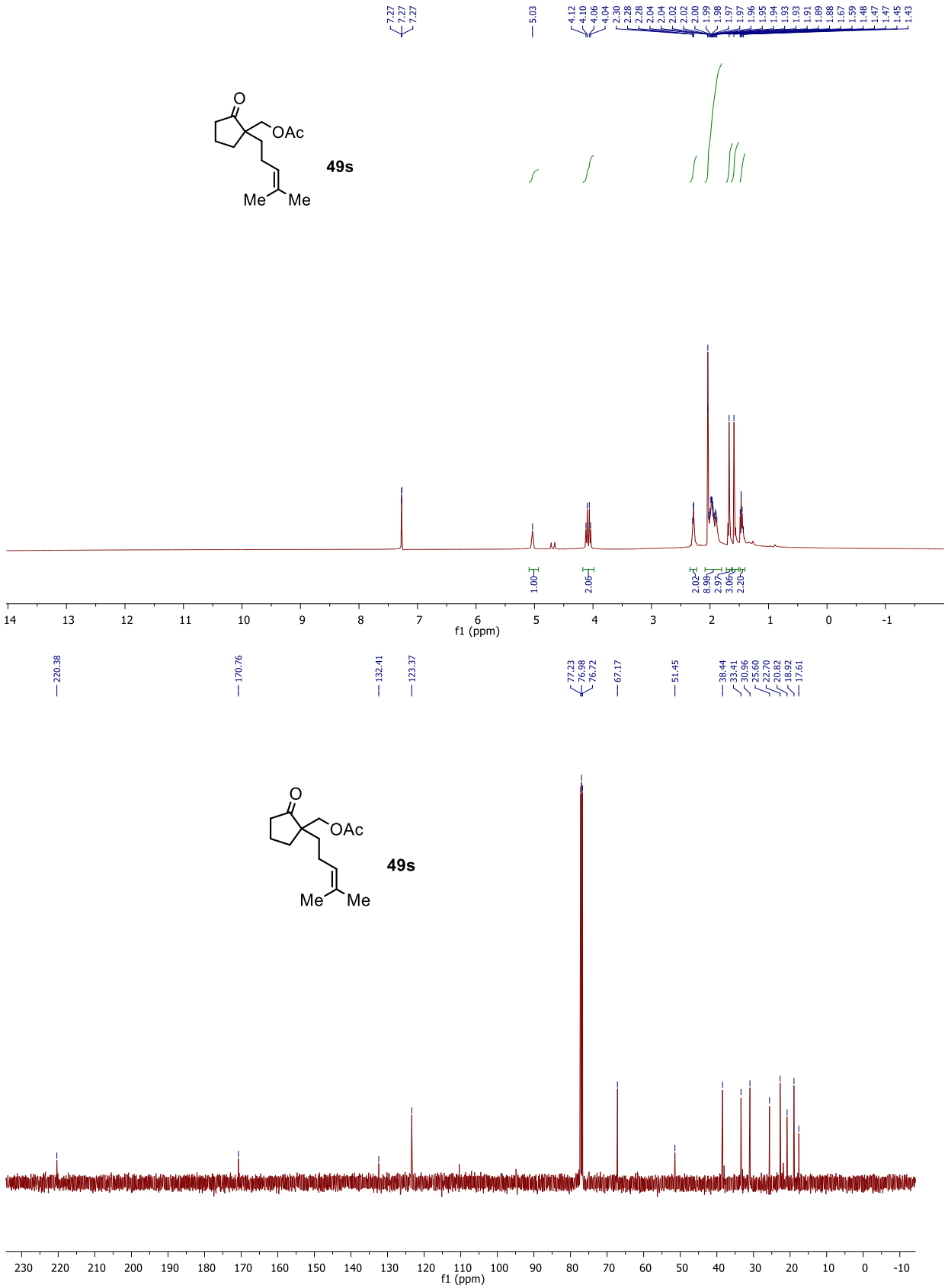
O
OAc
Me
Me
49s
f1 (ppm)
49s
f1 (ppm)

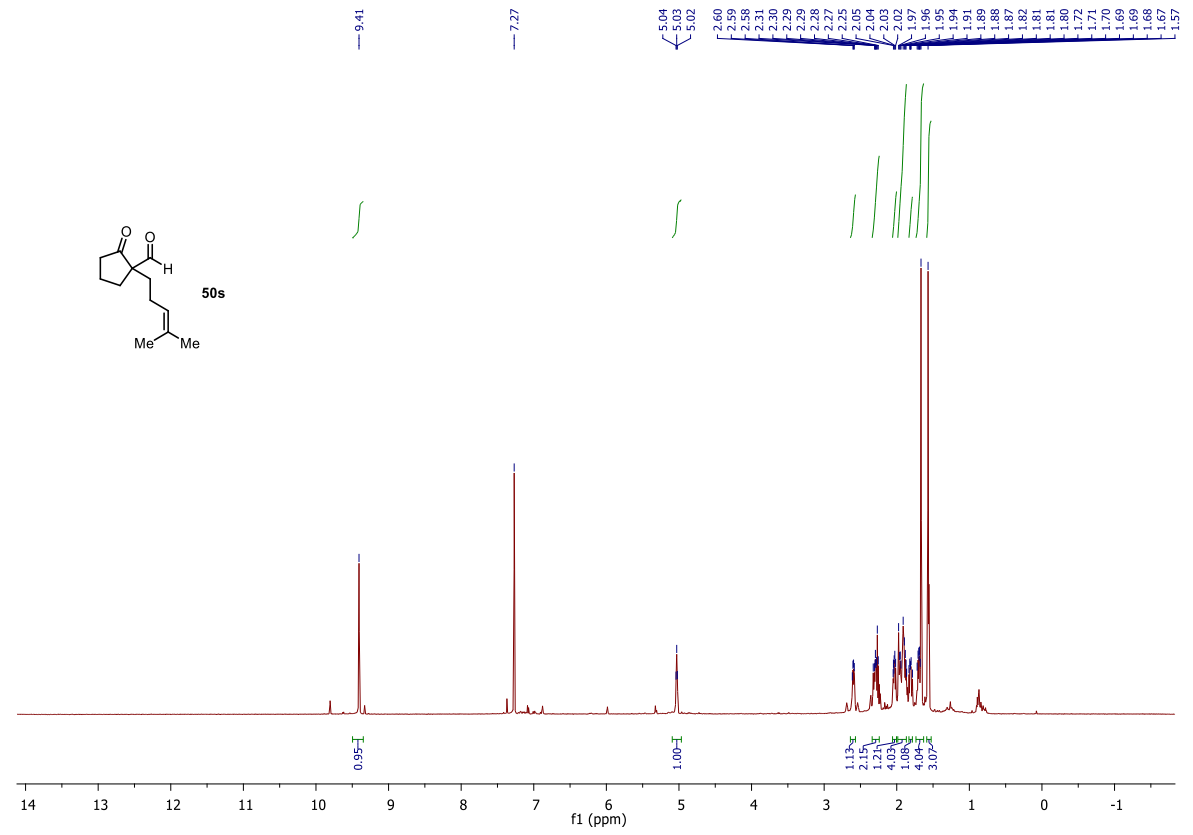
9.41
7.27
5.04
5.03
5.02
2.60
2.59
2.58
2.31
2.30
2.29
2.29
2.28
2.27
2.25
2.05
2.04
2.03
2.02
1.97
1.96
1.95
1.94
1.91
1.89
1.88
1.87
1.82
1.81
1.81
1.80
1.72
1.71
1.70
1.69
1.69
1.68
1.67
1.57
O
O
H
Me
Me
50s
0.95
1.00
1.13
2.15
1.21
4.03
1.08
4.04
3.07
14
13
12
11
10
9
8
7
6
5
4
3
2
1
0
-1
f1 (ppm)

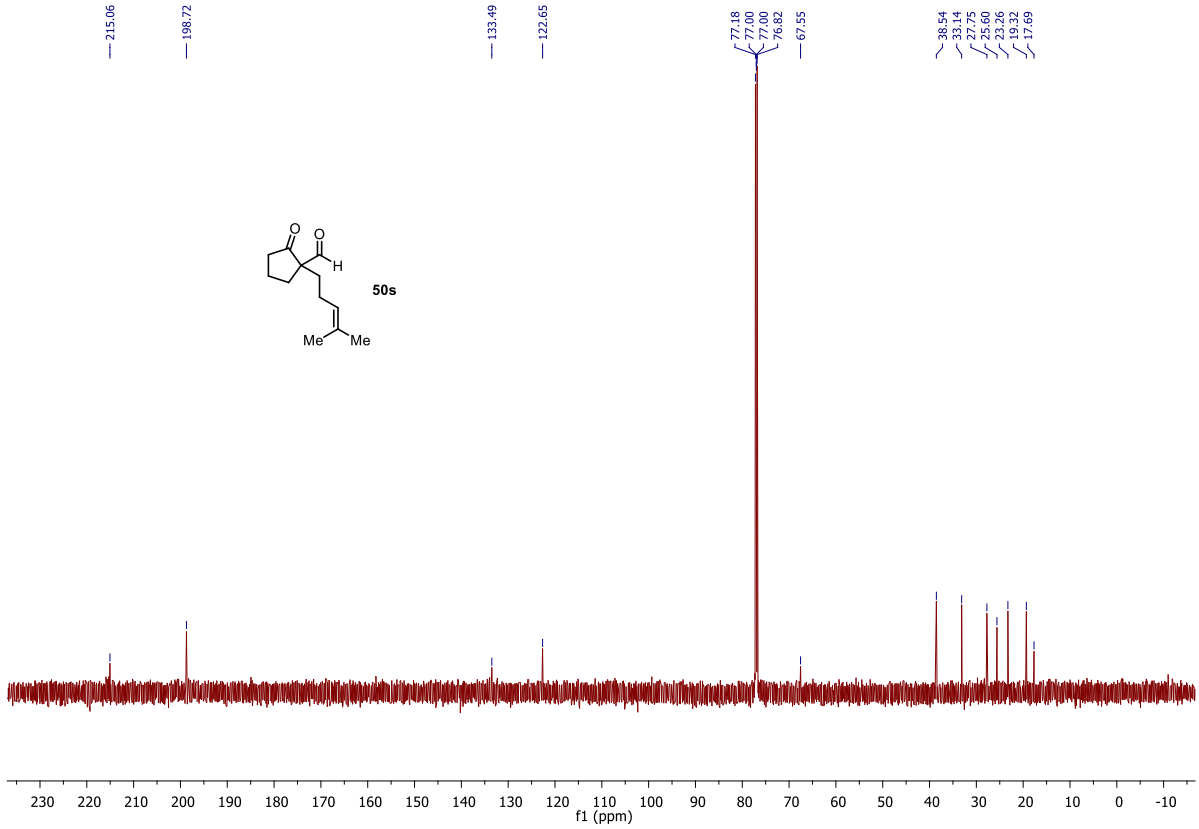
215.06
198.72
133.49
122.65
77.18
77.00
77.00
76.82
67.55
38.54
33.14
27.75
25.60
23.26
19.32
17.69
O
O
H
Me
Me
50s
230
220
210
200
190
180
170
160
150
140
130
120
110
100
90
80
70
60
50
40
30
20
10
0
-10
f1 (ppm)

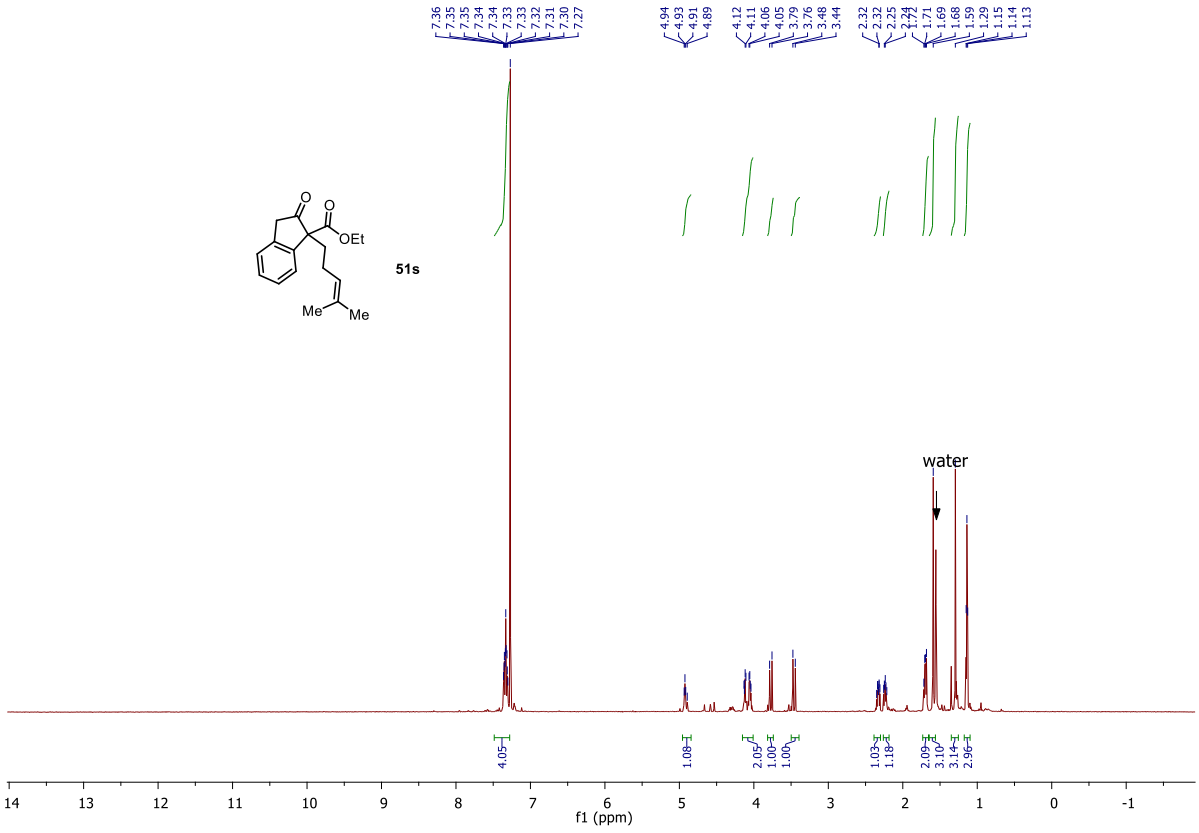
7.36
7.35
7.35
7.34
7.34
7.33
7.33
7.32
7.31
7.30
7.27
4.94
4.93
4.91
4.89
4.12
4.11
4.06
4.05
3.79
3.76
3.48
3.44
2.32
2.32
2.25
1.71
1.69
1.68
1.59
1.29
1.15
1.14
1.13
O
O
OEt
Me
Me
51s
water
4.05
1.08
2.05
1.00
1.00
1.03
1.18
2.09
3.10
3.14
2.96
14
13
12
11
10
9
8
7
6
5
4
3
2
1
0
-1
f1 (ppm)

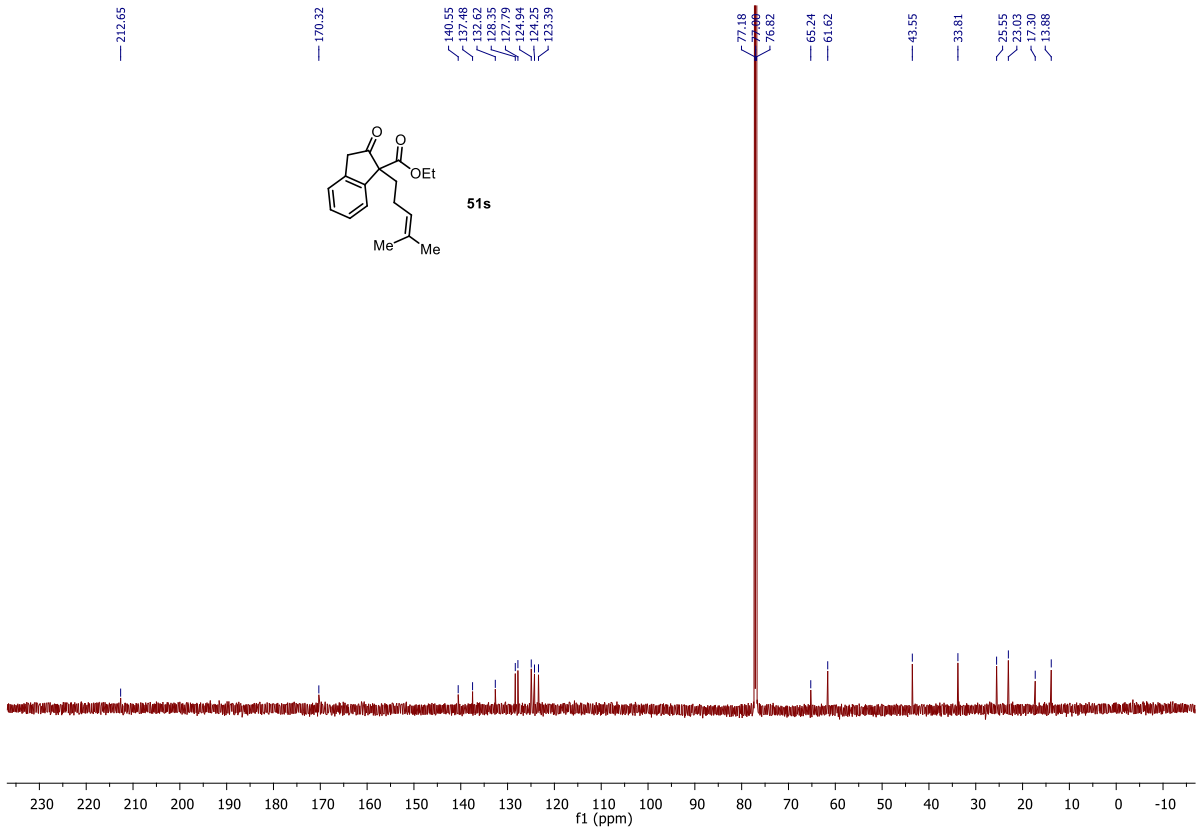
212.65
170.32
140.55
137.48
132.62
128.35
127.79
124.94
124.25
123.39
77.18
77.00
76.82
65.24
61.62
43.55
33.81
25.55
23.03
17.30
13.88
O
O
OEt
Me
Me
51s
230
220
210
200
190
180
170
160
150
140
130
120
110
100
90
80
70
60
50
40
30
20
10
0
-10
f1 (ppm)

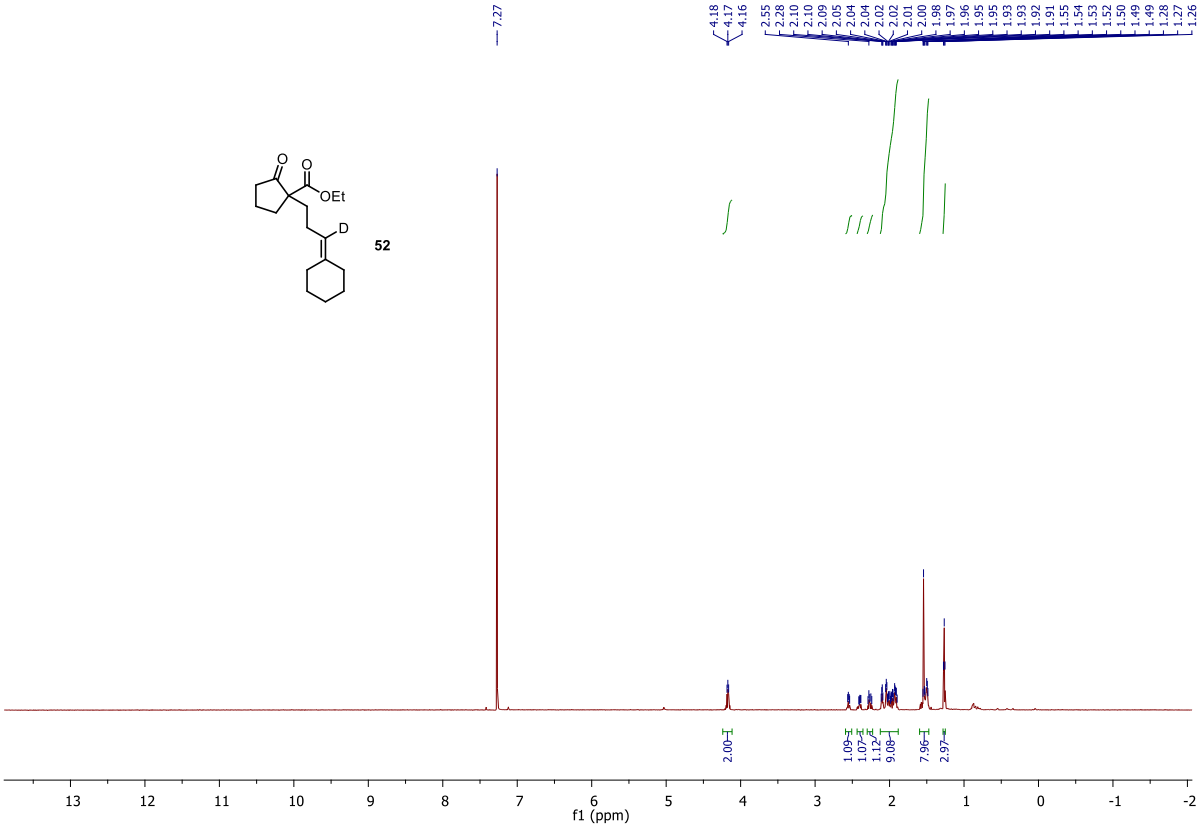
7.27
4.18
4.17
4.16
2.55
2.28
2.10
2.10
2.09
2.05
2.04
2.04
2.02
2.02
2.01
2.00
1.98
1.97
1.96
1.95
1.95
1.93
1.93
1.92
1.91
1.55
1.54
1.53
1.52
1.50
1.49
1.49
1.28
1.27
1.26
O
O
OEt
D
52
2.00
1.09
1.07
1.12
9.08
7.96
2.97
13
12
11
10
9
8
7
6
5
4
3
2
1
0
-1
-2
f1 (ppm)

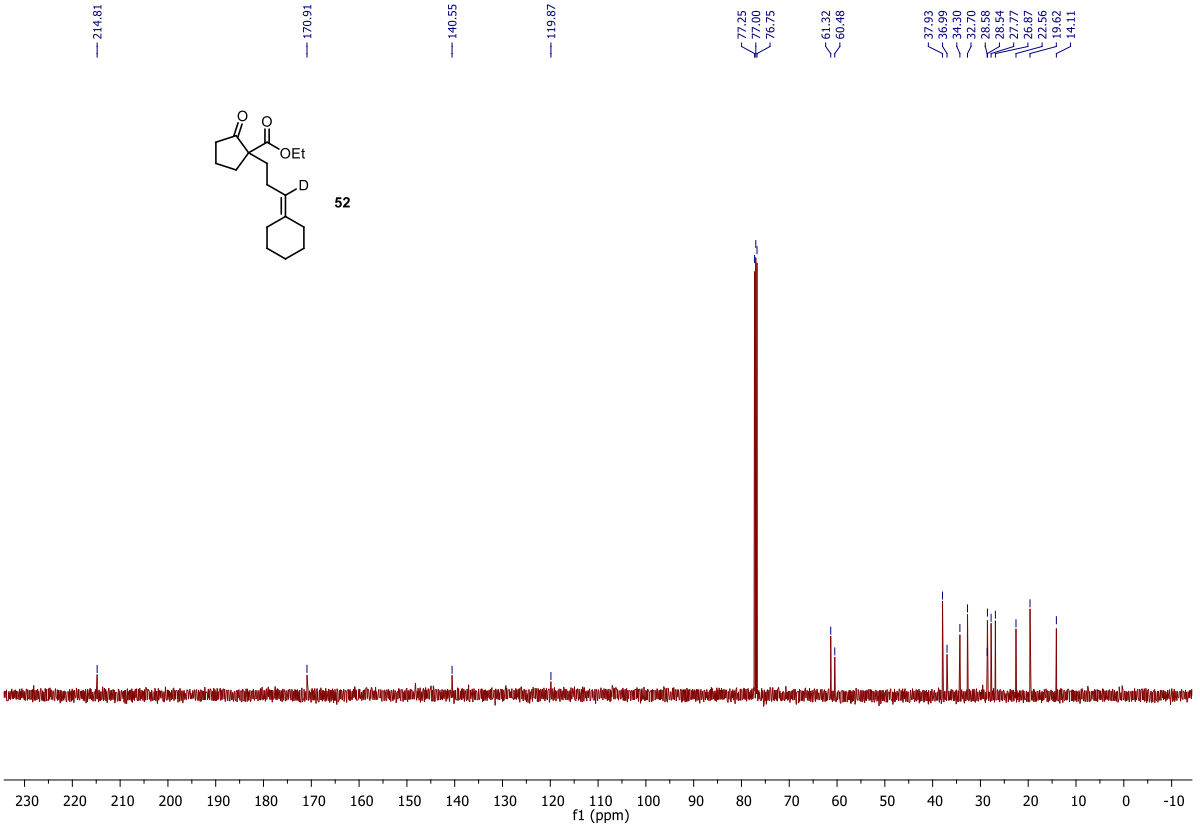
214.81
170.91
140.55
119.87
77.25
77.00
76.75
61.32
60.48
37.93
36.99
34.30
32.70
28.58
28.54
27.77
26.87
22.56
19.62
14.11
O
O
OEt
D
52
230
220
210
200
190
180
170
160
150
140
130
120
110
100
90
80
70
60
50
40
30
20
10
0
-10
f1 (ppm)

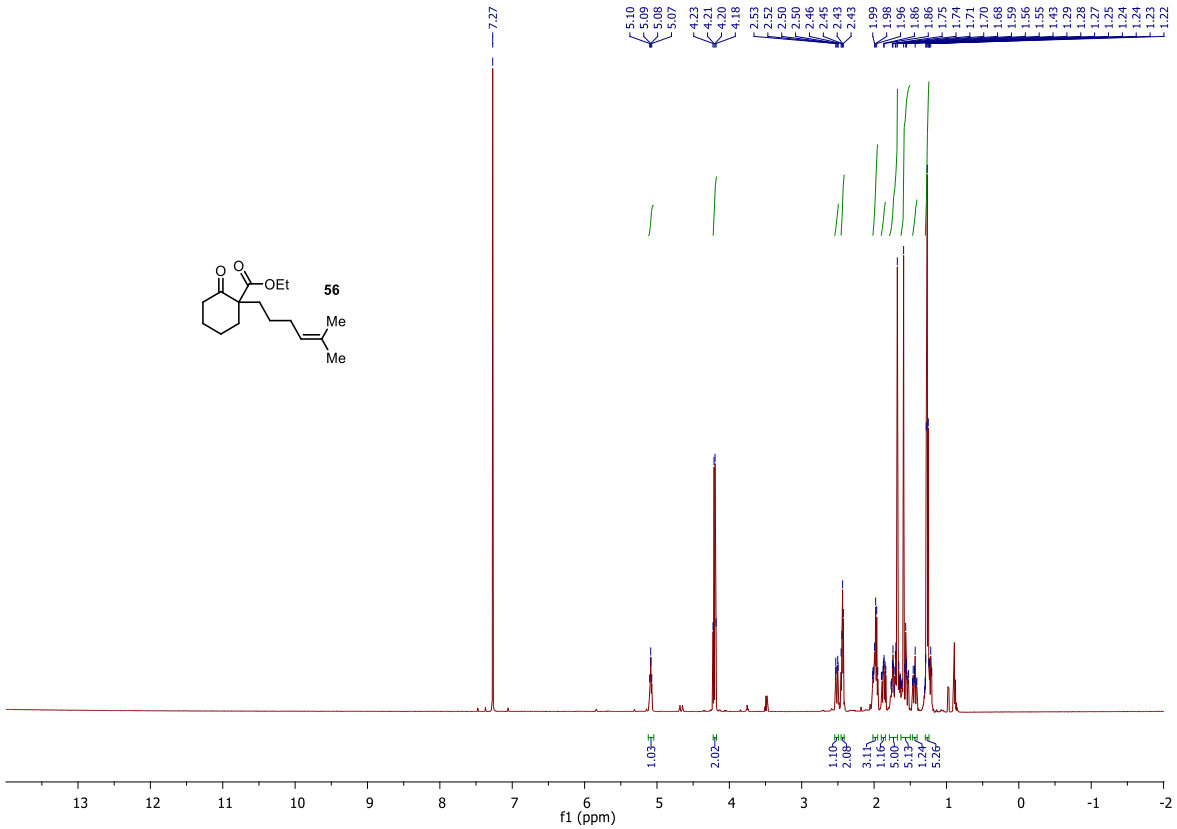
7.27
5.10
5.09
5.08
5.07
4.23
4.21
4.20
4.18
2.53
2.52
2.50
2.50
2.46
2.45
2.43
2.43
1.99
1.98
1.96
1.86
1.86
1.75
1.74
1.71
1.70
1.68
1.59
1.56
1.55
1.43
1.29
1.28
1.27
1.25
1.24
1.24
1.23
1.22
O
O
OEt
56
Me
Me
1.03
2.02
1.10
2.08
3.11
1.16
5.00
5.13
1.24
5.26
13
12
11
10
9
8
7
6
5
4
3
2
1
0
-1
-2
f1 (ppm)

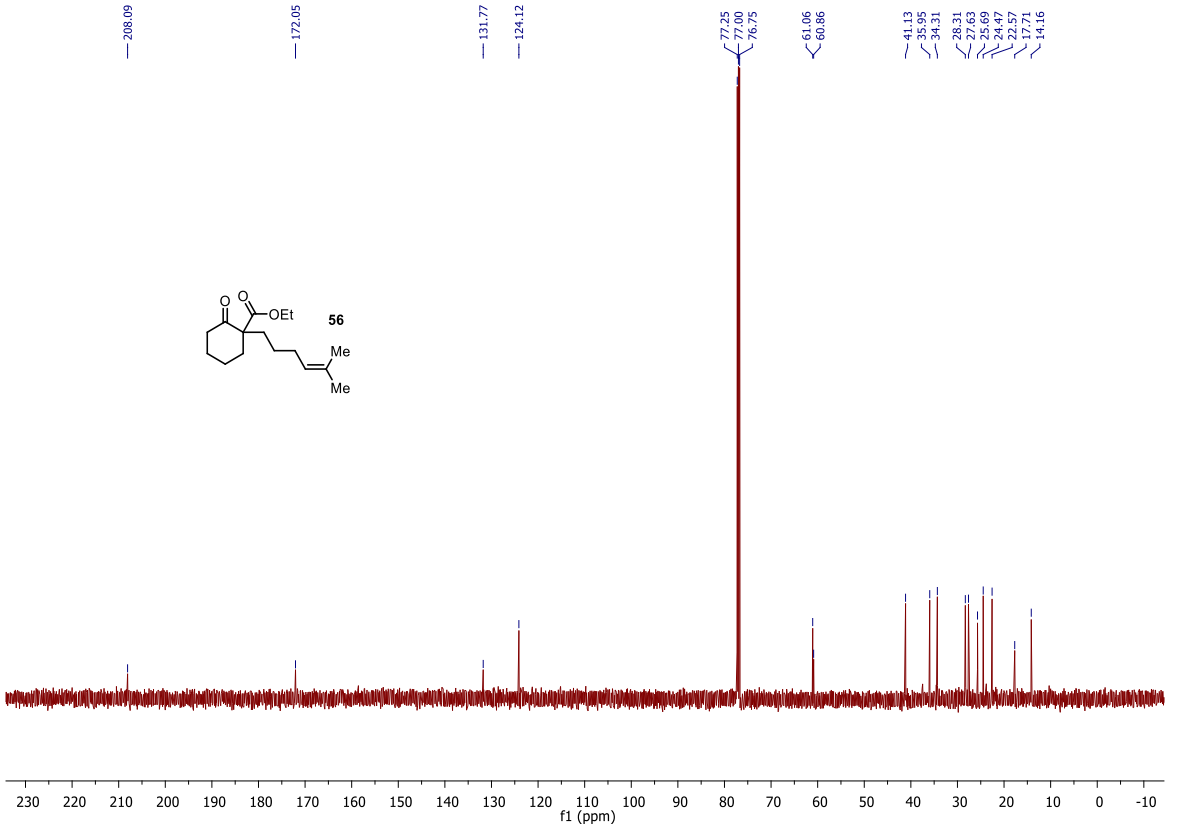
208.09
172.05
131.77
124.12
77.25
77.00
76.75
61.06
60.86
41.13
35.95
34.31
28.31
27.63
25.69
24.47
22.57
17.71
14.16
O
O
OEt
56
Me
Me
230
220
210
200
190
180
170
160
150
140
130
120
110
100
90
80
70
60
50
40
30
20
10
0
-10
f1 (ppm)

Carbocyclization Products

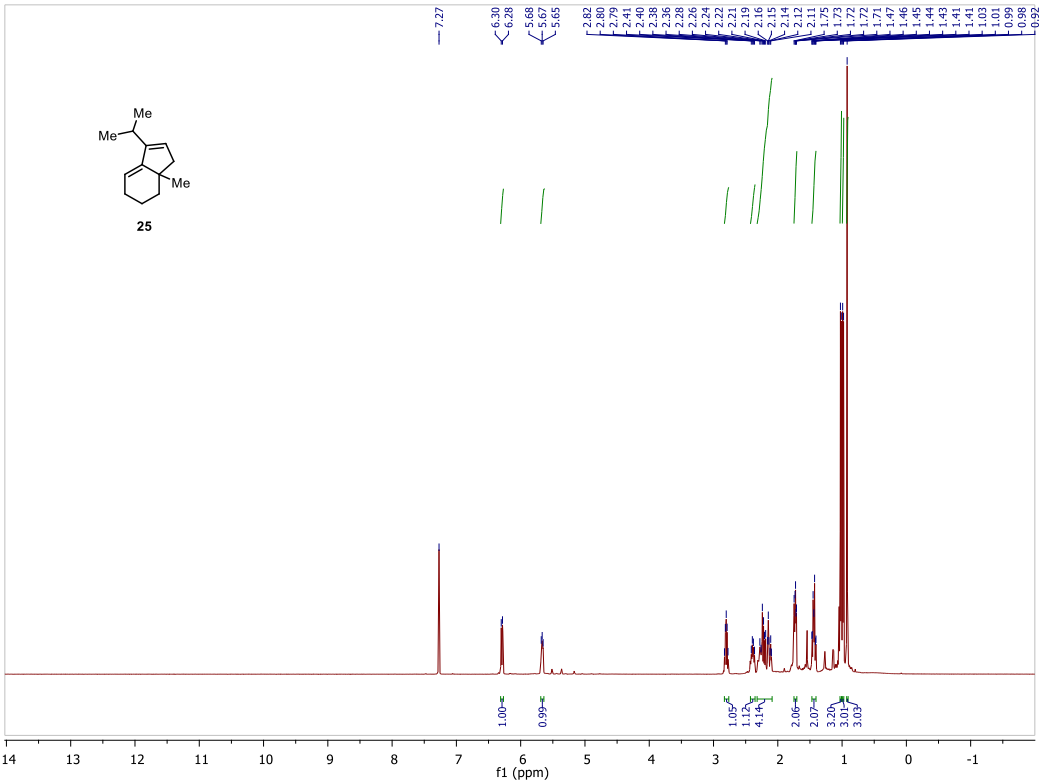
Me
Me
Me
25
7.27
6.30
6.28
5.68
5.67
5.65
2.82
2.80
2.79
2.41
2.40
2.38
2.36
2.28
2.26
2.24
2.22
2.21
2.19
2.16
2.15
2.14
2.12
2.11
1.75
1.73
1.72
1.72
1.71
1.47
1.46
1.45
1.44
1.43
1.41
1.41
1.03
1.01
0.99
0.98
0.92
1.00
0.99
1.05
1.12
4.14
2.06
2.07
3.20
3.01
3.03
14 13 12 11 10 9 8 7 6 5 4 3 2 1 0 -1
f1 (ppm)

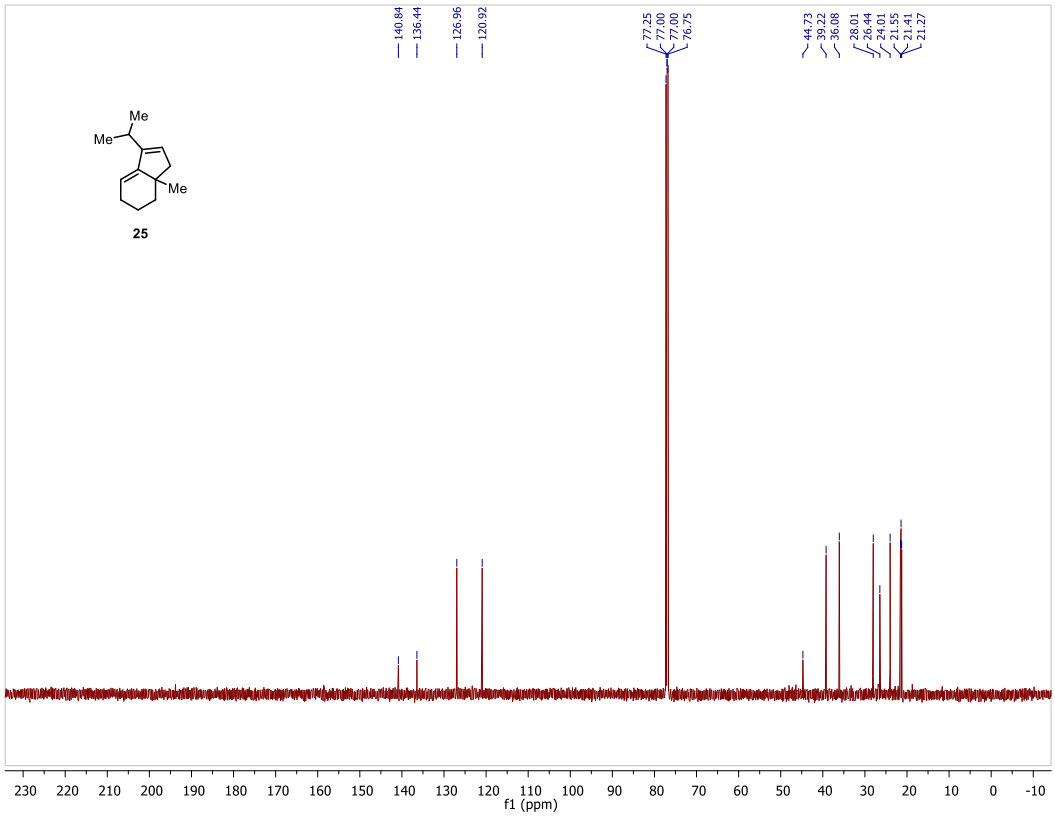
Me
Me
Me
25
140.84
136.44
126.96
120.92
77.25
77.00
77.00
76.75
44.73
39.22
36.08
28.01
26.44
24.01
21.55
21.41
21.27
230 220 210 200 190 180 170 160 150 140 130 120 110 100 90 80 70 60 50 40 30 20 10 0 -10
f1 (ppm)

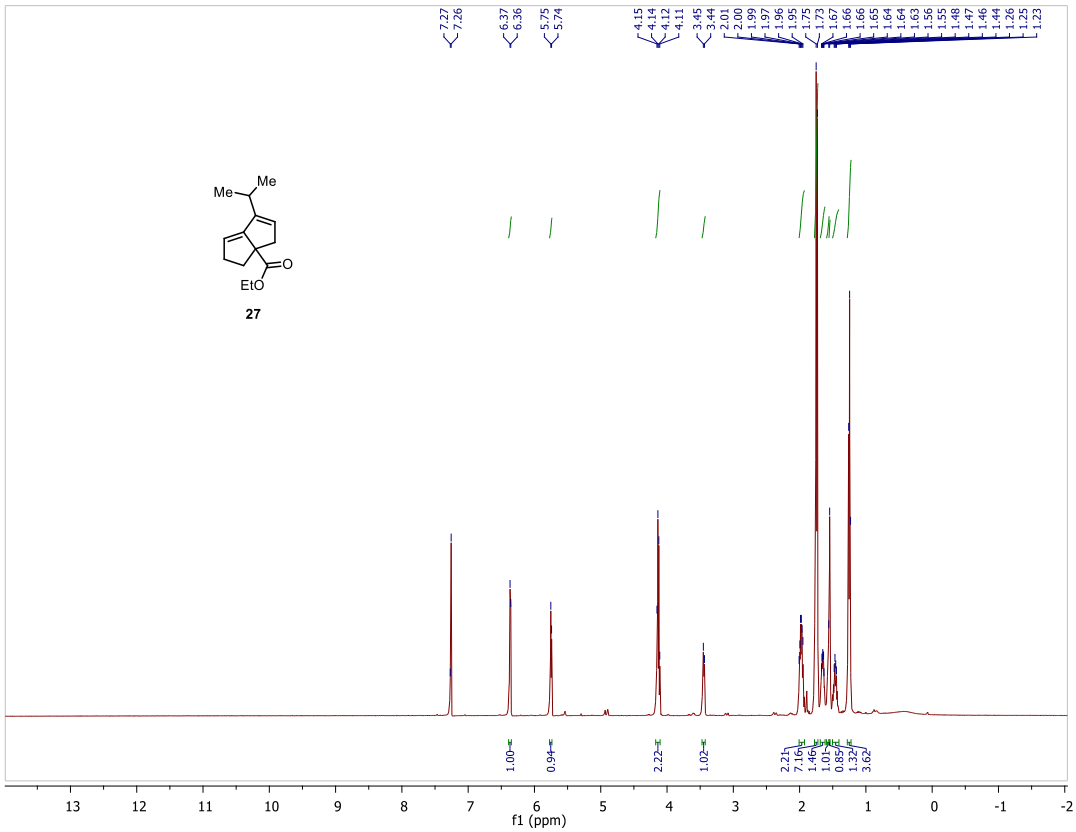
Me
Me
O
EtO
27
f1 (ppm)

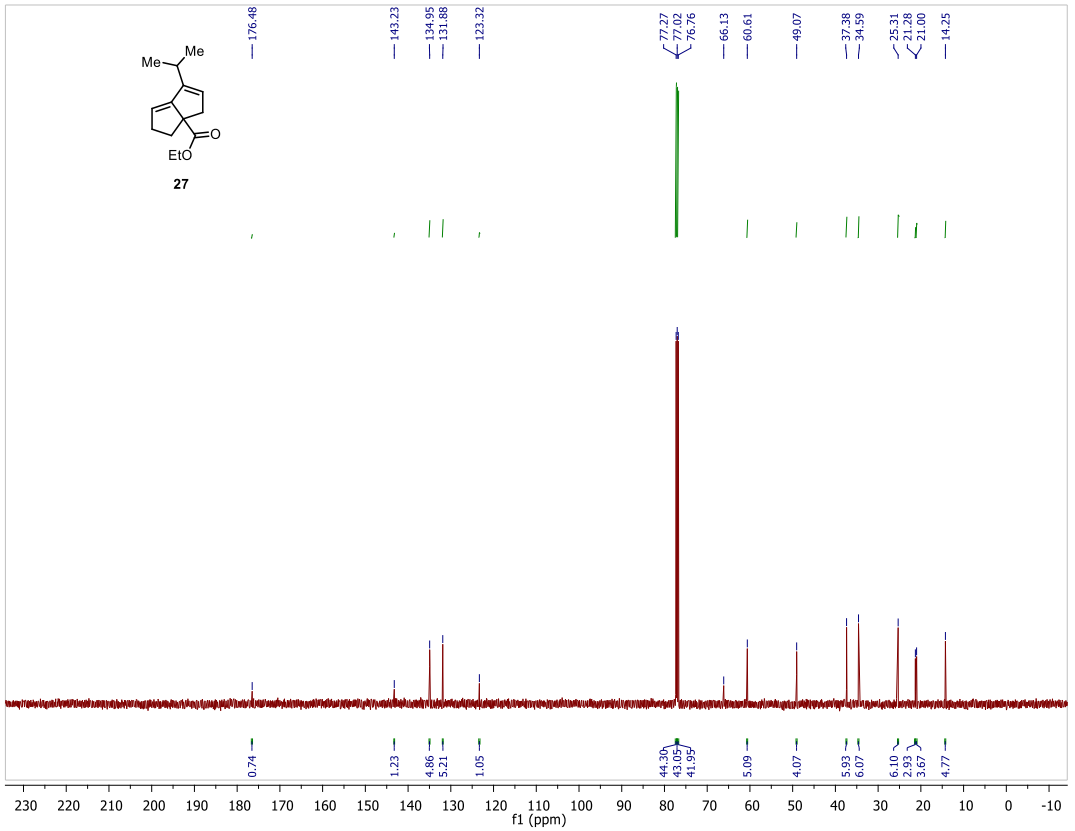
Me
Me
O
EtO
27
f1 (ppm)

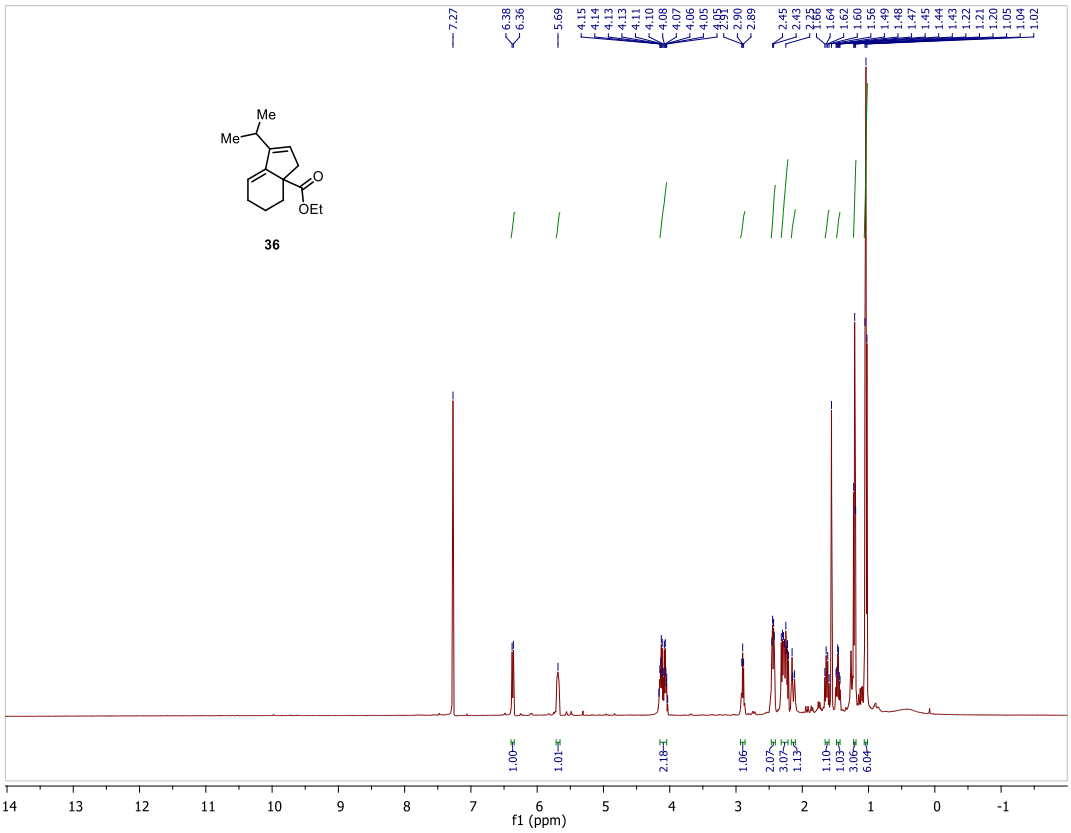
Me
Me
O
OEt
36
7.27
6.38
6.36
5.69
4.15
4.14
4.13
4.11
4.10
4.08
4.07
4.06
4.05
2.91
2.90
2.89
2.45
2.43
1.64
1.62
1.60
1.56
1.49
1.48
1.47
1.45
1.44
1.43
1.22
1.21
1.20
1.05
1.04
1.02
1.00
1.01
2.18
1.06
2.07
3.07
1.13
1.10
1.03
3.06
6.04
14 13 12 11 10 9 8 7 6 5 4 3 2 1 0 -1
f1 (ppm)

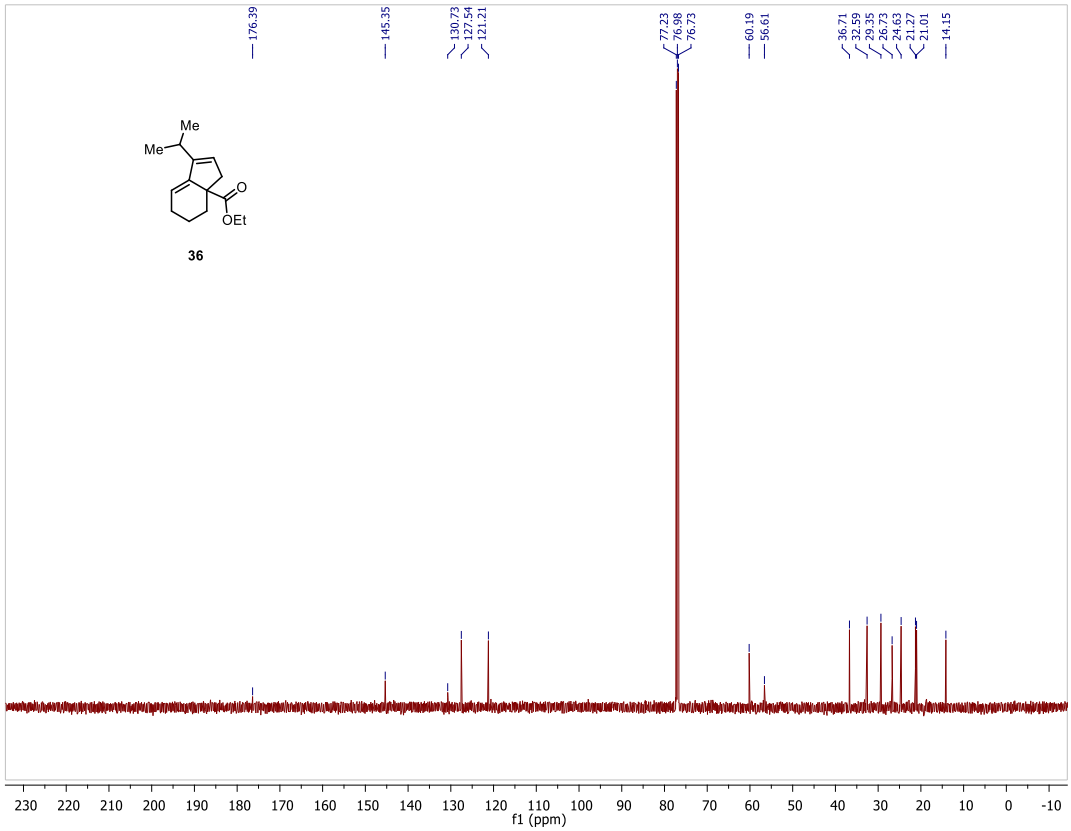
Me
Me
O
OEt
36
176.39
145.35
130.73
127.54
121.21
77.23
76.98
76.73
60.19
56.61
36.71
32.59
29.35
26.73
24.63
21.27
21.01
14.15
230 220 210 200 190 180 170 160 150 140 130 120 110 100 90 80 70 60 50 40 30 20 10 0 -10
f1 (ppm)

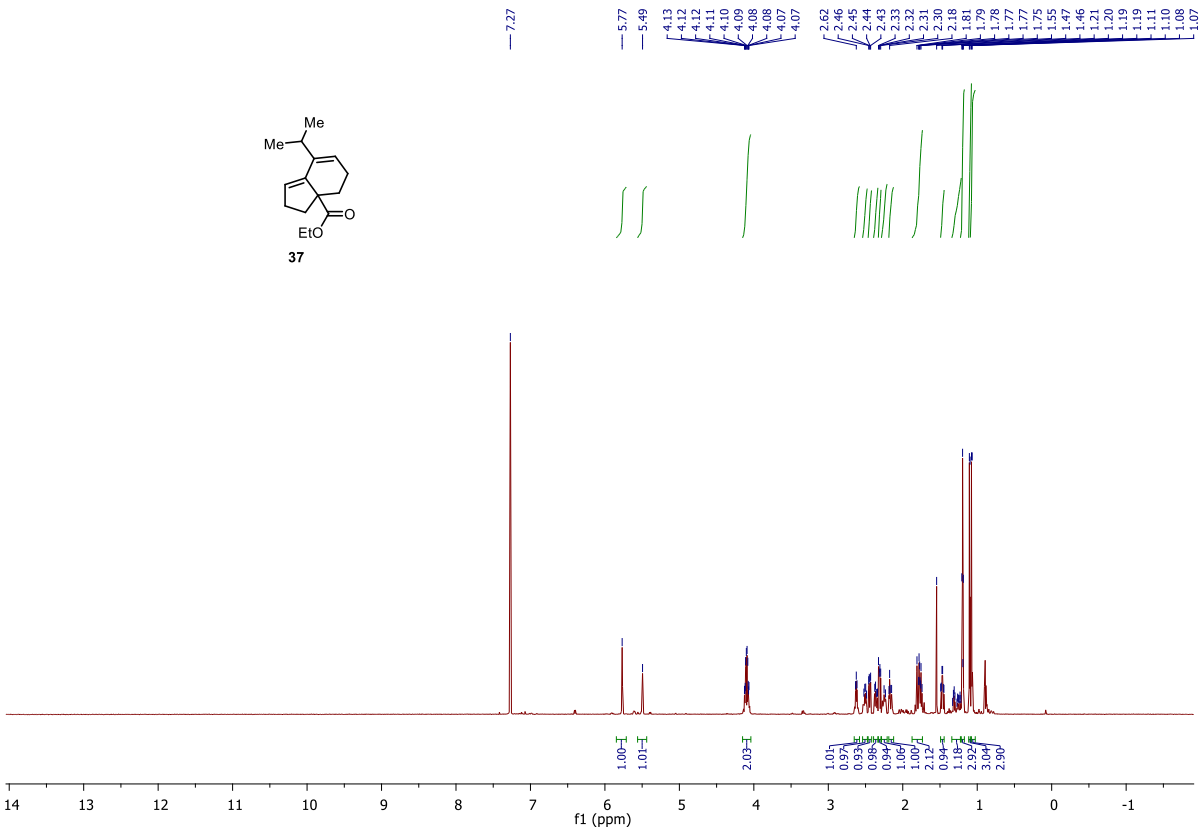
7.27
5.77
5.49
4.13
4.12
4.12
4.11
4.10
4.09
4.08
4.08
4.07
4.07
2.62
2.46
2.45
2.44
2.43
2.33
2.32
2.31
2.30
2.18
1.81
1.79
1.78
1.77
1.77
1.75
1.55
1.47
1.46
1.21
1.20
1.19
1.19
1.11
1.10
1.08
1.07
Me
Me
O
EtO
37
1.00
1.01
2.03
1.01
0.97
0.93
0.98
0.94
1.06
1.00
2.12
0.94
1.18
2.92
3.04
2.90
14
13
12
11
10
9
8
7
6
5
4
3
2
1
0
-1
f1 (ppm)

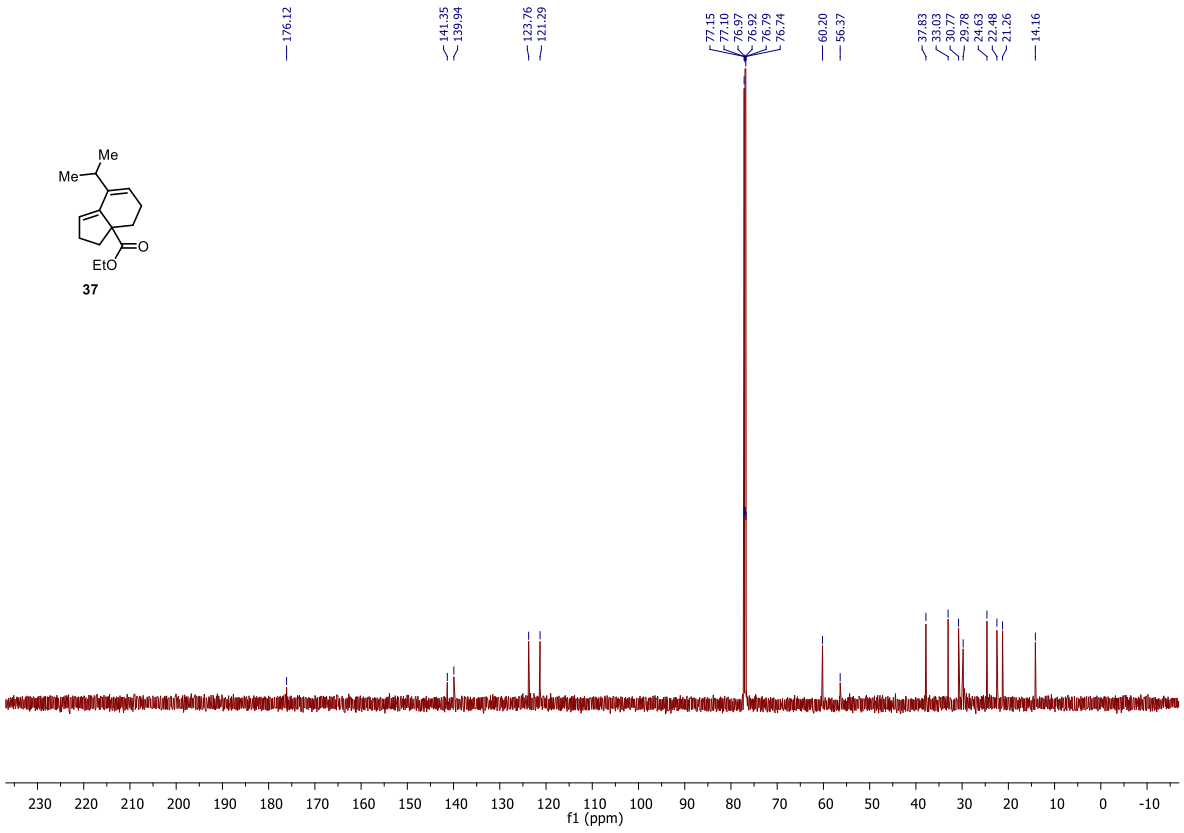
176.12
141.35
139.94
123.76
121.29
77.15
77.10
76.97
76.92
76.79
76.74
60.20
56.37
37.83
33.03
30.77
29.78
24.63
22.48
21.26
14.16
Me
Me
O
EtO
37
230
220
210
200
190
180
170
160
150
140
130
120
110
100
90
80
70
60
50
40
30
20
10
0
-10
f1 (ppm)

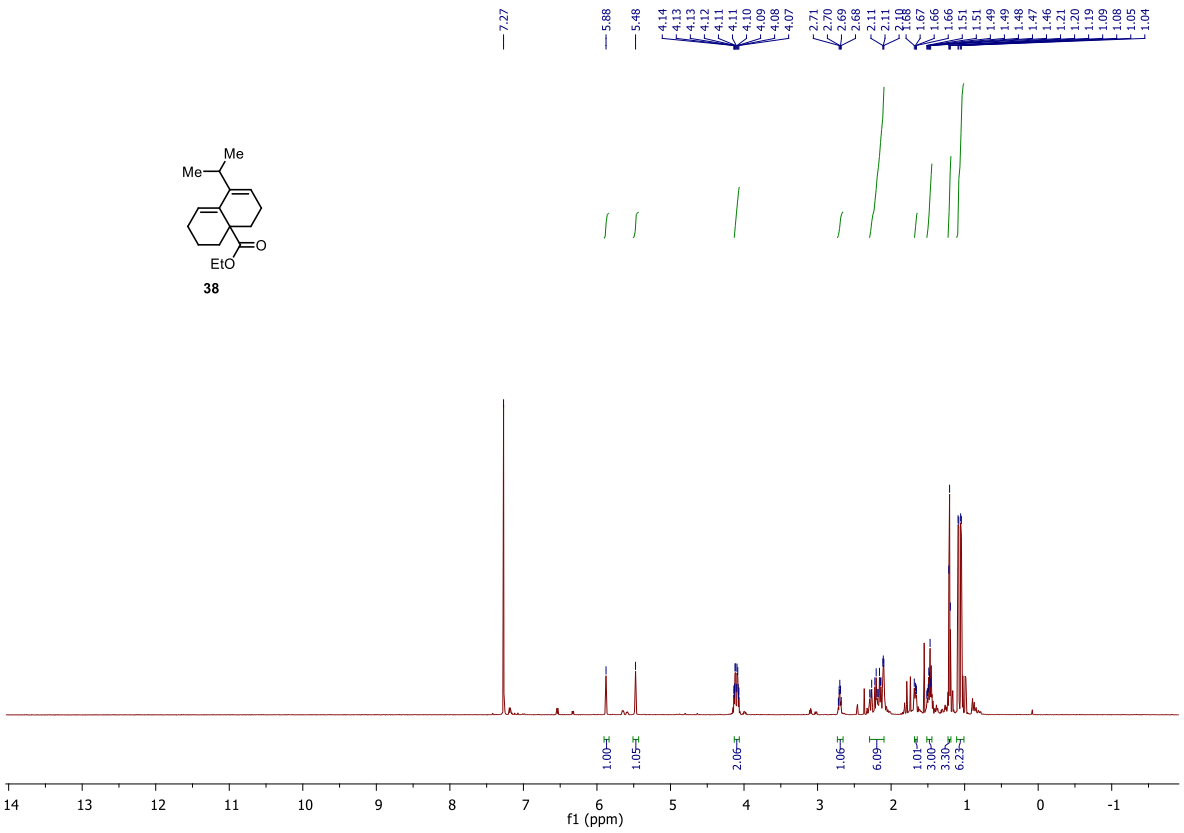
7.27
5.88
5.48
4.14
4.13
4.13
4.12
4.11
4.11
4.10
4.09
4.08
4.07
2.71
2.70
2.69
2.68
2.11
2.11
2.10
2.08
1.67
1.66
1.66
1.51
1.51
1.49
1.49
1.48
1.47
1.46
1.21
1.20
1.19
1.09
1.08
1.05
1.04
Me
Me
O
EtO
38
1.00
1.05
2.06
1.06
6.09
1.01
3.00
3.30
6.23
14
13
12
11
10
9
8
7
6
5
4
3
2
1
0
-1
f1 (ppm)

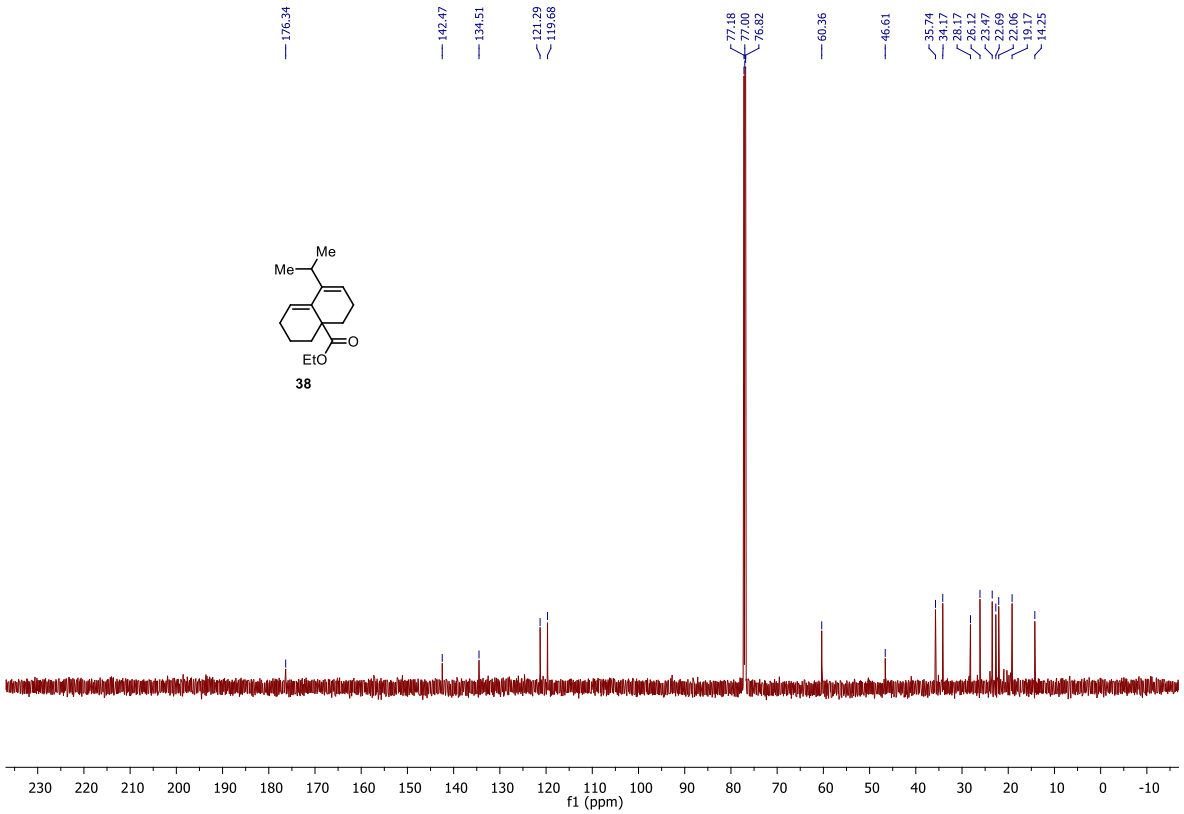
176.34
142.47
134.51
121.29
119.68
77.18
77.00
76.82
60.36
46.61
35.74
34.17
28.17
26.12
23.47
22.69
22.06
19.17
14.25
Me
Me
O
EtO
38
230
220
210
200
190
180
170
160
150
140
130
120
110
100
90
80
70
60
50
40
30
20
10
0
-10
f1 (ppm)

Me
Me
O
OEt

39

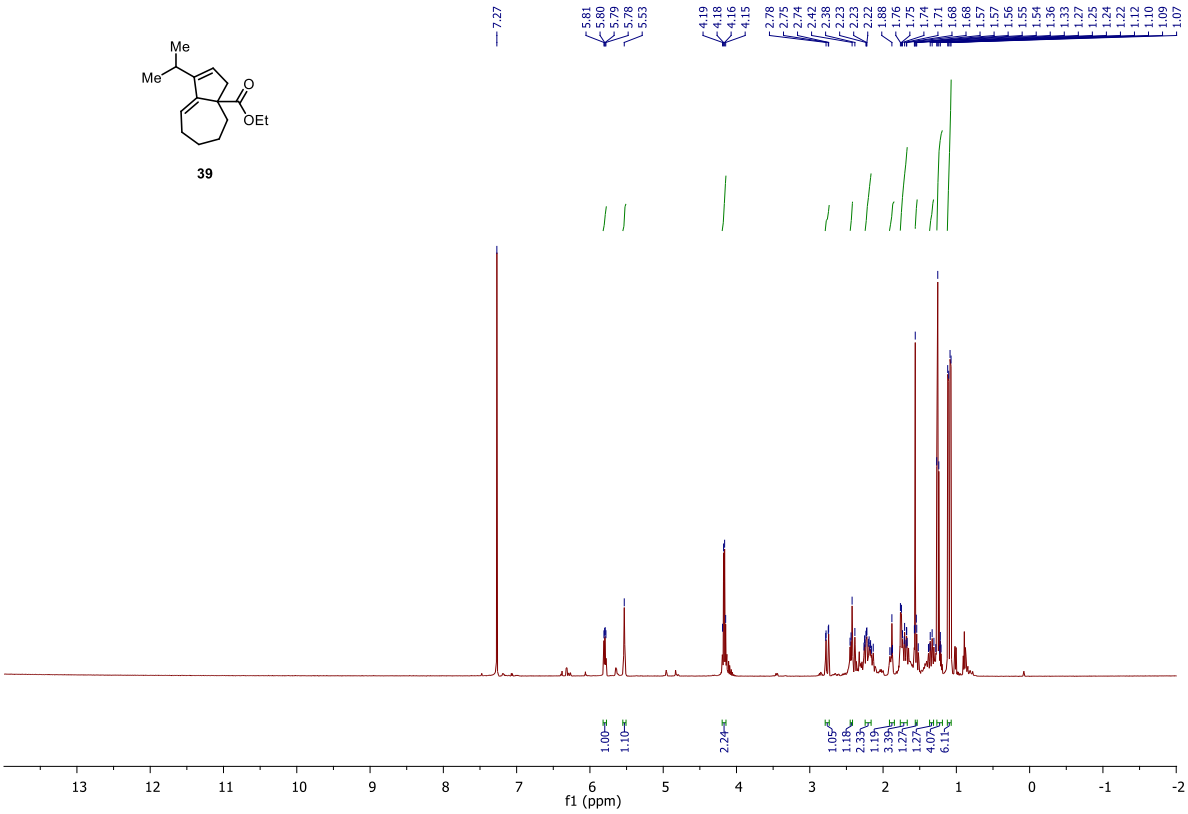
7.27
5.81
5.80
5.79
5.78
5.53
4.19
4.18
4.16
4.15
2.78
2.75
2.74
2.42
2.38
2.23
2.23
2.22
1.88
1.76
1.75
1.74
1.71
1.68
1.68
1.57
1.57
1.56
1.55
1.54
1.36
1.33
1.27
1.25
1.24
1.22
1.12
1.10
1.09
1.07
1.00
1.10
2.24
1.05
1.18
2.33
1.15
3.39
1.27
1.27
4.07
6.11
13
12
11
10
9
8
7
6
5
4
3
2
1
0
-1
-2
f1 (ppm)

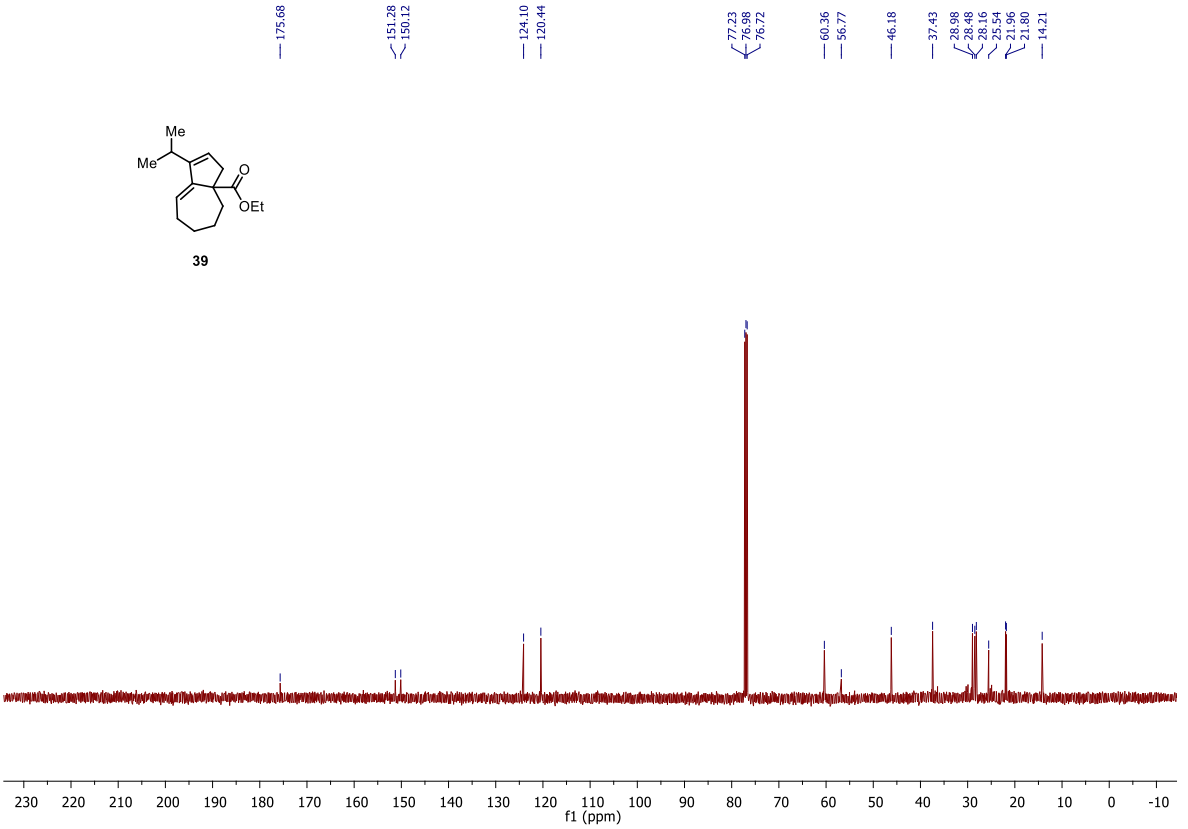
175.68
151.28
150.12
124.10
120.44
77.23
76.98
76.72
60.36
56.77
46.18
37.43
28.98
28.48
28.16
25.54
21.96
21.80
14.21
230
220
210
200
190
180
170
160
150
140
130
120
110
100
90
80
70
60
50
40
30
20
10
0
-10
f1 (ppm)

Me
Me
O
OEt

39

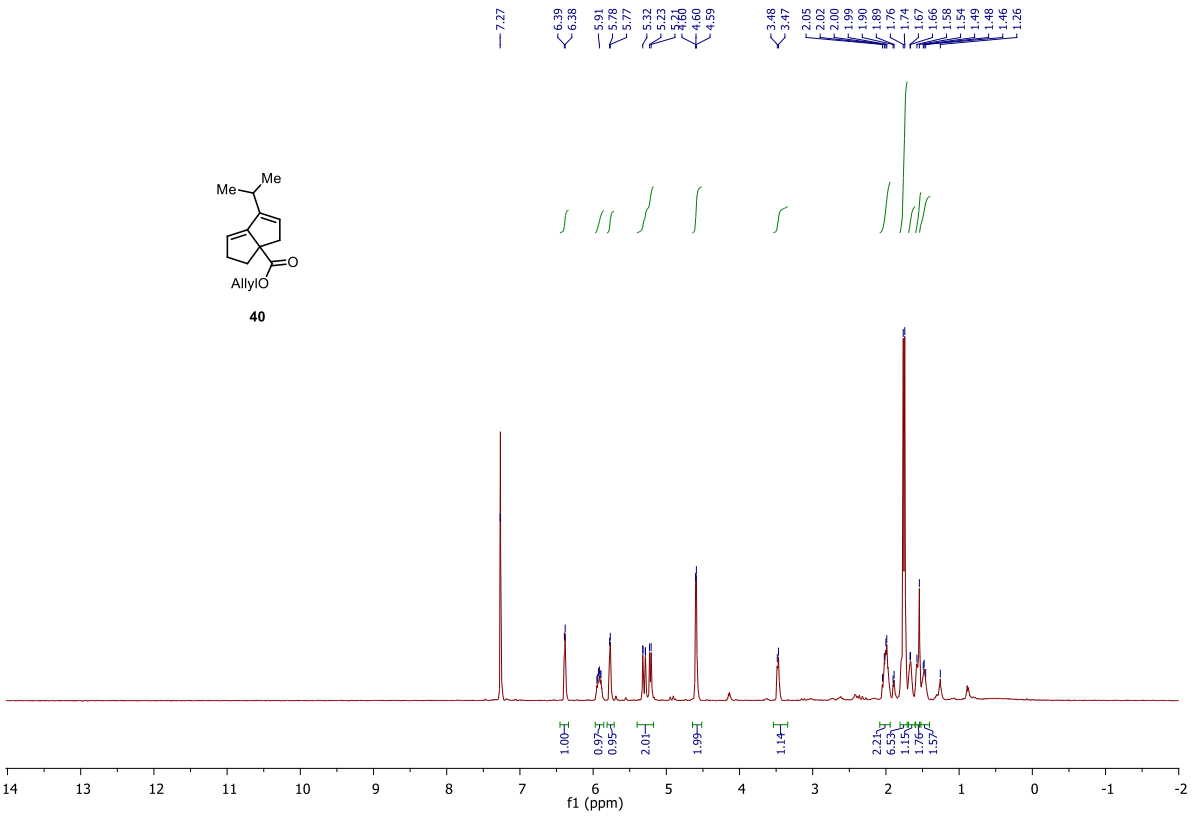
7.27
6.39
6.38
5.91
5.78
5.77
5.32
5.23
5.21
4.60
4.59
3.48
3.47
2.05
2.02
2.00
1.99
1.90
1.89
1.76
1.74
1.67
1.66
1.58
1.54
1.49
1.48
1.46
1.26
Me
Me
O
AllylO
40
1.00
0.97
0.95
2.01
1.99
1.14
2.21
6.53
1.15
1.76
1.57
f1 (ppm)

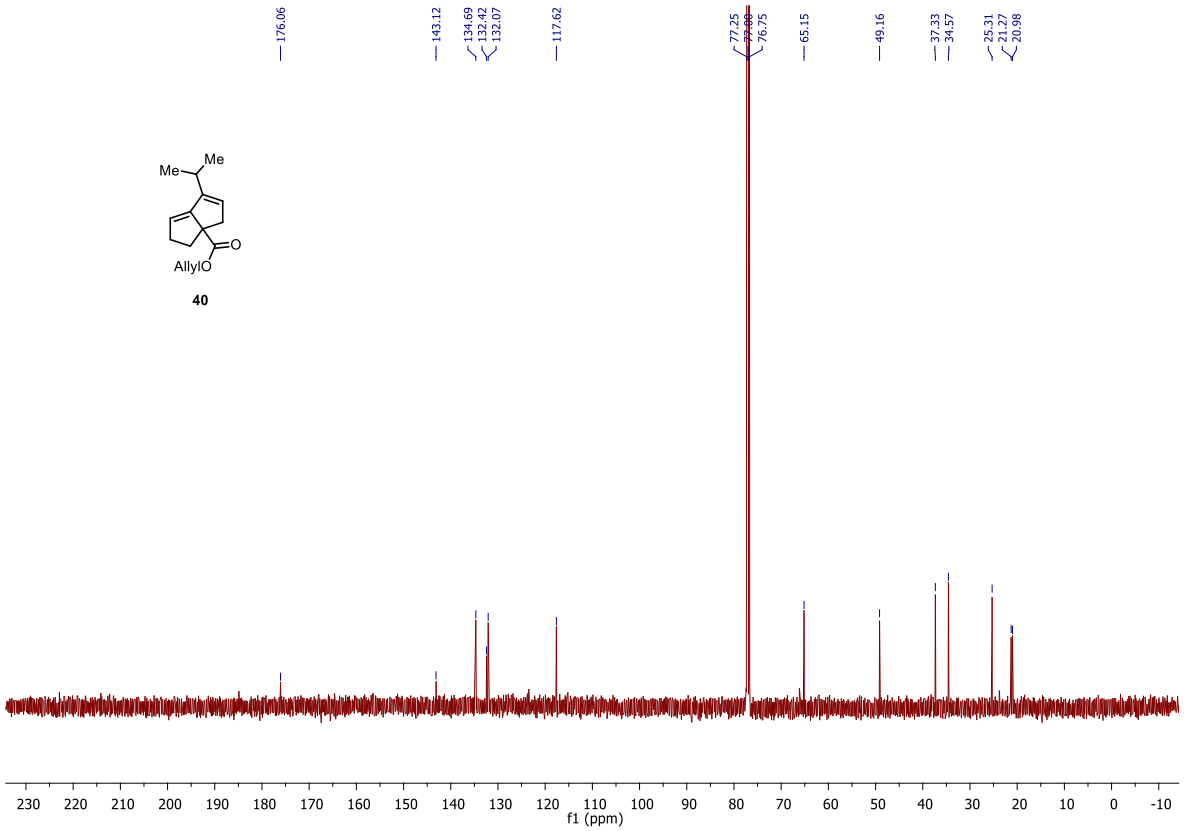
176.06
143.12
134.69
132.42
132.07
117.62
77.25
77.00
76.75
65.15
49.16
37.33
34.57
25.31
21.27
20.98
Me
Me
O
AllylO
40
f1 (ppm)

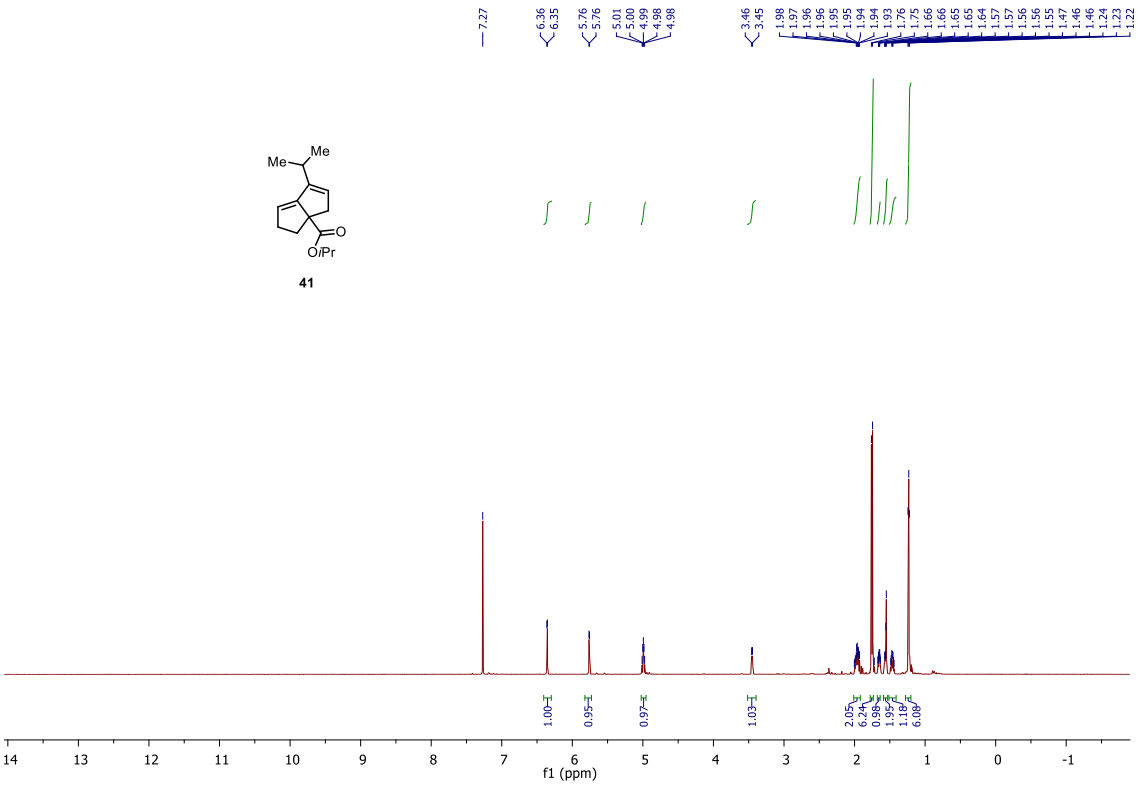
7.27
6.36
6.35
5.76
5.76
5.01
5.00
4.99
4.98
4.98
3.46
3.45
1.98
1.97
1.96
1.96
1.95
1.95
1.94
1.93
1.76
1.75
1.66
1.66
1.65
1.65
1.64
1.57
1.57
1.56
1.56
1.55
1.47
1.46
1.46
1.24
1.23
1.22
Me
Me
O
OiPr
41
1.00
0.95
0.97
1.03
2.05
6.24
0.98
1.95
1.18
6.08
14 13 12 11 10 9 8 7 6 5 4 3 2 1 0 -1
f1 (ppm)

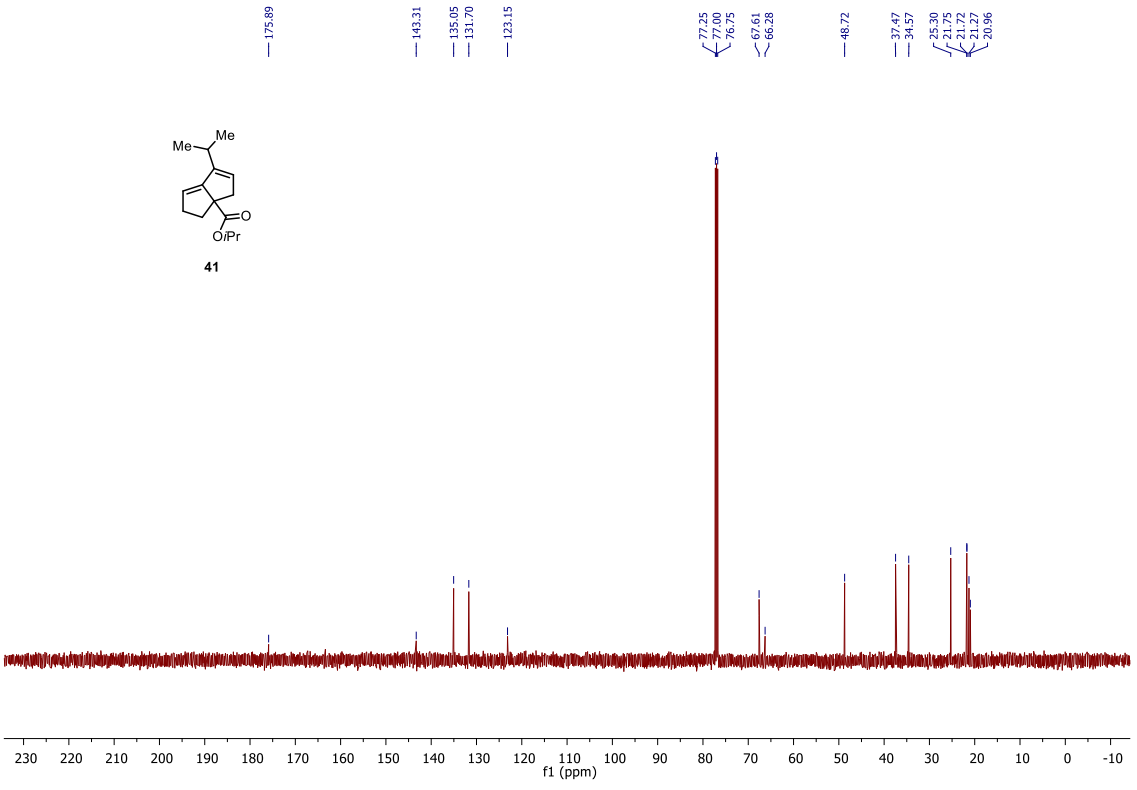
175.89
143.31
135.05
131.70
123.15
77.25
77.00
76.75
67.61
66.28
48.72
37.47
34.57
25.30
21.75
21.72
21.27
20.96
Me
Me
O
OiPr
41
230 220 210 200 190 180 170 160 150 140 130 120 110 100 90 80 70 60 50 40 30 20 10 0 -10
f1 (ppm)

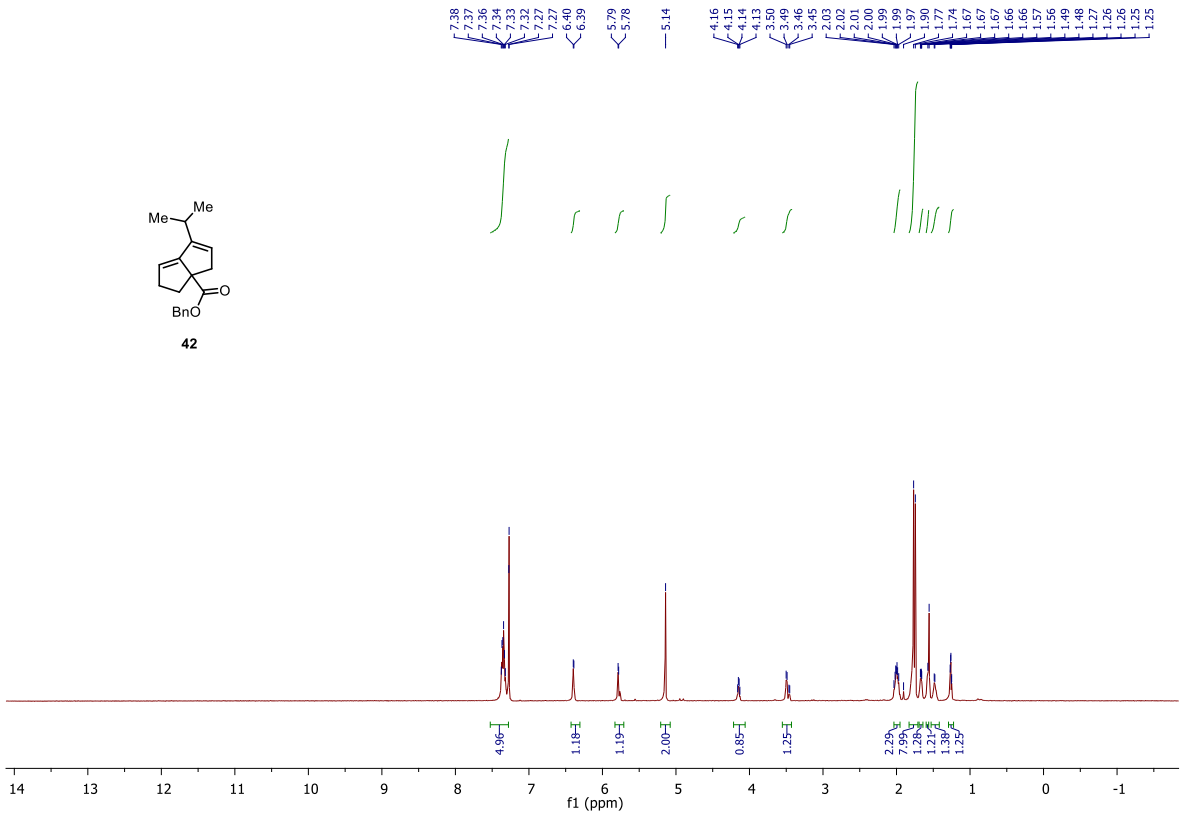
Me
Me
O
BnO
42
f1 (ppm)

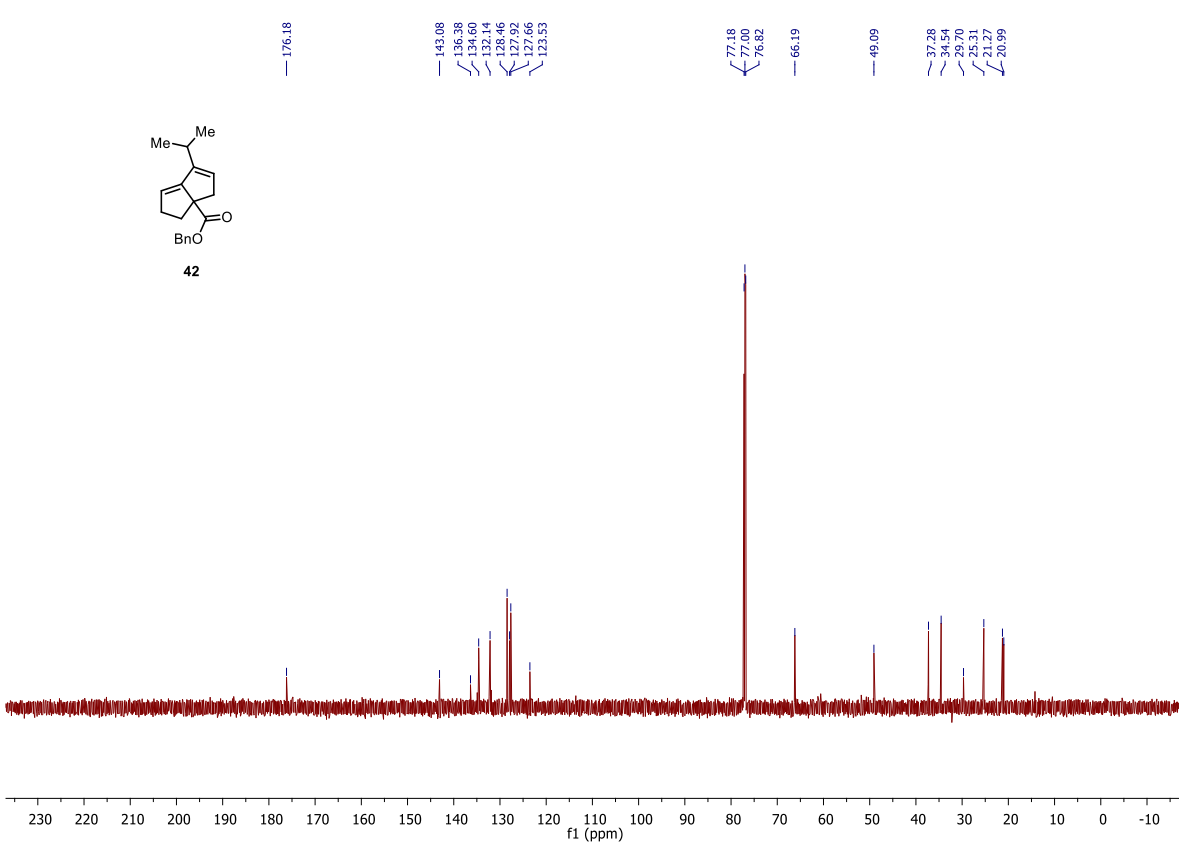
Me
Me
O
BnO
42
f1 (ppm)

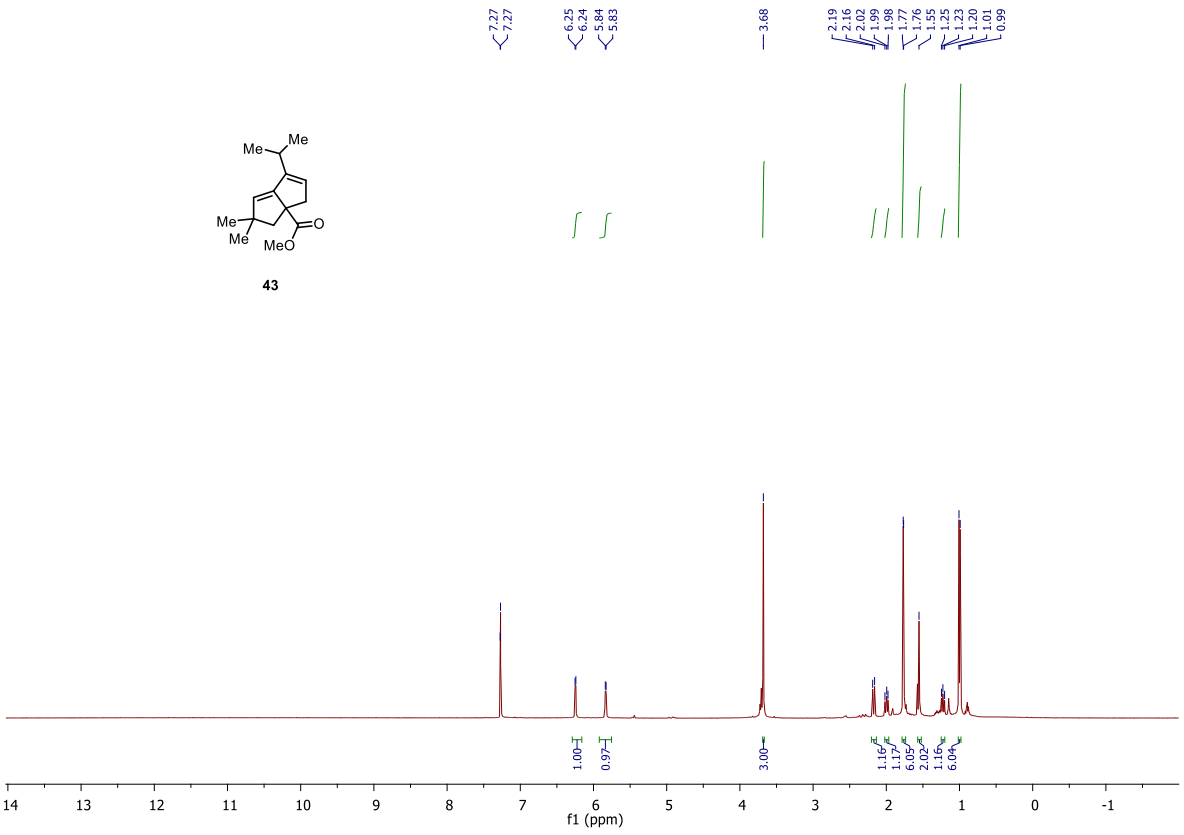
7.27
7.27
6.25
6.24
5.84
5.83
3.68
2.19
2.16
2.02
1.99
1.98
1.77
1.76
1.55
1.25
1.23
1.20
1.01
0.99
Me
Me
Me
Me
MeO
O
43
1.00
0.97
3.00
1.16
1.17
6.05
2.02
1.16
6.04
f1 (ppm)

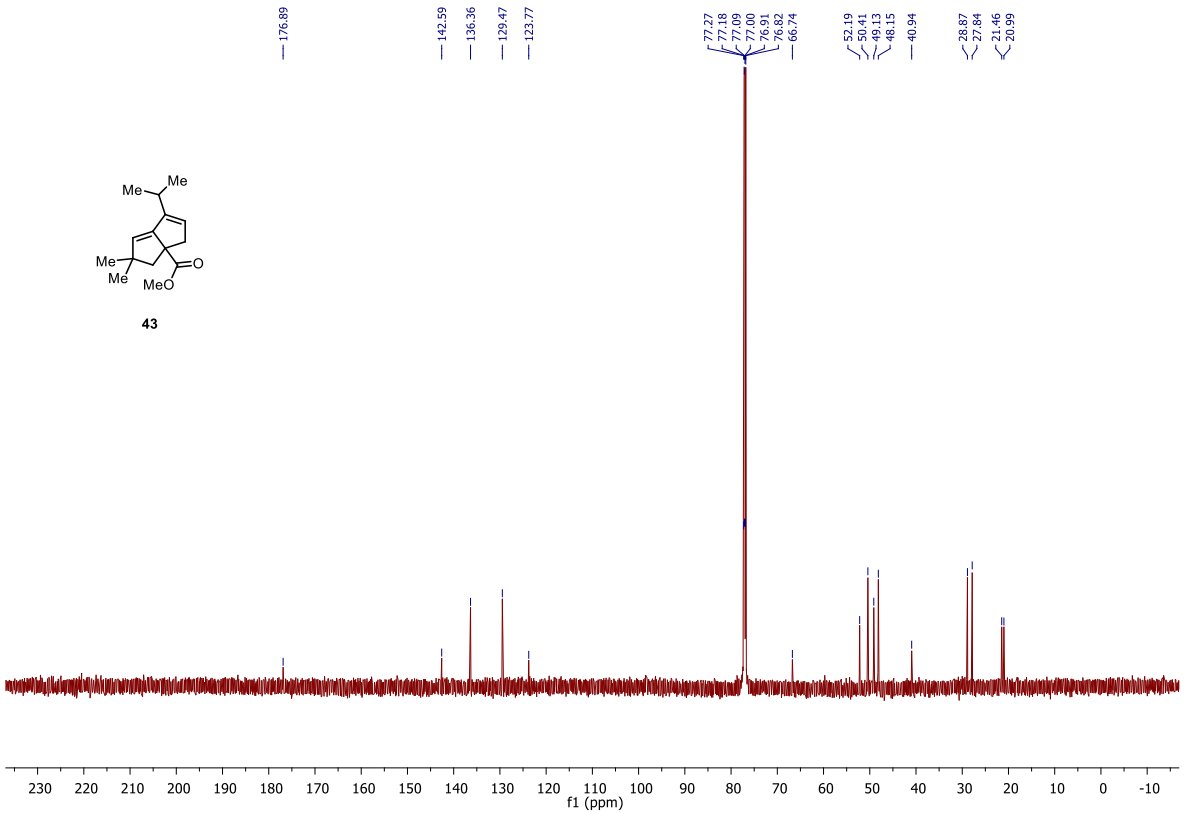
176.89
142.59
136.36
129.47
123.77
77.27
77.18
77.09
77.00
76.91
76.82
66.74
52.19
50.41
49.13
48.15
40.94
28.87
27.84
21.46
20.99
Me
Me
Me
Me
MeO
O
43
f1 (ppm)

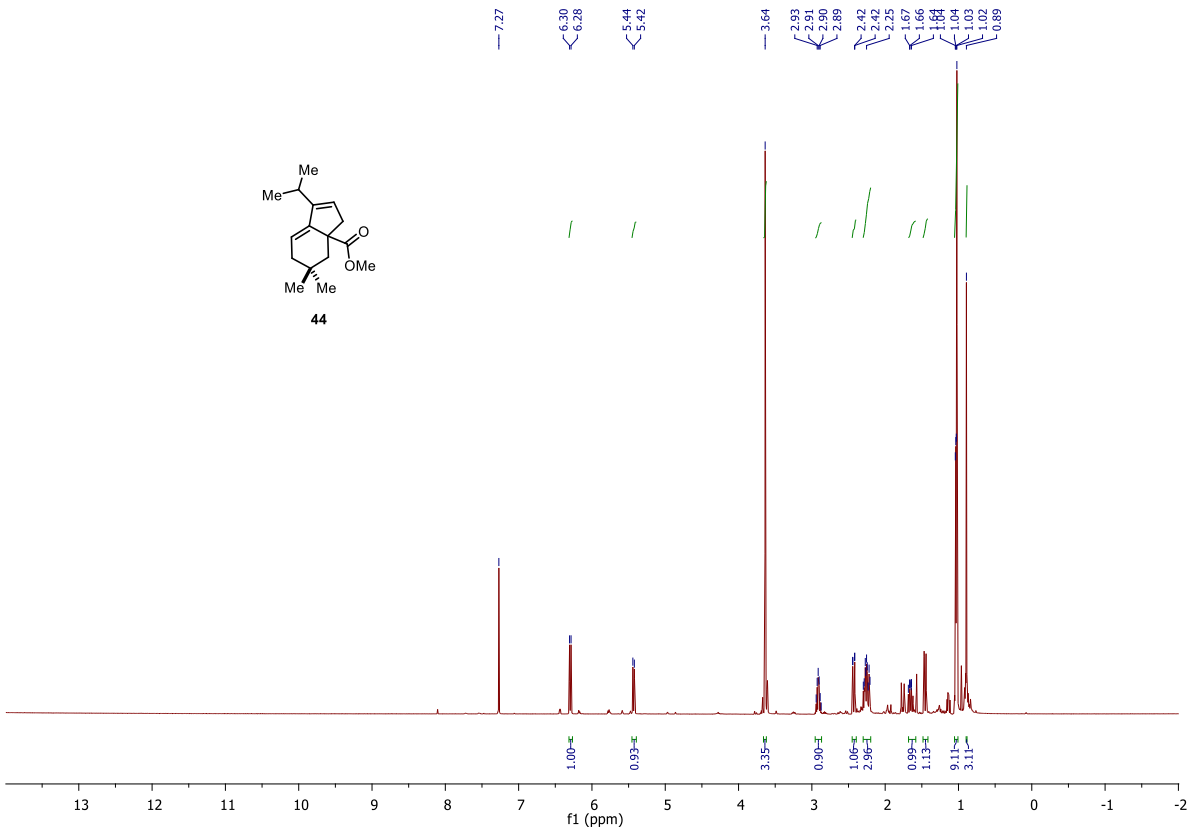
7.27
6.30
6.28
5.44
5.42
3.64
2.93
2.91
2.90
2.89
2.42
2.42
2.25
1.67
1.66
1.64
1.04
1.03
1.02
0.89
Me
Me
O
OMe
Me
Me
44
1.00
0.93
3.35
0.90
1.06
2.96
0.99
1.13
9.11
3.11
f1 (ppm)

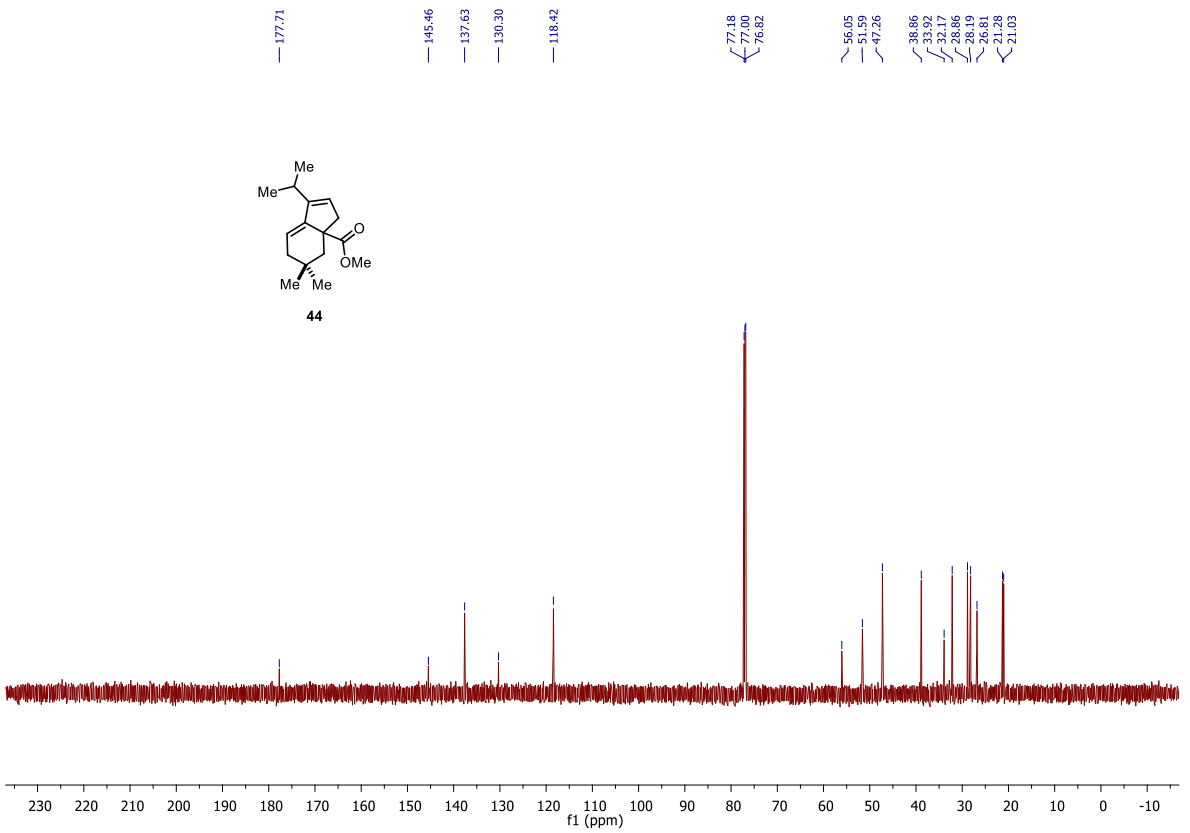
177.71
145.46
137.63
130.30
118.42
77.18
77.00
76.82
56.05
51.59
47.26
38.86
33.92
32.17
28.86
28.19
26.81
21.28
21.03
Me
Me
O
OMe
Me
Me
44
f1 (ppm)

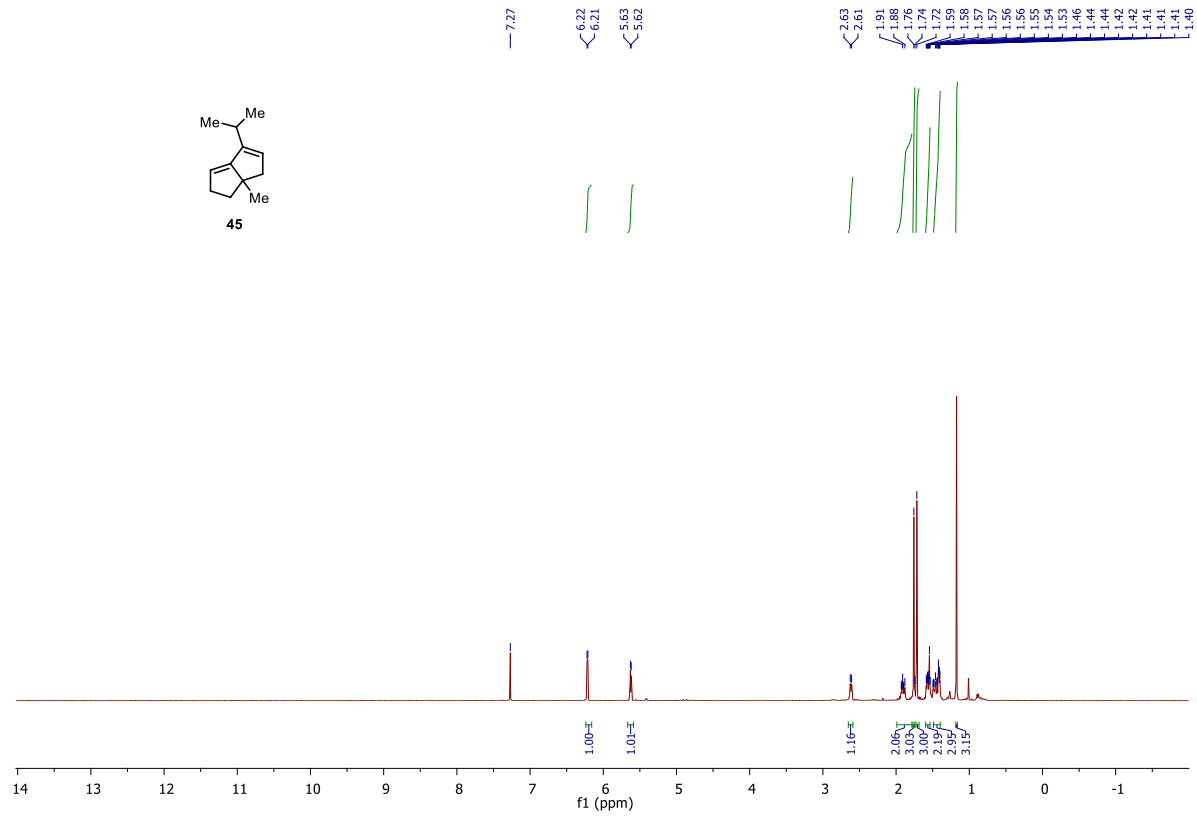
7.27
6.22
6.21
5.63
5.62
2.63
2.61
1.91
1.88
1.76
1.74
1.72
1.59
1.58
1.57
1.57
1.56
1.56
1.55
1.54
1.53
1.46
1.44
1.44
1.42
1.42
1.41
1.41
1.41
1.40
Me
Me
Me
45
1.00
1.01
1.16
2.06
3.03
3.00
2.19
2.95
3.15
14
13
12
11
10
9
8
7
6
5
4
3
2
1
0
-1
f1 (ppm)

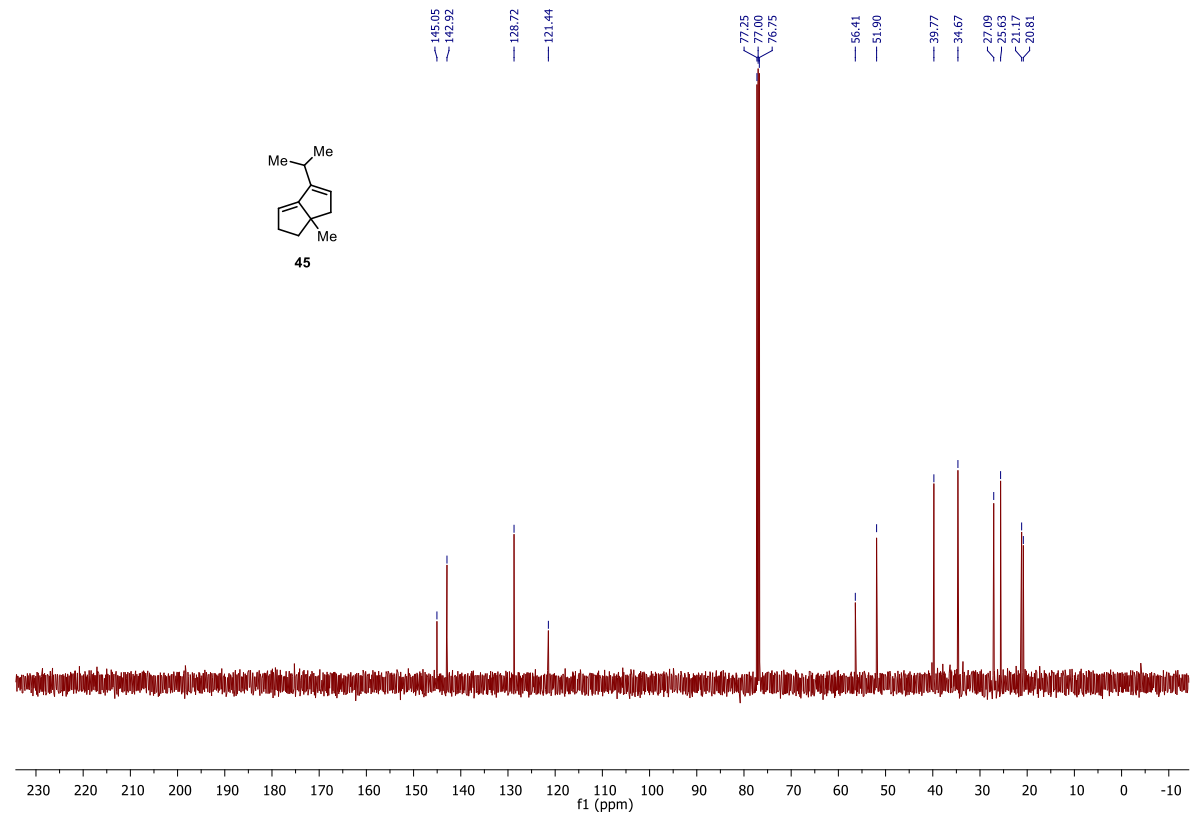
145.05
142.92
128.72
121.44
77.25
77.00
76.75
56.41
51.90
39.77
34.67
27.09
25.63
21.17
20.81
Me
Me
Me
45
230
220
210
200
190
180
170
160
150
140
130
120
110
100
90
80
70
60
50
40
30
20
10
0
-10
f1 (ppm)

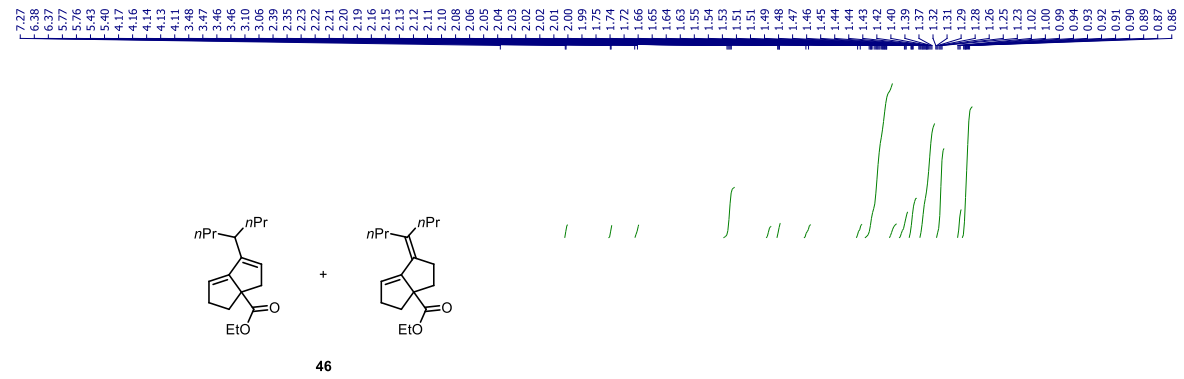
nPr
nPr
EtO
O
+
nPr
nPr
EtO
O

46

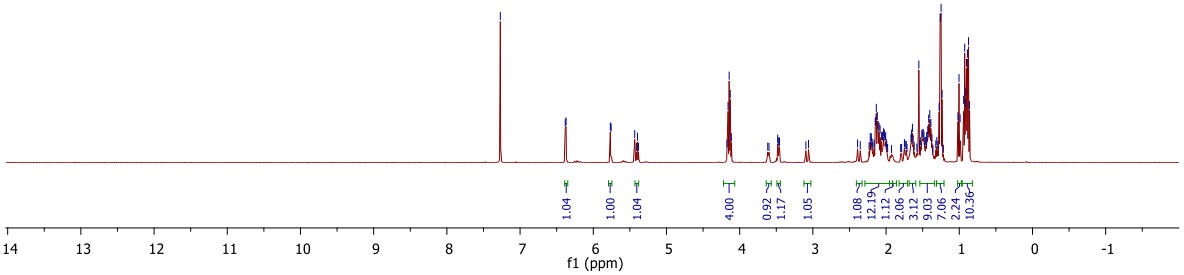
1.04
1.00
1.04
4.00
0.92
1.17
1.05
1.08
12.19
1.12
2.06
3.12
9.03
7.06
2.24
10.36
14 13 12 11 10 9 8 7 6 5 4 3 2 1 0 -1
f1 (ppm)

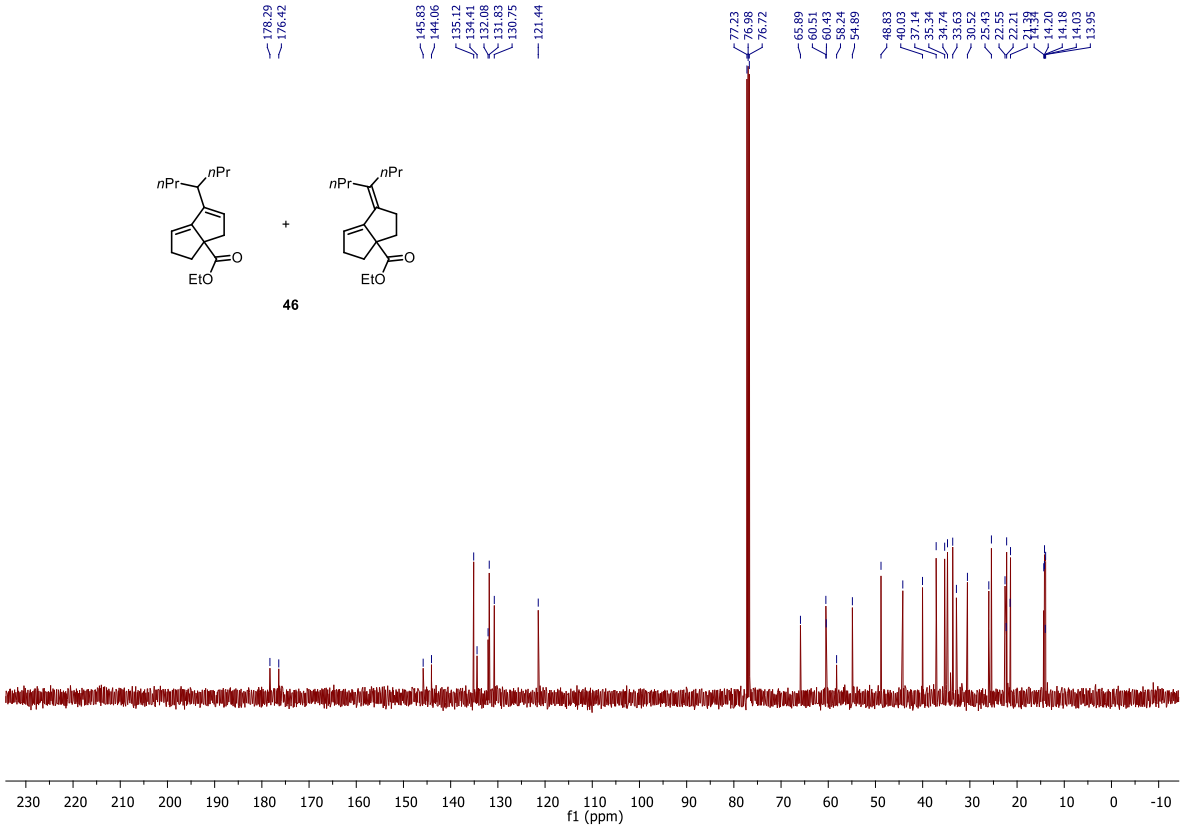
178.29
176.42
145.83
144.06
135.12
134.41
132.08
131.83
130.75
121.44
77.23
76.98
76.72
65.89
60.51
60.43
58.24
54.89
48.83
40.03
37.14
35.34
34.74
33.63
30.52
25.43
22.55
22.21
21.39
21.34
14.20
14.18
14.03
13.95
nPr
nPr
EtO
O
+
nPr
nPr
EtO
O
230 220 210 200 190 180 170 160 150 140 130 120 110 100 90 80 70 60 50 40 30 20 10 0 -10
f1 (ppm)

46

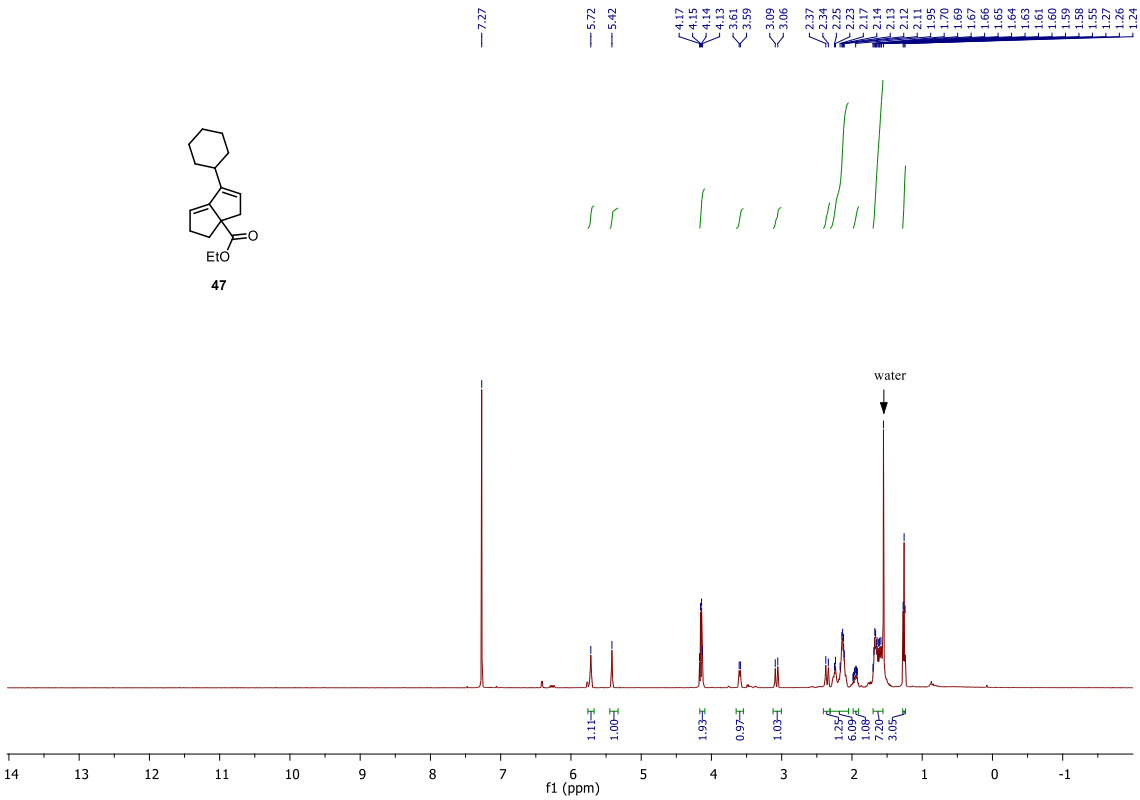
7.27
5.72
5.42
4.17
4.15
4.14
4.13
3.61
3.59
3.09
3.06
2.37
2.34
2.25
2.23
2.17
2.14
2.13
2.12
2.11
1.95
1.70
1.69
1.67
1.66
1.65
1.64
1.63
1.61
1.60
1.59
1.58
1.55
1.27
1.26
1.24
EtO
O
47
water
1.11
1.00
1.93
0.97
1.03
1.25
6.09
1.08
7.20
3.05
f1 (ppm)

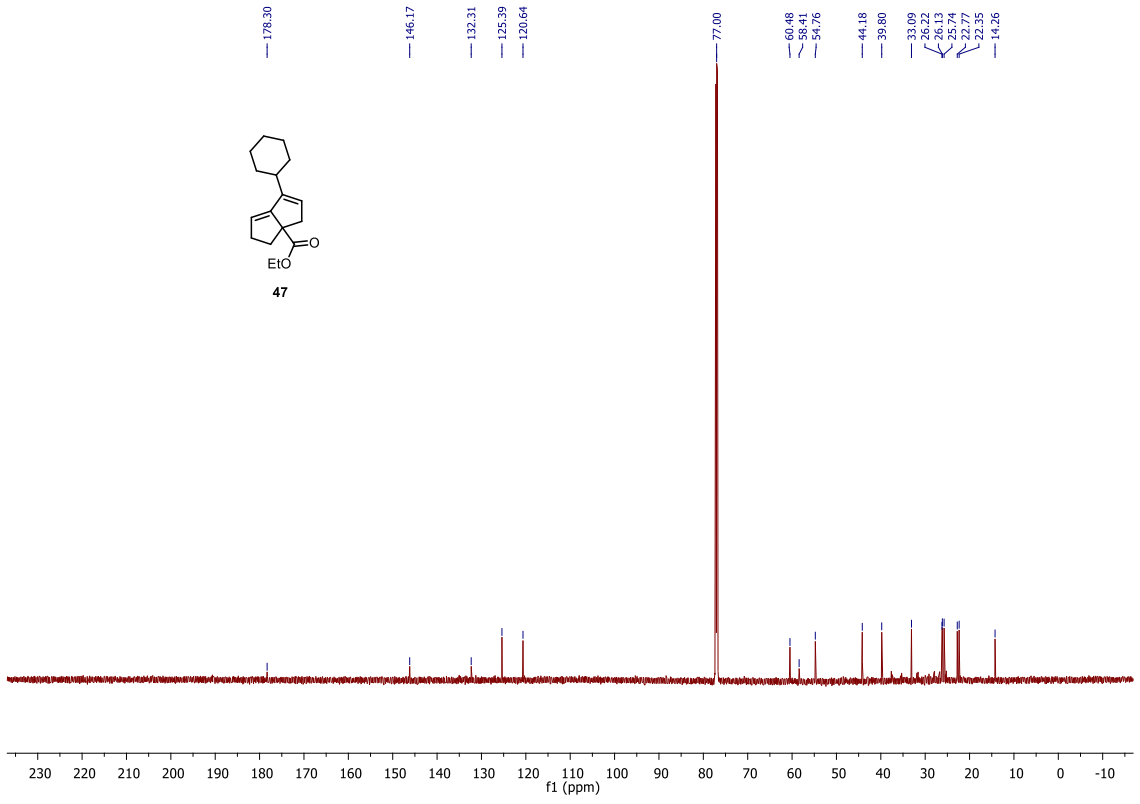
178.30
146.17
132.31
125.39
120.64
77.00
60.48
58.41
54.76
44.18
39.80
33.09
26.22
26.13
25.74
22.77
22.35
14.26
EtO
O
47
f1 (ppm)

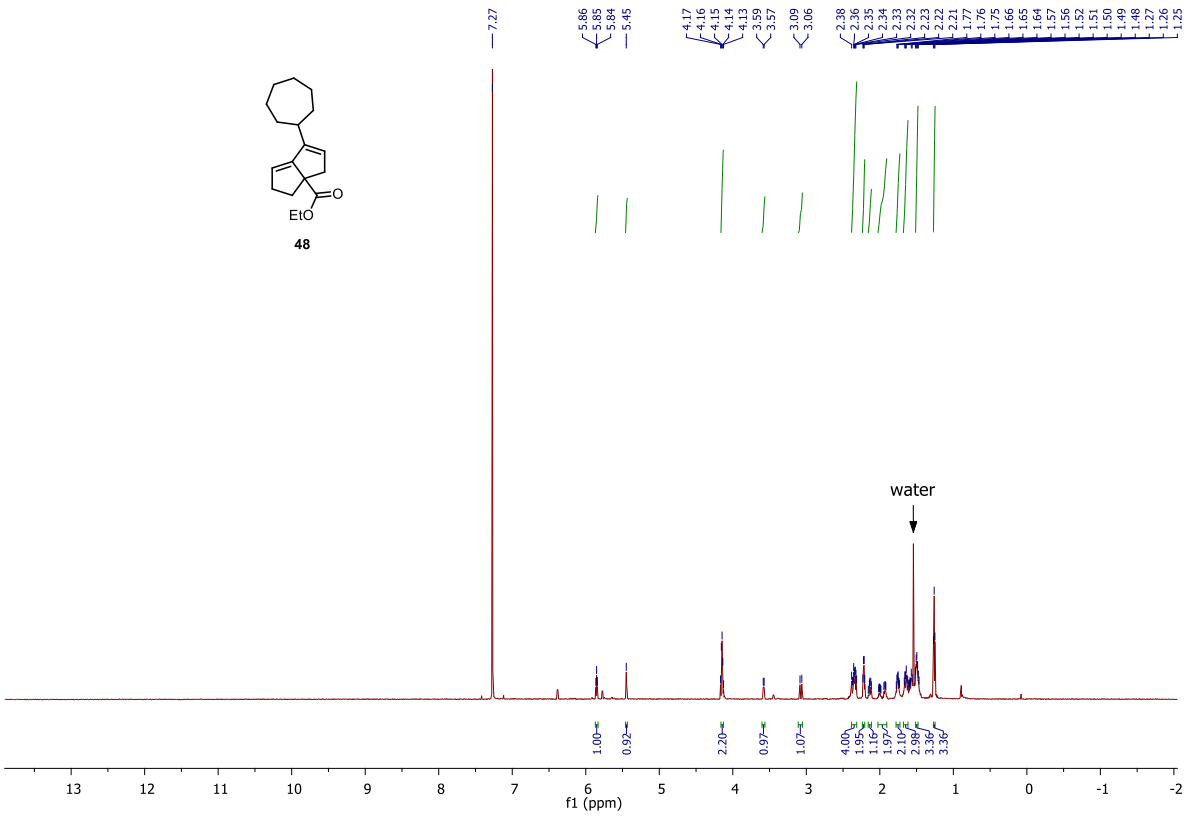
7.27
5.86
5.85
5.84
5.45
4.17
4.16
4.15
4.14
4.13
3.59
3.57
3.09
3.06
2.38
2.36
2.35
2.34
2.33
2.32
2.23
2.22
2.21
1.77
1.76
1.75
1.66
1.65
1.64
1.57
1.56
1.52
1.51
1.50
1.49
1.48
1.27
1.26
1.25
EtO
O
48
water
1.00
0.92
2.20
0.97
1.07
4.00
1.95
1.16
1.97
2.10
2.98
3.36
3.36
f1 (ppm)

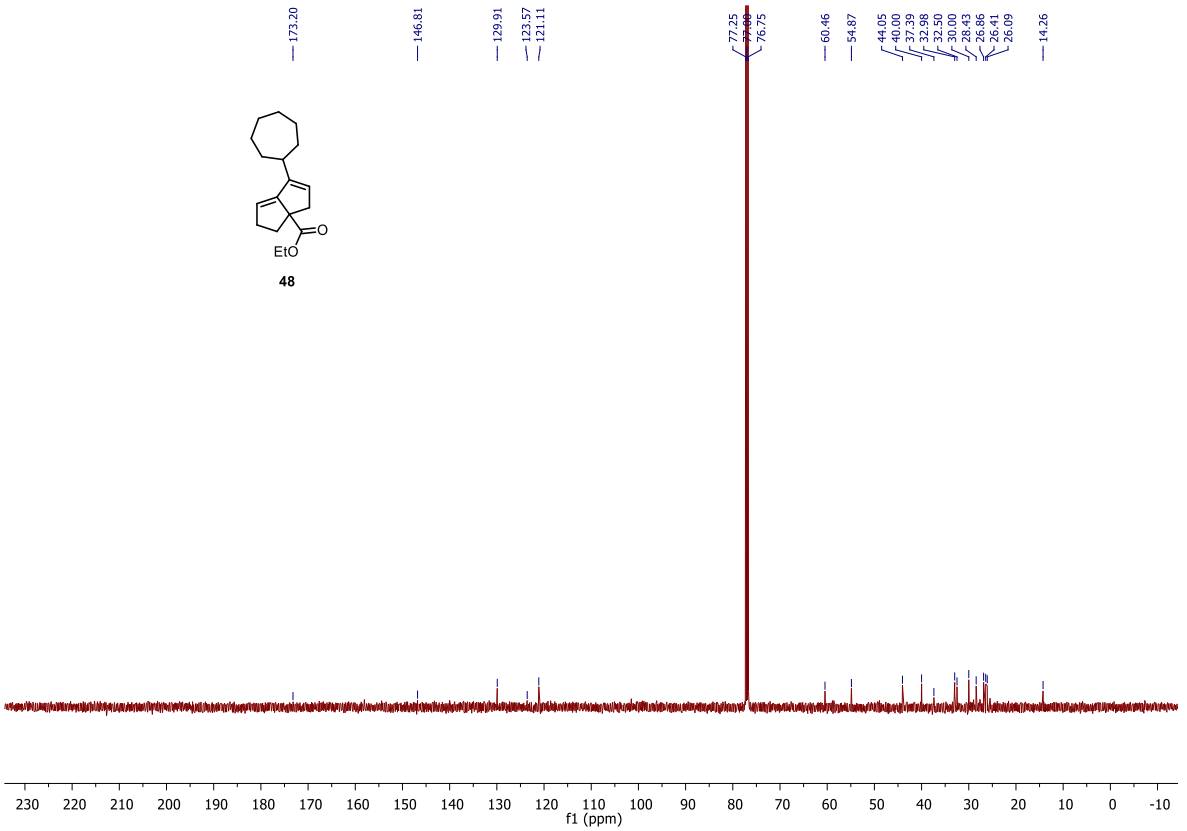
173.20
146.81
129.91
123.57
121.11
77.25
77.00
76.75
60.46
54.87
44.05
40.00
37.39
32.98
32.50
30.00
28.43
26.86
26.41
26.09
14.26
EtO
O
48
f1 (ppm)

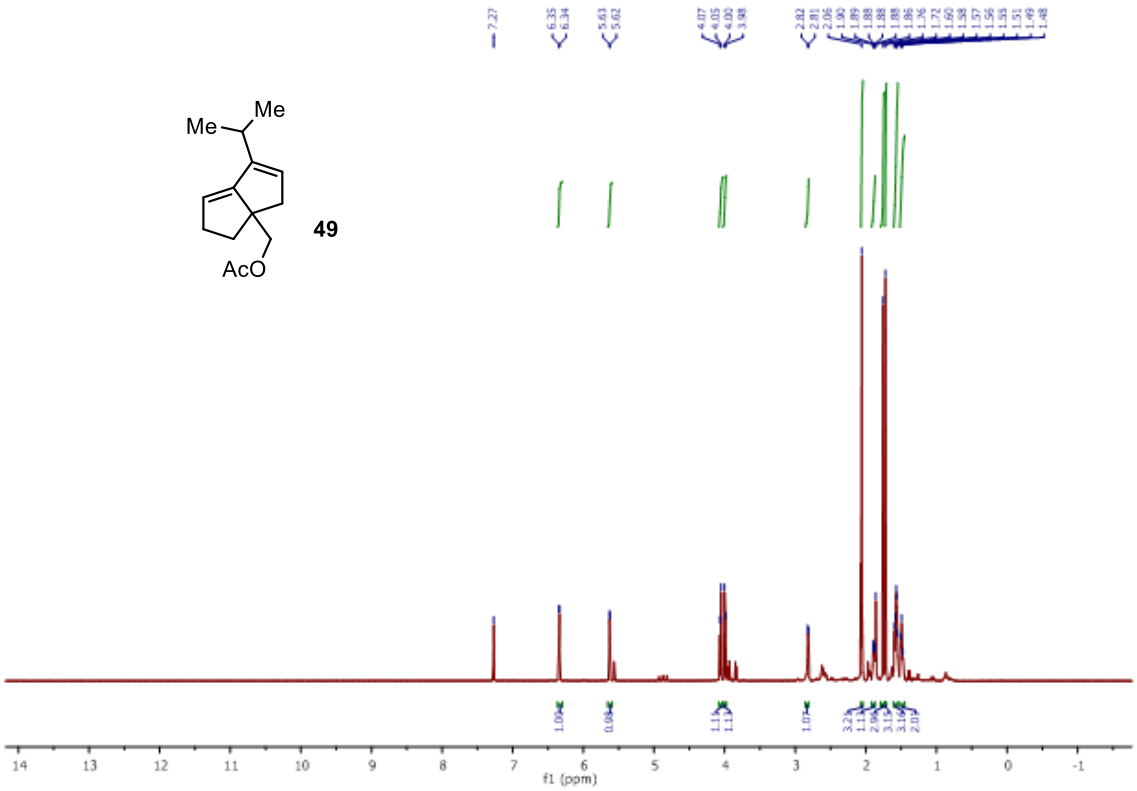
Me
Me
AcO
49
f1 (ppm)

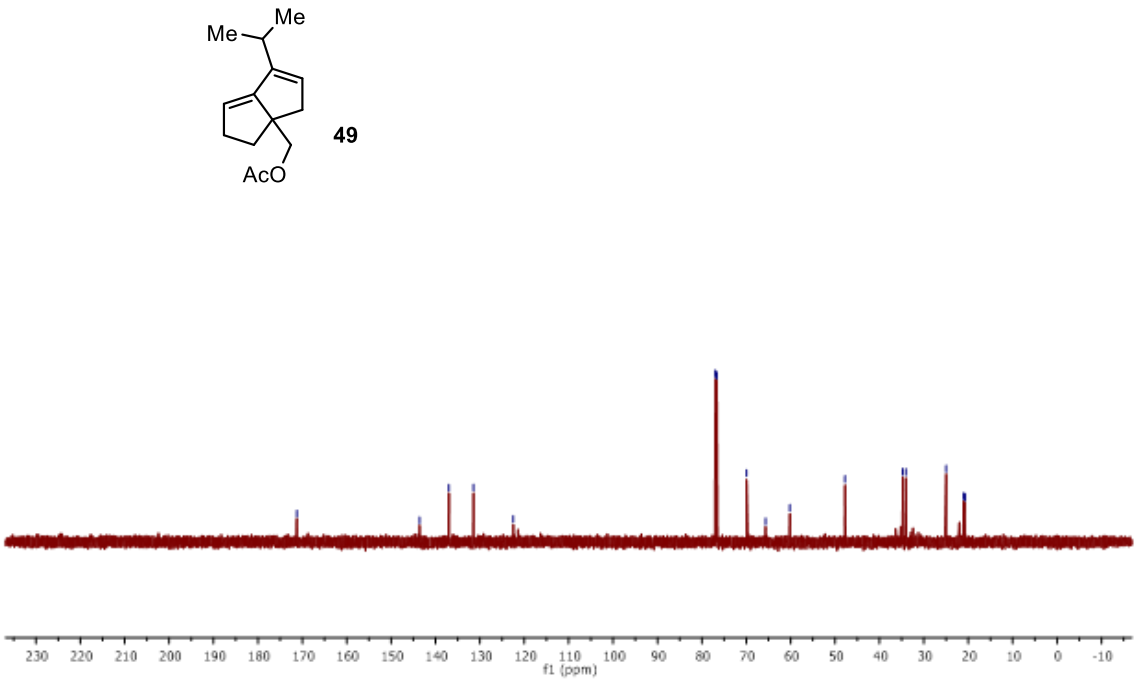
Me
Me
AcO
49
f1 (ppm)

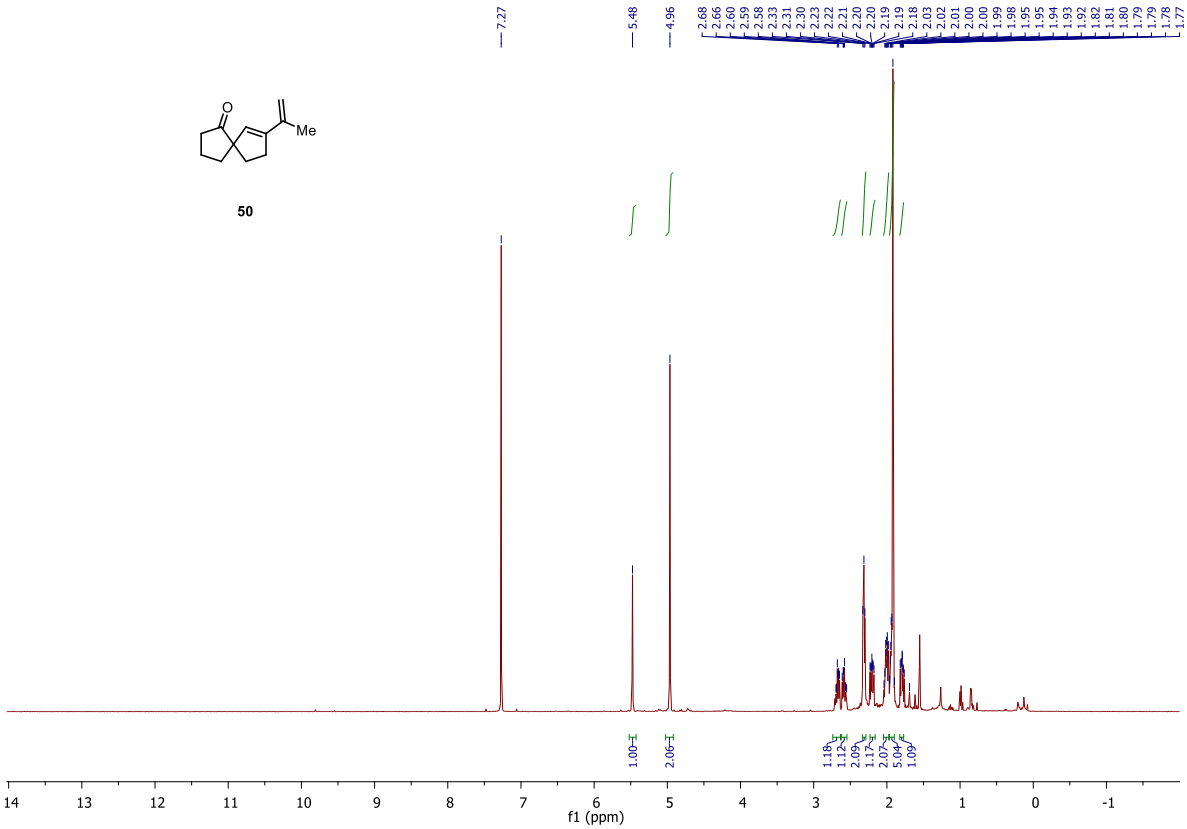
7.27
5.48
4.96
2.68 2.66 2.60 2.59 2.58 2.33 2.31 2.30 2.23 2.22 2.21 2.20 2.20 2.19 2.19 2.18 2.03 2.02 2.01 2.00 2.00 1.99 1.98 1.95 1.95 1.94 1.93 1.92 1.82 1.81 1.80 1.79 1.79 1.78 1.77
O
Me
50
1.00
2.06
1.18
1.12
2.05
1.17
2.07
5.04
1.09
14 13 12 11 10 9 8 7 6 5 4 3 2 1 0 -1
f1 (ppm)

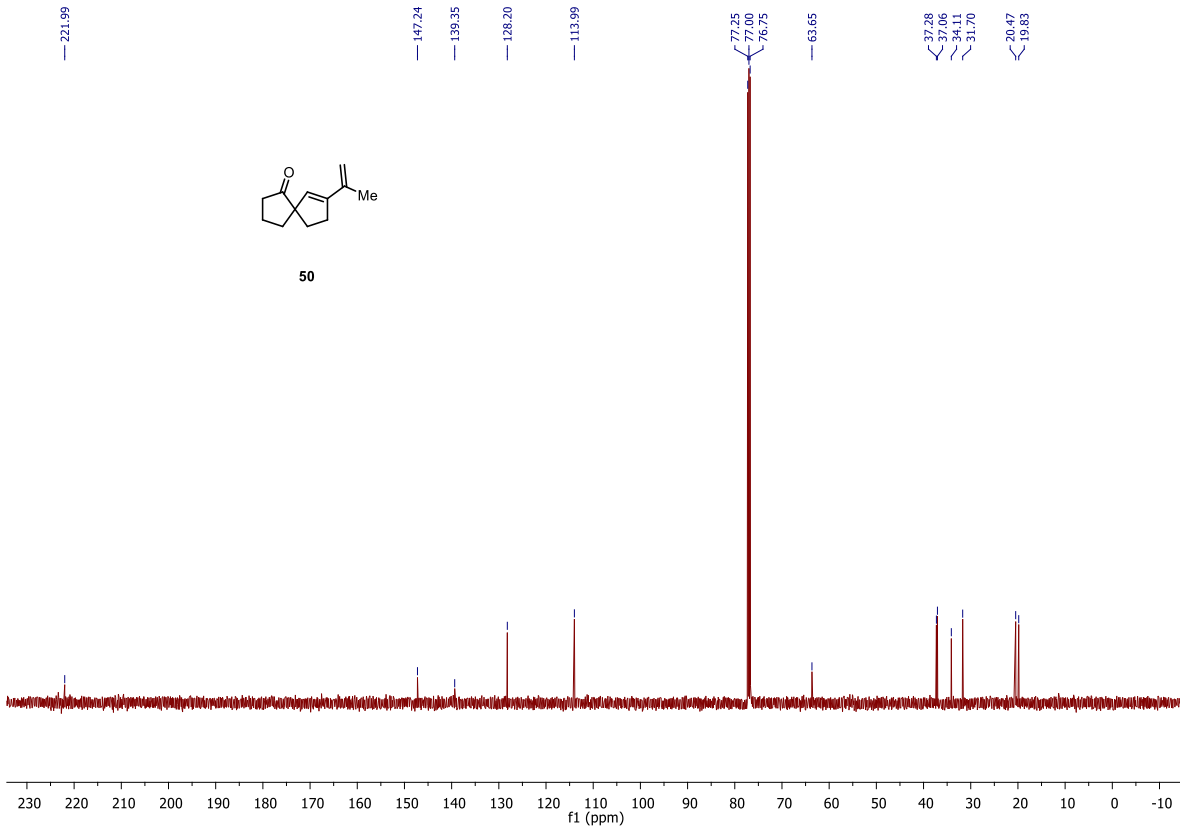
221.99
147.24
139.35
128.20
113.99
77.25
77.00
76.75
63.65
37.28
37.06
34.11
31.70
20.47
19.83
O
Me
50
230 220 210 200 190 180 170 160 150 140 130 120 110 100 90 80 70 60 50 40 30 20 10 0 -10
f1 (ppm)

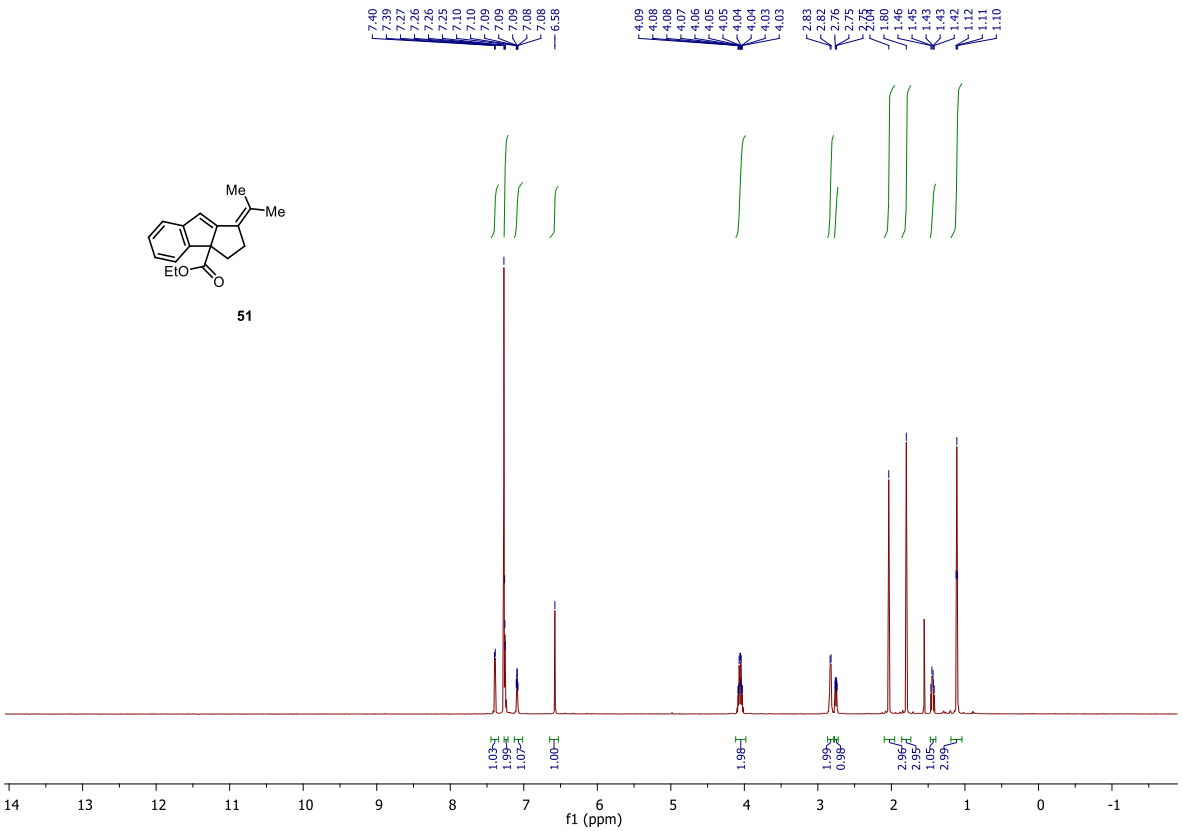
7.40
7.39
7.27
7.26
7.26
7.25
7.10
7.10
7.09
7.09
7.09
7.08
7.08
6.58
4.09
4.08
4.08
4.07
4.06
4.05
4.05
4.04
4.04
4.03
4.03
2.83
2.82
2.76
2.75
2.75
2.04
1.80
1.46
1.45
1.43
1.43
1.42
1.12
1.11
1.10
Me
Me
EtO
O
51
1.03
1.99
1.07
1.00
1.98
1.99
0.98
2.96
2.95
1.05
2.99
14
13
12
11
10
9
8
7
6
5
4
3
2
1
0
-1
f1 (ppm)

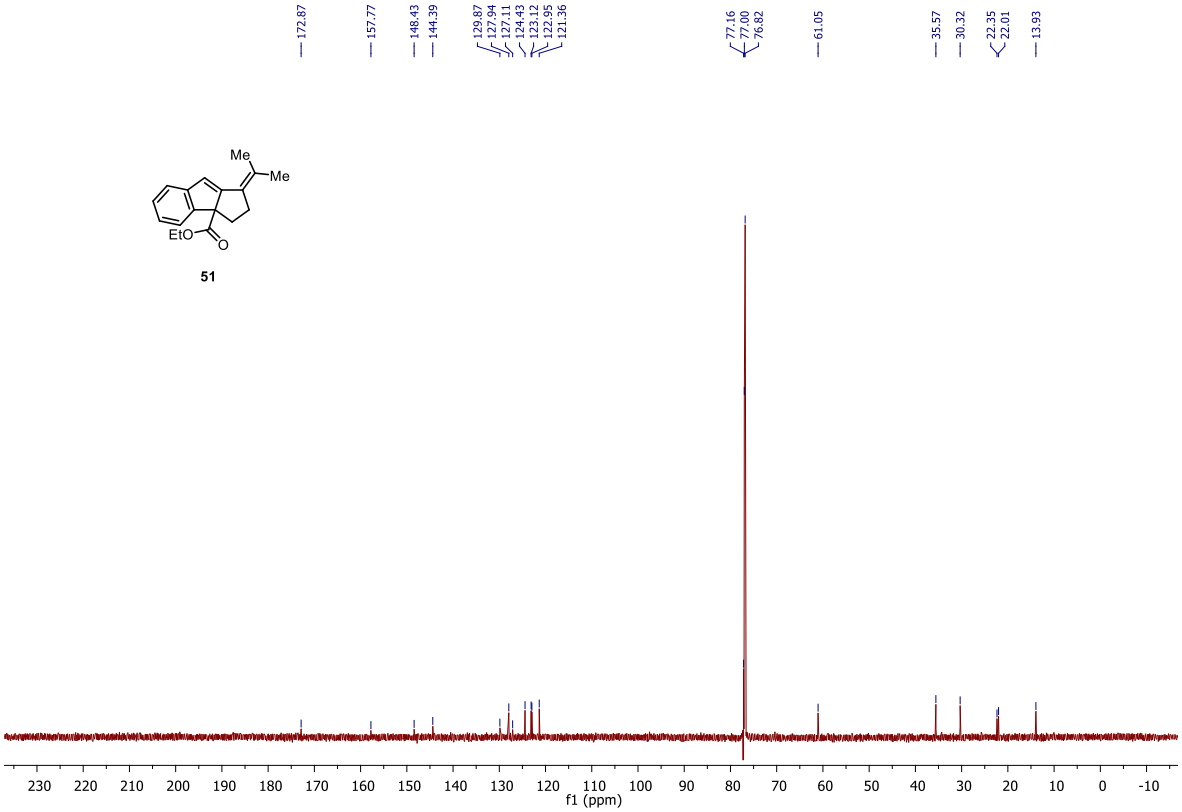
172.87
157.77
148.43
144.39
129.87
127.94
127.11
124.43
123.12
122.95
121.36
77.16
77.00
76.82
61.05
35.57
30.32
22.35
22.01
13.93
Me
Me
EtO
O
51
230
220
210
200
190
180
170
160
150
140
130
120
110
100
90
80
70
60
50
40
30
20
10
0
-10
f1 (ppm)

4.6 References

1. For selected examples of carbonyl-ene reactions, see: (a) Alder, K.; Pascher, F.; Schmitz, A. Über die Anlagerung von Maleinsäure-anhydrid und Azodicarbonsäure ester an einfach ungesättigte Kohlenwasserstoffe. Zur Kenntnis von Substitutionsvorgängen in der Allyl-Stellung *Ber. Dtsch. Chem. Ges. B Ser.* **1943**, *76*, 27−53. (b) Clarke, M. L.; France, M. B. The Carbonyl Ene Reaction. *Tetrahedron* **2008**, *64*, 9003−9031. (c) Mikami, K.; Shimizu, M. Asymmetric Ene Reactions in Organic Synthesis. *Chem. Rev*. **1992**, *92*, 1021−1050. (d) Ho, C.-Y.; Schleicher, K. D.; Chan, C.-W.; Jamison, T. F. Catalytic Addition of Simple Alkenes to Carbonyl Compounds by Use of Group 10 Metals. *Synlett* **2009**, *16*, 2565−2582. (e) Snider, B. B. in *Comp. Org. Synth*., B. M. Trost, I. Fleming, Eds. (Pergamon, Oxford, **1991**), Vol. 2, pp. 527−562.
2. For selected examples of Prins reaction, see: (a) Kriewitz, O. Ueber Addition von Formaldehyd an einige Terpene *Chem. Ber*. 1899, *32*, 57−60. (b) Prins, H.J. On the Condensation of Formaldehyde with some Unsaturated Compounds. *Chem. Weekblad* **1919**, *16*, 1510. (c) Arundale, E.; Mikeska, L.A. The Olefin-Aldehyde Condensation. The Prins Reaction. *Chem. Rev*. **1952**, *51*, 505−555. (d) Olier, C.; Kaafarani, M.; Gastaldi, S.; Betrand, M.P. Synthesis of Tetrahydropyrans and Related Heterocycles via Prins Cyclization; Extension to Aza-Prins Cyclization. *Tetrahedron* **2010**, *66*, 413−445. (e) Pastor, L.M.; Yus, M. The Prins Reaction: Advances and Applications. *Curr. Org. Chem.* **2007**, *11*, 925−957.
3. For carbonyl–olefin metathesis reactions proceeding via oxetane photoadducts, see: (a) Jones, G., II; Schwartz, S. B.; Marton, M. T. 374 Regiospecific Thermal Cleavage of Some Oxetan Photoadducts: Carbonyl–Olefin Metathesis in Sequential Photochemical and Thermal Steps. *J. Chem. Soc., Chem. Commun.* **1973**, *11*, 374−375. (b) Jones, G., II; Acquadro, M. A.; Carmody, M. A. Long-Chain Enals via Carbonyl–Olefin Metathesis. An Application in Pheromone Synthesis. *J. Chem. Soc., Chem. Commun.* **1975**, 206−207. (c) Carless, H. A. J.; Trivedi, H. S. New Ring Expansion Reaction of 2-tButyloxetans. *J. Chem. Soc., Chem. Commun.* **1979**, *8*, 382−383. (d) Pérez-Ruiz, R.; Gil, S.; Miranda, M. A. Stereodifferentiation in the Photochemical Cycloreversion of Diastereomeric Methoxynaphthalene-Oxetane Dyads. *J. Org. Chem.* **2005**, *70*, 1376−1381. (e) Pérez-Ruiz, R.; Miranda, M. A.; Alle, R.; Meerholz, K.; Griesbeck, A. G. An Efficient Carbonyl-Alkene Metathesis of Bicyclic Oxetanes: Photoinduced Electron Transfer Reduction of the Paternò−Büchi Adducts from 2,3-Dihydrofuran and Aromatic Aldehydes. *Photochem. Photobiol. Sci.* **2006**, *5*, 51−55. (f) Valiulin, R. A.; Kutateladze, A. G. Harvesting the Strain Installed by a Paternò−Büchi Step in a Synthetically Useful Way: High-Yielding Photoprotolytic Oxametathesis in Polycyclic Systems. *Org. Lett.* **2009**, *11*, 3886−3889. (g) D'Auria, M.; Racioppi, R.; Viggiani, L. Paternò−Büchi Reaction Between Furan and Heterocyclic Aldehydes: Oxetane Formation vs. Metathesis. *Photochem. Photobiol. Sci.* **2010**, *9*, 1134−1138. (h) Valiulin, R. A.; Arisco, T. M.; Kutateladze, A. G. Double-Tandem $[4_\pi+2_\pi]\cdot[2_\pi+2_\pi]\cdot[4_\pi+2_\pi]\cdot[2_\pi+2_\pi]$ Synthetic Sequence with Photoprotolytic Oxametathesis and Photoepoxidation in the Chromone Series. *J. Org. Chem.* **2011**, *76*, 1319−1332. (i) Valiulin, R. A.; Arisco, T. M.; Kutateladze, A. G. Photoinduced Intramolecular Cyclopentanation vs Photoprotolytic Oxametathesis in Polycyclic Alkenes Outfitted with Conformationally Constrained Aroylmethyl Chromophores.
4. For Brønsted and Lewis acid mediated carbonyl–olefin metathesis reactions, see: (a) Schopov, I.; Jossifov, C. A Carbonyl–Olefin Exchange Reaction – New Route to Polyconjugated Polymers, 1. A New Synthesis of Polyphenylacetylene. *Makromol. Chem., Rapid Commun.* **1983**, *4*, 659−662. (b) Jackson, A. C.; Goldman, B. E.; Snider, B. B. Intramolecular and

Intermolecular Lewis Acid Catalyzed Ene Reactions Using Ketones as Enophiles. *J. Org. Chem.* **1984**, *49*, 3988–3994. (c) van Schiak, H.-P.; Vijn, R.-J.; Bickelhaupt, F. Acid-Catalyzed Olefination of Benzaldehyde. *Angew. Chem. Int. Ed.* **1994**, *33*, 1611–1612. (d) Jossifov, C.; Kalinova, R.; Demonceau, A. Carbonyl Olefin Metathesis. *Chim. Oggi* **2009**, *40*, 85−87. (e) Soicke, A.; Slavov, N.; Neudörfl, J.-M.; Schmalz, H.-G. Metal-Free Intramolecular Carbonyl–Olefin Metathesis of *ortho*-Prenylaryl Ketones. *Synlett* **2011**, *2011*, 2487−2490.

5. For a stoichiometric approach relying on molybdenum alkylidenes, see: Fu, G. C.; Grubbs, R. H. Synthesis of Cycloalkenes via Alkylidene-Mediated Olefin Metathesis and Carbonyl Olefination. *J. Am. Chem. Soc.* **1993**, *115*, 3800-3801.
6. For organocatalytic approaches, see: (a) Griffith, A. K.; Vanos, C. M.; Lambert, T. H. Organocatalytic Carbonyl–Olefin Metathesis. *J. Am. Chem. Soc.* **2012**, *134*, 18581−18584. (b) Hong, X.; Liang, Y.; Griffith, A. K.; Lambert, T. H.; Houk, K. N. Distortion-Accelerated Cycloadditions and Strain-Release-Promoted Cycloreversions in the Organocatalytic Carbonyl–Olefin Metathesis. *Chem. Sci.* **2014**, *5*, 471−475. (c) Zhang, Y.; Jermaks, J.; MacMillan, S. N.; Lambert, T. H. Synthesis of 2H Chromenes via Hydrazine-Catalyzed Ring-Closing Carbonyl–Olefin Metathesis. *ACS Catal.* **2019**, *9*, 9259−9264. (d) Lambert, T. H. Development of a Hydrazine-Catalyzed Carbonyl–Olefin Metathesis Reaction. *Synlett* **2019**, *30*, 1954−1965. (e) Jermaks, J.; Quach, P. K.; Seibel, Z. M.; Pomarole, J.; Lambert, T. H. Ring-Opening Carbonyl–Olefin Metathesis of Norbornenes. *Chem. Sci.*, **2020**, *11*, 7884-7895.
7. For Brønsted acid-catalyzed approaches, see: (a) Catti, L.; Tiefenbacher, K. Brønsted Acid-Catalyzed Carbonyl–Olefin Metathesis Inside a Self-Assembled Supramolecular Host. *Angew. Chem., Int. Ed.* **2018**, *57*, 14589−14592. (b) To, T. A.; Pei, C.; Koenigs, R.; Nguyen, T. V. Hydrogen Bonding Networks Enable Brønsted Acid-Catalyzed Carbonyl–Olefin Metathesis. *Preprint at* https://chemrxiv.org/engage/chemrxiv/article-details/615d8156f718df1626d54e8c.
8. For other approaches, see: (a) Pitzer, L.; Sandfort, F.; Strieth-Kalthoff, F.; Glorius, F. Carbonyl–Olefin Cross-Metathesis Through a Visible-Light-Induced 1,3-Diol Formation and Fragmentation Sequence. *Angew. Chem., Int. Ed.* **2018**, *57*, 16219−16223. (b) Rivero-Crespo, M.A.; Tejeda Serrano, M.; Perez-Sanchez, H.; Ceron-Carrasco, J. P.; Leyva-Perez, A. Intermolecular Carbonyl–Olefin Metathesis with Vinyl Ethers Catalyzed by Homogeneous and Solid Acids in Flow. *Angew. Chem., Int. Ed.* **2020**, 59, 3846−3849.
9. For a review on Lewis acid-catalyzed carbonyl–olefin metathesis reactions, see: [‡]Albright, H.; [‡]Davis, A. J.; [‡]Gomez-Lopez, J. L.; [‡]Vonesh, H. L.; Quach, P; Lambert, T. H.; Schindler, C. S. Carbonyl–Olefin Metathesis Reactions. *Chem. Rev.* **2021**, *121*, 9359–9406. [‡]Authors contributed equally.
10. For Lewis acid-catalyzed approaches, see: (a) Ludwig, J. R.; Zimmerman, P. M.; Gianino, J. B.; Schindler, C. S. Iron(III)-Catalysed Carbonyl–Olefin Metathesis. *Nature* **2016**, *533*, 374−379. (b) McAtee, C. M.; Riehl, P. S.; Schindler, C. S. Polycyclic Aromatic Hydrocarbons via Iron(III)-Catalyzed Carbonyl–Olefin Metathesis. *J. Am. Chem. Soc.* **2017**, *139*, 2960−2963. (c) Ludwig, J. R.; Phan, S.; McAtee, C. M.; Zimmerman, P. M.; Devery, J. J.; Schindler, C. S. Mechanistic Investigations of the Iron(III)-Catalyzed Carbonyl–Olefin Metathesis Reaction. *J. Am. Chem. Soc.* **2017**, *139*, 10832−10842. (d) Groso, E. J.; Golonka, A. N.; Harding, R. A.; Alexander, B. W.; Sodano, T. M.; Schindler, C. S. 3-Aryl-2,5-Dihydropyrroles via Catalytic Carbonyl–Olefin Metathesis. *ACS Catal.* **2018**, *8*, 2006−2011. (e) Albright, H.; Vonesh, H. L.; Becker, M. R.; Alexander, B. W.; Ludwig, J. L.; Wiscons, R. A.; Schindler, C. S. $GaCl_3$-Catalyzed Ring-Opening Carbonyl–Olefin Metathesis. *Org. Lett.* **2018**, *20*, 4954−4958. (f)

Albright, H.; Riehl, P. S.; McAtee, C. M.; Reid, J. P.; Ludwig, J. R.; Karp, L. A.; Zimmerman, P. M.; Sigman, M. S.; Schindler, C. S. Catalytic Carbonyl–Olefin Metathesis of Aliphatic Ketones: Iron(III) Homo-Dimers as Lewis Acidic Superelectrophiles. *J. Am. Chem. Soc.* **2019**, *141*, 1690−1700. (g) Riehl, P. S.; Nasrallah, D. J.; Schindler, C. S. Catalytic Transannular Carbonyl–Olefin Metathesis Reactions. *Chem. Sci.* **2019**, *10*, 10267−10274. (h) Rykaczewski, K. A.; Groso, E. J.; Vonesh, H. L.; Gaviria, M. A.; Richardson, A. D.; Zehnder, T. E.; Schindler, C. S. Tetrahydropyridines via $FeCl_3$-Catalyzed Carbonyl−Olefin Metathesis. *Org. Lett.* **2020**, *22*, 7, 2844−2848. (i) Albright, H.; Vonesh, H. L.; Schindler, C. S. Superelectrophilic Fe(III)-Ion Pairs as Stronger Lewis Acid Catalysts for (*E*)-Selective Intermolecular Carbonyl−Olefin Metathesis. *Org. Lett.* **2020**, *22*, 3155−3160. (j) Davis, A. J.; Watson, R. B.; Nasrallah, D. J.; Gomez-Lopez, J. L.; Schindler, C. S. *Nat. Catal.* **2020**, *3*, 787−796. (k) Naidu, V. R.; Bah, J.; Franzén, J. Direct Organocatalytic Oxo-Metathesis, a *trans*-Selective Carbocation-Catalyzed Olefination of Aldehydes. *Eur. J. Org. Chem.* **2015**, *2015*, 1834−1839. (l) Ma, L.; Li, W.; Xi, H.; Bai, X.; Ma, E.; Yan, X.; Li, Z. $FeCl_3$-Catalyzed Ring-Closing Carbonyl–Olefin Metathesis. *Angew. Chem., Int. Ed.* **2016**, *55*, 10410−10413. (m) Ni, S.; Franzén, J. Carbocation Catalysed Ring Closing Aldehyde-Olefin Metathesis. *Chem. Commun.* **2018**, *54*, 12982−12985. (n) Tran, U. P. N.; Oss, G.; Pace, D. P.; Ho, J.; Nguyen, T. V. Tropylium-Promoted Carbonyl–Olefin Metathesis Reactions. *Chem. Sci.* **2018**, *9*, 5145−5151. (o) Tran, U. P. M.; Oss, G.; Breugst, M.; Detmar, E.; Pace, D. P.; Liyanto, K.; Nguyen, T. V. Carbonyl–Olefin Metathesis Catalyzed by Molecular Iodine. *ACS Catal.* **2019**, *9*, 912−919. (p) Hanson, C. S.; Psaltakis, M. C.; Cortes, J. J.; Devery, J. J. Catalyst Behavior in Metal-Catalyzed Carbonyl–Olefin Metathesis. *J. Am. Chem. Soc.* **2019**, *141*, 11870−11880. (q) Djurovic, A.; Vayer, M.; Li, Z.; Guillot, R.; Blataze, J.-P.; Gandon, V.; Bour, C. Synthesis of Medium-Sized Carbocycles by Gallium-Catalysed Tandem Carbonyl–Olefin Metathesis/Transfer Hydrogenation. *Org. Lett.* **2019**, *21*, 8132–8137. (r)Wang, R.; Chen, Y.; Shu, M.; Zhao, W.; Tao, M.; Du, C.; Fu, X.; Li, A.; Lin, Z. $AuCl_3$-Catalyzed Ring-Closing Carbonyl–Olefin Metathesis. *Chem. Eur. J.* **2020**, *26*, 1941–1946. (s) Hanson, C. S.; Psaltakis, M. C.; Cortes, J. J.; Siddiqi, S. S.; Devery, J. J. Investigation of Lewis Acid-Carbonyl Solution Interactions via Infrared-Monitored Titration. *J. Org. Chem.* **2020**, *85*, 820−832.

11. Ludwig, J.R.; Watson, R.B.; Nasrallah, D.J.; Gianino, J.B.; Zimmerman, P.M.; Wiscons, R.A.; Schindler, C.S. Interrupted Carbonyl–Olefin Metathesis via Oxygen Atom Transfer. *Science* **2018**, *361*, 1363-1369.
12. (a) Crews, P.; Klein, T. E.; Hogue, E. R.; Myers, B. L. Tricyclic Diterpenes from the Brown Marine Algae Dictyota divaricata and Dictyota linearis. *J. Org. Chem.* **1982**, *47*, 811-815. (b) Piers, E.; Friesen, R. W. Annulations Leading to Diene Systems. Total Synthesis of the Diterpenoid (±)-(14S)-Dolasta-1(15),7,9-trien-14-ol. *J. Org. Chem.* **1986**, *51*, 3405-3406. (c) Piers, E.; Friesen, R. W. Annulations Leading to Diene Systems. Total Syntheses of the Dolastane-type Diterpenoids (±)-(5S,12R,14S)-Dolasta-1(15),7,9-trien-14-ol and (±)-Amijitrienol. *Can. J. Chem.* **1992**, *70*, 1204-1220. (d) Leung, L. T.; Chiu, P. Total Synthesis of (−)-Dolastatrienol. *Chem. Asian J.* **2015**, *10*, 1042-1049.
13. (a) Urones ,J. G.; Marcos, I. S.; Basabe, P.; Alonso, C.; Olivia, I. M.; Garrido, N. M.; Martin, D. D.; Lithgow, A. M. Diterpenes with a Valparane Skeleton. *Phytochemistry* **1993**, *34*, 747-750. (b) Rodilla, J. M. L.; De Mendonca, D. I. M.; Urones, J. G.; Moro, R. F., Williams, D. J. Tricyclic Diterpenes from Halimium viscosum. *Phytochemistry* **1998**, *47*, 1545-1549.
14. (a) Peng, J.; Walsh, K.; Weedman, V.; Bergthold, J. D.; Lynch, J.; Lieu, K. L.; Braude, I. A., Kelly, M.; Hamann, M. T. The New Bioactive Diterpenes Cyanthiwigins E–AA from the

Jamaican Sponge *Myrmekioderma styx*. *Tetrahedron* **2002**, *58*, 7809-7819. (b) Peng, J.; Kasanah, N.; Stanley, C. E.; Chadwick, J.; Fronczek, F. R.; Hamann, M. T. Microbial Metabolism Studies of Cyanthiwigin B and Synergetic Antibiotic Effects. *J. Nat. Prod.* **2006**, *69*, 727-730.

15. Ohta, T.; TakakoKita, T.; Kobayashi, N.; Obara, Y.; Nakahata, N.; Ohizumi, O.; Takaya, Y.; Oshima, Y. Scabronine A, A Novel Diterpenoid Having Potent Inductive Activity of the Nerve Growth Factor Synthesis, Isolated from the Mushroom, Sarcodon scabrosus *Tet. Lett.* **1998**, *39*, 6229-6232.
16. Marcos, I. S.; Moro, R. F.; Gil-Mesón, A.; Díez, D. Chapter 5 - 7-6-5 Tricarbocyclic Diterpenes: Valparanes, Mulinanes, Cyathanes, Homoverrucosanes, and Related Ones. *St. Nat. Prod. Chem.* **2016**, *48*, 137-207.
17. Dixon, T.; Schweibenz, A.; Hight, B.; Kang, A.; Dailey, S.; Kim, M.-Y.; Chen, Y.; Kim, S.; Neale, A.; Groth, T.; Ike, S.; Khan, B.; Lieu, D.; Stone, T.; Orellana, R.; Couch, J. Bacteria-Induced Static Batch Fungal Fermentation of the Diterpenoid Cyathin A_3, a Small-Molecule Inducer of Nerve Growth Factor. *Ind. Microbiol. Biotechnol.* **2011**, *38*, 607-615.
18. (a) Sun, H. H.; McConnell, O. J.; Fenical, W. Tricyclic Diterpenoids of the Dolastane Ring System from the Marine Alga *Dictyota divaricataI. Tetrahedron* **1981**, *37*, 1237-1242. (b) Pattenden, G.; Robertson, G. M. Free Radical Reactions in Synthesis. Total Synthesis of Isoamijiol. *Tet. Lett.* **1986**, *27*, 399-402. (c) Mehta, G.; Krishnamurthy, N. An Enantioselective Approach to Dolastane Diterpenes. Total Synthesis of Marine Natural Products (+)-Isoamijiol and (+)-Dolasta-1(15),7,9-trien-14-OL. *Tet. Lett.* **1987**, *28*, 5945-5948. (d) Tori, M.; Toyoda, N.; Sono, M. Total Synthesis of Allocyathin B2, a Metabolite of Bird's Nest Fungi. *J. Org. Chem.* **1998**, *63*, 306-313. (e) Waters, S. P.; Tian, Y.; Li, Y.-M.; Danishefsky, S. J. Total Synthesis of (−)-Scabronine G, an Inducer of Neurotrophic Factor Production. *J. Am. Chem. Soc.* **2005**, *127*, 13514-13515. (f) Kobaykawa, Y.; Makada, M. Total Syntheses of (−)-Scabronines G and A, and (−)-Episcabronine A *Angew. Chem. Int. Ed.* **2013**, *52*, 7569-7573.
19. Enquis, Jr, J. A.; Stoltz, B. M. Synthetic Efforts Roward Cyathane Diterpenoid Natural Products. *Nat. Prod. Rep.* **2009**, *26*, 661-680.
20. Jackson, A. C.; Goldman, B. E.; Snider, B. B. Intramolecular and Intermolecular Lewis acid Catalyzed Ene Reactions Using Ketones as Enophiles. *J. Org. Chem.* **1984**, *49*, 3988-3994.
21. Gou, X.; May, H. Manifestation of Polar Reaction Pathways of 2,3-Dichloro-5,6-dicyano-p-benzoquinone. *J. Am. Chem. Soc.* **2013**, *135*, 12377-12387.
22. Huang, J.-W.; Shi, M. Ring-Opening Reaction of Methylenecyclopropanes with LiCl, LiBr or NaI in Acetic Acid. *Tetrahedron* **2004**, *60*, 2057-2062.
23. Fisher, M. J.; Overman, L. E. Intramolecular N-(Acyloxy)iminium Ion-Alkyne Cycloadditions. A New Route to Bicyclic α-Amino Ketones. *J. Org. Chem.* **1990**, *55*, 1447-1459.
24. Green, J. C.; Brown, E. R.; Pettus, T. R. R. Intramolecular Condensation via an o-Quinone Methide: Total Synthesis of (±)-Heliol. *Org. Lett.* **2012**, *14*, 2929-2931.
25. Cocker, W.; Geraghty, N. W. A.; McMurry, T. B. H.; Shannon, P. V. R. An Investigation of the Thermal Decomposition of the Methohydroxides and Methodeuterio-oxides of some 5-N,N-Dimethylaminopent-1-enes *J. Chem. Soc., Perkin Trans. 1* **1984**, *0*, 2245-2254.
26. Yadav, J. S.; Reddy, B. V. S.; Krishna, A. D.; Reddy, C. S.; Marsaiah, A. V. Triphenylphosphine: An Efficient Catalyst for Transesterification of β-Ketoesters. *J. Mol. Catal. A: Chem.* **2007**, 93-97.

27. Ros, A.; Magriz, A.; Dietrich, H.; Lassaletta, J. M.; Fernandez, R. Stereoselective Synthesis of *syn β*-Hydroxy Cycloalkane Carboxylates: Transfer Hydrogenation of Cyclic β-Keto Esters via Dynamic Kinetic Resolution *Tetrahedron* **2007,** *63,* 7532-7537.

Chapter 5: Stepwise Carbonyl–Olefin Metathesis

5.1 Introduction

In carbonyl–olefin metathesis, two π-bonds undergo a cycloaddition-cycloreversion process to form valuable olefins from simple precursors.[1-16] Although this synthetic methodology has advanced significantly, it remains unclear whether carbonyl–olefin metathesis occur via a stepwise or concerted pathway. Shown here, $^{12}C/^{13}C$ kinetic isotope effect (KIE) measurements definitively establish prototypical iron(III)-catalyzed carbonyl–olefin metathesis as being stepwise. Although this mechanism is well-supported by additional $^{1}H/^{2}H$ KIE and Hammett experiments, conventional computational models incorrectly predict a concerted mechanism. This failure is traced to the use of implicit solvation models, and it is further demonstrated that when solvent molecules are explicitly[17,18] represented, the correct stepwise mechanism is predicted. These findings call into question prior proposals of concerted carbonyl–olefin metathesis, suggest possible avenues for future reaction development, and highlight the importance of explicit solvent representations when modeling charged intermediates.

Significant advances in computational methodology have revolutionized the study of organic reaction mechanisms.[19] In particular, many accurate and efficient methods based on density functional theory (DFT) are now available, allowing mechanistic predictions to be made before detailed experimental studies can be conducted.[20] For example, DFT studies predicting that many nucleophilic aromatic substitution (S_NAr) reactions are concerted preceded confirmation by $^{12}C/^{13}C$ KIE measurements.[21] Thus, calculations provided the impetus to re-evaluate the existing mechanistic consensus, while experiments demonstrated the remarkable veracity of the DFT predictions across a range of S_NAr substrates.

In the area of carbonyl–olefin metathesis, a variety of stepwise and concerted mechanisms have been proposed (Figure 5.1). For example, stepwise proposals have been made by analogy to known polar mechanisms by the Snider, Bickelhaupt, Schmalz, and Franzén groups in aluminum-,[1] zinc-,[2] boron-,[3] and trityl-based[5] catalyst systems. To confirm the existence of a betaine intermediate in related systems, trapping experiments have been conducted by the groups of

Tiefenbacher,[9] Li,[7] Lin,[14] Schindler, Devery, and Zimmerman.[6,8] In some cases, trapping was observed; in others, carbonyl–olefin metathesis proceeded normally. However, the mechanistic implications of these observations are unclear. While trapping could be consistent with betaine capture, Lewis acids are known to catalyze oxetane-opening reactions.[22,23] As such, trapping could also be consistent with opening of the oxetane intermediate that is present in both the stepwise and concerted pathways. Furthermore, while the absence of trapping might reflect the absence of a betaine intermediate, such a negative result might also be explained by a short-lived betaine or an inefficient trapping agent.

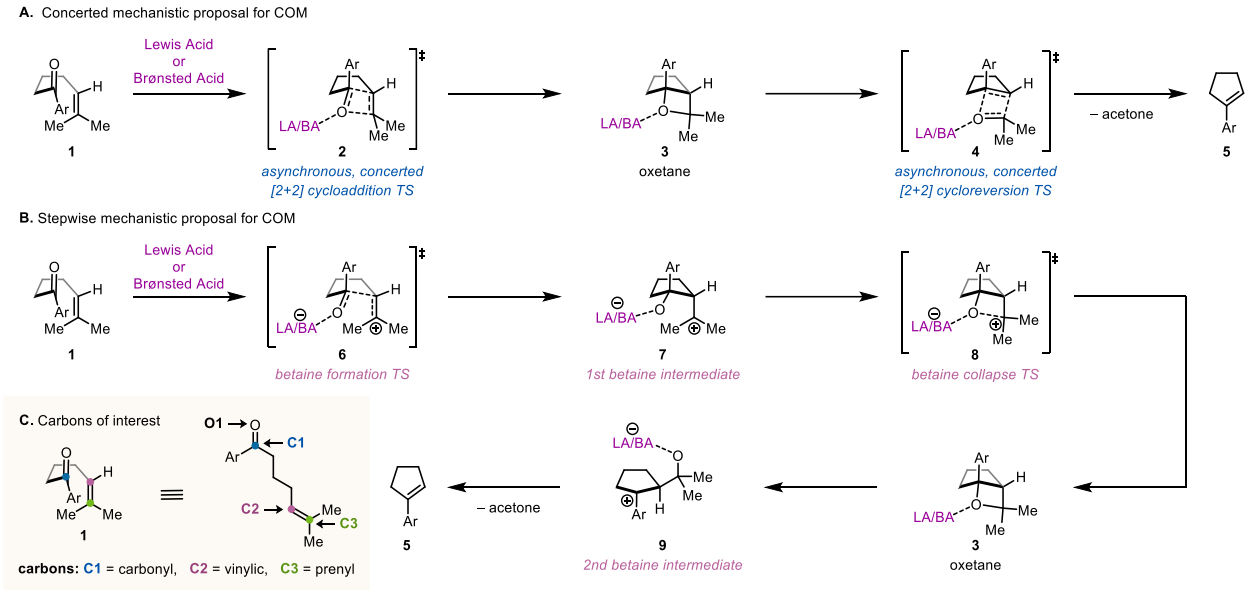

Figure 5.1: Mechanistic proposals for carbonyl–olefin metathesis.

Given the equivocal nature of the experimental evidence and the demonstrated ability of DFT to make accurate predictions, many groups have sought to support their mechanistic proposals with theoretical studies.[10,11,13,15] For example, the Nguyen and Bour groups reported calculations that support fully stepwise mechanisms for tropylium-,[10] iodine-,[11] pTSA-HFIP$_3$-[15] and gallium-catalyzed[13] carbonyl–olefin metathesis, while the Lin group used DFT to propose a mixed mechanism involving stepwise cycloaddition and concerted cycloreversion for gold-catalyzed[14] carbonyl–olefin metathesis. In contrast, in iron-based systems,[6,8,12] the Schindler, Devery, and Zimmerman groups predicted a fully concerted mechanism for prenyl-derived substrates but a mixed mechanism for styrenyl-derived substrates.

5.2. Revisiting Gas Phase and Implicit Solvent DFT Computations

To assess the ability of computational methods to make accurate mechanistic predictions, a full suite of experimental and computational data for a prototypical iron-catalyzed carbonyl–olefin metathesis reaction was gathered (Figure 5.2). Following conventional best practices,[24,25] the optimal model chemistry was selected from a variety of standard methods. Specifically, we compared the performance of DFT/basis set combinations in the gas phase to data from high-level coupled cluster calculations (DLPNO-CCSD(T_1)/aug-cc-pVTZ/TightPNO).[26] Structures were generated across a range of C1–C2 and C3–O1 distances (Figure 5.1C) such that the resulting test set spanned the stepwise-concerted continuum, including both charge-separated betaines and potentially concerted transition states. DFT and coupled cluster energies were nearly identical (see section 5.6.7 for more details), with T_1 diagnostic values indicating the appropriateness of a single-reference wavefunction for these high-spin iron(III) species.[27,28] On this basis, B3LYP-D3(BJ)/jul-cc-pVDZ was selected as an appropriate model chemistry in terms of dynamic correlation, basis set completeness, and static correlation.

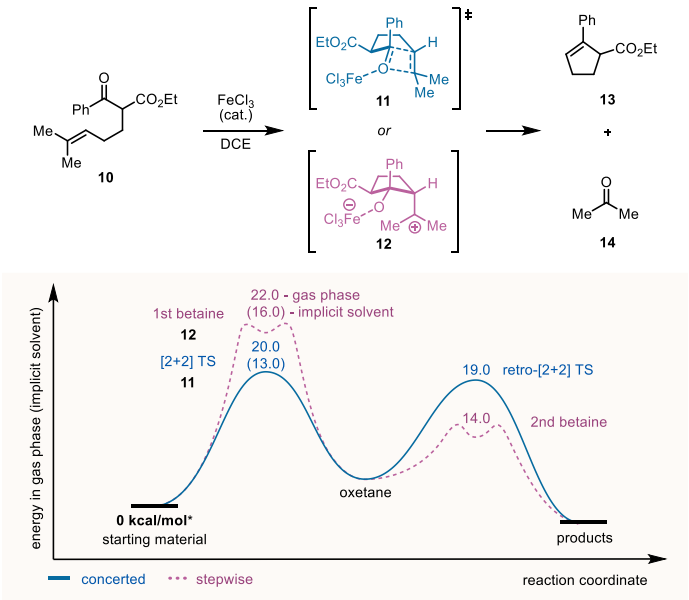

Figure 5.2: Conventional DFT calculations (B3LYP-D3(BJ)/jul-cc-pVDZ) predict concerted carbonyl–olefin metathesis in implicit solvent. *Electronic energies are shown as gas phase (implicit solvent) and are referenced to the pre-complex. Implicit solvent refers to the polarizable continuum model (PCM)[29] with DCE. Some energies have been omitted for clarity.

Then the mechanism for the prototypical carbonyl–olefin metathesis of prenyl substrate **10** catalyzed by $FeCl_3$ in 1,2-dichloroethane (DCE) was predicted. In both the gas phase and implicit

solvent, it was predicted that the concerted pathway is favored over the stepwise pathway, with cycloaddition being rate-determining (Figure 5.2). Interestingly, the predicted barriers are low, despite the fact that this [2+2]-cycloaddition is the doubly suprafacial approach of two 2-electron π-systems and thus should be thermally forbidden. However, the reaction could also be considered to be a relatively facile C–C bond formation between a carbonyl group activated by $FeCl_3$ and an olefin. Barrierless collapse of the resulting betaine (**14**), through attack of the iron alkoxide at O1 on the tertiary carbocation at C3, would generate the oxetane.

5.3 Experimental Mechanistic Investigations

This computed pathway for concerted carbonyl–olefin metathesis leads to concrete predictions of primary carbon KIEs at C1, C2, and C3 that can be tested experimentally. To accomplish this, intermolecular competition experiments were conducted on substrate **10** at natural abundance and the isotope ratios of the unreacted and remaining starting material at ~80% conversion were compared (Figure 5.3A). Because the traditional quantitative single-pulse NMR method[30] of determining site-specific isotopic fractionations is limited by the poor sensitivity of ^{13}C as an NMR nucleus, a recently-developed DEPT methodology was utilized to measure the ^{13}C KIEs (Figure 5.3B).[31] The DEPT method requires attached protons for sensitivity enhancement, so the carbonyl and olefin moieties in **10** were reduced in a two-step sequence with a sufficiently high yield to avoid perturbing the isotopic ratios at C1 and C3 (Figure 5.1C).

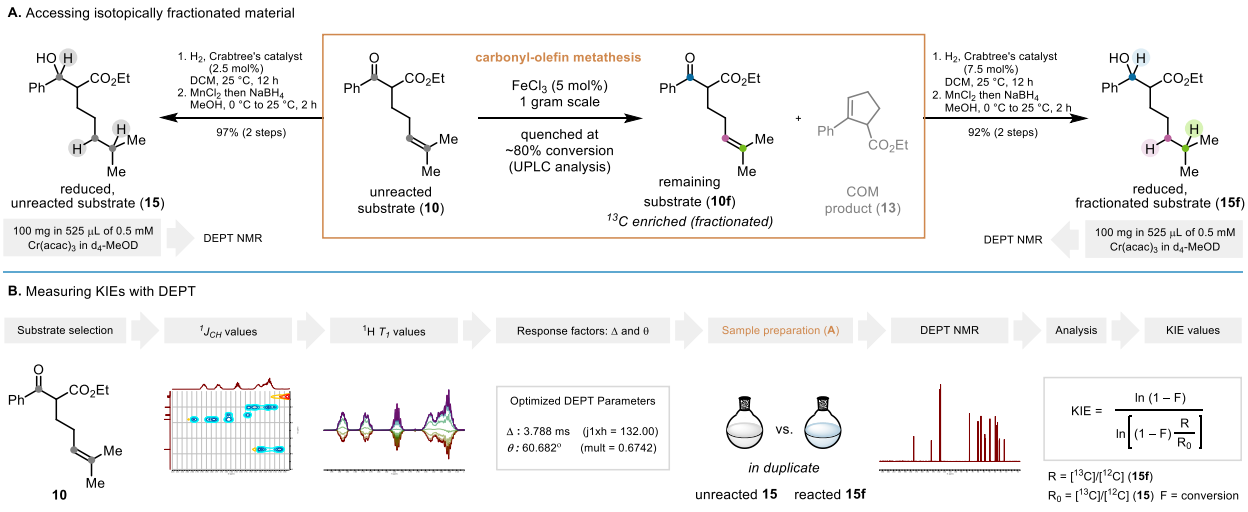

Figure 5.3: Workflow for $^{12}C/^{13}C$ KIE measurements. **A.** KIEs were measured at natural abundance by assessing the isotopic fractionation of recovered vs. unreacted starting materials. Attached protons at the carbons of interest (colored circles) were introduced by a high-yielding two-step reduction sequence that did not affect isotope ratios. **B.** Isotope

ratios were measured by DEPT NMR. To ensure that signal:noise was maximized for each carbon of interest, optimal values of the polarization transfer delay (Δ) and read angle (θ) were chosen based on measured $^{1}J_{CH}$ values. Spectroscopic data were collected over 6 days (15 blocks/sample for 4 samples) using a randomized block design. For additional details on data acquisition and analysis, please see 5.6.4.

Despite the careful choice of computational method, the predicted KIEs for the concerted cycloaddition and the experimental KIEs disagreed substantially (**11** vs **10**, Figure 5.4A). In particular, the discrepancies in the KIEs at the olefinic carbons (C2 and C3) were much larger than the variation between different model chemistries (see section 5.6.7 for more details).[31] Therefore, the KIEs are inconsistent with the concerted mechanism. Interestingly, the predicted equilibrium isotope effects (EIEs) for prenyl betaine **12** matched the experimental values better, suggesting the rate-determining transition state is betaine-like. Unfortunately, because charge separation in both the gas phase and implicit solvent is highly unfavorable, both the formation and collapse of this betaine are barrierless on the potential energy surface, and it is not possible to predict the KIEs for either step directly.

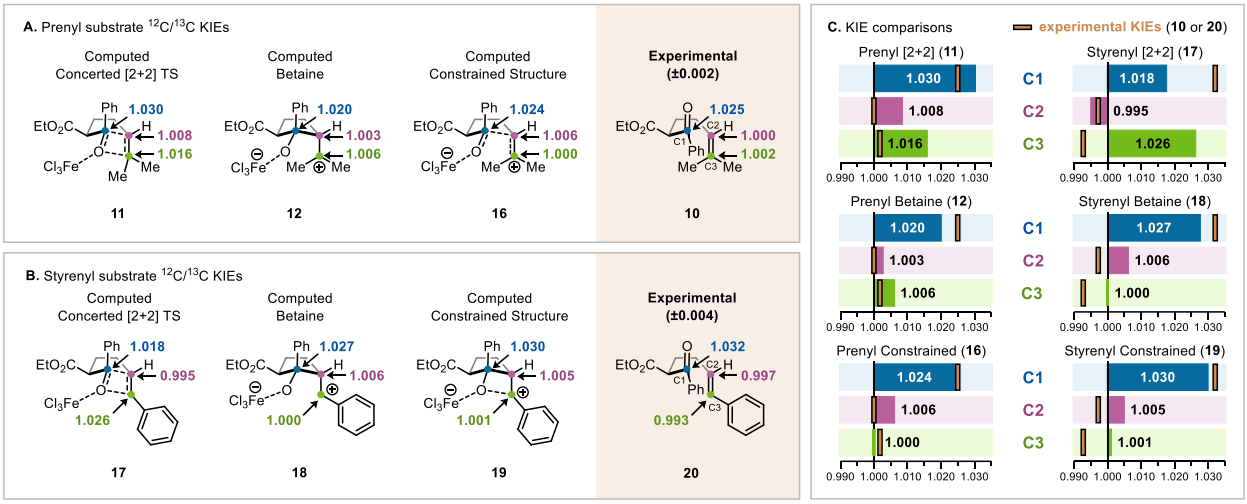

Figure 5.4: Experimental $^{12}C/^{13}C$ KIEs support a stepwise mechanism. **A.** Prenyl substrate computational and experimental carbon KIEs. **B.** Styrenyl substrate computational and experimental carbon KIEs. **C.** The KIEs do not match a concerted [2+2] transition state, are closer to the predicted EIEs for the first betaines, and match a constrained structure corresponding to first betaine formation (prenyl substrate **16**) or collapse (styrenyl substrate **19**).

However, it was possible to generate transition state proxies for these steps by using the known approach of conducting constrained geometry optimizations.[32] Although this approach relies on non-stationary structures, it benefits from a remarkable degree of error cancellation and has been successfully applied in many systems,[33] and is particularly well-suited for this system as several independent primary KIEs are available. Furthermore, the well-defined mechanistic

continuum allows a range of constrained structures to be considered, reducing the chances of a spurious correlation.[34] A structure with a C1–C2 distance of 2.2 Å and a C3–O1 distance of 3.0 Å gave predicted KIEs that agreed well with experimental values (**16** vs **10**). This structure corresponds to rate-determining betaine formation in a stepwise pathway.

To corroborate this analysis, an analogous natural abundance $^{12}C/^{13}C$ KIE experiment was conducted on styrenyl substrate **20** (Figure 5.4B). Once again, small olefinic KIEs were observed that were inconsistent with those predicted for a concerted mechanism (**17** vs **20**). These experimental KIEs were also closer to the predicted EIEs for a betaine (**18**). Despite larger residuals, which may reflect the larger experimental error bars (±0.004 for styrenyl substrate **20** vs. ±0.002 for prenyl substrate **10**), the observed KIEs are consistent with a constrained structure with C1–C2 and C3–O1 bond distances of 1.6 and 2.7 Å, respectively (**19** vs **20**). Once again, this betaine-like structure supports a stepwise pathway. However, this structure corresponds to rate-determining betaine collapse, rather than formation. This change in rate-determining step may reflect the reduced electrophilicity of the stabilized benzyl cation generated in the styrenyl substrate vs. the tertiary alkyl cation generated in the prenyl substrate.[35]

If a betaine is indeed collapsing in the rate-determining step, then there must be an increase in the amount of positive charge at C3 (see **23**) in the corresponding transition state relative to the ground state (Figure 5.5). This charge should be detectable in a Hammett study by varying the electronic properties of the styrene. A range of potential substituents was evaluated and it was found that electron-rich substrates gave decomposition, while electron-poor substrates were unreactive.[36] When intermolecular competition experiments were conducted within the accessible range (Figure 5.5A), the inferred relative rate varied as a function of conversion, which was potentially due to interference between substrates. Therefore, the study was conducted via initial rate analyses with multiple replicates to reduce error.

A good correlation with the Hammett σ parameter was found ($\rho = -2.5 \pm 0.5$; $R^2 = 0.88$). The considerable rate acceleration afforded by electron-donating substituents is consistent with the generation of substantial positive charge at C3. Interestingly, we only found a modest correlation with the Hammett σ^+ parameter. This decreased correlation might indicate that the cation is stabilized more by field effects, via the proximity between the positive charge at C3 and the negative charge at O1, and less by resonance effects from the neighboring aromatic ring. However, the incompatibility of the reaction with strongly electron-donating substituents precludes a more

detailed interpretation. Overall, the rate of carbonyl–olefin metathesis is greatly increased by electron-donating substituents, to an extent that is much larger than would be expected for a concerted cycloaddition (Figure 5.5B) but is consistent with a stepwise mechanism.[37]

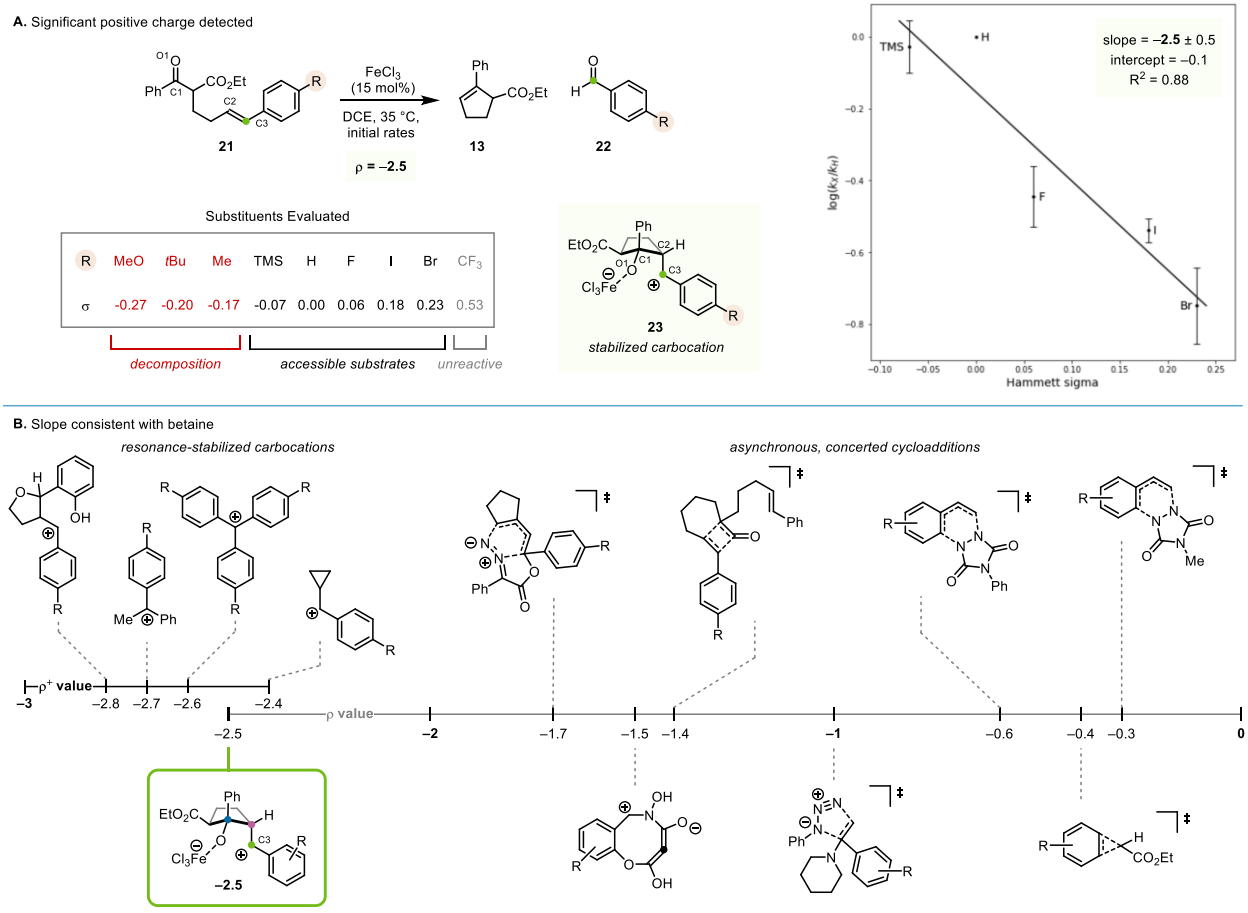

Figure 5.5: Hammett studies. **A.** Initial rate data were gathered for the indicated substrates with 7 aliquots per replicate and 3–5 replicates per substrate. **B.** Relevant Hammett ρ and ρ+ values from the literature. The observed slope is consistent with the generation of a stabilized carbocation (left), but not consistent with a concerted cycloaddition (right).

While these $^{12}C/^{13}C$ KIE and Hammett studies provide strong evidence for a stepwise mechanism, one possible discrepancy comes from a finding made by the Schindler, Devery, and Zimmerman groups in 2017.[8] They previously conducted a β-secondary deuterium KIE (SDKIE) study on α-methyl styrene **24** and found an unusual inverse value of 0.65 (Figure 5.6A). However, a normal KIE would be expected for deuterium substitution adjacent to a carbocation. At the time, the inverse KIE was taken as evidence for a change in hybridization from sp^2 to sp^3, but such an interpretation[38] is usually only applied to α-SDKIEs, rather than β-SDKIEs. While it is possible that an inverse β-SDKIE could arise from steric compression[39] in the transition state, such an effect

is not predicted by DFT. Instead, a simpler explanation would be that the unusual value arose from the relatively large experimental error that is inherent to absolute rate measurements.

To evaluate the β-SDKIE with more accuracy in a related system, intermolecular competition experiment between isotopologues **10** and **25** were conducted and a KIE of 1.08±0.05 was observed (Figure 5.6B). As with the $^{12}C/^{13}C$ KIEs, we found that the experimental β-SDKIE was inconsistent with the predicted value of 1.40 for a concerted reaction (**11**, Figure 5.6C). In contrast, the predicted value of 1.03 from grid structure **16** agreed well,[40] providing further support for a stepwise mechanism. This normal β-SDKIE is expected to arise from transition state hyperconjugation at C3 (Figure 5.6D): as the betaine forms, a vacant p-orbital develops that can serve as an excellent hyperconjugative acceptor for the C–H bonds of the adjacent methyl groups. Because C–H bonds are better donors than C–D bonds,[41] the positive charge in the protiated substrate is better stabilized. Thus, the protiated substrate reacts faster, and a normal β-SDKIE results. Similar β-SDKIEs have been observed for olefin addition to Lewis acid-activated carbonyls.[42]

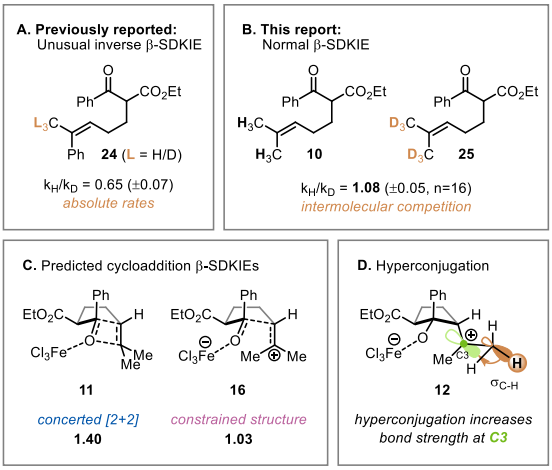

Figure 5.6: Secondary $^{1}H/^{2}H$ KIE studies. **A.** The previously reported inverse β-SDKIE is unusual, but was measured with absolute rates. **B.** Intermolecular competition studies in this report show that the β-SDKIE in a related system is normal. **C.** The normal β-SDKIE is inconsistent with a concerted cycloaddition, but matches the grid structure for rate-determining betaine formation. **D.** Transition state hyperconjugation increases the bond strength at C3, which counters the loss of the C2=C3 π bond. As a result, the KIE at C3 is nearly unity.[43]

5.4 Explicit Solvent Molecular Dynamics

Overall, this body of experimental evidence strongly supports the existence of a betaine intermediate and a stepwise pathway (Figure 5.7A). However, the fact that DFT calculations that

are nearly of coupled-cluster quality instead predict a concerted mechanism is troubling. We propose that this error is due to deficiencies in the treatment of solvation. While implicit solvent models perform well for neutral species, predicting their solvation energies with best-case root-mean-squared deviations of ~1 kcal/mol, such models perform much worse for ionic solutes (~6 kcal/mol).[44] As a result, implicit solvation is expected to be accurate for the relatively unpolarized ground state, but inaccurate for the charge-separated betaine. Hence, the cancellation of solvation errors is likely to be poor.

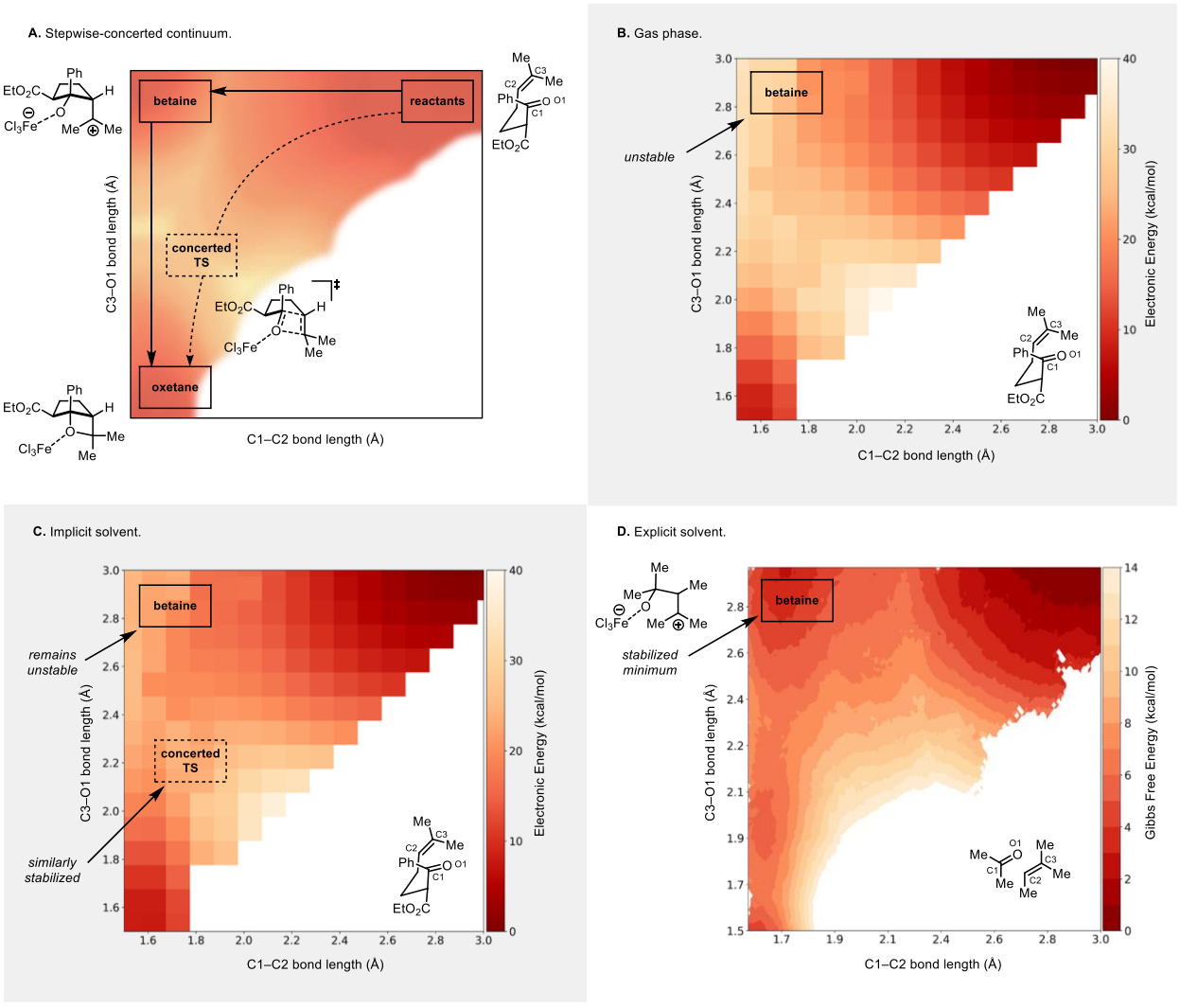

Figure 5.7: Solvation method affects the predicted mechanism. **A.** Shows an idealized More O'Ferrall–Jencks plot. **B.** The betaine is unstable (B3LYP-D3(BJ)/jul-cc-pVDZ) in both the gas phase and **C.** in implicit solvent. **D.** When explicit solvent is included, the betaine becomes visible in the upper left-hand corner (AIMD with B3LYP-D3(BJ)/MIDI!-LANL2DZ(Fe,Cl) for solutes and GFN0-xtb[45] for solvents).

This effect leads to the erroneous prediction that the betaine and the concerted transition state have a similar stability relative to one another in solution as they do in the gas phase (Figure 5.2). Further consequences of insufficient betaine stabilization can be seen by comparing Figure 5.7B to 5.7C. When implicit solvation is applied, the betaine is modestly lowered in energy (the upper left region darkens) but does not become a minimum. Because of this, and the fact that both the betaine and the concerted region are similarly stabilized, the minimum energy path remains a concerted one. This systematic error arises because implicit solvation models represent the solvent as a continuous medium and are therefore unable to account for specific solute-solvent interactions.[25]

While the natural remedy is to model the solvent explicitly,[46-50] this introduces many new degrees of freedom that require extensive sampling. Here, the model system was immersed in a sphere of 100 molecules of DCE[51] and the resulting ensemble was sampled by using *ab initio* molecular dynamics (AIMD).[52-55] To run the required simulations, *presto*[56] was developed, an open-source Python program that enables the setup, running, and analysis of AIMD trajectories. Following equilibration, 130 replicates were constrained to various C1–C2 and C3–O1 bond distances and allowed to evolve for 20 ps each, for a total of 2.6 ns of simulation time. Then, a two-dimensional free energy surface was dervied by using the weighted histogram analysis method (WHAM).[57] In contrast to the predictions made in the gas phase or implicit solvent, these explicitly solvated calculations predict that the betaine exists as a stable intermediate (Figure 5.7D). While these calculations are subject to the recognized limitations of current explicit solvent methodology (approximate energies, incomplete sampling,[58] and possible non-equilibrium solvation effects[59]), the distinct betaine minimum is interpreted as support for a classical "Prins-like" stepwise mechanism.[60]

Both the failure of implicit solvation to predict the correct stepwise mechanism and the influence of this error on the predicted KIEs can be understood by using Marcus theory.[61] In general, the minimum energy path for cycloaddition can be regarded as the intersection of potentials for the reactants, betaine, and oxetane. In implicit solvent, the betaine curve is too high, causing the minimum energy path to involve only the reactants and oxetane (Figure 5.8A). The resulting concerted transition state is positioned centrally between these species, involves a significant degree of bond cleavage and formation, and thus generates relatively large predicted KIEs for the concerted mechanism.

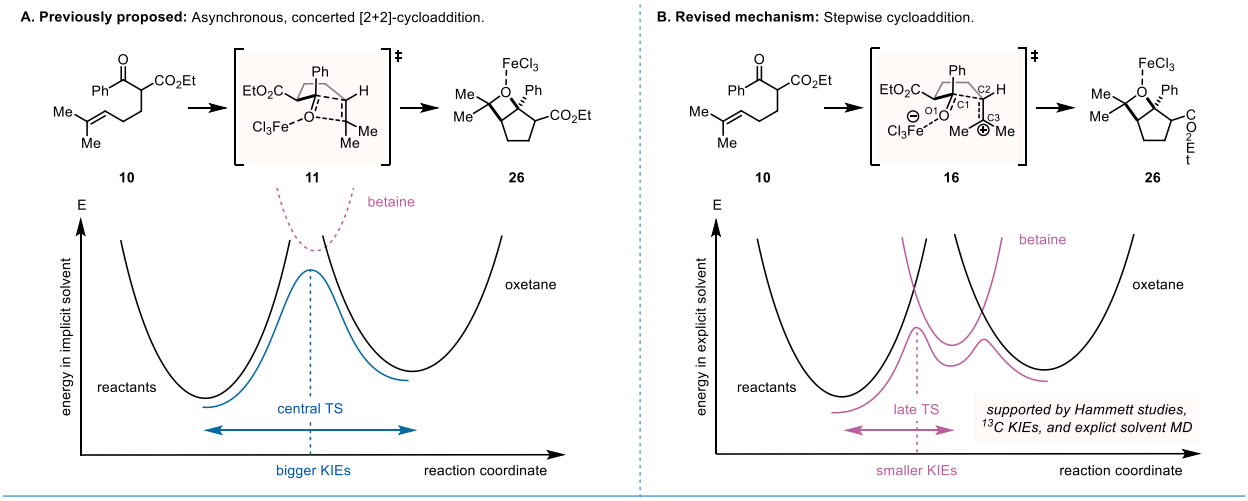

Figure 5.8: Marcus analysis. **A.** In implicit solvent, the betaine curve is too high in energy to contribute to the minimum energy path and a concerted mechanism is predicted. The corresponding transition state is central between the reactants and oxetane and thus large KIEs are erroneously predicted. **B.** In explicit solvent, the betaine curve is stabilized and intersects the reactant and oxetane potentials, resulting in the prediction of a stepwise mechanism. In the case depicted, betaine formation is rate-determining, the corresponding transition state is late and betaine-like, and small KIEs are correctly predicted.

In explicit solvent, the betaine curve is much lower, causing it to intersect the minimum energy path as an intermediate with two flanking transition states. In Figure 5.8B, the first transition state (betaine formation, **16**) is depicted as rate-limiting, as is the case for prenyl substrate **10**. This transition state is late with respect to the reactants and the betaine and is thus betaine-like. Alternatively, the second transition state (betaine collapse, **19**) could be rate-limiting, as it is for the styrenyl substrate **20**. This transition state is positioned early with respect to the betaine and oxetane and is thus also betaine-like. In both structures, the bonds are nearly completely formed or broken, and thus give relatively small predicted KIEs for the stepwise mechanism.

This Marcus picture conceptualizes the concerted mechanism as the limit of the stepwise mechanism as the lifetime of the intermediate approaches zero. The poor stabilization of the betaine in implicit solvent leads any developing carbocationic character to be immediately quenched by attack of the iron alkoxide, such that addition and collapse occur concomitantly. This is analogous to another formally forbidden process, concerted S_NAr, which is observed for substrates lacking strongly electron-withdrawing groups.[21] In both cases, the instability of the intermediate means that subsequent transformations occur faster than the timescale of molecular vibrations, enforcing a concerted transition state in a manifold that is conventionally stepwise.[62,63]

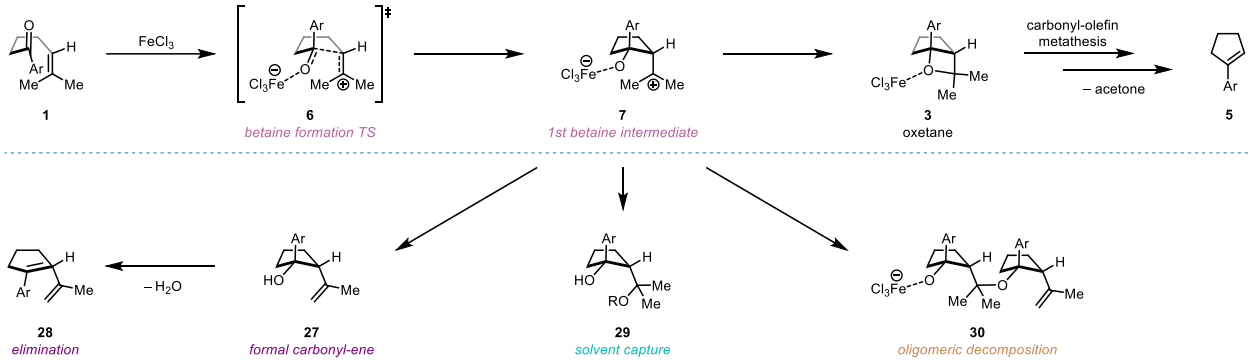

Figure 5.9: Selectivity for the carbonyl–olefin metathesis pathway.

In reality, the betaine is a solvent-stabilized intermediate, and the sum of the experimental evidence strongly supports a stepwise mechanism for carbonyl–olefin metathesis. However, alternative reaction outcomes can occur. For example, the fate of an analogous betaine has been previously characterized by the Singleton group in the Lewis acid-catalyzed carbonyl-ene reaction between 2-methyl-2-butene and formaldehyde.[64] In that case, fast addition of the olefin to the polarized carbonyl group led to betaine formation and was followed by slow elimination to generate the product. Thus, Lewis acids can generate betaine intermediates that can partition between many possible pathways (Figure 5.9): desired collapse to the oxetane, giving eventual carbonyl–olefin metathesis (**5**) or undesired solvent capture (**29**), carbonyl-ene reaction (**27**)/elimination[65] (**28**), or decomposition[66] (**30**).

The existence of these diverging paths implies that achieving efficient carbonyl–olefin metathesis requires that the betaine be stable enough to be energetically accessible, but not so persistent that it can react with other bases or nucleophiles. Accordingly, carbonyl–olefin metathesis is inefficient with electron-poor styrenes (as observed in the Hammett study), primary olefins, and nonpolar solvents (e.g. toluene, benzene, or hexanes), while electron-rich styrenes lead to decomposition. Furthermore, the high sensitivity of the optimal carbonyl–olefin metathesis conditions to the nature of the substrate across many catalyst systems may be explained by another balance between competing requirements: sufficient Lewis acidity to promote addition of the olefin to the carbonyl group but adequate nucleophilicity in the resulting metal alkoxide to permit betaine collapse.[16]

5.5 Conclusions

While further studies will be needed to understand the factors that control reaction efficiency and the selectivity for carbonyl–olefin metathesis over other pathways, the experimental evidence presented in this study rules out a thermally forbidden [2+2]-cycloaddition pathway in iron(III)-based carbonyl–olefin metathesis. These findings suggests that concerted proposals in other carbonyl–olefin metathesis systems should be re-evaluated, and may offer opportunities for synthetic advances. For example, catalysts that can stabilize the charge-separation inherent to betaines, while taking advantage of the modest geometric and steric constraints of forming one bond at a time, might be able to improve both the selectivity for the carbonyl–olefin metathesis pathway and the substrate scope of the reaction.

Furthermore, these findings highlight the limitations of computational models and the power of $^{12}C/^{13}C$ KIE experiments to confirm or refute mechanistic proposals. Historically, the accuracy of predictions has been primarily constrained by the underestimation of electron correlation and basis set incompleteness. Now, with the advent of sophisticated density functionals, balanced basis sets, and greater computational power, these errors have been greatly reduced.[20,24,26] In this case, the model chemistry is nearly of coupled-cluster/complete-basis-set quality and, by this conventional metric, could have been declared "chemically accurate."[26] Nonetheless, other significant errors remain. Implicit solvation models cannot account for specific solute-solvent interactions and overestimate the energy of the betaine. As a result, the betaine does not contribute to the minimum energy path and a concerted mechanism is erroneously predicted.

This error reveals a hidden failure mode of conventional computational protocols that may be rather common: when charge separation develops along the reaction path, poor error cancellation between the ground and transition states can lead to qualitatively incorrect predictions. In contrast, explicit solvation models do not suffer from this bias. While this approach is complex and costly today, I hope that it will become practical in the near future.[46,58,60,67,68] More broadly, this strategy of making more realistic computational models and evaluating their predictions experimentally will serve as a useful framework for studying carbonyl–olefin metathesis and other reactions involving polarized intermediates.

5.6 Experimental Procedures and Supplemental Information

5.6.1 General Information

General Laboratory Procedures

All moisture-sensitive reactions were performed under an atmosphere of nitrogen in flame-dried round bottom flasks or glass vials fitted with rubber septa and/or septa equipped screw caps. Stainless steel syringes were used to transfer air or moisture-sensitive liquids. Flash chromatography was performed using silica gel SiliaFlash® 40-63 micron (230-400 mesh) from Silicycle.

Materials and Instrumentation

All chemicals were purchased from Sigma-Aldrich, VWR, Oakwood or Acros and were used as received unless otherwise stated. Tetrahydrofuran was dried by being passed through columns of activated alumina. Proton Nuclear Magnetic Resonance NMR (^{1}H NMR) spectra and carbon nuclear magnetic resonance (^{13}C NMR) spectra were recorded on a Varian Inova 400, Varian MR400, Varian vnmrs 500, Varian Inova 500, Varian Mercury 500, Bruker Avance Neo 500, Varian Vnmrs 600, and Varian vnmrs 700 spectrometers. Chemical shifts for protons are reported in parts per million and are references to the NMR solvent peak ($CDCl_3$: δ_H 7.27). Chemical shifts for carbons are reported in parts per million and are referenced to the carbon resonances of the NMR solvent ($CDCl_3$: δ_C 77.0). Data are represented as follows: chemical shift, integration, multiplicity (br = broad, s = singlet, d = doublet, t = triplet, q = quartet, p = pentet, m = multiplet), and coupling constants in Hertz (Hz). Ultra-high performance liquid chromatography (UPLC) was performed on an Agilent 1290 Infinity II LC System using an ZORBAX RRHD Eclipse Plus C18 column, 95 Å, 2.1 x 50 mm, 1.8 µm, 1200 bar pressure limit. Mass spectroscopic (MS) data was recorded at the Mass Spectrometry Facility at the Department of Chemistry of the University of Michigan in Ann Arbor, MI on an Agilent Q-TOF HPLC-MS with ESI high resolution mass spectrometer. Infrared (IR) spectra were obtained using a Perkin Elmer Frontier MIR spectrometer. IR data are represented as frequency of absorption (cm^{-1}).

Data Availability

Experimental procedures, compound characterization data, and computational details are provided below for this work. Additional NMR spectroscopic and computational data, scripts, and analyses are available at https://github.com/ekwan/carbonyl_olefin_metathesis_SI. *presto* is available at https://github.com/corinwagen/presto under the GPL 3.0 license.

Acknowledgements

I thank Dr. Eugenio Alvarado for helpful guidance with setting up NMR experiments. I thank Katherine Forbes, Marcus Sak, Hayden Sharma, and Daniel Singleton for helpful discussions. Additionally, I thank Haley Albright, Lara Cala Alvares, Melodie Christensen, Ashlee Davis, Marion Emmert, Joe Gair, Mario Gaviria, Shane Grosser, Dennis Kutateladze, Colin Lam, Richard Liu, Daniel Nasrallah, John Ovian, Paul Riehl, Rebecca Ruck, Jonathon Ryan, Daniel Steigerwald, Alexandra Sun, Shannon Wilkens, Jonathan Wong, and Charles Yeung for providing useful feedback.

5.6.2 General Procedures

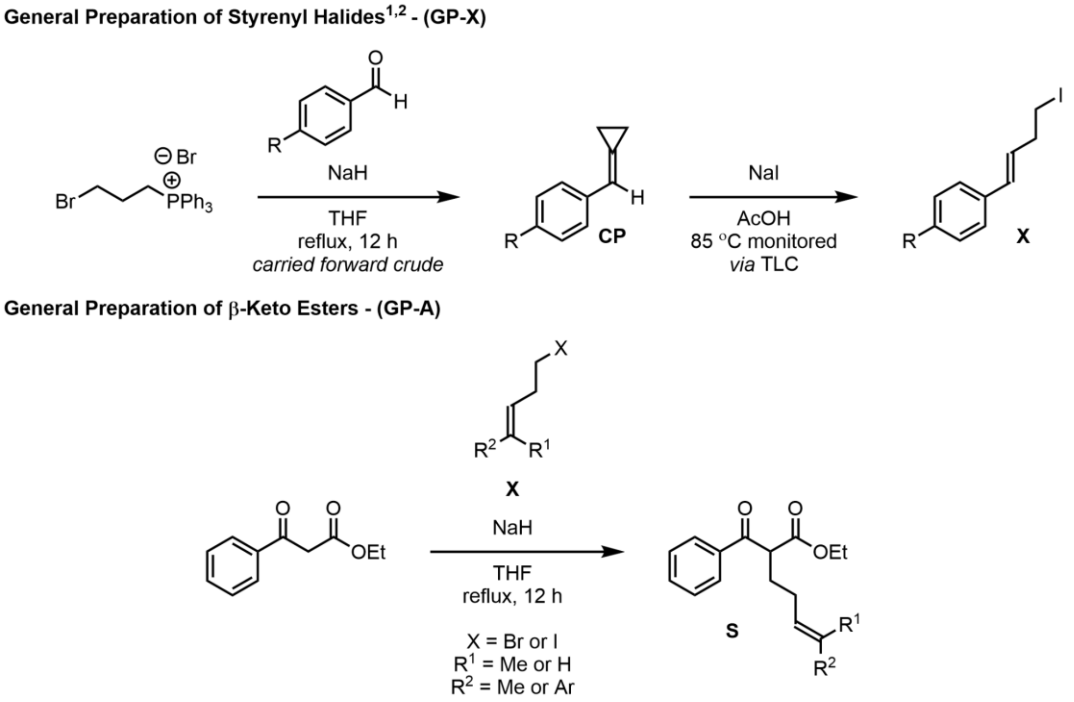

General Preparation of Styrenyl Halides (GP-X)[69,70]

(3-Bromopropyl)triphenylphosphonium bromide[69] (1.1 equiv.) was dissolved in THF (0.5 M) in a flame dried round bottom flask equipped with a stir bar, under N_2, and stirred at room temperature for 0.5 h. Sodium hydride (1.105 equiv.) was added to the solution slowly, then reaction mixture was allowed to stir at room temperature for an additional 0.5 h, then was heated to reflux for 1.5 h. Carbonyl (1.0 equiv.) was added, and the reaction was allowed to stir at 70 °C overnight. The reaction was removed from the heat and allowed to cool to room temperature, diluted with water, and extracted 3 times with pentanes. The organics were collected, washed with brine, and dried over Na_2SO_4. The organic phase was filtered and concentrated under vacuum. The crude product **CP** was used in the next step without purification.

Cyclopropylidene **CP** (1.0 equiv.) was dissolved in acetic acid (0.5 M) in a flame dried round bottom flask equipped with a stir bar and under N_2. The solution was treated with sodium iodide (1.50 equiv.) and heated to 85 °C until TLC showed complete consumption of the starting material. Upon completion, the reaction was quenched with water. The aqueous solution was extracted with Et_2O 3 times. The organics were collected and washed with Na_2CO_3 until all acid was consumed, then water and brine, and dried over Na_2SO_4. The organics were filtered and concentrated under

vacuum to afford a colorless oil. The crude product was purified by flash column chromatography in 100% hexanes to afford the desired alkyl halide substrate **X**.

General Preparation of Alkyl or Styrenyl β-Keto Esters (GP-A)

A flask was charged with sodium hydride (1.2 equiv.) and anhydrous THF (0.32 M) was added to the mixture under N_2. The suspension was cooled to 0 °C and stirred for 10 minutes. Aryl β-keto ester was added (1.0 equiv.) dropwise to the mixture and stirred for another 10 minutes at 0 °C. A solution of alkyl halide **X** (1.05 equiv.) in anhydrous THF (0.63 M) was added dropwise to the mixture at 0 °C. Then, the mixture was heated to 72 °C for 16 h. The reaction was quenched by the addition of saturated aqueous NH_4Cl (100 mL). The mixture was extracted with Et_2O (3 x 50 mL). The combined organic phases were washed with brine and dried over Na_2SO_4. The organic phase was filtered and concentrated under vacuum. The crude product was purified by flash column chromatography in 1-3% EtOAc/pentanes with a 2% DCM additive to obtain the desired β-keto ester substrate **S**.

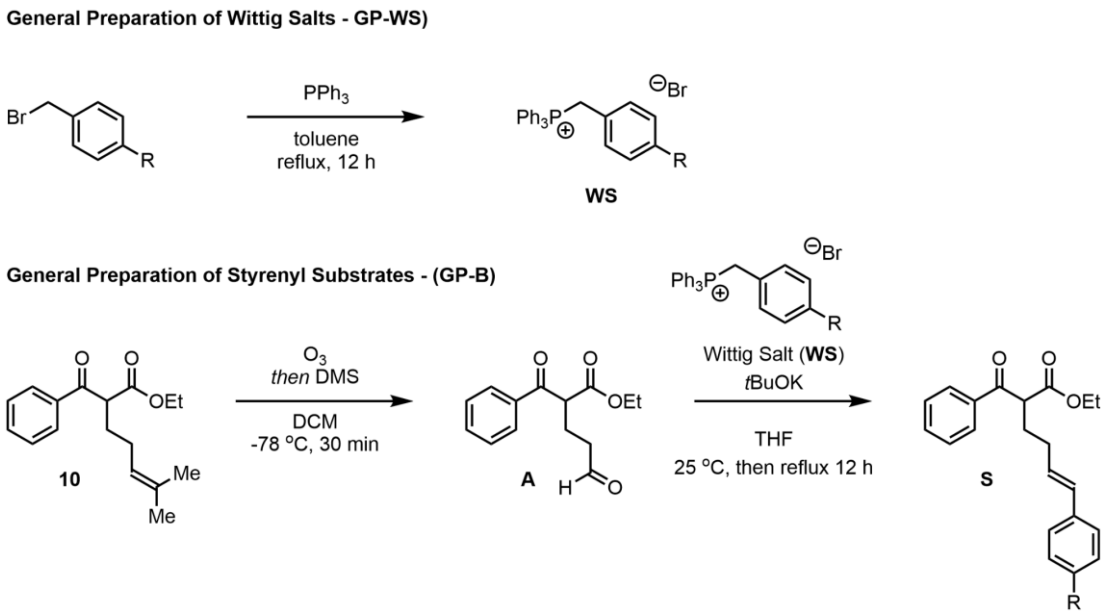

General Preparation of Wittig Salts (GP-WS)

Equimolar amounts of aryl benzyl bromide (1.0 equiv.) and triphenylphosphine (1.0 equiv.) were combined in flame dried round bottom flask equipped with a stir bar, under N_2, and heated in toluene (0.5 M) at 110 °C for 16 h. After 16 h, the reaction was cooled to 25 °C and the solid was filtered and placed under vacuum to dry for 8 h, yielding the desired Wittig salt **WS**.

General Preparation of Styrenyl β-Keto Ester Substrates (GP-B)

A solution of potassium *tert*-butoxide (1.5 equiv.) in THF (1.3 M) was slowly added to a solution of **WS** (1.5 equiv) in THF (0.5 M) and stirred at 70 °C for 1 h under N_2. Then **A** (1.0 equiv.) in THF (2.0 M) was added dropwise and the mixture was refluxed for 16 h. After cooling, the suspension was filtered, and the solvent of the filtrate was removed under vacuum. The products were purified by column chromatography on silica gel, eluting with 1-3% EtOAc/hexanes to afford the desired styrenyl β-keto ester substrate **S**.

5.6.3 Synthesis and Characterization

ethyl 2-benzoyl-6-methylhept-5-enoate (**10**)

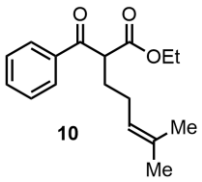

10

Pure starting material:

Prepared according to **GP-A** using 60 wt% sodium hydride (999 mg, 1.2 equiv., 25.0 mmol), ethyl 3-oxo-3-phenylpropanoate (4.00 g, 1.0 equiv., 20.8 mmol), 5-iodo-2-methylpent-2-ene[71] (4.59 g, 1.05 equiv., 21.9 mmol), and THF (99 mL, 0.2 M) with a reaction time of 16 h. Purification by flash column chromatography afforded the pure compound as a colorless oil (3.25 g, 57%).

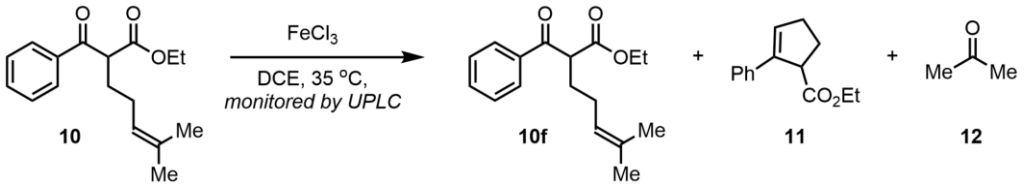

10 **10f** **11** **12**

1 g scale carbonyl–olefin metathesis reaction:

A flame-dried round bottom flask under N_2 was charged with $FeCl_3$ (29.6 mg, 0.05 equiv., 0.182 mmol), freshly distilled DCE (36.0 mL, 0.1 M), and stirred at 35 °C for 10 min. To this solution was added **10** (1.00 g, 1.0 equiv., 3.64 mmol), and the resultant mixture was monitored by UPLC

until about 80% conversion. Then the reaction mixture was passed through a short silica plug eluting with DCM (50 mL) and the filtrate was concentrated under reduced pressure. **10f** (180 mg, 18%) and ethyl 2-phenylcyclopent-2-ene-1-carboxylate (carbonyl–olefin metathesis product, **11**) (653 mg, 82 %) were carried forward without purification. The procedure was repeated for the preparation of an additional sample. Conversions (82% and 78%) were determined by UPLC with caffeine as an internal standard and later confirmed by crude mass of **10f** and **11** and mass recovery of **15f** and **11**.

Calibration of caffeine (C: caffeine) and **10** for UPLC analysis; 6 different samples were prepared. In each sample, the concentration of C was held constant (1.94 mg/mL) but the concentration of **10** was varied from 0.14 mg to 3.43 mg/mL. The integral ratio of **10** and C plotted against the known concentration of **10**. A linear correlation (R^2 = 0.9994) was observed, which implies that the response factor of **10** does not change over this range of concentrations.

	Concentration of **10** [mM]	Ratio (**10**/C)
Sample 1	0.5000	0.1261
Sample 2	2.5000	0.6114
Sample 3	5.0000	1.2289
Sample 4	7.5000	1.8176
Sample 5	10.000	2.4594
Sample 6	12.5000	2.9752

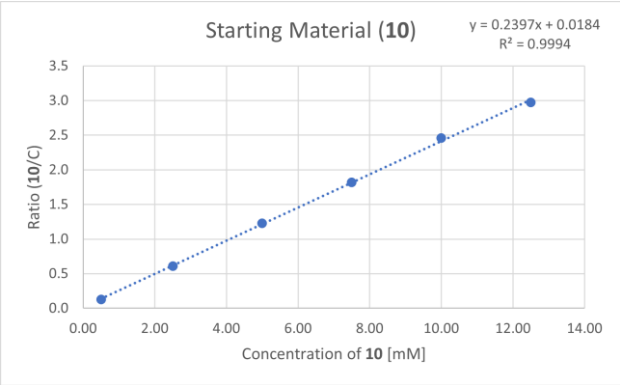

[C] = 1.94 mg/mL , RF = 0.41

UPLC Conditions: 60-80% acetonitrile in water (0.1% formic acid), 0.400 mL/min, 4 min method, 254 nm

Retention time: T_C = 0.389 min; $T_{\mathbf{10}}$ = 3.252 min

Determination of the conversion **10f**: Small aliquots (50 µL) where taken from the reaction at various time points and combined with C (47 µL, concentration of C ~ 1.94 mg/mL) were diluted with acetonitrile and measured by UPLC; each sample was run twice and the average was used. Final aliquots were taken immediately prior to quenching the reaction.

	Sample 1 - 82%				Sample 2 - 78%		
	Average Area of **10f**	Average Area of C	Conversion		Average Area of **10f**	Average Area of C	Conversion
Aliquot 1	708.48	1083.32	73.18%	Aliquot 1	815.945	956.99	65.03%
Aliquot 2	485.65	1029.515	80.6%	Aliquot 2	509.75	973.615	78.53%
Aliquot 3 (final)	444.535	1010.9875	81.97%	Aliquot 3 (final)	556.47	1033.235	77.91%

Conversion: F = [1 - (R_f ∗ (average area **10f** / average area C) ∗ (mol C per aliquot / mol **10f** per aliquot)] ∗ 100 = [1 - (0.41 ∗ (444.535 / 1010.9875) ∗ (0.00001 / 0.00001)] ∗ 100 = 81.97%

Characterization of **10**

^{1}H NMR (700 MHz; $CDCl_3$) δ_H 7.98 (d, J = 7.7 Hz, 2H), 7.59 (t, J = 7.4 Hz, 1H), 7.48 (t, J = 7.3 Hz, 2H), 7.27 (d, J = 2.0 Hz, 1H), 5.11 (d, J = 7.0 Hz, 1H), 4.34 – 4.29 (m, 1H), 4.16 (q, J = 7.2 Hz, 2H), 2.11 – 2.03 (m, 4H), 1.68 (s, 3H), 1.53 (s, 3H), 1.19 (t, J = 7.0 Hz, 3H).

^{13}C NMR (176 MHz, $CDCl_3$) δ_C 195.4, 170.0, 136.3, 133.32, 133.29, 128.6, 128.5, 123.0, 61.2, 53.4, 29.0, 25.9, 25.7, 17.6, 14.0.

Spectroscopic data matches literature report.[6]

^{1}H NMR spectrum of **10**:

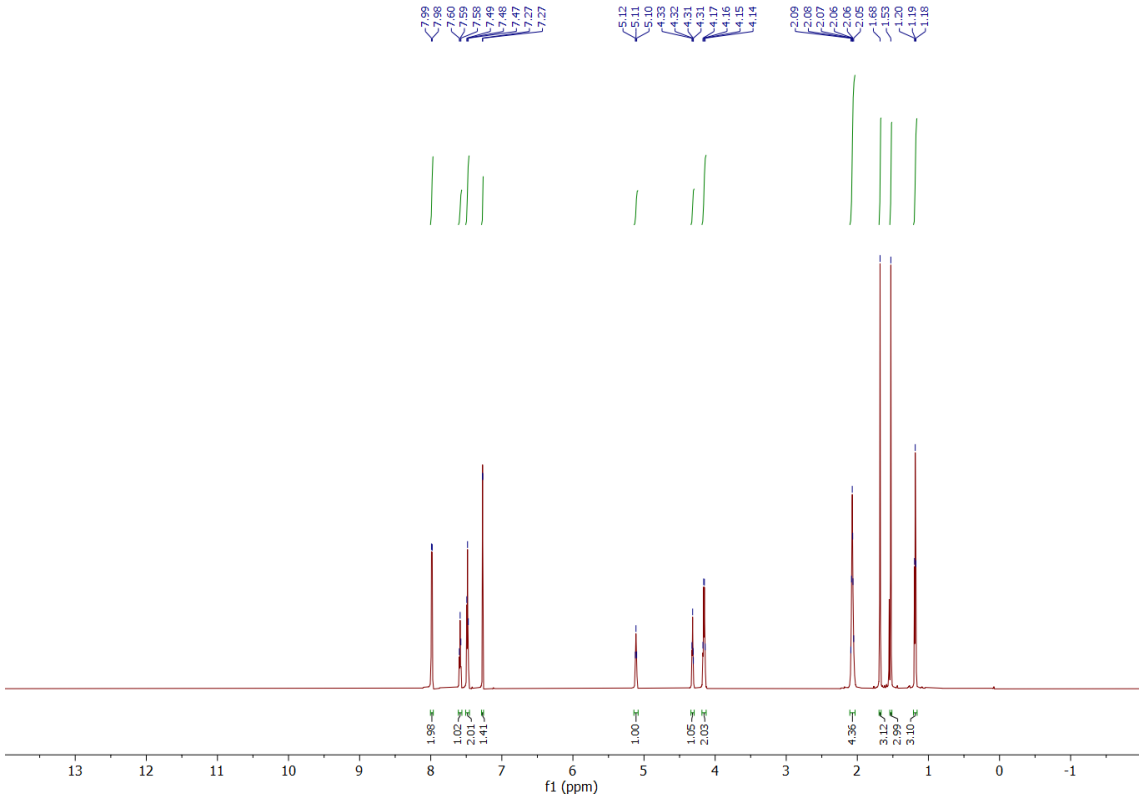

^{13}C NMR spectrum of **10**:

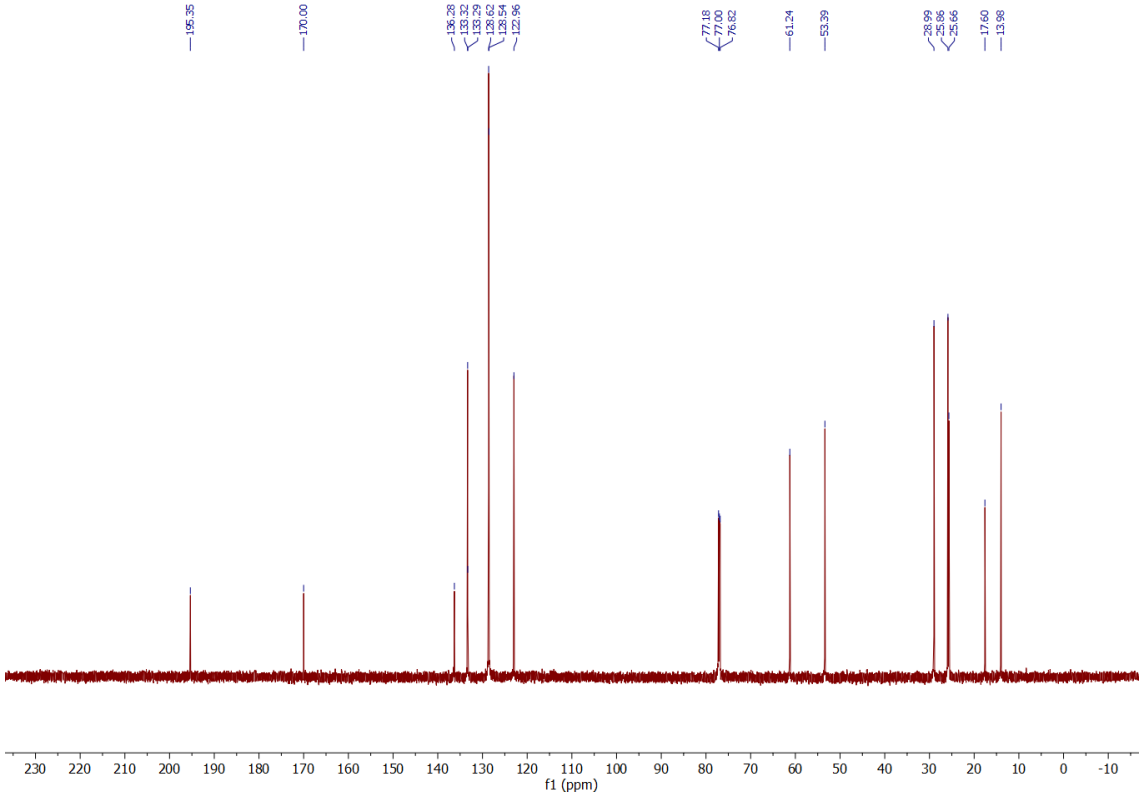

ethyl 2-benzoyl-6-methylheptanoate (**15r**)

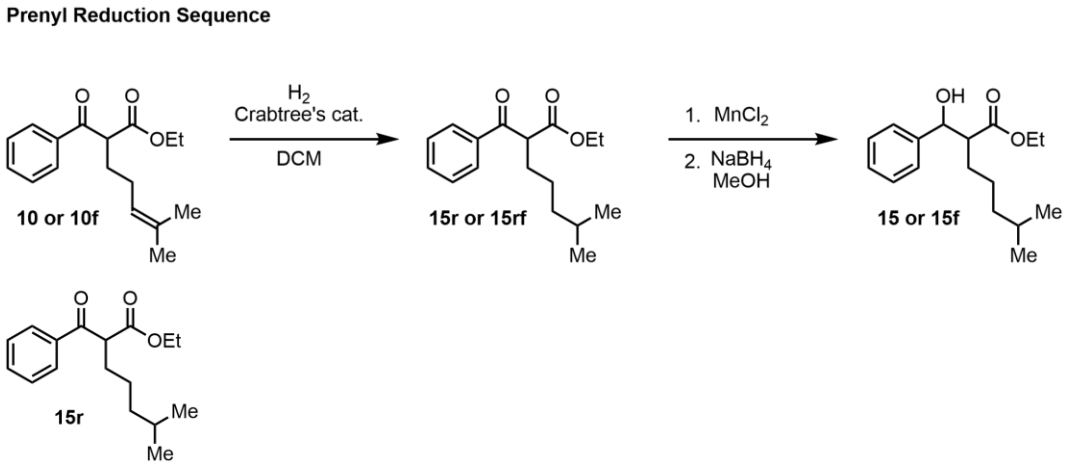

Small scale, pure starting material:

To a flame dried vial was added (1,5-Cyclooctadiene)(pyridine)(tricyclohexylphosphine)-iridium(I) hexafluorophosphate (18.3 mg, 0.025 equiv., 22.8 µmol). The catalyst was added to a solution of the **10** (250 mg, 1.00 equiv., 911 µmol) in DCM (3.0 mL, 0.3 M). The flask was evacuated, and a balloon of H_2 was introduced. The flask was evacuated and refilled with H_2 3 times to ensure sufficient incorporation of the gas. The reaction solution started as a bright orange and turned a deep yellow. After 12 h, the DCM was evaporated, and the residue treated with Et_2O (5 mL) and filtered through a silica plug to remove the precipitated metal salts. The filtrate was concentrated under vacuum, providing the crude product quantitatively as a colorless oil, **15r** (252 mg, 912 µmol, 100 %), used crude in the next step of the reduction sequence. The procedure was repeated for the preparation of an additional sample.

1 g scale, crude mixture from 1 g carbonyl–olefin metathesis reaction:

To a flame dried vial was added (1,5-Cyclooctadiene)(pyridine)(tricyclohexylphosphine)-iridium(I) hexafluorophosphate (182 mg, 0.075 equiv., 226 µmol). The catalyst was added to solution of the **10f** (180 mg, 0.217 equiv., 656 µmol) and ethyl 2-phenylcyclopent-2-ene-1-carboxylate (carbonyl–olefin metathesis product, **11**) (653 mg, 1.00 equiv., 3.02 mmol) in DCM (12.0 mL, 0.3 M). The flask was evacuated, and a balloon of H_2 was introduced. The flask was evacuated and refilled with H_2 3 times to ensure sufficient incorporation of the gas. The reaction solution started as a bright orange and turned a deep yellow. After 12 h, the DCM was evaporated,

and the residue treated with Et_2O (20 mL) and filtered through a silica plug to remove the precipitated metal salts. The filtrate was concentrated under vacuum, providing the crude products quantitatively as yellow oils, **15rf** (181 mg, 655 µmol, 99.8 %) and ethyl 2-phenylcyclopent-2-ene-1-carboxylate (carbonyl–olefin metathesis product, **11**) (653 mg, 3.02 mmol, 100 %), used crude in the next step of the reduction sequence.

Characterization of **15r**

^{1}H NMR (600 MHz; $CDCl_3$) δ_H 8.00 (d, J = 7.3 Hz, 2H), 7.59 (t, J = 7.4 Hz, 1H), 7.49 (t, J = 7.8 Hz, 2H), 4.29 (t, J = 7.1 Hz, 1H), 4.16 (qd, J = 7.2, 2.7 Hz, 2H), 1.99 (tdd, J = 15.7, 10.8, 6.4 Hz, 2H), 1.54 (dp, J = 13.3, 6.6 Hz, 1H), 1.35 (h, J = 6.9 Hz, 2H), 1.22 (tt, J = 10.0, 6.0 Hz, 2H), 1.18 (t, J = 7.1 Hz, 3H), 0.86 (dd, J = 6.6, 2.4 Hz, 6H).

^{13}C NMR (176 MHz, $CDCl_3$) δ_C 195.3, 170.1, 136.4, 133.4, 128.7, 128.6, 61.3, 54.4, 38.6, 29.2, 27.7, 25.4, 22.5, 22.5, 14.0.

Spectroscopic data matches literature report.[6]

^{1}H NMR spectrum of **15r**:

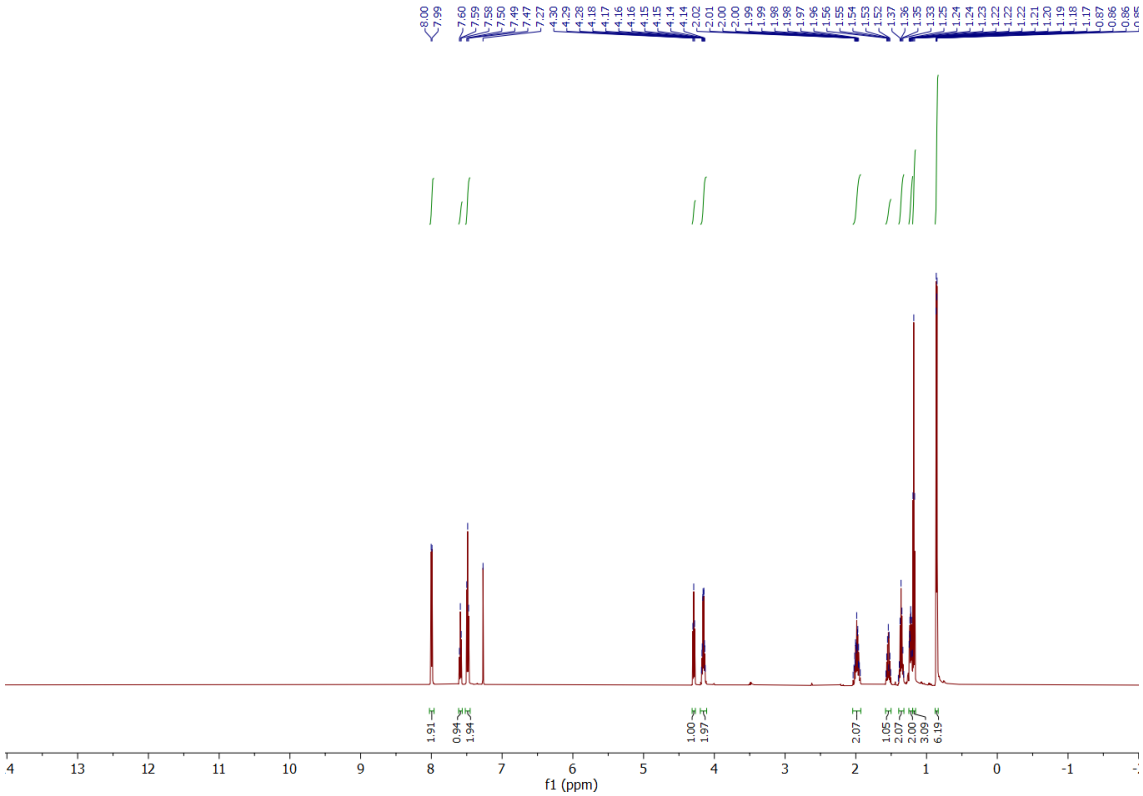

^{13}C NMR spectrum of **15r**:

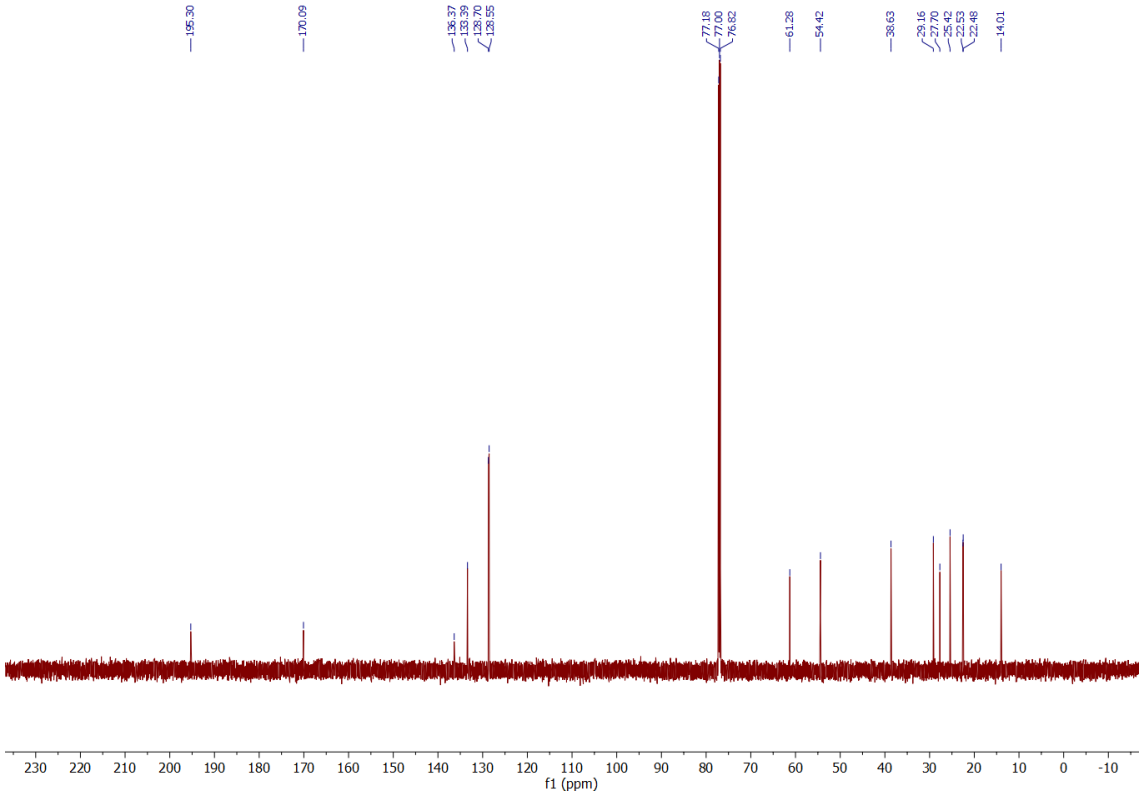

ethyl 2-(hydroxy(phenyl)methyl)-6-methylheptanoate (**15**)

Prenyl Reduction Sequence

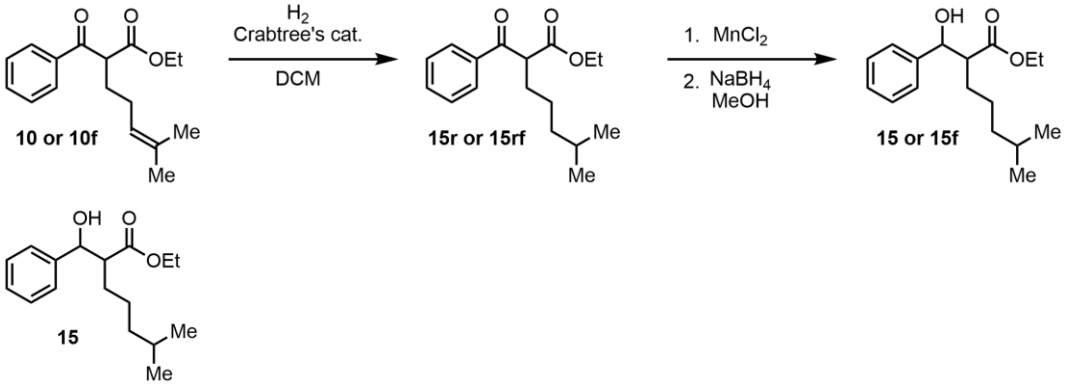

Small scale, pure starting material:

To a solution of **15r** (250 mg, 1 equiv., 905 µmol) in MeOH (6.80 mL, 0.133 M) were added manganese(II) chloride (232 mg, 2.04 equiv., 1.85 mmol). The mixture was stirred for 40 min and cooled to 0°C under N_2, sodium borohydride (34.9 mg, 1.02 equiv., 923 µmol) was added, and the mixture was stirred for 1 h at that temperature. The reaction was quenched and washed with 5% aqueous HCl (25 mL), then brine (25 mL) and EtOAc (25 mL) were added, and the mixture was vigorously shaken in a separatory funnel. The organic phase was separated, the aqueous phase was extracted with EtOAc (25 mL), and the extract was combined with the organic phase, washed with a solution of $NaHCO_3$ (2 x 25 mL) and brine (25 mL), dried over anhydrous Na_2SO_4, and concentrated. The product was purified by column chromatography on silica gel, eluting with 1-10% EtOAc/hexanes to afford the pure compound as a colorless oil (218 mg, 87%).

1 g scale, crude mixture from 1 g carbonyl–olefin metathesis reaction:

To a solution of **15rf** (180 mg, 0.216 equiv., 651 µmol) and ethyl 2-phenylcyclopent-2-ene-1-carboxylate (carbonyl–olefin metathesis product, **11**) (653 mg, 1.00 equiv., 3.02 mmol) in MeOH (22.5 mL, 0.133 M) were added manganese(II) chloride (775 mg, 2.04 equiv., 6.16 mmol). The mixture was stirred for 40 min and cooled to 0°C under N_2, sodium borohydride (117 mg, 1.02 equiv., 3.08 mmol) was added, and the mixture was stirred for 1 h at that temperature. The reaction was quenched and washed with 5% aqueous HCl (100 mL), then brine (100 mL) and EtOAc (100 mL) were added, and the mixture was vigorously shaken in a separatory funnel. The organic phase

was separated, the aqueous phase was extracted with EtOAc (100 mL), and the extract was combined with the organic phase, washed with a solution of $NaHCO_3$ (2 x 100 mL) and brine (100 mL), dried over anhydrous Na_2SO_4, and concentrated. The product was purified by column chromatography on silica gel, eluting with 1-10% EtOAc/hexanes to afford the pure compound **15f** as a colorless oil (146 mg, 81%).

Characterization of **15**

^{1}H NMR (600 MHz; CD_3OD) δ_H 7.35 – 7.28 (m, 4H), 7.24 (t, J = 6.9 Hz, 1H), 4.67 (d, J = 8.5 Hz, 1H), 3.88 (q, J = 7.1 Hz, 2H), 2.70 (ddd, J = 10.6, 8.5, 3.4 Hz, 1H), 1.88 (dddd, J = 13.7, 10.1, 6.1, 3.4 Hz, 1H), 1.73 (tdd, J = 13.7, 10.1, 4.9 Hz, 1H), 1.55 (dp, J = 13.2, 6.6 Hz, 1H), 1.38 – 1.16 (m, 4H), 1.00 (t, J = 7.1 Hz, 3H), 0.89 (dd, J = 6.6, 3.7 Hz, 6H).

^{13}C NMR (126 MHz, CD_3OD) δ_C 175.5, 144.2, 129.1, 128.6, 127.7, 76.3, 61.1, 55.8, 39.9, 30.3, 28.9, 26.4, 23.1, 22.8, 14.3.

ν_{max} (FTIR)/cm^{-1}: 3032, 2954, 2869, 2570, 1729, 1710, 1455, 1176, 1025, 699.

HRMS (ESI) m/z: $[M+Na]^+$ calculated for $C_{17}H_{26}O_3Na^+$: 301.1774; found: 301.1768.

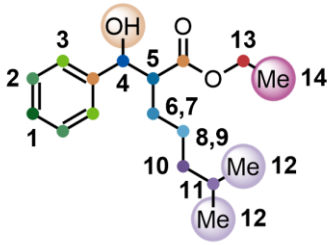

#	^{1}H (ppm)	^{13}C (ppm)	# of protons	^{1}H T_1 (sec)	Peak Widths (Hz)	$^{1}J_{CH}$ (Hz)
1	7.27	128.6	1	0.67	1.68	162
2	7.33	127.7	2	0.73	1.55	156
3	7.33	129.1	2	0.73	1.59	156
4	**4.67**	**76.3**	1	**0.82**	**1.69**	**144**
5	2.70	55.8	1	0.82	1.63	132
6	1.33	26.4	1	1.25	1.69	120
7	1.26	26.4	1	1.39	1.69	120
8	1.89	30.3	1	1.48	1.73	126
9	1.73	30.3	1	1.43	1.73	114
10	**1.22**	**39.9**	2	**1.10**	**1.51**	**120**
11	**1.55**	**28.9**	1	**0.66**	**1.41**	**120**
12	0.98	23.1, 22.8	6	0.86	1.62, 1.59	120, 120
13	3.90	61.1	2	0.71	1.88	144
14	1.00	14.3	3	0.63	1.55	126

Quanternary Carbons (ppm): 175.5, 144.2

$^{1}J_{CH}$ determined by cgHSQCAD (error bar is less than 1 Hz). T_1s determined by inversion recovery (error bar is less than 0.1 s). Assignments determined by ^{1}H NMR, proton-decoupled ^{13}C NMR, and gHSQCAD.

^{1}H NMR spectrum of **15**:

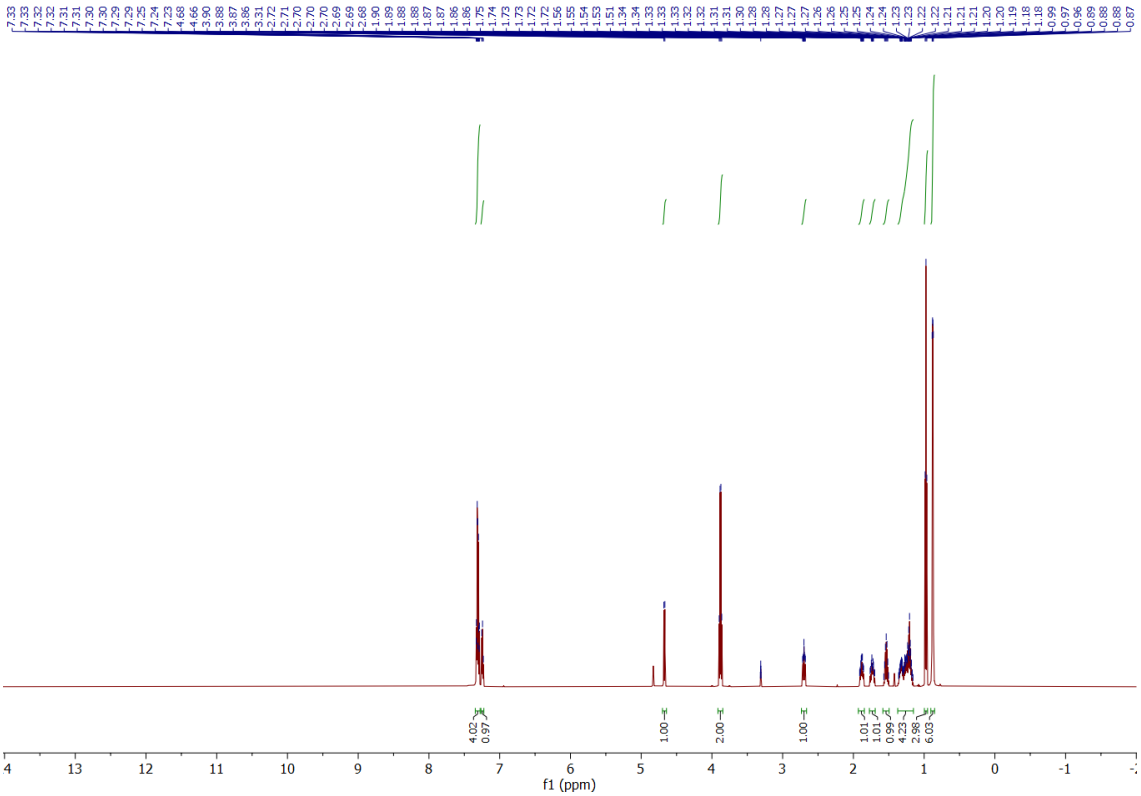

^{13}C NMR spectrum of **15**:

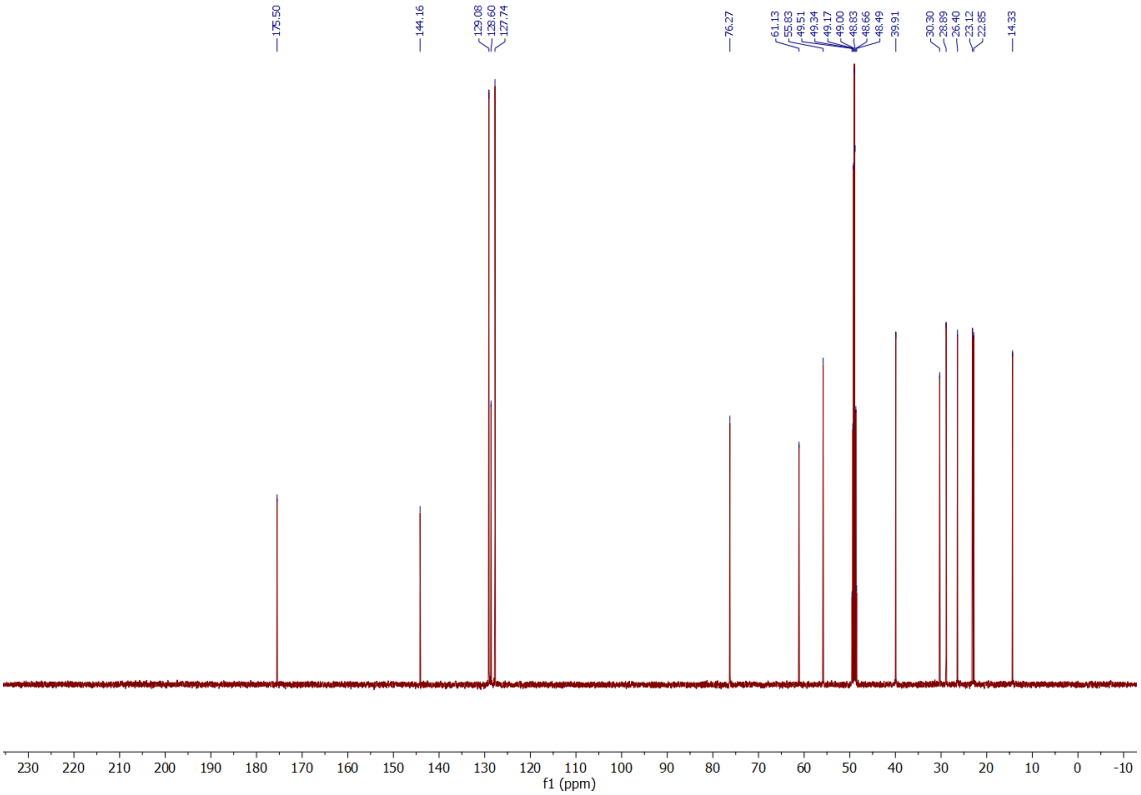

(*E*)-(4-iodobut-1-en-1-yl)benzene (**20X**)

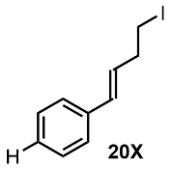

Prepared according to **GP-X** using (3-bromopropyl)triphenylphosphonium bromide (15.3 g, 1.1 equiv., 33 mmol), 60 wt% sodium hydride (1.32 g, 1.105 equiv., 33.1 mmol), benzaldehyde (3.06 mL, 1.0 equiv., 30.0 mmol), and THF (60 mL, 0.5 M) with a reaction time of 16 h. Afforded crude **20CP** (1.56 g, 40%). Using **20CP** (1.56 g, 1.00 equiv., 12.0 mmol), sodium iodide (2.69 g, 1.50 equiv. 18.0 mmol), and acetic acid (24 mL, 0.5 M) with a reaction time of 4 h. Purification by flash column chromatography afforded the pure compound as a colorless oil (2.25 g, 78%).

Characterization of **20X**

^{1}H NMR (700 MHz; $CDCl_3$) δ_H 7.38 (d, J = 7.7 Hz, 2H), 7.32 (t, J = 7.7 Hz, 2H), 7.25 (t, J = 7.4 Hz, 1H), 6.49 (d, J = 15.8 Hz, 1H), 6.16 (dt, J = 15.7, 6.8 Hz, 1H), 3.26 (t, J = 7.2 Hz, 2H), 2.80 (q, J = 6.7 Hz, 2H).

^{13}C NMR (176 MHz; $CDCl_3$) δ_C 137.0, 132.3, 128.6, 128.5, 127.4, 126.2, 37.0, 5.1.

Spectroscopic data matches literature report.[72]

^{1}H NMR spectrum of **20X**:

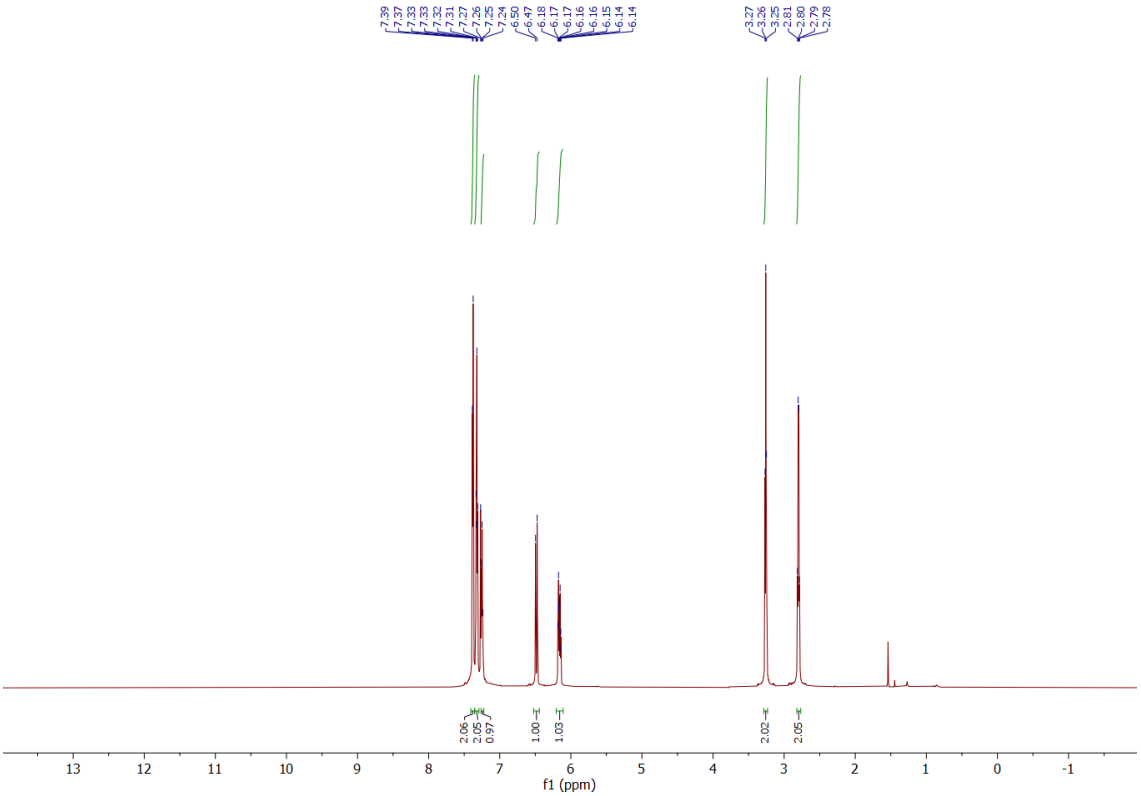

^{13}C NMR spectrum of **20X**:

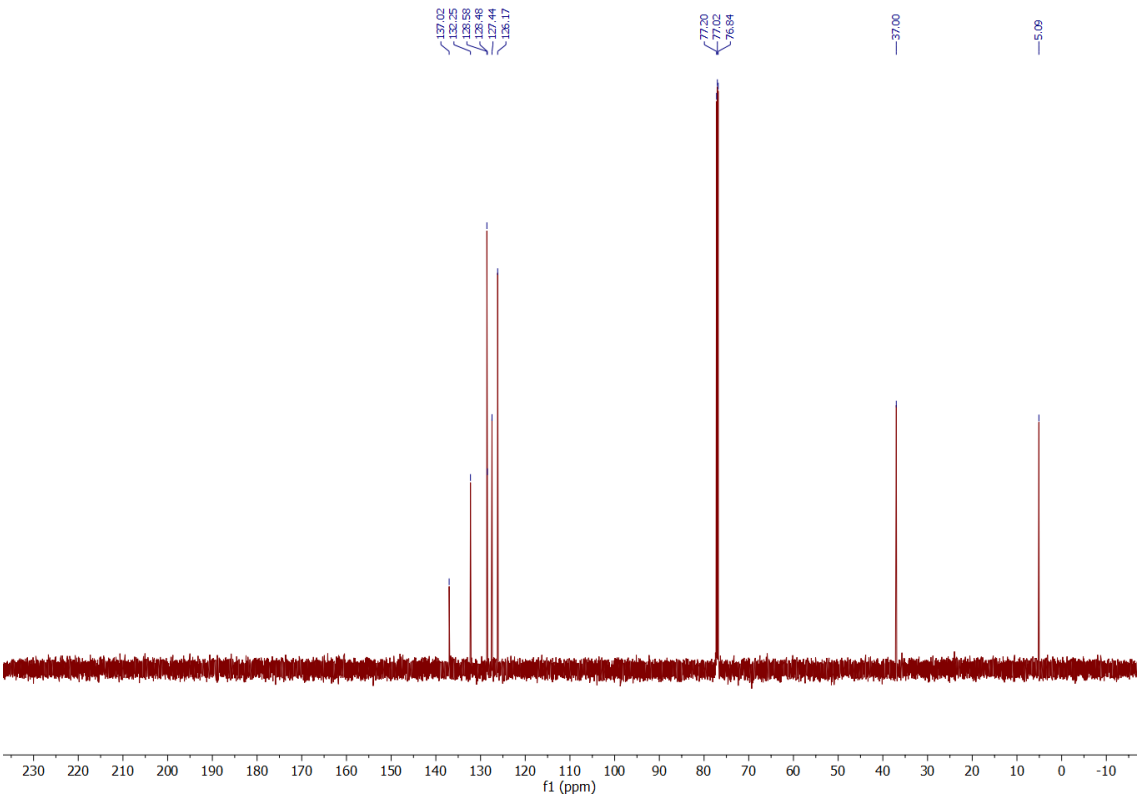

ethyl (*E*)-2-benzoyl-6-phenylhex-5-enoate (**20**)

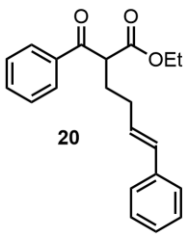

Pure starting material:

Prepared according to **GP-A** using 60 wt% sodium hydride (375 mg, 1.2 equiv., 9.36 mmol), ethyl 3-oxo-3-phenylpropanoate (1.50 g, 1.0 equiv., 7.80 mmol), **20X** (2.11 g, 1.05 equiv., 8.19 mmol), and THF (41 mL, 0.2 M) with a reaction time of 16 h. Purification by flash column chromatography afforded the pure compound as a white solid (1.21 g, 48%).

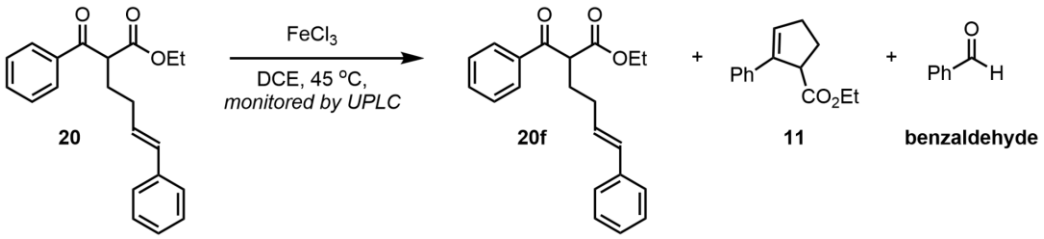

1 g scale carbonyl–olefin metathesis reaction:

A flame-dried round bottom flask under N_2 was charged with $FeCl_3$ (50.3 mg, 0.10 equiv., 0.310 mmol), freshly distilled DCE (72.0 mL, 0.05 M), and stirred at 45 °C for 10 min. To this solution was added **20** (1.00 g, 1.0 equiv., 3.10 mmol), and the resultant mixture was monitored by UPLC until the desired % conversion. Then the reaction mixture was passed through a short silica plug eluting with DCM (50 mL) and the filtrate was concentrated under reduced pressure. **20f** (200 mg, 20%), ethyl 2-phenylcyclopent-2-ene-1-carboxylate (carbonyl–olefin metathesis product, **11**) (537 mg, 80 %), and benzaldehyde (263 mg, 80 %) were carried forward without purification. The procedure was repeated for the preparation of an additional sample. Final conversions (80% and 67%) were determined by ^1H NMR with $PhSiMe_3$ as an internal standard and later confirmed by crude mass of **20f**, **11**, and benzaldehyde, and mass recovery of **20rf**, **11**, and benzyl alcohol.

Determination of the conversion **20f**: $PhSiMe_3$ (20 µL) was added directly into the concentrated reaction mixture, followed by 2 mL of $CDCl_3$. A small amount of the mixture was transferred to an NMR tube and subsequently diluted with another 0.5 mL of $CDCl_3$. Peaks corresponding to $PhSiMe_3$ were integrated and normalized to the appropriate amount of protons, then the peaks corresponding to **20f** were integrated.

	Sample 1 - 80%					Sample 1 - 67%			
	Integration of **20f**	$PhSiMe_3$ mol	**20f** mol	Conversion		Integration of **20f**	$PhSiMe_3$ mol	**20f** mol	Conversion
NMR 1	4.34	0.0001426	0.00310	80.04%	NMR 2	7.23	0.0001426	0.00310	66.74%

Conversion: F = [1 - (integration **20f** ∗ (mol $PhSiMe_3$ / mol **20f**)] ∗ 100 = [1 - (4.34 ∗ (0.0001426 / 0.00310)] ∗ 100 = 80.04%

Characterization of **20**

^{1}H NMR (500 MHz; $CDCl_3$) δ_H 7.99 (d, J = 7.7 Hz, 2H), 7.59 (t, J = 7.4 Hz, 1H), 7.47 (t, J = 7.7 Hz, 2H), 7.34 – 7.28 (m, 4H), 7.21 (t, J = 6.2 Hz, 1H), 6.36 (d, J = 15.8 Hz, 1H), 6.19 (dt, J = 15.7, 6.9 Hz, 1H), 4.39 (t, J = 7.0 Hz, 1H), 4.15 (q, J = 7.1 Hz, 2H), 2.37 – 2.27 (m, 2H), 2.22 (q, J = 7.1 Hz, 2H), 1.18 (t, J = 7.1 Hz, 3H).

^{13}C NMR (126 MHz, $CDCl_3$) δ_C 195.2, 169.9, 137.3, 136.3, 133.5, 131.4, 128.9, 128.7, 128.6, 128.5, 127.1, 126.0, 61.4, 53.2, 30.8, 28.5, 14.0.

ν_{max} (FTIR)/cm^{-1}: 2986, 1721, 1688, 1597, 1447, 1319, 1172, 1150, 970, 692.

HRMS (ESI) m/z: $[M+Na]^+$ calculated for $C_{21}H_{22}O_3Na^+$: 354.1461; found: 345.1457.

^{1}H NMR spectrum of **20**:

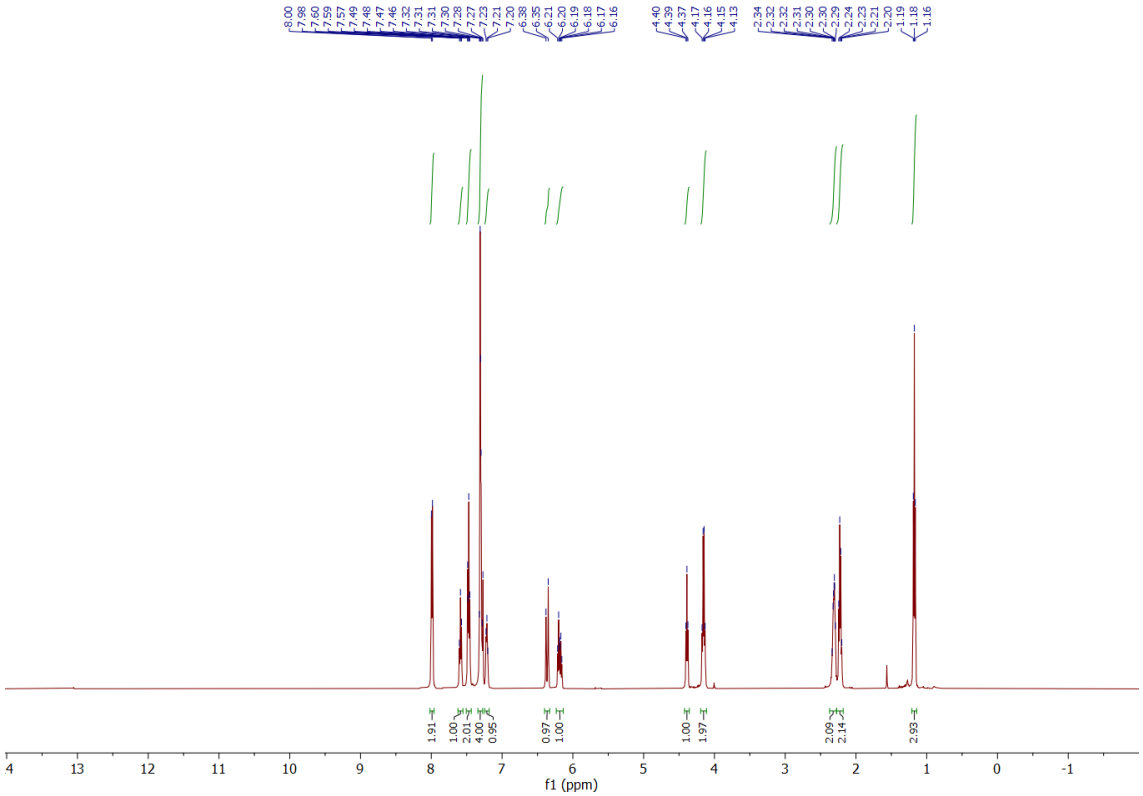

^{13}C NMR spectrum of **20**:

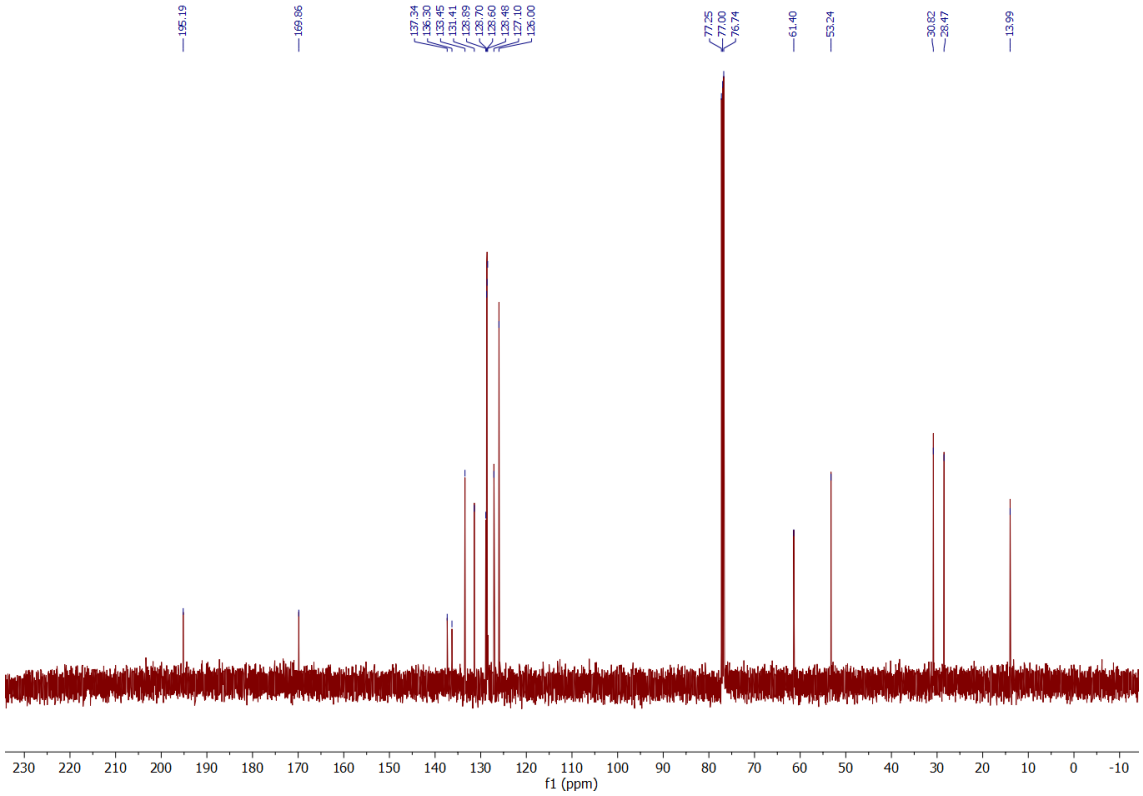

ethyl (*E*)-2-(hydroxy(phenyl)methyl)-6-phenylhex-5-enoate (**20r**)

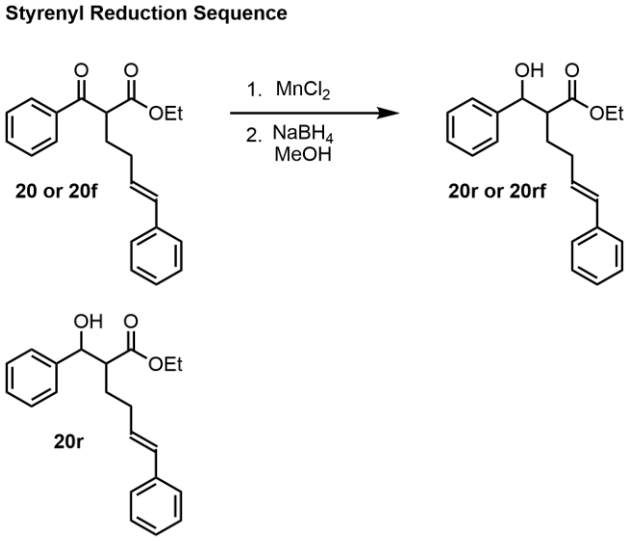

Small scale, pure starting material:

To a solution of **20** (150 mg, 1 equiv., 465 µmol) in MeOH (4.10 mL, 0.133 M) were added manganese(II) chloride (119mg, 2.04 equiv., 949 µmol). The mixture was stirred for 40 min and cooled to 0°C under N_2, sodium borohydride (18 mg, 1.02 equiv., 475 µmol) was added, and the mixture was stirred for 1 h at that temperature. The reaction was quenched and washed with 5% aqueous HCl (20 mL), then brine (20 mL) and EtOAc (20 mL) were added, and the mixture was vigorously shaken in a separatory funnel. The organic phase was separated, the aqueous phase was extracted with EtOAc (20 mL), and the extract was combined with the organic phase, washed with a solution of $NaHCO_3$ (2 x 20 mL) and brine (20 mL), dried over anhydrous Na_2SO_4, and concentrated. The product was purified by column chromatography on silica gel, eluting with 1-10% EtOAc/hexanes to afford the pure compound **20r** as a colorless oil (125 mg, 83%). The procedure was repeated for the preparation of an additional sample.

1 g scale, crude mixture from 1 g carbonyl–olefin metathesis reaction:

To a solution of **20f** (200 mg, 0.288 equiv., 716 µmol), ethyl 2-phenylcyclopent-2-ene-1-carboxylate (carbonyl–olefin metathesis product, **11**) (537 mg, 1.00 equiv., 2.48 mmol), and benzaldehyde (263 mg, 1.00 equiv., 2.48 mmol) in MeOH (19 mL, 0.133 M) were added manganese(II) chloride (637 mg, 2.04 equiv., 5.07 mmol). The mixture was stirred for 40 min and

cooled to 0°C under N_2, sodium borohydride (95.8 mg, 1.02 equiv., 2.53 mmol) was added, and the mixture was stirred for 1 h at that temperature. The reaction was quenched and washed with 5% aqueous HCl (100 mL), then brine (100 mL) and EtOAc (100 mL) were added, and the mixture was vigorously shaken in a separatory funnel. The organic phase was separated, the aqueous phase was extracted with EtOAc (100 mL), and the extract was combined with the organic phase, washed with a solution of $NaHCO_3$ (2 x 100 mL) and brine (100 mL), dried over anhydrous Na_2SO_4, and concentrated. Purification by preparative SCF (Sepiatec 2) on an OJ-H column (21x250 mm, 5 µm) eluting with 20% MeOH in water (0.1% NH_4OH) at 2.40 min (70 mL/min, 5.25 min method, 215 nm) afforded the pure compound as a colorless oil (151 mg, 65%).

Characterization of **20r**

^{1}H NMR (700 MHz; $CDCl_3$) δ_H 7.40 – 7.29 (m, 9H), 7.23 (t, J = 6.9 Hz, 1H), 6.36 (d, J = 15.8 Hz, 1H), 6.13 (dt, J = 15.7, 6.9 Hz, 1H), 4.97 (d, J = 5.8 Hz, 1H), 4.06 (q, J = 7.1 Hz, 2H), 3.00 (s, 1H), 2.81 (ddd, J = 10.0, 5.8, 3.6 Hz, 1H), 2.26 (dq, J = 14.5, 6.9 Hz, 1H), 2.17 (dq, J = 14.8, 7.5 Hz, 1H), 1.98 (dtd, J = 16.1, 8.6, 5.7 Hz, 1H), 1.88 (dddd, J = 13.2, 9.5, 7.1, 3.5 Hz, 1H), 1.14 (t, J = 7.1 Hz, 3H).

^{13}C NMR (176 MHz, $CDCl_3$) δ_C 174.7, 141.5, 137.4, 130.5, 129.4, 128.3, 128.2, 127.6, 126.8, 126.1, 125.8, 74.2, 60.5, 52.4, 30.9, 26.6, 13.9.

ν_{max} (FTIR)/cm^{-1}: 3463, 3028, 2936, 1724, 1710, 1449, 1178, 1024, 731, 693.

HRMS (ESI) m/z: $[M+Na]^+$ calculated for $C_{21}H_{24}O_3Na^+$: 347.1618; found: 347.1609.

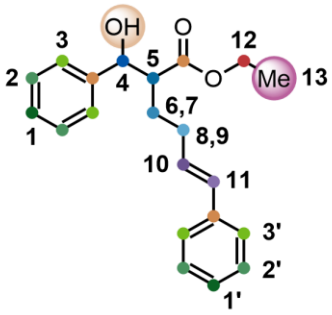

#	^{1}H (ppm)	^{13}C (ppm)	# of protons	^{1}H T_1 (sec)	Peak Widths (Hz)
1, 1'	7.23 , 7.41-7.29	126.8, 127.6	2	0.42, 0.62	1.90, 1.96
2, 2'	7.41-7.29	126.1, 125.9	4	0.42	1.90, 1.67
3, 3'	7.41-7.29	128.3, 128.2	4	0.42	1.34, 1.69
4	**4.97**	**74.2**	1	1.28	1.68
5	2.81	52.4	1	0.97	1.55
6	1.98	26.6	1	1.53	1.93
7	1.89	26.6	1	1.65	1.93
8	2.26	30.9	1	1.34	1.83
9	2.18	30.9	1	1.35	1.83
10	**6.13**	**129.4**	1	0.62	1.17
11	**6.36**	**130.5**	1	0.77	1.80
12	4.06	60.5	2	0.71	1.78
13	1.14	13.9	3	0.61	1.63
Quanternary Carbons (ppm): 174.7, 141.5, 137.5					

T_1s determined by inversion recovery (error bar is less than 0.1 s). Assignments determined by ^{1}H NMR, proton-decoupled ^{13}C NMR, and gHSQCAD.

^{1}H NMR spectrum of **20r**:

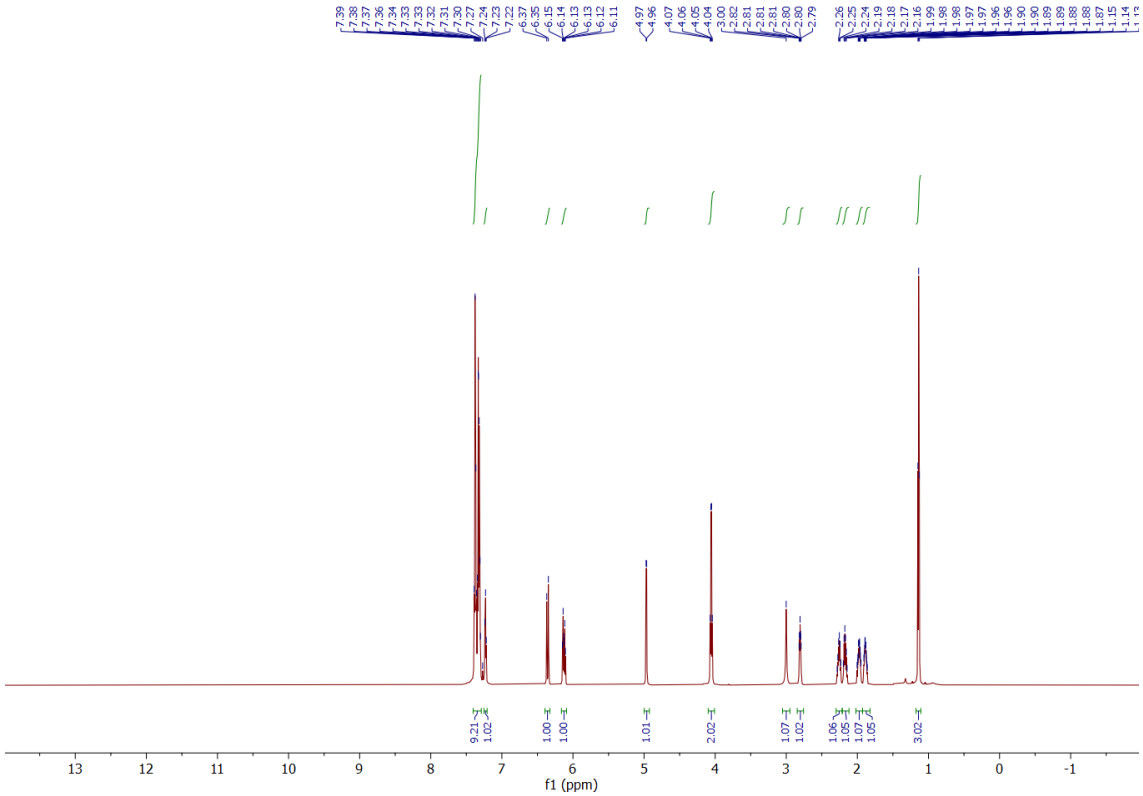

^{13}C NMR spectrum of **20r**:

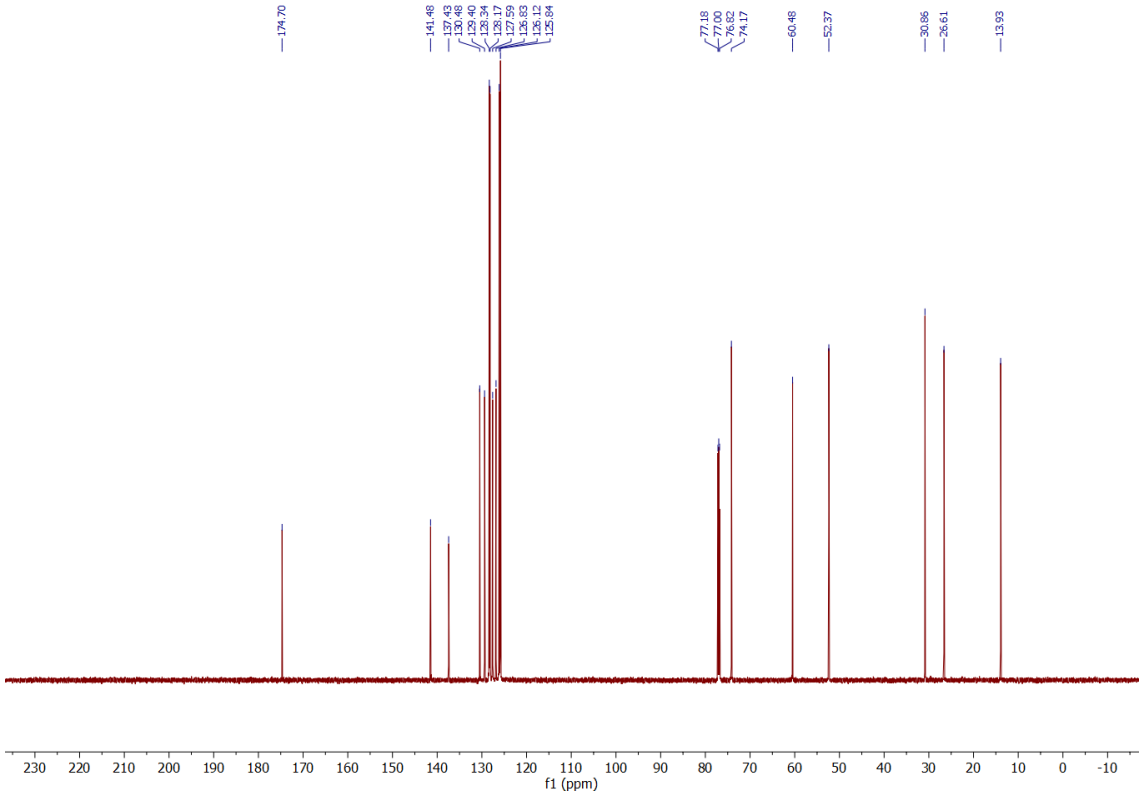

(*E*)-1-(4-iodobut-1-en-1-yl)-4-methoxybenzene (**21X-OMe**)

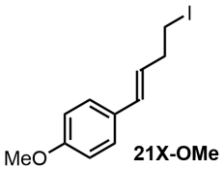

21X-OMe

Prepared according to **GP-X** using (3-bromopropyl)triphenylphosphonium bromide (15.0 g, 1.1 equiv., 32.3 mmol), 60 wt% sodium hydride (1.30 g, 1.105 equiv., 32.5 mmol), 4-methoxybenzaldehyde (3.57 mL, 1.0 equiv., 29.4 mmol), and THF (57 mL, 0.5 M) with a reaction time of 16 h. Afforded crude **21CP-OMe** (2.08 g, 44%). Using **21CP-OMe** (2.08 g, 1.00 equiv., 13.0 mmol), sodium iodide (2.92 g, 1.50 equiv. 19.5 mmol), and acetic acid (26 mL, 0.5 M) with a reaction time of 4 h. Purification by flash column chromatography afforded the pure compound as a pale yellow solid (1.99 g, 53%).

Characterization of **21X-OMe**

^{1}H NMR (700 MHz; $CDCl_3$) δ_H 7.31 (d, J = 8.5 Hz, 2H), 6.86 (d, J = 8.4 Hz, 2H), 6.42 (d, J = 15.8 Hz, 1H), 6.02 (dt, J = 15.9, 7.0 Hz, 1H), 3.82 (s, 3H), 3.24 (t, J = 7.3 Hz, 2H), 2.77 (q, J = 7.2 Hz, 2H).

^{13}C NMR (176 MHz, $CDCl_3$) δ_C 159.1, 131.6, 129.8, 127.3, 126.3, 114.0, 55.3, 37.1, 5.5.

Spectroscopic data matches literature report.[73]

^{1}H NMR spectrum of **21X-OMe**:

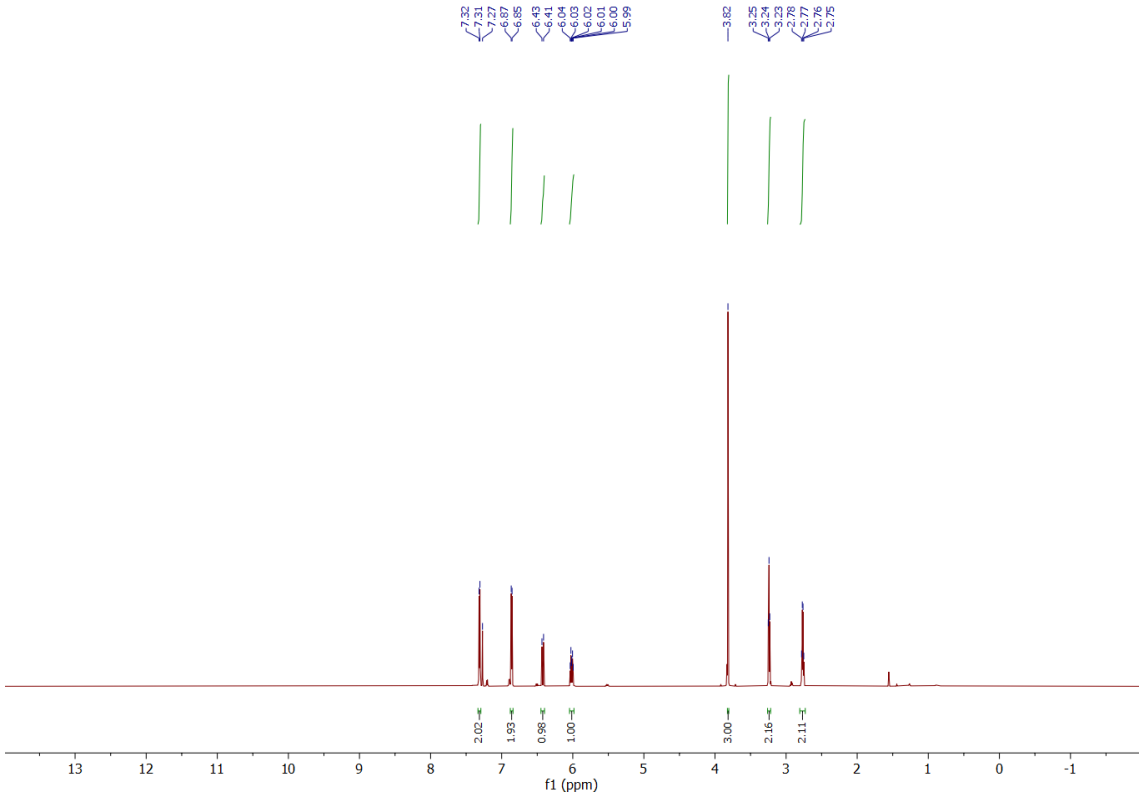

^{13}C NMR spectrum of **21X-OMe**:

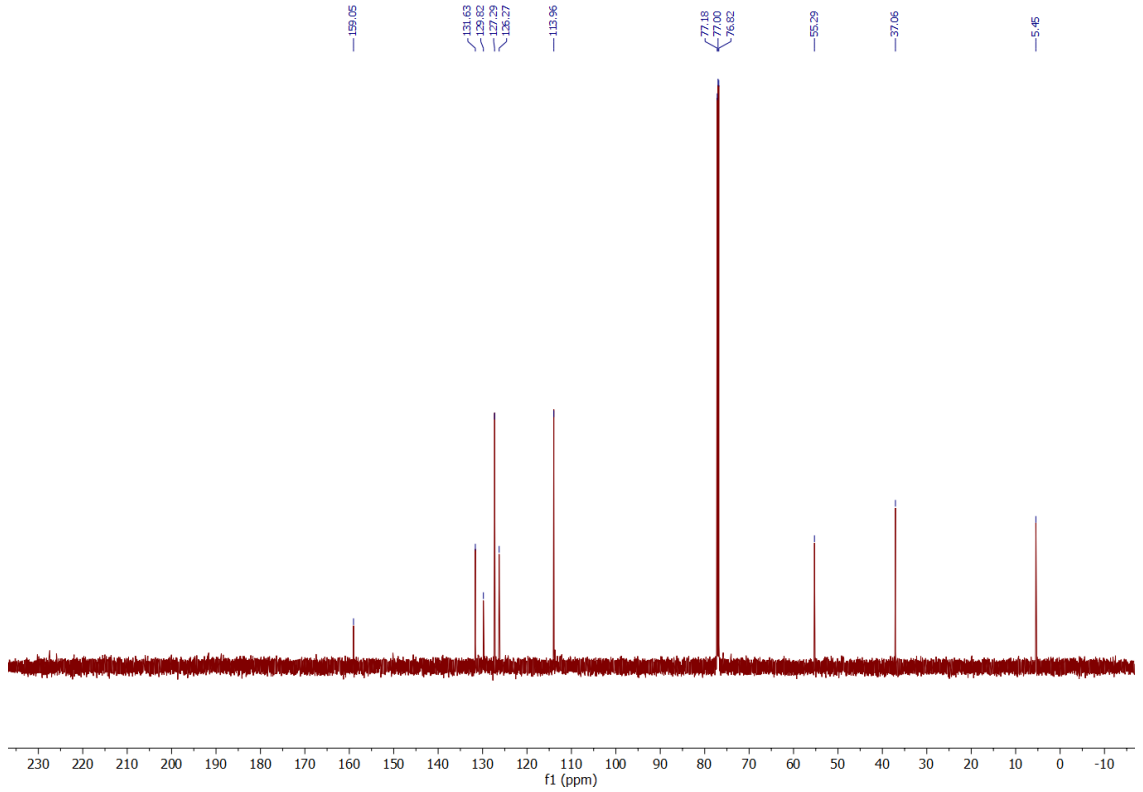

ethyl (*E*)-2-benzoyl-6-(4-(methoxy)phenyl)hex-5-enoate (**21-OMe**)

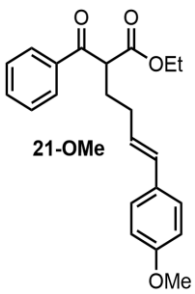

Prepared according to **GP-A** using 60 wt% sodium hydride (317 mg, 1.2 equiv., 7.93 mmol), ethyl 3-oxo-3-phenylpropanoate (1.27 g, 1.0 equiv., 6.61 mmol), **21X-OMe** (1.99 g, 1.05 equiv., 6.91 mmol), and THF (33 mL, 0.2 M) with a reaction time of 16 h. Purification by flash column chromatography afforded the pure compound as a colorless oil (1.17 g, 50%), E:Z ratio 18.5:1.

Characterization of **21-OMe**

^{1}H NMR (700 MHz; $CDCl_3$) δ_H 7.98 (d, J = 7.8 Hz, 2H), 7.58 (t, J = 7.4 Hz, 1H), 7.47 (t, J = 7.6 Hz, 2H), 7.24 (d, J = 8.3 Hz, 2H), 6.84 (d, J = 8.3 Hz, 2H), 6.30 (d, J = 15.8 Hz, 1H), 6.03 (dt, J = 15.0, 7.0 Hz, 1H), 4.38 (t, J = 7.0 Hz, 1H), 4.15 (tt, J = 7.1, 3.7 Hz, 2H), 3.81 (s, 3H), 2.28 (hept, J = 7.2 Hz, 2H), 2.20 (q, J = 7.3 Hz, 2H), 1.17 (t, J = 7.1 Hz, 3H).

^{13}C NMR (126 MHz, $CDCl_3$) δ_C 195.3, 169.9, 158.9, 136.3, 133.4, 130.8, 130.2, 128.7, 128.6, 127.1, 126.7, 113.9, 61.4, 55.3, 53.3, 30.8, 28.6, 14.0.

ν_{max} (FTIR)/cm^{-1}: 2936, 2837, 1732, 1683, 1607, 1510, 1447, 1244, 1174, 689.

HRMS (ESI) m/z: $[M+Na]^+$ calculated for $C_{22}H_{24}O_4Na^+$: 375.1567; found: 375.1575.

^{1}H NMR spectrum of **21-OMe**:

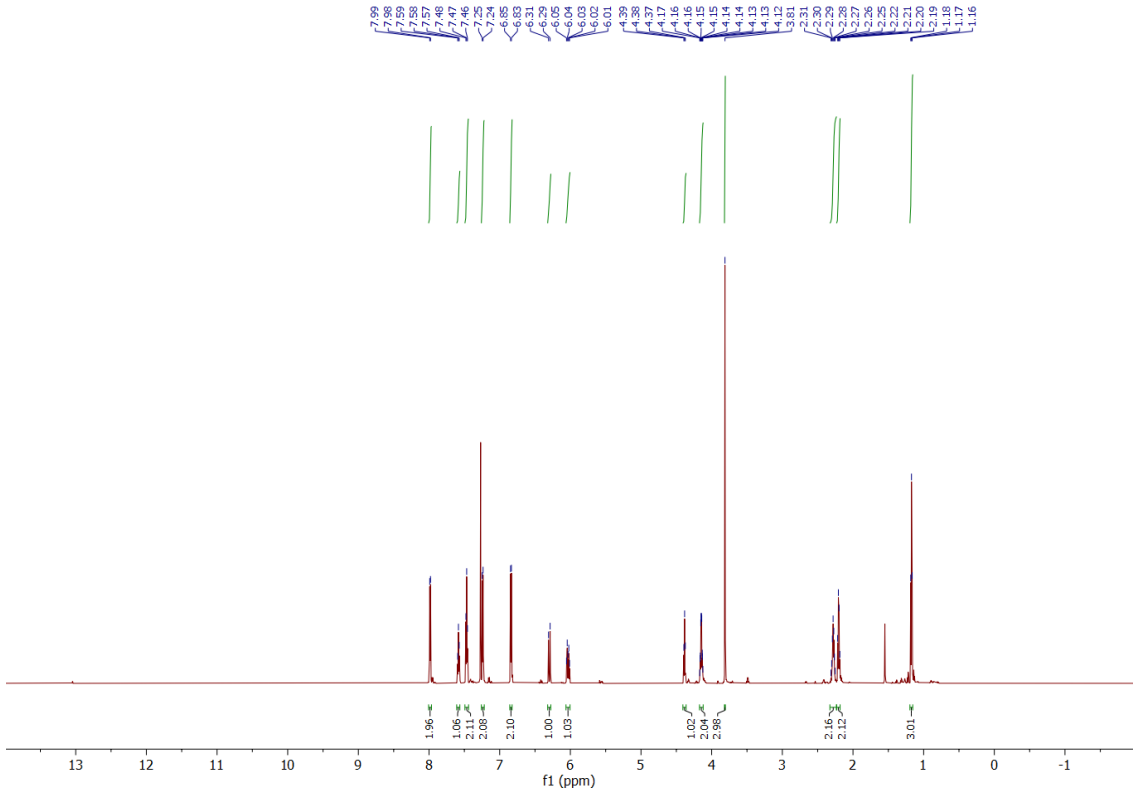

^{13}C NMR spectrum of **21-OMe**:

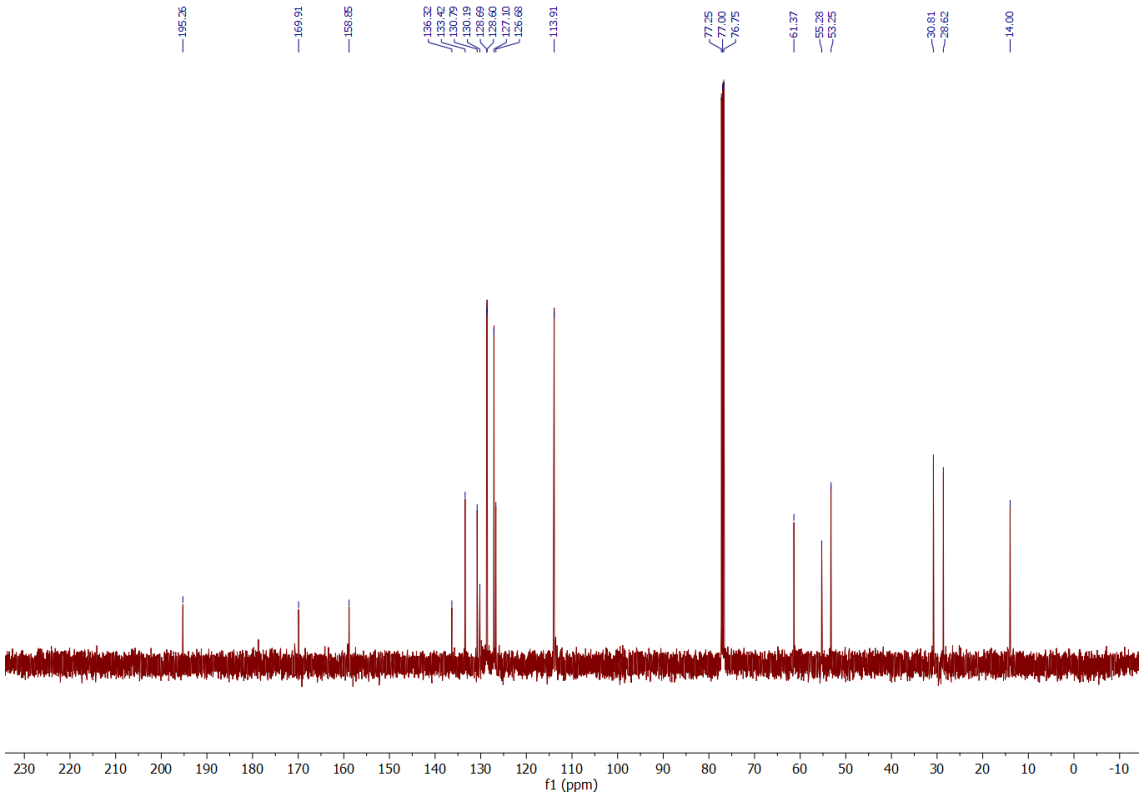

ethyl 2-benzoyl-5-oxopentanoate (**A**)

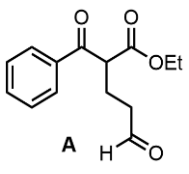

In a flame dried round bottom flask equipped with a stir bar, a solution of the ethyl 2-benzoyl-6-methylhept-5-enoate (6.50 g, 1.0 equiv., 23.7 mmol) in DCM (475 mL, 0.05 M) was cooled to -78 °C and sparged with O_3 till the solution turned blue (took about 40 minutes). Once the blue color appeared, the O_3 line was exchanged for a N_2 line and the solution was sparged until the blue color disappeared (10 minutes). Then the reaction mixture was quenched with dropwise addition of dimethyl sulfide (11.8 g, 14.0 mL, 8.0 equiv., 190 mmol) and stirred overnight at 25 °C under N_2. The reaction mixture was concentrated under vacuum and purified via column chromatography in 20% EtOAc/hexanes yielding **A** (4.99 g, 20.1 mmol, 84.8 %) as a colorless oil.

Characterization of **A**

^{1}H NMR (700 MHz; $CDCl_3$) δ_H 9.79 (s, 1H), 8.02 (d, J = 7.7 Hz, 2H), 7.61 (t, J = 7.4 Hz, 1H), 7.50 (t, J = 7.6 Hz, 2H), 4.44 (t, J = 7.1 Hz, 1H), 4.16 (qq, J = 7.6, 3.8 Hz, 2H), 2.63 (qt, J = 18.6, 7.0 Hz, 2H), 2.31 (dhept, J = 28.5, 7.0 Hz, 2H), 1.18 (t, J = 7.1 Hz, 3H).

^{13}C NMR (176 MHz, $CDCl_3$) δ_C 201.1, 194.8, 169.5, 135.9, 133.7, 128.8, 128.7, 61.6, 52.7, 41.2, 21.2, 14.0.

ν_{max} (FTIR)/cm^{-1}: 2982, 2728, 1724, 1682, 1597, 1581, 1448, 1226, 1158, 689.

HRMS (ESI) m/z: $[M+Na]^+$ calculated for $C_{14}H_{16}O_4Na^+$: 271.0941; found: 271.0939.

^{1}H NMR spectrum of **A**:

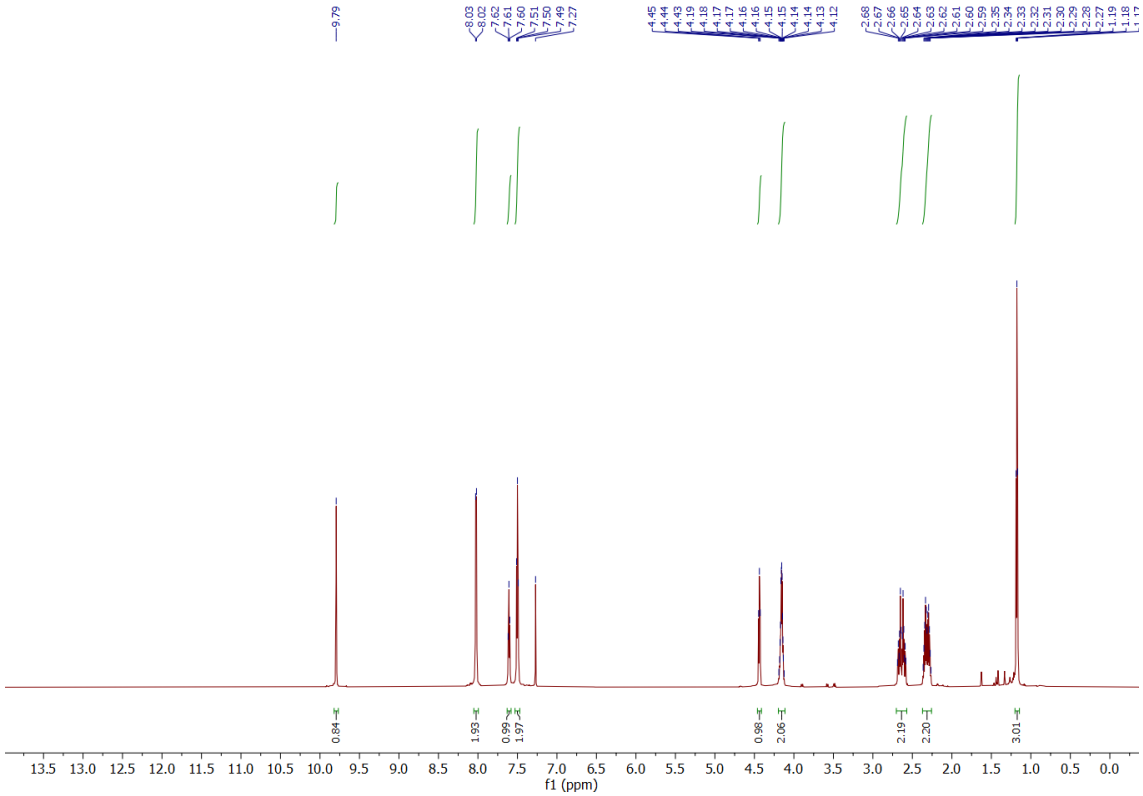

^{13}C NMR spectrum of **A**:

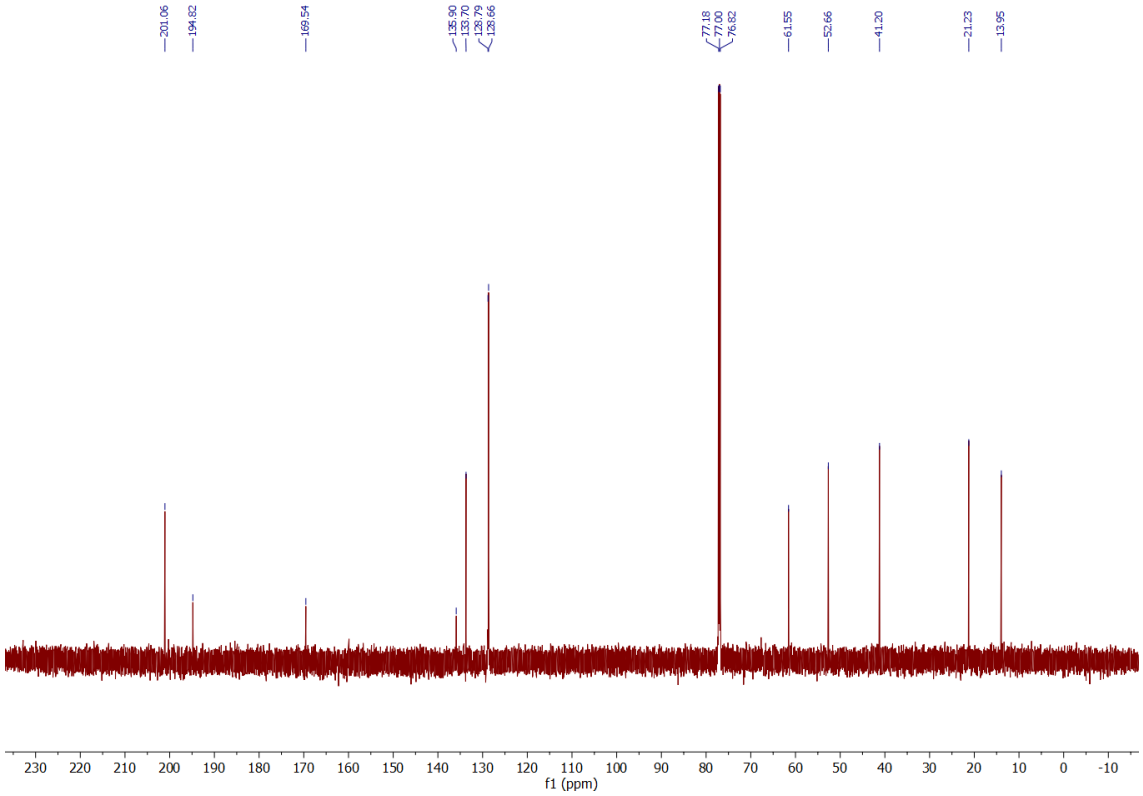

(4-(*tert*-butyl)benzyl)triphenylphosphonium bromide (**21WS-*t*Bu**)

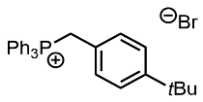

21WS-*t*Bu

Prepared according to **GP-WS** using 1-(bromomethyl)-4-(*tert*-butyl)benzene (5.00 g, 4.05 mL, 1.0 equiv., 22.0 mmol), triphenylphosphine (5.77 g, 1.0 equiv., 22.0 mmol), and toluene (45 mL, 0.5 M) with a reaction time of 16 h, afforded the pure compound as a white solid (10.8 g, 100%).

Characterization of **21WS-*t*Bu**

^{1}H NMR (400 MHz; $CDCl_3$) δ_H 7.75 (tt, J = 12.4, 6.9 Hz, 9H), 7.63 (td, J = 7.7, 3.4 Hz, 6H), 7.14 (d, J = 8.2 Hz, 2H), 7.01 (dd, J = 8.4, 2.6 Hz, 2H), 5.36 (d, J = 14.0 Hz, 2H), 1.24 (s, 9H).

Spectroscopic data matches literature report.[74]

^{1}H NMR spectrum of **21WS-*t*Bu**:

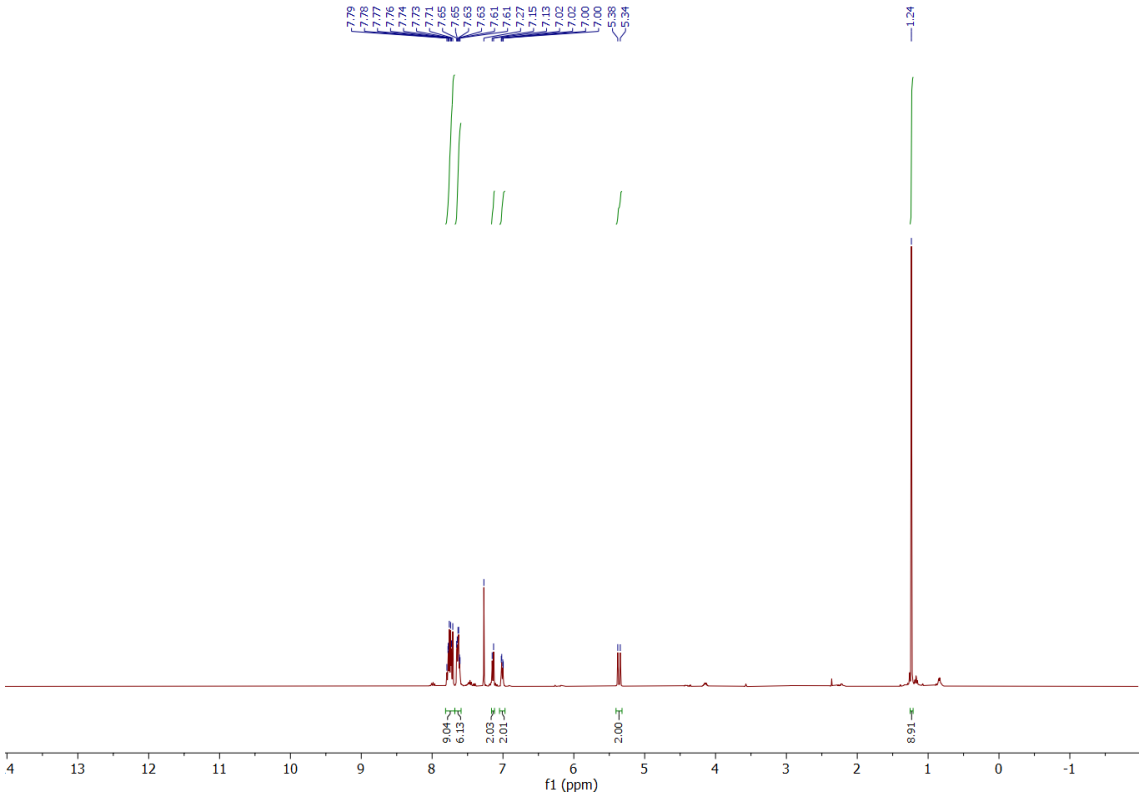

ethyl (*E*)-2-benzoyl-6-(4-(*tert*-butyl)phenyl)hex-5-enoate (**21-*t*Bu**)

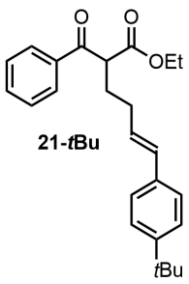

Prepared according to **GP-B** using potassium *tert*-butoxide (508 mg, 1.5 equiv., 4.53 mmol) in THF (3.5 mL, 1.3 M), **21WS-*t*Bu** (2.22 g, 1.5 equiv., 4.53 mmol) in THF (9 mL, 0.5 M), and **A** (750 mg, 1.0 equiv., 3.02 mmol) in THF (4.5 mL, 2.0 M) with a reaction time of 16 h. Purification by flash column chromatography afforded the pure compound as a colorless oil (125 mg, 11%), E:Z ratio 26:1.

Characterization of **21-*t*Bu**

^{1}H NMR (500 MHz; $CDCl_3$) δ_H 7.99 (d, J = 7.3 Hz, 2H), 7.59 (t, J = 7.4 Hz, 1H), 7.47 (t, J = 7.7 Hz, 2H), 7.33 (d, J = 8.3 Hz, 2H), 7.26 (d, J = 8.3 Hz, 2H), 6.34 (d, J = 15.8 Hz, 1H), 6.14 (dt, J = 15.9, 6.9 Hz, 1H), 4.39 (t, J = 6.9 Hz, 1H), 4.15 (q, J = 7.1 Hz, 2H), 2.30 (dq, J = 10.6, 6.5, 6.1 Hz, 2H), 2.21 (q, J = 7.2 Hz, 2H), 1.32 (s, 9H), 1.18 (t, J = 7.1 Hz, 3H).

^{13}C NMR (176 MHz, $CDCl_3$) δ_C 195.3, 169.9, 150.2, 136.3, 134.6, 133.4, 131.2, 128.7, 128.6, 128.1, 125.7, 125.4, 61.4, 53.1, 34.5, 31.3, 30.8, 28.5, 14.0.

ν_{max} (FTIR)/cm^{-1}: 2962, 2905, 2868, 1735, 1685, 1597, 1448, 1151, 968, 689.

HRMS (ESI) m/z: $[M+Na]^+$ calculated for $C_{25}H_{30}O_3Na^+$: 401.2087; found: 401.2081.

^{1}H NMR spectrum of **21-*t*Bu**:

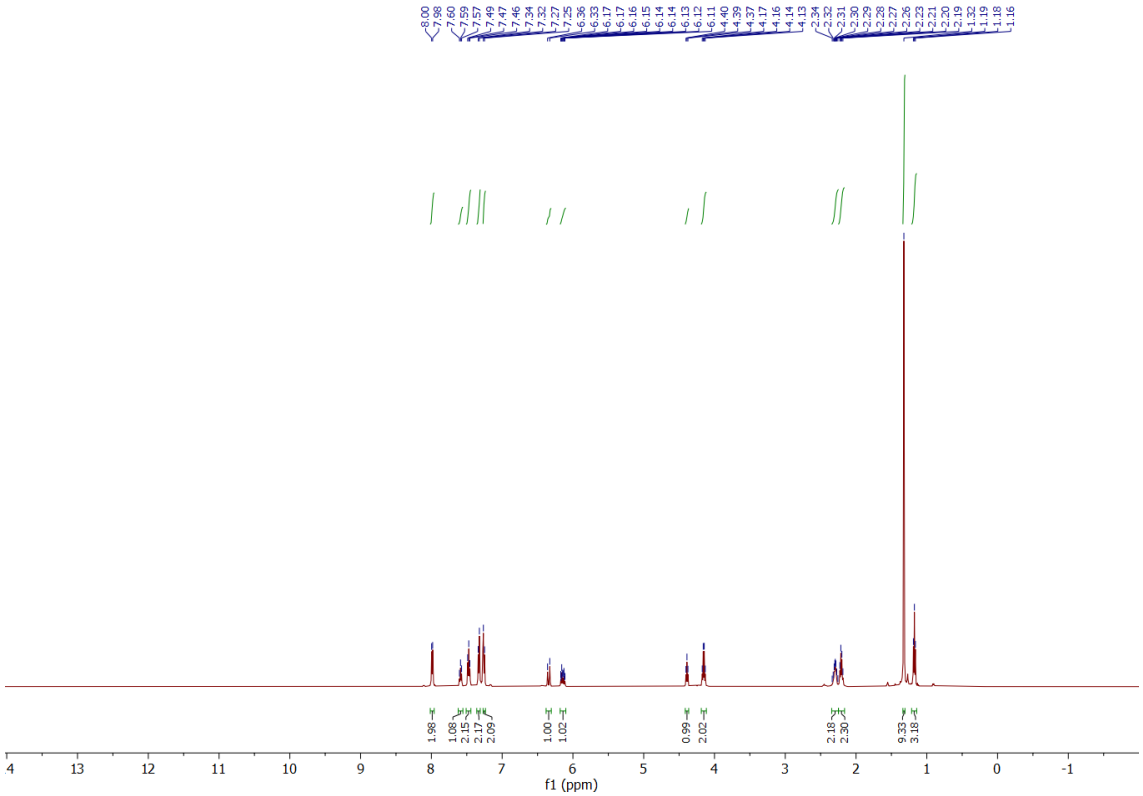

^{13}C NMR spectrum of **21-*t*Bu**:

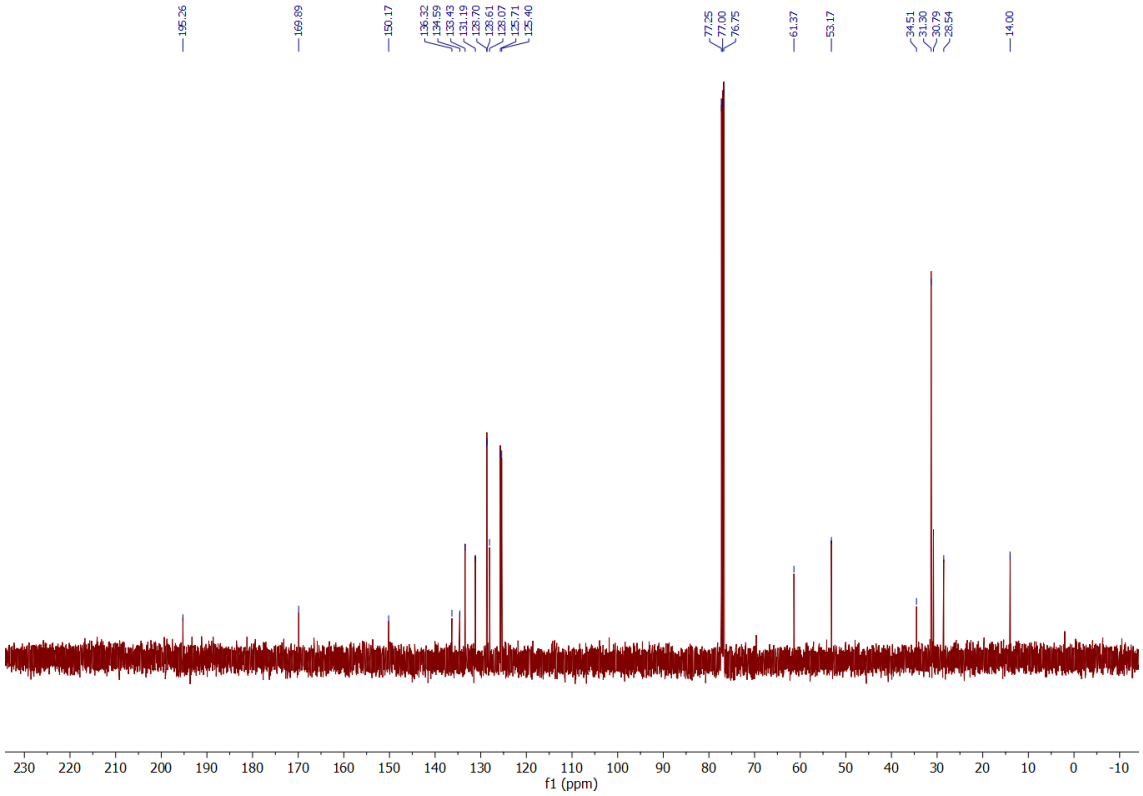

(4-methylbenzyl)triphenylphosphonium bromide (**21WS-Me**)

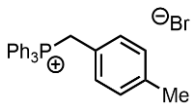

21WS-Me

Prepared according to **GP-WS** using 1-(bromomethyl)-4-methylbenzene (5.00 g, 1.0 equiv., 27.0 mmol), triphenylphosphine (7.09 g, 1.0 equiv., 27.0 mmol), and toluene (55 mL, 0.5 M) with a reaction time of 16 h, afforded the pure compound as a white solid (12.1 g, 100%).

Characterization of **21WS-Me**

^{1}H NMR (500 MHz; $CDCl_3$) δ_H 7.75 (td, J = 13.3, 12.5, 7.7 Hz, 9H), 7.63 (td, J = 7.8, 3.3 Hz, 6H), 6.96 (d, J = 7.8 Hz, 2H), 6.92 (d, J = 7.8 Hz, 2H), 5.33 (d, J = 14.1 Hz, 2H), 2.25 (s, 3H).

Spectroscopic data matches literature report.[74]

^{1}H NMR spectrum of **21WS-Me**:

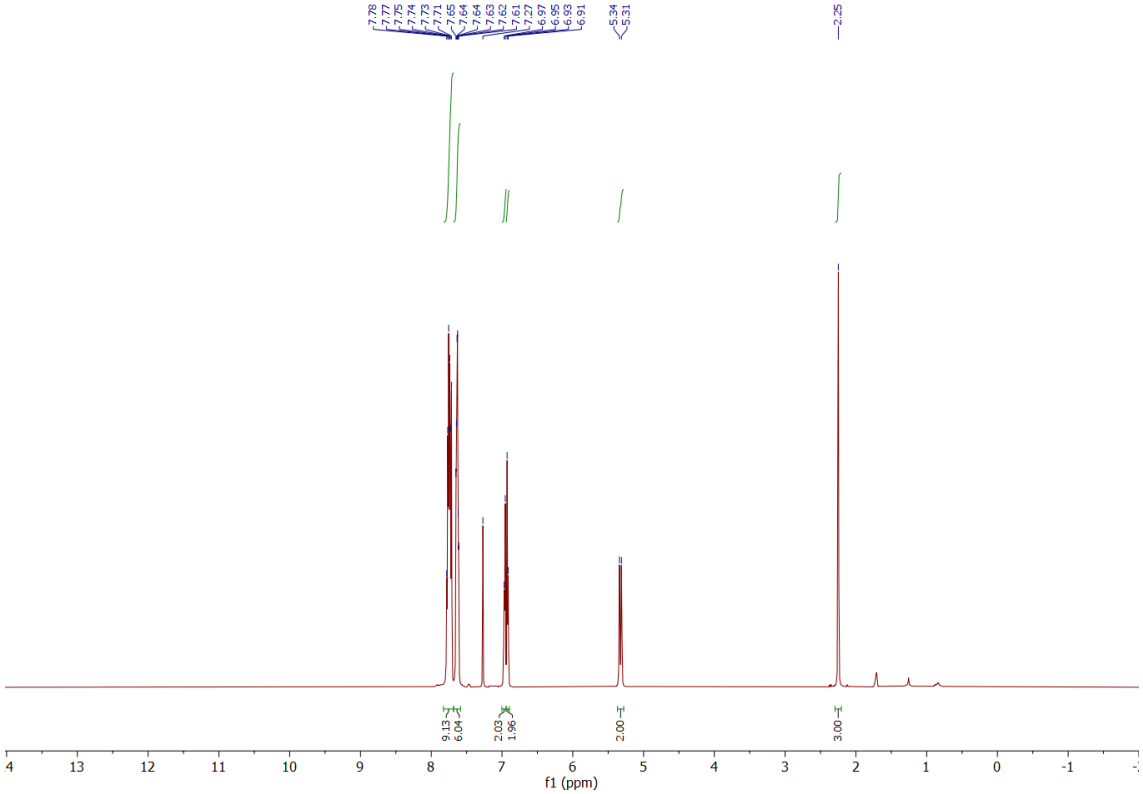

ethyl (*E*)-2-benzoyl-6-(p-tolyl)hex-5-enoate (**21-Me**)

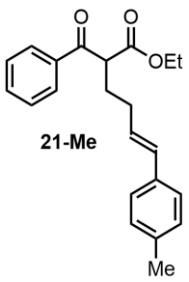

Prepared according to **GP-B** using potassium *tert*-butoxide (508 mg, 1.5 equiv., 4.53 mmol) in THF (3.5 mL, 1.3 M), **21WS-Me** (2.03 g, 1.5 equiv., 4.53 mmol) in THF (9 mL, 0.5 M), and **A** (750 mg, 1.0 equiv., 3.02 mmol) in THF (4.5 mL, 2.0 M) with a reaction time of 16 h. Purification by flash column chromatography afforded the pure compound as a colorless oil (250 mg, 25%), E:Z ratio 22:1.

Characterization of **21-Me**

^{1}H NMR (700 MHz; $CDCl_3$) δ_H 7.98 (d, J = 8.1 Hz, 2H), 7.59 (t, J = 7.3 Hz, 1H), 7.47 (t, J = 7.6 Hz, 2H), 7.21 (d, J = 7.8 Hz, 2H), 7.11 (d, J = 7.8 Hz, 2H), 6.33 (d, J = 15.8 Hz, 1H), 6.13 (dt, J = 16.0, 7.0 Hz, 1H), 4.38 (t, J = 7.0 Hz, 1H), 4.15 (qd, J = 7.2, 1.7 Hz, 2H), 2.34 (s, 3H), 2.29 (p, J = 7.1 Hz, 2H), 2.21 (q, J = 7.3 Hz, 2H), 1.17 (t, J = 7.1 Hz, 3H).

^{13}C NMR (176 MHz, $CDCl_3$) δ_C 195.3, 169.9, 136.9, 136.3, 134.6, 133.4, 131.3, 129.2, 128.7, 128.6, 127.8, 125.9, 61.4, 53.2, 30.8, 28.5, 21.1, 14.0.

ν_{max} (FTIR)/cm^{-1}: 2979, 1733, 1684, 1597, 1512, 1448, 1224, 1151, 968, 689.

HRMS (ESI) m/z: $[M+Na]^+$ calculated for $C_{22}H_{24}O_3Na^+$: 359.1618; found: 359.1617.

^{1}H NMR spectrum of **21-Me**:

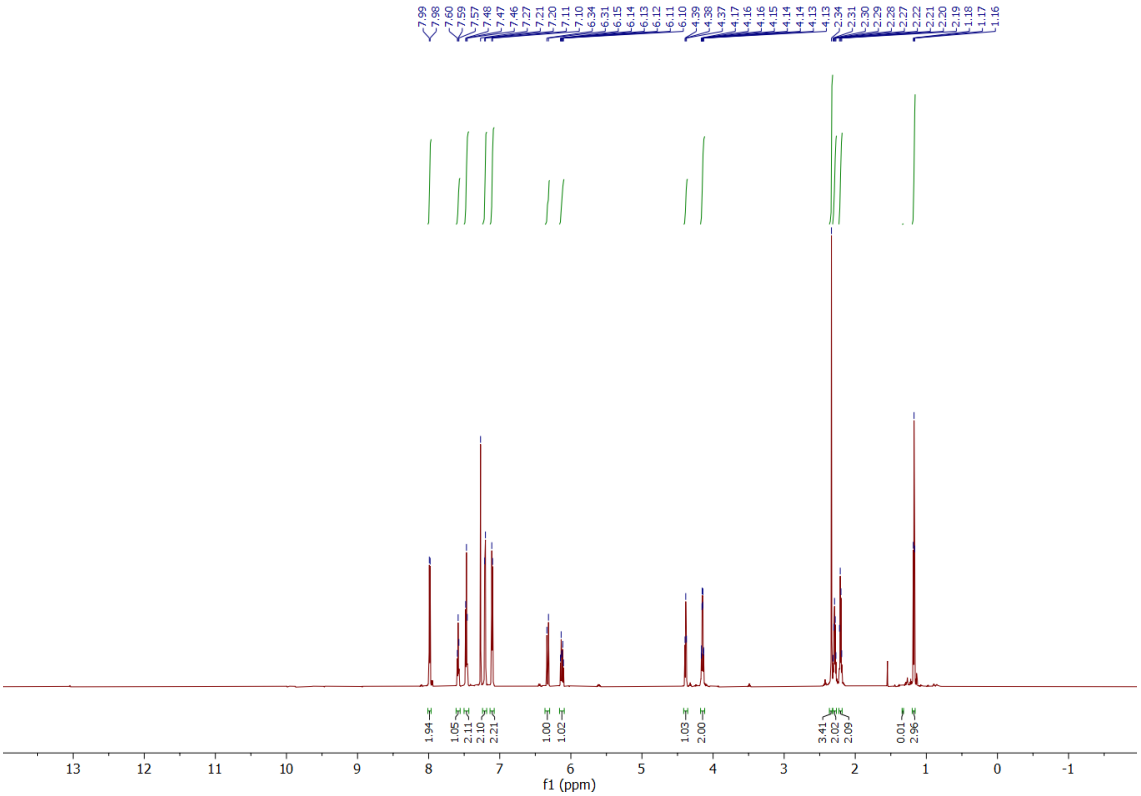

^{13}C NMR spectrum of **21-Me**:

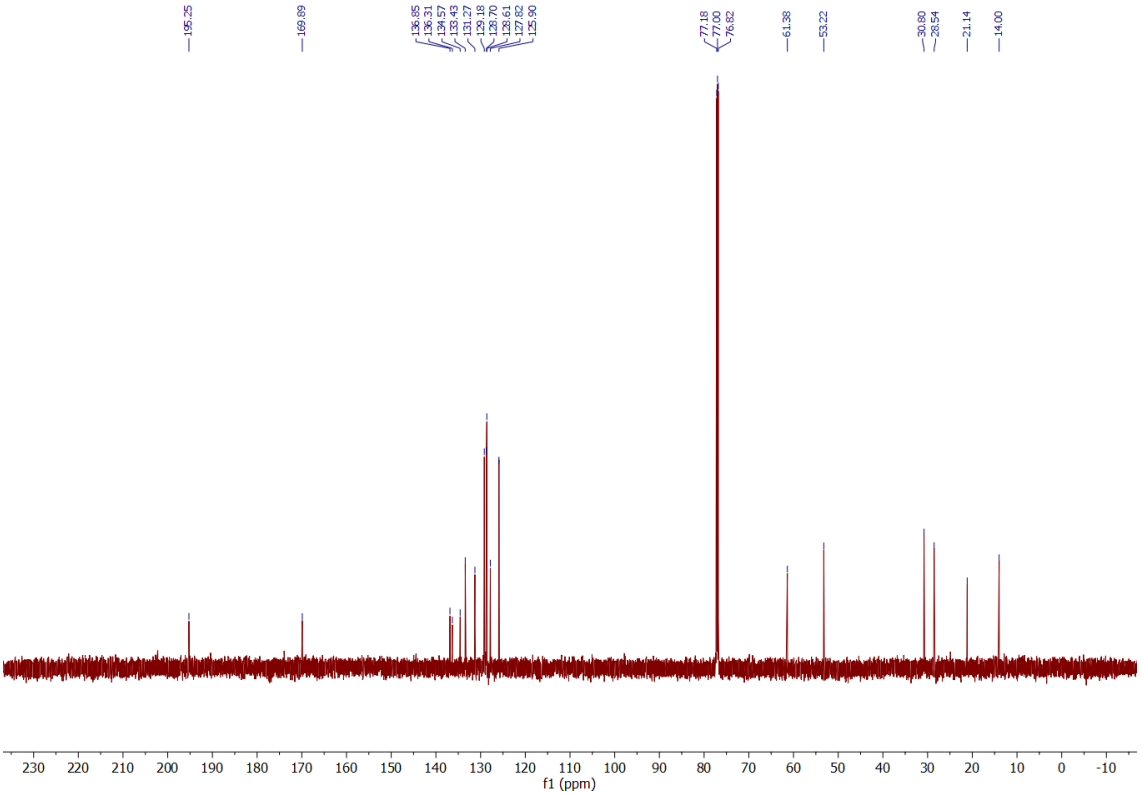

triphenyl(4-(trimethylsilyl)benzyl)phosphonium bromide (**21WS-TMS**)

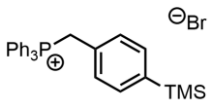

21WS-TMS

Prepared according to **GP-WS** using (4-(bromomethyl)phenyl)trimethylsilane[75] (6.50 g, 1.0 equiv., 26.7 mmol), triphenylphosphine (7.01 g, 1.0 equiv., 26.7 mmol), and toluene (55 mL, 0.5 M) with a reaction time of 16 h, afforded the pure compound as a white solid (12.1 g, 89%).

Characterization of **21WS-TMS**

^{1}H NMR (700 MHz; $CDCl_3$) δ_H 7.65 (t, J = 7.4 Hz, 3H), 7.57 (dd, J = 12.6, 7.8 Hz, 6H), 7.50 (td, J = 7.8, 3.4 Hz, 6H), 7.13 (d, J = 7.5 Hz, 2H), 6.94 (d, J = 6.1 Hz, 2H), 5.13 (d, J = 14.4 Hz, 2H), 0.07 (s, 9H).

^{13}C NMR (176 MHz, $CDCl_3$) δ_C 140.5 (d, J = 3.8 Hz), 134.7 (d, J = 3.0 Hz), 133.9 (d, J = 9.8 Hz), 133.3 (d, J = 3.3 Hz), 130.3 (d, J = 5.5 Hz), 129.8 (d, J = 12.5 Hz), 127.1 (d, J = 8.5 Hz), 117.2 (d, J = 85.8 Hz), 30.4 (d, J = 47.4 Hz), -1.6.

^{31}P NMR (283 MHz, $CDCl_3$) δ_P 22.81.

ν_{max} (FTIR)/cm^{-1}: 2955, 2844, 2773, 1600, 1486, 1436, 1247, 1108, 826, 750.

HRMS (ESI) m/z: $[M - Br + H]^+$ calculated for $C_{28}H_{31}PSi^+$: 426.1927; found: 426.1930.

^{1}H NMR spectrum of **21WS-TMS**:

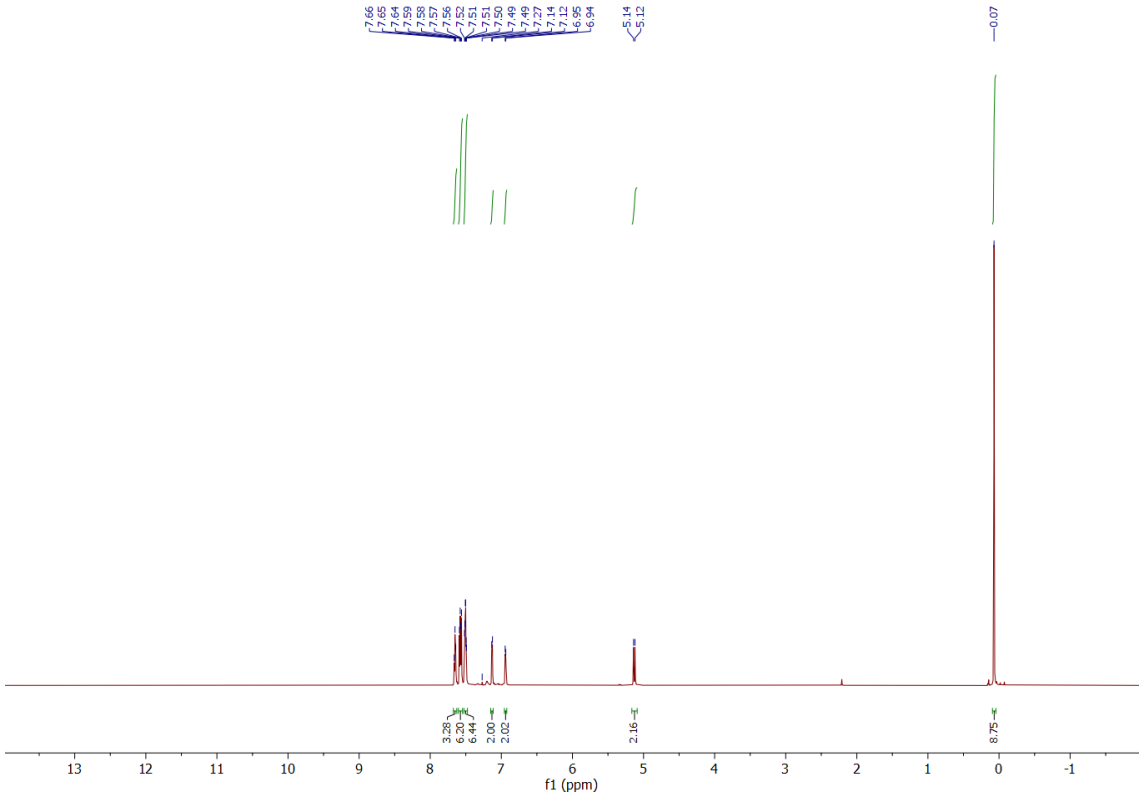

^{13}C NMR spectrum of **21WS-TMS**:

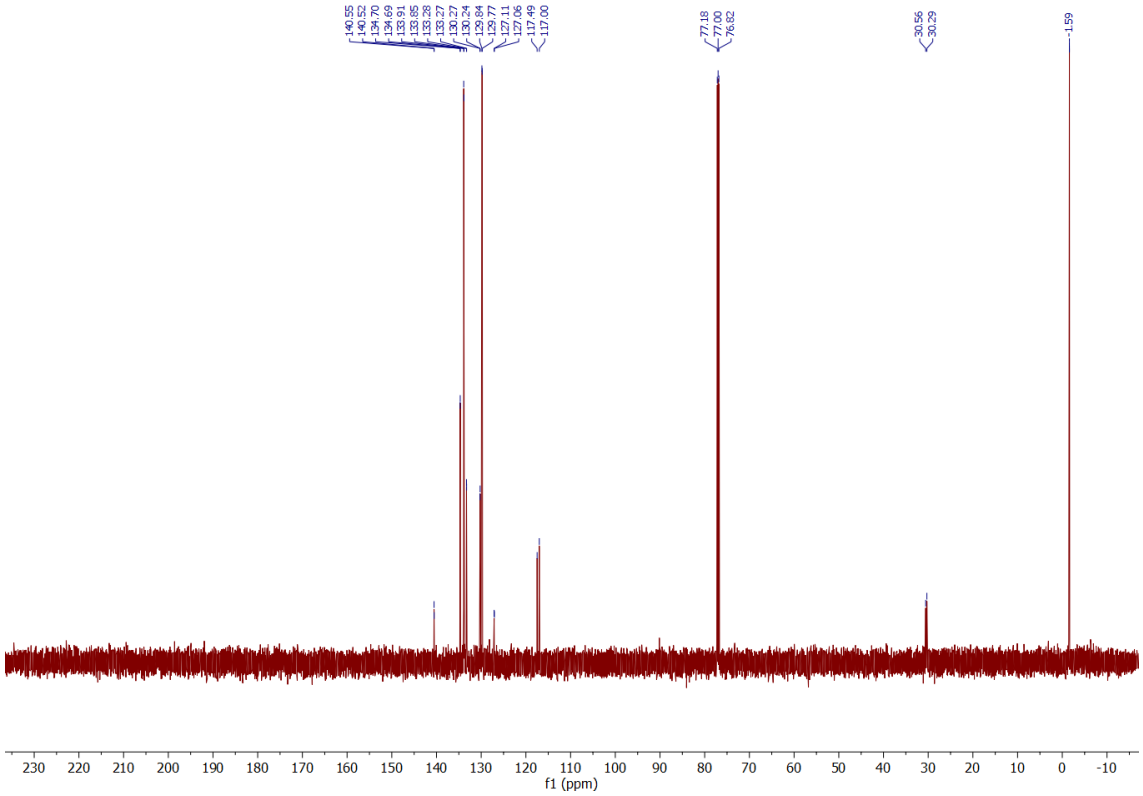

ethyl (*E*)-2-benzoyl-6-(4-(trimethylsilyl)phenyl)hex-5-enoate (**21-TMS**)

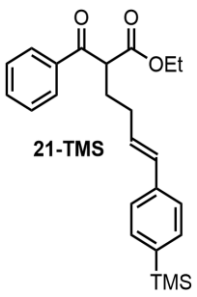

Prepared according to **GP-B** using potassium *tert*-butoxide (508 mg, 1.5 equiv., 4.53 mmol) in THF (3.5 mL, 1.3 M), **21WS-TMS** (2.29 g, 1.5 equiv., 4.53 mmol) in THF (9 mL, 0.5 M), and **A** (750 mg, 1.0 equiv., 3.02 mmol) in THF (4.5 mL, 2.0 M) with a reaction time of 16 h. Purification by flash column chromatography afforded the pure compound as a colorless oil (145 mg, 12%), E:Z ratio 16.5:1.

Characterization of **21-TMS**

^{1}H NMR (700 MHz; $CDCl_3$) δ_H 7.99 (d, J = 7.6 Hz, 2H), 7.59 (t, J = 7.3 Hz, 1H), 7.47 (dd, J = 11.5, 7.8 Hz, 4H), 7.30 (d, J = 7.6 Hz, 2H), 6.35 (d, J = 15.8 Hz, 1H), 6.21 (dt, J = 15.2, 6.9 Hz, 1H), 4.38 (t, J = 7.0 Hz, 1H), 4.15 (q, J = 7.0 Hz, 2H), 2.31 (hept, J = 7.1 Hz, 2H), 2.21 (q, J = 7.3 Hz, 2H), 1.17 (t, J = 7.1 Hz, 3H), 0.27 (s, 9H).

^{13}C NMR (176 MHz, $CDCl_3$) δ_C 195.2, 169.9, 139.3, 137.8, 136.3, 133.54, 133.46, 131.5, 129.2, 128.7, 128.6, 125.3, 61.4, 53.2, 30.8, 28.4, 14.0, -1.1.

ν_{max} (FTIR)/cm^{-1}: 2955, 1735, 1685, 1597, 1448, 1247, 1109, 969, 833, 688.

HRMS (ESI) m/z: $[M+Na]^+$ calculated for $C_{24}H_{30}O_3SiNa^+$: 417.1856; found: 417.1856.

^{1}H NMR spectrum of **21-TMS**:

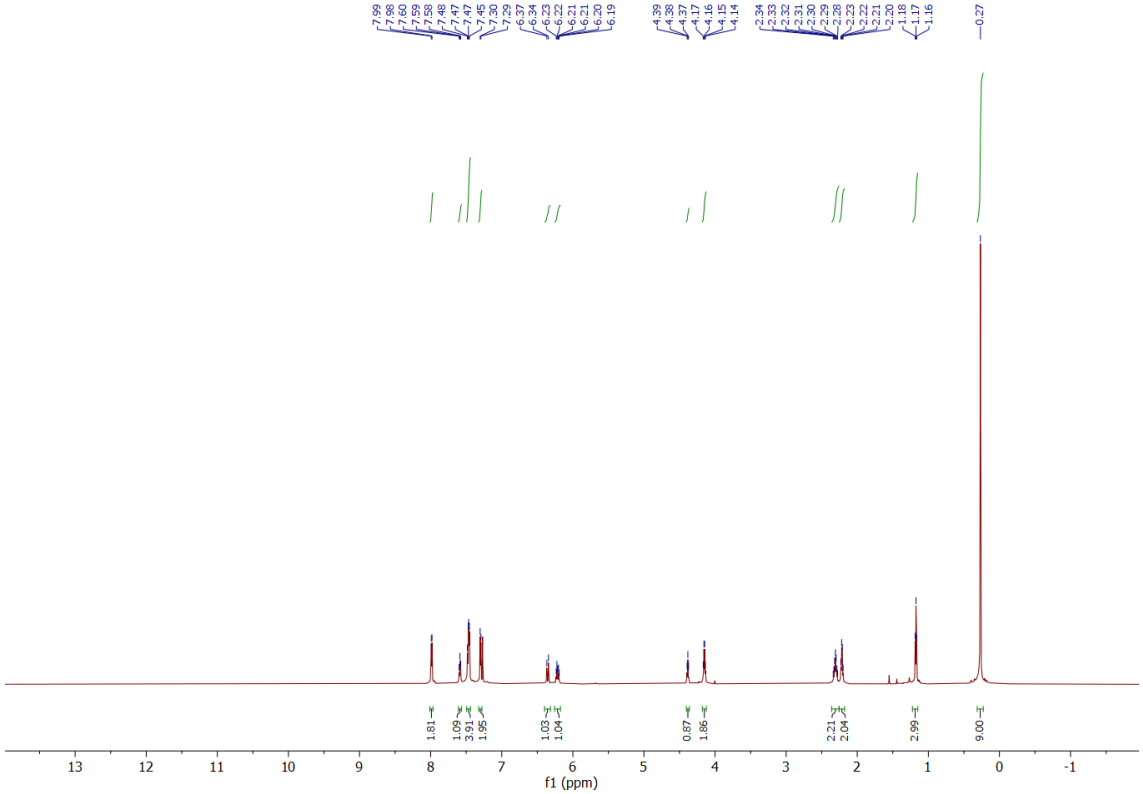

^{13}C NMR spectrum of **21-TMS**:

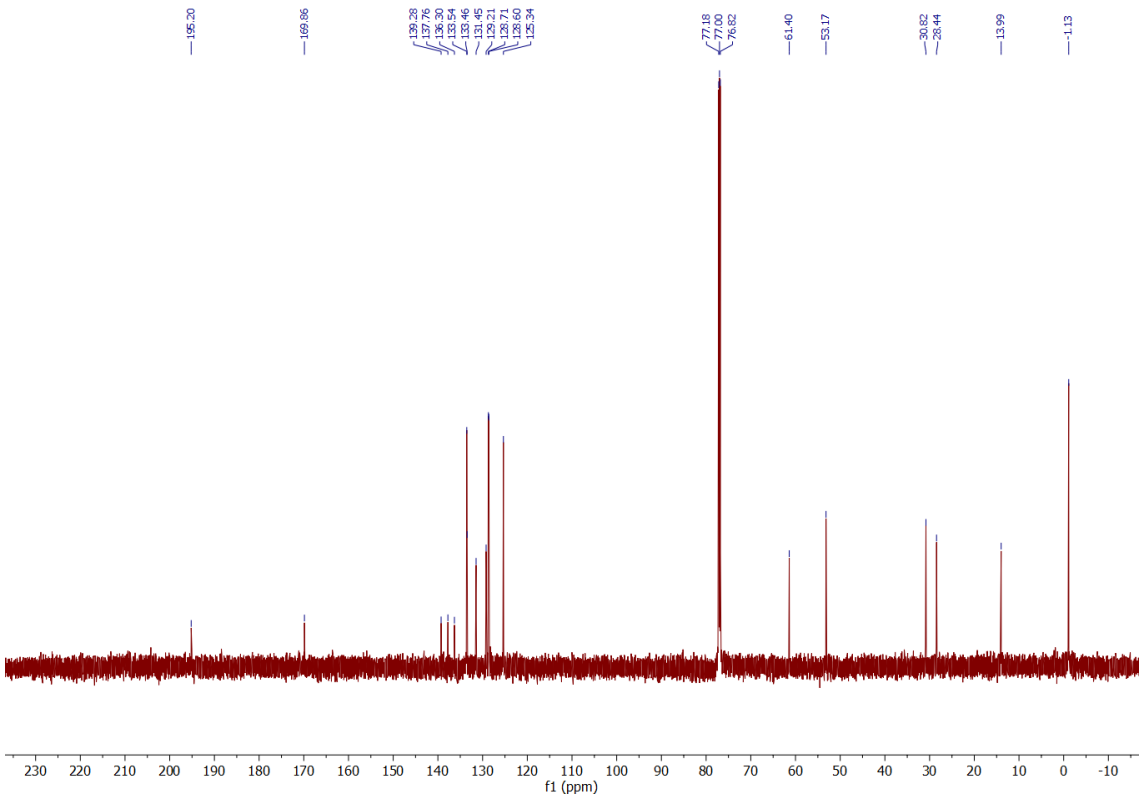

(4-fluorobenzyl)triphenylphosphonium bromide (**21WS-F**)

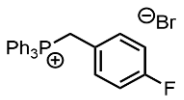

21WS-F

Prepared according to **GP-WS** using 1-(bromomethyl)-4-fluorobenzene (1.6 g, 1.04 mL, 1.0 equiv., 8.46 mmol), triphenylphosphine (2.22 g, 1.0 equiv., 8.46 mmol), and toluene 16 mL, 0.5 M) with a reaction time of 16 h, afforded the pure compound as a white solid (3.8 g, 99%).

Characterization of **21WS-F**

^{1}H NMR (600 MHz; $CDCl_3$) δ_H 7.85 – 7.72 (m, 9H), 7.62 (d, J = 7.8 Hz, 6H), 7.17 (td, J = 5.9, 2.8 Hz, 2H), 6.79 (t, J = 8.4 Hz, 2H), 5.56 (d, J = 14.2 Hz, 2H).

Spectroscopic data matches literature report.[74]

^{1}H NMR spectrum of **21WS-F**:

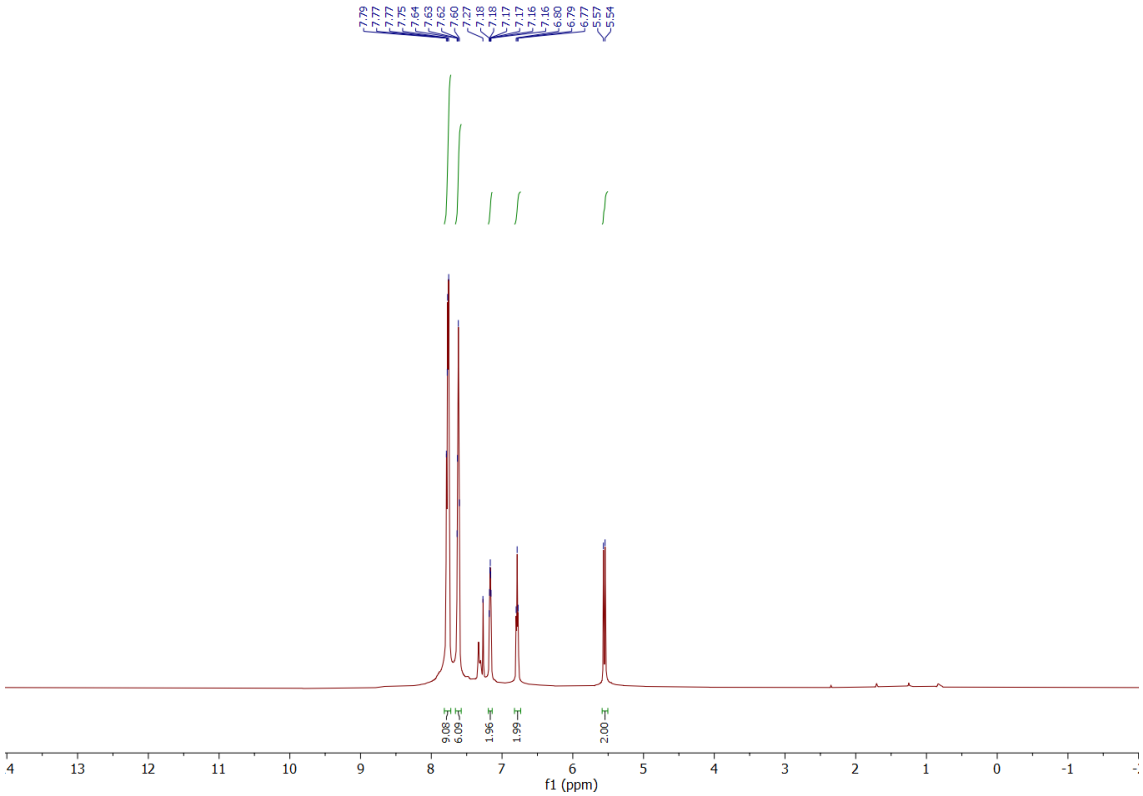

ethyl (*E*)-2-benzoyl-6-(4-fluorophenyl)hex-5-enoate (**21-F**)

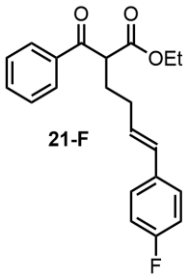

Prepared according to **GP-B** using potassium *tert*-butoxide (508 mg, 1.5 equiv., 4.53 mmol) in THF (3.5 mL, 1.3 M), **21WS-F** (2.05 g, 1.5 equiv., 4.53 mmol) in THF (9 mL, 0.5 M), and **A** (750 mg, 1.0 equiv., 3.02 mmol) in THF (4.5 mL, 2.0 M) with a reaction time of 16 h. Purification by flash column chromatography afforded the pure compound as a colorless oil (130 mg, 13%), E:Z ratio 28:1.

Characterization of **21-F**

^{1}H NMR 700 MHz; $CDCl_3$) δ_H 7.98 (d, J = 7.6 Hz, 2H), 7.59 (t, J = 7.4 Hz, 1H), 7.47 (t, J = 7.7 Hz, 2H), 7.27 – 7.23 (m, 2H), 6.98 (t, J = 8.6 Hz, 2H), 6.31 (d, J = 15.8 Hz, 1H), 6.09 (dt, J = 15.9, 6.9 Hz, 1H), 4.37 (t, J = 7.0 Hz, 1H), 4.15 (qd, J = 7.1, 2.8 Hz, 2H), 2.29 (dt, J = 9.2, 6.8 Hz, 2H), 2.21 (q, J = 7.3 Hz, 2H), 1.17 (t, J = 7.1 Hz, 3H).

^{13}C NMR (176 MHz, $CDCl_3$) δ_C 195.1, 169.8, 162.0 (d, J = 246.0 Hz), 136.3, 133.5, 130.18, 12k8.71, 128.66 (d, J = 2.2 Hz), 128.58, 127.4 (d, J = 7.9 Hz), 115.3 (d, J = 21.5 Hz), 61.4, 53.3, 30.8, 28.5, 14.0.

ν_{max} (FTIR)/cm^{-1}: 2981, 1733, 1683, 1598, 1507, 1448, 1223, 1156, 967, 689.

HRMS (ESI) m/z: $[M+Na]^+$ calculated for $C_{21}H_{21}O_3FNa^+$: 363.1367; found: 363.1360.

^{1}H NMR spectrum of **21-F**:

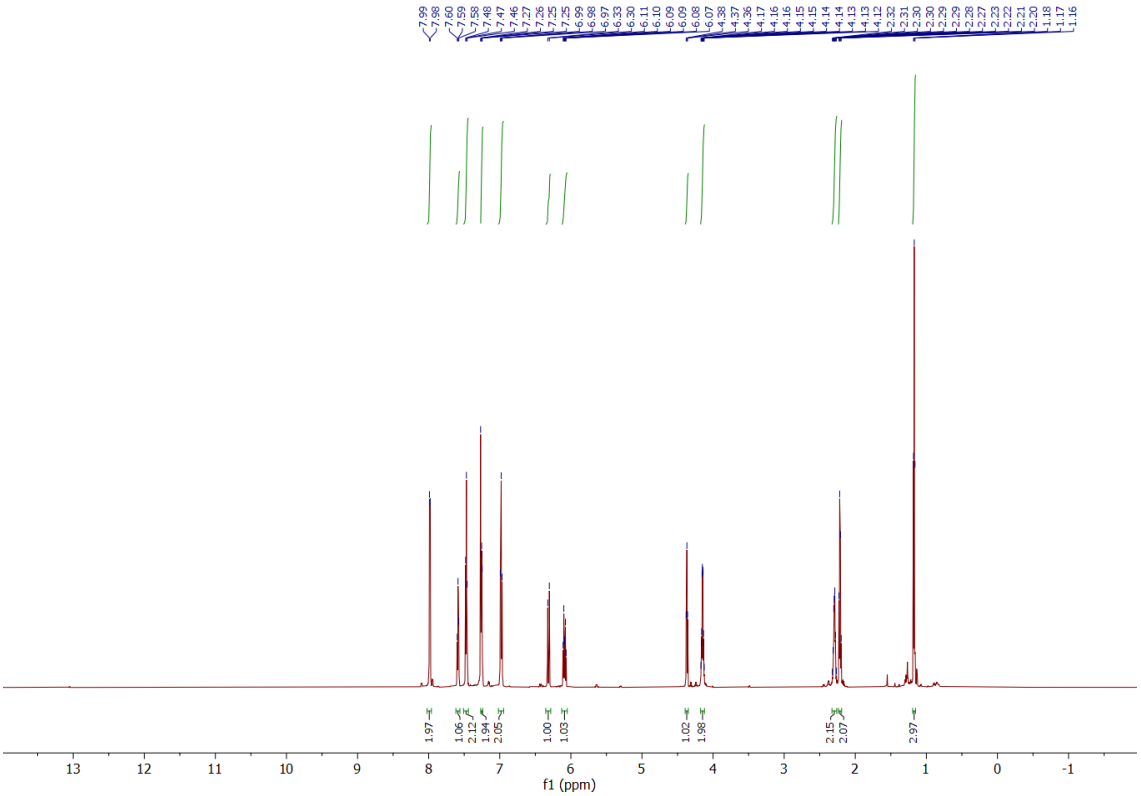

^{13}C NMR spectrum of **21-F**:

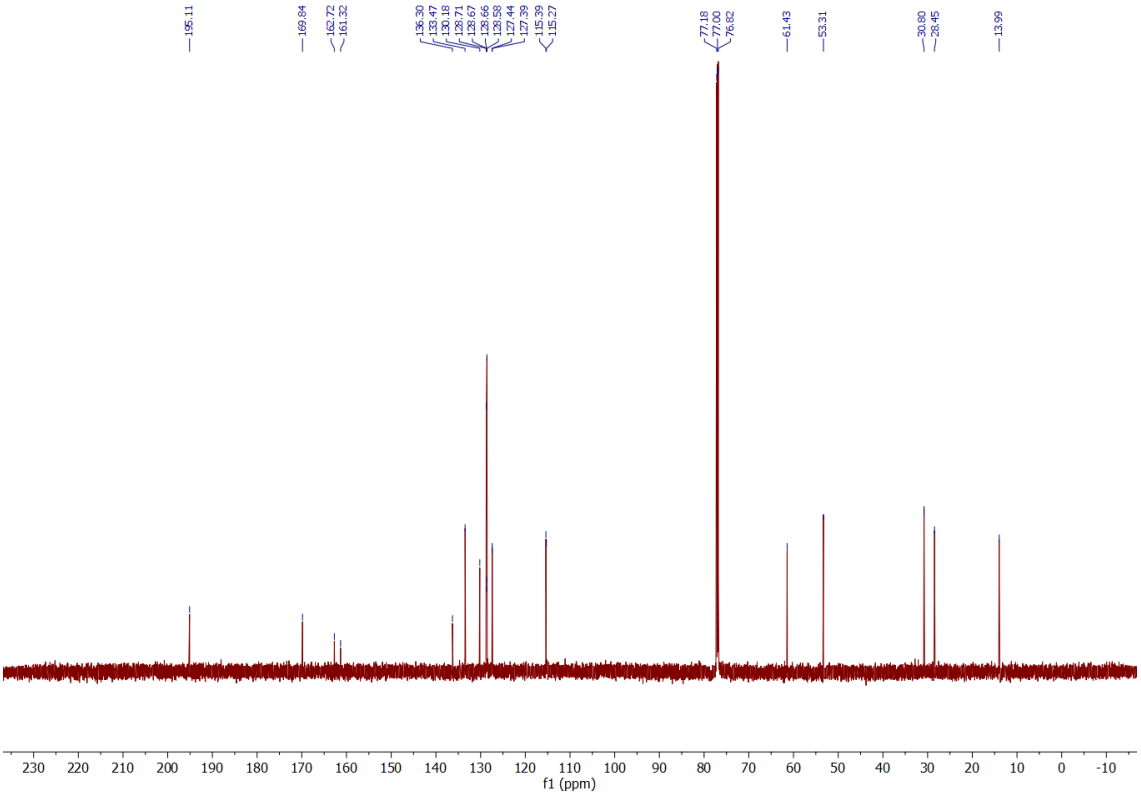

(4-iodobenzyl)triphenylphosphonium bromide (**21WS-I**)

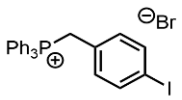

21WS-I

Prepared according to **GP-WS** using 1-(bromomethyl)-4-iodobenzene (2.80 g, 1.0 equiv., 9.43 mmol), triphenylphosphine (2.47 g, 1.0 equiv., 9.43 mmol), and toluene (19 mL, 0.5 M) with a reaction time of 16 h, afforded the pure compound as a brown solid (4.6g, 88%).

Characterization of **21WS-I**

^{1}H NMR (600 MHz; $CDCl_3$) δ_H 7.75 (td, J = 13.4, 12.8, 7.6 Hz, 9H), 7.65 – 7.59 (m, 6H), 7.40 (d, J = 7.8 Hz, 2H), 6.91 (d, J = 7.6 Hz, 2H), 5.37 (d, J = 14.6 Hz, 2H).

Spectroscopic data matches literature report.[76]

^{1}H NMR spectrum of **21WS-I**:

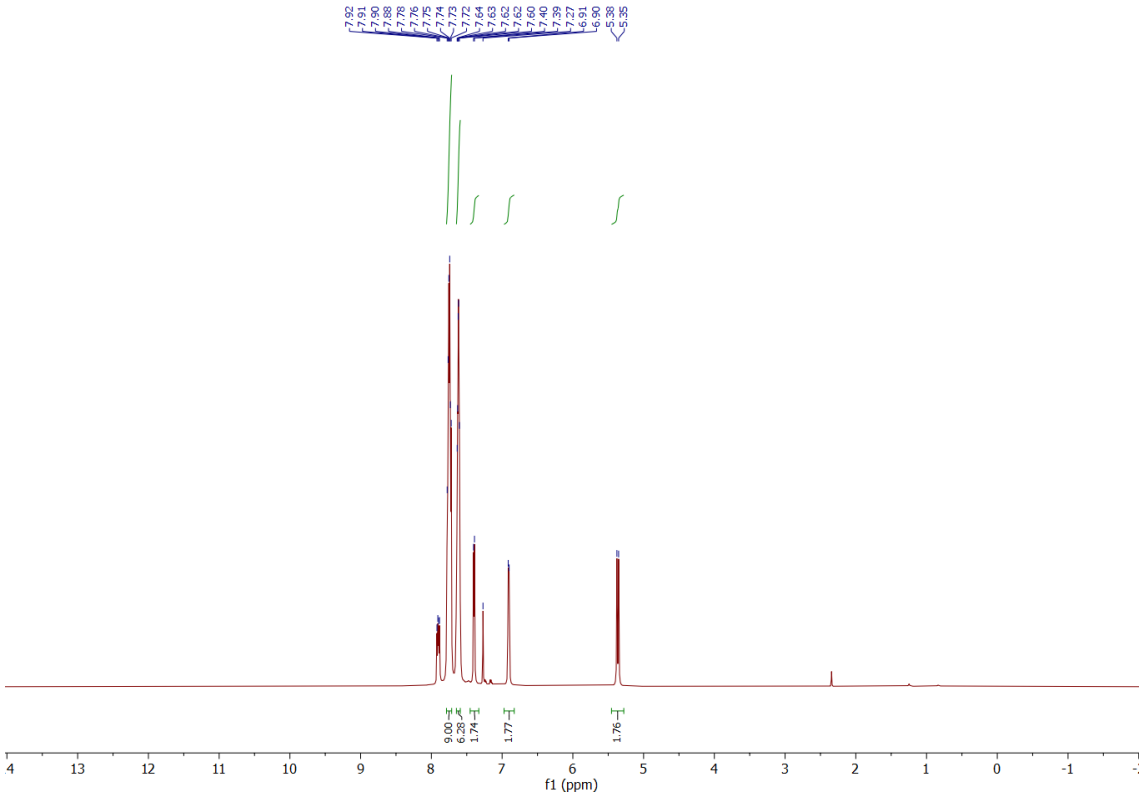

ethyl (*E*)-2-benzoyl-6-(4-iodophenyl)hex-5-enoate (**21-I**)

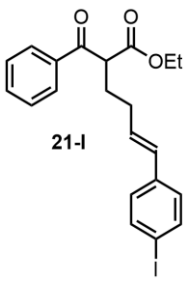

Prepared according to **GP-B** using potassium *tert*-butoxide (508 mg, 1.5 equiv., 4.53 mmol) in THF (3.5 mL, 1.3 M), **21WS-I**(2.53 g, 1.5 equiv., 4.53 mmol) in THF (9 mL, 0.5 M), and **A** (750 mg, 1.0 equiv., 3.02 mmol) in THF (4.5 mL, 2.0 M) with a reaction time of 16 h. Purification by flash column chromatography afforded the pure compound as a colorless oil (390 mg, 29%).

Characterization of **21-I**

^{1}H NMR (700 MHz; $CDCl_3$) δ_H 7.98 (d, J = 7.5 Hz, 2H), 7.61 (d, J = 8.3 Hz, 2H), 7.59 (t, J = 7.5 Hz, 1H), 7.47 (t, J = 7.8 Hz, 2H), 7.04 (d, J = 8.1 Hz, 2H), 6.27 (d, J = 15.8 Hz, 1H), 6.18 (dt, J = 15.8, 6.8 Hz, 1H), 4.36 (t, J = 7.0 Hz, 1H), 4.14 (qd, J = 7.2, 2.8 Hz, 2H), 2.34 – 2.25 (m, 2H), 2.25 – 2.18 (m, 2H), 1.17 (t, J = 7.1 Hz, 3H).

^{13}C NMR (176 MHz, $CDCl_3$) δ_C 195.1, 169.8, 137.5, 136.9, 136.3, 133.5, 130.3, 130.0, 128.7, 128.6, 127.8, 92.2, 61.5, 53.3, 30.8, 28.3, 14.0.

ν_{max} (FTIR)/cm^{-1}: 2977, 2934, 1732, 1683, 1483, 1447, 1151, 1002, 967, 688.

HRMS (ESI) m/z: $[M+Na]^+$ calculated for $C_{21}H_{21}O_3INa^+$: 471.0428; found: 471.0423.

^{1}H NMR spectrum of **21-I**:

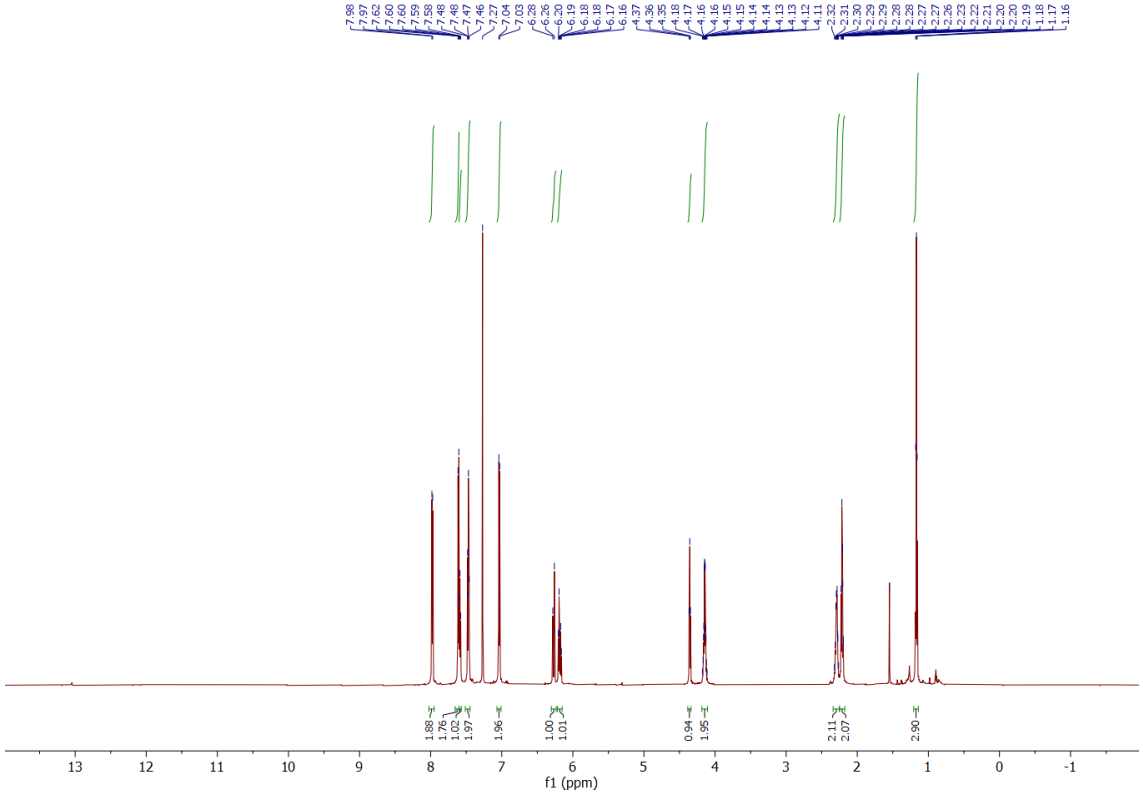

^{13}C NMR spectrum of **21-I**:

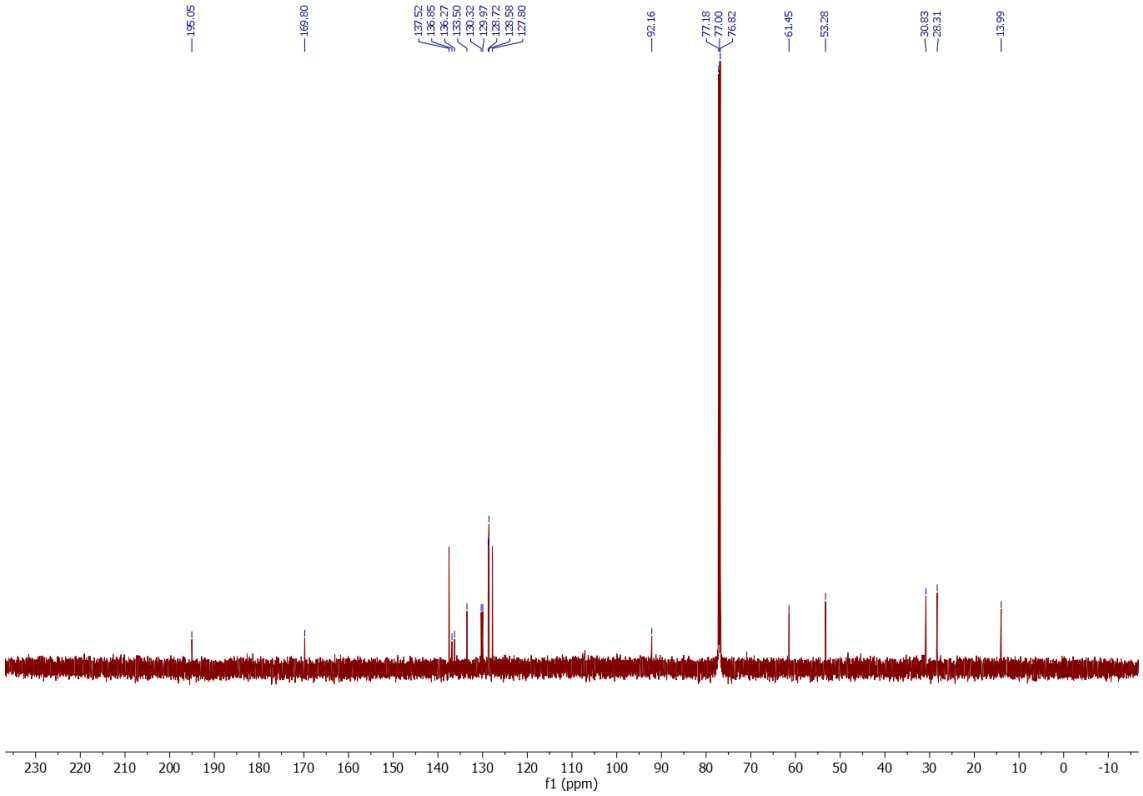

(4-bromobenzyl)triphenylphosphonium bromide (**21WS-Br**)

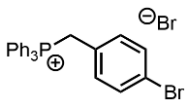

21WS-Br

Prepared according to **GP-WS** using 1-bromo-4-(bromomethyl)benzene (5.00 g, 1.0 equiv., 20.0 mmol), triphenylphosphine (5.25 g, 1.0 equiv., 20.0 mmol), and toluene (40 mL, 0.5 M) with a reaction time of 16 h, afforded the pure compound as a white solid (10.0 g, 98%).

Characterization of **21WS-Br**

^{1}H NMR (600 MHz; $CDCl_3$) δ_H 7.84 – 7.69 (m, 9H), 7.61 (dt, J = 10.3, 4.8 Hz, 6H), 7.19 (d, J = 8.0 Hz, 2H), 7.07 (d, J = 8.1 Hz, 2H), 5.60 (d, J = 14.7 Hz, 2H).

Spectroscopic data matches literature report.[74]

^{1}H NMR spectrum of **21WS-Br**:

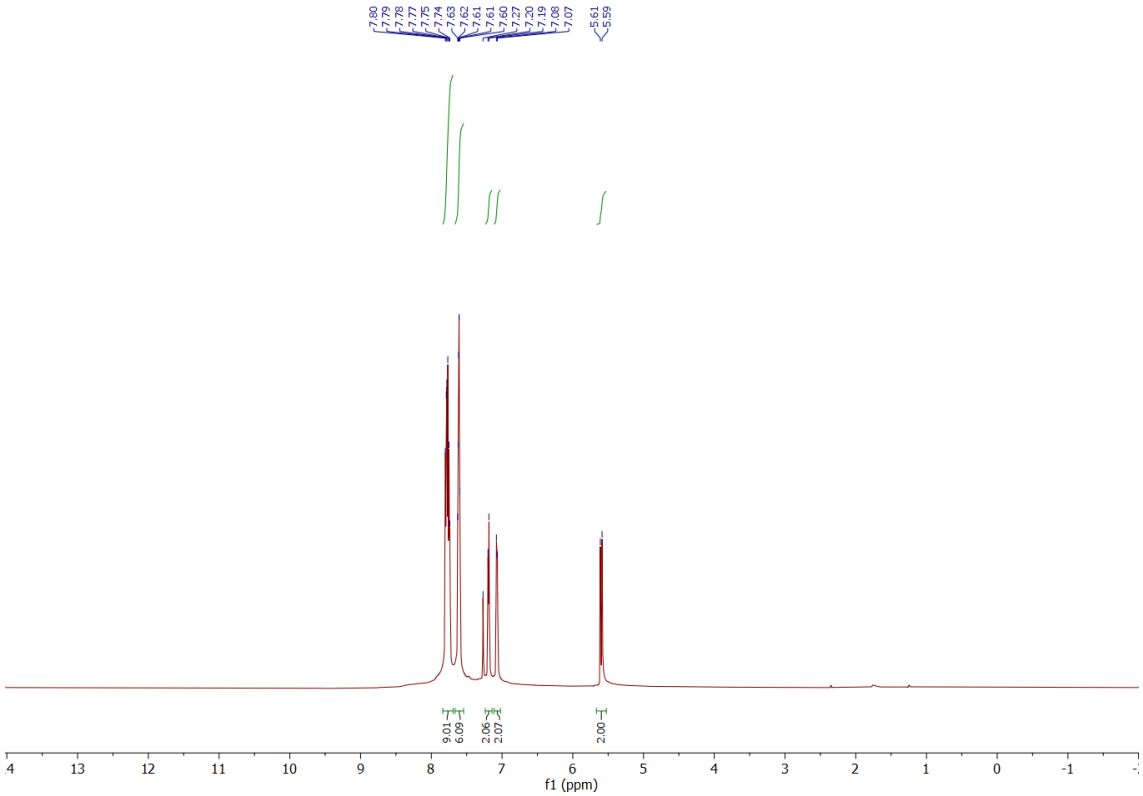

ethyl (*E*)-2-benzoyl-6-(4-bromophenyl)hex-5-enoate (**21-Br**)

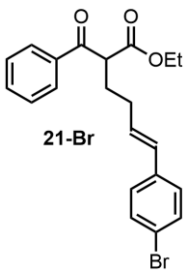

Prepared according to **GP-B** using potassium *tert*-butoxide (67.8 mg, 1.5 equiv., 0.60 mmol) in THF (0.46 mL, 1.3 M), **21WS-Br** (309 mg, 1.5 equiv., 0.60 mmol) in THF (1.2 mL, 0.5 M), and **A** (100 mg, 1.0 equiv., 0.40 mmol) in THF (0.6 mL, 2.0 M) with a reaction time of 16 h. Purification by flash column chromatography afforded the pure compound as a colorless oil (100 mg, 62%).

Characterization of **21-Br**

^{1}H NMR (700 MHz; $CDCl_3$) δ_H 7.98 (d, J = 7.7 Hz, 2H), 7.59 (t, J = 7.4 Hz, 1H), 7.47 (t, J = 7.6 Hz, 2H), 7.41 (d, J = 8.2 Hz, 2H), 7.16 (d, J = 8.2 Hz, 2H), 6.29 (d, J = 15.8 Hz, 1H),6.17 (dt, J = 15.5, 6.9 Hz, 1H), 4.36 (t, J = 7.0 Hz, 1H), 4.15 (qd, J = 7.2, 2.8 Hz, 2H), 2.29 (td, J = 7.5, 3.0 Hz, 2H), 2.21 (q, J = 7.3 Hz, 2H), 1.17 (t, J = 7.1 Hz, 3H).

^{13}C NMR (176 MHz, $CDCl_3$) δ_C 195.1, 169.8, 136.3, 133.5, 131.6, 130.2, 129.8, 128.7, 128.6, 127.5, 120.8, 61.5, 53.3, 30.8, 28.3, 14.0.

ν_{max} (FTIR)/cm^{-1}: 2964, 1721, 1689, 1447, 1320, 1252, 1173, 969, 804, 694.

HRMS (ESI) m/z: $[M+Na]^+$ calculated for $C_{21}H_{21}O_3BrNa^+$: 423.0566; found: 423.0563.

^{1}H NMR spectrum of **21-Br**:

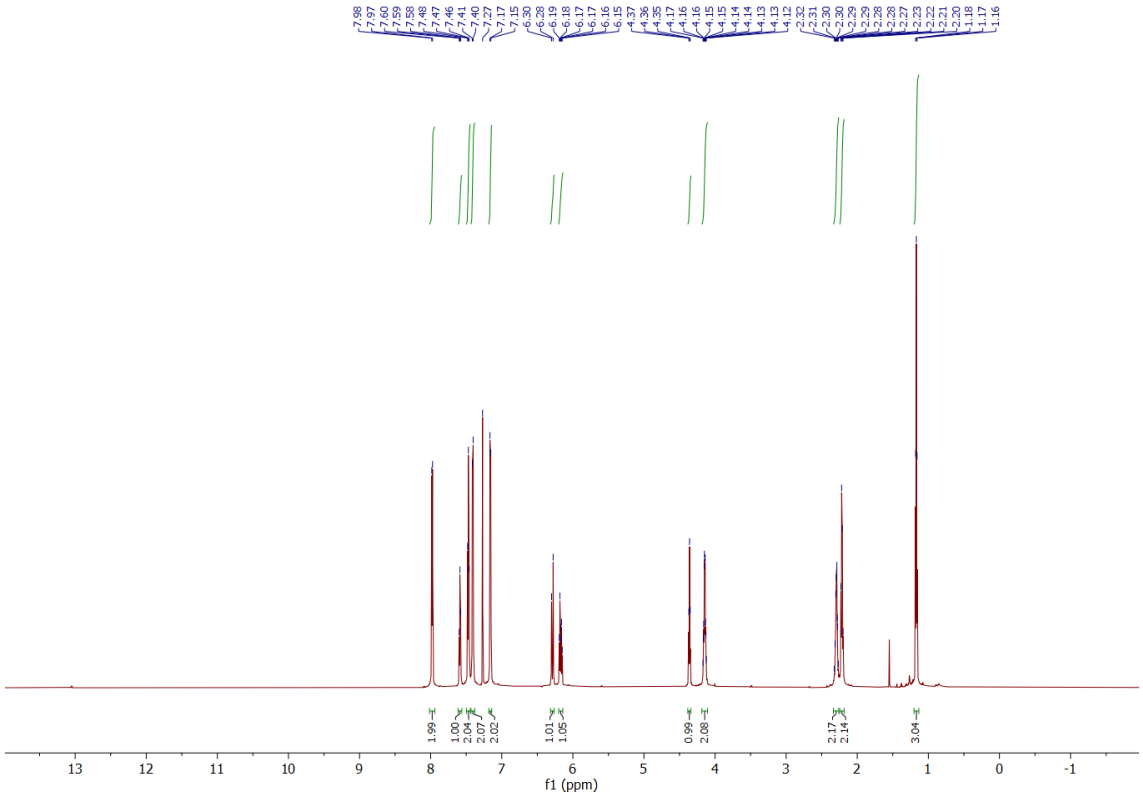

^{13}C NMR spectrum of **21-Br**:

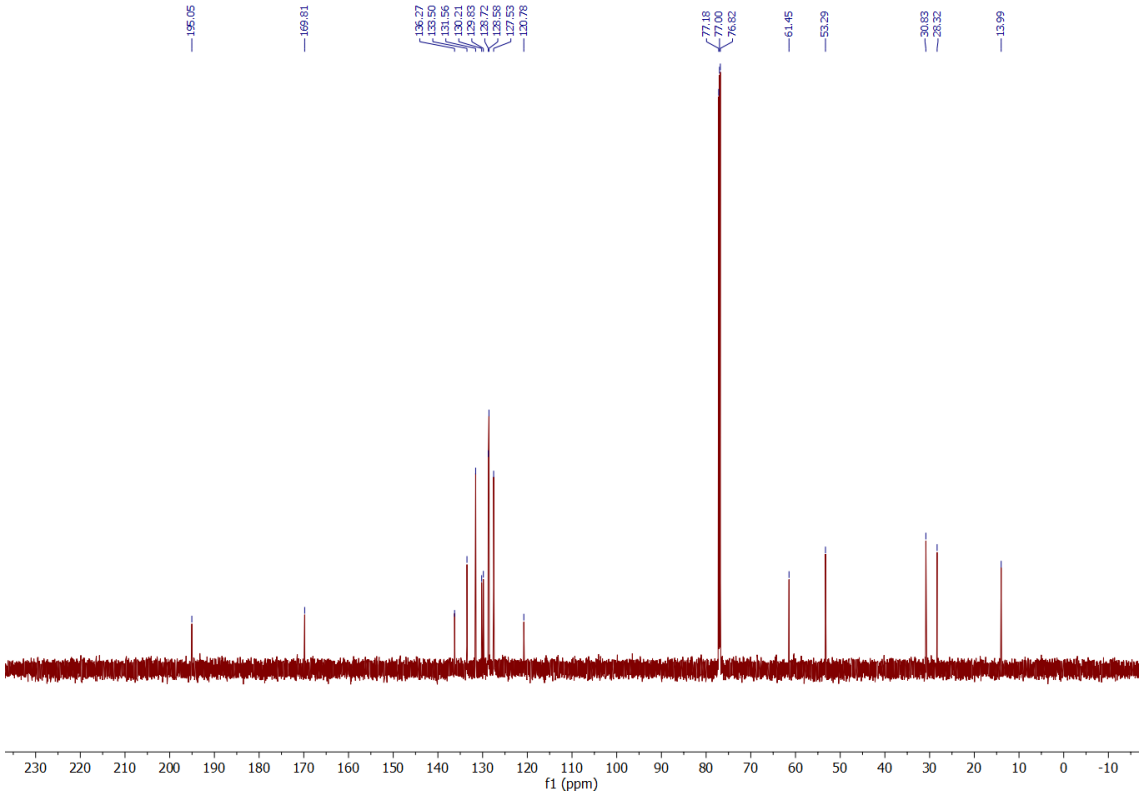

triphenyl(4-(trifluoromethyl)benzyl)phosphonium bromide (**21WS-CF$_3$**)

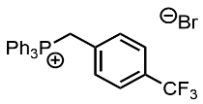

21WS-CF$_3$

Prepared according to **GP-WS** using 1-(bromomethyl)-4-(trifluoromethyl)benzene (5.00 g, 1.0 equiv., 20.9 mmol), triphenylphosphine (5.49 g, 1.0 equiv., 20.9 mmol), and toluene (42 mL, 0.5 M) with a reaction time of 16 h, afforded the pure compound as a white solid (10.5 g, 100%).

Characterization of **21WS-CF$_3$**

^{1}H NMR (600 MHz; CD_2Cl_2) δ_H 7.78 (dq, J = 14.9, 7.7 Hz, 9H), 7.58 (td, J = 7.8, 3.3 Hz, 6H), 7.36 (d, J = 7.8 Hz, 2H), 7.31 (d, J = 8.0 Hz, 2H), 5.82 (d, J = 15.5 Hz, 2H).

Spectroscopic data matches literature report.[77]

^{1}H NMR spectrum of **21WS-CF$_3$**:

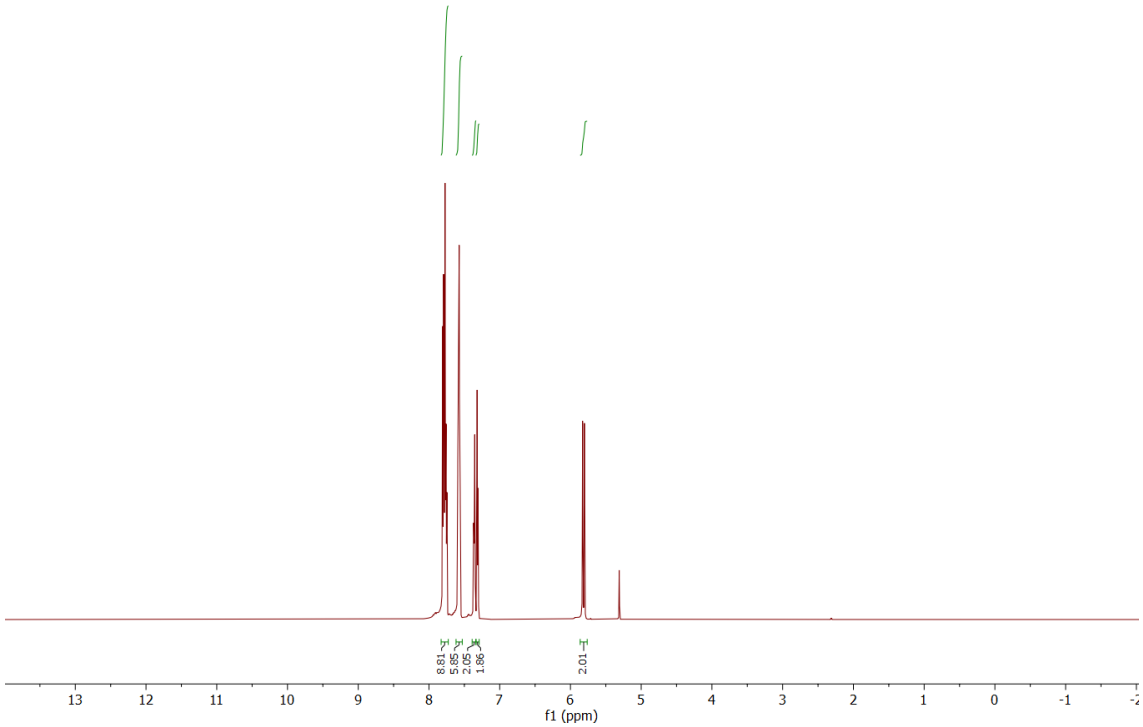

ethyl (*E*)-2-benzoyl-6-(4-(trifluoromethyl)phenyl)hex-5-enoate (**21-CF$_3$**)

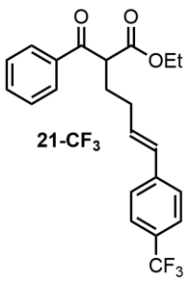

Prepared according to **GP-B** using potassium *tert*-butoxide (508 mg, 1.5 equiv., 4.53 mmol) in THF (3.5 mL, 1.3 M), **21WS-CF$_3$** (2.27 g, 1.5 equiv., 4.53 mmol) in THF (9 mL, 0.5 M), and **A** (750 mg, 1.0 equiv., 3.02 mmol) in THF (4.5 mL, 2.0 M) with a reaction time of 16 h. Purification by flash column chromatography afforded the pure compound as a colorless oil (420 mg, 36%), E:Z ratio 40:1.

Characterization of **21-CF$_3$**

^{1}H NMR (500 MHz; $CDCl_3$) δ_H 7.98 (d, J = 8.3 Hz, 2H), 7.59 (t, J = 7.4 Hz, 1H), 7.54 (d, J = 8.0 Hz, 2H), 7.47 (t, J = 7.6 Hz, 2H), 7.38 (d, J = 8.0 Hz, 2H), 6.39 (d, J = 15.9 Hz, 1H), 6.29 (dt, J = 15.3, 6.7 Hz, 1H), 4.36 (t, J = 6.9 Hz, 1H), 4.15 (q, J = 7.1 Hz, 2H), 2.34 (q, J = 7.2 Hz, 2H), 2.28 – 2.19 (m, 2H), 1.17 (t, J = 7.1 Hz, 3H).

^{13}C NMR (176 MHz, $CDCl_3$) δ_C 195.0, 169.8, 140.8, 136.3, 133.5, 131.8, 130.1, 129.0, 128.9 (d, J = 32.5 Hz), 128.7, 128.6, 126.10, 125.41 (q, J = 3.6 Hz), 124.21 (d, J = 271.4 Hz), 61.5, 53.3, 30.9, 28.2, 14.0.

ν_{max} (FTIR)/cm^{-1}: 2982, 1734, 1685, 1448, 1323, 1159, 1112, 1066, 856, 688.

HRMS (ESI) m/z: $[M+Na]^+$ calculated for $C_{22}H_{22}O_3F_3Na^+$: 413.1335; found: 413.1333.

^{1}H NMR spectrum of **21-CF$_3$**:

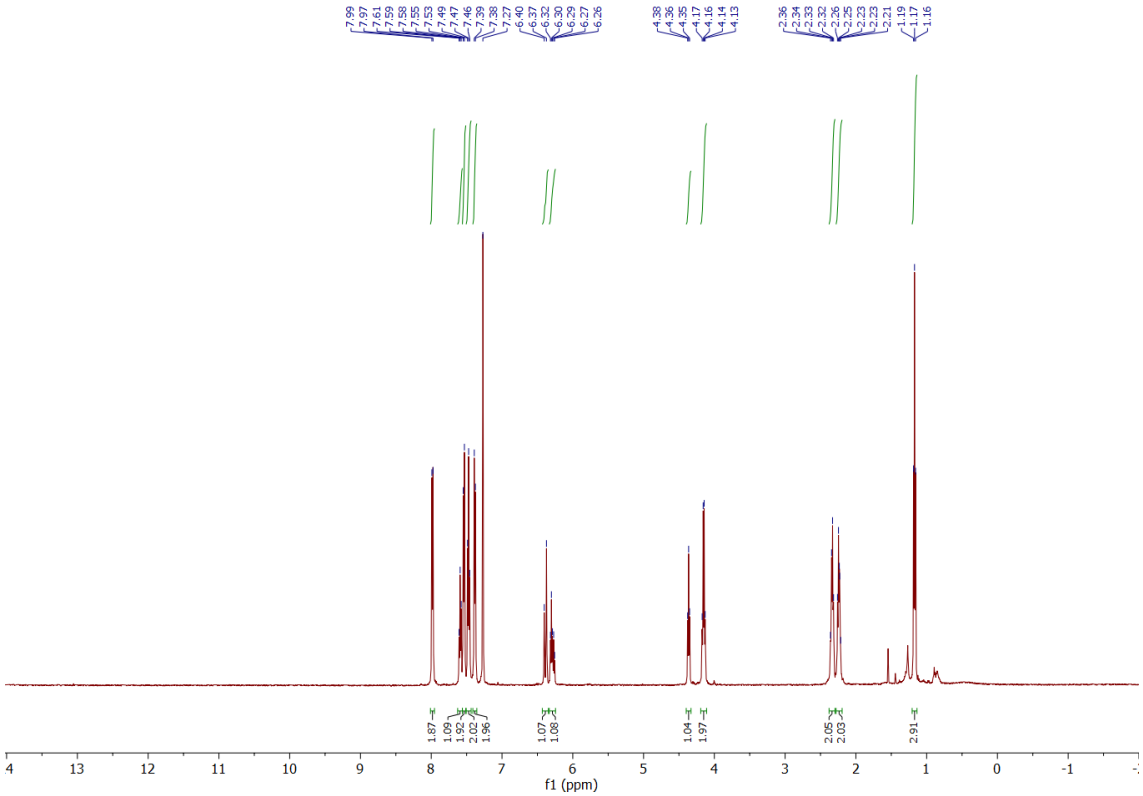

^{13}C NMR spectrum of **21-CF$_3$**:

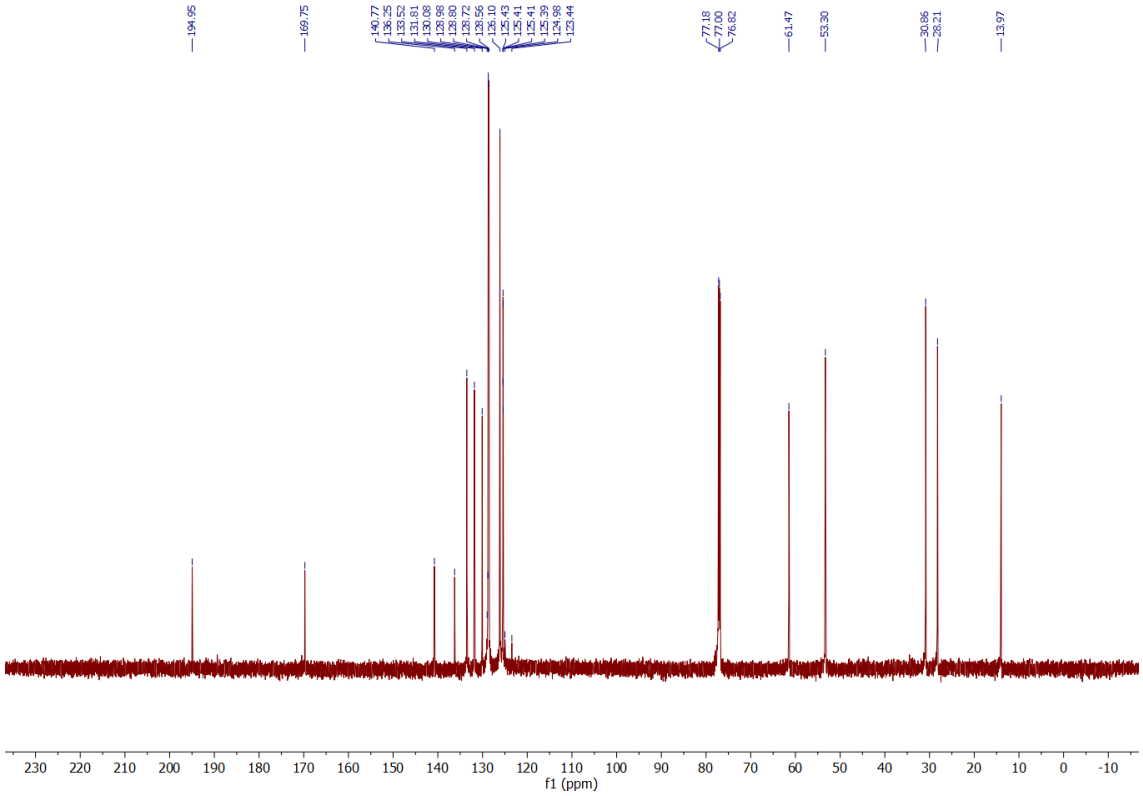

5-bromo-2-(methyl-*d*$_3$)pent-2-ene-1,1,1-*d*$_3$ (**25X**)

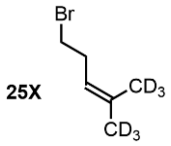

A solution of propan-2-one-*d*$_6$ (3.21 g, 1.00 equiv, 50.0 mmol) in Et_2O (25 mL, 2.0 M) was slowly added via addition funnel to a solution of cyclopropylmagnesium bromide (100.0 mL, 0.5 molar, 1.00 equiv., 50.0 mmol) in Et_2O (16 mL, 0.5 M) cooled to 0 °C under N_2. Once addition was complete, the solution was allowed to stir at room temperature for 1 h. After 1 h, a round-bottom flask was cooled to 0 °C, water (36 mL), then sulfuric acid (18.7 mL) was slowly added. Using a powder funnel, the slurry from the first round-bottom was transferred to the acidic solution and allowed to stir for overnight at room temperature. The aqueous layer was separated and extracted with Et_2O (2 x 30 ml). The combined organic layers were then washed with 5% hydrogen sulfite, brine, dried with Na_2SO_4, filtered, and concentrated under reduced pressure. The crude product was purified by flash column chromatography in 100% pentanes to obtain the desired pure compound as a pale yellow oil (1.80 g, 21%).

Characterization of **25X**

^{1}H NMR (700 MHz; $CDCl_3$) δ_H 5.14 (t, J = 7.1 Hz, 1H), 3.35 (t, J = 7.3 Hz, 2H), 2.57 (q, J = 7.3 Hz, 2H).

^{13}C NMR (176 MHz, $CDCl_3$) δ_C 134.8, 121.0, 32.9, 31.8.

ν_{max} (FTIR)/cm^{-1}: 2962, 2194, 2063, 1661, 1434, 1270, 1204, 1048, 869, 702.

HRMS (ESI) m/z: $[M-H]^-$ calculated for $C_6H_4D_6Br^-$: 167.0348; found: 167.0352.

^{1}H NMR spectrum of **25X**:

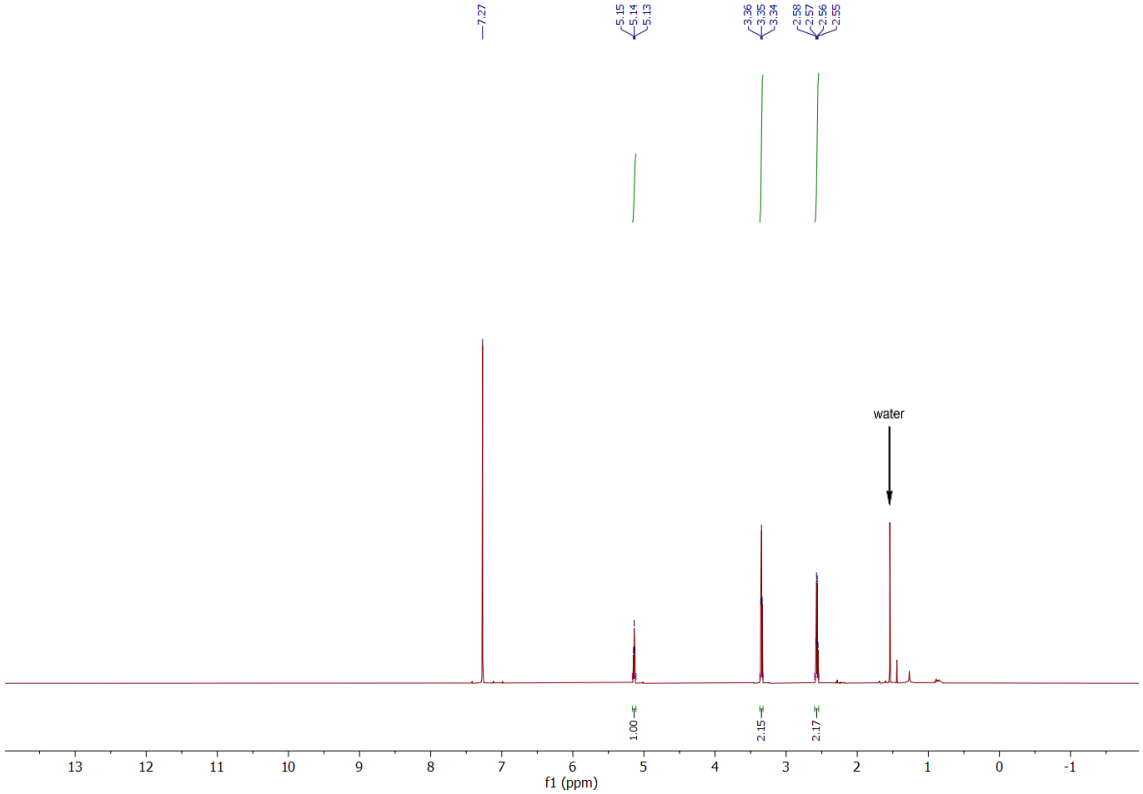

^{13}C NMR spectrum of **25X**:

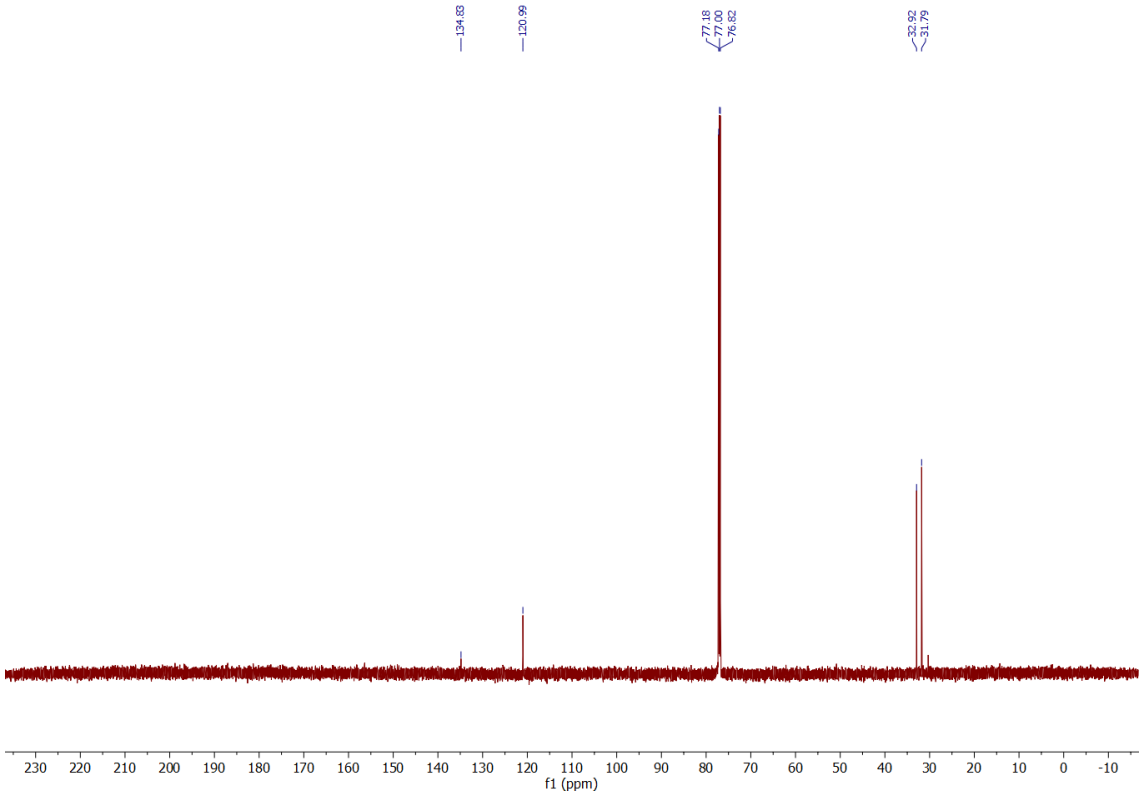

ethyl 2-benzoyl-6-(methyl-d_3)hept-5-enoate-7,7,7-d_3 (**25**)

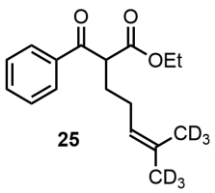

Prepared according to **GP-A** using 60 wt% sodium hydride (407 mg, 60% Wt, 1.2 equiv., 10.2 mmol), ethyl 3-oxo-3-phenylpropanoate (1.63 g, 1.47 mL, 1.00 equiv., 8.48 mmol), **25X** (1.51 g, 1.05 equiv., 8.90 mmol), and THF (47 mL, 0.2 M) with a reaction time of 16 h. Purification by preparative SCF (Sepiatec 2) on an AD-H column (21x250 mm, 5 µm) eluting with 10% MeOH in water (0.1% NH_4OH) at 1.60 min (70 mL/min, 4 min method, 215 nm) afforded the pure compound as a colorless oil (637 mg, 27 %).

Characterization of **25**

^{1}H NMR (700 MHz; $CDCl_3$) δ_H 7.98 (d, J = 7.8 Hz, 2H), 7.59 (t, J = 7.4 Hz, 1H), 7.48 (t, J = 7.6 Hz, 2H), 5.11 (t, J = 6.6 Hz, 1H), 4.32 (t, J = 6.4 Hz, 1H), 4.15 (tdd, J = 7.2, 6.4, 5.7, 2.2 Hz, 2H), 2.06 (dt, J = 10.2, 6.5 Hz, 4H), 1.18 (t, J = 7.1 Hz, 3H).

^{13}C NMR (176 MHz, CDCl3) δ_C 195.4, 170.1, 136.3, 133.4, 128.7, 128.6, 123.0, 53.4, 29.0, 25.9, 14.0.

ν_{max} (FTIR)/cm^{-1}: 2980, 2192, 2063, 1734, 1684, 1597, 1448, 1149, 1026, 689.

HRMS (ESI) m/z: $[M+Na]^+$ calculated for $C_{21}H_{16}D_6O_3Na^+$: 303.1838; found: 303.1831.

^{1}H NMR spectrum of **25**:

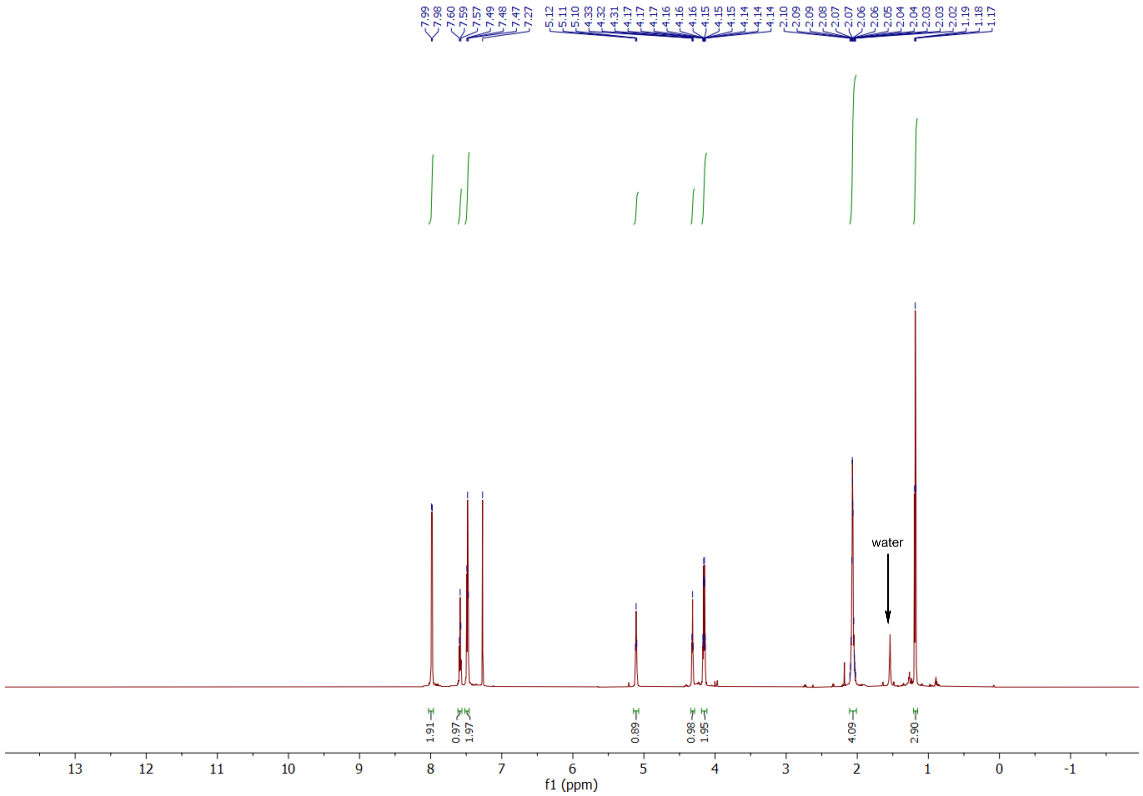

^{13}C NMR spectrum of **25**:

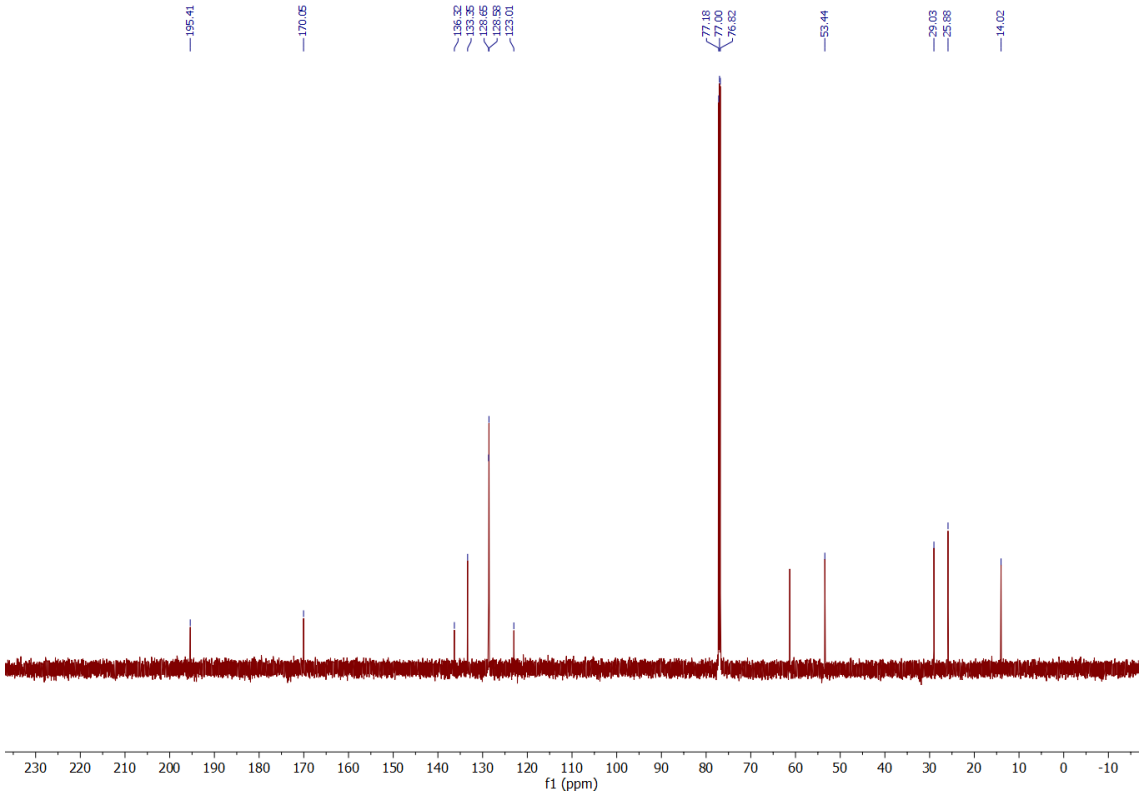

5.6.4 Kinetic Isotope Effects

Sample Preparation

For carbonyl–olefin metathesis reactions with **10**:

The carbonyl–olefin metathesis reaction was conducted with **10** (as described in 5.6.3). **10** or **10f** was subsequently reduced to **15** or **15f**, respectively (as described in 5.6.3).

Two sets of two samples were prepared (100 mg of **15** or **15f** in 525 μL of MeOD with 0.05 mM $Cr(acac)_3$). Two of the samples in each set were no conversion samples (**15**, F = 0%) and two were partial conversion samples (**15f**, F = 82% and F = 78%) with respect to the prenyl β-keto ester starting material (**10**).

For carbonyl–olefin metathesis reactions with **20**:

The carbonyl–olefin metathesis reaction was conducted with **20** (as described in 5.6.3). **20** or **20f** was subsequently reduced to **20r** or **20rf**, respectively (as described in 5.6.3).

Two sets of two samples were prepared (100 mg of **20r** or **20rf** in 525 μL of $CDCl_3$ with 0.05 mM $Cr(acac)_3$). Two of the samples in each set were no conversion samples (**20r**, F = 0%) and two were partial conversion samples (**20rf**, F = 80% and F = 67%) with respect to the styrenyl β-keto ester starting material (**20**).

All samples were prepared in Wilmad WG-1241-8-5 NMR tubes and subsequently hermetically sealed under air at room temperature.

Data Acquisition

The DEPT experiments were conducted over about a 5 to 6 day period for each set of samples. For the prenyl samples (**15** and **15f**), the set of 4 samples was run in 15 randomized iterations, and for the styrenyl samples (**20r** and **20rf**) the set of 4 samples was run in 20 randomized iterations. The pulse sequence, pulse sequence code, and detailed instructions for installing and running the DEPT experiments can be found at:

https://github.com/ekwan/carbonyl_olefin_metathesis_SI/tree/main/NMR/acquisition.

Processing Procedure

Detailed instructions on how to reference and phase spectra in TopSpin and how to process all the data in Jupyter Lab is located on:
https://github.com/ekwan/carbonyl_olefin_metathesis_SI/tree/main/NMR/processing.

Additionally, due to the file size, raw data for the prenyl (**15** and **15f**) and styrenyl (**20r** and **20rf**) samples and the corresponding Jupyter Lab notebooks can be found at the link provided above.

Analysis and KIEs

All processed raw data for prenyl (**15** and **15f**) and styrenyl (**20r** and **20rf**) samples, KIE calculations, and error can be found at:
https://github.com/ekwan/carbonyl_olefin_metathesis_SI/tree/main/NMR/analysis.

All KIE values for **10** and **20** are shown below.

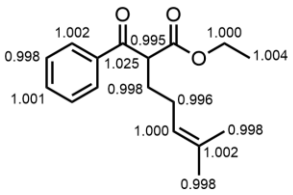

prenyl β-keto ester (**10**)

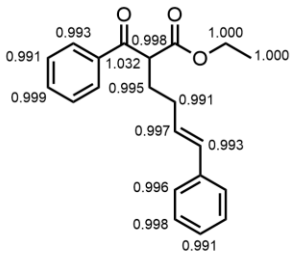

styrenyl β-keto ester (**20**)

5.6.5 Hammett Studies

Substrate Evaluation

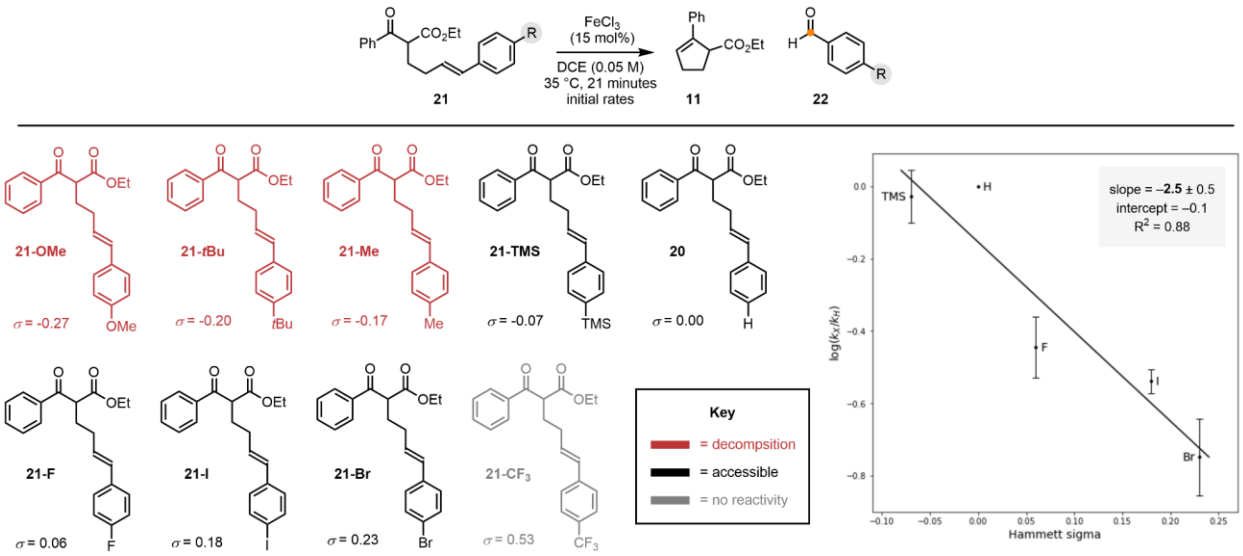

Substrates evaluated: 9 substrates were evaluated for the Hammett study (shown below). Initial investigations with **21-OMe**, **21-*t*Bu**, **21-Me**, showed significant decomposition by UPLC and were excluded from the study. There was no reactivity with **21-CF3** after a 24 h reaction time and was also excluded from the study. The Hammett study was then conducted with the remaining reactivity substrates: **21-TMS**, **20**, **21-F**, **21-I**, and **21-Br**. 3 to 5 replicates were conducted per substrate with a 7 aliquots per replicate (exception: 1 of 4 replicates for **21-Br** only has 4 aliquots).

Reaction Setup

Styrenyl β–keto ester substrate **S** (1.00 equiv.) was added to a flame dried 1 dram vial, equipped with a stir bar followed by freshly distilled DCE (final molarity was 0.05 M) and stirred for 10 minutes at 35 °C. Then, a homogeneous solution of $FeCl_3$ in freshly distilled DCE (0.15 equiv., 0.02 M) was added and the reaction was sampled every 3 minutes for 21 minutes. Aliquots (17 to 20 µL) were placed in a Captiva filter vial (filter vial, PTFE, 0.45 µm) with caffeine as an internal standard (~ 1.94 mg/mL), diluted with acetonitrile, and measured by UPLC; each sample was run twice and the average area values were used. All standard curves, raw UPLC data, the analysis and associated errors were calculated using an Excel and can be found at: https://github.com/ekwan/carbonyl_olefin_metathesis_SI/tree/main/spreadsheets.

21-TMS: UPLC Conditions: 60-90% acetonitrile in water (0.1% formic acid), 0.400 mL/min, 5 min method, 254 nm, retention time for **11** = 1.30 min, retention time for **21-TMS** = 3.39 min.

21-TMS (39.5 mg, 1.00 equiv., 100.0 µmol) and $FeCl_3$ (750 µL, 0.02 molar, 0.15 equiv., 15.0 µmol) in DCE (1.25 mL). Or, **21-TMS** (33.5 mg, 1.00 equiv., 84.9 µmol) and $FeCl_3$ (637 µL, 0.02 molar, 0.15 equiv., 12.7 µmol) in DCE (1.06 mL).

20: UPLC Conditions: 60-80% acetonitrile in water (0.1% formic acid), 0.400 mL/min, 4 min method, 254 nm, retention time for **11** = 1.30 min, retention time for **20** = 2.15 min.

20 (32.2 mg, 1.00 equiv., 100.0 µmol) and $FeCl_3$ (750 µL, 0.02 molar, 0.15 equiv., 15.0 µmol) in DCE (1.25 mL).

21-F: UPLC Conditions: 60-80% acetonitrile in water (0.1% formic acid), 0.400 mL/min, 4 min method, 254 nm, retention time for **11** = 1.30 min, retention time for **21-F** = 2.12 min.

21-F (34.0 mg, 1.00 equiv., 100.0 µmol) and $FeCl_3$ (750 µL, 0.02 molar, 0.15 equiv., 15.0 µmol) in DCE (1.25 mL). Or, **21-F** (29.0 mg, 1.00 equiv., 84.9 µmol) and $FeCl_3$ (637 µL, 0.02 molar, 0.15 equiv., 12.7 µmol) in DCE (1.06 mL).

21-I: UPLC Conditions: 60-80% acetonitrile in water (0.1% formic acid), 0.400 mL/min, 4 min method, 254 nm, retention time for **11** = 1.30 min, retention time for **21-I** = 3.13 min.

21-I (44.8 mg, 1.00 equiv., 100.0 µmol) and $FeCl_3$ (750 µL, 0.02 molar, 0.15 equiv., 15.0 µmol) in DCE (1.25 mL)

21-Br: UPLC Conditions: 60-80% acetonitrile in water (0.1% formic acid), 0.400 mL/min, 4 min method, 254 nm, retention time for **11** = 1.30 min, retention time for **21-Br** = 2.77 min.

21-Br (40.1 mg, 1.00 equiv., 100.0 µmol) and $FeCl_3$ (750 µL, 0.02 molar, 0.15 equiv., 15.0 µmol) in DCE (1.25 mL). Or, **21-Br** (38.0 mg, 1.00 equiv., 94.7 µmol) and $FeCl_3$ (710 µL, 0.02 molar, 0.15 equiv., 14.2 µmol) in DCE (1.19 mL).

5.6.6 Secondary Deuterium Kinetic Isotope Effects

Reaction Setup

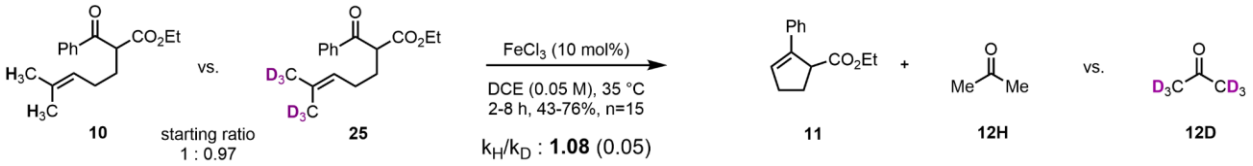

Initial Mixture of **10** and **25**: A mixture of **10** (225 mg, 1.00 equiv., 820 µmol) and **25** (230 mg, 1.00 equiv., 820 µmol) was prepared for these experiments. Five NMR samples were made of the initial mixture of **10**:**25** and the ratio was determined to be 1:0.97.

Reaction Setup: A 1:0.97 mixture of **10** (225 mg, 1.00 equiv., 46.0 µmol) and **25** (230 mg, 0.97 equiv., 44.6 µmol) were added to a flame dried 1 dram vial, equipped with a stir bar. Then a homogeneous solution of $FeCl_3$ in freshly distilled DCE (460 µL, 0.10 equiv., 0.01 M, 164 µmol) was added and the reaction was stirred for 2-8 h at 35 °C. After cooling, the reaction mixture was pushed through a silica plug to remove the iron. The silica plug was rinsed with 10 mL of DCM. The solvent was removed under vacuum and dried. The resulting crude mixture was diluted with 0.5 mL of benzene-d_6. All spectra were taken on a Bruker Avance Neo 500 with 4 scans (n = 4) and a 60 second relaxation delay (d1) to ensure full relaxation of the protons.

Spectra

Starting ratio of the 1:0.97 mixture of **10**:**25**

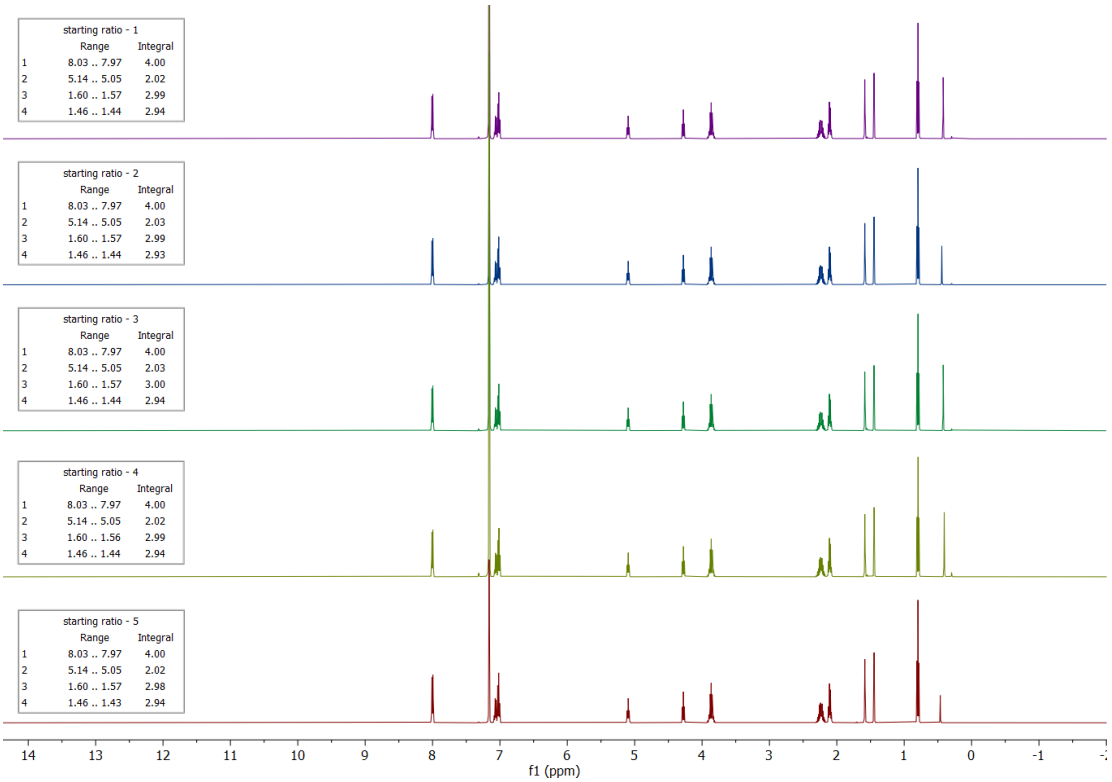

Experiments 1-4: 2.25 - 3 h

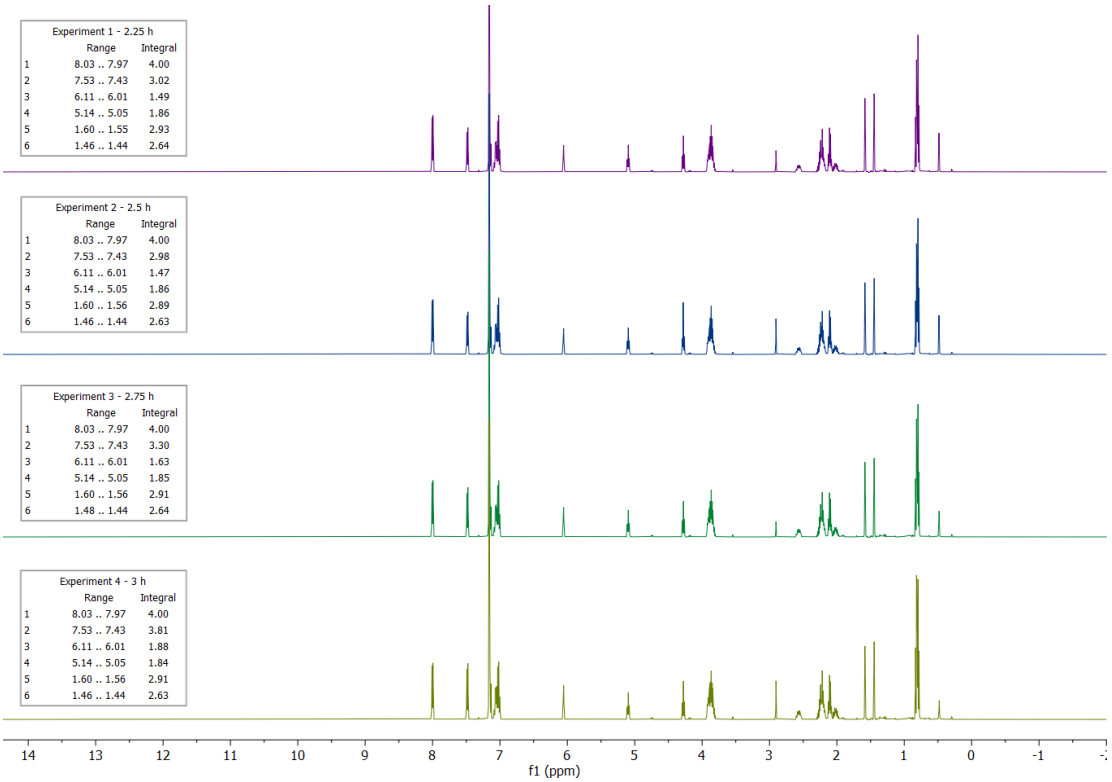

Experiments 5-8: 3.25 - 5 h

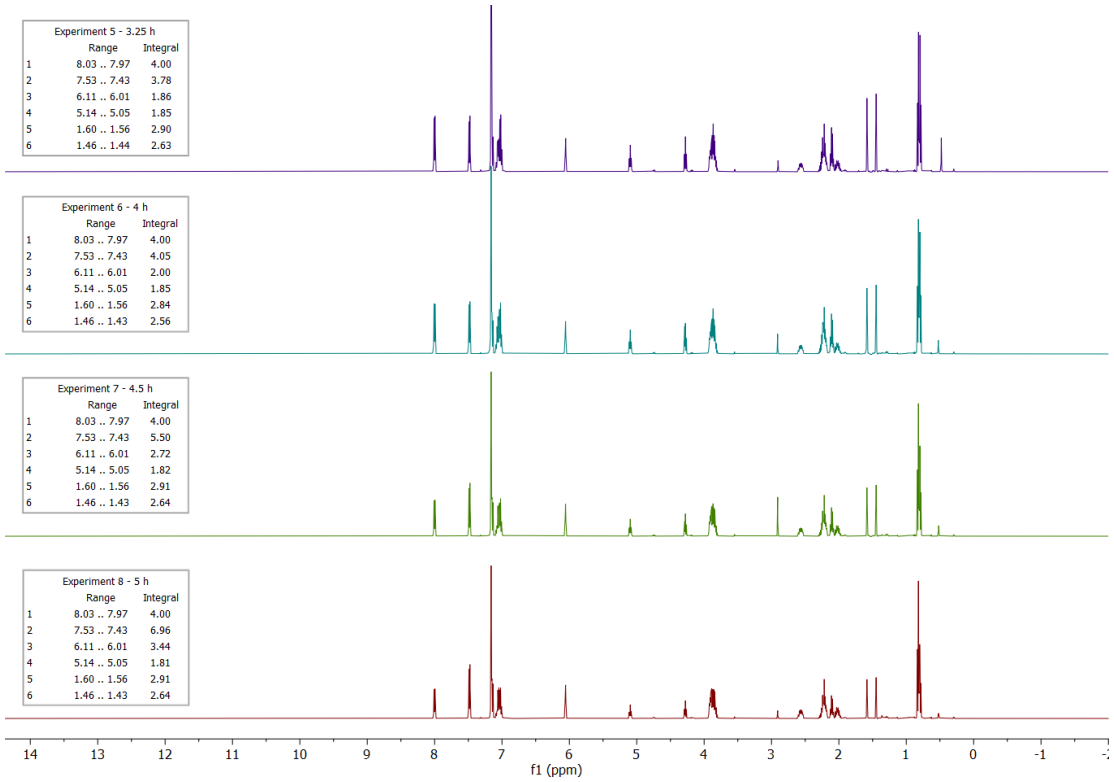

Experiments 9-12: 5.5 - 6.5 h

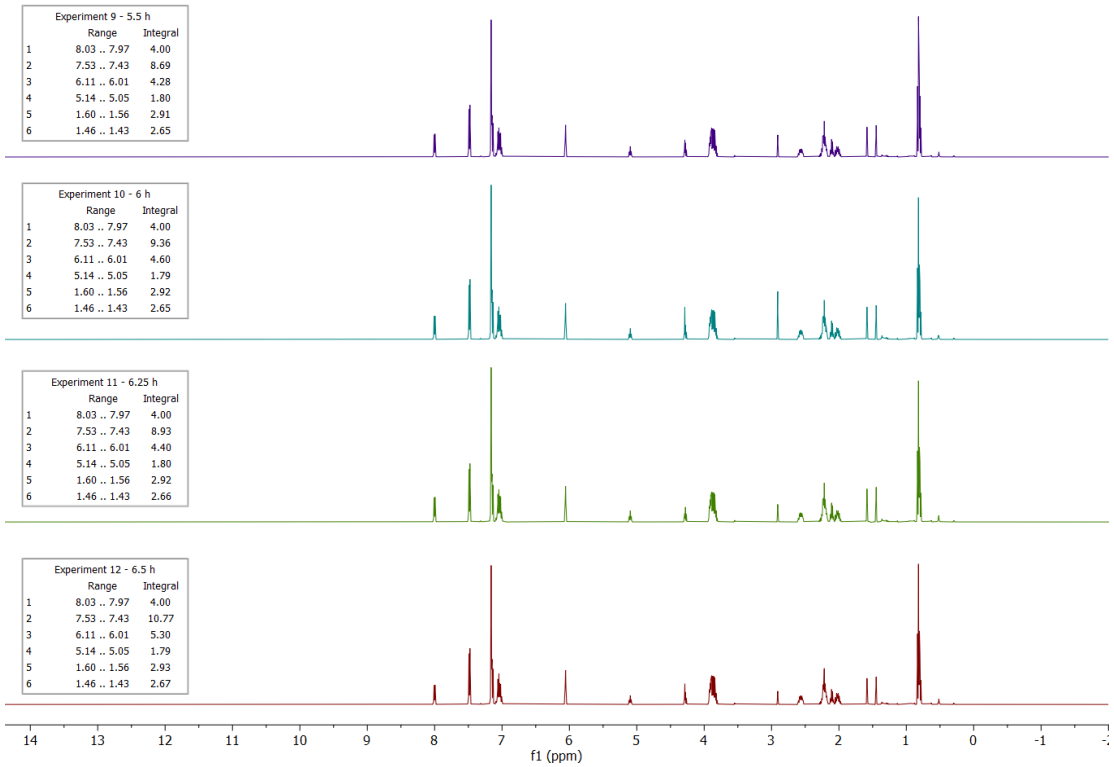

Experiments 13-16: 6.75 - 7.5 h

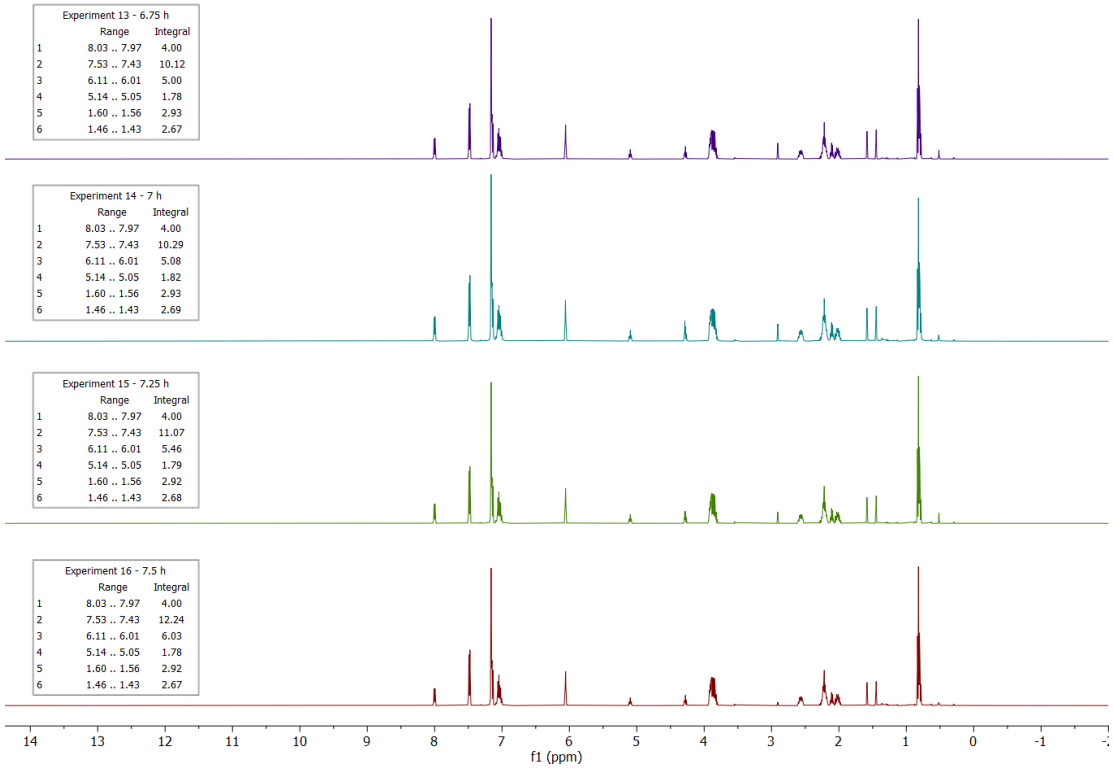

All experiments 1-16: 2.25 - 7.5 h

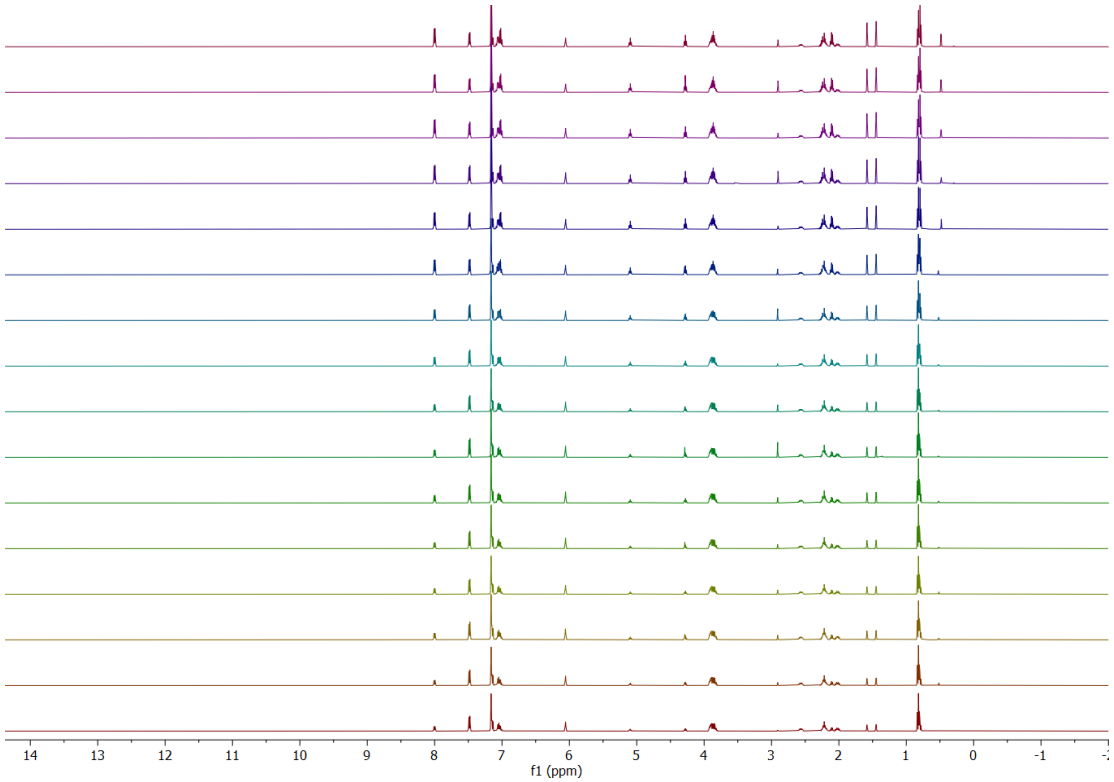

Experimental SDKIEs

Experimental SDKIEs for the sixteen intermolecular competition reactions between **10** and **25** are shown tabulated below. All raw and normalized integral data, KIEs, and their associated errors were calculated using Excel and can be found at: https://github.com/ekwan/carbonyl_olefin_metathesis_SI/tree/main/spreadsheets.

Reaction #	Time (h)	average conversion (%)	KIEs
1	2.25	43.75	1.12
2	2.5	43.42	1.16
3	2.75	46.02	1.12
4	3	49.66	1.11
5	3.25	49.36	1.12
6	4	51.13	1.19
7	4.5	58.86	1.07
8	5	64.51	1.06
9	5.5	69.44	1.04
10	6	71.02	1.04
11	6.25	70.02	1.04
12	6.5	73.84	1.03
13	6.75	72.71	1.02
14	7	72.82	1.03
15	7.25	74.38	1.03
16	7.5	76.29	1.02
		average = 1.08	
		standard deviation = 0.05	

5.6.7 Computations

General Procedures

DFT calculations were carried out using *Gaussian 16, Revision A.03*:

M. J. Frisch, G. W. Trucks, H. B. Schlegel, G. E. Scuseria, M. A. Robb, J. R. Cheeseman, G. Scalmani, V. Barone, G. A. Petersson, H. Nakatsuji, X. Li, M. Caricato, A. V. Marenich, J. Bloino, B. G. Janesko, R. Gomperts, B. Mennucci, H. P. Hratchian, J. V. Ortiz, A. F. Izmaylov, J. L. Sonnenberg, D. Williams-Young, F. Ding, F. Lipparini, F. Egidi, J. Goings, B. Peng, A. Petrone, T. Henderson, D. Ranasinghe, V. G. Zakrzewski, J. Gao, N. Rega, G. Zheng, W. Liang, M. Hada, M. Ehara, K. Toyota, R. Fukuda, J. Hasegawa, M. Ishida, T. Nakajima, Y. Honda, O. Kitao, H. Nakai, T. Vreven, K. Throssell, J. A. Montgomery, Jr., J. E. Peralta, F. Ogliaro, M. J. Bearpark, J. J. Heyd, E. N. Brothers, K. N. Kudin, V. N. Staroverov, T. A. Keith, R. Kobayashi, J. Normand, K. Raghavachari, A. P. Rendell, J. C. Burant, S. S. Iyengar, J. Tomasi, M. Cossi, J. M. Millam, M.

Klene, C. Adamo, R. Cammi, J. W. Ochterski, R. L. Martin, K. Morokuma, O. Farkas, J. B. Foresman, and D. J. Fox, Gaussian, Inc., Wallingford CT, 2016.

DLPNO-CCSD(T1) calculations were carried out in ORCA with TightPNO cutoffs.

All stationary points were verified to be true local minima or saddle points by frequency analysis. Due to substantial problems with numerical convergence in implicit solvent, non-essential parts of the potential energy surface (PES) such as second betaines, cycloreversion transition states, products, etc. were not comprehensively evaluated. Essential stationary points were converged to the best of our ability and satisfy normal convergence criteria in most cases. Original output files are available at:
www.github.com/ekwan/carbonyl_olefin_metathesis_SI

KIEs were calculated using *PyQuiver*, which is freely available from the collaborator Eugene E. Kwan at:
www.github.com/ekwan/PyQuiver

3D molecule structures were made in CLYView:
www.cylview.org

Benchmarks

The performance of a variety of DFTs was assessed by comparing single-point energies calculated in the gas phase on a grid of structures with constrained C1–C2 and C3–O1 structures for 2-methyl-2-butene + acetone + $FeCl_3$. Reference energies were calculated with DLPNO-CCSD(T1)/aug-cc-pVTZ/TightPNO. Single points were also calculated with DLPNO-CCSD(T1)/cc-pVTZ/TightPNO and we found an RMS error of 1.11 kcal/mol with a Pearson correlation coefficient of 0.99965, suggesting the importance of diffuse basis functions. Below, "kcal" refers to RMS errors and average time is in seconds. Although B3LYP-D3(BJ)/jul-cc-pVDZ was not the "best" by these metrics, it is a standard functional with excellent performance in this system, and we felt this choice for computing the PES was unlikely to be pathological. We further surveyed minimal basis sets for explicit solvent dynamics, as the solute layer dominates the

computational time. We found that B3LYP-D3(BJ) with MIDI! on the carbon, hydrogen, and oxygen atoms and the LANL2DZ ECPs and basis sets on iron and chlorine gave acceptable performance.

	6-31G*		6-31+G*		jul-cc-pVDZ		jun-cc-pVTZ		MIDI! on CHO, LANL2DZ on Fe,Cl		
	kcal	Pearson r	kcal	Pearson r	kcal	Pearson r	kcal	Pearson r	unscaled kcal	Pearson r	avg time
pbe0	2.14	0.98374	1.82	0.98668	1.69	0.98894			3.44	0.96167	44.8
pbe0_d3bj	2.10	0.98889	1.76	0.99142	1.63	0.99303			3.46	0.96773	44.7
b3lyp	1.08	0.99223	1.04	0.99254	0.93	0.99401			1.76	0.98853	44.4
b3lyp_d3bj	0.91	0.99651	0.73	0.99670	0.68	0.99721	1.34	0.99184	1.85	0.99288	44.4
b97d	1.52	0.98452	1.46	0.98522	1.36	0.98724			2.16	0.98229	46.6
b97d3	1.35	0.98741	1.34	0.98768	1.25	0.98930			1.91	0.98628	46.5
bhandhlyp	1.18	0.99322	0.94	0.99435	0.90	0.99451			2.18	0.98752	47.1
bhandh	3.73	0.95164	3.29	0.96326	3.18	0.96540			5.02	0.89331	47.1
lcwpbe_d3bj	2.45	0.97038	2.14	0.97584	2.08	0.97624					
bp86_d3bj	2.05	0.98506	1.78	0.98761	1.73	0.98995					
bmk_d3bj	1.76	0.99159	1.33	0.99448	1.29	0.99551					
cam_b3lyp_d3bj	1.25	0.99464	0.96	0.99575	0.93	0.99602					
m062x	1.41	0.99353	1.04	0.99502	1.00	0.99451	1.35	0.98858			
m062x_d3	1.40	0.99362	1.02	0.99506	0.99	0.99456					
m06_hf_d3	2.27	0.98959	1.85	0.99300	1.92	0.99272					
m06l_hf_d3	1.28	0.98865	1.35	0.98922	1.22	0.99110					
hf	2.15	0.96937	2.15	0.97466	2.29	0.97448			4.35	0.86748	15.1
blyp_d3bj	1.20	0.99029	1.15	0.99090	1.06	0.99216			1.81	0.98584	49.9
tpsstpss_d3bj	1.81	0.98832	1.52	0.99055	1.40	0.99261					
vsxc	2.17	0.97233	2.41	0.97451	2.76	0.97186					
b3p86	2.03	0.98434	1.74	0.98685	1.64	0.98914			3.17	0.96844	43.9
b98	1.43	0.99054	1.20	0.99177	1.08	0.99366			2.43	0.98154	47.9
b971	1.48	0.98996	1.24	0.99133	1.12	0.99326			2.5	0.97976	47.8

b972	1.38	0.98986	1.20	0.99084	1.07	0.99257			2.44	0.98057	46.4
o3lyp	1.49	0.98446	1.49	0.98508	1.38	0.98743			2.32	0.9741	45.3
mpw1pw91	2.00	0.98528	1.68	0.98790	1.56	0.99001			3.24	0.96702	45
mpw1lyp	0.95	0.99422	0.91	0.99433	0.81	0.99546			1.7	0.99072	45
mpw1pbe	2.14	0.98345	1.82	0.98650	1.69	0.98882			3.42	0.96161	44.9
mpw3pbe	1.98	0.98431	1.69	0.98674	1.58	0.98913					
m11	1.41	0.99407	1.08	0.99538	1.08	0.99491	1.25	0.98949			
n12sx	2.22	0.98273	1.93	0.98571	1.90	0.98782					
mn12sx	1.09	0.99555	0.82	0.99590	0.81	0.99614	1.18	0.99163			
b1b95	1.33	0.99275	1.07	0.99373	0.99	0.99454					
b3pw91	1.82	0.98535	1.56	0.98749	1.44	0.98978			2.95	0.97103	44.3
m06l_d3	1.28	0.98865	1.35	0.98922	1.22	0.99110					
b97d3_d3bj	1.34	0.98765	1.32	0.98792	1.24	0.98931			1.94	0.98539	46.5

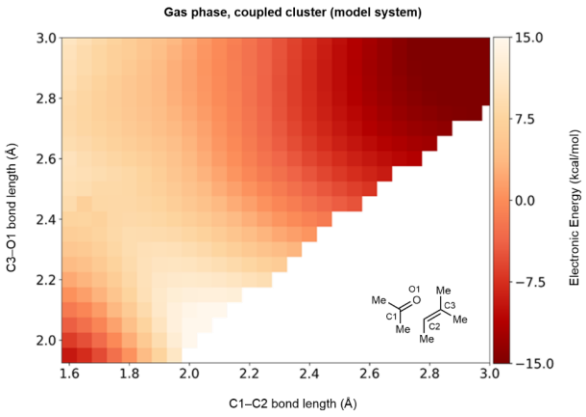

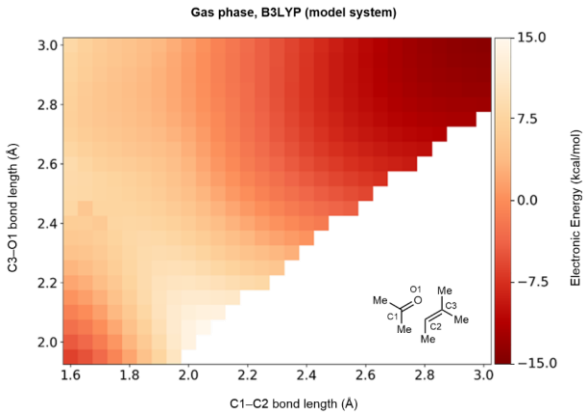

Energy Diagrams

Gibbs free energies at 298 K are shown below for the predicted concerted and stepwise pathways.

Prenyl System, Gas Phase (Concerted)

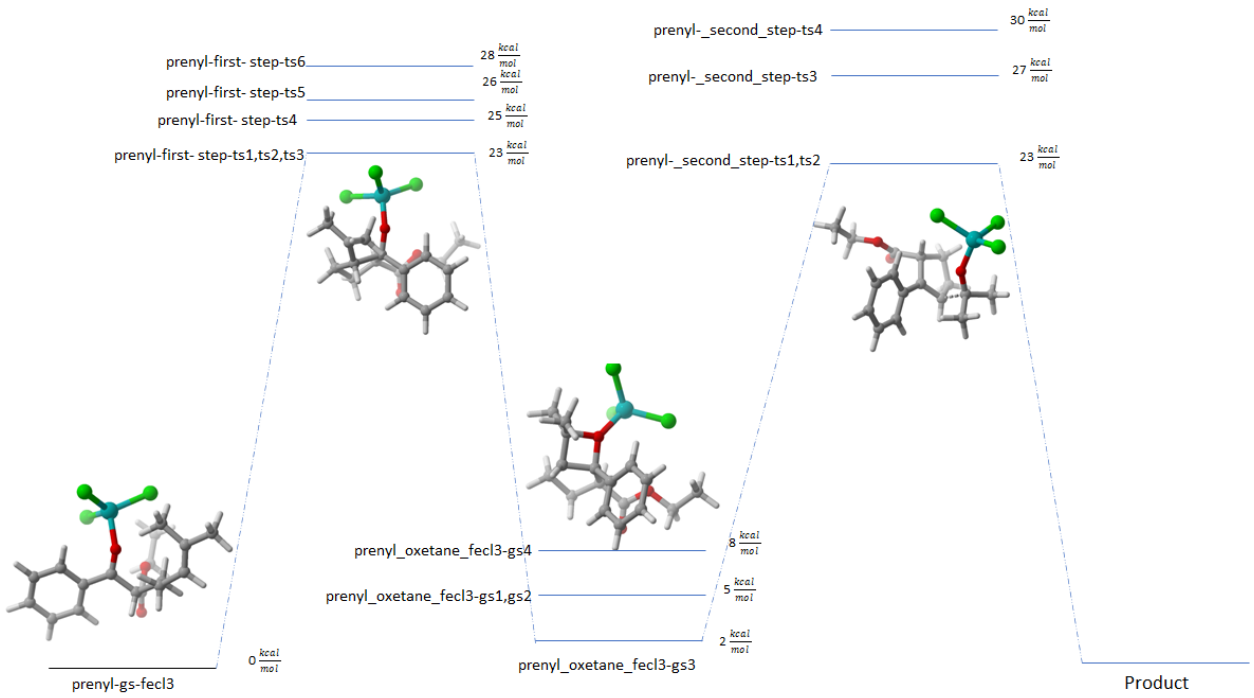

Prenyl System, Implicit DCE (Concerted)

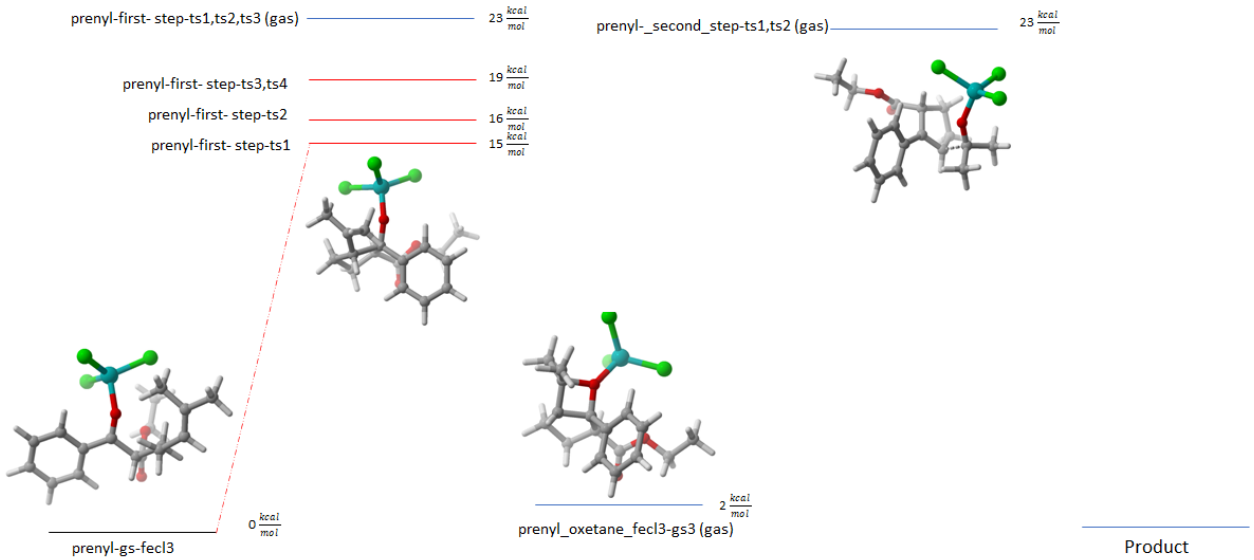

Prenyl System, Implicit Water (Concerted)

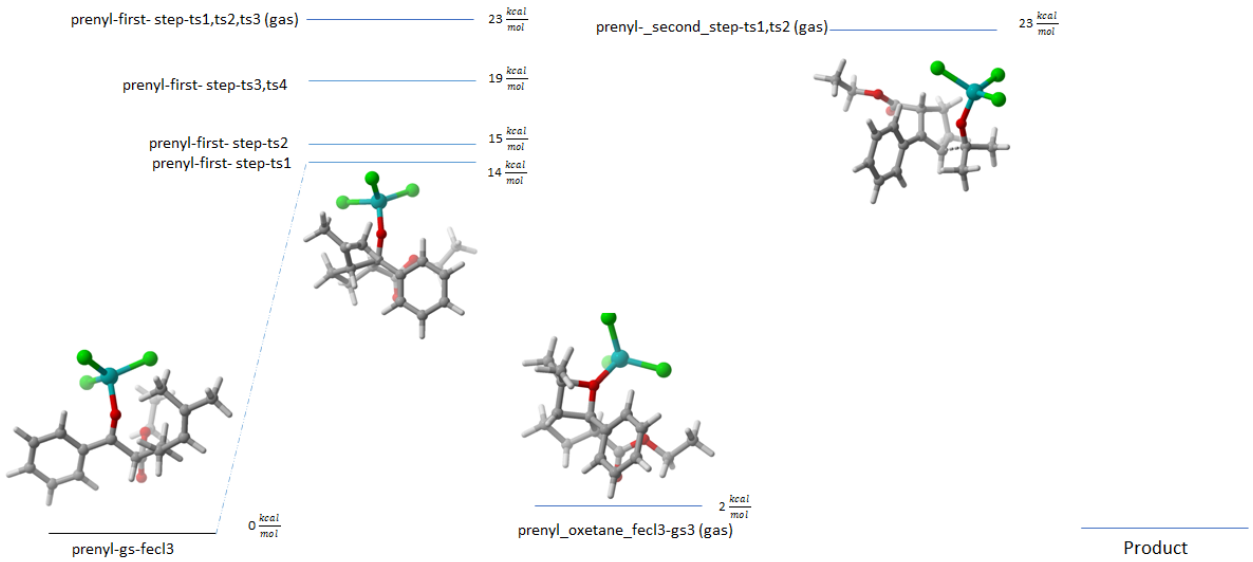

Prenyl System, Gas Phase (Stepwise)

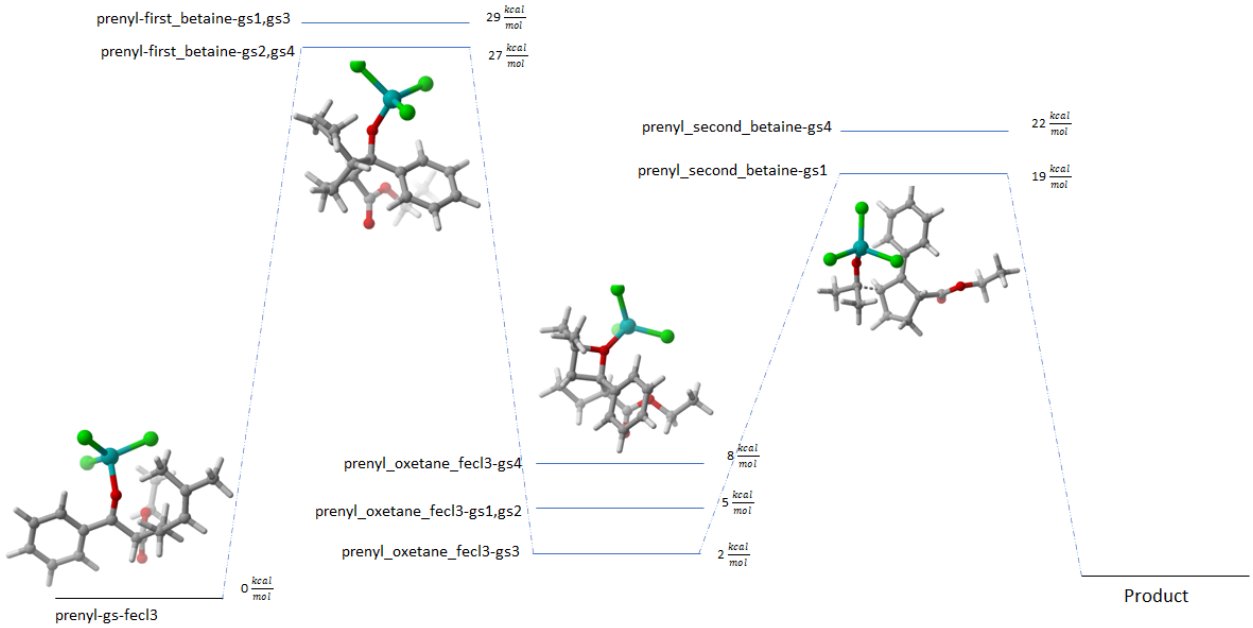

Prenyl System, Implicit DCE (Stepwise)

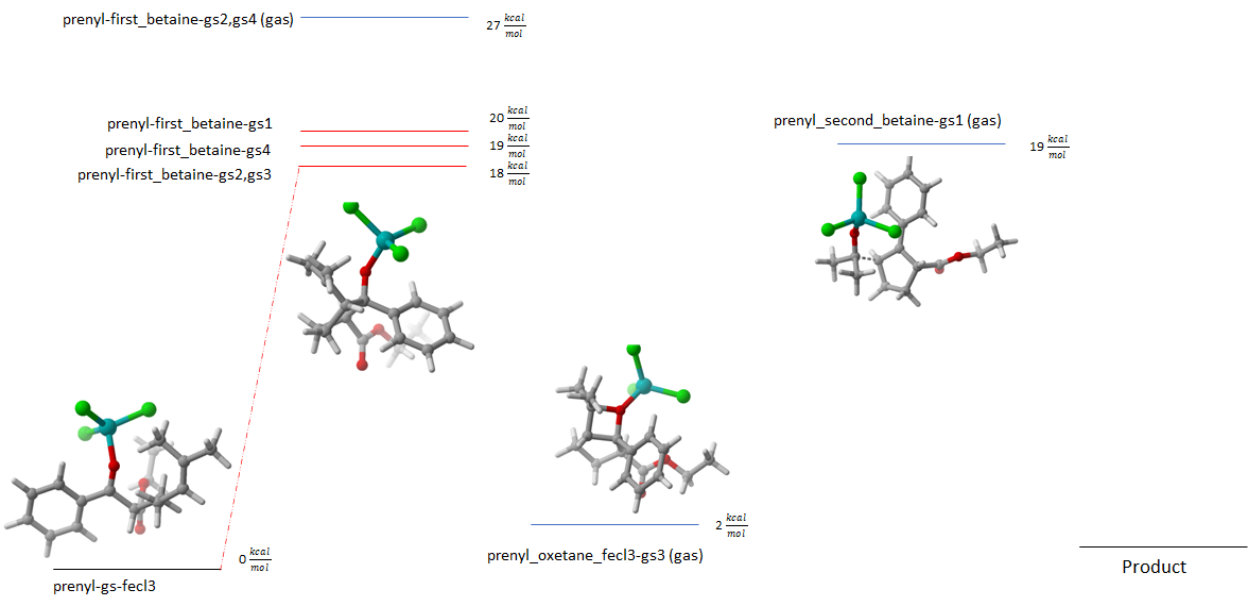

Prenyl System, Implicit Water (Stepwise)

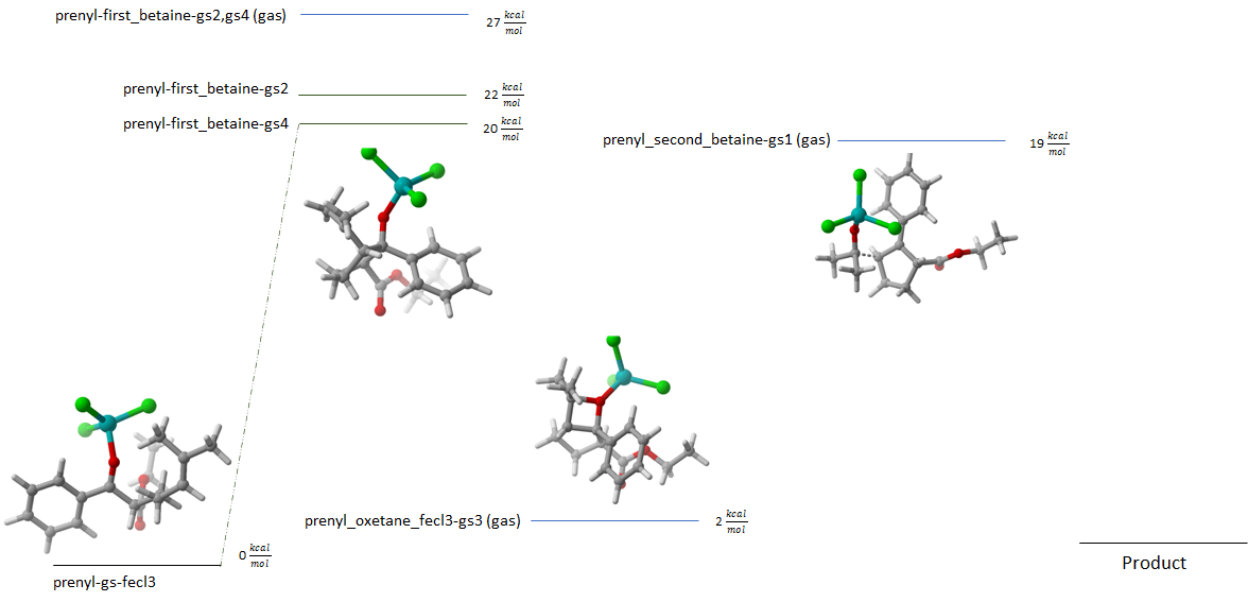

Styrenyl System, Gas Phase (Concerted)

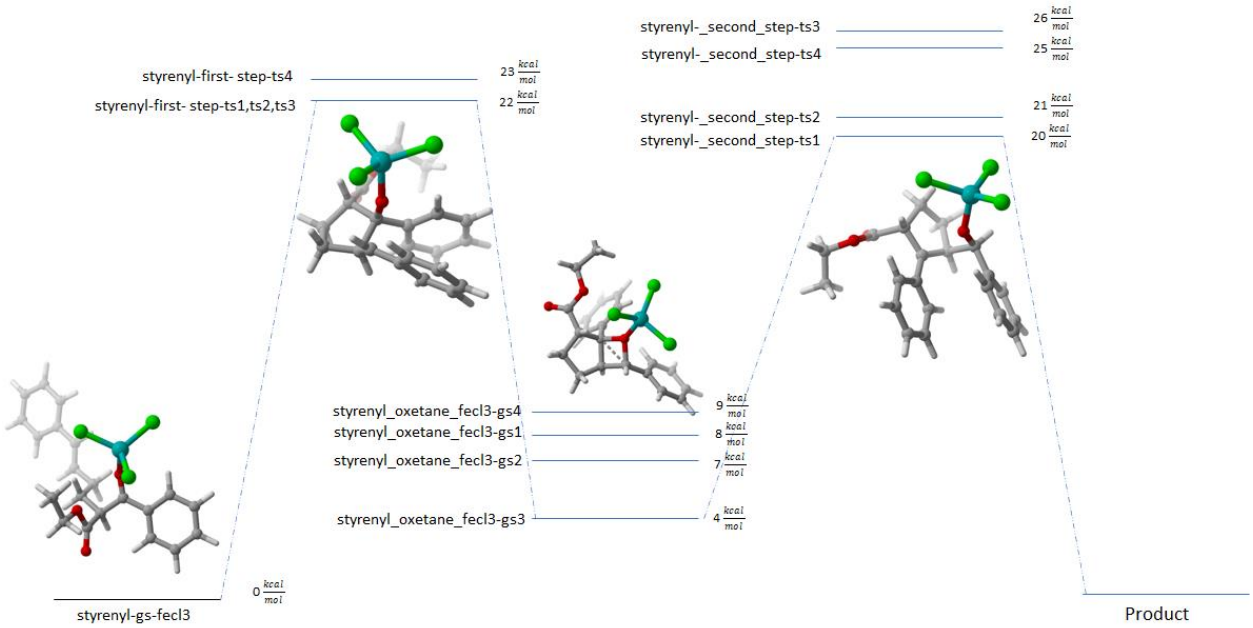

Styrenyl System, Implicit DCE (Concerted)

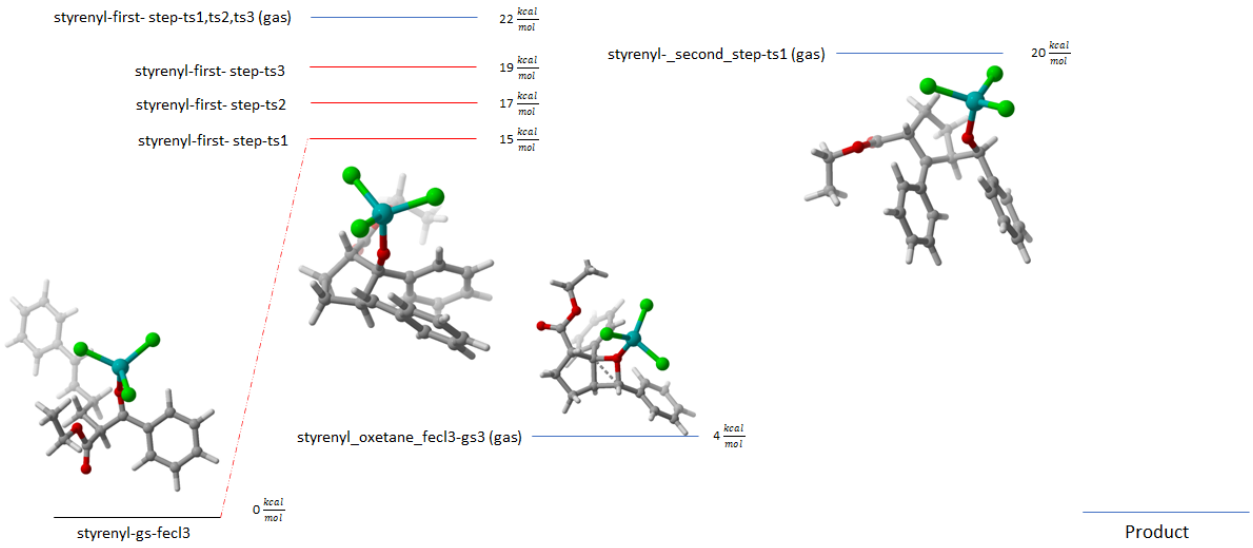

Styrenyl System, Implicit Water (Concerted)

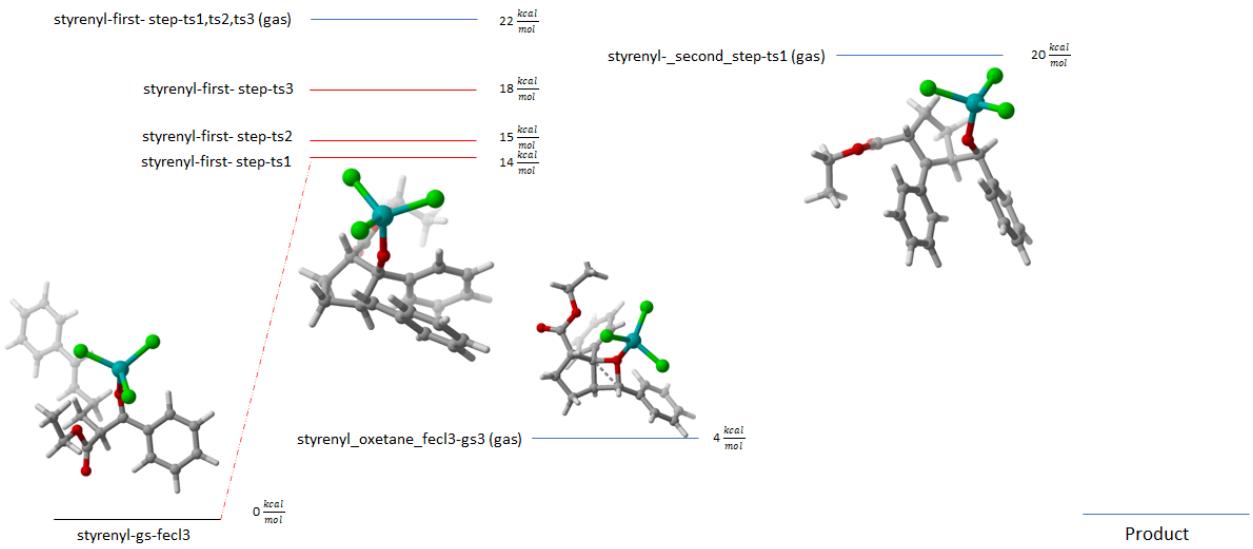

Styreneyl System, Gas Phase (Stepwise)

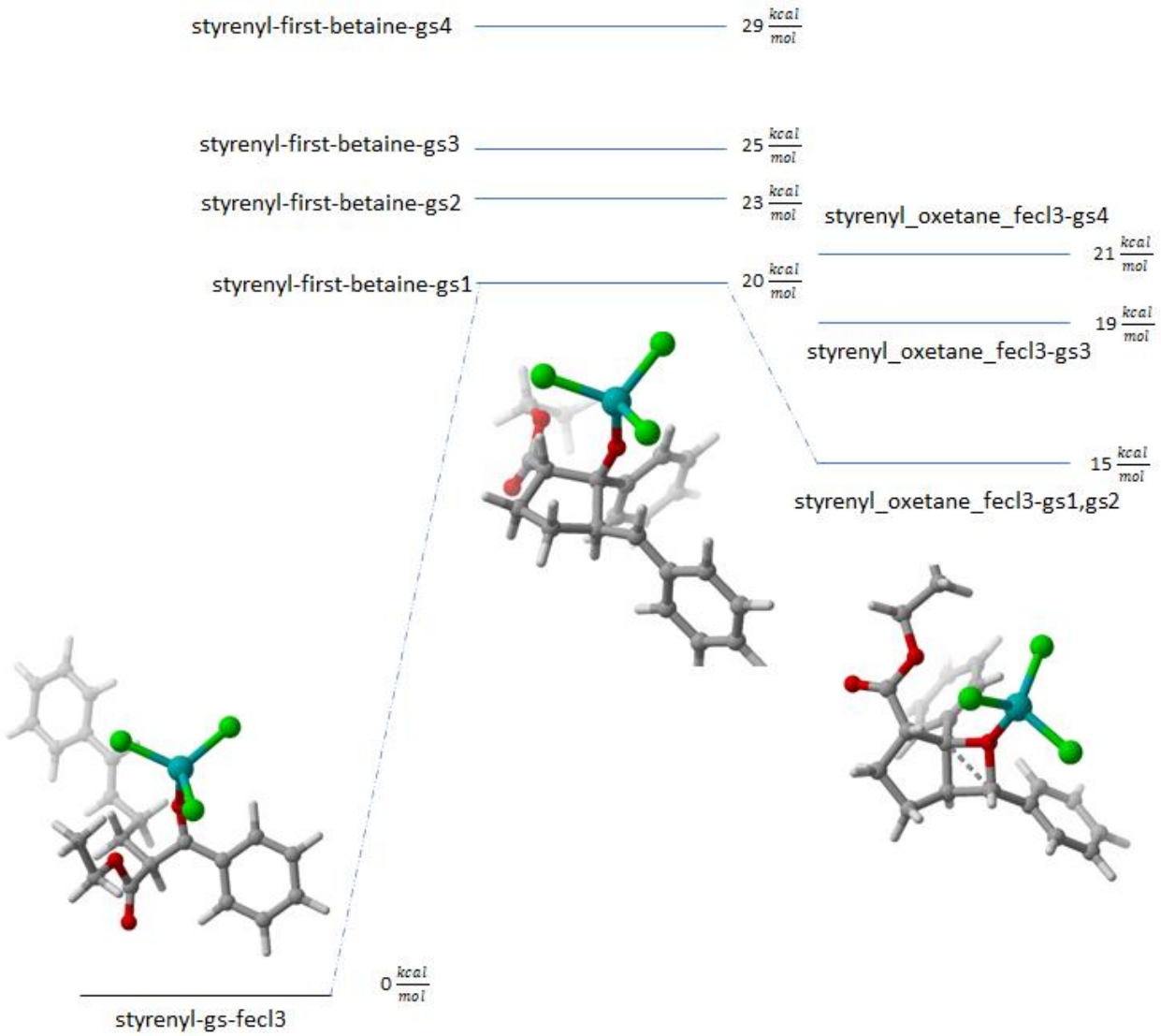

Styrenyl System, Implicit DCE (Stepwise)

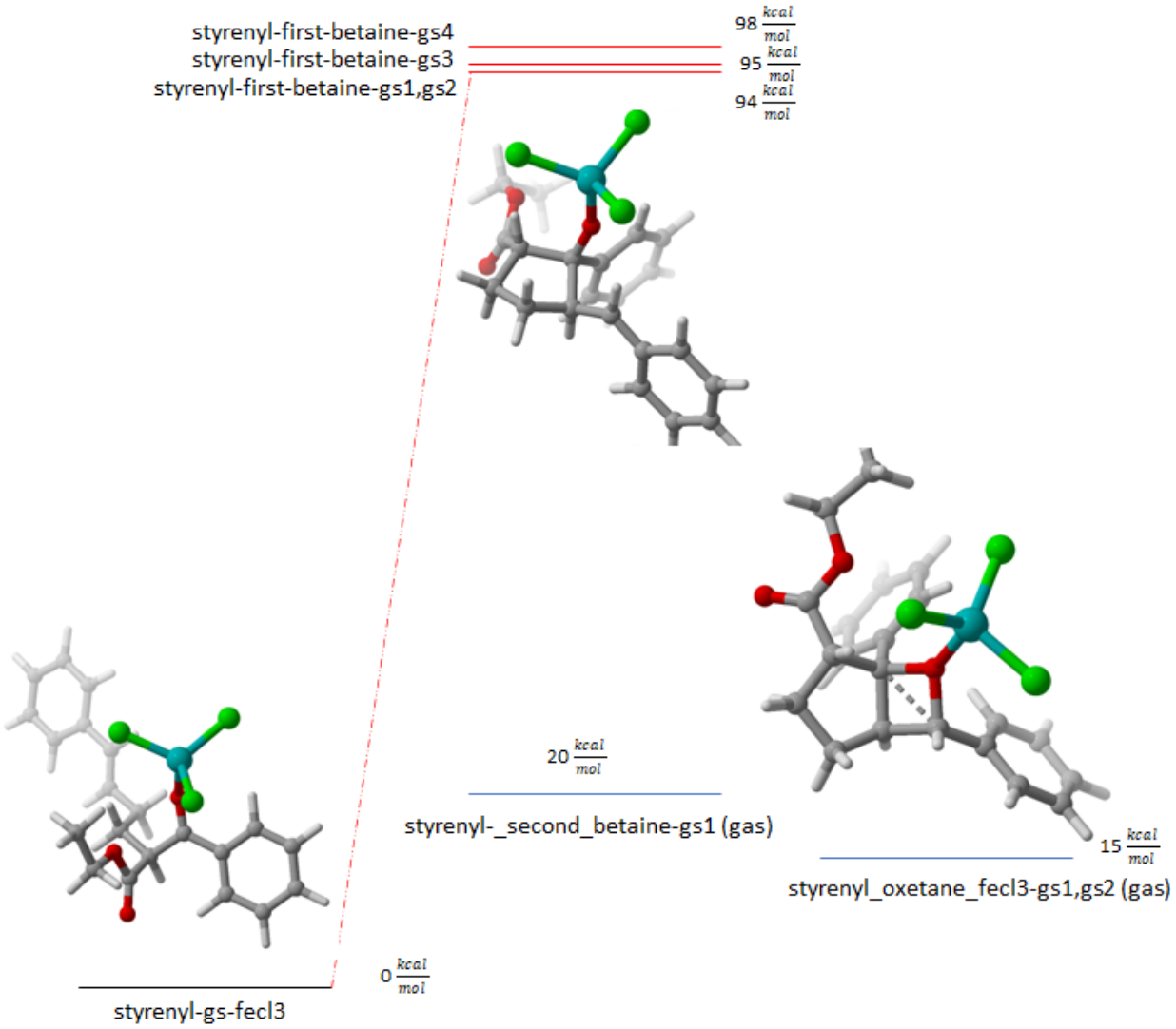

Styrenyl System, Implicit Water (Stepwise)

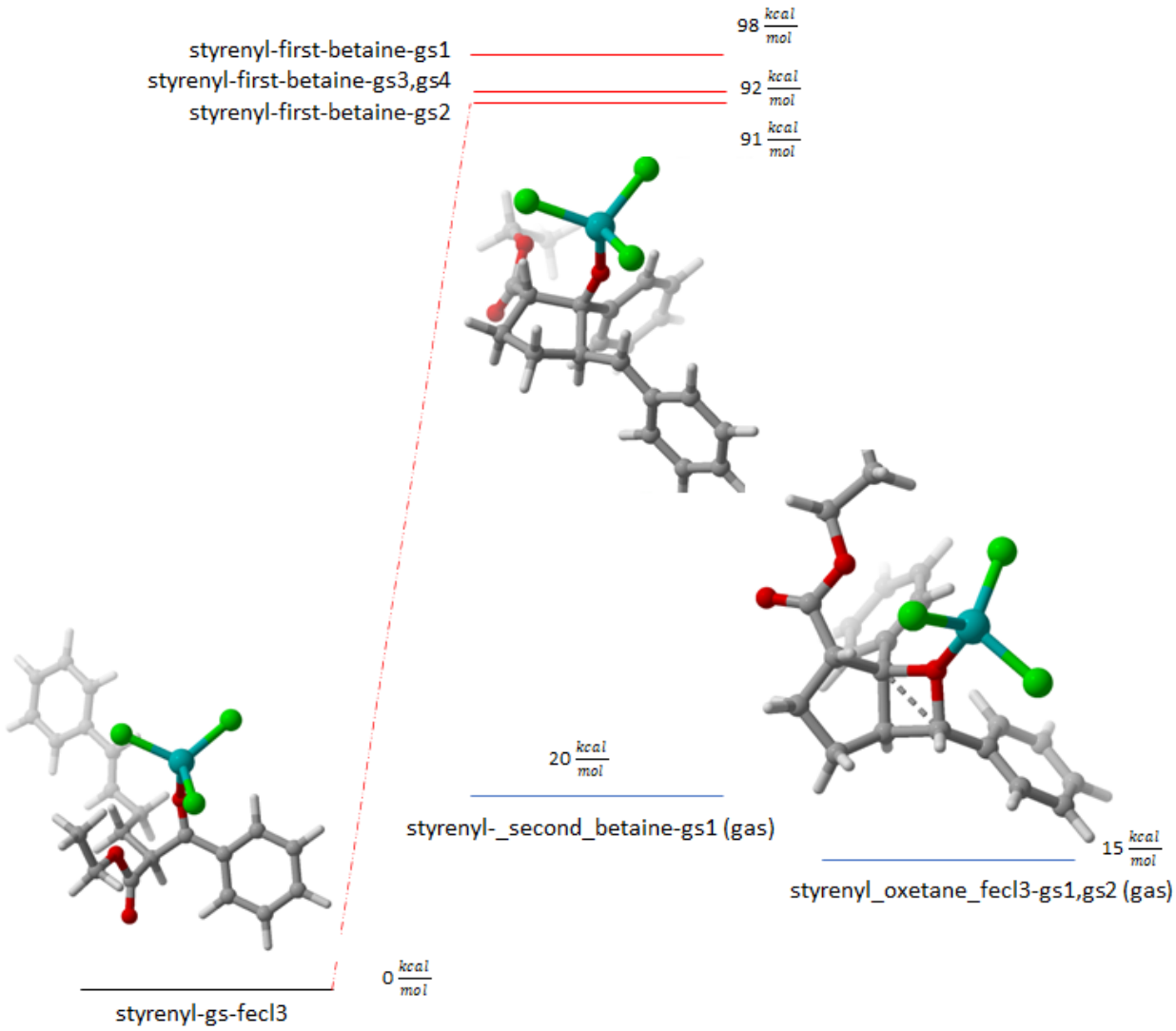

Table of Energies

Concerted Stationary Points

Compound		prenyl														styrenyl										
Phase		gas						dce				water				gas				dce			water			
File Number		1	2	3	4	5	6	1	2	3	4	1	2	3	4	1	2	3	4	1	2	3	1	2	3	4
COMPOUND-first_step-ts_FILENUMBER-b3lyp_d3bj-juldz-PHASE	Electronic (kcal/mol)	20	20	20	21	25	24	13	13	16	15	11	12	15	14	17	16	17	17	11	14	15	11	13	14	11
	Enthalpy (kcal/mol)	18	18	18	19	22	22	11	11	15	14	10	10	13	12	16	16	16	17	11	13	15	11	13	15	12
	Gibbs (kcal/mol)	23	23	23	25	28	26	15	16	19	19	14	15	19	19	22	22	22	23	15	17	19	14	15	18	15
COMPOUND-oxetane_fecl3-gs_FILENUMBER-b3lyp_d3bj-juldz-PHASE	Electronic (kcal/mol)	-1	-2	-5	0	-	-	-	-	-	-	-	-	-	-	2	1	-2	1	-	-	-	-	-	-	-
	Enthalpy (kcal/mol)	0	-1	-4	1	-	-	-	-	-	-	-	-	-	-	3	2	-1	2	-	-	-	-	-	-	-
	Gibbs (kcal/mol)	5	5	2	8	-	-	-	-	-	-	-	-	-	-	8	7	4	9	-	-	-	-	-	-	-
COMPOUND-second_step-ts_FILENUMBER-b3lyp_d3bj-juldz-PHASE	Electronic (kcal/mol)	19	20	22	26	-	-	-	-	-	-	-	-	-	-	16	16	19	18	-	-	-	-	-	-	-
	Enthalpy (kcal/mol)	18	19	21	24	-	-	-	-	-	-	-	-	-	-	15	15	18	18	-	-	-	-	-	-	-
	Gibbs (kcal/mol)	23	23	27	30	-	-	-	-	-	-	-	-	-	-	20	21	26	25	-	-	-	-	-	-	-

Stepwise Stationary Points

Compound		prenyl												styrenyl											
Phase		gas				dce				water				gas				dce				water			
File Number		1	2	3	4	1	2	3	4	1	2	3	4	1	2	3	4	1	2	3	4	1	2	3	4
COMPOUND-first_betaine-ts_FILENUMBER-b3lyp_d3bj-juldz-PHASE	Electronic (kcal/mol)	26	22	26	22	18	91	91	16	17	15	14	15	20	19	17	23	94	92	93	94	96	91	91	92
	Enthalpy (kcal/mol)	24	21	24	21	17	90	89	15	16	14	14	14	19	18	16	21	93	92	92	93	97	91	92	92
	Gibbs (kcal/mol)	29	27	29	27	22	92	92	20	20	18	18	19	25	23	20	29	94	94	95	98	96	91	92	92
COMPOUND-oxetane_fecl3-gs_FILENUMBER-b3lyp_d3bj-juldz-PHASE	Electronic (kcal/mol)	-1	-2	-5	0	-	-	-	-	-	-	-	-	17	16	12	16	-	-	-	-	-	-	-	-
	Enthalpy (kcal/mol)	0	-1	-4	1	-	-	-	-	-	-	-	-	19	17	14	18	-	-	-	-	-	-	-	-
	Gibbs (kcal/mol)	5	5	2	8	-	-	-	-	-	-	-	-	19	19	15	21	-	-	-	-	-	-	-	-
COMPOUND-second_betaine-ts_FILENMBER-b3lyp_d3bj-juldz-PHASE	Electronic (kcal/mol)	14			16	-	-	-	-	-	-	-	-	-	-	-	-	-	-	-	-	-	-	-	-
	Enthalpy (kcal/mol)	14			16	-	-	-	-	-	-	-	-	-	-	-	-	-	-	-	-	-	-	-	-
	Gibbs (kcal/mol)	19			22	-	-	-	-	-	-	-	-	-	-	-	-	-	-	-	-	-	-	-	-

Tables of KIEs

The impact of changing the DFT was assessed for the cycloaddition step. Unless otherwise indicated, the calculations were carried out in the gas phase.

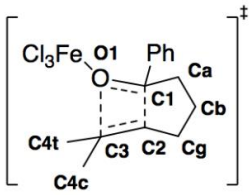

H2 refers to deuterium at position 2 (i.e., vinylic). Me_trans and Me_cis refer to the effects of CD_3 substitution at the indicated methyl groups. Distances are given in Angstroms and "imag_frq" is the imaginary frequency in cm^{-1}. The variation between DFTs is small, with the biggest difference being the size of the imaginary frequency, which will modestly affect the KIEs.

				predicted KIEs									
DFT	C1-C2 dist	C3-O1 dist	imag_frq	C1	C2	C3	Ca	Cb	Cg	C4c	C4t	H2	Me_trans	Me_cis
b1b95	1.663	2.329	308	1.036	1.015	1.029	0.996	0.996	1.000	1.000	1.003	0.864	1.185	1.138
b3lyp	1.676	2.369	343	1.040	1.018	1.029	0.996	0.996	1.001	1.000	1.002	0.852	1.149	1.108
b3lyp_d3bj	1.673	2.361	310	1.037	1.016	1.027	0.996	0.996	1.001	1.000	1.002	0.847	1.153	1.116
b3p86	1.663	2.364	305	1.037	1.015	1.027	0.996	0.996	1.001	1.000	1.003	0.854	1.226	1.138
b3pw91	1.665	2.365	322	1.038	1.015	1.028	0.996	0.996	1.000	1.000	1.002	0.855	1.208	1.123
b971	1.68	2.36	349	1.039	1.016	1.029	0.996	0.996	1.000	1.000	1.002	0.857	1.149	1.106
b972	1.663	2.367	323	1.038	1.015	1.028	0.996	0.996	1.000	1.000	1.002	0.852	1.166	1.112
b97d/CPCM	1.67	2.368	241	1.035	1.013	1.024	0.996	0.996	1.000	0.999	1.002	0.821	1.076	1.098
b97d/gas	1.69	2.318	416	1.042	1.019	1.030	0.996	0.996	1.001	0.999	1.000	0.843	1.115	1.105
b97d3	1.683	2.323	394	1.041	1.018	1.029	0.995	0.996	1.000	0.999	1.001	0.839	1.133	1.110
b97d3_d3bj	1.682	2.342	388	1.042	1.018	1.028	0.996	0.996	1.000	0.999	1.001	0.846	1.145	1.097
b98	1.679	2.359	347	1.039	1.017	1.029	0.996	0.996	1.001	1.000	1.002	0.856	1.145	1.102
bhandh	1.772	2.582	138	1.040	1.028	1.009	0.996	0.998	1.003	1.001	1.003	0.848	1.191	1.172
bhandhlyp	1.653	2.422	140	1.032	1.013	1.022	0.996	0.996	1.001	1.001	1.007	0.836	1.175	1.120

blyp_d3bj	1.696	2.351	417	1.044	1.020	1.029	0.996	0.996	1.001	1.000	1.001	0.856	1.150	1.100
bmk_d3bj	1.665	2.357	259	1.031	1.010	1.028	0.996	0.997	1.001	1.000	1.003	0.852	1.015	1.139
bp86_d3bj	1.679	2.354	373	1.040	1.017	1.029	0.996	0.996	1.001	1.000	1.001	0.861	1.236	1.130
cam_b3lyp_d3bj	1.659	2.418	184	1.032	1.013	1.023	0.996	0.997	1.001	1.000	1.005	0.843	1.189	1.149
hf	1.851	2.69	389	1.057	1.048	1.011	0.996	0.996	1.002	1.000	1.001	0.839	1.020	1.023
lcwpbe_d3bj	1.663	2.745	76	1.025	1.011	1.007	0.998	1.008	1.008	1.001	1.002	0.862	1.169	1.203
m062x	1.709	2.398	209	1.036	1.022	1.023	0.998	0.999	1.001	1.001	1.003	0.863	1.207	1.194
m062x_d3	1.709	2.397	208	1.036	1.022	1.023	0.998	0.999	1.001	1.001	1.003	0.863	1.215	1.191
m06_hf_d3	1.77	2.465	257	1.041	1.037	1.018	0.997	0.999	1.001	1.003	1.003	0.873	1.149	1.201
m06l_d3	1.646	2.311	334	1.038	1.013	1.030	0.996	0.996	1.000	1.000	1.002	0.854	1.200	1.145
m06l_hf_d3	1.646	2.311	334	1.038	1.013	1.030	0.996	0.996	1.000	1.000	1.002	0.855	1.200	1.145
m11	1.728	2.426	224	1.037	1.026	1.021	0.997	0.999	1.001	1.001	1.002	0.861	1.153	1.177
mn12sx	1.697	2.407	159	1.036	1.018	1.022	0.997	0.997	1.001	1.001	1.006	0.864	1.212	1.173
mpw1lyp	1.673	2.375	317	1.039	1.017	1.028	0.996	0.996	1.001	1.000	1.002	0.851	1.145	1.111
mpw1pbe	1.659	2.368	287	1.036	1.014	1.027	0.996	0.996	1.000	1.000	1.003	0.854	1.220	1.137
mpw1pw91	1.66	2.367	290	1.036	1.014	1.027	0.996	0.996	1.000	1.000	1.003	0.853	1.214	1.135
mpw3pbe	1.664	2.364	316	1.037	1.015	1.028	0.996	0.996	1.000	1.000	1.002	0.855	1.217	1.134
n12sx	1.661	2.361	304	1.036	1.015	1.028	0.996	0.996	1.000	1.000	1.003	0.851	1.178	1.126
o3lyp	1.673	2.364	412	1.044	1.017	1.031	0.997	0.995	1.000	1.000	1.002	0.854	1.123	1.088
pbe0	1.659	2.367	285	1.035	1.014	1.027	0.996	0.996	1.000	1.000	1.003	0.854	1.220	1.141
pbe0_d3bj	1.657	2.363	265	1.034	1.013	1.026	0.996	0.996	1.001	1.000	1.003	0.854	1.220	1.151
sogga11	1.694	2.345	571	1.057	1.025	1.036	0.997	0.995	1.000	1.000	1.001	0.881	1.032	1.043
tpsstpss_d3bj	1.693	2.344	395	1.043	1.020	1.028	0.996	0.996	1.000	1.000	1.002	0.862	1.188	1.108
vsxc	1.666	2.27	330	1.040	1.015	1.034	0.996	0.999	1.001	1.001	1.002	0.922	1.117	1.164

The same analysis was carried out for the cycloreversion step:

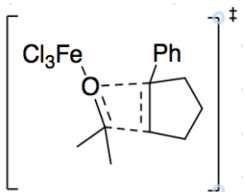

predicted KIEs

DFT	C1-C2 dist	C3-O1 dist	imag_frq	C1	C2	C3	Ca	Cb	Cg	C4c	C4t	H2	Me_trans	Me_cis
b1b95	1.778	2.441	275	1.027	1.03	1.037	1.002	0.997	0.998	0.999	0.998	0.914	0.927	0.982
b3lyp	1.749	2.548	233	1.027	1.028	1.034	1.004	0.996	0.999	0.999	0.998	0.889	0.896	0.959
b3lyp_d3bj	1.798	2.484	287	1.024	1.033	1.038	1.003	0.997	0.999	0.998	0.998	0.900	0.882	0.957
b3p86	1.771	2.533	223	1.025	1.028	1.033	1.004	0.997	0.999	0.999	0.998	0.904	0.914	0.964
b3pw91	1.757	2.532	222	1.027	1.027	1.032	1.004	0.996	0.999	0.999	0.998	0.904	0.913	0.960
b971	1.762	2.525	217	1.028	1.027	1.031	1.004	0.997	0.999	0.999	0.998	0.897	0.901	0.965
b972	1.749	2.539	215	1.028	1.027	1.031	1.004	0.996	0.998	0.999	0.998	0.900	0.905	0.957
b97d/CPCM	1.838	3.039	183	1.014	1.033	1.038	1.001	0.997	1.000	0.999	0.997	0.881	0.865	0.937
b97d/gas	1.751	2.445	377	1.03	1.029	1.041	1.001	0.997	0.998	0.999	0.998	0.888	0.878	0.980
b97d3	1.758	2.446	374	1.029	1.030	1.041	1.001	0.997	0.998	0.999	0.998	0.890	0.882	0.961
b97d3_d3bj	1.750	2.463	350	1.029	1.029	1.040	1.003	0.996	0.998	0.999	0.998	0.892	0.890	0.962
b98	1.758	2.525	219	1.029	1.027	1.031	1.004	0.996	0.999	0.999	0.998	0.897	0.901	0.960
bhandh	1.873	2.452	314	1.024	1.034	1.038	1.002	0.998	1.000	0.997	0.997	0.934	0.924	0.969
bhandhlyp	1.849	2.572	328	1.025	1.037	1.039	1.003	0.997	0.999	0.998	0.997	0.907	0.889	0.940
blyp_d3bj	1.744	2.485	363	1.030	1.028	1.041	1.003	0.997	0.998	0.999	0.998	0.892	0.874	0.970
bmk_d3bj	1.844	2.476	251	1.027	1.031	1.031	1.002	0.997	1.000	0.998	0.997	0.918	0.907	1.030
bp86_d3bj	1.755	2.470	324	1.029	1.027	1.038	1.003	0.997	0.998	0.999	0.998	0.908	0.904	0.976
cam_b3lyp_d3bj	1.845	2.510	325	1.023	1.035	1.04	1.003	0.997	0.999	0.998	0.997	0.912	0.891	0.956
hf	1.912	2.624	464	1.030	1.046	1.045	1.003	0.996	1.000	0.996	0.996	0.922	0.865	0.905
lcwpbe_d3bj	1.883	2.493	363	1.022	1.035	1.042	1.002	0.997	0.999	0.998	0.997	0.929	0.912	0.953
m062x	1.763	2.416	222	1.029	1.029	1.031	1.002	0.998	1.000	0.998	0.998	0.923	0.924	0.963
m062x_d3	1.762	2.416	221	1.029	1.029	1.031	1.002	0.998	1.000	0.998	0.998	0.922	0.924	0.963
m06_hf_d3	1.759	2.400	240	1.032	1.032	1.029	1.003	0.997	1.000	0.998	0.997	0.938	0.912	0.957

m06l_d3	1.758	2.444	273	1.027	1.028	1.037	1.003	0.997	0.998	0.999	0.999	0.899	0.939	0.980
m06l_hf_d3	1.758	2.444	273	1.027	1.028	1.037	1.003	0.997	0.998	0.999	0.999	0.899	0.939	0.980
m11	1.764	2.391	287	1.030	1.031	1.035	1.001	0.998	0.999	0.998	0.997	0.922	0.918	0.957
mn12sx	1.802	2.452	286	1.026	1.033	1.037	1.001	0.997	0.999	0.998	0.998	0.924	0.938	0.975
mpw1lyp	1.769	2.561	235	1.026	1.030	1.034	1.004	0.997	0.999	0.999	0.998	0.891	0.894	0.956
mpw1pbe	1.786	2.536	227	1.025	1.029	1.033	1.003	0.996	0.999	0.999	0.998	0.909	0.917	0.960
mpw1pw91	1.784	2.537	229	1.025	1.029	1.033	1.003	0.996	0.999	0.999	0.998	0.907	0.915	0.959
mpw3pbe	1.765	2.527	224	1.026	1.028	1.033	1.003	0.996	0.999	0.999	0.998	0.905	0.916	0.963
n12sx	1.778	2.535	207	1.025	1.028	1.032	1.004	0.997	0.999	0.999	0.998	0.900	0.894	0.962
o3lyp	1.695	2.506	286	1.035	1.022	1.031	1.003	0.995	0.998	1.000	0.999	0.894	0.886	0.937
pbe0	1.793	2.529	233	1.024	1.030	1.034	1.003	0.997	0.999	0.999	0.998	0.909	0.915	0.962
pbe0_d3bj	1.817	2.493	262	1.023	1.032	1.036	1.003	0.997	0.999	0.999	0.998	0.913	0.909	0.966

The predicted KIEs for the prenyl system in the gas phase are given below. "Me" refers to perdeuterated prenyl methyl groups.

filename	**C1**	**C2**	**C3**	**Ca**	**Cb**	**Cg**	**C4c**	**C4t**	**Me**
prenyl-first_step-ts1-b3lyp_d3bj-juldz-gas.out	1.033	1.009	1.021	0.998	0.996	0.997	1.000	1.001	1.397
prenyl-first_step-ts2-b3lyp_d3bj-juldz-gas.out	1.034	1.013	1.023	0.996	0.996	1.000	0.999	1.002	1.296
prenyl-first_step-ts3-b3lyp_d3bj-juldz-gas.out	1.038	1.014	1.018	0.998	0.998	1.000	0.999	1.003	1.313
prenyl-first_step-ts4-b3lyp_d3bj-juldz-gas.out	1.036	1.017	1.024	0.997	0.997	0.999	0.999	1.001	1.346
prenyl-first_step-ts5-b3lyp_d3bj-juldz-gas.out	1.023	1.010	1.012	0.995	0.998	1.000	1.000	1.008	2.271
prenyl-first_step-ts6-b3lyp_d3bj-juldz-gas.out	1.035	1.012	1.019	0.999	1.000	1.001	1.000	1.004	1.362
prenyl-first_betaine-gs1-b3lyp_d3bj-juldz-gas.out	1.022	1.003	1.005	1.001	0.998	1.008	1.000	1.000	1.676
prenyl-first_betaine-gs2-b3lyp_d3bj-juldz-gas.out	1.019	1.001	1.005	0.999	0.998	1.006	1.000	0.999	1.696
prenyl-first_betaine-gs3-b3lyp_d3bj-juldz-gas.out	1.022	1.003	1.005	1.001	0.998	1.008	1.000	1.000	1.677
prenyl-first_betaine-gs4-b3lyp_d3bj-juldz-gas.out	1.019	1.001	1.005	0.999	0.998	1.006	1.000	0.999	1.696

prenyl-second_step-ts1-b3lyp_d3bj-juldz-gas.out	1.017	1.030	1.036	1.001	0.997	0.999	0.997	0.997	0.844
prenyl-second_step-ts2-b3lyp_d3bj-juldz-gas.out	1.016	1.031	1.037	1.001	0.999	0.999	0.998	0.998	0.845
prenyl-second_step-ts3-b3lyp_d3bj-juldz-gas.out	1.018	1.030	1.038	1.000	0.996	0.998	0.997	0.996	0.827
prenyl-second_step-ts4-b3lyp_d3bj-juldz-gas.out	1.021	1.030	1.038	1.001	0.995	0.998	0.997	0.997	0.833
prenyl-second_betaine-gs1-b3lyp_d3bj-juldz-gas.out	1.009	1.012	1.019	1.000	0.998	0.998	0.996	0.997	0.782
prenyl-second_betaine-gs4-b3lyp_d3bj-juldz-gas.out	1.013	1.011	1.016	1.004	0.997	0.998	0.995	0.997	0.778

The predicted KIEs for the prenyl system in implicit solvent (PCM, DCE) are given below:

filename	**C1**	**C2**	**C3**	**Ca**	**Cb**	**Cg**	**C4c**	**C4t**	**Me**
prenyl-first_step-ts1-b3lyp_d3bj-juldz-dce.out	1.030	1.008	1.016	0.997	0.996	0.998	1.001	1.010	1.266
prenyl-first_step-ts1a-b3lyp_d3bj-juldz-dce.out	1.020	0.998	1.027	0.997	0.996	0.998	1.002	1.002	1.216
prenyl-first_step-ts3-b3lyp_d3bj-juldz-dce.out	1.031	1.007	1.021	0.999	0.999	0.999	1.000	1.003	1.229
prenyl-first_step-ts4-b3lyp_d3bj-juldz-dce.out	1.029	1.007	1.021	0.997	0.997	0.999	1.000	1.003	1.228
prenyl-first_betaine-gs1-b3lyp_d3bj-juldz-dce.out	1.017	1.001	1.005	0.999	0.997	1.010	1.000	1.000	1.149
prenyl-first_betaine-gs2-b3lyp_d3bj-juldz-dce.out	1.020	1.003	1.006	1.001	0.998	1.010	1.001	1.001	1.303
prenyl-first_betaine-gs3-b3lyp_d3bj-juldz-dce.out	1.020	1.005	1.006	0.997	0.998	1.012	1.001	1.001	1.296
prenyl-first_betaine-gs4-b3lyp_d3bj-juldz-dce.out	1.016	1.002	1.005	0.996	0.998	1.012	1.001	1.000	1.269

The predicted KIEs for the styrenyl system in the gas phase are given below:

filename	**C1**	**C2**	**C3**	**Ca**	**Cb**	**Cg**	**styrene_alpha**	**styrene_beta**
styrene-first_step-ts1-b3lyp_d3bj-juldz-gas.out	1.032	1.006	1.016	0.999	0.997	0.998	0.958	0.845
styrene-first_step-ts2-b3lyp_d3bj-juldz-gas.out	1.027	1.007	1.015	0.995	0.997	1.001	0.957	0.835

styrene-first_step-ts3-b3lyp_d3bj-juldz-gas.out	1.039	1.015	1.017	0.997	0.998	1.001	0.946	0.855
styrene-first_step-ts4-b3lyp_d3bj-juldz-gas.out	1.023	1.002	1.018	0.999	1.000	1.003	0.945	0.820
styrene-second_step-ts1-b3lyp_d3bj-juldz-gas.out	1.017	1.012	1.016	1.002	0.997	0.998	0.909	0.883
styrene-second_step-ts2-b3lyp_d3bj-juldz-gas.out	1.014	1.009	1.011	1.001	0.998	0.998	0.893	0.877
styrene-second_step-ts3-b3lyp_d3bj-juldz-gas.out	1.022	0.997	0.999	1.001	0.995	0.996	0.993	0.839
styrene-second_step-ts4-b3lyp_d3bj-juldz-gas.out	1.019	1.001	1.002	1.002	0.997	0.997	0.991	0.851

The predicted KIEs for the styrenyl system in implicit DCE are given below:

filename	**C1**	**C2**	**C3**	**Ca**	**Cb**	**Cg**	**styrene_alpha**	**styrene_beta**
styrene-first_betaine_gs1-b3lyp_d3bj-juldz-dce.out	1.026	1.006	1.000	1.000	0.997	1.004	0.956	0.796
styrene-first_betaine_gs2-b3lyp_d3bj-juldz-dce.out	1.024	1.006	1.001	0.999	1.000	1.007	0.960	0.794
styrene-first_betaine_gs3-b3lyp_d3bj-juldz-dce.out	1.026	1.005	1.001	1.002	0.998	1.004	0.960	0.807
styrene-first_betaine_gs4-b3lyp_d3bj-juldz-dce.out	1.027	1.006	1.001	1.002	0.998	1.004	0.966	0.790
styrene-first_step-ts1-b3lyp_d3bj-juldz-dce.out	1.018	0.995	1.026	0.997	0.997	0.998	0.936	0.829
styrene-first_step-ts2-b3lyp_d3bj-juldz-dce.out	1.019	0.995	1.025	0.998	0.998	0.999	0.926	0.840
styrene-first_step-ts3-b3lyp_d3bj-juldz-dce.out	1.020	0.996	1.026	0.999	1.000	0.999	0.928	0.823

Explicit Solvent Calculations

We performed *ab initio* molecular dynamics using *presto* v0.2.5. *presto* is an open-source Python package designed to make *ab initio* Born-Oppenheimer molecular dynamics simple and user-friendly. *presto* takes an initial xyz file containing the system of interest and a configuration file specifying various run parameters, and uses conventional numerical integration methods to propagate the systems forward in time. Force computations, which are the time-consuming step in most molecular dynamics programs, are performed by external electronic structure programs like Gaussian or *xtb*.

Benchmarking revealed that B3LYP-D3(BJ)/MIDI!-LANL2DZ(Fe,Cl) best balanced speed and accuracy for the solute (see above). For the solvent, we employed the semiempirical non-self-consistent GFN0-xtb method. The two layers were combined using Morokuma's ONIOM scheme.[48]

To accurately model solution phase reactivity, a thermostat is needed to keep the simulation in the canonical (*NVT*) ensemble. We employed a second-order Langevin integrator[78] with a timestep of 1 fs to model collisions with an external heat bath. Previous testing has demonstrated this thermostat to be very effective at keeping simulations in the canonical ensemble.[79]

Particles were confined to a sphere by applying a 10 kcal/mol•Å^2 restoring force to any particles which strayed farther than 14.7 Å from the origin. (14.7 Å was computed from the theoretical volume of the solute and the volume of each DCE molecule in bulk DCE.) The solute was tethered to the origin (via C2) by a 5 kcal/mol•Å^2 constraint, to prevent the solute from wandering to the edge of the sphere and experiencing unphysical edge effects.

To prevent unphysical side reactions of the betaine, two additional constraints were added: the methyl hydrogens on the prenyl group were attached to their corresponding carbons by 200 kcal/mol•Å^2 potential, and the iron was locked to the carbonyl oxygen by a 200 kcal/mol•Å^2 potential. Both potentials took effect only when the bond distance exceeded their equilibrium values of 1.1 Å and 1.8 Å, respectively, ensuring that the only effect would be to steepen the vibrational well for bond dissociation. (Additionally, the hydrogen–carbon constraint only operated on the furthest hydrogen from a given carbon, further lessening the impact on vibrational frequencies.) In the absence of these constraints, Fe–O dissociation sometimes occurred, followed by intramolecular proton abstraction to generate a homoallylic alcohol. These constraints are similar to those employed by Singleton to prevent unphysical side reactions in his study of diene hydrochlorination.[48]

To construct a free energy surface for carbonyl–olefin metathesis, we solvated our model system with 100 1,2-dichloroethane molecules using PACKMOL.[47] This starting configuration was first

initialized at 1000 K with frozen solute, and then slowly cooled to the desired temperature of 323 K over 10 ps. After an additional 10 ps of solvent equilibration at 323 K, the solute was unfrozen and the whole system was equilibrated for an additional 20 ps. A pairwise harmonic constraint kept the C–C and C–O distances to 2.90 Å and 2.90 Å, respectively, to prevent the reaction from progressing (k = 500 kcal/mol•Å^2) during equilibration.

Once equilibration was complete, the C–O and C–C distances were adjusted with *cctk* and new 500 kcal/mol•Å^2 constraints applied (new constraints were gradually initiated over the first 100 fs to prevent spikes in energy). The resulting 130 trajectories were run for 20 ps. The first 5 ps were discarded, to prevent strange effects from initialization, and the subsequent 15 ps analyzed through *wham2d*.[54] (The relatively slow molecular reorganization time of DCE, estimated to be around 3.5 ps,[80] implies that the solvent molecules need at least this much time to fully relax around the solute.)

The trajectories were given the following constraints:

Trajectory	**C2–C3** (Å)	**C1–O4** (Å)
1	3.00	3.00
2	3.00	2.80
3	2.95	2.85
4	2.90	2.95
5	2.90	2.75
6	2.85	2.85
7	2.80	3.00
8	2.80	2.80
9	2.75	3.00
10	2.75	2.80
11	2.75	2.60
12	2.70	2.85
13	2.70	2.65

14	2.65	2.90
15	2.65	2.70
16	2.60	3.00
17	2.60	2.80
18	2.60	2.60
19	2.55	2.95
20	2.55	2.75
21	2.55	2.55
22	2.50	2.95
23	2.50	2.75
24	2.50	2.55
25	2.45	2.95
26	2.45	2.75
27	2.45	2.55
28	2.40	3.00
29	2.40	2.80
30	2.40	2.60
31	2.40	2.40
32	2.35	2.90
33	2.35	2.70
34	2.35	2.50
35	2.35	2.30
36	2.30	2.85
37	2.30	2.65
38	2.30	2.45
39	2.30	2.25
40	2.25	2.85
41	2.25	2.65
42	2.25	2.45

43	2.25	2.25
44	2.20	2.90
45	2.20	2.70
46	2.20	2.50
47	2.20	2.30
48	2.15	2.95
49	2.15	2.75
50	2.15	2.55
51	2.15	2.35
52	2.15	2.15
53	2.10	2.85
54	2.10	2.65
55	2.10	2.45
56	2.10	2.25
57	2.05	3.00
58	2.05	2.80
59	2.05	2.60
60	2.05	2.40
61	2.05	2.20
62	2.00	3.00
63	2.00	2.80
64	2.00	2.60
65	2.00	2.40
66	2.00	2.20
67	2.00	2.00
68	1.95	2.85
69	1.95	2.65
70	1.95	2.45
71	1.95	2.25

72	1.95	2.05
73	1.90	2.95
74	1.90	2.75
75	1.90	2.55
76	1.90	2.35
77	1.90	2.15
78	1.90	1.95
79	1.85	2.85
80	1.85	2.65
81	1.85	2.45
82	1.85	2.25
83	1.85	2.05
84	1.80	2.95
85	1.80	2.75
86	1.80	2.55
87	1.80	2.35
88	1.80	2.15
89	1.80	1.95
90	1.75	2.85
91	1.75	2.65
92	1.75	2.45
93	1.75	2.25
94	1.75	2.05
95	1.70	2.95
96	1.70	2.75
97	1.70	2.55
98	1.70	2.35
99	1.70	2.15
100	1.70	1.95

101	1.65	2.85
102	1.65	2.65
103	1.65	2.45
104	1.65	2.25
105	1.65	2.05
106	1.60	3.00
107	1.60	2.80
108	1.60	2.60
109	1.60	2.40
110	1.60	2.20
111	1.60	2.00
112	1.90	2.15
113	1.85	2.20
114	1.70	2.30
115	1.85	2.50
116	1.85	2.60
117	1.85	2.70
118	1.80	2.75
119	1.90	2.80
120	1.90	2.85
121	1.95	2.90
122	1.90	2.00
123	1.55	2.00
124	1.55	2.15
125	1.55	2.30
126	1.55	2.45
127	1.55	2.60
128	1.55	2.75
129	1.55	2.90

130	1.77	2.46

All input files and data are available in the associated *git* repository.

5.7 References

14. Jackson, A. C.; Goldman, B. E.; Snider, B. B.; Intramolecular and Intermolecular Lewis Acid Catalyzed Ene Reactions Using Ketones as Enophiles. *J. Org. Chem.* **1984**, *49*, 3988–3994.
15. van Schiak, H.-P.; Vijn, R.-J.; Bickelhaupt, F. Acid-Catalyzed Olefination of Benzaldehyde. *Angew. Chem. Int. Ed.* **1994**, *33*, 1611–1612.
16. Soicke, A.; Slavov, N.; Neudörf, J.-M.; Schmalz, H.-G. Metal-Free Intramolecular Carbonyl–Olefin Metathesis of *ortho*-Prenylaryl Ketones. *Synlett* **2011**, *17*, 2487–2490.
17. Griffith, A. K.; Vanos, C. M.; Lambert, T. H. Organocatalytic Carbonyl−Olefin Metathesis. *J. Am. Chem. Soc.* **2012**, ***134***, 18581–18584.
18. Naidu, V. R.; Bah, J.; Franzén, J. Direct Organocatalytic Oxo-Metathesis, A *trans*-Selective Carbocation-Catalyzed Olefination of Aldehydes. *Eur. J. Org. Chem.* **2015**, *2015*, 1834–1839.
19. Ludwig, J. R.; Zimmerman, P. M.; Gianino, J. B.; Schindler, C. S. Iron(III)-Catalysed Carbonyl–Olefin Metathesis. *Nature* **2016**, ***533***, 374–379.
20. Ma, L.; Li, W.; Xi, H.; Bai, X.; Ma, E.; Yan, X.; Li, Z. $FeCl_3$-Catalysed Ring-Closing Carbonyl–Olefin Metathesis. *Angew. Chem. Int. Ed.* **2016**, *55*, 10410–10413.
21. Ludwig, J. R.; Phan, S.; McAtee, C. M.; Zimmerman, P. M.; Devery, J. J.; Schindler, C. S. Mechanistic Investigations of the Iron(III)-Catalyzed Carbonyl–Olefin Metathesis Reaction. *J. Am. Chem. Soc.* **2017**, *139*, 10832−10842.
22. Catti, L.; Tiefenbacher, K. Bronsted Acid-Catalyzed Carbonyl–Olefin Metathesis Inside a Self-Assembled Supramolecular Host. *Angew. Chem., Int. Ed.* **2018**, *57*, 14589−14592.
23. Tran, U. P. N.; Oss, G.; Pace, D. P.; Ho, J.; Nguyen, T. V. Tropylium-Promoted Carbonyl–Olefin Metathesis Reactions. *Chem. Sci.* **2018**, *9*, 5145–5151.
24. Tran, U. P. M.; Oss, G.; Breugst, M.; Detmar, E.; Pace, D. P.; Liyanto, K.; Nguyen, T. V. Carbonyl–Olefin Metathesis Catalyzed by Molecular Iodine. *ACS Catal.* **2019**, *9*, 912−919.
25. Hanson, C. S.; Psaltakis, M. C.; Cortes, J. J.; Devery, J. J. Catalyst Behavior in Metal-Catalyzed Carbonyl–Olefin Metathesis. *J. Am. Chem. Soc.* **2019**, *141*, 11870–11880.
26. Djurovic, A.; Vayer, M.; Li, Z.; Guillot, R.; Blataze, J.-P.; Gandon, V.; Bour, C. Synthesis of Medium-Sized Carbocycles by Gallium-Catalysed Tandem Carbonyl–Olefin Metathesis/Transfer Hydrogenation. *Org. Lett.* **2019**, *21*, 8132–8137.
27. Wang, R.; Chen, Y.; Shu, M.; Zhao, W.; Tao, M.; Du, C.; Fu, X.; Li, A.; Lin, Z. $AuCl_3$-Catalyzed Ring-Closing Carbonyl–Olefin Metathesis. *Chem. Eur. J.* **2020**, *26*, 1941–1946.
28. To, T. A.; Pei, C.; Koenigs, R.; Nguyen, T. V. Hydrogen bonding networks enable Brønsted acid-catalyzed carbonyl–olefin metathesis. **2021**, *Preprint at* https://chemrxiv.org/engage/chemrxiv/article-details/615d8156f718df1626d54e8c.
29. For a review on Lewis acid-catalyzed carbonyl–olefin metathesis reactions, see: [‡]Albright, H.; [‡]Davis, A. J.; [‡]Gomez-Lopez, J. L.; [‡]Vonesh, H. L.; Quach, P; Lambert, T. H.; Schindler, C. S. Carbonyl–Olefin Metathesis Reactions. *Chem. Rev.* **2021**, *121*, 9359–9406. [‡]Authors contributed equally.
30. Gao, J. Hybrid Quantum and Molecular Mechanical Simulations: An Alternative Avenue to Solvent Effects in Organic Chemistry. *Acc. Chem. Res.* **1996**, *29*, 298–305.
31. Jorgensen, W. L. Free Energy Calculations: A Breakthrough for Modeling Organic Chemistry in Solution. *Acc. Chem. Res.* **1989**, *22*, 184–189.
32. Cheng, G.-J.; Zhang, X.; Chung, L. W.; Xu, L.; Wu, Y.-D. Computational Organic Chemistry: Bridging Theory and Experiment in Establishing the Mechanisms of Chemical Reactions. *J. Am. Chem. Soc.* **2015**, *137*, 1706–1725.

33. Becke, A. D. Perspective: Fifty Years of Density-Functional Theory in Chemical Physics. *J. Chem. Phys.* **2014**, *140*, 18A301.
34. Kwan, E. E.; Zeng, Y.; Besser, H. A.; Jacobsen, E. N. Concerted Nucleophilic Aromatic Substitutions. *Nat. Chem.* **2018**, *10*, 917–923.
35. Adames, G.; Bibby, C.; Grigg, R. Rhodium(I) Catalysed Rearrangements of Vinyl Epoxides and Oxetans. *J. Chem. Soc., Chem. Commun.*, **1972**, 491–492.
36. Carless, H. A. J.; Trivedi, H. S. New Ring Expansion Reaction of 2-*t*-Butyloxetanes. *J. Chem. Soc., Chem. Commun.*, **1979**, 382–383.
37. Mata, R. A.; Suhm, M. A. Benchmarking Quantum Chemical Methods: Are We Heading in the Right Direction? *Angew. Chem. Int. Ed.* **2017**, *56*, 11011–11018.
38. Ryu, H.; Park, J.; Kim, H. K.; Park, J. Y.; Kim, S.-T.; Baik, M. Pitfalls in Computational Modeling of Chemical Reactions and How to Avoid Them. *Organometallics* **2018**, *37*, 3228–3239.
39. Guo, Y.; Riplinger, C.; Becker, U.; Liakos, D. G.; Minenkov, Y.; Cavallo, L.; Nesse, F. Communication: An Improved Linear Scaling Perturbative Triples Correction for the Domain Based Local Pair-Natural Orbital Based Singles and Doubles Coupled Cluster Method [DLPNO-CCSD(T)]. *J. Chem. Phys.* **2018**, *148*, 011101.
40. Lee, T. J.; Taylor, P. R. A Diagnostic for Determining the Quality of Single-Reference Electron Correlation Methods. *Int. J. Quantum Chem.* **1989**, *36*, 199–207.
41. Li, B.; Li, Y.; Dang, Y.; Houk, K. N. Post-Transition State Bifurcation in Iron-Catalyzed Arene Aminations. *ACS Catal.* **2021**, *11*, 6816–6824.
42. Mennucci, B. Polarizable Continuum Model. *Wiley Interdiscip. Rev. Comput. Mol. Sci.* **2012**, *2*, 386–404.
43. Singleton, D. A.; Thomas, A. A. High-Precision Simultaneous Determination of Multiple Small Kinetic Isotope Effects at Natural Abundance. *J. Am. Chem. Soc.* **1995**, *117*, 9357–9358.
44. Kwan, E. E.; Park, Y.; Besser, H. A.; Anderson, T. L.; Jacobsen, E. N. Sensitive and Accurate ^{13}C Kinetic Isotope Effect Measurements Enabled by Polarization Transfer. *J. Am. Chem. Soc.* **2017**, *139*, 43–46.
45. Hirschi, J. S.; Takeya, T.; Hang, C.; Singleton, D. A. Transition-State Geometry Measurements from ^{13}C Isotope Effects. The Experimental Transition State for the Epoxidation of Alkenes with Oxaziridines. *J. Am. Chem. Soc.* **2009**, *131*, 2397–2403.
46. Schramm, V. L. Enzymatic Transition States, Transition-State Analogs, Dynamics, Thermodynamics, and Lifetimes. *Annu. Rev. Biochem.* **2011**, *80*, 703–732.
47. Zhuo, M.-H.; Wilbur, D. J.; Kwan, E. E.; Bennet, C. S. Matching Glycosyl Donor Reactivity to Sulfonate Leaving Group Ability Permits S_N2 Glycosylations. *J. Am. Chem. Soc.* **2019**, *141*, 16743–16754.
48. Mayr, H.; Patz, M.; Gotta, M. F.; Ofial, A. R. Reactivities and Selectivities of Free and Metal-Coordinated Carbocations. *Pure & Appl. Chem.* **1998**, *70*, 1993–2000.
49. Source of Hammett rho values: Hansch, C.; Leo, A.; Taft, R. W. A Survey of Hammett Substituent Constants and Resonance and Field Parameters. *Chem. Rev.* **1991**, *91*, 165–195.
50. Hammet rho values from left to right: (a) Nielsen, C. D.-T.; Mooij, W. J.; Sale, D.; Rzepa, H. S.; Burés, J.; Spivey, A. C. Reversibility and Reactivity in an Acid Catalyzed Cyclocondensation to give Furanochromanes – A Reaction at the 'Oxonium-Prins' vs. '*ortho*-Quinone Methide Cycloaddition' Mechanistic Nexus. *Chem. Sci.* **2019**, *10*, 406–412. (b) Brown, H. C., Okamoto, Y. Electrophilic substituent constants. *J. Am. Chem. Soc.* **1958**, *80*, 4979–4987. (c) Hallett-Tapley, G.; Cozens, F. L.; Schepp, N. P. Absolute Reactivity of

Arylallyl Carbocations. *J. Phys. Org. Chem.* **2009**, *22*, 343–348. (d) Qiu, H.; Srinivas, H. D.; Zavalij, P. Y.; Doyle, M. P. Unprecedented Intramolecular [4 + 2]-Cycloaddition Between a 1,3-Diene and a Diazo Ester. *J. Am. Chem. Soc.* **2016**, *138*, 1808–1811. (e) Bonsignore, L.; Loy, G.; Secci, M.; Cabiddu, S.; Gelli, G. Novel Reactions of Carbon Suboxide. Part 8. Kinetic Study of the Reaction with Substituted 2-Hydroxybenzaldehyde Oximes. *J. Chem. Soc., Perkin Trans. 2*, **1988**, *1988*, 1247–1250. (f) Bélanger, G.; Lévesque, F.; Pâquet, J.; Barbe, G. Competition Between Alkenes in Intramolecular Ketene−Alkene [2 + 2] Cycloaddition: What Does it Take to Win? *J. Org. Chem.* **2005**, *70*, 291–296. (g) Meilahn, M. K.; Cox, B.; Munk, M. E. Polar [.pi.4 + .pi.2] Cycloaddition Reaction. Enamines as Dipolarophiles in 1,3-Dipolar Additions. *J. Org. Chem.* **1975**, *40*, 819–824. (h) Laila, A. Concerted Cycloaddition of Triazolinediones to Substituted Styrenes in the Initial 1:1 Adduct Formation: Kinetic Evidence. *J. Prakt. Chem.* **1995**, *337*, 655–658. (i) Baldwin, J. E.; Smith, R. A. Cycloadditions. XII. The Relative Reactivity of Carbethoxycarbene and Carbethoxynitrene in Cycloadditions with Aromatics. *J. Am. Chem. Soc.* **1967**, *89*, 1886–1890.

51. Streitwieser Jr., A.; Jagow, R. H.; Fahey, R. C.; Suzuki, S. Kinetic Isotope Effects in the Acetolyses of Deuterated Cyclopentyl Tosylates.[1,2] *J. Am. Chem. Soc.* **1958**, *80*, 2326–2332.
52. Bartell, L. S. The Role of Non-Bonded Repulsions in Secondary Isotope Effects. I. Alpha and Beta Substitution Effects.[1] *J. Am. Chem. Soc.* **1961**, *83*, 3567–3571.
53. Meyer, M. P.; DelMonte, A. J.; Singleton, D. A. Reinvestigation of the Isotope Effects for the Claisen and Aromatic Claisen Rearrangements: The nature of the Claisen Transition States. *J. Am. Chem. Soc.* **1999**, *121*, 10865–10874.
54. Shiner, Jr., V. J. Deuterium Isotope Effects and Hyperconjugation. *Tetrahedron* **1959**, *5*, 243–252.
55. Stephenson, L. M.; Orfanopoulos, M. Changes in Ene Reaction Mechanisms with Lewis Acid Catalysis. *J. Org. Chem.* **1981**, *46*, 2200–2201.
56. Kresge, A. J.; Lichtin, N. N.; Rao, K. N.; Weston, Jr., R. E. The Primary Carbon Isotope Effect on the Ionization of Triphenylmethyl Chloride. Experimental Determination, Theoretical Justification, and Implications for Carbon Isotope Effects on Nucleophilic Substitution at Saturated Carbon.[1-3] *J. Am. Chem. Soc.* **1965**, *87*, 437–445.
57. Marenich, A. V.; Cramer, C. J.; Truhlar, D. G. Universal Solvation Model Based on Solute Electron Density and on a Continuum Model of the Solvent Defined by the Bulk Dielectric Constant and Atomic Surface Tensions. *J. Phys. Chem. B* **2009**, *113*, 6378–6396.
58. Roytman, V. A.; Singleton, D. A. Solvation Dynamics and the Nature of Reaction Barriers and Ion-Pair Intermediates in Carbocation Reactions. *J. Am. Chem. Soc.* **2020**, *142*, 12865–12877.
59. Nieves-Quinones, Y.; Singleton, D. A. Dynamics and Regiochemistry of Nitration of Toluene. *J. Am. Chem. Soc.* **2016**, *138*, 15167–15176.
60. Eilmes, A.; Kubisiak, P.; Brela, M. Explicit Solvent Modelling of IR and UV–Vis Spectra of 1-Ethyl-3-methylimidazolium Bis(trifluoromethylsulfonyl)imide Ionic Liquid. *J. Phys. Chem. B* **2016**, *120*, 11026–11034.
61. Fu, Y.; Bernasconi, L.; Liu, P. Ab Initio Molecular Dynamics Simulations of the S_N1/S_N2 Mechanistic Continuum in Glycosylation Reactions. *J. Am. Chem. Soc.* **2021**, *143*, 1577–1589.
62. Van Lommel, R.; Bock, J.; Daniliuc, C. G.; Hennecke, U.; De Proft, F. A Dynamic Picture of the Halolactonization Reaction Through a Combination of *ab Initio* Metadynamics and Experimental Investigations. *Chem. Sci.* **2021**, *12*, 7746–7757.
63. Martínez, L.; Andrade, R.; Bergin, E. G.; Martínez, J. M. PACKMOL: A Package for Building Initial Configurations for Molecular Dynamics Simulations. *J. Comput. Chem.* **2009**, *30*,

2157–2164.
64. Chung, L. W.; Sameera, W. M. C.; Ramozzi, R.; Page, A. J.; Hatanaka, M.; Petrova, G. P.; Harris, T. V.; Li, X.; Ke, Z.; Liu, F.; Li, H.-B.; Ding, L.; Morokuma, K. The ONIOM Method and Its Applications. *Chem. Rev.* **2015**, *115*, 5678–5796.
65. Bannwarth, C.; Caldeweyher, E.; Ehlert, S.; Hansen, A.; Pracht, P.; Seibert, J.; Spicher, S.; Grimme, S. Extended Tight-Binding Quantum Chemistry Methods. *Wiley Interdiscip. Rev. Comput. Mol. Sci.* **2021**, *11*, e1493.
66. Vidossich, P.; Lledós, A.; Ujaque, G. First-Principles Molecular Dynamics Studies of Organometallic Complexes and Homogeneous Catalytic Processes. *Acc. Chem. Res.* **2016**, *49*, 1271–1278.
67. Peltzer, R. M.; Gauss, J.; Eisenstein, O.; Cascella, M. The Grignard Reaction – Unraveling a Chemical Puzzle. *J. Am. Chem. Soc.* **2020**, *142*, 2984–2994.
68. Kühne, T. D. Second Generation Car–Parrinello Molecular Dynamics. *Wiley Interdiscip. Rev. Comput. Mol. Sci.* **2014**, *4*, 391–406.
69. Wagen, C. C. *presto*. **2021**, github.com/corinwagen/presto.
70. Grossfeld, A. WHAM: The Weighted Histogram Analysis Method, version 2.0.11, http://membrane.urmc.rochester.edu/wordpress/?page_id=126.
71. Crabb, E.; France-Lanord, A.; Leverick, G.; Stephens, R.; Shao-Horn,Y.; Grossman, J. C. Importance of Equilibration Method and Sampling for *ab Initio* Molecular Dynamics Simulations of Solvent–Lithium-Salt Systems in Lithium-Oxygen Batteries. *J. Chem. Theory Comput.* **2020**, *16*, 7255–7266.
72. Chen, Z.; Nieves-Quinones, Y.; Waas, J. R.; Singleton. D. A. Isotope Effects, Dynamic Matching, and Solvent Dynamics in a Wittig Reaction. Betaines as Bypassed Intermediates. *J. Am. Chem. Soc.* **2014**, *136*, 13122–13125.
73. Plata, R. E.; Singleton, D. A. A Case Study of the Mechanism of Alcohol-Mediated Morita Baylis–Hillman Reactions. The Importance of Experimental Observations. *J. Am. Chem. Soc.* **2015**, *137*, 3811–3826.
74. Marcus, R. A.; Sutin, N. Electron Transfers in Chemistry and Biology. *Biochim. Biophys. Acta* **1985**, *811*, 265–322.
75. Jencks, W. P. When is an Intermediate Not an Intermediate? Enforced Mechanisms of General Acid-Base, Catalyzed, Carbocation, Carbanion, and Ligand Exchange Reaction. *Acc. Chem. Res.* **1980**, *13*, 161–169.
76. Williams, A. The Diagnosis of Concerted Organic Mechanisms. *Chem. Soc. Rev.* **1994**, *23*, 93–100.
77. Singleton, D. A.; Chao Hang, C. ^{13}C and ^{2}H kinetic Isotope Effects and the Mechanism of Lewis Acid-Catalyzed Ene Reactions of Formaldehyde. *J. Org. Chem.* **2000**, *65*, 895–899.
78. Albright, H.; Vonesh, H. L.; Becker, M. R.; Alexander, B. W.; Ludwig, J. L.; Wiscons, R. A.; Schindler, C. S. $GaCl_3$-Catalyzed Ring-Opening Carbonyl–Olefin Metathesis. *Org. Lett.* **2018**, *20*, 4954−4958.
79. Albright, H.; Vonesh, H. L.; Schindler, C. S. Superelectrophilic Fe(III)-Ion Pairs as Stronger Lewis Acid Catalysts for (*E*)-Selective Intermolecular Carbonyl–Olefin Metathesis. *Org. Lett.* **2020**, **22**, 3155–3160.
80. Yang, Y. I.; Shao, Q.; Zhang, J.; Yang, L.; Gao, Y. Q. Enhanced Sampling in Molecular Dynamics. *J. Chem. Phys.* **2016**, *151*, 070902.
81. Souaille, M.; Roux, B. Extension to the Weighted Histogram Analysis Method: Combining Umbrella Sampling with Free Energy Calculations. *Comput. Phys. Commun.* **2001**, *135*, 40–

57.
82. Utimoto, K.; Tamura, M.; Sisido, K. Preparation and Reaction of Cyclopropyltriphenylphosphonium Salt. *Tetrahedron* **1973**, *29*, 1169–1171.
83. Huang, J.-W.; Shi, M. Ring-Opening Reaction of Methylenecyclopropanes with LiCl, LiBr or NaI in Acetic Acid. *Tetrahedron* **2004**, *60*, 2057–2062.
84. Placzek, A. T.; Gibbs, R. A. New Synthetic Methodology for the Construction of 7-Substituted Farnesyl Diphosphate Analogs. *Org. Lett.* **2011**, *13*, 3576–3579.
85. Leškovskis, K.; Gulbe, K.; Mishnev, A.; Turks, M. Ring Opening of Methylenecyclopropanes with Halides in Liquid Sulfur Dioxide. *Tetrahedron Lett.* **2020**, *61*, 1525282.
86. Spell, M. L.; Deveaux, K.; Bresnahan, C. G.; Bernard, B. L.; Sheffield, W.; Kumar, R.; Ragains, J. R. A Visible-Light-Promoted O-glycosylation with a Thioglycoside Donor. *Angew. Chem. Int. Ed.* **2016**, *55*, 6515–6519.
87. Nomura, S.; Endo-Umeda, K.; Aoyama, A.; Makishima, M.; Hashimoto, Y.; Ishikawa, M. Styrylphenylphthalimides as Novel Transrepression-Selective Liver X receptor (LXR) Modulators. *ACS Med. Chem. Lett.* **2015**, *6*, 902–907.
88. Stanetty, P.; Koller, H.; Pürstinger, G.; Grubner S. Synthese Neuer 7-Benzofuranmethanamine Als Heterocyclische Analoga des Squalenepoxidasehemmers Butenafine. *Arch. Pharm. (Weinheim)* **1993**, *326*, 351–358.
89. Karamzadeh, B.; Eaton, T.; Cebula, I.; Torres, D. M.; Neuburger, M.; Mayor, M.; Buck, B. Bestowing Structure Upon the Pores of a Supramolecular Network. *Chem. Commun.* **2014**, *50*, 14175–14178.
90. Ammer, J.; Nolte, C.; Karaghiosoff, K.; Thallmair, S.; Mayer, P.; de Vivie-Riedle, R.; Mayr, H. Ion-Pairing of Phosphonium Salts in Solution: C–H···Halogen and C–H···π Hydrogen Bonds. *Chem. Eur. J.* **2013**, *19*, 14612–14630.
91. Vanden-Eijnden, E., Ciccotti, G. Second-Order Integrators for Langevin Equations with Holonomic Constraints. *Chem. Phys. Lett.* **2006**, *429*, 310–316.
92. Wagen, C. C. *presto* validation. **2021**, github.com/corinwagen/presto/blob/master/VALIDATION.md.
93. Bock, E.; Tomchuk, E. Spin–Lattice Relaxation of 1,2-Dichloroethane in Different Solvents. *Can. J. Chem.* **1969**, *47*, *4365–5368*.